Durham University

Durham E-Theses

Influence of the micro-environment on the maintenance and differentiation of pluripotent stem cells

ELEANOR GRACE KNIGHT

How to cite:

KNIGHT, ELEANOR GRACE (2013) Influence of the micro-environment on the maintenance and differentiation of pluripotent stem cells. Doctoral thesis, Durham University.

Use policy

The full-text may be used and/or reproduced, and given to third parties in any format or medium, without prior permission or charge, for personal research or study, educational, or not-for-profit purposes provided that:

- a full bibliographic reference is made to the original source
- a https://etheses.durham.ac.uk/id/eprint/9462/ is made to the metadata record in Durham E-Theses
- the full-text is not changed in any way

The full-text must not be sold in any format or medium without the formal permission of the copyright holders.

Please consult the full Durham E-Theses policy for further details.

Academic Support Office, The Palatine Centre, Durham University, Stockton Road, Durham, DH1 3LE
e-mail: e-theses.admin@durham.ac.uk Tel: +44 0191 334 6107
https://etheses.durham.ac.uk

Durham University

School of Biological and Biomedical Sciences

Influence of the Micro-Environment on the Maintenance and Differentiation of Pluripotent Stem Cells.

Eleanor Grace Knight

September 2013

A thesis submitted for the degree of Doctor of Philosophy

Abstract

Routine cell culture in two dimensions forces cells to adopt an unnatural flattened morphology. This is unrepresentative of their *in vivo* microenvironment. When primary cells are placed onto standard tissue culture plastic, they tend to become over-proliferative, they stretch out across the rigid surface and become overly adherent to the substrate [1]. Since the development of the glass Petri dish in the early 20th century, standard 2D cell cultureware has been optimised for a range of adherent cells to best mimic their *in vivo* microenvironment. This has often involved the modification of the surface to enhance cell adhesion. However a flat rigid surface that allows for limited cell interactions is not a true representation. Three dimensional (3D) cell culture models are necessary to better understand cell behaviour *in vitro* and to mimic the *in vivo* microenvironment.

A stem cells ability to form multiple cells types and their potential use in therapies to cure diseases; however the cell culture environment is limited. The application of a 3D environment to stem cell biology is of particular interest. Developmental processes involving stem cells rely on signalling between cells to determine cell fate. An increasing effort is focused on the development of new technologies to improve the standard culture environment to allow such signalling and cell interaction to occur. Using a non-degradable porous polystyrene scaffold it has been possible to optimise the 3D culture conditions for a range of cell types including pluripotent stem cells. This knowledge has permitted the long term culture of stem cells in 3D and led to the development of a 3D neuronal differentiation model.

A modified version of the scaffold was also able to mimic the stem cell niche. This allowed for self-renewal and prolonged propagation of a range of pluripotent stem cell lines and human embryonic stem cells in 3D. The prolonged culture in 3D permitted the cells to adapt to the environment. Such adaptation was demonstrated by increased levels of pluripotency markers, a change in cell shape, and increased differentiation potential of the stem cells. This 3D culture system was also assessed as a potential alternative to the teratoma assay. Using the 3D membrane to support terminal differentiation of embryoid bodies led to complex structure formation and differentiation into all three germ layers.

Acknowledgements

I would like to acknowledge funding from the MRC and Reinnervate Ltd without which this work would not have been possible.

I would also like to thank the following people:

My supervisor, Professor Stefan Przyborski for supervision and support over the past four years.

Helen Bradburn and John Gardner at Roslin Cellab for their assistance with ES/EB work.

Prof M Lako at Newcastle University for assistance with the teratoma study and for providing H9 cells.

All members of Office 234, who have made the last four years so much easier; including Dan, Rachel, David, Rosie, Sarah, Bridie and Ally who are always willing to provide tea and/or wine. Especially Rosie, who has rescued me from many ridiculous situations over the past few years and James, for his help with confocal microscopy.

Finally I would like to thank my family – Mum, Dad, Roisin and Jack for their support during my studies and Jonathan for love, support, patience and willingness to travel.

Declaration

The work described herein was carried out in the Department of Chemistry, or the School of Biological and Biomedical Sciences, University of Durham between October 2009 and September 2013. All of the work is my own, except where specifically stated otherwise. No part has previously been submitted for a degree at this or any other university.

Statement of Copyright

The copyright of this thesis rests with the author. No quotation from it should be published without the prior written consent and information derived from it should be acknowledged.

Publications arising from this work:

Knight, Eleanor., Murray, Bridgid., Carnachan, Ross., Przyborski, Stefan,. **Alvetex®:polystyrene scaffold technology for routine three dimensional cell culture.** Methods Mol Biol, 2011. 695:p.323-40.

Oral Presentations:

Developing a 3D Model for the Propagation and Differentiation of Stem Cells in 3D. (2012) Cell Control in a Petri Dish Early Stage Researchers Forum, Nottingham, UK.

Neural Differentiation by Human Pluripotent Stem Cells is Regulated by Scaffold Presentation. (2012) 3rd TERMIS World Congress, Vienna, Austria.

Neural Differentiation of Pluripotent Stem Cells is Regulated by Scaffold Format. (2012) Tissue and Cell Engineering Society conference, Liverpool, UK.

Neural Differentiation During 3D Culture is Regulated by Scaffold Presentation (2011). 13th Annual White Rose Biomaterials and Tissue Engineering Work in Progress Meeting, Sheffield, UK

Published abstracts:

Neural differentiation by human pluripotent stem cells is regulated by scaffold presentation. Knight E.G., Przyborski S.A, TERMIS World Congress, Vienna, Austria. J Tissue Eng Regen Med 2012; **6 (Suppl.1): p.256**

Neural differentiation of pluripotent stem cells is regulated by scaffold format. Knight E.G., Przyborski S.A., TCES conference, Liverpool, UK European Cells and Materials, **23**, supplement 4, 2012

Alvetex® ®: Technology that Enables Routine 3D Cell Culture for Use in Research Knight E., Przyborski S. TCES annual meeting, Leeds, UK. European Cells and Materials, **22,** supplement 3, 2011

Posters presented:

Neural Differentiation by Human Pluripotent Stem Cell is Enhanced During 3D Culture. Knight E., Przyborski S., (2011) Strategies for Successful Tissue Regeneration: NESCI Research Day, Durham, UK

Considering the Metabolic Demands of Cells When Grown in Three Dimensional Cultures. Knight E., Przyborski S., (2010) 12th Annual White Rose Biomaterials and Tissue Engineering Work in Progress Meeting, Leeds, UK

Enhanced Differentiation of Human Pluripotent Stem Cells using Alvetex® – a Unique Technology for 3D Cell Culture. Knight E.G., Maltman D.J., Christie V.B., Carnachan R., Parchure A., Murray, B.A., Przyborski S.A., (2010). Revolutionizing drug discovery with stem cell technology, Biochemical Society Focused Meeting, Stevenage, UK

Table of Contents

List of Figures

List of Tables

List of Abbreviations

2D ..... Two Dimensional

3D..... Three Dimensional

3Rs ..... Replacement, Reduction & Refinement

A2B5 ..... Ganglioside epitope, marker for early neuronal differentiation

AFP ..... Alpha-fetoprotein

ATCC ..... American Type Culture Collection

ATRA ..... *all-trans* Retinoic Acid

bFGF ..... basic Fibroblast Growth Factor

BrdU ..... Bromodeoxyuridine

BSA ..... Bovine Serum Albumin

DAPI ..... 4',6-diamidino-2-phenylindole

dH_2O ..... Distilled water

DMEM ..... Dulbecco´s Modified Eagle Medium

DMSO ..... Dimethyl sulfoxide

DNA ..... Deoxyribonucleic Acid

D_p ..... Penetration Depth

dsDNA ..... double stranded Deoxyribonucleic Acid

EB ..... Embryoid Body

EC ..... Embryonal Carcinoma

EC23 ..... Photostable synthetic retinoid

ECM ..... Extracellular Matrix

EDTA ..... Ethylenediaminetetraacetic acid

ES ..... Embryonic stem cells

FACS ..... Fluorescence-activated Cell Sorting

FCS ..... Fetal Calf Serum

H&E ..... Haematoxylin and Eosin

H9 ..... Human embryonic stem cell line

HA ..... Hyaluronic Acid

HEMA..... 2-hydroxyethyl methacrylate

hESCs ..... human Embryonic Stem cells

HIPE ..... High Internal Phase Emulsion

hMSC ..... human Mesenchymal Stem Cell

ICM ..... Inner Cell Mass

iPSC ..... induced Pluripotent Stem Cell

Ki-67 ..... Proliferation marker

LIF ..... Leukaemia Inhibitory Factor

MC ..... Media Change

MEF ..... Mouse Embryonic Fibroblasts

mESC ..... Mouse Embryonic Stem Cell

MET 4 ..... Squamous cell carcinoma line

mTeSR1 ..... Defined ES media

MTS ... 3-(4,5-dimethylthiazol-2-yl)-5-(3-carboxymethoxyphenyl)-2-(4-sulfophenyl)-2H-tetrazolium

MTT ..... 3-(4,5-dimethylthiazol-2-yl)-2,5-diphenyltetrazolium bromide

NAD+ ..... Nicotinamide adenine dinucleotide

NF-200 ..... Neurofilament-200

NICD ..... Notch intracellular domain

NIH ..... National Institutes of Health

NIH 3T3 ..... Mouse embryonic fibroblast cell line

NPC ..... Neural Progenitor Cells

NSC ..... Neural Stem Cells

Oct 4 ..... Embryonic stem cell marker

PBS ..... Phosphate Buffered Saline

PFA ..... Paraformaldehyde

PLGA ..... Poly(lactic-co-glycolic acid)

PLA ..... Polylactic acid

qPCR ..... quantitative Polymerase Chain Reaction

RC-6 ..... Human ES cell line provided by Roslin Cellab

RC-10 ..... Human ES cell line provided by Roslin Cellab

RNA ..... Ribonucleic Acid

ROS ..... Reactive Oxygen Species

RPM ..... Rotations Per Minute

SCID ..... Severe Combined Immunodeficiency

SEM ..... Standard Error of the Mean

SEM ..... Scanning Electron Micrograph

Shh ..... Sonic Hedgehog Protein

SMA ..... Smooth Muscle Actin

SSEA-3 ..... Stage-specific embryonic antigen 3

TCA ..... TriCarboxylic Acid

TCP ..... Tissue Culture Plastic

TERA2.cl.SP12 ..... Human embryonal carcinoma cell line

TGCT ..... Testicular Germ Cell Tumour

TRA-1-60 ..... Pluripotency marker

TUJ-1 ..... Neuronal Class III beta-tubulin

UV ..... UltraViolet

Y-27632 ..... ROCK inhibitor

ZPA ..... Zone of Polarising Activity

Influence of the Micro-Environment on the Maintenance and Differentiation of Pluripotent Stem Cells.

1 Introduction

1.1 Overview

This study is focused on the development and application of new technologies to modify the growth environment for stem cells in culture and to enhance differentiation of their derivatives. It has long been recognised that 2D culture systems are not sufficient for the complex differentiation of stem cells *in vitro*. There have been many attempts to mimic the *in vivo* environment using extracellular matrix proteins [2] and more recently these have involved the development of 3D systems [3-5]. However none of these methods have produced defined conditions for stem cell maintenance and differentiation in 3D. To fully optimise such a system it is necessary to blend technology development, with knowledge of engineering and biology.

Adoption of 3D culture technologies has been slow. This is due to a range of reasons as identified by Comley in Drug Discovery World [6]. These include:

1. Poor reproducibility between batches of biomimetic scaffolds.
2. Limited ability to scale up or down.
3. Difficulty in post-culture processing.
4. Difficulty of extractions from the matrix.
5. Little flexibility in accommodating different cell lines and types.
6. Characterising cell in 3D geometries is difficult.
7. Poor visualisation of cells.
8. Limited stability in long term experiments.
9. 3D matrices have too many components and creation of constructs is difficult and laborious.
10. Lack of consistency between cultures especially when using primary cultures and stem cells.

A fully optimised, non-degradable, ready-to-use scaffold would overcome the majority of these issues for routine 3D culture.

In this work I provide a background to highlight the need for reproducible 3D cell culture and demonstrate how such a system will enhance the *in vitro* environment. This will be achieved by replicating cell contact and cell signalling *in vivo*. The work then highlights developmental

processes that require the 3D environment and therefore cannot be replicated in standard cell culture. Attempts to mimic the *in vivo* environment during standard 2D culture are discussed and also previous attempts at creating 3D culture environments. Finally, it details a model pluripotent stem cell line which will be ideal for optimisation of 3D substrates for stem cell culture.

Detailed literature reviews have been incorporated into the beginning of each chapter and provide a detailed description and justification for each area of study. Due to the wide ranging scope of this thesis through protocol development, tissue engineering challenges and biological applications individual reviews of the literature for each topic provided a better insight into the purpose of the research.

Chapter 2 establishes defined culture conditions in 3D. The literature review gives examples of surface coating used to enhance cell attachment and details previous attempts at optimising scaffold cultures. The review concludes that the vast majority of 3D culture systems have previously been optimised for use with osteoblast or bone-like cells. This is consistent with the previously mentioned issue 5. Experiments detailed in this chapter help to overcome the issues mentioned in points 1, 3, 5, 7, & 9. The porous polystyrene scaffold used throughout this study demonstrates high reproducibility. This is due to it not being biodegradable. The scaffold is produced with defined pore and interconnect size. Batches of scaffolds are also quality controlled to confirm biocompatibility and require minimal treatment prior to cell seeding (issue 1 & 9). I have also developed standard protocols for use with the 3D scaffold system. These are detailed in the method sections throughout this work (issue 3) and include protocols for the visualisation of cells in 3D culture which have been published (Knight et al, 2011 [7]) (issue 7). Finally this chapter adapts cell seeding methods, cell density and surface treatment for 3D cultures as well as producing 3D growth profiles for a range of cell lines. This demonstrates the flexibility of the porous polystyrene scaffold for accommodating different cell types (issue 5). The scaffold's flexibility gives it potential for use in a range of cell culture models including developmental and cancer models and also models for *in vitro* testing.

Chapter 3 incorporates a detailed optimisation of 3D stem cell cultures. The literature review highlights issues that are unique to 3D cultures due to the increased space for cell expansion provided by the scaffold. This includes the rapid build-up of waste products and nutrient diffusion as well as poor cell infiltration into the scaffold interior. Poor optimisation of a scaffold system can lead to either a build-up of cells at the surface of a construct or a necrotic area at the centre of a construct. Gradients of nutrients and waste products are a particular issue during stem cell cultures and they affect differentiation. I demonstrate opportunities for scale up of 3D cultures to produce large numbers of cells (11 million cells per scaffold within 5 days) (issue 2) and also

methods for the extraction of cells from the matrices for downstream processing, this is also covered in Chapter 4 using a modified scaffold (issue 4). After modification of the scaffold support system it was possible to combine all the knowledge gained in the previous chapter with the modified scaffold presentation and nutrient profile to produce a 3D model of neuronal differentiation. TERA2.cl.SP12 cells were differentiated in 3D for up to 16 days and displayed enhanced differentiation. This suggests that the 3D system is suitable for long term culture (issue 8) and demonstrated an application for the scaffold for research into the differentiation of stem cells in a 3D environment.

Chapter 4 displays a change in tactics. Instead of using the 3D environment to promote differentiation, a 3D system was developed to maintain stem cell self-renewal. This involved modification of the 3D system by reducing pore and interconnect size while retaining scaffold reproducibility. In this chapter I demonstrate methods for assessing the geometry of cells from 3D cultures (issue 6). The literature review details attempts to establish a stem niche during standard 2D culture. The 2D culture environment has profound effect on stem cells and not only affects cell shape and proliferation but can also lead to karyotypic changes and increased tumorigenesis [8-10]. After establishment of an optimised model for the prolonged propagation of stem cells *in vitro* we were able to adapt the protocols for the growth of hESCs. The 3D culture environment enhanced their differentiation potential both *in vitro* and *in vivo*.

Finally, Chapter 5 demonstrates how a fully optimised 3D environment has the potential to be used as a replacement for *in vivo* testing. The assay that was identified for replacement was the teratoma assay. I demonstrate that the 3D environment afforded by a scaffold goes part of the way to producing an alternative testing method. This process would need only simple validation before it could be implemented as an alternative *in vitro* assay.

I have developed protocols for use with 3D constructs and have overcome many technical engineering challenges to produce fully optimised and defined systems for the 3D culture of stem cells. I have also demonstrated the biological applications of the 3D system. In the discussions for each chapter I highlight the further opportunities for biological characterisation and applications of the 3D culture system.

1.2 Background

It is well established that cells adapt to their environments by responding to local signals and cues, this has consequences on cell proliferation, differentiation and function. For example cells grown *in vitro* on conventional two dimensional (2D) polystyrene substrates adopt an unnatural geometry, remodel their cytoskeleton and change their growth characteristics. This in turn affects their ability to function and differentiate and they become poor delegates of their native counterparts [11]. When cells are grown as a monolayer, the majority of their surface area is either exposed to a plastic substrate or to the culture medium. This leads to minimal opportunities for interactions with neighbouring cells. This situation is far-removed from *in vivo* conditions. This has significant impact on cell performance and consequently influences the representation of any biological assays. Many existing cell lines used in research today have become far removed from their source of origin and are no longer truly representative as an effective model.

Structural re-organisation of cell shape and the limited scope for cell-cell interaction also impacts on the degree of differentiation of cells grown in conventional 2D culture plates [12]. Developmental processes rely on signalling between cells to determine cell fate [13]. This has major relevance for stem cell biology as it is the objective to reproduce developmental processes and engineer specific cells and tissue types *in vitro*. An increasing amount of effort is focused on the research and development of new technologies to improve the standard culture environment in an attempt to mirror *in vivo* conditions. This will enable cells to interact more readily and differentiate into representative functional tissues. Previous research has demonstrated that a three dimensional (3D) environment may be necessary to model morphogenetic and remodelling events. These include demonstrating that 3D architecture is necessary for the production of functional tissue such as in epithelial acinar formation [14] and studies of mammary [15] and kidney [16]. A seminal work by Roskelley et al. demonstrates the link between a mammary phenotype and 3D culture conditions by forming rounded cell cluster on non-adhesive polyHEMA (poly(2-hydroxyethyl methacrylate) coated plates [17]. By placing cells into a 3D environment and allowing the production of dense tissue-like structures, it is possible to create molecular gradients and study the impact of naturally arising concentration gradients. Such gradients can affect cells in one of two ways. Firstly it can cause the central areas of tissue to behave differently to surface cells due to differences in factors such as oxygen and nutrient concentration or secondly it can lead to chemotactic migration, for examples towards a richer nutrient source.

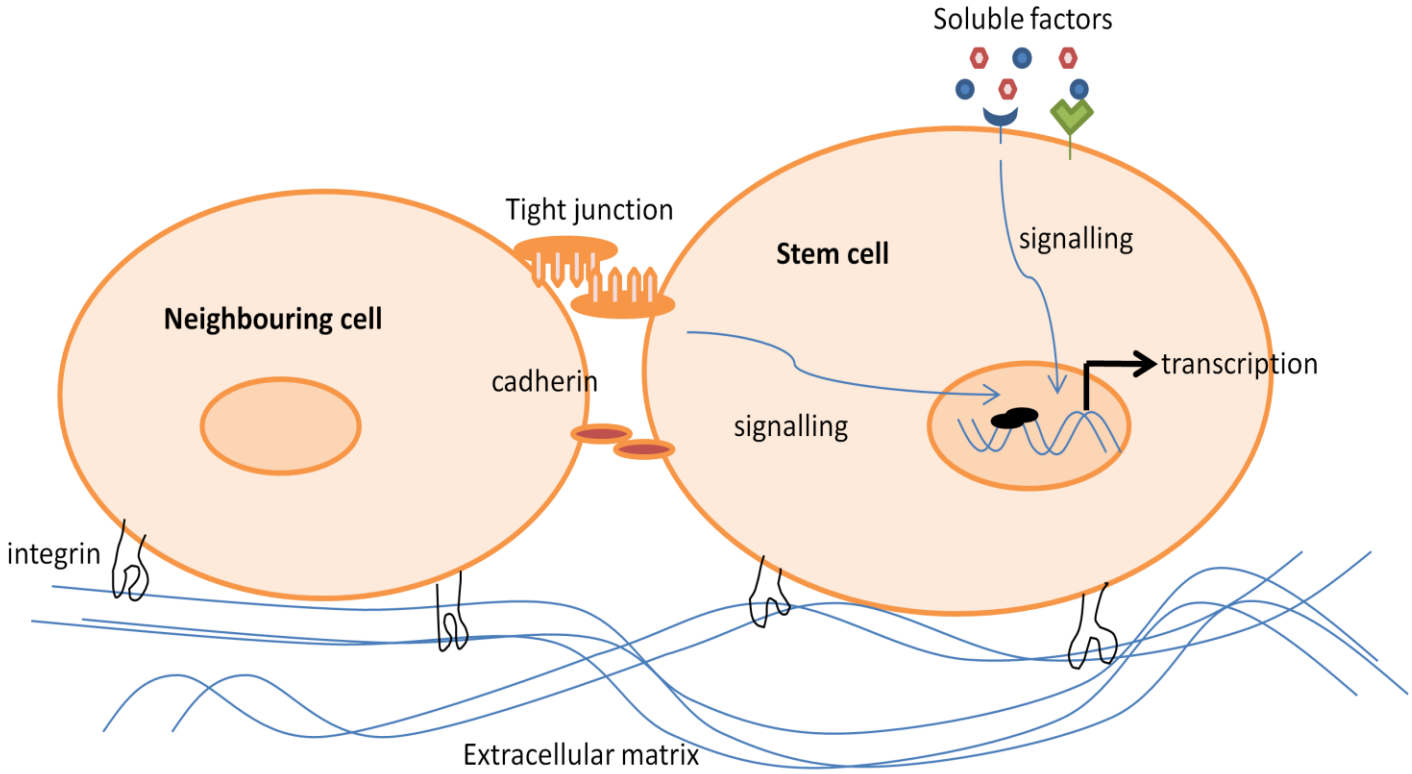

Figure 1.1 Schematic of stem cell interactions with the extracellular microenvironment. Adapted from Haque et al.[18]. Stem cell fate is influenced by a range of soluble factors such as cytokines and growth factors, by the extracellular matrix via integrin binding to extracellular matrix proteins such as collagen and fibronectin and finally signals from neighbouring cells via cadherins and other cell adhesion molecules.

Such differences in oxygen and nutrient concentration across a 3D culture have led to the development of well inserts. The inserts help to lift cells to near the air liquid interface which also allows nutrients to diffuse upwards through scaffold cultures [19].

This study is focused on the development and application of new technologies to modify the growth environment for stem cells in culture and to enhance differentiation of their derivatives. Further examples demonstrating the importance of spatial environment and how it influences cell-cell interactions and developmental processes will be reviewed. This investigation will examine three dimensional (3D) cell culture models to overcome the limitations of existing methods of 3D cell culture and enable cells to grow and function in a more realistic manner. Much of the initial work requires understanding and technical development of the culture environment to provide an optimised system for stem cell growth, proliferation, self-renewal and differentiation.

1.2.1 Cell environment

The extracellular microenvironment affects cell behaviour. The microenvironment or niche in which a stem cell resides regulates the cells survival, self-renewal and differentiation [20]. There are many components that form the stem cell niche including insoluble natural matrix molecules such as laminin [21], collagen [22, 23] and fibronectin [24], soluble macromolecules including cytokines and growth factors [25] that assist in the signalling between cells and the environment and finally proteins on the surface of adjoining cells (e.g. cadherins) [26]. These are shown schematically in Figure 1.1. All these factors can lead to changes in gene transcription which ultimately affects cell shape, proliferation, differentiation and possibly even apoptosis.

1.2.1.1 Cell signalling within the microenvironment

A cell can only perform its function if it can ascertain its location with respect to neighbouring cells. Cells communicate and probe their environment via juxtacrine signalling (by direct cell contact), autocrine or paracrine signalling. Processes such as embryogenesis are highly orchestrated by interactions of various cell signalling pathways. Cues from paracrine signalling pathways determine both cell fate and tissue organisation [27] and autocrine signalling allows cells to respond to the microenvironment [28]. Cells are also influenced by factors such as cell shape, cell contact, and are affected by the chemical and mechanical properties of the surrounding fluid and extracellular matrix (ECM). All of these factors are particularly important in the case of stem cell cultures and will be reviewed further. Embryonic stem cells (ESCs) differentiate into a range of adult cell types and form complex structures. Recent research has shown their ability to differentiate *in vitro* but there are limits to the complexity that they can achieve with limited signalling capabilities and interactions with their environment [29]. When

studying stem cells *in vitro*, conventional cell culture only allows for limited cell-cell and cell-matrix interactions as demonstrated in Figure 1.2. Embryonic stem cell differentiation in 2D culture does not mimic the *in vivo* environment and can lead to inefficient and highly heterogeneous differentiation. There have also been many studies which demonstrate a difference in differentiation between 2D and 3D culture. Tanaka et al. demonstrated that the culture of mouse embryonic stem cells (mESCs) in 3D micromass cultures led to enhanced expression of cartilage marker genes compared to their 2D counterparts [30]. Similarly Hwang et al. used polyethylene glycol (PEG) hydrogels to culture mESC derived embryoid bodies (EBs) and compared these to monolayer cultures [31]. Differentiation in 3D led to upregulation of cartilage relevant markers. It has also been suggested that a 3D microenvironment can lead to selective differentiation [32].

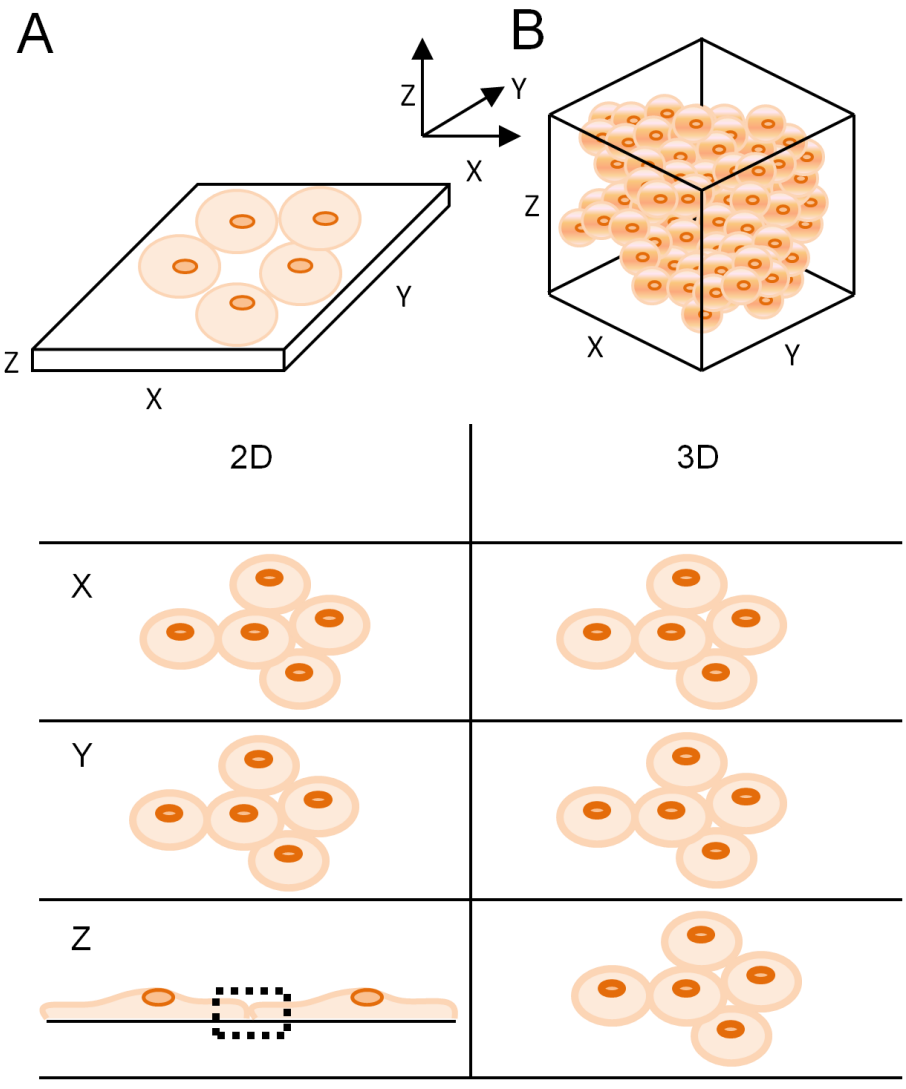

Figure 1.2. Differences between 2D and 3D cell growth. During standard monolayer culture cells exhibit an unnatural flattened morphology and are only able to signal with a limited number of cells **(A). B** highlights the advantages of 3D cell culture or *in vivo* environment. These cells have a more rounded morphology and interact with many more neighbouring cells which allows for more complex cell to cell interactions. The second half of the diagram shows cross-sections through each plane and highlights the differences between 2D and 3D cell growth. In vitro (2D) cells do have a '3D' structure but the height of cells is minimal and unnatural. The dotted box highlight the limited areas of cell contact in the 2D culture environment.

1.2.1.2 Cell-to-cell signalling

There are many examples of cell-to-cell signalling including Notch signalling. Notch is a contact-dependent signalling pathway involved in lateral inhibition, mutual inhibition and lateral specification [33] and has also been demonstrated to control cell fate decisions [34]. During asymmetrical division of stem cells, one cell retains it stem cell phenotype while the daughter cell adopts an altered cell type which drives it towards proliferation and differentiation. As this new cell fate is adopted Notch signalling amplifies small differences in the population and suppresses neighbouring cells from adopting a similar cell type (Figure 1.3). For example in the ventricular zone of the developing chick spinal cord, the activation of Notch signalling prevents neighbouring neuroepithelial cells from undergoing neuronal differentiation [35]. One of the most important features of the Notch protein is that it is both a transmembrane receptor and a transcription factor. Notch as a transmembrane protein comprises of a large extracellular domain, a transmembrane domain and an intracellular domain. The transmembrane linker region prevents premature activation of the receptor and the Notch intracellular domain (NICD) contains a nuclear localisation signal and is a transcription factor. Notch does not become active until it is modified by cleavage of the S1 site in the Golgi apparatus [36], Notch's binding affinity to Delta/Jagged is also modified in the Golgi through glycosylation by Fringe. Delta or Jagged interacts with a Notch receptor on a neighbouring cell causing cleavage of Notch and endocytosis of the Delta/Jagged–Notch complex. This leaves the linker and intracellular domain, the linker is cleaved by presenilin containing enzyme complex γ-secretase releasing the NICD [37]. Leaving NICD free to translocate to the nucleus and bind to CSL (CBF-1, Suppressor of Hairless, Lag-1) which disassembles the repression complex and forms an activation complex with Mastermind (MAM). This process is detailed schematically in Figure 1.4. Gene activation gives rise to increased transcription of Notch genes including repressors responsible for expressing tissue specific proteins and inhibit differentiation [38].

Regulation of Notch signalling is vital in development as demonstrated by Notch mutant flies not developing past the embryonic stage [39]. More recent studies have shown that although Notch is not required for propagation of undifferentiated hESCs it is required for the maintenance of differentiating cell types [40]. Although this does not appear to be the case in embryonic carcinoma (EC) cells where studies into the inhibition of the Notch signalling pathway by γ-secretase inhibitors (GSIs) suggests that cell proliferation is affected by Notch [41].

The Notch signalling pathway has been shown to affect stem cell expansion both *in vivo* and *in vitro*. Androutsellis-Theotokis et al. demonstrated that Notch ligands regulate stem cell expansion through a pathway that is fundamental to both development and cancer [42]. Fox et al. also demonstrated that Notch signalling regulates cell proliferation of hESCs and their malignant

equivalents – embryonal carcinoma cells [41]. If small interfering RNA was used to knockdown NOTCH1 and NOTCH2 then there was a reduction in cell growth without evidence of differentiation. This may account for the slow proliferation of stem cells *in vitro* and therefore the problems producing a large of cells for stem cell therapies. For Notch signalling to be effective, it requires cell-cell contact [33]. In Figure 1.2 the red boxes highlight the extent of cell contact during standard monolayer culture and demonstrate it may not be sufficient for successful maintenance of stem cells. In addition to this Notch signalling is also required for neuronal differentiation as it has been shown to promote neural lineage entry of pluripotent stem cells. Lowell et al. found that pharmacological or genetic interference of Notch signalling suppressed neural fate choice and limiting its activation led to heterogeneous lineage commitment [43]. It is clear from the wide ranging affects of this pathway, in both stem cell development and differentiation and human diseases [44, 45], if Notch signalling is limited then normal development is not possible. The minimal cell contact provided by conventional 2D monolayer culture cannot provide a true model of cells *in vivo* especially when studying stem cell differentiation. It is therefore necessary to enhance the culture environment by developing 3D models for stem cell maintenance and neuronal differentiation.

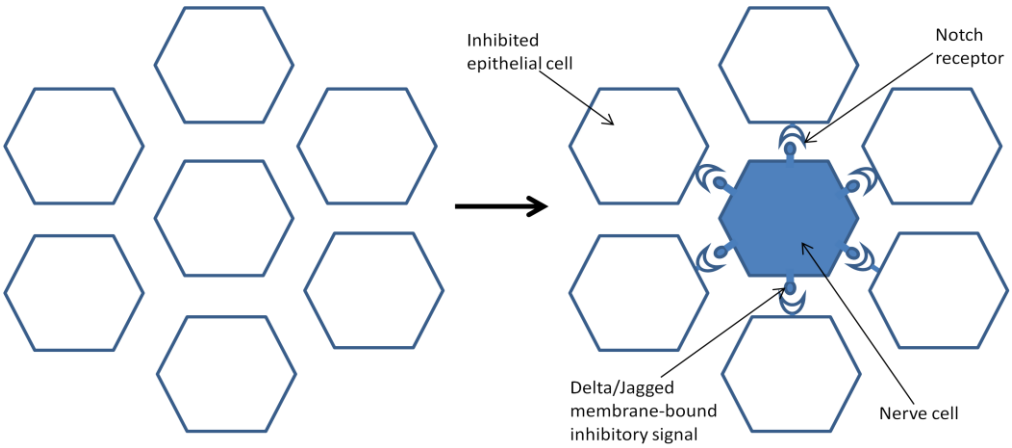

Figure 1.3 Lateral inhibition in an epithelial sheet. If one cell in the epithelial sheets starts to display a neuronal phenotype this leads to the expression of Delta/Jagged receptors on the surface of this cell. When Delta binds to Notch on adjoining cells this inhibits the expression of neuronal genes in the neighbouring cells and allows them to express genes to produce supporting cells to the nerve cell. An example of such nerve epithelium interactions occurs during olfactory nerve formation [46].

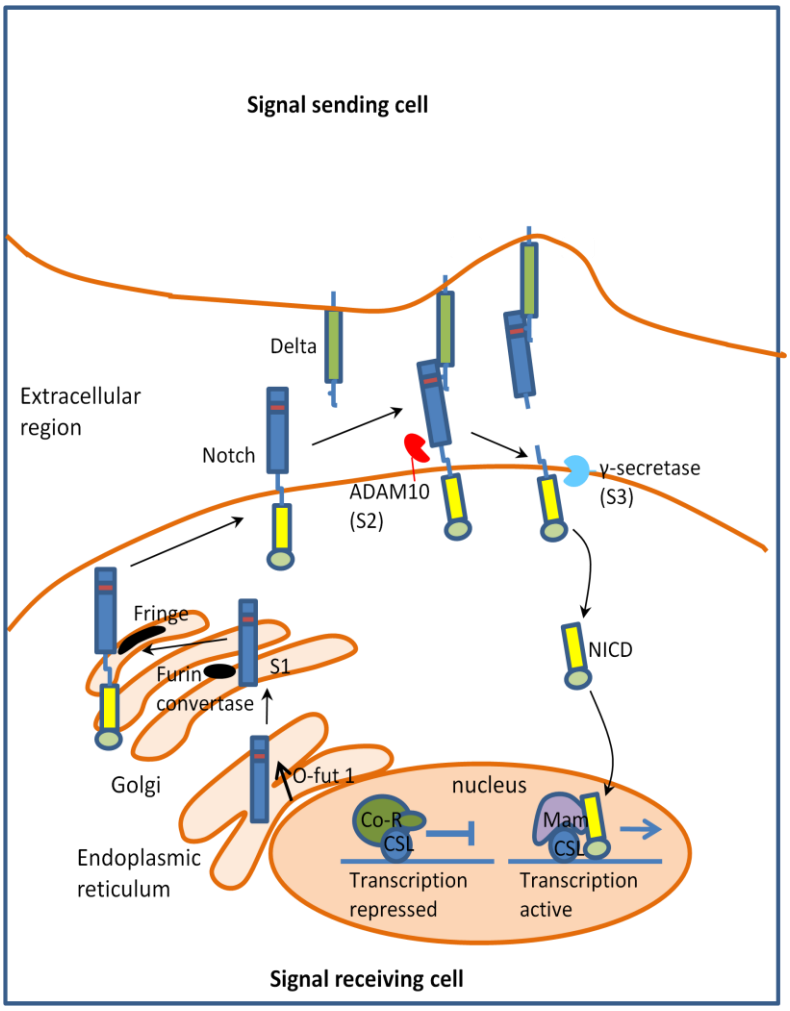

Figure 1.4 Canonical Notch signalling pathway. Binding of a **Delta** ligand on the signal sending cell to a Notch receptor on the signal receiving cell leads to the proteolytic cleavage by **ADAM 10** metalloprotease this catalyses cleavage at **S2** and **S3** by **γ-secretase**. This releases the Notch intracellular domain which translocates to the nucleus where it dislodges the repressors, allowing **CSL** to form a ternary complex with **NICD** and Mastermind. This recruits transcription factors activating target gene expression. Abbreviations: **O-fut 1**=O-fucosyltransferase, **NICD**=Notch Intracellular Domain, **Co-R**=co-repressor, **CSL**= CBF-1, Suppressor of Hairless, Lag-1, **Mam**=mastermind

1.2.1.3 Interactions with the extracellular matrix

Cell-cell adhesions and cell-extracellular matrix adhesions also help to determine cell fate. Proteins involved in adhesion include selectins, cadherins, and integrins. Integrins are heterodimer receptors for ECM proteins such as fibronectin and collagen [47]. The ECM has 5 main functions during development they include as an adhesive substrate, to provide structure, to present growth factors to their receptors, sequester and store growth factors and finally to sense and transduce mechanical signals. The importance of various ECM proteins has further been demonstrated by studying the loss of function phenotypes during development, examples of which are summarised by Rozario and DeSimone and can lead to death [48]. They also help to define cell shape and regulate the cell cycle. Integrins are crucial in cell migration. More specifically during development, β1 integrins are required for the maintenance of epidermal stem cells and due to their role in controlling differentiation and morphogenesis in the epidermis, they are also used as epidermal stem cell markers [49]. Loss or alteration of integrins can cause departure of stem cells from their niche and leads to differentiation or apoptosis. As previously mentioned, it is also possible for the ECM to adjust local concentrations of secreted factors within the stem cell niche [50], when considering that some of these molecules such as hedgehog proteins are dose-dependent, the ECMs role in signalling and maintaining the cell microenvironment is of great importance. During normal cell culture there are limited ECM interactions due to only being a monolayer of cells.

1.2.2 Stem cells and the developmental 3D environment.

Embryonic stem cells (ESCs) are pluripotent stem cells from the inner cell mass (ICM) of blastocyst stage embryos. The isolation of human ESCs in 1998 [51] led to elevated interest in stem cells for cell therapy. Such cells are considered as a novel and unlimited source of cells and tissue for transplantation and treatment of a range of human diseases. Keller suggests this is partly due to their ability to retain a normal karyotype[52]. However, recent studies have suggested that adaptation of hESCs to cell culture leads to a changes in karyotype [10]. The greatest challenge for using hESC in clinical applications and stem cell therapies is the lack of knowledge in directing their differentiation. Although there are many studies that have developed protocols for the generation of specific cell types *in vitro*, they are not able to display uniform differentiation into a particular cell type. Korin and Levenberg attribute this to the absence of proper temporal and spatial signals from the surrounding environment [53]. The environment that they are referring to is the standard cell culture environment which has limitations for stem cell culture due to its lack of morphogenetic processes and the absence of a temporal dimension [54]. Such signals are vital for stem cell development as they lead to morphogenesis – the reorganisation of cells and tissue into new forms – which is essential for animal development. This process requires a 3D

microenvironment. Specific examples of the need for a 3D environment include determining the regional characteristics of neural progenitor cells (NPCs) [55] and neural tube development. This is specified by a range of morphogens including sonic hedgehog (Shh), as well as retinoic acid and Wnts. These molecules lead to patterning along the dorsal-ventral and anterior-posterior axes. Hedgehog proteins are short range signalling proteins. There limited signalling range means that in traditional cell culture, hedgehog proteins are only able to reach a very small number of cells. Hedgehog signalling is also concentration dependent. The concentration gradient is thought to be important in tissue development as differing concentrations produce different responses. For example during neural tube development a morphogen concentration induces different types of ventral neurons, this morphogen is the signalling protein sonic hedgehog [56]. This is demonstrated schematically in Figure 1.5. Other examples of concentration dependent effect of sonic hedgehog have been reported in vertebrate limb development specifically in a chick wing model where a morphogen gradient is produced from the zone of polarising activity (ZPA). Cells closest to the source form the posterior digits whereas cells further from the ZPA form the thumb [57]. It has also been suggested that *in vitro* systems limit the activity of Shh demonstrated by cells grown in conventional cell culture systems requiring 20-30 times higher concentrations of Shh to produce the same degree of differentiation that is observed *in vivo* [58].

It is not only morphogens that require a 3D environment to develop tissue; a 3D environment is also required to regulate cell shape during tissue formation. An example of such a system is also during neural tube formation. During this process hinge point cells in the neuroepithelium apically constrict to bend the neural plate. The cells undergo a change in cell shape which causes them to wedge and their apical surface narrows [59]. Neural tube closure is a of particular importance as it is one of the most common human birth defects [60]. Sawyer et al. suggest that cell adhesion, at both cell-cell junctions and cell-matrix junctions is important in such processes [61]. It is not possible to mimic such complex differentiation of cells in the current cell culture environment. By placing cells in 3D they are surrounded by neighbouring cells and extracellular matrix which is considered necessary for tissue development and short range morphogens would be able to reach a larger number of cells than in a 2D cell culture environment. By increasing the possibilities for cell interactions it may be possible to produce more uniform differentiation *in vitro*. A 3D cell culture environment will potentially be useful in both the production of stem cells for cell therapies and to produce models of embryogenesis. Such models will lead to further understanding of developmental processes which in turn could help to prevent birth defects such as neural tube defects.

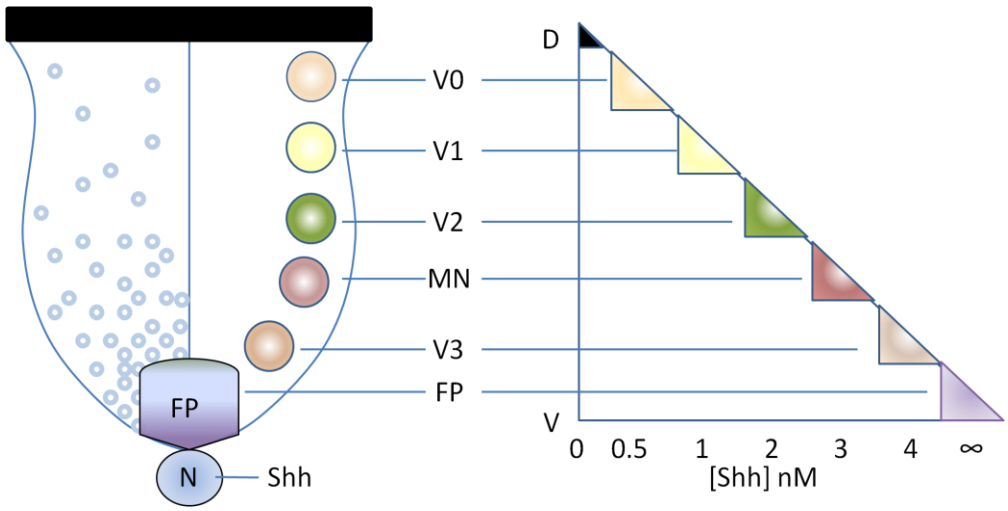

Figure 1.5 An example of the concentration dependent effects of Sonic Hedgehog signalling. A model proposed by Jessell for the influence of Shh on ventral neuronal fates. The left shows presumed gradient of Shh activity in the ventral neural tube. Shh distribution (shown by blue dots) is ventral-high to dorsal-low in the ventral neural epithelium, where five classes of neurons are generated in response to Shh signalling. This coincides with the profile on the right which shows neuronal generation in intermediate neural plate explants grown in different concentrations of Shh-N. The more dorsal the position of neuronal subtype generation *in vivo* the lower concentration of Shh is required to induce the neuronal subpopulation *in vitro*. Abbreviations: **V0-V3**=4 classes of ventral interneurons, **MN**=motor neurons, **FP**=floor plate, **D**=dorsal neural tube, **V**=ventral neural tube. Adapted from Jessell[62]

1.2.3 Cell culture environment

Conventional cell culture in two-dimensions places cells under topographical stress due to the unnatural, flattened morphologies that they assume (Figure 1.2). Cells grown on tissue culture polystyrene have limited cell contact, exaggerated cell adhesions, as well as the cell monolayer being more susceptible to therapeutic agents [63, 64]. Two-dimensional cultures on rigid surfaces have also shown enhanced cell proliferation but also inhibit cell differentiation due to limited cell interactions [65]. A primary purpose of the cell culture environment is to mimic the *in vivo* microenvironment. The standard and simplest model to achieve this in conventional cell culture on rigid plastic substrates is with soluble factors and nutrients in the surrounding cell culture media. Modification of this environment is helpful in identifying the effects of individual niche components on cell fate [66]. Attempts at producing a more relevant cell culture substrate have led to modification of the surface topography.

1.2.3.1 Attempts to mimic the extracellular matrix

Surface topography has been demonstrated to affect such parameters as cellular adhesion, mediation of stem cell differentiation and initiation of intracellular signalling [67]. This includes changing cell geometry by seeding onto a nanograted surface. Such surface contains nano-sized peaks and troughs which represent ECM constituents such as collagen fibrils. Such nanotopographic surface had been shown to effect cells in culture. For example, both epithelial cells [68] and bovine pulmonary artery smooth muscle cells [69] respond to the nanopatterned surfaces by alignment and elongation of the cells along the axis of the grating. Whereas Yim et al. suggested that nano-gratings were able to assist in the transdifferentiation of human mesenchymal stem cells (hMSCs) toward neuronal lineages [70].

A different approach is the immobilisation of ECM proteins onto the substrate, this also helps recreate *in vivo* growth conditions. Successes have included culture of mES cells on plates coated with a fusion protein of E-cadherin and IgG Fc domain [71]. The mES cells displayed high proliferative ability and required less leukaemia inhibitory factor (LIF) than colony forming cells. Pierret et al. immobilised the ECM proteins – entactin, collagen and laminin and coupled with modified culture medium allowed the differentiation of mES cells, which led to the formation of structures that exhibit properties of a neural stem cell (NSC) niche [72].

1.2.3.2 The effect of cell shape

Deposition of ECM is also used to control cell shape. Many previous studies have determined that the ECM regulates proliferation and apoptosis [73], however these studies fail to address whether the adhesive microenvironment formed by the ECM or the differences in cell shape produced were responsible for the decrease in apoptosis. Chen at al. demonstrated that cell shape appears

to regulate cell function with more rounded cells having increased levels of apoptosis [74]. Regulation of shape by micropatterned islands affects cell differentiation. McBeath et al. found that the area of the islands determines the differentiation program of hMSCs. Large islands allowed for cell spreading which favoured osteogenesis whereas small islands promoted cell rounding and led to adipogenesis [75]. Mei et al. used geometrical cell shape to promote the self-renewal of hESCs in the absence of feeder layers and suggest that this is possible due to enhancement of juxtacrine and autocrine signalling [76].

The changes in cell shape that affect cells in culture are not surprising considering the vital role of cell shape *in vivo.* For example during morphogenesis, the formation of the neural tube occurs when contraction of microfilaments cause columnar cells of the neural plate to become wedge-shaped allowing them to act of hinges and assist in the rolling of the plate into the neural tube [77]. It has also been proven that cell shape is a regulator of DNA synthesis and cell growth *in vitro* [78].

As demonstrated above there are many factors that can be controlled during cell culture including modification of the substrate with ECM proteins, substrate topography, and cell shape. These factors help to mimic the *in vivo* microenvironment. But the 2D culture system is simplified and even with these additions, it still does not allow for sufficient cell communication. To overcome these limitations there is increasing research into the possibility of culturing cells in 3D. The third dimension allows for greater cell to cell contact - increasing cell-cell signalling and allows cells to differentiate into more complex structures. It may also allow cells to begin to organise into tissue through the uniformed expression of adhesion molecules across the cell surface [65]. In 3D culture, receptors and adhesion molecules are spread across the cell surface whereas in 2D culture they tend to be concentrated on the ventral surface where they attach to the tissue culture plastic [79]. Optimisation of 3D culture methods will produce more relevant assays which have the potential to reduce testing on animals. However, there are concerns that the multiple cell layers produced during 3D culture may lead to an insufficient supply of oxygen and nutrients to the core of the cell cultures. In addition to this there is also the possibility of accumulation of toxic metabolites which may lead to necrosis of the central areas. Therefore, 3D cell models need to be well characterized and maintained under optimized and standardized culture conditions [80].

1.2.4 Examples of three dimensional cell culture systems.

There are currently many techniques to produce 3D cell cultures which are summarised in Table 1.1. The simplest and oldest method is the hanging drop technique [81]. Cells are cultured in a

Method of 3D cell culture	Advantages	Disadvantages	References
Hanging drop technique	• Simple method requires no additional cultureware • Permits long term survival and maintenance of stem cell phenotype • Allows for homogenous differentiation compared to standard monolayers	• Aggregates formed using this method are relatively small and unsupported • Increase in aggregate size can lead to necrotic centres • Difficulties with media changes and the addtion of exogenous factors	[82-85]
Hydrogels	• Can be designed to support specific cell types. • Can support cell migration into the material. • Similar to *in vivo* ECM. • Helps to maintain functionality of primary cells.	• Often biodegradable so unsuitable for *in vitro* testing. • Can lead to the growth of isolate aggregates embedded within the gel which are unable communicate with other cells. • Ability to form ordered layered structures is limited. • Suggested that there is a limited period of time for the culture of cells due to limited	[86-90]

		• nutrient diffusion. • Variability between batches	
Electrospun fibres	• Can be formed from both synthetic and natural materials • Biologically active agents can be incorporated • Can be produced as aligned fibres for specific applications such as nerve guide conduits	• Large pore size – leads to curvature of cells rather than true 3D structures • Organic solvents are often required • Mechanical properties of electrospun fibres is generally pore	[91-98]
Porogen leaching	• Simple method with no special equipment required • Sponge-like porous scaffold is produced • Have previous been used for the culture of human embryonic stem cells • Can be produced from biodegradable materials	• Difficult to achieve full interconnectivity of pores, this can lead to cell build up at surface of the scaffold • Difficult to produce uniform pore size • Due to biodegradability cannot be used for standardised *in vitro* tests	[3, 99, 100]

Table 1.1 Summary of the advantages and disadvantages of techniques for 3D cell culture.

drop of media which is suspended on the lid of a cell culture dish. The cells are unable to adhere and therefore form three-dimensional spheroids at the apex of the drop of media. This method of culture has been shown to permit long term cell survival and maintenance of the stem cell phenotype of bone marrow stromal cells [83], and also allows for more homogenous differentiation compared to standard cell monolayers [84]. It has also been proposed that the hanging drop method maintains a high local concentration of endogenous factors such as the hedgehog proteins and therefore able to sustain tissue function better than a monolayer culture [85]. This is a simple method for producing a 3D microenvironment, but aggregates formed using this method, are relatively small and unsupported.

1.2.4.1 Hydrogel-based 3D matrices

Other 3D cell culture models focus on providing a matrix for cells to adhere or embed into, which will encourage cell growth proliferation and differentiation. Examples of such a material are hydrogels. Hydrogels have been well established for growth of various cell types including hMSCs, mouse embryonic fibroblast line – NIH 3T3, and the human endothelial cell line – HUVEC [87]. Cells are either embedded into the gel [87, 88] or allowed to migrate into the interior of the gel from the surface [89]. Hydrogels are considered to be similar to the extracellular matrix *in vivo*. This hydrogel extracellular matrix can be modified depending on what the embedded cells secrete into the surrounding environment. Hydrogels can consist of protein fibres and/or cross-linked polymer chains [101]. Between the fibres or polymer chains there is a high water content of up to 90% (Figure 1.6) [102]. Cells are encapsulated into the gels by self-assembly, ionic cross linking or radical polymerisations by UV exposure. Three dimensional cell culture hydrogels have proved useful in the testing of drugs *in vitro*. For example by embedding hepatic cells in synthetic peptide scaffolds, liver specific functions such as the synthesis of enzymes which metabolise drugs are maintained for longer in comparison to hepatocytes grown in 2D [90]. However, there are inherent disadvantages of hydrogels including the previously mentioned, use of UV light for curing of the gel. Such a procedure may have a detrimental effect on cells [103]. In addition, there are also studies that suggest cells can only be cultured for short periods of time due to problems with the diffusion of nutrients through the hydrogel [87]. Many hydrogel-based scaffolds are biodegradable [104]. This means that the niche in which the cell resides is forever changing, making these scaffolds non-optimal for drug discovery and development. Hydrogels have been tested as *in vitro* substitutes for the stem cell niche: Gerecht et al. used hyaluronic acid hydrogels to culture hES cells [105]. Hyaluronic acid was chosen because it supports hES cells and also co-

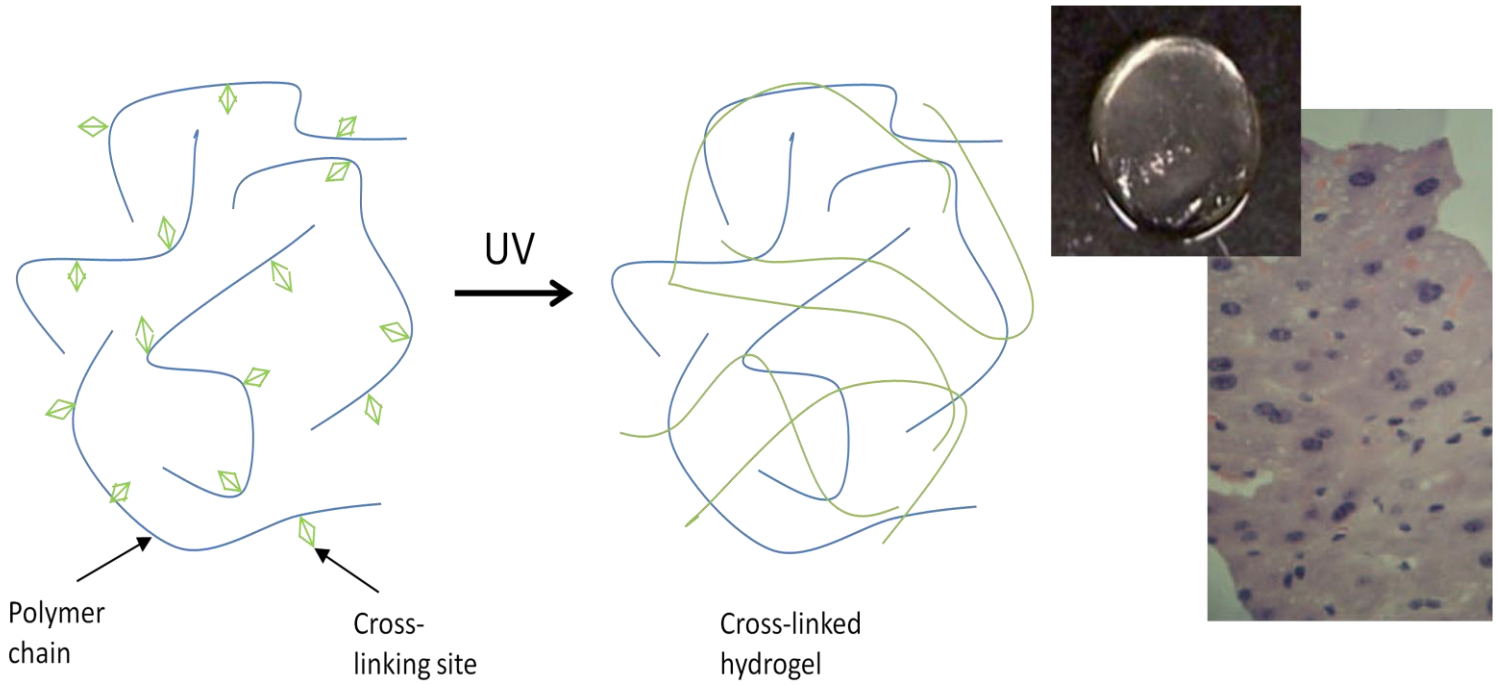

Figure 1.6 Example of 3D culture using hydrogels. polymer chains with reactive groups are cross-linked trapping water and producing a swollen network as shown in the H&E stained section of hESC – hyaluronic acid construct cultured for 20 days showing undifferentiated colony within 3D networks, Histological images adapted from Gerecht et al.[105] Schematic adapted from Marklein et al.[106]

regulates gene expression, proliferation, and morphogenesis of hES cells *in vivo* [107]. The hyaluronic acid hydrogel was able to maintain a state of self-renewal in hESCs and with the introduction of angiogenic factors readily induced vascular differentiation.

1.2.4.2 Scaffolds formed from electrospun fibres

Another option of 3D culture matrices are fibrous scaffolds manufactured via electrospinning [108]. These fibres can be formed from a variety of synthetic polymers such polycaprolactone [109] or polystyrene [91] or natural fibres such as silk [92], alginate and chitosan [93] or even combinations of synthetic and natural materials [94]. Electrospun scaffolds are produced by a polymer jet passing through an electric field and collecting on a grounded surface(Figure 1.7). This process produces a mesh of fibres. It is possible to use two or more jetting materials to produce heterogeneous scaffolds. Biologically active materials can also be incorporated into the polymer mesh. For example, the incorporation of DNA into poly(ethylene glycol) (PEG) electrospun scaffolds [95] or for the delivery of antibiotics for controlled release [96] or anticancer agents [97]. There are also examples of electrospun scaffolds which are biodegradable *in vitro* usually formed from poly(lactic acid) (PLA), poly(glycolic acid) (PGA) and there copolymer (PLGA). There have been successes in the culture of skin cells in 3D on these types of scaffolds. Sun et al. used poly L-lactic acid fibres for the growth of human dermal fibroblasts [98]. This study and other studies from the same group have suggested that cytotoxic agents have reduced effects on cells cultured in 3D on electrospun scaffolds compared to their 2D counterparts [64]. Such findings could lead to a reduced amount of drug failures in expensive clinical trials. By developing 3D culture methods that are more realistic than the 2D monolayer culture, it may be possible to detect potential failures at an earlier less expensive stage in drug development. Unfortunately cells grown on fibres are not considered to truly represent three-dimensional cell growth; due to the large gaps between individual fibres it is often not possible for cells to bridge the gap. Cells are therefore similar to cells grown in a monolayer but with a curvature to the membrane caused by their adhesions to rounded fibres.

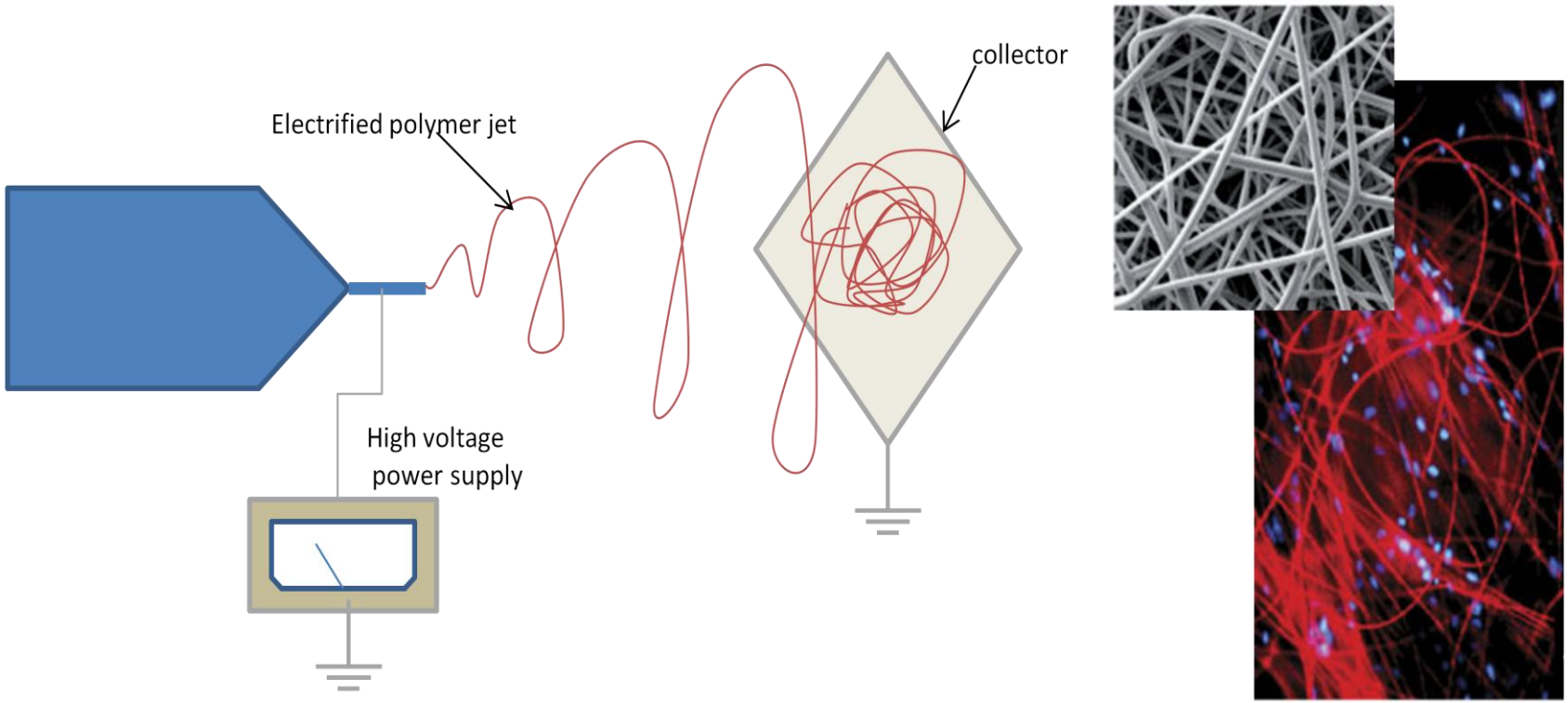

Figure 1.7 Formation of electrospun mats for 3D cell culture. Electrospun fibres produced by an electrically charged polymer jet being spun into an irregular mesh on a grounded collector. Image shows DAPI stained human dermal fibroblasts on polystyrene electrospun fibres from Sun et al.[91]**.** Schematic adapted from Marklein et al.[106]

1.2.4.3 Porous scaffolds for 3D cell culture

To produce scaffolds where it is possible for cells to bridge the pores and therefore produce a more three dimensional morphology, it is necessary to monitor the pore size of the material. Scaffolds with defined pore size can be produced by particulate leaching [99]. Particulate leaching involves casting polymer around soluble beads known as porogens. The polymer and porogen need to be soluble in different solvents, often the porogens used are soluble in water whereas the polymer is only soluble in organic solvents. Commonly used porogens are salt [3], sugar [100] or paraffin spheres [99]. Using this method a sponge-like porous polymer is produced as demonstrated by the schematic in Figure 1.8. Levenberg et al. used salt leached poly(lactic-co-glycolic acid) (PLGA) and poly(L-lactic acid) (PLA) to form scaffolds to produce an artificial microenvironment for differentiating human embryonic stem cells [3]. The two polymers used to produce these scaffolds were carefully chosen for their properties. PLGA degrades quickly in culture (~3 weeks), which was thought to encourage cell growth throughout the scaffolds and the PLA was chosen for its mechanical stiffness. Due to this scaffold being biodegradable it again would be unsuitable for standardised *in vitro* assays. This is due to the cell environment constantly changing and localised areas of high lactic acid concentration within the scaffold. Another disadvantage of the particulate leaching process is that it is possible to produce pores that are not interconnected to neighbouring pores, as seen in left hand corner of the diagram in Figure 1.8. Levenberg et al. demonstrated the difficulties of getting the cells to infiltrate and fill the scaffold [3]. They describe how undifferentiated hESCs tended to build up at the surface of the polymer scaffold and only infiltrate the scaffold when they were given a cue to differentiate. This could be due to the cells not having any ECM to bind to, and suggests that 3D culture matrices may also require coating with ECM proteins in a similar way to standard tissue culture plastic.

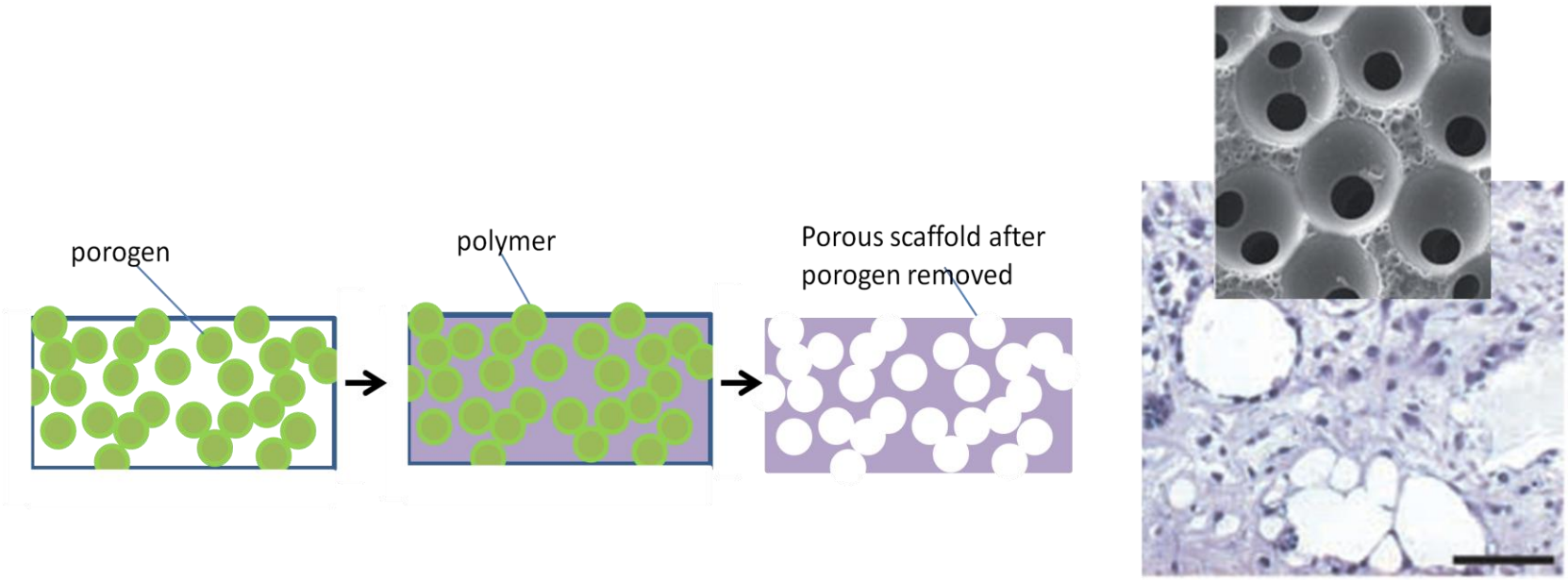

Figure 1.8 Porous polymeric scaffolds formed using particulate leaching. The process involves selection of porogen that is soluble in a different solvent to the polymer scaffold. This porogen is usually soluble in an aqueous solvent for example salts or sugars and the polymer is soluble in organic solvent. Once the polymer has formed round the porogens they are dissolved leaving a porous polymer scaffold. Histological image shows differentiated hESCs grown on a PLLA/PLGA porogen scaffold supported using Matrigel (a commercial basement membrane matrix) (Levenberg et al.[3]). This schematic is adapted from Marklein et al.[106]

There are also other methods of producing porous scaffolds and these include emulsion templating [110]. As with particulate leaching, it is possible to produce pores of defined size as demonstrated by Carnachan et al. [111] and unlike porogen leaching all voids are connected to neighbouring voids via interconnects. The particular scaffold described by Carnachan et al. [111] and Bokhari et al. [110] is manufactured from polystyrene which is the same material as standard cultures dishes. The scaffold is non-biodegradable and therefore ideal for the production of a standardised cell culture environment for use in long term culture in 3D. Similar scaffolds produced using this method have already been used to culture a range of cell types in 3D, including hepatocytes [79, 112], osteoblasts [110] pluripotent stem cell derived neurons [113, 114], and a similar poly(ε-caprolactone) scaffolds for the growth of fibroblasts [115]. The previously mentioned porous polystyrene scaffold has been developed into a commercial product called Alvetex® [116] and this thesis will concentrate on the optimisation of the reproducible scaffold for the self-renewal, proliferation and differentiation of pluripotent stem cells in 3D.

1.2.5 3D culture and tissue engineering.

Although there are many methods of 3D culture described above many of the methods described are intended to form tissue prior to implantation *in vivo*. For example there have been studies demonstrating that co-cultures of endothelial cells with either fibroblasts [117] or myoblasts [118] on porous scaffolds have been able to form microvessels – like endothelial networks after implantation into nude mice and were able to carry blood. However, it is not known if these structures were functional *in vitro* prior to implantation or whether the chemical and biophysical cues from the environment promoted functionality. As suggested by Griffith and Swartz, 3D culture approaches that are derived from therapeutic tissue engineering may be unsuitable for *in vitro* models [19]. It is therefore necessary to optimise 3D cultures specifically for *in vitro* tests that provide a reproducible microenvironment. Such models could eventually be used to replace animal tests. For example changes to ISO 10993:10 – Tests for irritation and skin sensitisation in 2010 included an alternative *in vitro* assay for the rabbit skin irritation test [119]. Due to implementation of the 3Rs framework to replace, reduce and refine scientific experiments using animals [120] it is also necessary to find *in vitro* alternatives to other *in vivo* testing methods. An *in vivo* test which could benefit from a 3D stem cell alternative is the teratoma assay. This assay is used to assess the pluripotency of stem cells [121] and there is currently no suitable method of early screening to prevent the use of large numbers of mice. In this study I will also investigate the possibility of alternative 3D culture methods for testing pluripotency.

1.2.6 Development and investigation of novel technology to enhance the 3D microenvironment for the growth and differentiation of pluripotent stem cells.

A source of pluripotent stem cells can be found in teratocarcinomas, these are tumours arising from transformed germ cells which occur spontaneously in either the ovary or the testis [122]. Primordial germ cells display abnormal proliferation and start to form an embryonic ectoderm-like structure, subsequently this structure becomes disorganised. Most of the tumours formed are benign but occasionally they contain undifferentiated cells. This was proven by Kleinsmith and Pierce in 1964 when they demonstrated that implantation of a single one of these undifferentiated cells into a nude mouse, could give rise to a heterogeneous structure known as a teratoma [123]. These undifferentiated cells are known as embryonal carcinoma (EC) cells. EC cells have the ability to differentiate into all three germ layers (ectoderm, mesoderm and endoderm) and are believed to be the malignant counterparts of embryonic stem cells. Recognition that EC cells were the malignant counterparts of cells found in the inner cell mass (ICM) of the blastocyst stage of mouse embryos plus an understanding of the culture conditions required to maintain EC cells led to the isolation of ES cell lines [124, 125]. Embryonic carcinoma cells are a caricature of embryogenesis as they are able to produce distinct cell types but in a disordered manner. This is demonstrated by the implantation of EC cells into mice, leading to teratoma formation [126]. The EC cells are a simpler and more robust experimental system for the study of stem cells *in vitro* [127]. This model system is often used for *in vitro* studies of development and recent findings suggest that ES cells may develop in culture in ways that mimic changes occurring in EC cells during tumour progression [128]. Unfortunately due to their tumour properties they are not useful in clinical medicine.

There are many EC cell lines in existence which all show different abilities to differentiate into specific lineages even when derived from the same teratoma lineage. Such cell lines include GCT27, NTERA2.cl.D1 and TERA2.cl.SP12. GCT27 cells require a feeder layer for proliferation [129] whereas NTERA2 cells and also TERA2.cl.SP12 are independent of feeder layers. This is ideal for the initial optimisation of 3D cultures systems. However the cells show more restricted differentiation as demonstrated by Pleasure et al. who suggest that they are representative of neuronal progenitor cells [130]. EC cells display similar traits to ES cell including high levels of expression of SSEA-3, SSEA-4, TRA-1-60, TRA-1-81 and Oct 4 [131, 132].

The TERA2 cell line was first isolated in 1975 from a metastasis of a human testicular teratocarcinoma. They display pluripotent characteristics but were initially overlooked as a potential EC cell line due to their requirement of specific culture conditions [122]. In contrast to previously isolated mouse EC lines, TERA2.cl.SP12 cells require a high cell density and to remain in clumps during passaging to prevent spontaneous differentiation. Immunomagnetic isolation of

TERA2 cells allowed for the isolation of SSEA-3 positive cells and single positive cells were cloned to establish new cell lines [133]. TERA2.cl.SP12 is one of these clonal lines, it displays high levels of Oct 4, SSEA-3 and TRA-1-60 expression and commits to differentiation after 2-3 days of treatment with retinoic acid. Transplantation of TERA2.cl.SP12 cells into nude mice results in the formation of epidermal and neural tissues [134] suggesting that the plasticity of these cells is limited to ectodermal derivatives. This makes them an ideal model for the study of neurogenesis *in vitro*.

By studying a model system such as the embryonal carcinoma cell line TERA2.cl.SP12 it may be possible to develop a routine three dimensional stem cell culture for the expansion and differentiation of stem cells. TERA2.cl.SP12 display limited spontaneous differentiation *in vitro* compared to other EC lines [135] as long as they are kept at high confluency. Unfortunately this may become a problem in polymer scaffolds as it is difficult to seed high density cultures uniformly throughout a scaffold which may lead to spontaneous differentiation in 3D. At low density EC cell lines tend to differentiate due to loss of cell-cell contact [136]. However the 3D environment will provide increase cell contact in all axes which will help to prevent spontaneous differentiation. More recently it has been suggested that the Notch signalling pathway provides a cell-cell proliferation signal for EC cells and hES cells [41] which is another difference when compared with their murine counterparts who do not require cell-cell contact. Notch signalling promotes the transcription factors including basic helix-loop-helix factors (bHLH) such as the proneural gene NeuroD1 [137] and promotes neural lineage entry [43]. NeuroD1 is a marker of proneural cells which are preparing to exit the cell cycle, migrate and differentiate into neural cells. The transcription of NeuroD1 correlates with the expression of A2B5 – a neural cell surface antigen in NTERA-2 cells [138]. The increased cell-cell contact achieved during 3D scaffold culture may promote enhanced differentiation and neurogenesis but could also assist in maintaining the stem cell self-renewal. Xu et al. have demonstrated that the physical structure of ES cells such as their 2D, 3D morphology or compactness plays a role in their self-renewal, as cell-ECM interaction modulates growth factor signalling promoting hES cell survival and self-renewal [26].

1.3 Aims and Objectives

1.3.1 Aims

The aim of this thesis is to fully optimise 3D scaffold environments for the growth, differentiation and self-renewal of pluripotent stem cells. Optimisation will include development of standard culture conditions for a range of cell lines. This will establish how the changes in the microenvironment affect cell behaviour. The presentation of the scaffold will also be modified in order to establish an efficient presentation for both long term differentiation and short term screening experiments. The 3D microenvironment provided by the scaffold can also be modified in attempt to promote self-renewal of pluripotent stem cells. This study will establish if there is an effect on cell shape, proliferation and stem cell marker expression during prolonged 3D culture. Being able to maintain pluripotent stem cells in 3D may provide a source of cells that are adapted to a 3D environment. This will be useful for transplantation *in vivo* or for use in other complex 3D models and will reduce the time required for adaptation of cells to the 3D environment. Finally I will investigate the possibility of developing an alternative method for assessing pluripotency without the use of animal models.

1.3.2 Objectives

- Optimisation of a standard 3D culture environment for a range of cell lines.
- Assess nutrient requirements and the removal of waste products from 3D cultures.
- Modify the scaffold presentation to produce optimal 3D culture conditions.
- Development of a model for neuronal differentiation using the optimised culture conditions.
- Establish a model for the 3D stem cell propagation.
- Determine the effects of long-term stem cell propagation in 3D compared to 2D culture.
- Assess if 3D propagation of stem cells affects developmental potential.
- Use the 3D microenvironment provided by the scaffold to develop an *in vitro* pluripotency assay.

2 Scaffold optimisation: Producing the optimal culture environment for stem cells.

2.1 Introduction

Routine cell culture in two dimensions forces cells to adopt an unnatural morphology that is unrepresentative of their *in vivo* microenvironment. *In vivo* cells reside within a niche and interact with neighbouring cells and their extracellular matrix, once placed onto 2D culture plastic cells tend to become over-proliferative, stretch out across the rigid surface and become overly adherent to the tissue culture substrate [139]. Before a 3D culture system is widely adopted is necessary to demonstrate that is adaptable for a range of cell lines and can be as routine as 2D cultures.

The principle of tissue culture was first developed in 1885 when Wilhelm Roux grew portions of the medullary plate of an embryonic chicken in warm saline solution for several days on a flat glass plate. This was further developed by Julius Richard Petri who is credited with the development of the glass Petri dish in 1887. More recently with the advances in polymer technology, disposable Petri dishes have been developed for single use with cell lines and primary cells. Further development of the Petri dish has led to the production of flasks such as T25's and T75's seen in most cell culture labs today and also conical flasks and disposable bags used in bioreactors. Flasks for cell culture have undergone extensive optimisation since their development including coating with extracellular matrix components for specific cell lines [140] and surface treatment to enhance cell adhesion [141] such as plasma treatment and the immobilisation of ECM proteins on the culture surface [142].

2.1.1 Surface treatment of growth substrates.

Enhancing cell adhesion can be achieved using a range of methods including surface oxidisation [143], addition of extracellular matrix proteins by coating with animal proteins [140] or other methods[142] and plasma treatment[144]. Surface oxidation often involves bacteriological dishes being treated with a range of acids including chloric acid, sulphuric acid or hydrochloric acid. Curtis et al. tested these methods to promote cell adhesion to polystyrene substrates and compared with other methods such as ozonolysis and treatment with UV light [143]. Previous to this study it had been suggested that sulphonate [145] and carboxyl groups [146] were the crucial binding groups involved in the adhesion of cells to culture substrates. However Curtis et al. blocked both of these functional groups and found that the increase in cell adhesion attributed to this treatment was actually due to the increased deposition of serum proteins. As an alternative method for the treatment of tissue culture polystyrene they suggest hydroxylation. The

hydroxylation method has proved to be advantageous to range of cell lines including leukocytes and baby hamster kidney cells.

More recently, plasma modification has been used as a method for treatment of tissue culture plastic. Plasma is composed of highly excited atomic, ionic and radical species. It is achieved when gases are excited by high energy radio frequencies[147]. Most frequently the increase in cell adhesion is achieved by the addition of oxygen-containing functional groups to a polymer surface; these include hydroxyl, carboxyl and carbonyl groups. By selectively treating surfaces or modifying the time of plasma treatment it is possible to control wettability of the surface of 3D culture scaffolds which in turn affects surface adhesions and cell shape. Cell shape is important during stem cell differentiation for example cell rounding has been shown to promote adipogenesis of embryonic stem cells [148]. Unexpectedly prolonged periods of plasma treatment can lead to a decrease in cell adhesion [141].

Plasma modification is the chosen surface modification method for commercial tissue culture surfaces. This includes the Primaria® surface chemistry used by BD Falcon. This method involves the deposition of oxygen plus nitrogen containing groups on the polystyrene surface [144]. Other commercially available culture surfaces use corona treatment, this is an atmospheric plasma that increases the surface energy of polymeric surfaces [143]. Barker and LaRocca stated that plasma treatment of any type of tissue culture vessel requires a complex and highly controlled manufacturing process [144]. Due to this it may be of limited use when optimising scaffolds for 3D culture.

All of the treatments detailed above are based on the fact that a more hydrophilic surface [149, 150] and a negative charge facilitates protein adhesion and therefore promotes cell adhesion[151]. Surface treatment affects more than cell attachment, different surfaces lead to differences in cell survival, proliferation, migration and differentiation[152]. There are many examples of surface treatment affecting proliferation, cell adhesion and the development of tissues especially when using biomaterials and 3D culture matrices. Oxygen plasma is the most commonly used surface modification. It has previously been demonstrated that increasing the incorporation of oxygen onto the bacteriological culture dishes leads to increased proliferation of human umbilical vein endothelial cells (HUVEC)[153]. Alternatively oxygen plasma treatment can be used to modify the surface of poly (chloro-para-xylylene) (Parylene-C). This material has become the representative coating material for insulating neural electrodes; however it is hydrophobic and therefore does not support cell growth. The oxygen plasma treatment renders the surface hydrophilic and improves the adhesiveness of neuronal cells to a level which is comparable to tissue culture plastic [154]. Finally the deposition of an oxygen functional

hydrocarbon coating onto poly(ε-caprolactone) electrospun fibres can lead to myotube differentiation from the mouse skeletal myoblast cell line C2C12 [109].

It is evident that surface modification allows standard 2D culture surfaces to better mimic cells in vivo. Unfortunately even with the modification of the cultures surfaces they are still far removed from a cells *in vivo* microenvironment. Scaffolds provide a more realistic 3D environment but have undergone limited optimisation due to existing naturally-derived and synthetic scaffolds often not being reproducible. Due to the increased surface area provided by a scaffold both surface treatment plus more basic parameters such as an understanding of the cells growth profile, seeding density and seeding method require optimisation specifically for the 3D environment. Optimisation of these parameters will lead to a well-defined model for future experiments.

2.1.2 Optimisation of parameters for 3D cell culture.

Previous studies to optimise 3D cultures have focussed on optimisation of the materials used rather than the cell- based parameters. Such materials optimisation often includes optimising bulk properties such as pore size and void fraction as well as the previously mentioned surface treatment. A material with limited porosity can affect both the proliferation and differentiation of cells seeded on it. The low porosity is often paired with a low interconnectivity which effects the movement of cells through a scaffold and also the diffusion of nutrients. The porosity of a material for 3D culture is important but the pore size has been shown to be a crucial parameter requiring optimisation. Kuboki et al. found that pore size affected the differentiation of osteoblasts in extracellular matrices used to repair bone defects. The matrices with small pore sizes of between 90-120µm led to chondrogenesis prior to osteogenesis whereas the larger void sizes (~350µm) resulted in osteogenesis and increased vascularisation [155]. Similar phenomena are also observed when using microsphere based scaffolds where smaller void sizes were found to be more permissible to mineralisation throughout the entire defect [156]. In contrast to these findings other cell types such as dermal fibroblast appear to show no selectivity for a specific pore size when cultured on porous poly(l-lactic acid) scaffolds but microvascular epithelial cells formed different types of cultures depending on void fraction and pore size. This ranged from webs of tissue with sparse extracellular matrix in scaffolds of 38-150µm but at the lower void sizes of <38µm they formed a multilayered lining on the scaffold surface [157]. This leads Zeltinger et al. to suggest that specification of pore size could be used to preferentially promote or exclude the ingrowth of specific cell types into an engineered tissue. Interestingly other studies have suggested that dermal fibroblasts need a pore size of less than 160µm for optimal cell growth [158].

Cell-based parameters that need optimisation are seeding density and seeding method along with an understanding of the growth profile of cells in 3D. This is important due to many polymeric-

based scaffolds not allowing the visualisation of cells through standard phase contrast microscopy. Van den Dolder et al. suggested a range of seeding methods that are alternatives to the standard method of seeding 2D cultures in a large suspension of media[159]. The seeding method used include seeding as a dense cell droplet, and high and low density cell suspension these parameters as well as dynamic seeding were teamed with glow discharge surface treatments to provide a comprehensive range of parameters that affect cell growth profiles, and differentiation potential.

Bokhari et al. demonstrated that seeding techniques onto porous polystyrene scaffolds can affect mass transfer of both nutrients and waste products [160]. Static methods for seeding primary osteoblasts led to accumulation of cells at the scaffold surface. At early timepoints cells were seen within the scaffold but there is a preference for the cells to remain at the surface where nutrient concentrations are high.

Many of the examples described above use osteoblasts or bone-like cell lines for the optimisation of scaffolds for 3D culture. This is due to the translational nature of this research that allows for many opportunities for implantation of biodegradable scaffolds. An alternative use of scaffolds for 3D culture is providing a more realistic environment for *in vitro* testing. For this purpose a range of relevant cell lines needs to be optimised for 3D culture. Relevant cell lines will include those used as cancer models to provide a 3D environment for drugs testing. A range of 3D cancer models have been reviewed by Kimlin et al. [161] but many include animal derived-products such as Matrigel which can lead to inconsistencies between batches. Such culture systems cannot be validated as models for drug testing in 3D. Another model for *in vitro* testing could include 3D skin-epidermal models to test the skin barrier function. For this purpose a co-culture system would be ideal but this will require initial optimisation of polymeric scaffolds for individual epidermal cell types. Finally 3D scaffolds can be used to mimic the stem cell niche to assess how the 3D environment increases cell signalling and therefore leads to enhanced differentiation, such studies have previously been conducted using a range of 3D environments [106, 162, 163]. Three dimensional scaffolds provide a unique tool for developmental biologist to study early developmental processes without interference from early patterning information. This information is still present in alternative 3D systems such as the formation of embryoid bodies (EBs)

2.2 Aims of chapter

To optimise the 3D environment for a range of cell lines for their specific properties (Table 2.1). These cell lines are the mouse embryonic fibroblast line: NIH 3T3, squamous cell carcinoma – MET 4 and the pluripotent stem cell line – TERA2.cl.SP12. These cell lines can all form the basis of more complex 3D models. By placing cells in a novel 3D environment it is not possible to monitor their growth and viability on a daily basis using phase contrast microscopy. Due to this 3D cultures need to fully optimised to ensure high quality cells throughout an experiment and produce a well-defined model.

2.3 Objectives

1. Produce growth curves of cells grown in 3D to compare with standard 2D cultures.
2. Establish optimal seeding densities for all cell lines.
3. Establish optimal seeding method for all cell lines.
4. Establish whether 3D culture scaffold require surface treatment to produce a dense slab of tissue and assess the most suitable surface modification for each cell line.
5. Assess requirements of specific cell lines during 3D culture.

Cell Line	Cell type	Properties to consider when optimising conditions for 3D cell culture			References
		Cell size in 2D on TCP	Features	Growth	
NIH 3T3	Mouse Embryonic Fibroblast	~100µm	• Contact inhibited	• Should only reach 80% confluency or less (ATCC) • Saturation density 0.5-0.6 x10^6 cells per 10cm^2	Jainchill et al. 1969
MET 4	Human Metastasis of Squamous Cell Carcinoma – keratinocyte-like	~50µm	• Highly invasive • Dissociated keratinocyte morphology	• Rapid doubling time	Proby et al. 2000
TERA2.cl.SP12	Human Embryonal Carcinoma Stem Cell	~20µm	• Clone of the TERA-2 cell line	• Must be cultured at high confluency to maintain stem cell phenotype	Przyborski 2001

Table 2.1 Properties of the three cell lines NIH3T3, MET-4, and TERA2.cl.SP12 that need to be addressed to produce optimal 3D culture

2.4 Materials and Methods

2.4.1 Scaffold production

Highly porous scaffolds were manufactured and prepared as detailed by Carnachan et al.[111] A schematic of the process is detailed in Figure 2.1. In summary, an oil phase containing styrene, 2-ethylhexyl acrylate, divinylbenzene and the surfactant sorbitan monooleate (Span 80) were placed in a round bottomed flask. The oil phase was stirred continuously using an overhead stirrer while the aqueous phase was added until a high internal phase emulsion (HIPE) was formed. The aqueous phase consists of deionised water and the initiator potassium persulphate. The HIPE is then transferred to a 50ml centrifuge tube and placed in an oven at 60°C for 24 hours. The resulting monolith was extracted from the tube and washed in acetone using a soxhlet apparatus. The monoliths were sectioned into 200µm membranes using a vibratome (Leica VT1000S) to produce thin discs which are suitable for cell culture. The scaffold discs fit into 12-well plates and are sterilised in 70% ethanol followed by two phosphate buffered saline (PBS) washes prior to cell culture. The scaffold which is produced is commercially available as Alvetex®. It is an inert non-degradable scaffold constructed from porous polystyrene. Each void is connected to the neighbouring voids via interconnects and when the monolith is cut into 200µm slices there is an open surface structure (Figure 2.4B). The open surface allows cells into the interior of the scaffold and helps address issues of mass transfer concerning exchange of gases and nutrients[111].

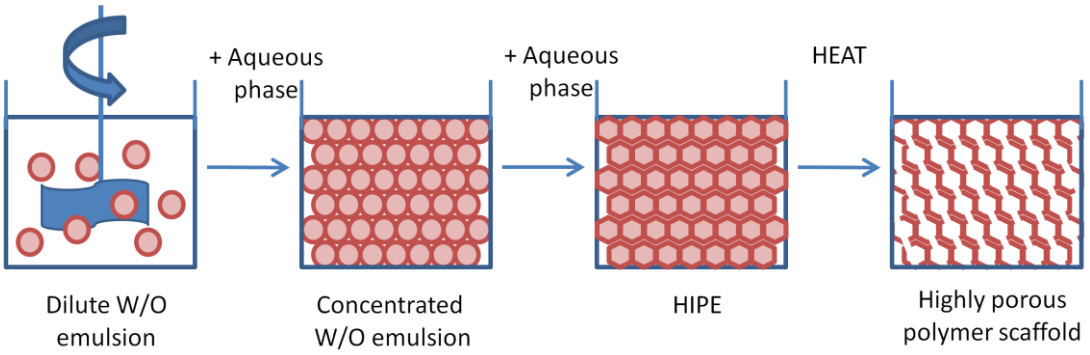

Figure 2.1 Schematic summarising the production of polyHIPE scaffolds from a water in oil (w/o) emulsion.

This method was later modified for production on a large scale to produce the economically viable commercial product.

2.4.2 Analysis of scaffold structure

2.4.2.1 Scanning electron microscopy

The void size of the polyHIPE scaffold was assessed as previously described by Bokhari et al. [110]. Segments of the polyHIPE monolith were mounted onto carbon fibre pads and attached to aluminium stubs prior to gold coating using an Edwards Pirani 501 Sputter coater. The scaffold morphology was assessed using a FEI XL30 ESEM. Average void size was calculated

using ImageJ (NIH) image analysis software, the diameter of fifty voids were chosen at random from SEM images to give a distribution plot of frequency versus diameter. It is necessary to statistically correct void size measurements as it is unlikely that the surface bisects the centre of each void.

2.4.2.2 Mercury intrusion porosimetry

Mercury intrusion porosimetry was used to assess interconnect diameter as previously described [110]. Interconnect diameter was determined using a Micrometrics Autopore III 9420. Intrusion and extrusion mercury contact angles were 130°. A penetrometer of stem volume of 1.836ml and bulb volume of 5ml was used.

2.4.3 Cell culture

2.4.3.1 Maintenance and passaging of MET 4

The squamous cell carcinoma cell line MET 4 was cultured in high glucose Dulbecco's modified Eagle Medium (DMEM) with 10% heat treated fetal calf serum (FCS), 2mM L-glutamine and 100U/ml Penicillin/streptomycin. Cultures were placed in a humidified incubator at 37°C and 5% CO_2 until they reached a confluency of 80%. Cultures were grown in T75 flasks (Nunc) and passaged using 0.25% Trypsin EDTA for 5 minutes and split 1:4.

2.4.3.2 Maintenance and passaging of NIH 3T3

The mouse embryonic fibroblast cell line NIH 3T3 was cultured in high glucose Dulbecco's modified Eagle Medium (DMEM) with 10% heat treated fetal calf serum (FCS), 2mM L-glutamine and 100U/ml Penicillin/streptomycin. Cultures were placed in a humidified incubator at 37°C and 5% CO_2 until they reached 70% confluency, as suggested by the American Type Culture Collection (ATCC). Cultures were grown in T75 flasks (Nunc) and passaged using 0.25% Trypsin EDTA for 2 minutes and split 1:3.

2.4.3.3 Maintenance and passaging of TERA2.cl.SP12

The pluripotent embryonal carcinoma cell line TERA2.cl.SP12 were cultured as previously described [133] in T75 flasks (BD Bioscience) in high glucose DMEM supplemented with 10% heat treated FCS, 2mM L-glutamine and 100U/ml penicillin/streptomycin. Cultures were placed in a humidified incubator at 37°C and 5% CO_2 until they reached confluency. Cultures were passaged at 95% confluent by rolling acid-washed glass beads over the confluent cultures and splitting 1:3 before replating.

2.4.4 Culturing cells in three dimensions

Prior to seeding onto the scaffolds, each cell line was removed from T75 culture flasks using 0.25% Trypsin EDTA and centrifuged at 1000 rpm for 3 minutes in a centrifuge tube. Cells were seeded onto the scaffold using one of two methods: concentrated seeding or dispersed seeding (Figure 2.2). The final PBS wash from the scaffold preparation steps was immediately

removed just prior to cell seeding to prevent the scaffold drying out. The dispersed seeding method (Figure 2.2A) is similar to seeding a standard 2D culture. The required number of cells per scaffold was resuspended in 4ml of media which is added to one well of a 12-well plate containing the scaffold. This allows the cells to settle evenly across the scaffold while being incubated at 37°c and 5% CO_2. For the concentrated seeding technique (Figure 2.2B) the required number of cells per scaffold was resuspended in 100µl of DMEM. The 100µl droplet of cell suspension was added directly to the centre of scaffold disc. Scaffolds containing cells were incubated at 37°C and 5% CO_2 for 15 minutes prior to the addition of the remaining 4ml of cell culture media. Media was replenished every 24 hours.

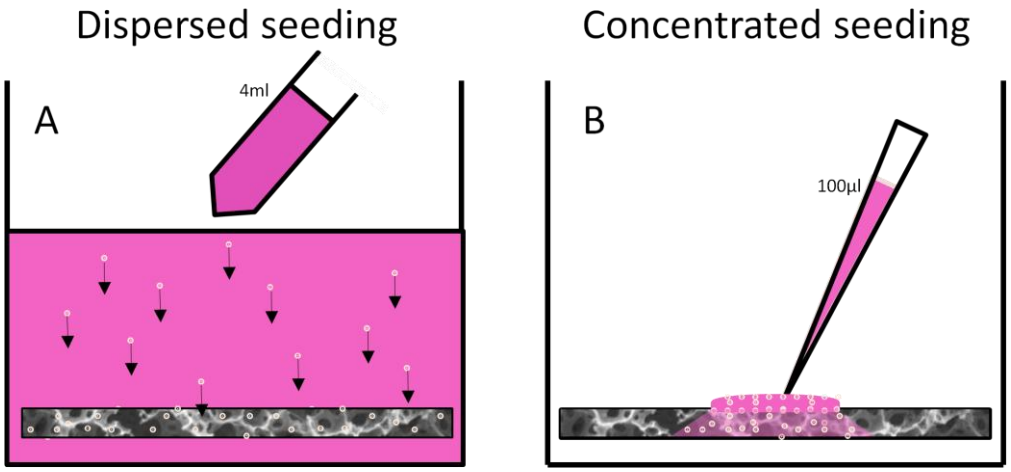

Figure 2.2 Schematics showing different methods of seeding onto porous scaffolds.

2.4.5 Surface treatment to promote cell attachment

Discs of Alvetex® were deemed hydrophilic by either ethanol wetting or plasma treatment. Ethanol wetting involves treating the scaffold as previously described. Individual discs were placed in the bottom of 12-plates and 70% ethanol was added, removed and then followed by two washes in sterile PBS. Scaffolds remain in PBS until just before the cell suspension was added. Alternatively plasma treatment can produce a hydrophilic surface. Scaffolds were sterilised in 70% ethanol and left to dry overnight prior to plasma treatment. Plasma ashing was achieved using the Emitech plasma asher K1050X, parameters were kept constant with a bleed delay time of 15 minutes, the vent valve unrestricted and pump spin down time at 15 minutes. The power applied was investigated at two different conditions of 40 Watts for 5 minutes and 10 Watts for 30 minutes.

2.4.6 Testing for cell viability

Cell viability was determined using a commercially available kit: CellTiter 96® AQueous One Solution Cell Proliferation (Promega). This assay is based upon Cory's method for measuring cell activity [164], and is a simple single step process. It is a basic MTS assay that measures

mitochondrial reductase activity, cells reduce the MTS compound to produce a formazan compound which is released by the cells. This salt compound can be quantified by measuring absorbance at 490nm this is directly proportional to the number of cells. Modifications of the protocol were required for use with the porous polystyrene scaffolds.

To assess viability, scaffolds were removed from their culture media and placed into a new 12-well plate. To each well containing a scaffold plus an empty control well, 1.2 ml of MTS solution was added, the plate was placed in the dark in a humidified incubator at 37°C and 5% CO_2 for one hour. MTS solution comprises 1ml of DMEM plus 200µl of the CellTiter 96® AQueous One Solution. After the hour incubation the solution on the scaffold was diluted 1 in 10 and 200µl of the solution was placed in a 96-well plate. Absorbance was measured at 490nm using a Biotek ELx800 microplate reader. For 2D cultures the protocol remains the same but the cell culture media is removed before the addition of new media containing MTS solution.

2.4.7 Processing of scaffold cultures for histology

Scaffolds containing cells were fixed, dehydrated and embedded as previously described by Knight et al.[7]. Scaffolds were preserved in Bouin's fixative (70% (v/v) saturated picric acid; 25% (v/v) formalin (37%) and 5% (v/v) glacial acetic acid) or 4% paraformaldehyde (4% PFA) in PBS overnight at 4°C. Fixed samples were gradually dehydrated through a series of ethanols, starting with 30% ethanol in distilled water for 15 minutes to prevent cell shrinkage. This was replaced with 50%, 70%, 80%, 90%, 95% and 100% each for 15 minutes. Samples were then cut in half and cleared in Histoclear for 15 minutes then incubated at 60°C in Histoclear/paraffin wax (1:1) for 30 minutes. Finally the solution was removed and samples were incubated in paraffin wax for 1 hour prior to embedding in dispomoulds. The cut surface is placed perpendicular to the bottom of the mould. Scaffolds were sectioned at 10µm using a Leica Microtome RM2125RT prior to floating on a 40°C histology water bath and mounting onto electrostatically charged SuperFrost+ slides.

2.4.7.1 Haematoxylin and Eosin staining

Scaffolds were stained for visualisation the cells using Haematoxylin and Eosin (H&E) staining. Haematoxylin stains cell nuclei purple whereas the Eosin stains the cytoplasm pink. Slides were de-waxed in Histoclear for 5 minutes then rehydrated through 100% ethanol (2 minutes), 95% ethanol, 70% ethanol and distilled H_2O (dH_2O) for 1 minute each. Nuclei were stained using Mayer's Haematoxylin (Sigma) for 5 minutes prior to being washed in dH_2O and subsequently blued using alkaline ethanol (30ml ammonia in 970ml 70% ethanol) for 30 seconds. Slides were dehydrated through 70% and 95% ethanol for 30 seconds each and the cytoplasm was stained using Eosin Y (5g in 1L of 70% ethanol) for 1 minute. Sections were washed twice in 95%

ethanol for 10 seconds and twice in 100% ethanol for 15 seconds and 30 seconds. Finally sections were cleared for 2x 3 minutes in Histoclear prior to mounting in DPX mountant.

2.4.7.2 Immunohistochemistry

Scaffold that had been fixed in PFA, embedded and sectioned were de-waxed and rehydrated as previously described for H&E staining. Antigen retrieval was performed by microwaving the slides for 3 x 2 min at 800W in 10mM citrate buffer at pH6 (10x stock: 19.2g anhydrous citric acid in 1000ml dH_2O). Slides were left to stand in the warm citrate buffer for 20 minutes and subsequently incubated in permeabilisation solution (0.1% (v/v) Triton X-100 in PBS) for 15 minutes. Sections were blocked using blocking buffer (0.1% Tween-20, and 1% normal goat serum in PBS) for 30 minutes prior to the addition of primary antibodies diluted in blocking buffer (Table 2.2). Sections were incubated at 4°C in a humidified chamber overnight before washing for 3 x 10 minutes in blocking buffer on a rotator plate at 40rpm. Fluorescent-conjugated antibodies were diluted in blocking buffer with Hoescht 33342 (Table 2.2) to stain nuclei and incubated on the sections for 1 hour at room temperature. Immuno-stained scaffolds were washed as before for 3 x 10 minutes and mounted using Vectashield mounting media (Vector Labs), coverslips were attached using nail varnish. The slides were then examined using fluorescence microscopy. Figure 2.3 shows the negative control for immunostaining for Oct 4.

Reagent	Antibody	Supplier	Dilution
Primary antibody	Oct 4 Rabbit polyclonal	Abcam (ab19857)	1:250
Secondary antibody	Cy3-AffiniPure Donkey Anti-Rabbit IgG (H+L)	Jackson ImmunoResearch	1:600
Nuclear stain	Hoescht 33342	Molecular Probes (H3570)	1:1000

Table 2.2 Dilutions of antibodies for immunostaining

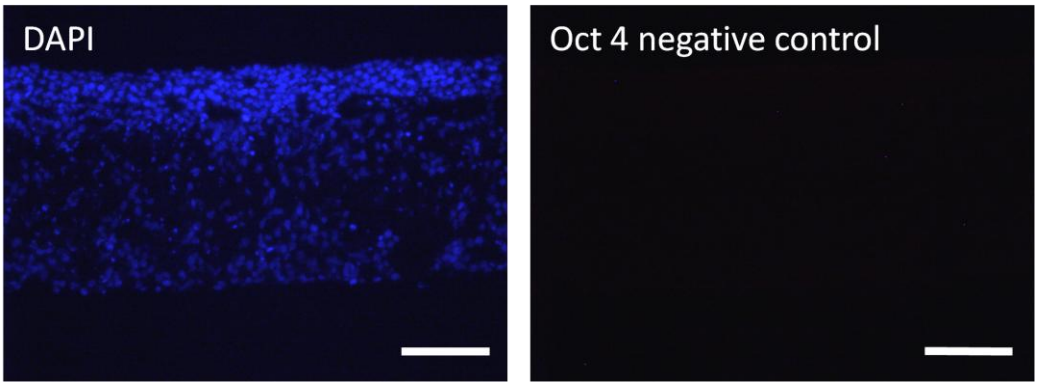

Figure 2.3 Negative control for Oct 4 staining of Alvetex® Scaffold. The standard immunohistochemistry protocol was performed without the addition of the primary antibody, to demonstrate the degree of background staining. Scale bar=100µm

2.4.8 Imaging

All images were captured using the Nikon Diaphoto 300 with connected digital camera and ACT1 image capture software.

2.4.8.1 Measurements of images

Measurements were taken from images using the ImageJ software (http://rsb.info.nih.gov/ij/) and setting the scale within the program. Measurements were taken as described below:

2.4.8.1.1 Calculating cell density

Cell density was established using scaffold sections stained with Hoescht 33342. The number of nuclei was counted in five randomly selected 100µm squares across a 10µm sections. This was repeated for 6 separate sections for each sample.

2.4.8.1.2 Calculating cell penetration into the scaffold

Measurement of cell penetration was taken from H&E stained sections. ImageJ was calibrated for the selected image and 15 measurements were taken across the entire length of the scaffold. Measurements were taken from the top surface of the scaffold and measured perpendicular from this surface until the cells that had penetrated the furthest was reached. This was repeated for three separate scaffold samples per timepoint.

2.5 Results

2.5.1 Characterisation of 3D scaffolds

Alvetex® is the inert non-degradable scaffold constructed from porous polystyrene polyHIPE. Each void of the scaffold is connected to the neighbouring voids via interconnects, this can be clearly visualised on the SEM micrograph in Figure 2.4A where large voids are highlighted in red. Voids are linked to multiple neighbouring voids through a network of smaller interconnects, outlined in blue. The scaffold monolith is sliced into membranes which are 200µm thick and 22mm in diameter. These membranes have an open surface structure which is shown in the SEM micrograph in Figure 2.4B; this will ensure the movement of cells and media into the scaffold interior. Alvetex® membranes can be fitted into the bottom of 12-well plates ready for cell culture. Polystyrene clips have been designed to hold the scaffold in place on the bottom of the well plate and prevent it from floating when immersed in media (Figure 2.4C). The clips can be readily removed using a pair of forceps and the two paddles which are seen at the bottom right of each of the wells. This allows the scaffold to be removed from the plate for processing.

Alvetex® Scaffolds undergo quality control procedures to ensure a consistent scaffold is produced. Void size is determined from analysis of SEM micrographs and statistical correction of the measured diameters. Average void diameter is plotted against frequency to establish the modal void size of the polyHIPE scaffold. Figure 2.4D shows an example of void size analysis; all Alvetex® Scaffolds have a modal void size of 40µm, although the voids range from 30µm - 90µm. Interconnect size is monitored using mercury porosimetry. The diameter of interconnects is between 11µm and 14µm (Figure 2.4E).

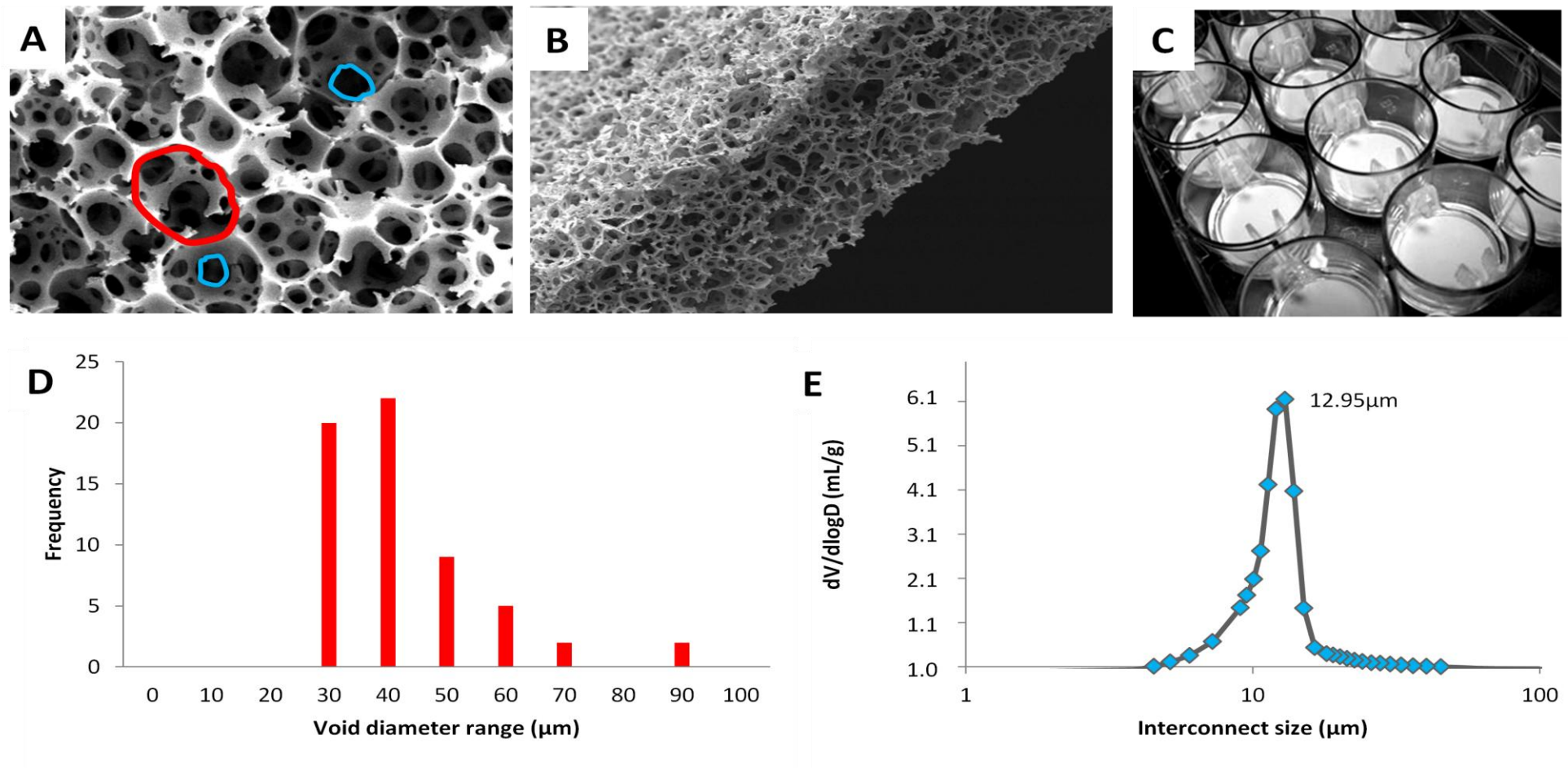

Figure 2.4 Characterisation of the structure of Alvetex® Scaffolds. Scanning electron micrograph of polyHIPE foam. A shows voids (red) linked by interconnects (blue). This structure can be cut into 200µm thick discs **(B)** which have an open surface structure. This disk can then be placed into to the bottom of a 12 well plate and held down with a well clip ready for cell culture **(C).** The scaffolds have a consistent structure with an average void **(A red)** size of 40µm **(D)** (determined by measurement of voids from SEM images) and 13µm interconnects **(A blue)** which is determined using mercury porosimetry **(E)** Data courtesy of R.Carnachan

2.5.2 The method of cell seeding onto scaffolds affects cell distribution.

Two techniques for seeding onto 3D scaffolds were assessed for use with the Alvetex® Scaffolds. The dispersed seeding method (Figure 2.5A) is similar to seeding cells in standard 2D culture. Cells are added to the scaffold suspended in the final volume of media (usually 4ml for a 12-well plate); they are then allowed to settle onto the surface of the scaffold. This leads to a uniform coverage of cells across the entire surface of the membrane as shown by the MTT staining and the graph of cell number across a scaffold section. For a scaffold seeded using the dispersed method, cell number is consistent across the entire length of the scaffold: 100 cells in each image across a 10µm section (Figure 2.5A).

An alternative method for seeding onto 3D constructs is the concentrated seeding method previously described by van den Dolder et al.[159]. This involves concentrating cells in a small volume of media such as 100µl before addition to the centre of the scaffold disc. This is followed by a short incubation at 37°C to promote cell attachment prior to addition of the final volume of cell culture media. This method leads to a concentrated area of cell growth in the centre of the scaffold. From the staining using the MTT solution (Figure 2.5B) there is very little migration of cells away from the initial seeding area. However from the cell counts on 10µm scaffold sections there appears to be small numbers of cell that are not situated in the centre of the disc with numbers ranging from 40 cells per image at the edge of the scaffold through to 240 cells per image in the centre of the scaffold disc. This profile differs greatly from the dispersed seeding method. The difference between the two seeding methods is clearly visible in Haematoxylin and Eosin stained sections of scaffolds (Figure 2.6). Example images were captured at the centre of the scaffold section, at the edge of the scaffold section and an area between these two points. Figure 2.6D shows the areas of initial seeding using the concentrated seeding method. The concentrated seeding method allows cells to fill the entire width of the scaffold but this is only in the central area of the scaffold. As you move towards the edge of the scaffold membrane, cell number decreases and cells infiltrate less than half the width of the scaffold (Figure 2.6E) and at the edge there are a few sparsely seeded cells (Figure 2.6F). This is in contrast to the dispersed seeded scaffold, the Haematoxylin and Eosin stained scaffold sections show a uniformed distribution of cells across the three areas with no dense area of cells (Figure 2.6G-I) at the centre of the disc; this is consistent with the graph of cell number in Figure 2.5A.

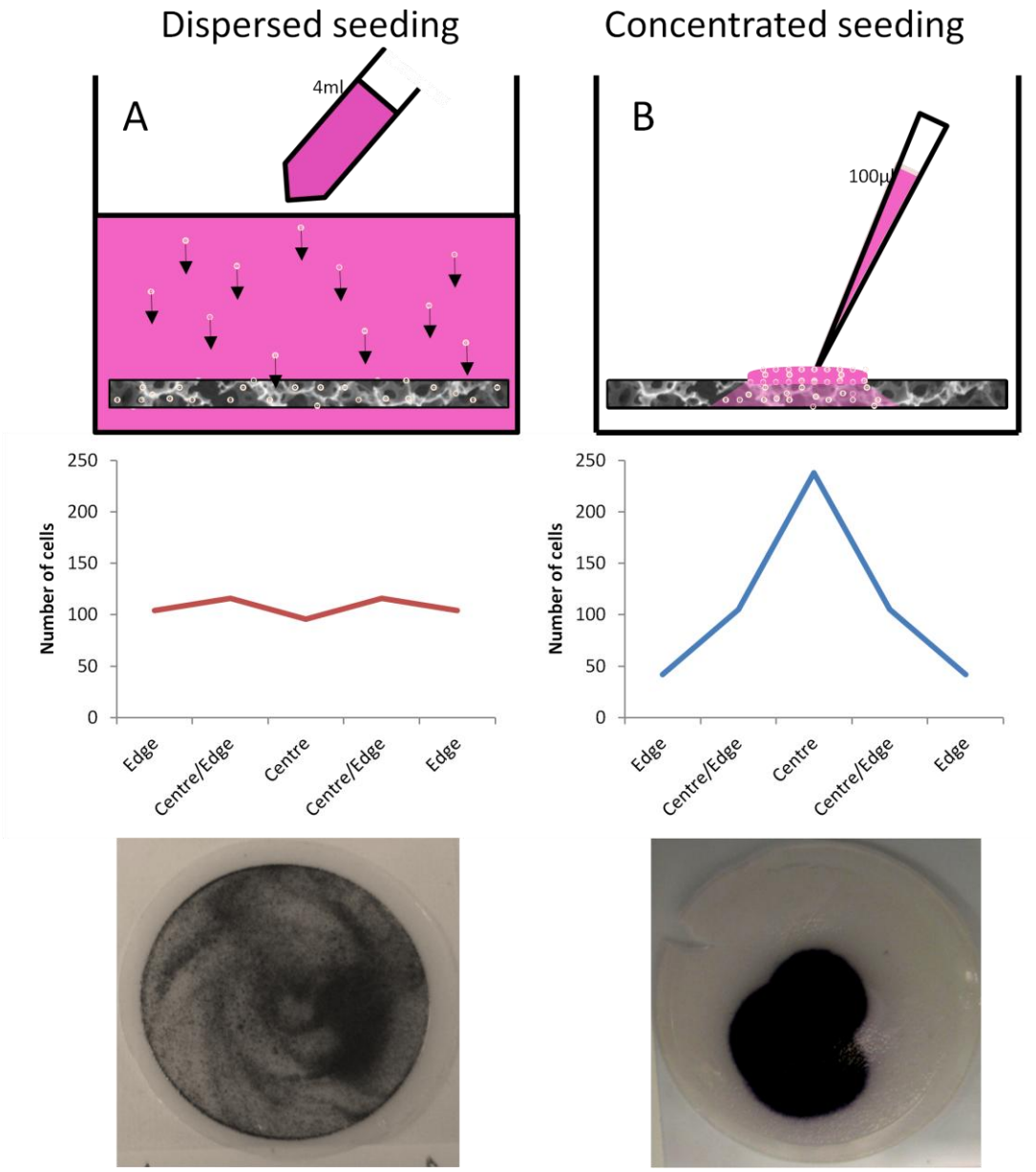

Figure 2.5 Two different approaches have been developed for cell seeding onto Alvetex® Scaffolds. 0.5 x 10^6 cells were added to each scaffold and cultured for 4 days. Method **A** shows the disperse seeding method where cells are added to the scaffold in a 4ml suspension and allowed to settle more evenly over the scaffold, this is similar to seeding on standard 2D cultureware. Method B is a concentrated seeding method where cells are suspended in a concentrated 100µl droplet and added to the centre to the scaffold. This allows cells to rapidly infiltrate the scaffold and the remaining cell culture media is added after a 15 minute incubation at 37°C. Method **B** has previously been reported for seeding cells on 3D constructs [159]. Cell numbers were counted across 10µm sections as described in section 2.4.8.1.1.

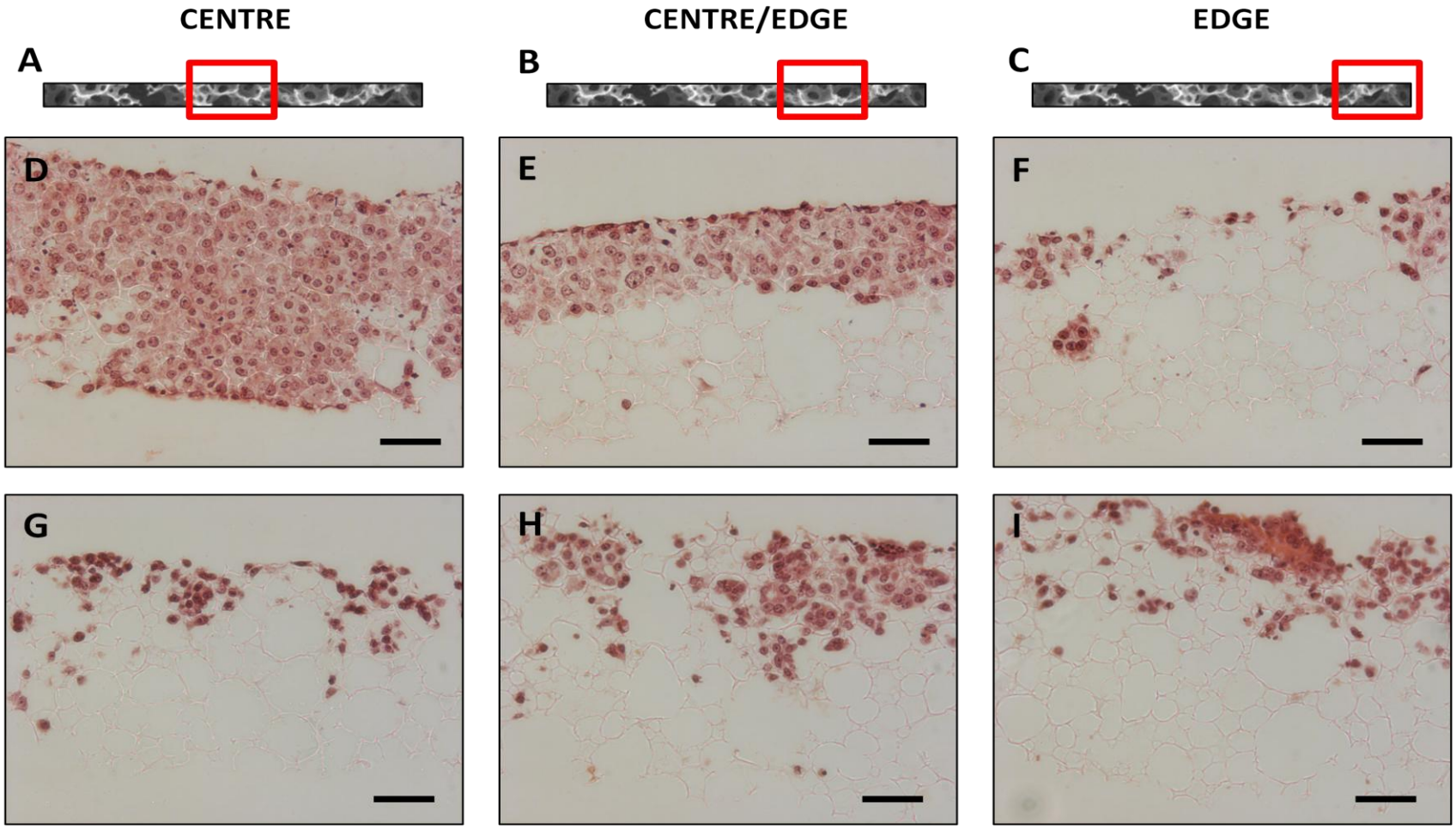

Figure 2.6 Seeding method affects cell density and distribution over the entire width of the scaffold. TERA2.cl.SP12 cells were seeded onto scaffolds in a 12 well plate using the two different seeding methods. **A-C** shows the area on a scaffold section that is being viewed in the photos below. **D-F** show a scaffold seeded using the concentrated seeding method. Cell distribution on a dispersed seeded scaffold is much more uniform across the entire disk **(G-I). Scale bars: D-I=50µm.**

2.5.3 Seeding method and initial cell density affect cell viability in 3D.

All three cell types: NIH 3T3, MET 4, and TERA2.cl.SP12 were cultured on the scaffold and seeded using the two seeding techniques. Two initial cell seeding densities of 0.5 $x10^6$ and 1 $x10^6$ cells were assessed. Cell viability was tested after 7 days using the MTS assay.

After 7 days of culture in the 3D environment, the initial seeding density has very little effect on the growth of NIH 3T3 cells. Although initially there was a difference in cell seeding density, by day 7, the two conditions show an almost identical level of cell viability (Figure 2.7A). This is also the case when looking at the two methods of seeding by day 7 there are no noticeable effects on cell viability.

The MET 4 cell line shows more of a difference between the different seeding methods especially at the higher cell density. There appears to be a higher degree of cell viability when cells are seeded at 1 x 10^6 using the dispersed method. There is no significant difference in NIH 3T3 cell viability between the two seeding methods at the lower initial seeding density (Figure 2.7B). In contrast, the seeding method does affect the viability of TERA2.cl.SP12 grown in three dimensions with both seeding densities showing higher cell viability when using the concentrated seeding method compared to the dispersed method (Figure 2.7C).

2.5.4 Seeding method has an effect on cell density

Cell density was calculated from sections of 3D cultures stained with DAPI to highlight the nuclei. Although there was no difference in cell viability (Figure 2.7A) using the two seeding techniques and densities for NIH 3T3 cells, when cell density was assessed there were differences between the conditions. The higher initial seeding density of 1 x 10^6 NIH 3T3 cells maintained a high cell density up to day 7 and also showed a difference in density between the two seeding methods. As expected the concentrated method led to a higher cell density than the dispersed method and they displayed a greater difference in density at the high initial seeding density, a difference of 5 cells per 100μm^2 (Figure 2.8A). This was in comparison with the 0.5 x 10^6 cells where the difference between the two seeding methods was less than 2 cells per 100μm^2.

In contrast with the NIH 3T3 data, the cell density of MET 4 cells correlated with the cell viability data. Interestingly the high initial seeding density leads to a lower cell density after 7 days of 3D culture. At 1 x 10^6 cells the dispersed seeding method produced an increased cell density of 7 cells per 100μm^2 compared to the concentrated method which only has 5 cells per 100μm^2. This was in contrast to the low seeding density (0.5 x 10^6 cells) where the concentrated method led to a higher cell density at 7 days (13 cells per 100μm^2) compared to the 10 cells per 100μm^2 on dispersed seeded scaffold, both of these values are higher than the

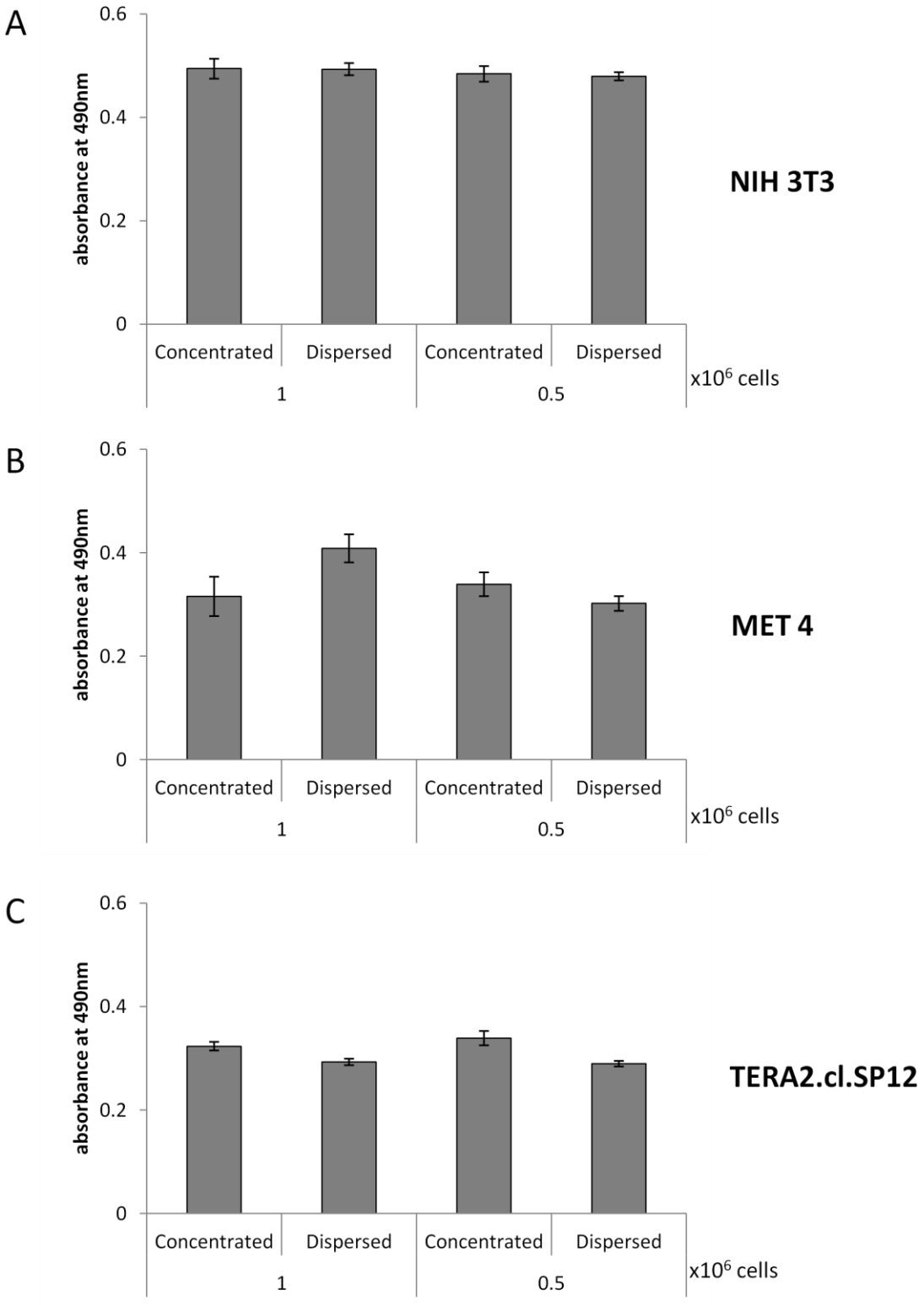

Figure 2.7 Initial cell seeding has little effect on overall cell viability using an MTS assay. Cell viability was assessed for the two seeding methods at different seeding densities after 7 days of culture. NIH 3T3 cells are viable independent of seeding method whereas MET 4 and TERA2.cl.SP12 cells are affected by initial seeding method**. n=3, ±SEM**

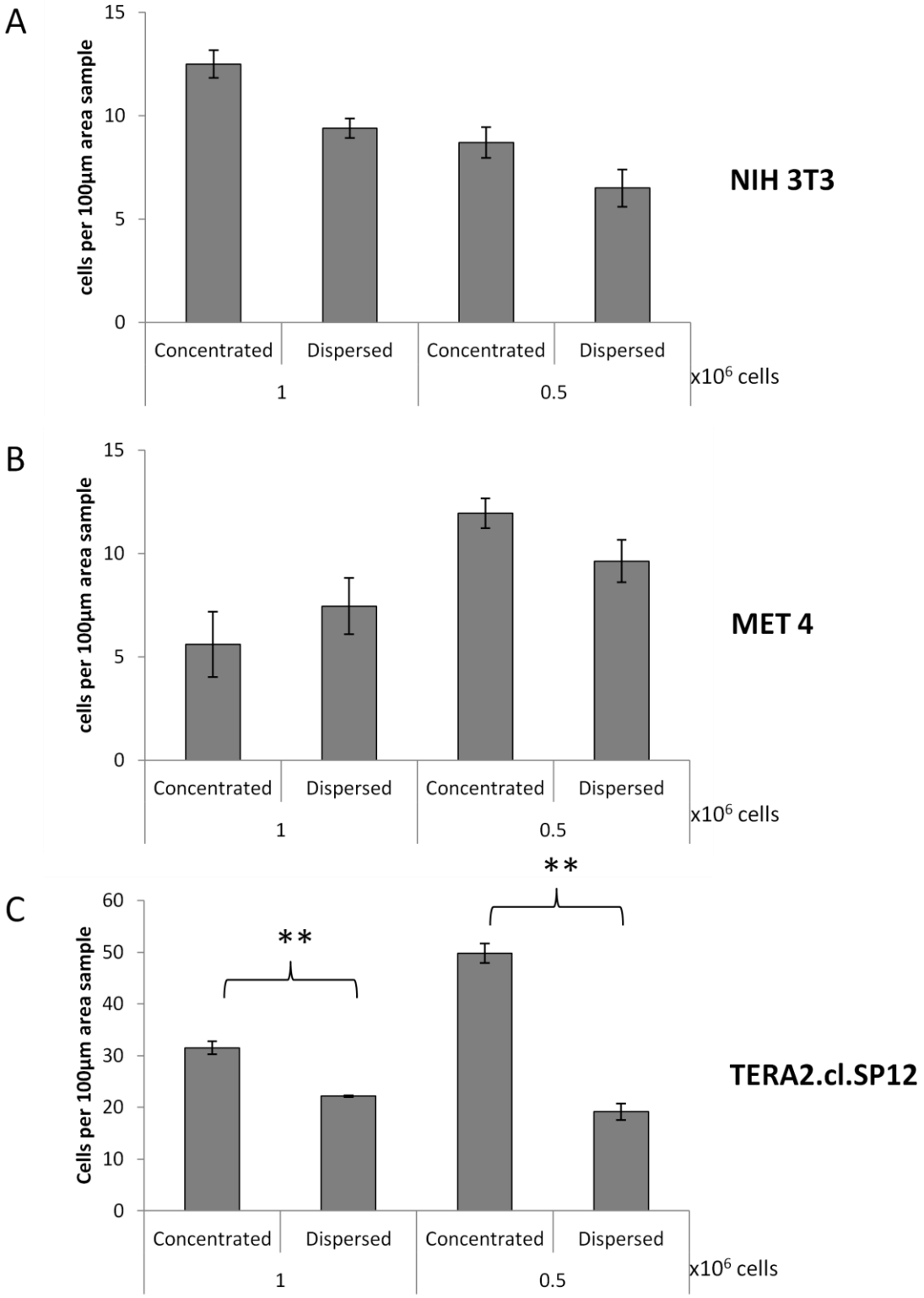

Figure 2.8 Seeding methods affects cell density. Cells were seeded on the scaffold in the 12-well plate format using the both seeding methods. Cell density was calculated by counting the number of DAPI stained nuclei in five randomly selected 100µm squares across a 10µm section. Note that in cultures of MET 4 cells higher initial seeding lead to a lower cell density and TERA2.cl.SP12 have a higher cell density in all condition compared to the other two cell types and this is significantly different between the two seeding methods. ****:p=0.01 n=3 ±SEM**

1 x 10^6 seeded scaffolds (Figure 2.8B).

The cell density for TERA2.cl.SP12 cells after 7 days was significantly greater than the other two cells lines; with even the lowest cell density achieved by disperse seeding 0.5 x 10^6 cells being more than the other two cell lines (Figure 2.8). The stem cell line also displayed the greatest difference between the two seeding methods. Concentrated seeding led to a significantly higher cell density (p=0.01) compared to dispersed seeding for both the initial seeding densities. Cells that were seeded at 0.5 x 10^6 cells using the concentrated seeding method were able to reach a density of 50 cells per 100µm^2 after just 7 days in 3D culture (Figure 2.8C).

2.5.5 Initial seeding density affects cell viability in 3D scaffolds.

A more detailed study was required to determine the ideal seeding density for cells on Alvetex® Scaffolds. A higher seeding density than 2D culture should be required due to the increased surface area for cell growth. Cell viability was assessed in all three cell lines using an MTS assay, for a range of cell densities between 0.1 x 10^6 cells and 0.75 x 10^6 cells at both day 3 and 6.

Initial seeding density affects the viability of NIH 3T3 cells. At the two lower cell densities (0.1 x 10^6 and 0.25 x 10^6 cells) there was a drop in cell viability between days 3 and 6 presumably due to a lack of cell communication. There was a drop in viability for the highest initial seeding density, whereas for 0.5 x 10^6 cells there was an increase in cell viability between day 3 and 6. This is the ideal situation but there is only small increase in viability considering the further 3 days for cell growth (Figure 2.9A). Histological analysis of NIH 3T3 cells on Alvetex® Scaffold after 3 and 6 days (Figure 2.10A&B) showed there is no significant increase in cell number within the scaffold but after 6 days a thick layer of cells started to form at the surface of the scaffold (Figure 2.10B).

MET 4 and TERA2.cl.SP12 cells display a more linear relationship between initial seeding density and cell viability. For the MET 4 cells, viability increases between days 3 and 6 for seeding densities between 0.1-0.5 x 10^6 cells but there was no increase for the 0.75 x 10^6 initial seeding density (Figure 2.9B). Cell viability increases between the two time points for all seeding densities of TERA2.cl.SP12 cells with the lower initial seeding densities producing fewer viable cells than the higher cell densities as would be expected (Figure 2.9C). Even though there was an increase in cell viability between the two time points for the TERA2.cl.SP12 cells, the H&E stained sections in Figure 2.10C&D show a similar feature to the NIH 3T3 seeded scaffolds (Figure 2.10A&B). At the later timepoint TERA2.cl.SP12

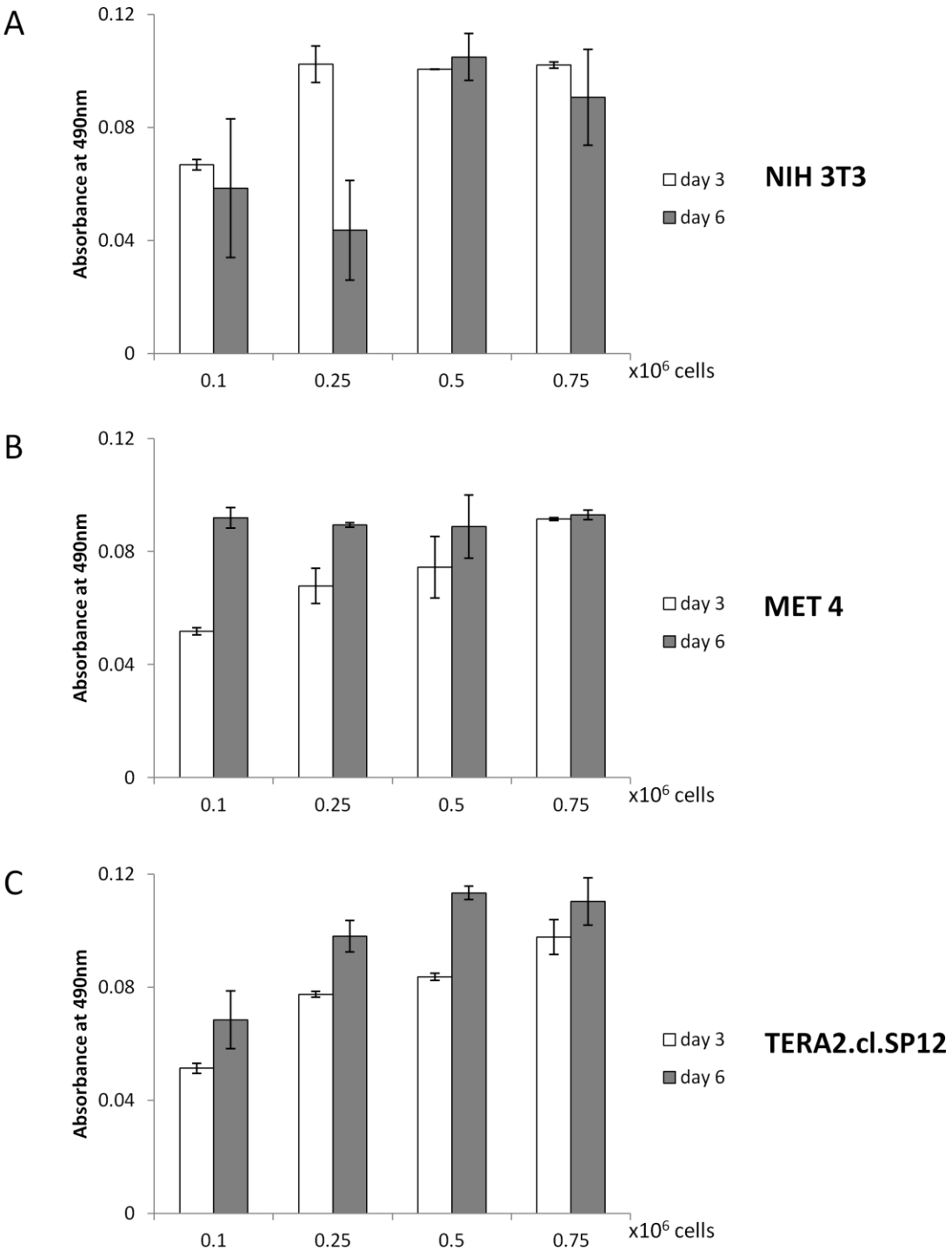

Figure 2.9 Growth and viability of alternative cell types grown in 3D using Alvetex® Scaffold. Cell viability was assessed after 3 and 6 days using an MTS assay. Each data point represents the mean and standard error of 3 separate samples. Note the decrease in viability between 3 and 6 days when NIH 3T3 cells are seeded at high cell density. Viability of MET 4 cells does not increase between the two timepoints when $0.75x10^6$ cells are seeded. Growth of TERA2.cl.SP12 cells shows a good example of a linear relationship as cell number increases. The differences in these viability profiles is due to the specific characteristics of each cell line as detailed in Table 2.1.

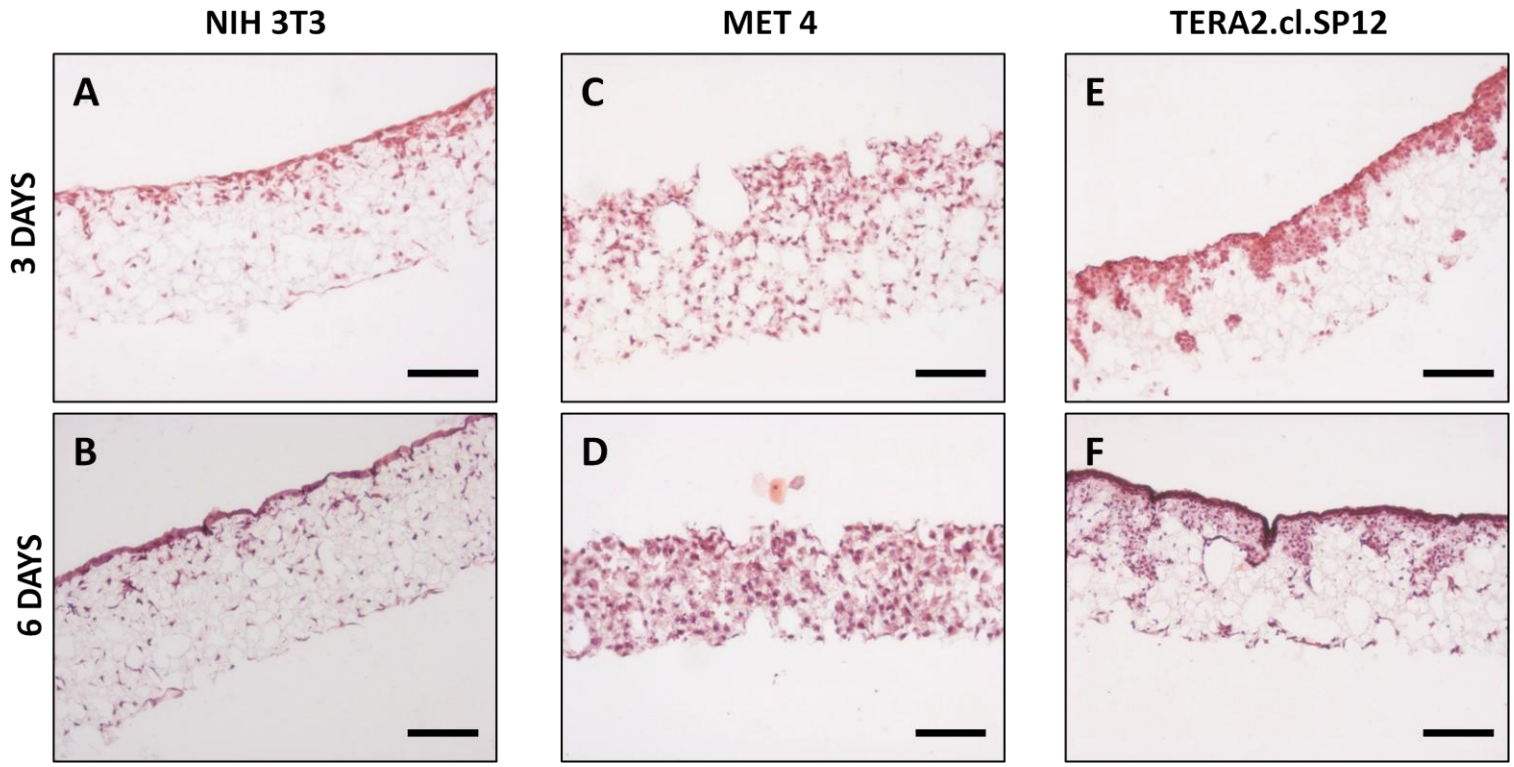

Figure 2.10 Histological analysis of alternate cell types grown in 3D culture using Alvetex® technology, 3 (A,C,E) and 6 (B,D,F) days culture: Data show typical cell distribution of NIH 3T3 **(A,B),** MET 4 **(C,D)** and TERA2.cl.SP12 cells **(E,F)** when cells are seeded at an initial seeding density of 0.5 x 10^6 cells per scaffold. Samples were taken from central location of the Alvetex® disc. All sections were stained with Haematoxylin and Eosin Scale bars: **A-F**=100µm.

cells have started to produce a dense layer at the surface of the scaffold rather than continuing to infiltrate the scaffold interior. This phenomenon does not appear in the MET 4 seeded scaffolds where there was evidence of an increased cell density between day 3 and 6. At day 6, the scaffold was completely filled with a dense slab of MET 4 cells (Figure 2.10E&F).

2.5.6 Growth profiles in 2D and 3D differ depending on cell type

Growth profiles were obtained for all three cell lines by assessing cell viability over a 9 day period. The initial seeding density for 2D and 3D cultures was 0.5 x 10^6 cells. Scaffolds were seeded using the concentrated seeding method. The 3D scaffold environment does not appear to affect the growth of NIH 3T3 cells which displayed a similar growth profile in both 2D and 3D cultures (Figure 2.11A). MET 4 cells showed a slight difference in growth profiles between the 2D and 3D environments. Cells in 2D showed greater viability at days 2 and 4 when compared with their 3D counterparts, however at day 9 the viability of the 3D cells is still increasing whereas in 2D the viability has begun to decrease (Figure 2.11B) presumably due to the lack of space for further expansion.

In contrast to the other two cell lines there is a significant difference in cell viability between the 2D and 3D cultures of TERA2.cl.SP12 cells. The 3D cultures showed a delay in proliferation when compared to the 2D cultures. The 2D cultures behave as expected the cell viability which is proportional to cell number rapidly increased between days 1-5 but the viability plateaued by day 9. The growth profile for the 3D cultures is radically different, the viability of the cells remained constant between days 1 and 5 but there is a rapid increase in cell viability by day 9, but the cell numbers seen in the 2D cultures are not reached in the 3D cultures in the 9 day growth period (Figure 2.11C).

2.5.7 The confluency of cells remains important during 3D culture

Figure 2.12 displays phase contrast images of typical NIH 3T3 cells grown on standard 2D tissue culture plastic. At day 1, cells are sparse with few points of contacts between neighbouring cells. The NIH 3T3 cells are long spindle-like cells, as they became confluent the cells lost this morphology and began to squash together; this is visible in the phase micrograph at day 5. When the cells are grown on 3D scaffolds they retained their long spindle-like structure as they stretched along the top surface of the scaffold and cells which entered the scaffold interior remained stretched across the voids as shown in the image after one day in 3D culture. In a similar way to the 2D cultures, the fibroblasts grown in 3D have started to lose their distinctive shape by day 5. Cells at the surface of the scaffold appeared more rounded and the cells which had moved through the scaffold to the bottom surface also appeared rounded. The similarity

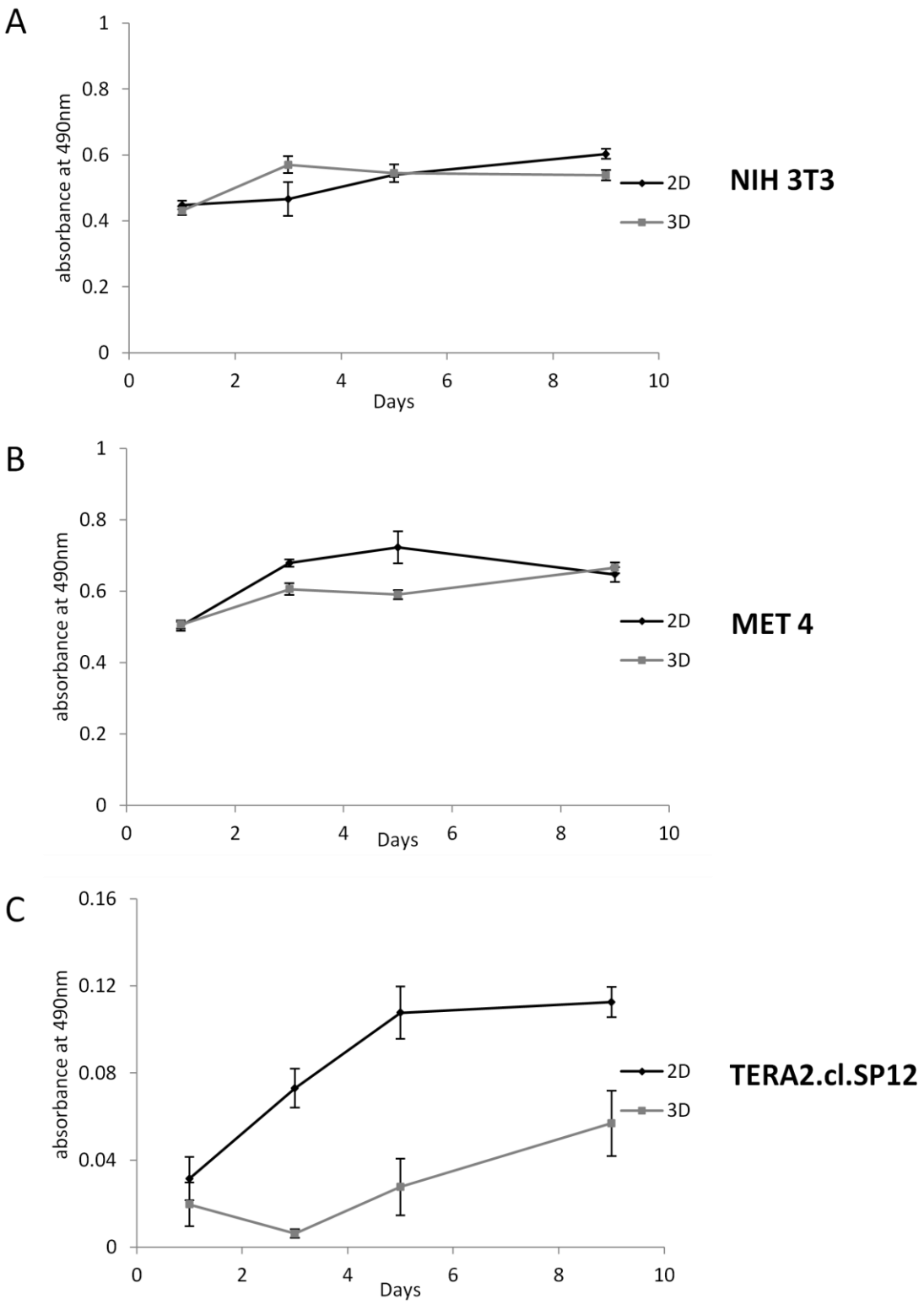

Figure 2.11 Cell growth profiles in 2D and 3D culture differ depending on cell type. 2D cultures and scaffolds were seeded with 0.5 million cells using the concentrated seeding method. NIH 3T3 **(A)** and MET 4 **(B)** cells show little difference in cell growth between 2D and 3D culture. Interestingly, TERA2.cl.SP12 cells show delay in proliferation when grown in 3D **(C).** Each data point represents the mean and standard error of 3 separate samples.

between the two culture methods is also evident when cell density is calculated. The densities of the cultures at day 1 are identical with both types of culture having a density of 4 cells per 100µm^2. For the 2D cultures the density rapidly increases up to day 3 when it reaches 13 cells per 100µm^2 this is maintained for another 2 days before there was a decrease in cell density to less than at day 1. The 3D cultures show a similar profile but delayed: the cultures do not reach their maximum cell density until day 5 and this was maintained up to day 9. It is likely that a decrease in cell density would occur soon after the day 9 timepoint. This data provides evidence that percentage confluency of a culture remains important when growing cells in 3D.

MET 4 cells have a different cell density profile in 2D culture compared to 3D culture. The phase contrast micrographs in Figure 2.13 show the keratinocyte-like cell line after one day in culture, the cells tend to grow in colonies but show no close cell contact. By day 5 the cells have produced a confluent cell layer and unlike the 3T3 cells they do not change morphology to fill the gaps in the cell layer this is consistent with their dissociated keratinocyte morphology which has previously been described [165]. Cell density approximately doubled every 2 day for the first few days of culture and reached a density of 12 cells per 100µm^2 at day 9; this greatly differred to the cell density profile in 3D.

When the MET 4 cells are cultured on the Alvetex® Scaffold their cell density rapidly increased from 3 cells per 100µm^2 at day 1 to 16.5 cells per 100µm^2 at day 3, this was a higher cell density than was possible during standard 2D culture. However the scaffold does not appear to be able to maintain the cells at this high density and there was a drop in density by day 5 to closer to the level of 2D cultures. H&E stained sections showed that the MET 4 cells started to infiltrate the scaffold as early as day 1 and unlike the 3T3 cells the entire cell layer infiltrated the scaffold rather than single cell migration, by day 5 approximately 150µm of the 200µm scaffold membrane is filled with cells.

TERA2.cl.SP12 are able to reach higher cell densities than the other two cell lines and showed the greatest difference between 2D and 3D cell culture (Figure 2.14). At day 1, the 2D culture was already ~70% confluent and by day 5 the phase micrograph showed a dense confluent layer of cells which in some areas consisted of more than one cell layer. This accounted for the high cell density at day 5 of 23 cells per 100µm^2. In 3D, the TERA2.cl.SP12 ability to form cell layers is also evident. At day 1, the cells are dispersed in the top quarter of the scaffold membrane but as they reach day 5 the gaps between cells have been filled with a densely packed slab of tissue. In a similar way to the MET 4 cultures there is limited single cell migration through the scaffold. Significantly higher cell densities are possible in the 3D cultures

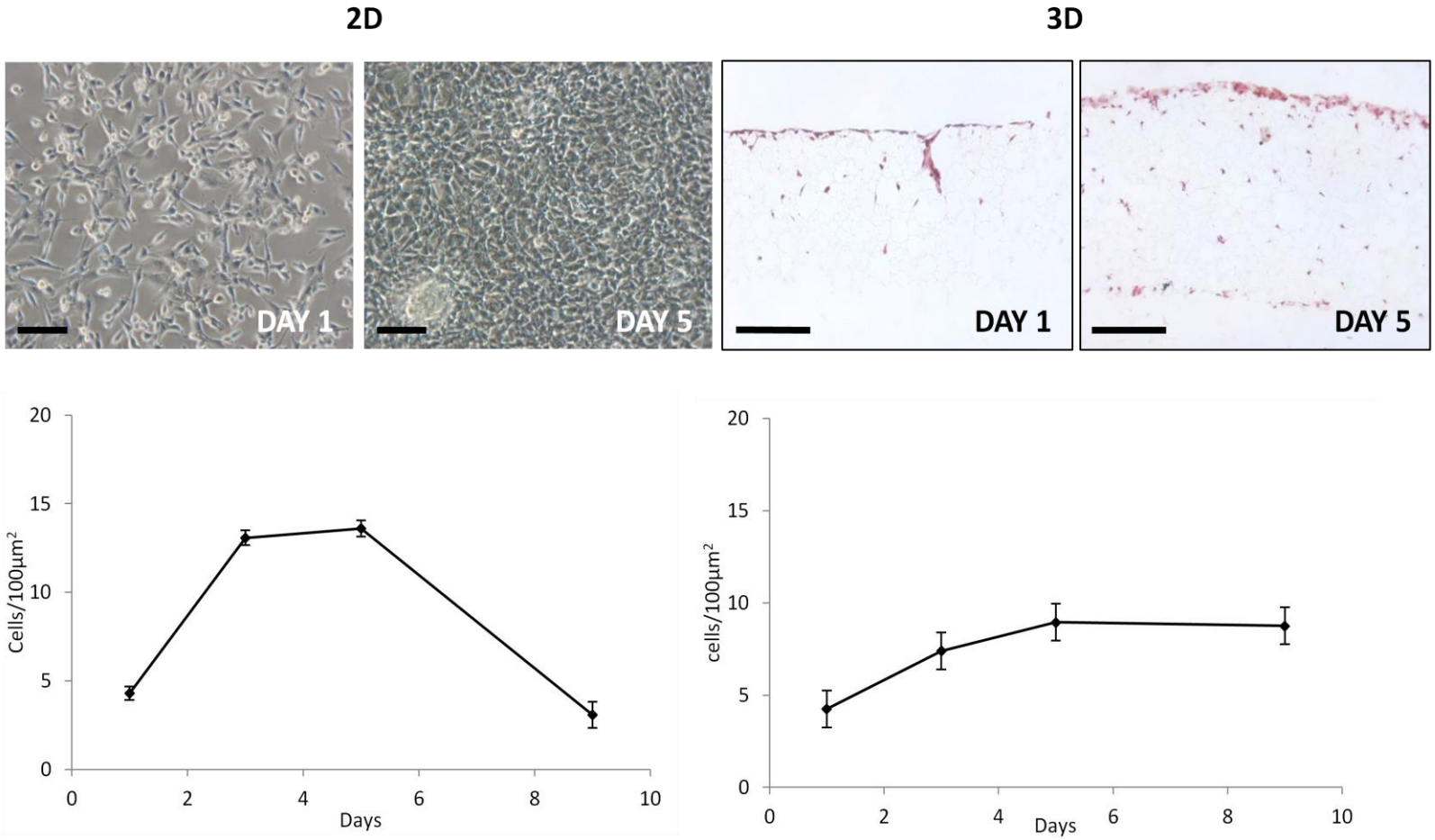

Figure 2.12 Comparison of cell density of NIH 3T3 in 2D and 3D culture. Cells were seeded in 2D in a 6 well plate and in 3D scaffold in the 12-well plate format using the concentrated seeding method. Density was calculated by counting the number of DAPI stained nuclei in five 100µm squares on 6 separate samples. It was noticeable that contact inhibition appears to affect the growth of NIH 3T3 in 3D. The cells do not grow together and compact in 3D leading to a difference in the rate of confluency between the two growth conditions **Scale bar = 100µm**

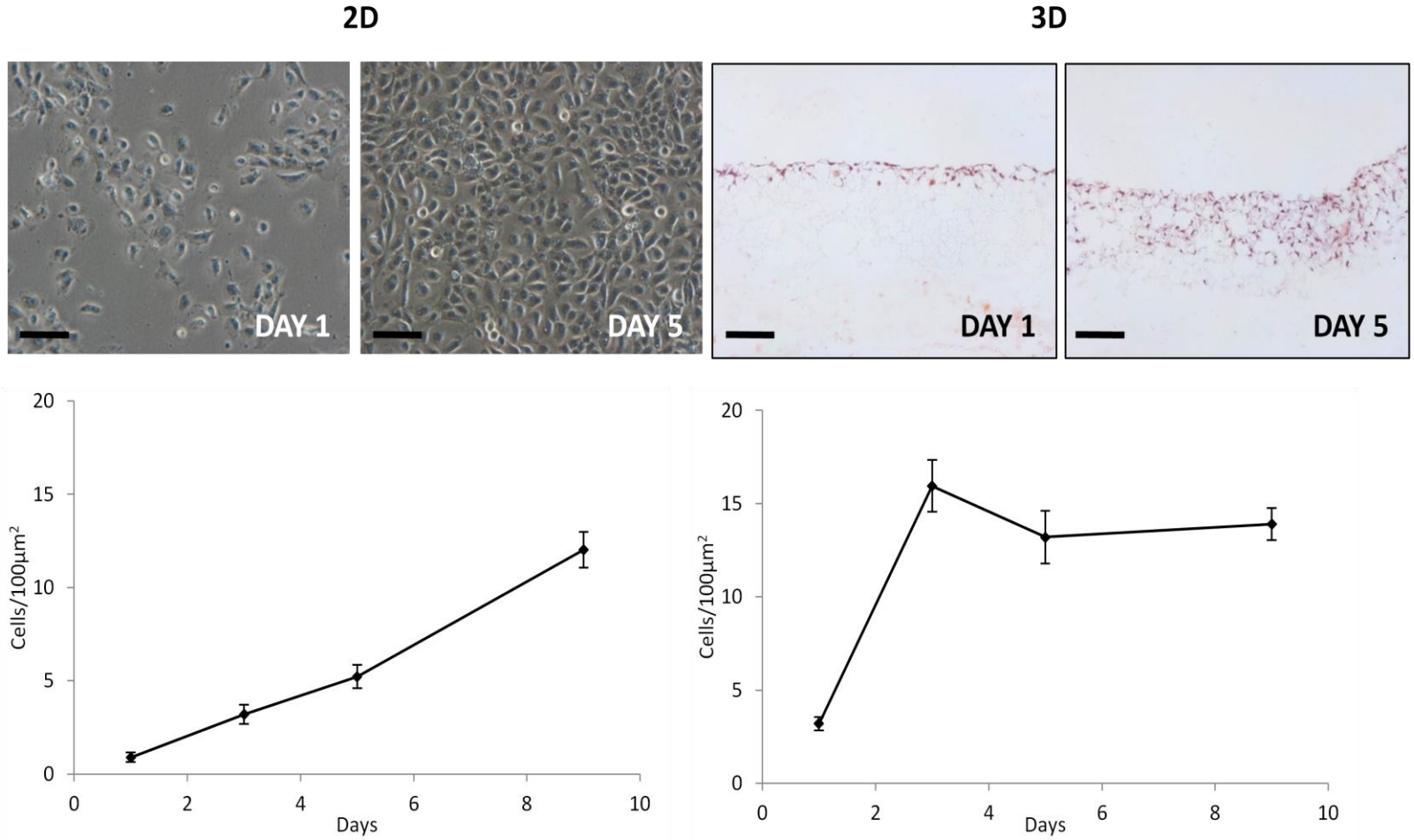

Figure 2.13 Comparison of cell density of MET 4 in 2D and 3D culture. Cells were seeded in 2D in a 6 well plate and in 3D scaffold in the 12-well plate format using the concentrated seeding method. Density was calculated by counting the number of DAPI stained nuclei in five 100µm squares on 6 separate samples. A higher cell density is reached at an earlier timepoint in 3D compared to 2D cultures. **Scale bar = 100µm.**

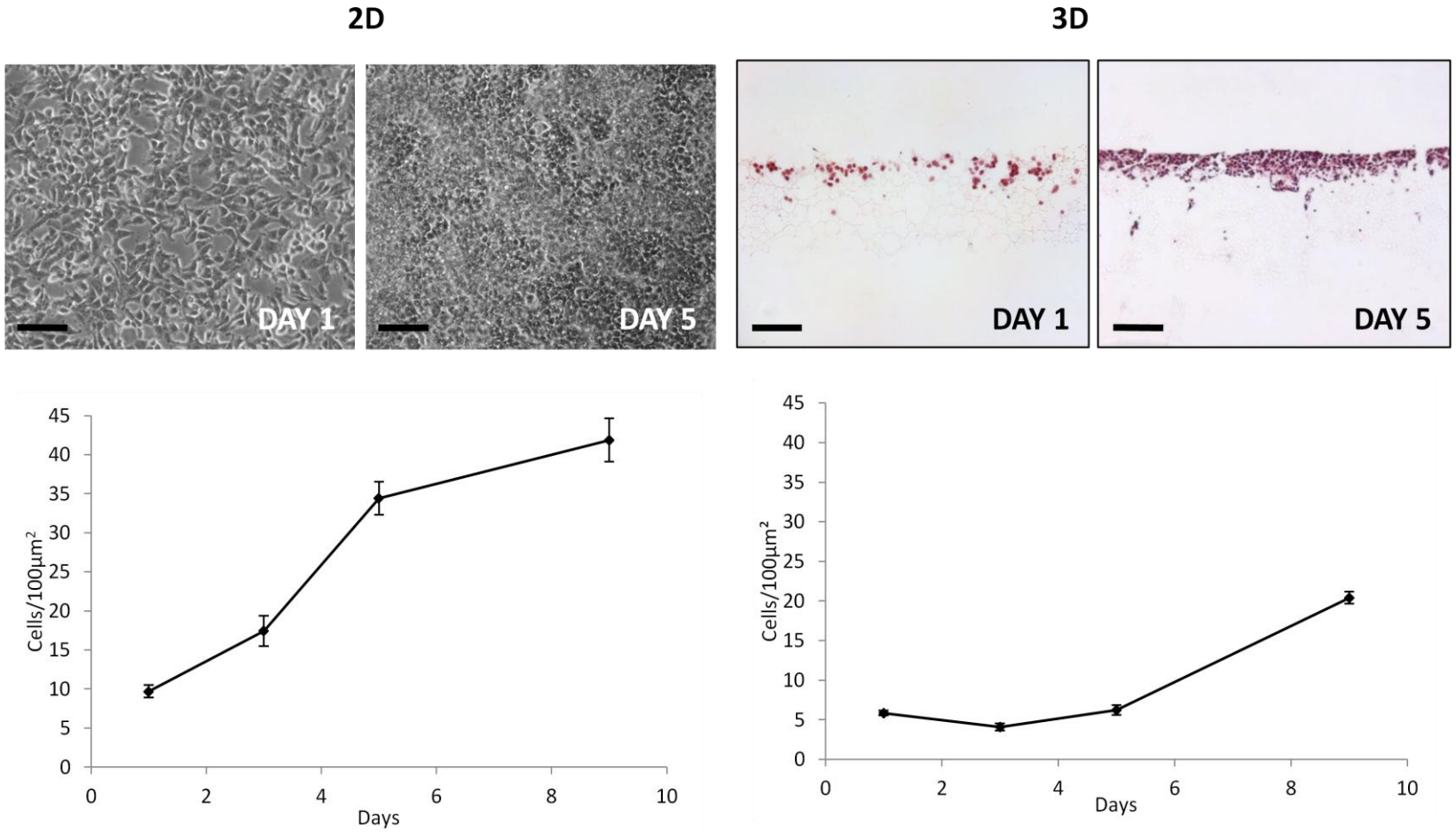

Figure 2.14 Comparison of cell density of TERA2.cl.SP12 in 2D and 3D culture. Cells were seeded in 2D in a 6 well plate and in 3D scaffold in the 12-well plate format using the concentrated seeding method. Density was calculated by counting the number of DAPI stained nuclei in five 100µm squares on 6 separate samples. 3D cultures of TERA2.cl.SP12 cells are able to reach higher cell densities than 2D cultures. **Scale bar = 100µm**

compared to the 2D cultures. By day 3, the cell density in the 3D cultures has already reached the density at 9 days in 2D culture. Cell density continued to increase up to day 5 where it reached 35 cells per 100μm^2. This is more than twice as many cells as MET 4 cultures and over three times as many as 3D cultures of NIH 3T3 cells.

2.5.8 Maximum cell penetration into the scaffold interior is independent of cell type

The average maximum penetration of cells into the scaffold interior was calculated from H&E stained sections of the 3D cultures. For each timepoint, three separate scaffold samples were assessed; fifteen measurements were taken across the entire length of each of the scaffold samples.

Maximum cell penetration appears to be independent of cell type as all three cell lines reach a maximum of 140μm into the scaffold interior during the 9 day period (Figure 2.15). NIH 3T3 rapidly migrated into the scaffold and have reached a quarter of the scaffold depth after one day in culture. By day 3, the cells are half way through the scaffold but the rate of infiltration decreased as cells are only able to reach the 140μm (Figure 2.15A). MET 4 cells displayed a similar profile to the NIH 3T3 cells but initial cell penetration was slower with only 25μm of the scaffold contained cells after one day in the 3D environment. By day 5, MET 4 cells have infiltrated to 140μm into the scaffold and there was no increase in cell penetration between day 5 and 9 (Figure 2.15B). In a similar way to the MET 4 cells, the TERA2.cl.SP12 cells are able to infiltrate into the scaffold interior almost immediately, cells reached a quarter of the way through the scaffold after 24 hours. Further migration was slower than the other two cell lines as the TERA2.cl.SP12 cells grow into dense layers before spreading further into the scaffold this is demonstrated by the cells not yet reaching 100μm by day 5 (Figure 2.15C). The TERA2.cl.SP12 cells do continue to infiltrate up to day 9 where they have reached 140μm which appears to be the limit of all three cell lines.

2.5.9 Surface treatment of 3D polystyrene scaffolds

Alvetex® Scaffolds are provided untreated and are therefore hydrophobic. As with all tissue culture plastic they require treatment to render them hydrophilic before the addition of cells. The simplest method of ensuring the disc is hydrophilic is ethanol treatment. This involves wetting the discs with 70% ethanol followed by two washes in PBS prior to addition of cells. This method means that the scaffold is full of PBS when the 100μl of cell suspension is added; this leads to the cells remaining close to the top surface of the scaffold (Figure 2.16A). Another method to ensure the discs are hydrophilic is plasma treatment. We tested a plasma ashing procedure using oxygen gas which is similar to the methods used for commercial 2D tissue culture polystyrene and helps to promote cell adhesion. This increased cell adhesion is

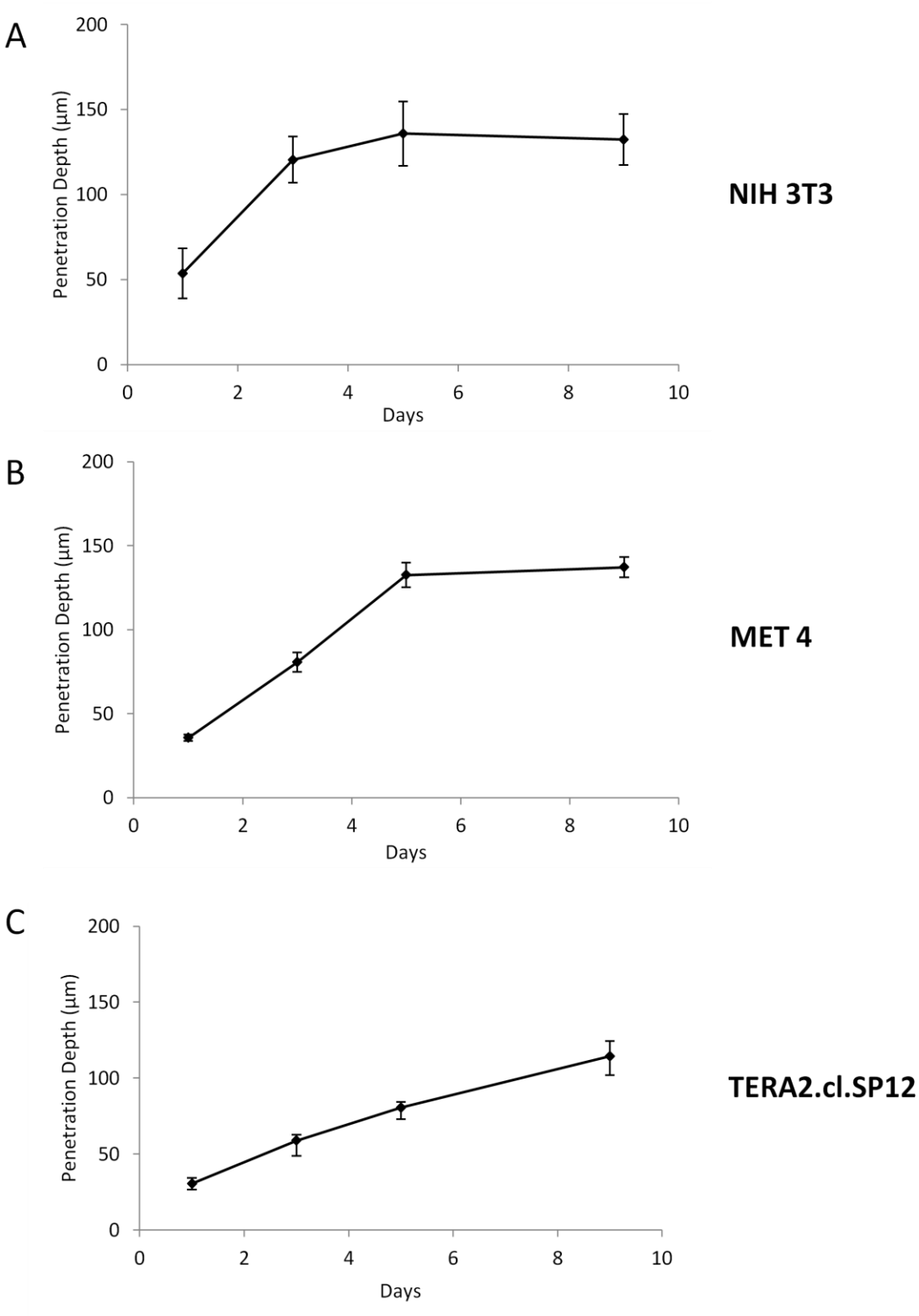

Figure 2.15 Penetration of cells into the scaffold is independent of cell type. Cells were seeded in the 12-well plate format using the concentrated seeding method. The average maximum penetration depth of cells was calculated by taking 15 measurements per scaffold for three separate scaffold samples for each timepoint. NIH 3T3 **(A),** MET 4 **(B)** reach a maximum of 140µm into the scaffold by day 5. Whereas TERA2.cl.SP12 **(C)** do not reach this depth until 9 days of culture.

achieved by the addition of oxygen-containing functional groups to the polymer surface; these include hydroxyl, carboxyl and carbonyl functional groups [166]. It is possible to plasma treat the porous polystyrene scaffold surface to improve wettability. This method means that ethanol treatment is not required before the addition of cells but it may still be required for sterilisation of the scaffolds. Due to this the scaffold is dry when the 100µl cell suspension droplet is added which allows the 100µl to be pulled into the scaffold interior and allows cells to infiltrate further into the scaffold (Figure 2.16B).

To assess the effect of surface treatment scaffold discs were suspended in standard well insert so as the movement of media and nutrients through the scaffold did not affect the degree into which the cells would infiltrate the scaffold. Hydrophobic non-treated scaffolds were compared with ethanol treated and plasma treated scaffolds using two different sets of conditions: 10 Watts for 30 minutes and 40 Watts for 5 minutes. After both lengths of plasma treatment half the scaffolds were subsequently ethanol-sterilised.

The effect of surface treatment was assessed by studying H&E stained sections of treated scaffolds which have been seeded with TERA2.cl.SP12 using the concentrated seeding method. As expected when cells were added to untreated hydrophobic scaffolds there were a few patches of cells on the scaffold but they are sparse and show little evidence of infiltration into the scaffold (Figure 2.17A). Cell penetration into the scaffold was enhanced by making the scaffold hydrophilic using ethanol treatment, this led to a dense layer of cells at the surface of the scaffold and allowed cells into the scaffold interior (Figure 2.17B). To further increase cell growth into the scaffold interior, plasma treatment can be used. The treatment at 10W for 30 minutes led to a dense layer of cells throughout the scaffold (Figure 2.17C). This layer of cells can also be achieved when treating at the higher power for a shorter period of time (Figure 2.17E). The 40W treatment had no detrimental effect on the structure of the scaffold disc. Ethanol sterilisation post plasma treatment affected the infiltration of cells into the porous scaffold. When the scaffolds were treated for 30 minutes at 10W and then sterilised, a dense cell layer was still produced but it did not fill the entire depth of the scaffold (Figure 2.17D) this was in contrast with 40W for 5 minutes treatment where ethanol sterilisation had more of an effect and the cells showed limited cell infiltration into the scaffold (Figure 2.17F).

The effect of surface treatment was quantified by measuring the average maximum penetration into the scaffolds. Again this was achieved by taking 15 measurements across the entire length of the treated scaffold discs. Hydrophilic non-treated scaffolds allowed cells to infiltrate less than 50µm into the scaffold so any additional treatment significantly enhanced the degree of infiltration. Ethanol treatment did allow more cells to reach the interior of the

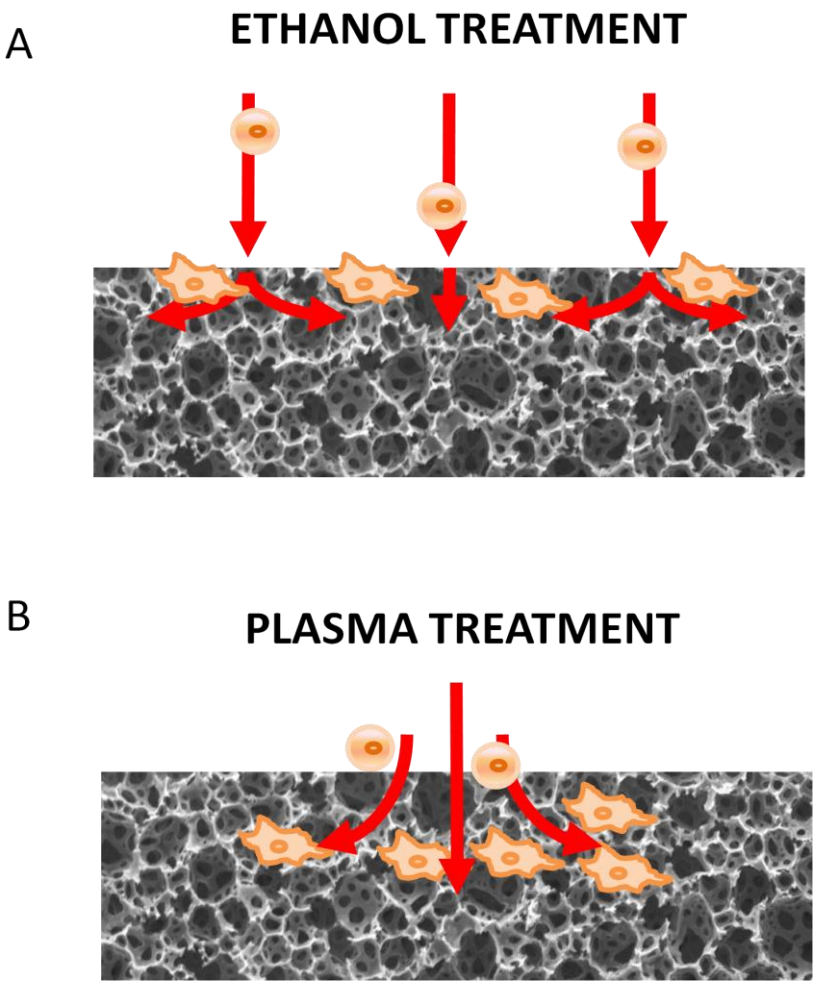

Figure 2.16 Cell penetration is dependent on surface treatment. This schematic diagram illustrates the behaviour of cells in the two conditions tested. When scaffolds are plasma treated to increase their hydrophilicity cells are added to a dry scaffold and are rapidly drawn into the scaffold interior. When ethanol treatment is used the scaffold is already filled with PBS so cells come to rest on the top surface of the scaffold and slowly make their way into the scaffold.

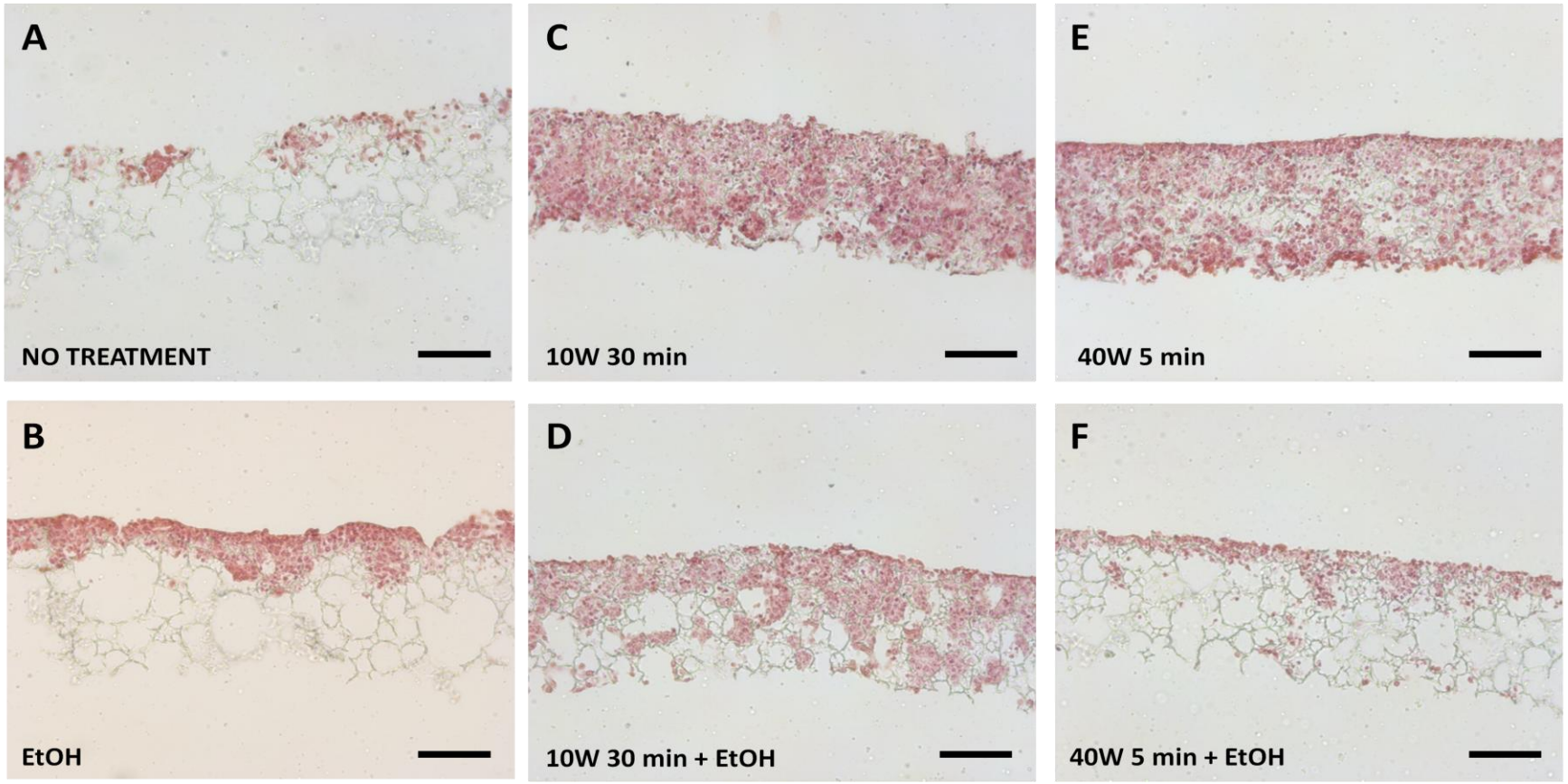

Figure 2.17 Surface plasma treatment affects cell growth and infiltration into the porous polystyrene scaffold. Scaffolds were seeded with 1 million TERA2.cl.SP12 cells and cultured for 7 days. Scaffolds are hydrophobic and require surface treatment prior to cell culture. When cells are added to non-treated scaffolds there is little cell adhesion and proliferation **(A).** Ethanol wetting the scaffold allows more cells to adhere the scaffold **(B).** Alternatively scaffolds can be plasma treated using an oxygen plasma. This method was tested at two different powers of 10W for 30 minutes **(C,D)** and 40 W for 5 minutes **(E,F).** Plasma treatment increases cell infiltration into the scaffold. An additional ethanol wetting step prior to seeding a plasma treated scaffold reduces the amount of cell penetration into the scaffold for both 10W **(D)** and 40 W **(F),** this could be due to the scaffold already being filled with PBS so cells are not pulled into the scaffold interior. **Scale bars: A-F=100µm**

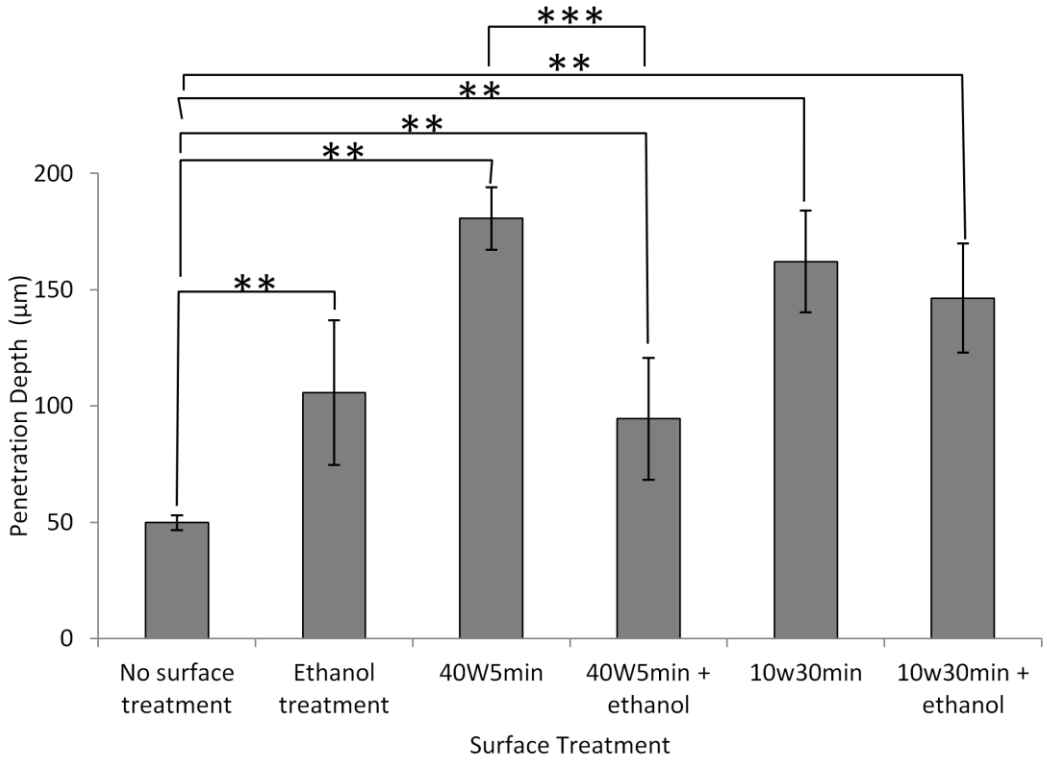

Figure 2.18 Surface treatment affects the depth of cell penetration into the scaffold. Scaffolds were treated and seeded with 0.5 million TERA2.clSP12 cells using the concentrated method and cultured for 7 days prior to being fixed, sectioned and stained prior to measurement of cell penetration. The average maximum penetration depth of cells was calculated by taking 15 measurements per scaffold for three separate samples for each surface treatment types. ** p=0.001, ***p=0.0001.

scaffold and led to a cell penetration depth of 110µm over twice the distance of a non-treated scaffold (Figure 2.18). Plasma treatment increased the penetration depth to 180µm for the 40W for 5 minutes treatment and slightly less cell penetration (160µm) for the low power treatment. An additional ethanol sterilisation step led to reduced cell penetration, with a decrease of 20µm in the low power treatment, but there was a significant effect on the 40W for 5 minutes surface treatment with ethanol sterilisation leading to a 100µm decrease in cell penetration.

Scaffold which had been surface treated were also seeded with MET 4 and NIH 3T3 cells. Scaffolds were either ethanol treated or plasma treated for 40W for 5 minutes. For both cell lines the treatment did not affect the degree of penetration. Both cells lines were able to reach the underneath surface of the scaffold with both treatments. This can be clearly visualised in the histological analysis of sections in Figure 2.19. Surface treatment has an effect on cell viability and cell density of both MET 4 and NIH 3T3 cells. MET 4 cells showed a significantly higher cell viability after 4 day of culture on plasma treated scaffolds when compared to ethanol treated scaffolds (Figure 2.19A). The plasma treatment led to a higher density of MET 4 cells within the scaffold interior (Figure 2.19B) whereas ethanol treatment allowed cells to penetrate throughout the scaffold they appeared at a much lower density (Figure 2.19C). NIH 3T3 cells are less affected by surface treatment with no significant difference in viability between the two treatments (Figure 2.19A), however the H&E stained sections showed a difference in cell morphology. Plasma treated scaffolds showed dense colonies of spindle-like cells within the scaffold interior (Figure 2.19D) whereas when the scaffold is ethanol treated there are rounded cells at both surfaces of the scaffold and a few rounded cells in the scaffold interior (Figure 2.19E).

2.5.10 Seeding method onto 3D scaffold affects the pluripotency of stem cells

An additional property of the TERA2.cl.SP12 cells was their need to maintain their stem cell phenotype. This is achieved in 2D cultures by allowing the cells to grow at a high confluency but if cells are passaged and split too harshly the cells tend to differentiate [133]. The need to maintain the stem cell phenotype and pluripotency will also be necessary when culturing this pluripotent stem cell line in 3D. Pluripotency of TERA2.cl.SP12 cells was assessed using immunohistochemistry to stain for the embryonic stem cell marker – Oct 4. All 3D cultures displayed cells that were positive for the embryonic stem cell marker (Figure 2.20). However both initial seeding density and seeding methods affected the number of positive cells. White arrows on the images highlight areas of cells which are negative for Oct 4. Almost all cells in the scaffold seeded using the concentrated method and an initial seeding density of 0.5×10^6 cells were positive for Oct 4, but at the higher initial cell seeding density (1×10^6 cells) there

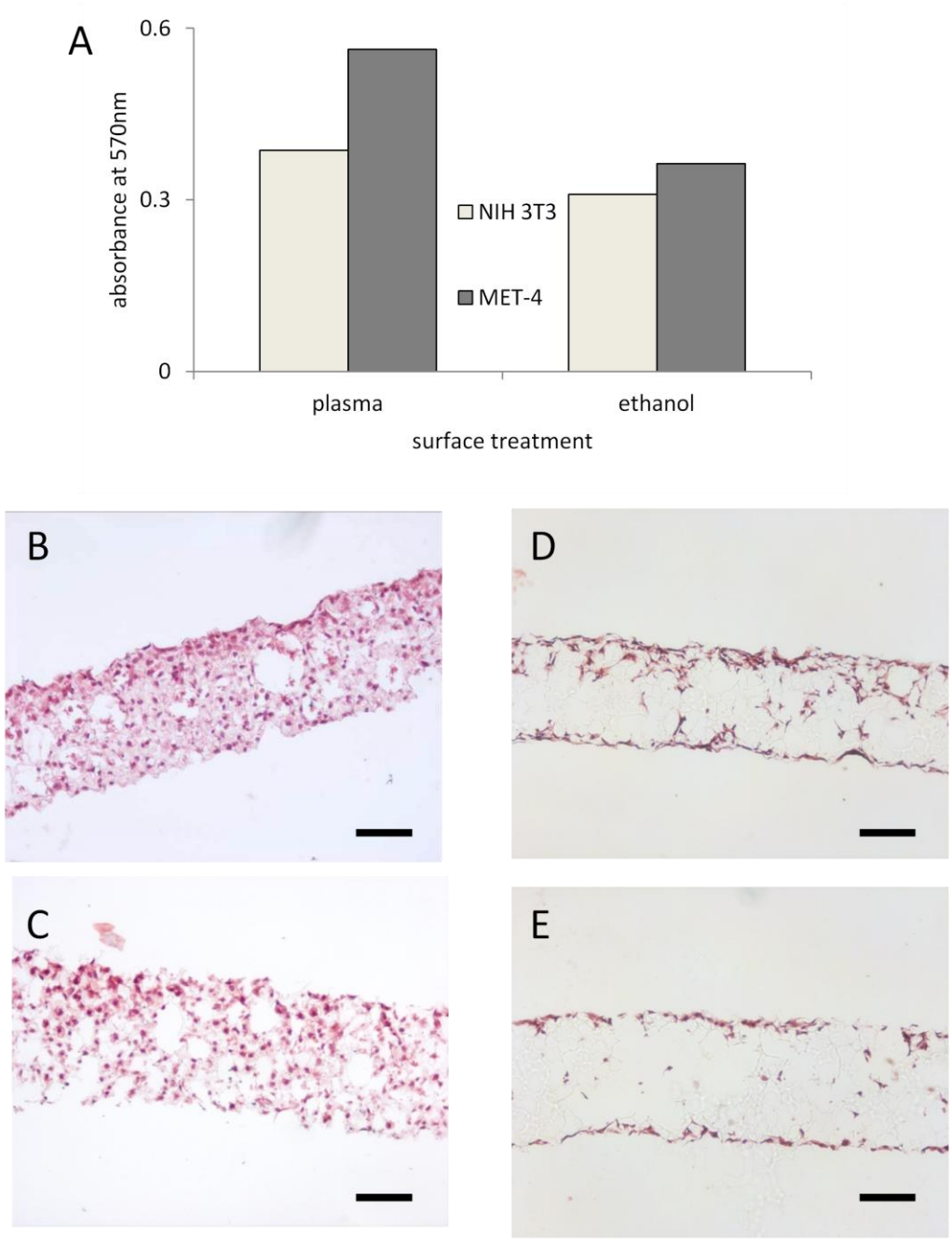

Figure 2.19 Surface treatment of the scaffold affects growth of MET 4 and NIH 3T3. Cells were seeded on the scaffold in the 12-well plate format using the concentrated seeding method and cultured for 4 days. Cell viability is affected by surface treatment for both MET 4 and NIH 3T3 **(A).** Plasma treatment leads to cells throughout the scaffold for MET 4 **(B)** and NIH 3T3 **(D)** whereas ethanol treatment leads to a less densely packed scaffold **(C,E)** over the same time period. **Scale bars: 100µm.**

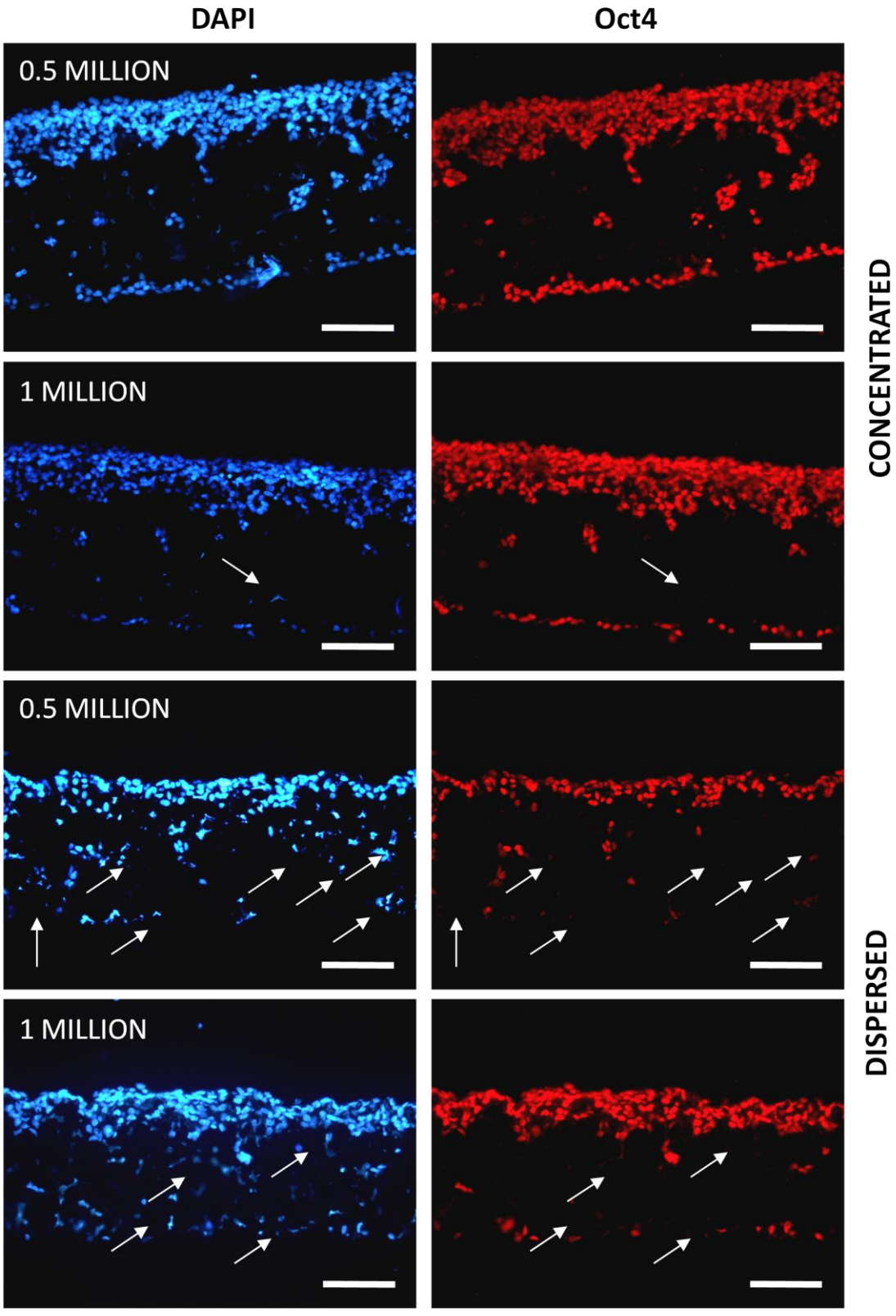

Figure 2.20 Immunofluorescence staining to show the maintenance of pluripotency in 3D using the two different seeding methods. Oct 4 expression is maintained in cells seeded in a concentrated drop but cells towards the bottom of the scaffold in disperse seeded scaffolds do not express Oct 4. White arrows highlight cells which are not positive for Oct 4. Note that cells in low density areas within the scaffold interior are often negative for Oct 4. **Scale bar=100µm**

were more areas of cells that do not stain for Oct 4. When scaffolds were seeded using the dispersed seeding method there are large areas of cells that are negative for Oct 4 especially within the scaffold interior. There were no significant differences between the two initial seeding densities when using the dispersed method but the scaffold seeded with 1×10^6 cells also showed cells that are negative for Oct 4 in the dense cell layer at the surface of the scaffold, this was not observed in any other condition.

2.6 Discussion

Cell culture has moved on significantly since Roux was culturing on flat glass plates but it is still not representative of processes that occur *in vivo*. Many methods for three dimensional cell culture have started to be developed but few have undergone significant optimisation for use with a range of cell lines. An example of a 3D environment which has undergone extensive optimisation are fibrin scaffolds. Optimal conditions have previously been determined for use with fibrin scaffolds for chick dorsal root ganglia [167, 168], fibroblasts [169, 170], mesenchymal stem cells [171] and neural progenitors from mouse ES cells [172]. These papers suggest that the scaffold needed to be optimised to limit cell death, promote proliferation, facilitate cell adhesion, and aid in cell migration.

Alvetex® Scaffold technology has been developed and has already been shown to be useful for the growth of three main cell types: HepG2 – a liver hepatocellular carcinoma [79, 112], MG63 – osteosarcoma cell line [110] and TERA2.cl.SP12 cells [113, 114]. Each of these cases demonstrated enhanced cell viability and functionality when cells were grown in 3D compared to their 2D counterparts. Hayman et al. demonstrated the need to coat 3D culture matrices. Untreated scaffolds were unable to support viable neurons whereas with the addition of poly-D-lysine and laminin they were able to support a large number of viable neurons [114]. Although the scaffold has been demonstrated for use with a range of cell types, specific parameters for culture in 3D for enhanced *in vitro* testing have not been established. Here I have demonstrated how 3D scaffolds can be optimised for a range of cell types with specific requirements (Table 2.1) to develop standard operating procedure for 3D culture.

2.6.1 The structure of Alvetex® Scaffolds.

It has previously been demonstrated that it is possible to tailor the morphology of emulsion-templated porous polymers [111]. Once the required morphology and void size is decided it is possible to manufacture the polystyrene polyHIPE scaffolds for a specific void and interconnect size. The chosen void size of 40µm and interconnect size of 13µm (Figure 2.4) are ideal to allow a range of cell types into the scaffold interior. Void size has previously been shown to affect cell adhesion, cell viability [157], ingrowth, distribution [173] and formation of extra-cellular matrix [156]. The open surface provided by Alvetex® Scaffolds allows cells into the interior of the scaffold and helps to address issues of mass transfer concerning exchange of gases, nutrients and waste products. All three of the cell lines I tested (NIH 3T3, MET 4 and TERA2.cl.SP12) demonstrate the ability to infiltrate into the scaffold interior (Figure 2.10 & Figure 2.15). However their size on 2D tissue culture plastic (TCP) greatly differs. The embryonic fibroblast cell line NIH 3T3 are long, thin and stretch up to 100µm on TCP [174] this is clearly visible in Figure 2.12 but they are still able to infiltrate the scaffold. Previous research

has demonstrated that similar cells such as dermal fibroblast grow well in scaffolds with pore sizes ranging from 20-150µm [175] or less than 160µm[158]. When cells are grown on the 3D scaffolds they are no longer stretched as this is often an artefact of the exaggerated cell adherence in 2D culture. 3D cultures allow NIH 3T3 cells to infiltrate the scaffold even though the void size is smaller than the previously suggested optimal void size. The cells are able to stretch across individual voids and therefore maintain their cell morphology (Figure 2.19D). MET 4 cells are half the size of the NIH 3T3 cells and are able to rapidly infiltrate into the scaffold interior whereas TERA2.cl.SP12 which are the smallest cells are able to infiltrate the scaffold but not as rapidly as the MET 4 cell line. This may be due to the tendency of the TERA2.cl.SP12 cells to require cell contact whereas MET 4 cells are more dissociated [165].

The chosen void size allowed all cells types to infiltrate the scaffold but they were not able to consistently fill the entire width of the scaffold and were limited to 140µm into the scaffold (Figure 2.15). As this is the case for all cell types a factor independent of the materials structure and the optimised parameters have an effect on cell penetration. It is most likely due to the scaffold being pinned to the bottom of a 12-well plate using the polystyrene clips. By placing the scaffold at the bottom of the well we are expecting cells in 3D only to be fed from the top surface. This is similar to 2D culture but in 3D there are increased number of cells and further for nutrients and waste product to diffuse. There is also a limited amount of media considering the high cell numbers achieved. The problem of nutrient diffusion is an issue that needs further investigation and may require the scaffold to be presented in a different manner to ensure the scaffold can be filled with cells.

2.6.2 Optimisation of 3D scaffold for specific cell types

From the data presented in this chapter it is possible to suggest parameters for optimal cultures of the three cell lines in 3D. These parameters include initial seeding density, seeding method, and surface treatment. The data presented also suggests possible lengths of experiments when scaffold are presented on the bottom of a 12-well plate. This basic format does not allow for the long-term culture of cells in 3D. The optimal conditions for culture of all three cell lines are presented in Table 2.3 and have been chosen by considering the data presented in this chapter and the properties of each cell line detailed in the aims for this chapter and in Table 2.1.

2.6.3 Optimal culture conditions for the growth of NIH 3T3 cells on Alvetex® Scaffolds.

Attempts to optimise culture surfaces for the growth of NIH 3T3 has been occurring since the early 1970s. Simple experiments by NG Maroudas were able to suggest that 3T3 fibroblasts do not adhere to either rigid hydrophobic or yielding hydrophilic surfaces [176]. From such

observations it suggests that the cell line will require significant optimisation to provide ideal conditions for the 3D culture of NIH 3T3 cells. Firstly I assessed the method of seeding of 3T3 cells. From analysis of the MTS assay in Figure 2.7A there is little difference in cell viability between the cell seeding methods for the two initial seeding densities. However when cell density is assessed, the concentrated seeding method leads to a higher cell density (Figure 2.8A). Due to the need to keep the density of NIH 3T3 cultures low in order to limit the possibilities of contact inhibition it is suggested that NIH 3T3 cells are seeded using the disperse seeding method. This is consistent with findings by Thevenot et al. who test the use of the concentrated seeding method (referred to as surface seeding) for seeding NIH 3T3 cells onto salt-leached poly(lactide co glycolide) degradable porous constructs. They find that a concentrated seeding method leads to limited cell penetration into the scaffold [177].

Initial seeding density also needs to be considered to maintain optimal cultures. It was expected that scaffold containing NIH 3T3 cells would need to be seeded at a low initial seeding density. This would allow cells to be maintained for as long as possible before the effects of contact inhibition. Unexpectedly the lowest seeding density of 0.1×10^6 cells leads to a drop in cell viability between 3 and 6 days. This is also the case for a seeding density of 0.25×10^6 cells (Figure 2.9A). This suggests that the lower seeding densities lead to small colonies of localised cells within the scaffold which are unable to communicate with each other and die within the 3 day period between the two timepoints. Cell death is confirmed by the large error bars at day 6 on both of these seeding densities. Large error bars on cell viability data are indicative of localised areas of cell death.

Interestingly there is also a drop in cell viability between days 3 and 6 in the highest initial seeding density suggesting that the high density leads to too many cells within the scaffolds and cells begin to die due to lack of nutrients or problems of diffusion through a dense cell layer. This is confirmed by the H&E images in Figure 2.10. After 6 days in culture a dense layer of cells is visible at the surface of the scaffold (Figure 2.10B) this prevents the cells that have infiltrated the scaffold interior from receiving nutrients and will also cause a localised build-up of waste products at the surface of the scaffold.

From the data in Figure 2.9 and Figure 2.10 it would suggest that an initial seeding density of 0.5×10^6 cells is ideal for the culture of NIH 3T3 cells. This density allows for cultures to be maintained for at least 7 days. The growth profile comparing 2D and 3D culture also confirm these findings (Figure 2.11A). The 3D cultures of NIH 3T3 cells have a similar growth profile to the 2D cells and the cells remain viable for at least 9 days. Cells were seeded for the growth profile using the concentrated seeding method, if the disperse method had been used the

period of cell viability is likely to be extended. Unlike the 2D cultures which have a rapid drop in cell density at day 5 (Figure 2.12), the 3D cultures maintain their cell density suggesting there is still space within the scaffold for further cell proliferation. Interestingly the cell density profile of the 2D NIH 3T3 cells with the rapid increase between days 1 and 3 is very similar to a profile of cell density for NIH 3T3 cells grown on electrospun membranes [178]. This suggests that electrospun fibres provide a very similar environment to 2D culture.

Surface treatment of the scaffold is necessary to promote attachment of NIH 3T3 cells. This is consistent with previous reports where plasma polymerised acrylic acid coating have been use to promote the adhesion of fibroblasts to cell culture surfaces [179]. The two methods of surface treatment ethanol wetting and oxygen plasma treatment both allow for cell ingrowth and display approximately the same viability after 4 days in culture. However from analysis of the H&E images (Figure 2.19D&E), plasma treatment is preferable for the culture of NIH 3T3 cells as it allows the cells to maintain their fibroblastic morphology as they stretch across the voids of the scaffold. In contrast to this, ethanol treatment leads to rounded cell in the scaffold interior (Figure 2.19E). It is likely that this is due to the plasma treatment presenting a charged functional group to the cell which provides a point for cell adhesion.

In conclusion, for the culture of NIH 3T3 cells on Alvetex® Scaffold, pre-treatment of the scaffold is required using the plasma ashing process at 40 Watts for 5 minutes. Cells should then be added to the scaffold at a density of 0.5 x 10^6 cells per scaffold using the dispersed seeding method. These parameters allow cells to be cultured at a low cell density to prevent contact inhibition and also allow the cells to maintain their spindle-like morphology.

2.6.4 Optimal culture conditions for the growth of MET 4 cells on Alvetex® Scaffolds.

MET 4 cells are the final stage of a metastatic squamous cell carcinoma cell series. They represent the advanced stages of malignant transformation of the epidermis. They have an unlimited ability to proliferate in culture, are anchorage dependent and dissociate from neighbouring cells [165]. Squamous cell carcinomas are a substantial clinical problem and are prolific in transplant patients and immunosuppressed individuals [180, 181]. Commandeur et al. suggest that development of a representative *in vitro* squamous cell carcinoma model system would allow for better understanding of the carcinogenesis mechanism and could be used as a validated pre-screening platform for drugs [182].

To develop a model for *in vitro* testing, a fully optimised system first needs to be produced. A polymeric scaffold such as Alvetex® is well defined and undergoes quality control procedures to ensure consistency; this makes it an ideal scaffold to be used for *in vitro* testing. Proby et al.

describe the MET 4 cells as dissociated without close contacts between neighbouring cells [165]. This accounts for the cells being more viable when grown at low cell density. This is consistent with the histology images in Figure 2.10C&D. After 3 days, the MET 4 cells appear healthier than after 6 days. Considering this data it would suggest that a low cell seeding density would be beneficial for long term cultures of MET4 (Figure 2.9B). Figure 2.7 suggests that where MET 4 cells show no preference towards either seeding technique; however Figure 2.8B highlights that if the dispersed seeding method is used after 7 days there is still a low cell density. This leads to the recommendation of a low seeding density of 0.25×10^6 cells using the dispersed seeding method would be ideal for a squamous cell carcinoma model. This is supported by the growth curve (Figure 2.11B) and the cell density profile for MET 4 cells (Figure 2.13). There is little difference in growth profiles between 2D and 3D cultures but the cell density profile which is calculated from concentrated seeded scaffolds greatly differs with the 3D cultures reaching a high cell density by day 3 which cannot be maintained.

Previous 3D models of squamous cell carcinoma have used collagen gels and are often co-cultures with fibroblast [183, 184]. Although less reproducible than a synthetic scaffold, Nystrom et al. [183] produced a 3D co-culture which recapitulated the *in vivo* pathology of an invasive squamous cell carcinoma. Interestingly cell invasion into the interior of the 3D environment only occurred when the fibroblast cell line was present. This was also the case in the 3D collagen environment created by Borchers et al.[184]. Control gels containing only keratinocyte-like cells led to a dense layer of cells at the surface. Both of the models described are intended for the screening of anti-invasive therapies but are both complex models. A simpler model containing only one cell type may be beneficial for initial drug screening. Alvetex® Scaffolds containing MET 4 cells would be ideal as I have already demonstrated that cells infiltrate into the scaffold interior (Figure 2.15). Further development of the model would be required which would allow cells to penetrate the entire scaffold, this could be achieved by placing the scaffold in a well insert and using an ethanol treatment to ensure hydrophilicity rather than plasma treatment which may promote infiltration into the scaffold interior (Figure 2.19B&C).

In conclusion to produce a functional *in vitro* 3D model of a human squamous cell carcinoma, MET 4 cells would be seeded at a low cell density (0.25×10^6 cells) using the dispersed seeding method onto ethanol-treated scaffolds. This model could be used to test anti-invasive therapies by assessing cell penetration into the scaffold; it could also be combined with the optimised 3D fibroblast model detailed previously to produce a more complex model.

2.6.5 Optimal culture conditions for the growth of TERA2.cl.SP12 cells on Alvetex® Scaffolds.

Stem cell differentiation can be induced in a 2D monolayer culture and does lead to the formation of a range of cell types [185, 186]. Such systems have been suggested as a model to study human embryology and as a source of cells for stem cell therapy [187]. But it has also been recognised that the formation of complex structures is not possible in 2D culture. To overcome this issue embryonic stem cells are often removed from their feeder layer and grown in suspension to form embryoid bodies (EBs). This allows the cells to differentiate into all three germ layers[188] but EBs are known to have many disadvantages when studying stem cell differentiation. These include methods which are not suitable for producing cells on a large scale, limited control of cell aggregation and cell density [189] which leads to low efficiency in EB formation and finally during differentiation of EBs to specific lineages such as ectodermal differentiation the EB forms a layer of visceral endoderm at the periphery [190]. *In vivo* this is a source of patterning and differentiation signalling but for experiments looking to control embryonic stem cell differentiation it is necessary to eliminate early patterning information [191].

There are many examples of the use of polymeric scaffolds for the culture of stem cells. Scaffolds allow for the formation of complex 3D tissues and unlike EBs they are able to provide physical cues for cell orientation and spreading and also provide space for remodelling of structures [192]. This has been demonstrated by Levenberg et al. who used biodegradable salt-leached PLGA/PLLA sponges to provide a structure for the culture of H9 ES cells taken from embryoid bodies [3]. This approach leads to the formation of complex structures but it does not provide the well-defined conditions for the maintenance of stem cell phenotype in 3D. In the experiments I have assessed the well-defined conditions to produce a stem cell model which can maintain stem cell phenotype but can also be used for differentiation studies.

Initial cell seeding density was extremely important when culturing TERA2.cl.SP12 cells on the polystyrene scaffolds this is because in 2D the cells must be maintained at high confluency to maintain their stem cell phenotype but also when cells are differentiated towards neuronal lineages, a high cell density may influence the degree of differentiation. Tonge and Andrews demonstrated that a high seeding density promotes differentiation using a cell density gradient monolayer culture [193]. This culture involved seeding a concentrated area of cells at the centre of the well plate; this is similar to the concentrated seeding technique on Alvetex® Scaffolds. Initial cell viability data suggested that there was little difference between seeding densities and seeding techniques for TERA2.cl.SP12 cells on to the scaffolds (Figure 2.7C). In contrast, analysis of density displayed a significant difference in cell density between the two

seeding methods (Figure 2.8C). This combined with the immunohistochemical analysis in Figure 2.20 leads to the recommendation that TERA2.cl.SP12 cells should be seeded using the concentrated seeding method. This leads to a high cell density and more Oct 4 positive cells. Unfortunately this seeding technique does not lead to uniform cell coverage of the entire scaffold surface. Figure 2.6 demonstrates the similarity between this concentrated seeding technique and seeding of EC cells by Tonge and Andrews to promote neuronal differentiation.

From Figure 2.9C it would suggest that a high initial cell seeding density is required for the growth of TERA2.cl.SP12 cells. For other methods of 3D culture such as fibrin scaffold it has been suggested that a density of 0.75×10^6 stem cells per well is ideal as it leads to increased viability, cell infiltration and differentiation towards neuronal lineages [172]. From the cell viability data in Figure 2.8C either the 0.5×10^6 or 0.75×10^6 cells per scaffold would be suitable. Both seeding densities lead to an increase in cell viability between days 3 and 6 (Figure 2.9C). However, if cells are seeded at the higher seeding density then there is a build-up of cells at the scaffold surface which will compromise the cells which have infiltrated the scaffold (Figure 2.10F).

TERA2.cl.SP12 cells are the only cell line that shows a significantly different growth profile between 2D and 3D culture (Figure 2.11C). When grown in 3D, the EC cells take up to 5 days before they begin to proliferate on the scaffold whereas in 2D the cells proliferate immediately. This suggests that TERA2.cl.SP12 cells are the only cell line which requires significant adaptation to return to a 3D environment. This is consistent with the cell density profiles (Figure 2.14). Cell density rapidly increases in 2D but the 3D cell density does not increase until after 5 days. This delay in cell proliferation also coincides with slow infiltration into the scaffold when compared with the other two cell lines. At day 5, TERA2.cl.SP12 cells have only reached 75µm into the scaffold and they do not reach the 140µm limit (Figure 2.15C).

Surface treatment of the Alvetex® Scaffold is also necessary for the attachment of pluripotent stem cells. A range of treatments were tested to encourage the attachment of TERA2.cl.SP12 to the scaffold. Figure 2.17A highlights the need for surface treatment to render the scaffold hydrophilic. Ethanol treatment shows some benefit to cell attachment and penetration but is still limited for this cell line (Figure 2.17B). Ethanol treatment after plasma treatment also affects the cell coverage (Figure 2.17D&F). Previous work has already been undertaken to determine parameters suitable for the polystyrene scaffold membranes to prevent charring of the scaffold and to ensure even surface coverage [194]. TERA2.cl.SP12 cells were tested on two types of plasma treated scaffold, one that had been treated for a prolonged period at a

low power (10W for 30 minutes) and one at a high power for a short time period (40W for 5 minutes). Previous studies suggest that the length of time for oxygen plasma surface modification affects parameters such as hydrophilicity, total surface energy and surface roughness. These in turn affect proliferation and differentiation of cells. Yildirim et al. found that a plasma modification time of 3 minutes more than doubled the number of osteoblast cells attached to a polycaprolactone surface compared to other lengths of treatment between 30 seconds and 7 minutes [195]. The 3 minutes of treatment with oxygen plasma also affects the differentiation of osteoblast cells. It effects calcium mineralisation and alkaline phosphatase activity even after 21 days in culture when compared to unmodified samples. Histological analysis reveals little difference between the two types of surface treatment with both treatments allowing cells into the centre of the scaffold and to infiltrate the entire 200µm of scaffold (Figure 2.17C&E). Quantitative analysis of the images reveals that the shorter plasma treatment appears to promote infiltration into the scaffold when compared to the longer treatment at a low power. Interestingly the shorter plasma treatment also appears to be more affected by a post treatment ethanol sterilisation step. Due to there being no significant difference in the degrees of cell penetration between the two treatments it is advised that the shorter plasma modification without subsequent ethanol sterilisation to be used to reduce discrepancies between large numbers of scaffold that may be used for further experiments.

Analysis of a wide range of optimisation experiments for TERA2.cl.SP12 cells has made it possible to recommend cell culture parameters which will ensure the cells are maintained at a high confluency to maintain stem cell phenotype and also to allow for cell penetration into scaffold. The cells should be seeded at an initial cell density of 0.5×10^6 cells using the concentrated seeding technique. The scaffold needs to be pre-treated using plasma modification at 40W for 5 minutes. Cultures should also be grown for at least 4 days to allow the cells to adapt to the 3D microenvironment.

2.7 Conclusions

The 3D environment provided by the polystyrene scaffold has been fully optimised for the range of cell lines. Comprehensive optimisation of the scaffold for the three cell lines takes into account the properties in Table 2.1 and has led to the recommendation of culture conditions summarised in Table 2.3. These conditions will allow for the culture of cells in three dimensions without the need for the daily monitoring of cultures using phase microscopy. The optimised 3D models that have been produced will now be useful for further experimentation. The fibroblast model could be used to develop a 3D epidermal model for the skin penetration and irritation testing or as the basis of a range of co-culture models. This could also include combining the optimised NIH 3T3 cultures with 3D cultures of the MET 4 cell line. This has the potential to lead to a model of a squamous cell carcinoma that could eventually be used to test anti-invasive agents. Finally the optimised pluripotent stem cell model will be used to assess the affect the 3D environment has on differentiation of TERA2.cl.SP12 cells.

Demonstrating that a 3D scaffold is adaptable for a range of cell lines is key to encouraging the widespread adoption of the system in cell culture laboratories. However for cells that require a complex *in vitro* environment such as primary cells and stem cells further optimisation is required. I have already demonstrated that it is possible to maintain stem cell phenotype in the 3D environment. For homogenous differentiation across the layer of tissue it is necessary to ensure a homogenous cell culture environment surrounding the scaffold. The following chapter addresses this requirement and demonstrates opportunities for scale up of 3D cultures.

Cell Line	Properties to consider when optimising conditions for 3D cell culture	Seeding Density	Seeding Method	Surface Treatment	Optimal conditions
NIH 3T3	• Contact inhibited • Should not be allowed to become confluent.	• 0.5 x 10^6 cells per scaffold. • High cell densities lead to high confluency within the scaffold	• Dispersed • Maintain low cell density	• Plasma treatment • Allow cells to infiltrate into the scaffold interior	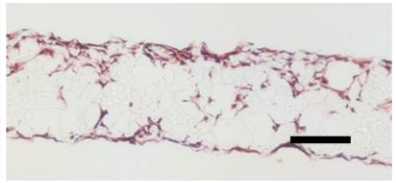
MET 4	• Highly invasive • Rapid doubling time .	• 0.25 x 10^6 cells per scaffold. • A lower seeding allows for longer term cultures.	• Dispersed	• Ethanol • Prevent cells from overgrowing	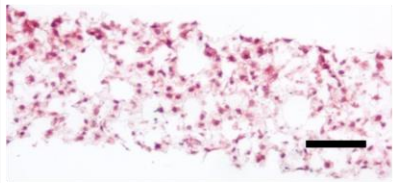
TERA2.cl. SP12	• Must be cultured at high confluency to maintain stem cell phenotype.	• 0.5 x 10^6 cells per scaffold. •High confluency helps to maintain pluripotency	• Concentrated • Maintains pluripotency	• Plasma treatment – 40W 5 min • Allows cells to adhere to scaffold	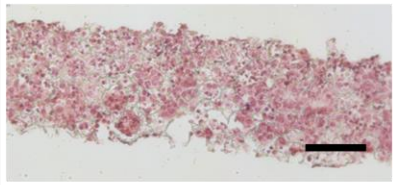

Table 2.3 Optimised parameters for successful 3D culture of NIH 3T3, MET 4, and TERA2.cl.SP12 cells. Scale bars: 100µm

3 How presentation of the scaffold influences stem cell metabolism and differentiation.

3.1 Introduction

During optimisation of the scaffold for cell growth it became apparent that there are many more parameters that need to be considered during culture in 3D in comparison to standard 2D culture. These include the mass diffusion of nutrients and waste products which are not normally considered in monolayer cultures. This parameter becomes important when large slabs of densely packed cells are produced during 3D cell cultures. It is necessary to provide sufficient cell culture media to maintain high number of cells throughout a scaffold construct. It is not feasible to thoroughly redesign current cell cultureware for use with 3D cultures. However simple modification of existing systems provides a viable option for producing optimised 3D cultures.

Standard cell cultures often utilise high glucose (4.5g/L) DMEM supplemented with L-glutamine. The excess glucose concentration is both a source of carbon and a source of energy for cells in culture. Due to the artificial nature of the cell culture environment there is an inefficient union between glycolysis and the tricaboxylic acid (TCA) cycle. This allows lactic acid to rapidly accumulate in the culture medium [196]. Recently the necessity for a more realistic 3D culture environment has increased leading to an even greater demand on cell culture media. Three dimensional cultures have been shown to display differing metabolic activity to two-dimensional (2D) cultures, more specifically an increase in glycolysis and lactic acid production [197]. Lactic acid accumulation on its own is toxic to mammalian cells and the change in pH associated with its production further limits glucose metabolism [198]. On top of these issues it is also necessary to consider cell migration and cell colonisation of the scaffold. Such factors are not normally considered during standard 2D cultures.

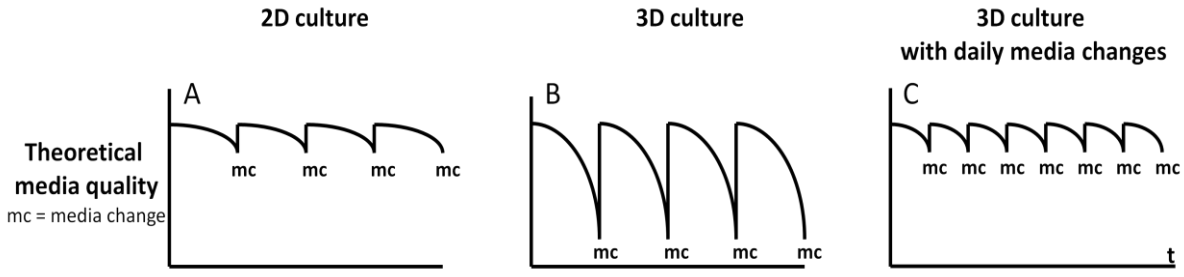

Figure 3.1 Theoretical media quality profiles for 2D and 3D cell culture. Cell culture media profile for 2D culture **(A)** and during standard 3D culture **(B)** note the rapid drop in media quality in 3D cultures. This is usually overcome by frequent possibly daily media changes **(C)**. The regular disturbance of cells can lead to cell detachment from the scaffold and is detrimental to cell health as it removes cell secreted agents from the surrounding area.

Many currently available commercial medium formulations are not able to support the number of cells achieved during 3D cell culture and the number of cells attained in a tissue-engineered construct is dependent on the nutritional value of the media. Many batch-fed systems such as standard 2D culture and 3D scaffold cultures which use commercially available cell culture media are only able to support approximately 1-5 million cells/ml [199]. During 2D cell culture, media is changed every 2-3 days and over this time there is a gradual decrease in media quality as glucose is consumed and lactic acid is produced. A theoretical media quality profile for such cultures is detailed in Figure 3.1A. For 3D cell culture using scaffolds or other methods such as hydrogels, there are more cells per millilitre of media. This leads to a more severe drop in media quality than in monolayer cultures (Figure 3.1B). It is possible to overcome this decrease in media quality by changing media daily. This produces a media quality profile similar to that shown in Figure 3.1C. This method is most frequently used for scaffold cultures as it is the simplest method for ensuring a regular high media quality. The method detailed in Figure 3.1C maintains media quality but also regularly disturbs the cell layer. Regular removal of media surrounding the scaffolds can lead to cell detachment and can prevent cells from producing a dense cell layer within the scaffolds.

3.1.1 Glucose and lactic acid metabolism

Glucose and lactic acid metabolism are closely related to cell density: it is difficult to completely fill a scaffold with cells if media quality is not kept at a constant high quality [200]. A lactic acid concentration of above 20mM inhibits cell growth, when accompanied with the drop in pH, this effect had been observed in a range of cells including mouse embryonic stem cells on microcarriers [201] and haematopoietic cells in 2D [202]. However when the increase in lactic acid concentration is accompanied by a controlled pH there is a lesser effect on cell proliferation [202] – this suggests that the media used for 3D culture may require complex buffering capabilities. Interestingly Zhu et al. have recently suggested that adipose-derived stem cells grown in three dimensions are no longer inhibited by a 20mM concentration of lactic acid this was compared with the 2D counterparts which were cultured under standard conditions and lactic acid concentrations did not exceed 20mM [5].

Other suggestions to maintain cell viability in 3D have been the additional supplementation of excess glucose to cell culture media. Heywood et al. have used what they consider an exceptionally high concentration of glucose (20.4mM = 3.7g/L) to increase cell viability of chondrocytes in alginate constructs [203]. However this in turn may leads to high lactic acid concentrations which further inhibit cell viability and affects matrix production. Razaq et al. demonstrated that a drop in pH from pH 7.2 to pH 6.4 (which is often caused by the build-up of lactic acid in cultures) can lead to a 50% decrease in matrix production in cells isolated from

bovine nucleus pulposus [204]. The production of extracellular matrix proteins is required for the infiltration of cells into 3D constructs [205].

Many biopharmaceutical companies routinely monitor glucose consumption and lactate production in order to ensure the viability of cells in cultures. This is due to both lactate and glucose being chemically stable in cell culture media and the concentration of both metabolites can be simply and reliably monitored. By monitoring cell growth curves in comparison with glucose consumption and lactic acid production it is possible to optimise the cell growth media and the scaffold environment for optimal 3D culture using porous scaffolds. By optimising and understanding the metabolism of cells in tissue-engineered constructs it will enable a greater cell yield which in turn will provide successful tissue models for research analysis using a wide range of techniques and will prevent the loss off function that often occurs when cells are transplanted *in vivo* [206].

3.1.2 Cell migration through 3D constructs

In order to produce a functional tissue *in vitro*, it is necessary for cells to form contacts and be able to signal with neighbouring cells. While doing this they also need to maintain metabolic activity even in areas that are far from the scaffold/media interface. In Alvetex® scaffolds cells are never more than 200µm from this interface which helps to maintain cell viability. Providing cells in 3D constructs with nutrients and channels for the removal of waste products ensures that cells are capable of synthesising and maintaining an extracellular matrix. Unfortunately the uppermost layers of cells in porous scaffolds tend to consume most of the available oxygen and nutrients; this in turn limits diffusion of media throughout the entire scaffold. A lack of diffusion of both nutrients to the cells and waste products away from the cells and 3D constructs limits the migration of pioneering cells into the scaffold interior and impacts on the length of time cells can be maintained optimally in 3D. The perfusion of nutrients and oxygen through scaffolds is a problem observed in all types of tissue engineering constructs [207] and is outlined schematically in Figure 3.2. This problem is directly applicable to the porous Alvetex® scaffolds used in this study. As described in the previous Chapter, Alvetex® is 90% porous and has an open pore structure that will allow the movement of cells and nutrient throughout the 200µm thick scaffold (Figure 3.2A). When cells are seeded onto the surface of the scaffold using the concentrated seeding method, which is recommended for use with stem cells (Table 2.3), they begin to produce the dense cell layer at the surface of the scaffold (Figure 3.2B). Initially this has very little effect on the diffusion of nutrients through the scaffold as it is often only one cell thick but as the culture progresses more cells build up and this starts to limit the penetration depth for nutrient diffusion (D_p) (Figure 3.2C). As more cells build up in the top half of the scaffold they put down more extra-cellular matrix (ECM) proteins and this cause an even greater decrease in D_p. Even-

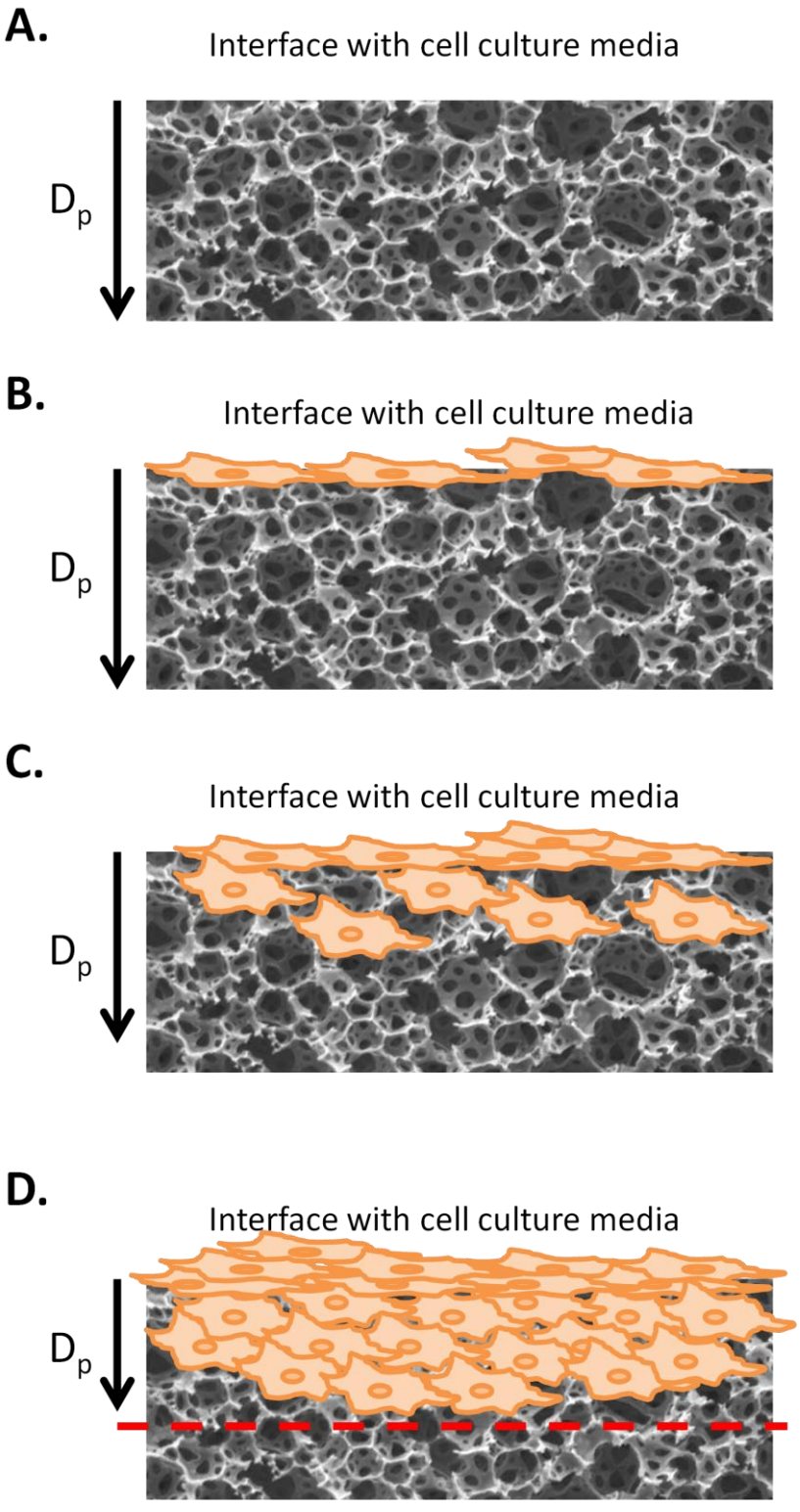

Figure 3.2 Nutrient diffusion through cell culture scaffolds. A scaffold with an open pore structure **(A)** allows for the diffusion of nutrients throughout. The distance nutrients and oxygen can pass through the scaffold is known as the penetration depth (D_p). When cells are seeded onto scaffold **(B)** initially they have little effect on the passage of oxygen, nutrients (e.g. glucose) and waste products through the scaffold. As pioneering cells begin proliferate and are able to migrate through the scaffold **(C)** they put down ECM proteins causing a decrease in D_p. Diffusion through the dense cell layer is limited preventing pioneering cells from colonising the entire width on the scaffold **(D).** This also can potentially lead to problems of diffusion of waste products away from the scaffold.

-tually this lack of diffusion of nutrients and waste products may prevent pioneering cells from colonising the entire width of the scaffold (Figure 3.2D).

Bokhari et al. demonstrated that the seeding techniques chosen for 3D cultures also affect mass transfer of nutrients. At early timepoints, osteoblast cells were observed in the scaffold interior but the cells preferentially grow at the surface at longer timepoints, due to this being where nutrient concentrations are high [160]. It is possible to overcome problems with diffusion through scaffolds by determining the ideal presentation of the scaffold to ensure cells are in close contact with the media. This ensures efficient mass diffusion of nutrients and waste products. Gstraunthaler et al. have previously demonstrated that media volume during standard 2D cultures influences cell metabolic rates and the levels of enzyme activity. These differences occur due to changes in nutrient supply and oxygenation and have been shown to influence the biochemistry and metabolic differentiation of renal epithelial cells from pigs and possums [208]. Exceptionally high volumes of culture media are also an option to support tissue development in engineered constructs. Heywood et al. used chondrocyte seeded alginate scaffolds to study cell viability across the entire section of a construct. It was found that homogeneity could only be achieved when the media volume reached 6.4ml per 1 x 10^6 cells [209] Although this method was effective and involved placing the constructs in 85mm Petri dishes it does not take into account the diffusion of waste products away from the immediate areas surrounding the constructs.

An obvious method to increase cellular activity in 3D constructs is the use of media perfusion systems. Such systems for use with 3D porous cellular constructs have been previously described by Cartmell et al. but they require very precise control of flow rate: High flow rates of 1ml/min resulted in substantial death of MC3T3-E1 osteoblast-like cells [210]. Unfortunately this may not be an option for the culture of stem cell in 3D as it is already well established that fluid shear stress caused by the flow of medium affects the differentiation of embryonic stem cells [211-214]. Interestingly diffusion through the cell layers during 3D cell culture also affects cell differentiation. A dense cell layer prevents molecules such as cytokines and signalling proteins from diffusing uniformly to all cells within the culture. Raghavan et al. investigated whether the rate at which growth factors diffused to cells in extracellular matrix microgels affects tubulogenesis of kidney cells rather than the dimensionality of the matrix itself. Cellular responses such as the activation of ERK (extracellular-signal-related kinase), were dominated by the stimulation rate but other responses including myosin II light-chain (MLC) activation leading to tubulogenesis were dominated by dimensionality [215].

To produce optimal cultures for the differentiation of stem cells in 3D it is necessary to produce cell-filled scaffolds where cells have easy access to nutrients. This needs to be teamed with rapid

diffusion of waste products away from the engineered construct. This is necessary as the build up of waste products such as lactic acid can lead to localised areas of low pH. Such changes in pH and the build-up of metabolites cause changes to the cell microenvironment. This is known to affect both differentiation and maintenance of stem cell phenotype of human embryonic stem cells [216].

3.2 Aims of Chapter

Using the Alvetex® Scaffold, the effect of media volume and how scaffold presentation affect on cell metabolism is investigated and its influence of cell viability, and overall cell number in 3D is assessed. In doing this optimisation, conditions for homogeneous cell distribution throughout the porous scaffold are determined and the development of a system to allow for minimal disturbance of cells in tissue engineered matrices. Using this information and the conditions established in the previous Chapter it will be possible to develop a model for the differentiation of TERA2.cl.SP12 cells in 3D towards neural derivatives in particular.

3.3 Objectives

1. Monitor the quality of cell culture media to determine the ideal time frame for media changes
2. To assess how scaffold presentation affects cell viability and infiltration into the scaffold interior
3. Assess the requirement for further modifications of scaffold presentation to produce a dense layer of homogenous tissue *in vitro*.
4. Using the optimised conditions for the growth of TERA2.cl.SP12 and the optimal scaffold presentation, develop a model for the differentiation of stem cells in 3D.

3.4 Materials and Methods

3.4.1 Cell culture

The pluripotent embryonal carcinoma cell line TERA2.cl.SP12 was cultured as described in Chapter 2. Cells were maintained in T75 flasks (BD Bioscience) in high glucose Dulbecco's Modified Eagle Medium (DMEM) supplemented with 10% fetal calf serum (DMEM and FCS Invitrogen), 2mM L-glutamine and penicillin/streptomycin. Cultures were passaged by rolling acid washed glass beads over the confluent cultures. All cultures were placed in a humidified incubator at 37°C and 5% CO_2

3.4.2 Culture of stem cells in 3D

3D cultures of TERA2.cl.SP12 cells were established using the optimised conditions described in the previous Chapter. Prior to cell seeding Alvetex® Scaffolds were washed with 70% ethanol, left to dry overnight and plasma treated at 40W for 5 minutes. 0.5 x10^6 cells were seeded onto each scaffold using the concentrated seeding method.

3.4.3 Inducing stem cell differentiation in 3D

The 3D stem cell cultures were induced to differentiate using either 1µM *all-trans* retinoic acid (ATRA) (Sigma) or 1µM photostable synthetic retinoid EC23 (Reinnervate Ltd). Control cultures contained equal volumes of dimethyl sulfoxide (DMSO). The required retinoid or DMSO control was added to the cultures four days after initial seeding of the scaffolds, during the first media change. This allows time for the 3D cultures to become well-established and therefore less susceptible to the toxic effects of retinoids. For the varying of lactate concentrations, cultures were supplemented with sodium L- lactate (Sigma-Aldrich, UK). This was to imitate a build-up of lactate ions in the cultures. This method has previously been described by both Patel et al. [202] and Wohnsland et al.[217] Sodium lactate was made as a 2M stock solution in sterile dH_2O and filter sterilised before addition of the appropriate amount of stock solution to each culture.

3.4.4 Scaffold presentation

In contrast to the previous Chapter, scaffolds were presented in a range of formats in an attempt to enhance the viability of 3D cultures. Scaffolds were presented either on the bottom of a 12-well plate or in well inserts suspended in either a 6-well plate or a deep well Petri dish. These formats are detailed in Figure 3.3. The deep well Petri dish allows for a large reservoir of media to support 3 inserts in one dish. The inserts used are a standard well inserts with closed walls. The inserts were later redesigned to incorporate windows in the walls of the insert. The windowed open wall inserts require more media. The amounts of media required for each scaffold format is detailed in Table 3.1

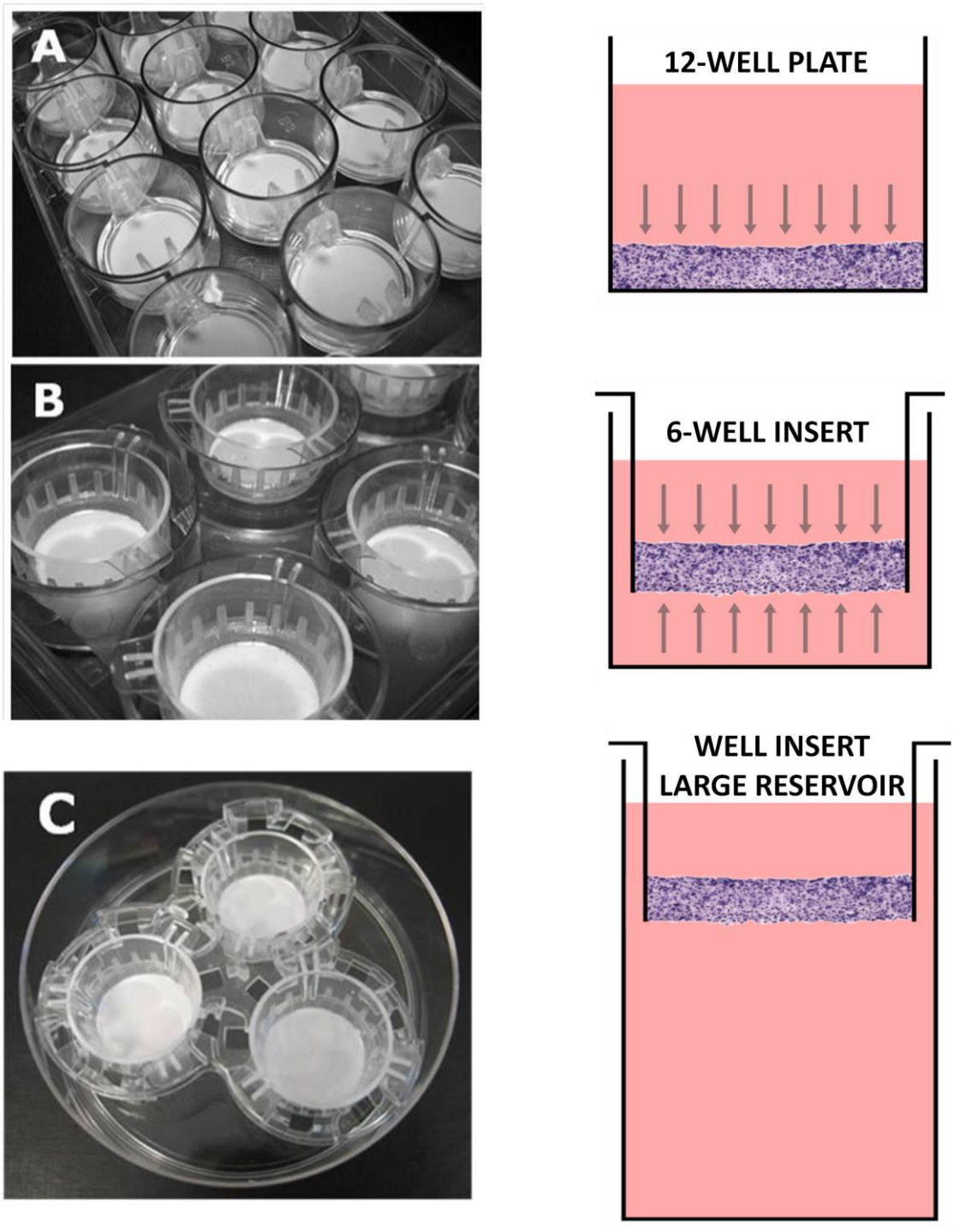

Figure 3.3 Alternative formats for the Alvetex® Scaffold to increase cell penetration: In the 12-well format, scaffolds sit at the bottom of wells secured in place by a polystyrene clip **(A).** Alvetex® Scaffold placed into closed-wall inserts which fit in a 6-well plate **(B)** allow cells within the scaffold more access to the cell culture media. Arrows indicate that is possible for the cells to feed from both above and below in inserts. Alternatively the inserts can be placed in a large reservoir Petri dish **(C)** allowing three inserts per dish and a larger volume of media per scaffold which is ideal for long term experiments.

Scaffold Format	Amount of media required
12-well plate	4 ml
6-well insert	10 ml
Standard closed wall insert in large reservoir Petri dish	50 ml
Windowed open wall insert in large reservoir Petri dish	75 ml

Table 3.1 Media required for different scaffold presentations

3.4.5 Testing media quality

Cells were grown in scaffolds for 5 days with no media changes. Samples of media were taken from around the scaffold at the beginning of the experiment and every 24 hours thereafter. For scaffolds presented in inserts, two media samples were taken per timepoint, one from inside the insert and one from the surrounding media (Figure 3.9). Each sample was subsequently tested to determine glucose concentration, lactic acid concentration and pH.

3.4.5.1 Glucose consumption

Glucose concentration of cell culture media was determined using the GlucCell® glucose monitoring system (Bellco Glass Inc., Vineland, NJ) according to the manufacturer's protocol. Media samples of 10µl were taken from the cultures at each time point to allow for repeats. Samples were tested by loading 2µl of media onto the glucose testing strips. This system has previously been optimised for use with cell culture media containing FBS [218].

3.4.5.2 Lactic acid production

Lactate production in cell culture media was assessed using a commercially available kit for the detection of L-lactic acid (Megazyme International Ireland Ltd) as previously described by Klawitter et al.[219] Quantification of lactic acid requires two enzyme reactions. One catalysed by L-lactate dehydrogenase where the lactic acid if oxidised to pyruvate by nicotinamide-adenine dinucleotide (NAD+). The second reaction converts pyruvate to D-alanine and 2 oxoglutarate with the enzyme D-glutamate-pyruvate transaminase. The amount of NADH formed in the two reactions is directly proportional to the amount of L-lactic acid present. NADH is measured by the increase in absorbance at 340nm.

The manufacturer modified microtitre plate protocol was used and the absorbance of each sample was read using a Biotek ELx800 plate reader. The concentration of lactate was calculated using the following equation:

$$c = \frac{V \times MW}{\varepsilon \times d \times v} \times \Delta A_{L-lactic\ acid}$$

Where: V = final volume (ml), MW = molecular weight of L-lactic acid = 90.1g/mol, ε = extinction coefficient of NADH at 340nm = 6300 l x mol^{-1} x cm^{-1}, d = light path (cm), v = sample volume (ml).

3.4.5.3 Assessing pH of cell culture media.

The pH of the cell culture media was assessed by directly testing the cell culture media in situ. Using a Hanna HI 2212 pH meter and a microprobe which was briefly sterilised by spraying with 70% ethanol, pH was measured every 24 hours.

3.4.6 Determination of cell viability

Cell viability was determined using an MTT assay which is more closely based on the assay described by Mossmann [220] than the MTS assay [164]. This assay is similar to the MTS assay described in the previous chapter but involves a two-step process to lyse cells and dissolve the substrate.

Whole Alvetex® Scaffolds were removed from inserts and briefly washed in PBS without calcium and magnesium before being placed in the bottom of a 12-well plate. 1ml of MTT solution was added to each scaffold and one control scaffold containing no cells. MTT solution consists of 1mg/ml (3-(4,5-dimethylthiazol-2-yl)-2,5 diphenyl tetrazolium bromide (MTT substrate) dissolved in phenol-red free DMEM (Sigma Aldrich UK). Scaffolds were incubated at 37°C and 5% CO_2 in the dark for 1 hour. After incubation, the purple MTT substrate is clearly visible in the areas of the scaffold that contain cells. The MTT solution was removed and the insoluble formazan salt solubilised using 1ml of acidified isopropanol (1µl/ml conc. hydrochloric acid) (Sigma Aldrich UK). Scaffolds were agitated for 10 minutes on a rotary plate shaker at 100rpm. The resulting isopropanol solution was diluted 1:10 and 200µl of the solution was placed into wells of a 96-well plate. The absorbance of each sample was read at 570nm using a Biotek ELx800 absorbance microplate reader.

3.4.7 Determination of cell number

Cell number was determined using the commercially available Quant-iT™ PicoGreen® dsDNA Kit (Invitrogen) as originally described by Rye et al. [221] and suggested for 3D culture by Ng et al. [222] The PicoGreen assay tests for the amount of double standard DNA (dsDNA) and is less sensitive to single stranded DNA and RNA than other types of stains such as DAPI, Hoescht and ethidium bromide. The amount of dsDNA can be related to a standard curve of cell number. The standard curve was produced by trypsinising TERA2.cl.SP12 cells from T75 flasks and determining cell number using a Trypan blue assay and a haemocytometer. Suitable numbers of cells were centrifuged at 1000rpm for 3 minutes, the supernatant was removed and 600µl of PicoGreen lysis buffer was used to resuspend the cell pellet. PicoGreen lysis buffer is an RNase-free buffer

containing 10mM Tris pH 8.0, 1mM EDTA and 0.2% (v/v) Triton-X100. Cell samples were stored at -80°C.

Cells within scaffolds were lysed by cutting the scaffold into 8 equal segments and placing in an RNase-free microcentrifuge tube prior to the addition of 600µl of PicoGreen lysis buffer. Samples were then stored at -80°C to aid in cell lysis. Prior to quantification all samples were thawed on ice and homogenised using a 1ml syringe and a 21-gauge needle. Samples and standards were diluted 1:10 using the PicoGreen lysis buffer. 100µl of each sample was added to wells of a black-walled microtitre 96-well plate prior to the addition of 100µl of the PicoGreen reagent. PicoGreen reagent consists of a 1:200 dilution of the concentrated DMSO reagent in TE buffer (10mM Tris-HCl, 1mM EDTA, pH 7.5) The plate was incubated at room temperature for 5 minutes prior to measuring the fluorescence at excitation and emission wavelengths of 460nm and 540nm, respectively using a Biotek FLx800 fluorescence microplate reader. Cell number was calculated using a standard curve prepared in the same manner. The fluorescence is directly proportional to cell number (Figure 3.4).

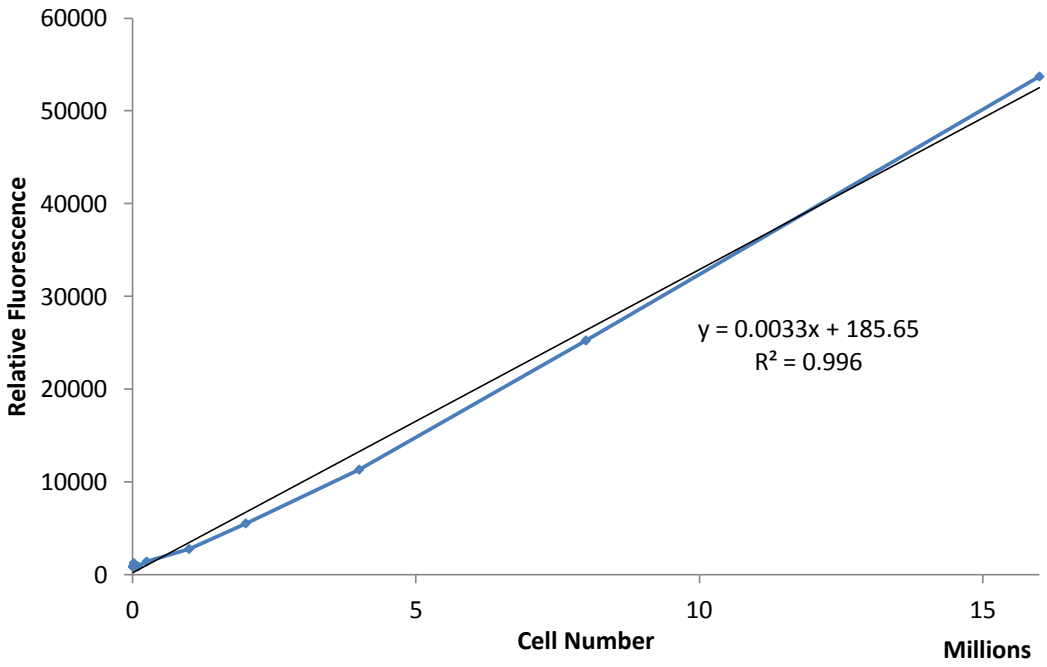

Figure 3.4 Standard curve to assess cell number using the PicoGreen assay. TERA2.cl.SP12 cells were cultured in T75 flasks then trysinised, counted using a haemocytometer and then appropriate numbers of cells were lysed to produce a standard curve.

Using the assessment of dsDNA to determine cell number is particularly useful in 3D constructs. Other simple methods of assessing cell viability which can be related to cell number such as the MTT & MTS assay are reliant on cell metabolism. However, metabolism can differ between the 2D and 3D environment making it difficult to produce a standard of curve of cell number. The

amount of dsDNA does not vary depending on culture conditions and therefore can be used as a method for calculating cell number within 3D constructs.

3.4.8 Immunofluorescence staining of paraffin-embedded scaffold sections

Scaffolds were fixed in PFA, embedded and sectioned. Slides containing sections were de-waxed and rehydrated as previously described. Antigen retrieval was performed by microwaving the slides for 3 x 2 min at 800W in 10mM citrate buffer at pH6 (10x stock: 19.2g anhydrous citric acid in 1L dH_2O). Slides were left to stand in the warm citrate buffer for 20 minutes and subsequently incubated in permeabilisation solution (0.1% (v/v) Triton X-100 in PBS) for 15 minutes. Sections were blocked using blocking buffer (0.1% Tween-20, and 1% normal goat serum in PBS) for 30 minutes prior to the addition of primary antibodies diluted in blocking buffer (see Table 3.2). Sections were incubated at 4°C in a humidified chamber overnight before washing for 3 x 10 minutes in blocking buffer on a rotator plate at 40rpm. Fluorescent-conjugated secondary antibodies were diluted in blocking buffer with Hoescht 33342 to stain nuclei (Table 3.2) and incubated on the sections for 1 hour at room temperature in the dark. Immuno-stained scaffolds were washed as before for 3 x 10 minutes and mounting using Vectashield mounting media (Vector Labs). Coverslips were attached using nail varnish. The slides were examined using fluorescence microscopy. All images were captured using the Nikon Diaphoto 300 with connected digital camera and ACT1 image capture software. Negative controls were produced by following the protocol but without the primary antibody (Figure 3.5).

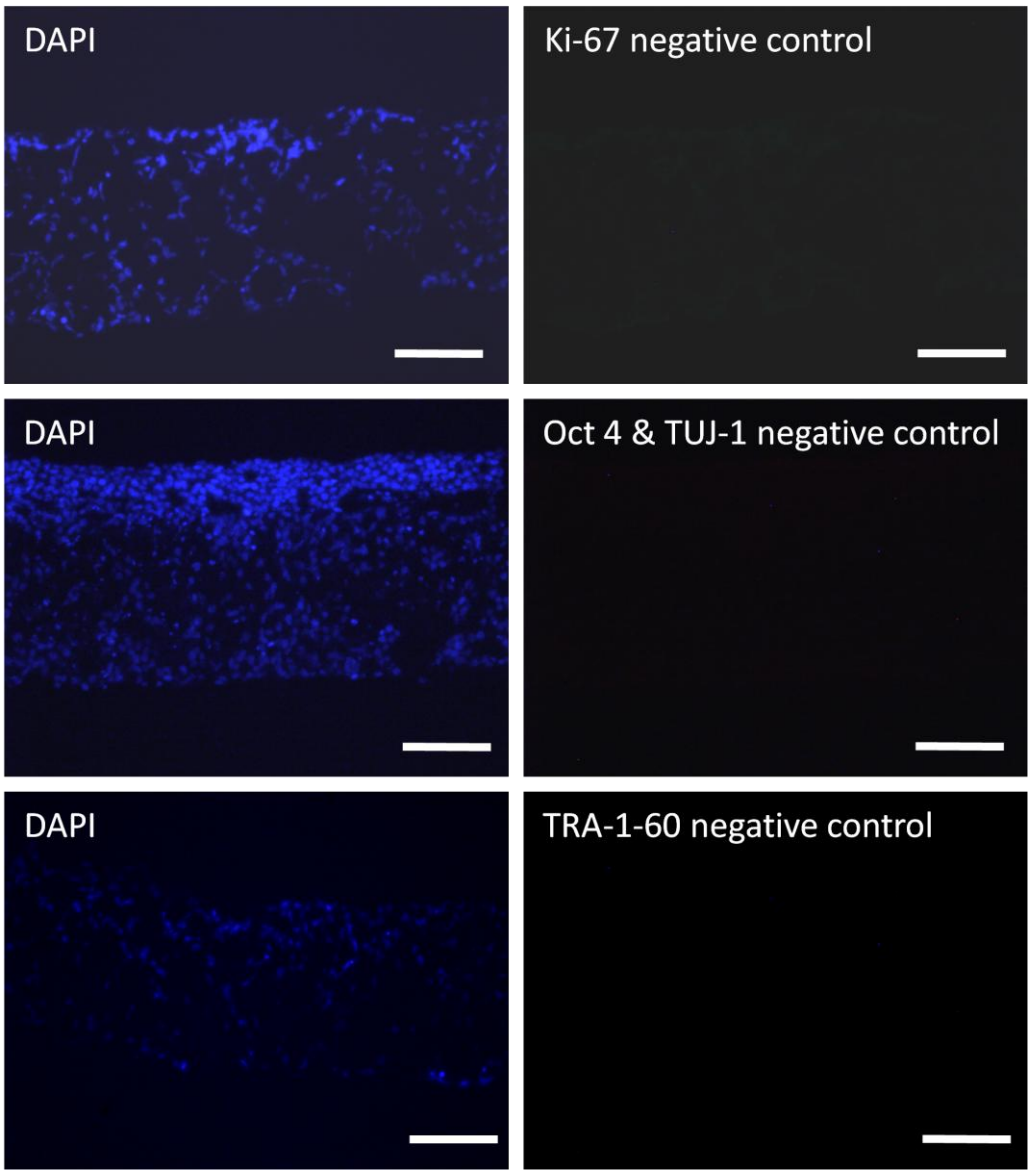

Figure 3.5 Negative control for Ki-67, TUJ-1 and TRA-1-60 staining on Alvetex® Scaffold. The standard immunohistochemistry protocol was performed without the addition of the primary antibody, to demonstrate the degree of background staining. Scale bar=100µm

Primary Antibody	Supplier	Dilution	Secondary Antibody	Supplier	Dilution
Ki-67 Mouse Monoclonal	Leica (NCL-Ki67-MM1) http://www.leicabiosystems.com/ihc-ish/novocastra-reagents/primary-antibodies/	1:100	Goat anti-mouse IgG (H+L) Alexafluor 488	Invitrogen (A1101) http://www.lifetechnologies.com	1:600
Oct 4 Rabbit polyclonal	Abcam (ab19857) http://www.abcam.com/	1:250	Cy3-AffiniPure Donkey Anti-Rabbit IgG (H+L)	Jackson ImmunoResearch http://www.jacksonimmuno.com/	1:600
Rabbit Polyclonal neuronal Class III β tubulin (TuJ-1)	Cambridge Bioscience (PRB-435P-100) http://www.bioscience.co.uk	1:600	Cy3-AffiniPure Donkey Anti-Rabbit IgG (H+L)	Jackson ImmunoResearch http://www.jacksonimmuno.com/	1:600
TRA-1-60 Mouse IgM	P Andrews, University of Sheffield	1:10	Anti-Mouse IgM (μ-chain specific)–FITC antibody produced in goat	Sigma-Aldrich (F9259) http://www.sigmaaldrich.com	1:100
Nuclear stain			Hoescht 33342	Molecular Probes (H3570) http://www.lifetechnologies.com	1:1000

Table 3.2 Antibody dilutions for immunostaining of scaffold sections

3.4.9 Cell retrieval from Alvetex® Scaffold

Cells were retrieved from the Alvetex® Scaffold in order to undergo further processing. Scaffolds were removed from inserts and washed briefly in PBS without calcium and magnesium before being cut into 8 equal segments. The scaffold segments were placed in a 3ml screw cap cryovial containing 2ml of trypsin EDTA. The tubes were incubated at 37°C and 5% CO_2 for 5 minutes while turning on a rotor. After incubation the 2ml of trypsin EDTA was removed and neutralised by placing into a centrifuge tube containing 5ml of DMEM containing 10% FBS. This step allowed cells at the surface of the scaffold to be removed without prolonged exposure to trypsin it also allows for a staged cell removal from the scaffold which overcomes issue caused by diffusion of trypsin through the dense cells layer. A further 1ml of trypsin EDTA was added to the cryovial containing scaffold sections and they were incubated on the rotor for a further 10 minutes before removal of the trypsin into the tube containing media and a further 10 minute incubation in an extra 1ml of trypsin. After the final incubation centrifuge tubes containing the cells removed from the scaffold were centrifuged at 1000 rpm for 3 minutes and were then processed for flow cytometry.

3.4.10 Flow cytometrical analysis of cells from 3D cultures

All tubes containing cells removed from scaffolds and media were centrifuged at 1000 rpm for 3 minutes, media was aspirated and cells were washed twice in 2ml of PBS without calcium and magnesium, centrifuging after each wash. The cell pellet was resuspended in suitable volume of blocking buffer (0.1% bovine serum albumin in PBS). A suitable volume should contain 0.2 x 10^6 cells usually suspended in 200µl of buffer for each antibody requiring testing. This 200µl of cell suspension was added to wells of a U-bottomed 96-well plate. The plate was then centrifuged at 1000rpm for 3 minutes at 4°C. The supernatant was removed from all wells. The pellet in each well was resuspended in 50µl of the appropriate primary antibody diluted in blocking buffer as detailed in Table 3.3

Antibody	Supplier	Working dilution
P3X mouse IgM	Developmental Studies Hybridoma Bank	1:10
SSEA-3 mouse IgM (MC-631)	Developmental Studies Hybridoma Bank	1:5
TRA-1-60 mouse IgM	P. Andrews, University of Sheffield	1:10
A2B5 Monoclonal mouse IgM (MAB1416)	R&D systems	1:20
Secondary antibody - Anti-Mouse IgM (μ-chain specific)–FITC antibody produced in goat	Sigma Aldrich, UK (F9259)	1:100

Table 3.3 Antibody dilutions for flow cytometrical analysis.

Cells were incubated with the primary antibody for 1 hour on ice before unbound excess antibody was removed by the addition of 100μl of the BSA solution and centrifugation at 4°C. Cells were washed twice more with 180μl blocking buffer before incubation with 50μl of the diluted secondary antibody – antimouse-IgM (Sigma) at a 1:100 dilution in BSA for 1 hour on ice in the dark. Cells were washed as previously described and resuspended in 200μl blocking buffer for analysis. Immunolabelled cells were analysed using Guava technologies EasyCyte Plus system and determination of positive cells were set against the negative control antibody, P3X.

3.5 Results

3.5.1 Assessment of cell number and viability in 3D scaffolds

To determine the optimal method for assessing cell viability in the Alvetex® Scaffold, three options were assessed – an MTS assay, an MTT assay and the PicoGreen assay. MTT and MTS assess the activity of mitochondrial reductase which is relative to cell number. The PicoGreen assay measures the amount of double stranded DNA which is compared to a standard curve of cell number. To assess how quickly the assays can detect levels of cell death, TERA2.cl.SP12 were seeded onto scaffolds in 6-well inserts. Cell culture media was not changed for 5 days to induce a drop in cell viability. It was then replenished daily after this timepoint to promote further cell growth. Cell viability was tested every other day using all of the methods. Figure 3.6 shows the growth profiles for all three methods. The MTT assay (Figure 3.6B) and PicoGreen assay (Figure 3.6C) are able to detect the decrease in cell viability as expected both showing a dip in cell number at 5 days which then increased after the media change up to day 9, there was little difference between day 7 and 9 presumably due to the scaffold being packed full of cells. At day 9 there are approximately 9 million cells within the scaffold which is similar to the number of cells achieved in a confluent 2D culture of TERA2.cl.SP12 cells in a T25 flask but in 3D this number of cells was being maintained in a significantly smaller area. In contrast the growth profile using the MTS assay greatly differs (Figure 3.6A). The MTS assay was unable to detect the drop in viability at day 5 but showed a delay as it detected a drop in viability at day 7. The MTS assay was originally described by Cory et al. as a one-step process and a simplified alternative to the MTT assay [164]. The MTS assay has proven to be a lot less sensitive to differences in cell viability during 3D culture this is due to this assay depending on the diffusion of the coloured substrate back into the cell culture media whereas the other two assays (MTT and PicoGreen) require cell lysis before the assay was read.

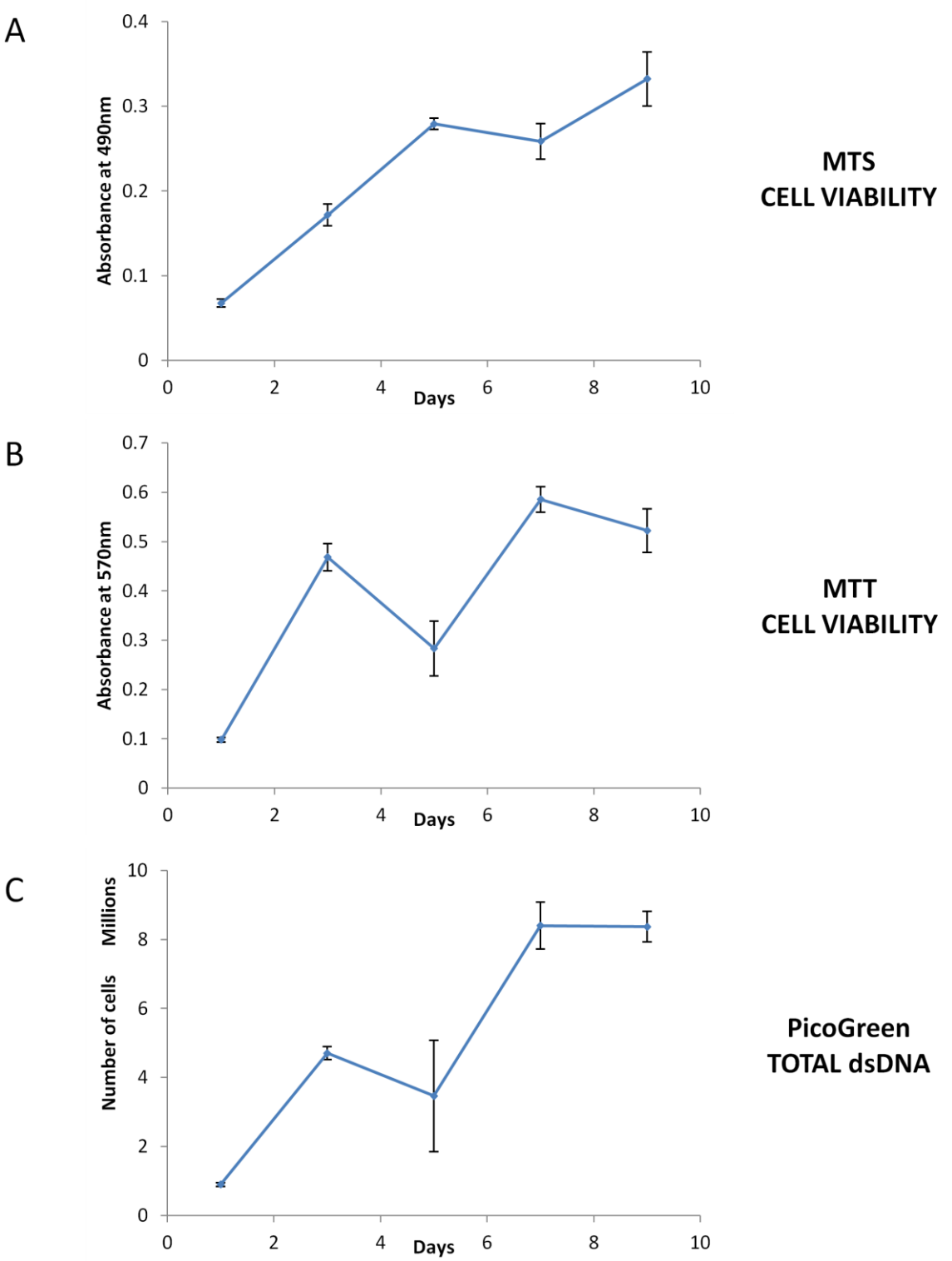

Figure 3.6 Differences between methods to assess cell number and viability in 3D. Scaffolds were seeded with 0.5 million TERA2.cl.SP12 and cultured for 5 days before the media was changed. Cell viability was assessed on a separate sample for each method using either an MTS assay **(A)** or an MTT assay **(B).** Separate samples were also lysed and the PicoGreen assay was used to assess total DNA **(C)** this can then be converted to cell number. Data represent mean **±SEM, n=3.**

3.5.2 Cell retrieval from Alvetex® Scaffolds

Removal of cells from the Alvetex® Scaffold is necessary for downstream processing. The removal of cells from the scaffold requires 3 trypsinisation steps. These three steps ensured that cells which are removed from the surfaces of the scaffold are not overexposed to trypsin EDTA. This would lead to a drop in cell viability and also allowed the trypsin to permeate into the scaffold interior to reach all cells. Figure 3.7 shows the effect of all three steps on the number of cells removed from the scaffold and highlights the requirement for each step. Figure 3.7A shows a TERA2.cl.SP12 seeded scaffold after four days in culture. It is necessary to remove cells from the scaffolds in a step-by-step process to ensure that retrieved cells are viable and can therefore be processed for flow cytometry. Figure 3.7B highlights the need for a short initial incubation in trypsin as after 5 minutes, cells that are at the surface of the scaffold are readily removed and prolonged exposure to trypsin would lead to a decrease in cell viability. Figure 3.7C shows further stages of cell removal, almost all cells were removed and there are only localised areas of shrunken cells remaining on the scaffold after the third trypsinisation step (Figure 3.7D)

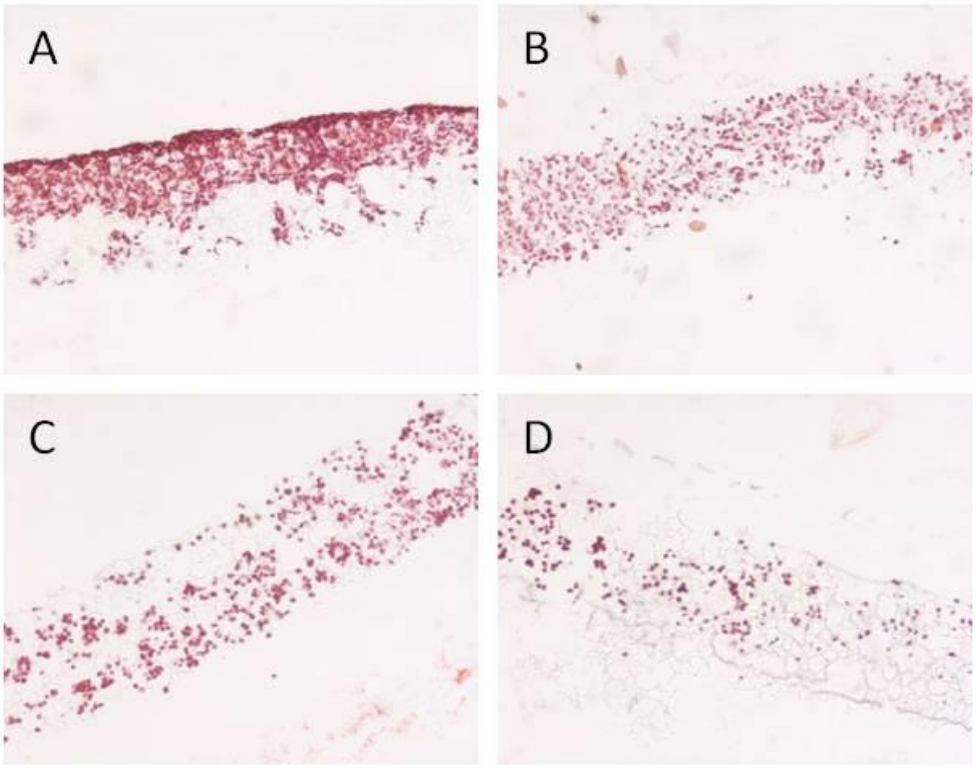

Figure 3.7 Cell removal from Alvetex® Scaffolds. TERA2.cl.SP12 cells were seeded onto Alvetex® Scaffolds and cultured for 4 days **(A).** Scaffolds then underwent a series of trypsinisation steps to remove cells from the scaffolds. **B** shows a scaffold after 5 minute of trypsin treatment, this step allows cells are the surface of the scaffold to be removed. After a further 10 minutes of trypsin treatment there a few cell left within the scaffold interior **(C).** After the full cell removal protocol **(D)** there are localised areas of scaffold which still contain a few cells.

3.5.3 Media quality profiles for 2D and 3D culture

Figure 3.8 shows profiles of glucose consumption and lactic acid production for both 2D and 3D culture in comparison to the predictive profiles previously presented in Figure 3.1. During 3D culture there are significantly more cells seeded than standard 2D culture due to the increased surface area for cell growth. This increase in cell number can lead to a huge drop in the quality of cell culture media (Figure 3.8B) or cultures have to undergo daily media changes (Figure 3.8C) this disturbs cells and can lead to cell detachment from the scaffold. TERA2.cl.SP12 cells were seeded onto Alvetex® Scaffolds placed in the bottom of 12-well plates, samples of media were taken every 24 hours for 8 days for two types of 3D cultures, one with media changes every 3 days similar to 2D cultures and one with daily media changes. The same number of cells was also seeded in 2D in 12-well plates and the media was changed in accordance with standard 2D culture protocols. Cell culture media samples were tested for both glucose concentration and lactic acid concentration. The experimental media quality profiles (Figure 3.8) differ from the theoretical profiles (Figure 3.1) in all cases, as the theoretical values do not take into account the increased drop in glucose concentration and increase in lactic acid concentration caused by further cell growth. For example during standard 2D culture at the first media change there was only a drop in glucose concentration of 0.2g/L and lactic acid production of 4mM. Whereas at the second media change there was a glucose concentration of 1.2g/L and the production of 12mM lactic acid. The increase in cell number that caused this progressive drop in media quality is more apparent in the 3D cultures with daily media changes. By changing the media too regularly on 3D cultures, this led to a drop in culture media quality which got progressively worse. This was so severe that by day 4 similar concentrations of lactic acid (12mM) are observed every 24 hours in the 3D culture as are observed in the 2D culture after 72 hours.

3.5.4 Presentation of the scaffold influences 3D cell culture medium quality.

The metabolic demand of TERA2.cl.SP12 cells grown within the scaffold in the three different formats (Figure 3.3) was assessed over a 5 day period. The cell culture media was not changed during the experiment and glucose concentration, lactic acid concentration and pH in the media was recorded every 24 hours. Cell viability was also assessed every 24 hours using the MTT assay. Figure 3.9 shows the media profiles for the three scaffold formats. Significantly higher glucose levels are observed in the large reservoir format both inside and outside the well inserts when compared to the other two formats (Figure 3.9A). The relatively high concentrations of glucose (2.2g/L) were still available in the large reservoir system after 5 days in culture. This is also interesting considering the large Petri dish system contains three inserts per dish. There was also a difference in the glucose concentration between the two sides of the insert. This was apparent in both insert systems which both had a difference of approximately 0.2g/L between the two areas. This suggests that there is limited diffusion through the scaffold containing cells.

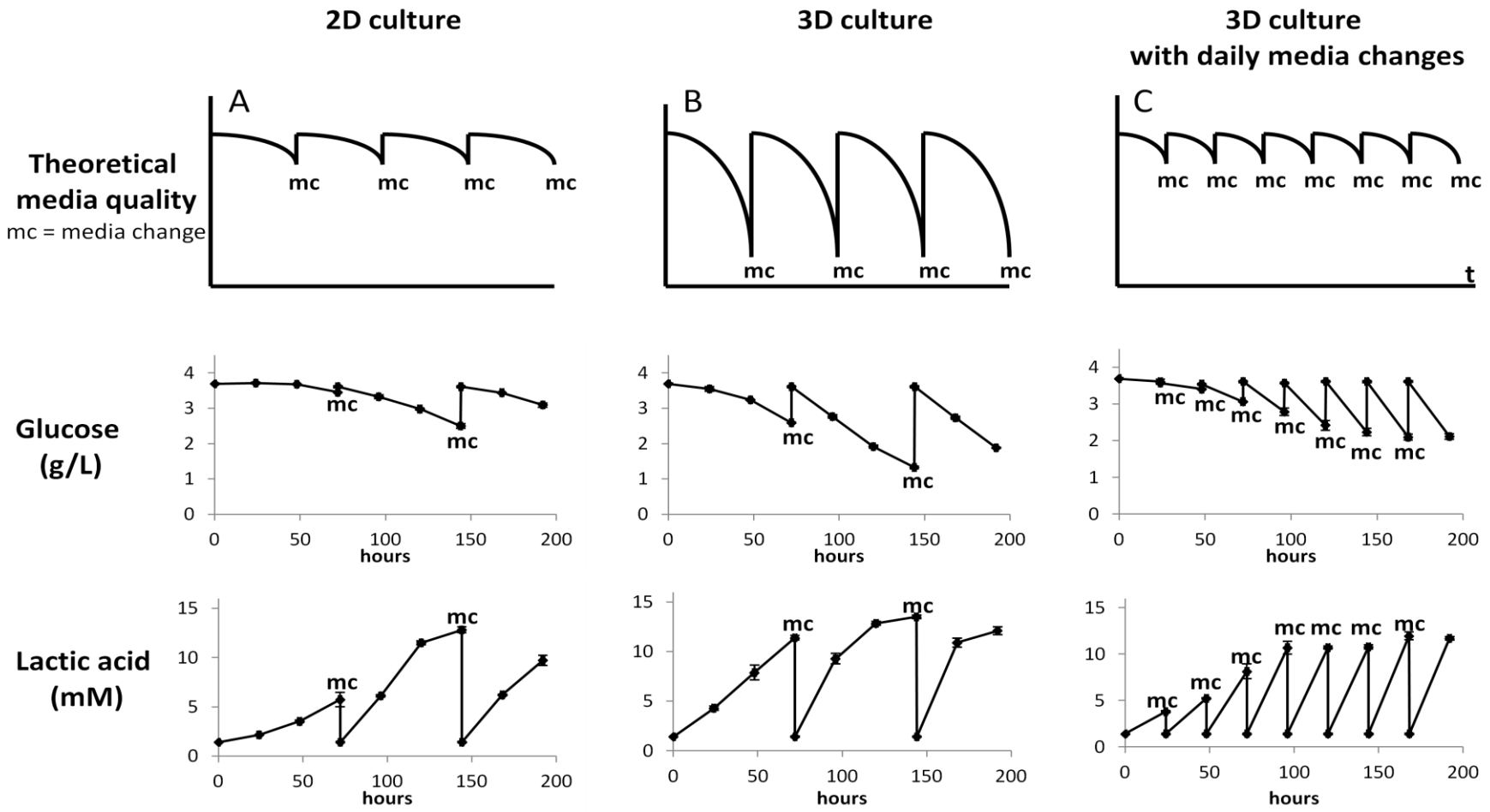

Figure 3.8 Media quality profiles for 2D and 3D cell culture. Cell culture media profile for growth of TERA2.cl.SP12 cells during 2D culture **(A)** and during standard 3D culture **(B)** the rapid drop in media quality is usually overcome by changing the media more often **(C),** the regular disturbance of cells can lead to cell detachment from the scaffold. Experimental data shows that when media is changed too regularly the drop in media quality gets progressively worse until it reaches a similar level of lactic acid (12mM) as a 3 days culture but within 24 hours. Data represents mean **±SEM, n=3.**

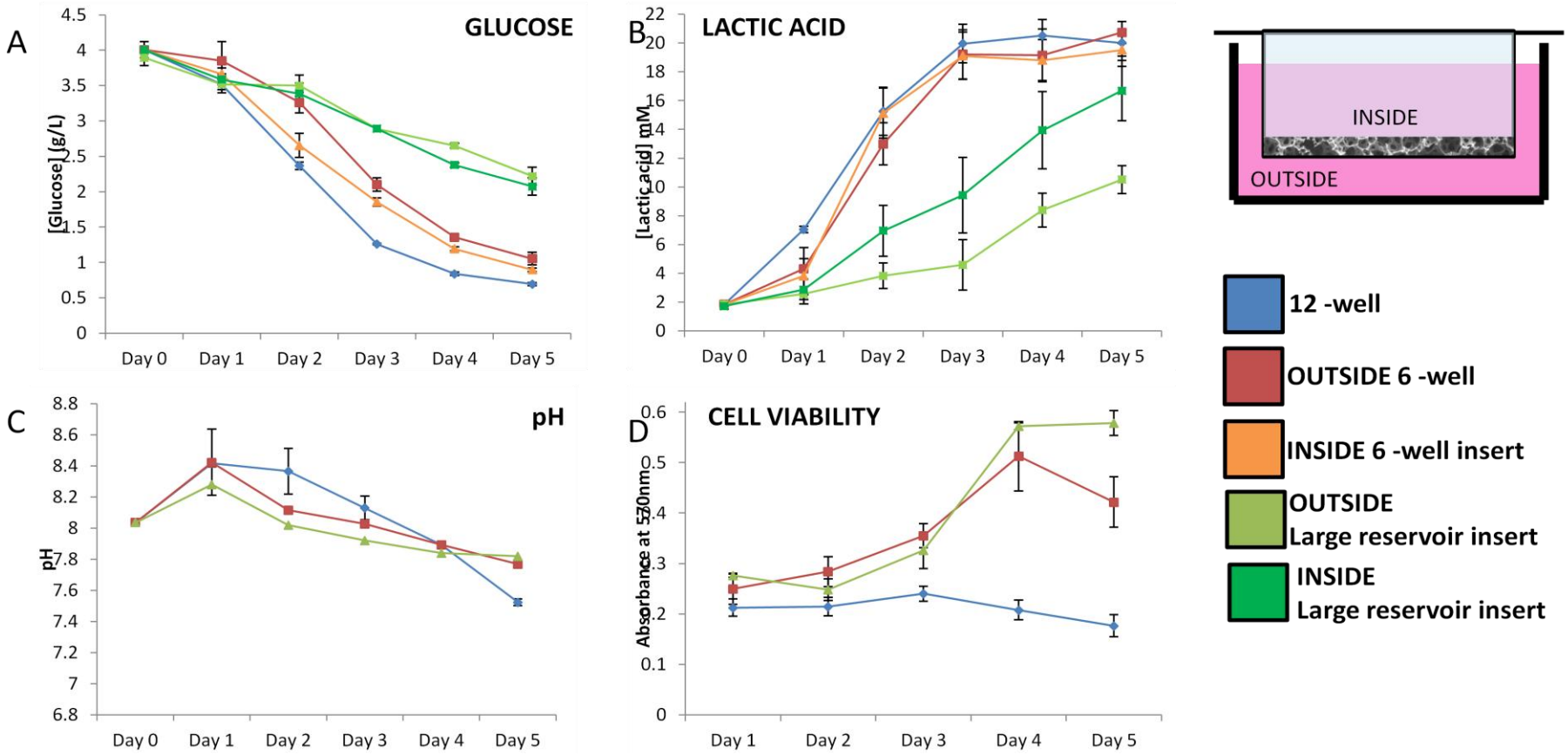

Figure 3.9 Scaffold formats affect cell culture media quality and cell viability. TERA2.cl.SP12 cells were cultured in the three scaffold formats for 5 days without media changes using optimum conditions established in previous chapter. During the 'stress test' media samples were collected and tested for glucose consumption **(A)** lactic acid production **(B)** and pH **(C)** every 24 hours. Cell viability was assessed using an MTT assay **(D).** Data represent means **±SEM, n=3.**

As expected the rapid consumption of glucose in the 12-well system (a decrease of 3.31g/L over the 5 day period) led to a rapid increase in lactic acid concentrations. In the 12-well system, the inhibitory concentration of 20mM of lactic acid in the cell culture media was reached by day 3 (Figure 3.9B) and this limited further cell growth (Figure 3.9D). The increase in lactic acid concentration was accompanied by a decrease in pH. Cell growth is enhanced in both the insert systems, but there was a build-up of lactic acid inside the insert (Figure 3.9B). The inserts in the 6-well plate displayed a difference of 1.2mM lactic acid between the inside and outside of the insert whereas there was a greater difference in the large reservoir format (6.2mM). To accompany the production of lactic acid there was a rapid drop in pH of the media in all the scaffold formats (Figure 3.9C)

3.5.5 Scaffold presentation affects cell viability.

The viability profiles of TERA2.cl.SP12 grown within the scaffolds are shown in Figure 3.9D. All scaffolds were seeded with identical numbers of cells, however after only one day in culture there were already differences in cell viability between the three scaffold presentations. Both insert systems performed better than the 12-well system. Cells remained viable in the 12-well system but limited new growth occurred after the first 24 hours of culture and by 3 days the viability had started to decrease. This drop in viability was also evident in histological samples of 12-well cultures where cells only showed limited migration into the scaffold at day 3 and there were already large areas of cell death by day 5 (Figure 3.10). The 6-well format and the large reservoir system showed similar viability profiles up to day 4 (Figure 3.9D). By day 5 there was a drop in cell viability in the 6-well insert system. Again this was evident when the cultures were stained with Haematoxylin and Eosin; there was evidence of cell death shown by areas of shrunken nuclei (Figure 3.10). There was limited new cell growth in the large reservoir system (Figure 3.9D) between day 4 and day 5 presumably due to the build-up of waste products. Interestingly there were no areas of cell death in the large reservoir cultures. Cells were able to penetrate throughout the scaffold and had begun to produce a dense slab of tissue within the scaffold and at the scaffold surface (Figure 3.10)

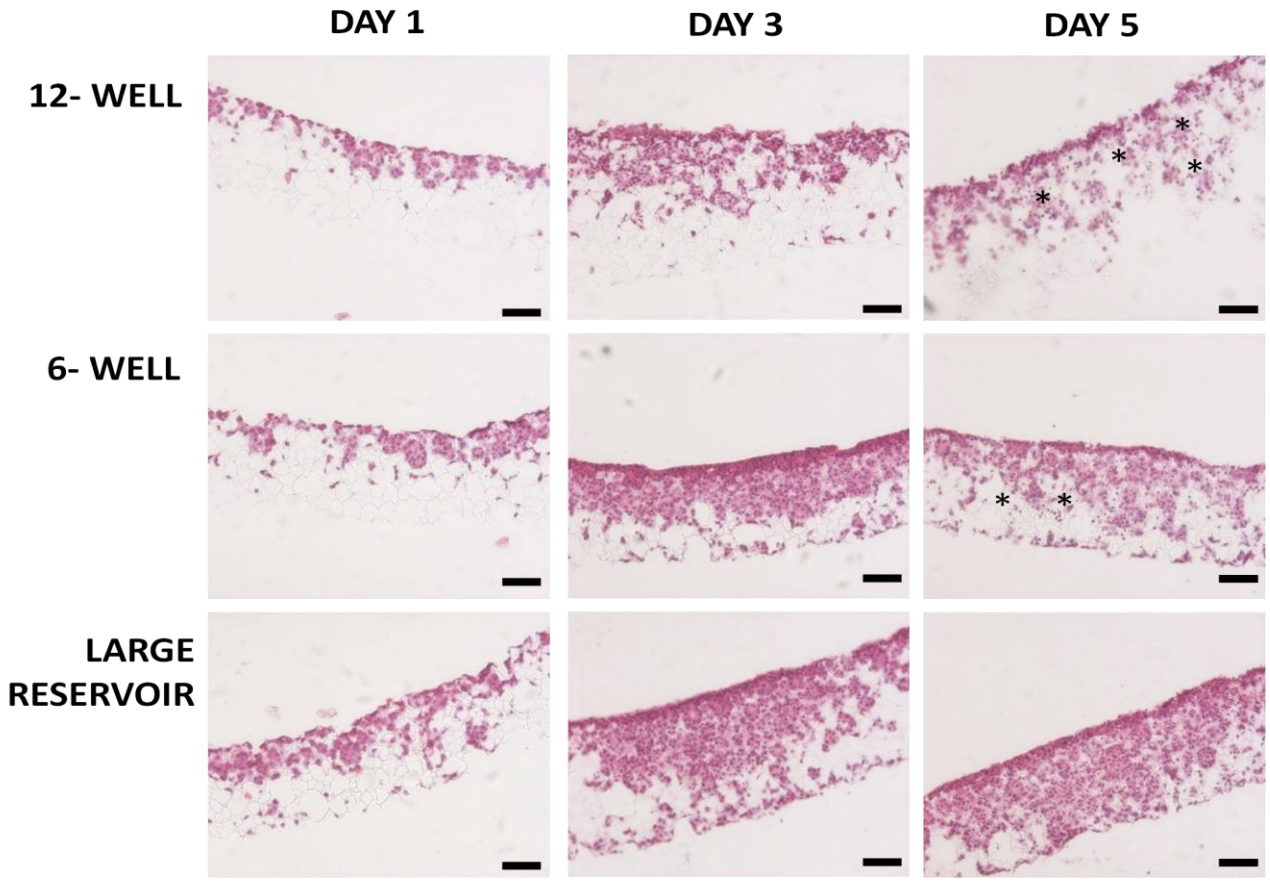

Figure 3.10 Histological analysis of cells grown in different scaffold presentations. Histological H&E analysis shows the penetration of TERA2.cl.SP12 cells through the scaffold in each formats over a 5 day period. * highlight areas of localised cell death (shrunken cytoplasm and nuclei) which occur in the cultures with limited cell culture media. In the two formats that use well inserts it is possible for cells to penetrate through the entire width of the scaffold. Scale bar:100µm

3.5.6 Scaffold presentation affects cell number and penetration through the scaffold.

Cell number was assessed using Quant-iT™ PicoGreen® dsDNA kit (Invitrogen, Molecular Probes). Whole scaffolds from each of the four formats were lysed to assess the total amount of double stranded DNA. Cell number can then be determined using a standard curve (Figure 3.4). The 12-well format demonstrated cell growth was limited, the number of cells only increased from the initial seeding density of 0.5 x 10^6 cells to 3.9 x 10^6 after the 5 day culture. However, cell number increased in a linear fashion over the 5 days (Figure 3.11A). This is in contrast with the 6-well system where the increase in cell number slowed after 3 days. Although the total cell number is significantly higher than the 12-well system. An increase of approximately 6.2 x 10^6 cells was observed in the 6-well insert system between days 1 and 5 (Figure 3.11A). The large reservoir Petri dish produced an interesting cell number profile over the 5 days. Between days 1 and 3 the cell number was almost identical to the 6-well insert cultures but as the 6-well cultures began to slow, the cell number in the Petri dish continued to increase. The 3D cultures in the large reservoir are able to support 1.1 x10^7 cells per scaffold after 5 days (Figure 3.11A).

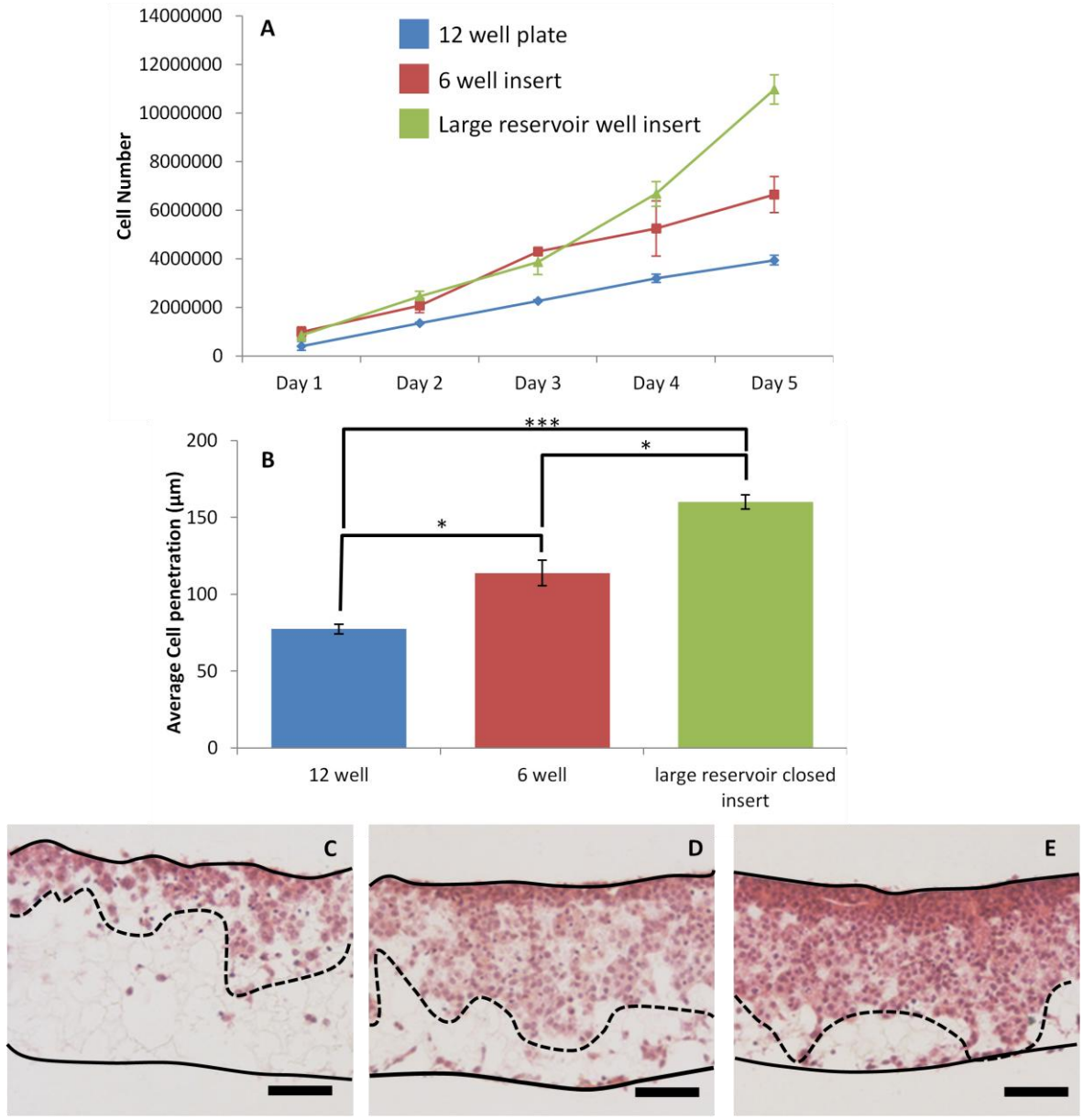

Figure 3.11 Effect of scaffold presentation on cell number and cell penetration (D_p). The number of cells within the Alvetex® Scaffold was assessed using Quant-iT™ PicoGreen® dsDNA kit and a standard curve of cell number. Scaffolds containing cells grown in the three different scaffold presentations were lysed to assess cell number which is greatly affected by scaffold presentation **(A).** Data represents mean ±SEM n=3. At day 4, scaffolds were fixed in 4% paraformaldehyde and processed for H&E staining to assess cell penetration **(B)** D_p was assessed by taking 15 measurements per scaffold from 3 separate scaffolds. There is a significant difference in the amount of cell penetration achieved in the different formats. H&E images highlight this difference between the 12 well format (C) and the two insert formats – 6 well (D) and large reservoir Petri dish (E) *p=0.05, ***p=0.001. Scale bar = 50µm.

The increase in cell number between the different formats is related to the distance a pioneering cell can migrate into the scaffold interior. The penetration depth (D_p) was assessed using histological sections, a selection of which are presented in Figure 3.10. Maximum cell penetration was assessed at day 4 due to the areas of cell death visible at day 5 in two of the formats. In the 12 well system, cell migration was limited to less than half of the Alvetex® Scaffold (80µm of the 200µm thick scaffold) shown in Figure 3.11B&C. The insert systems and the increase in cell number allowed for increased penetration of cells into the scaffold interior. The 6-well system displayed healthy viable cells but there were limited areas of migration through the entire width of the scaffold, this was evident in the H&E image in Figure 3.11B&D. On average cell migration was limited to 120µm into the scaffold. The large reservoir Petri dish allowed for increased cell penetration into the scaffold and there were areas of the section which clearly showed cells which have migrated through the entire width of the scaffold (Figure 3.11B&E). This may be due to the significantly larger cell number.

3.5.7 Redesign of well insert housing Alvetex® Scaffold for enhanced 3D culture

The metabolism profiles in Figure 3.9 showed a build-up of lactic acid concentration in the inside of the insert for the two insert systems. To address this issue the well insert was redesigned to incorporate three open areas in the walls of the device (Figure 3.12). These openings/windows allow for the passage of media from the area surrounding the scaffold to the reservoir on top of the scaffold without the need to pass through the scaffold. It may also prevent a gradient of nutrients and waste products forming across the scaffold. To ensure the reservoir on top of the scaffold is connected to the main culture media reservoir, Petri dishes containing the open-wall inserts require 75ml DMEM. Figure 3.12 compares the two types of well insert. Figure 3.12A shows the insert used in experiments up to this point. This is referred to as a closed wall insert as the media chamber above and surrounding the inserts are separated by the scaffold. The closed wall insert is based on a standard transwell insert which is used for various commercial products such as transwell insert by Corning and Millicell culture inserts by Millipore. Figure 3.12B shows the redesigned insert which allows movement of media around the scaffold to prevent the build-up of lactic acid, these are open wall inserts.

The quality of cell culture media was assessed by placing scaffolds in the two types of inserts in the large reservoir Petri dish system containing 75ml DMEM. For consistency with previous experiments cultures were grown for 5 days without media changes, samples of cell culture media were taken every 24 hours. Samples were tested for glucose consumption and lactic acid production. Cell metabolism was assessed in the new open-walled inserts in comparison to the original closed wall inserts (Figure 3.12A). There was no significant different in glucose metabolism between the two types of inserts, but the open-wall inserts appeared to deplete the

glucose concentration more rapidly than the closed-wall inserts (Figure 3.13A). There was a difference in the lactic acid profiles for both types of insert. As previously described the closed-wall insert allowed for a build-up of lactic acid in the centre of the insert this was shown by a difference of 7mM lactic acid between the two areas of the culture by day 5 (Difference between the green lines in Figure 3.13B). The redesign of the insert was intended to reduce this difference in lactic acid concentration across the cell culture scaffold. The open-insert was effective as shown by Figure 3.13B, there was no difference between the inside and the outside of the well insert. The homogenous lactic acid concentration means that the overall lactic acid concentration is lower in the large reservoir Petri dish containing the open-wall inserts.

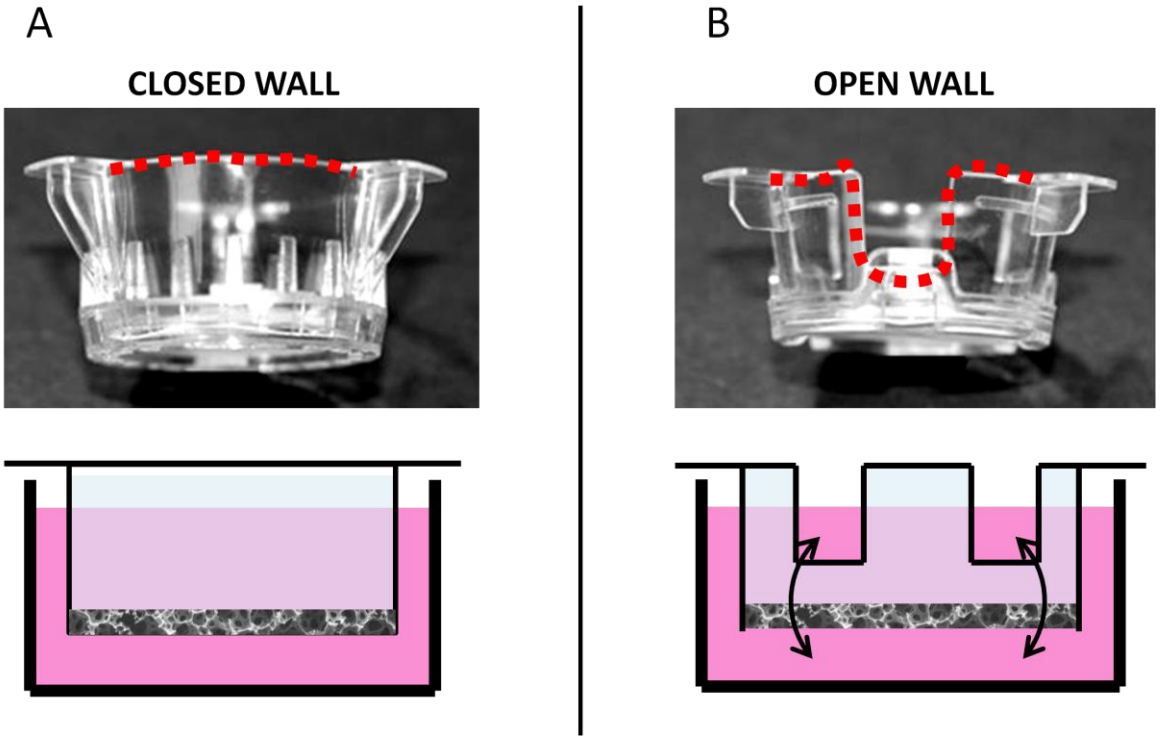

Figure 3.12 Comparison of well inserts. The standard well insert known as the closed wall insert **(A)** was redesigned incorporating windows in the side of the insert - open wall insert **(B).** This allows media to pass from reservoir above the scaffold to the reservoir surrounding the scaffold preventing the build-up of lactic acid on the inside of the insert, which allows for longer term cultures. This will also allow for equilibration of lactic acid concentration across the membrane.

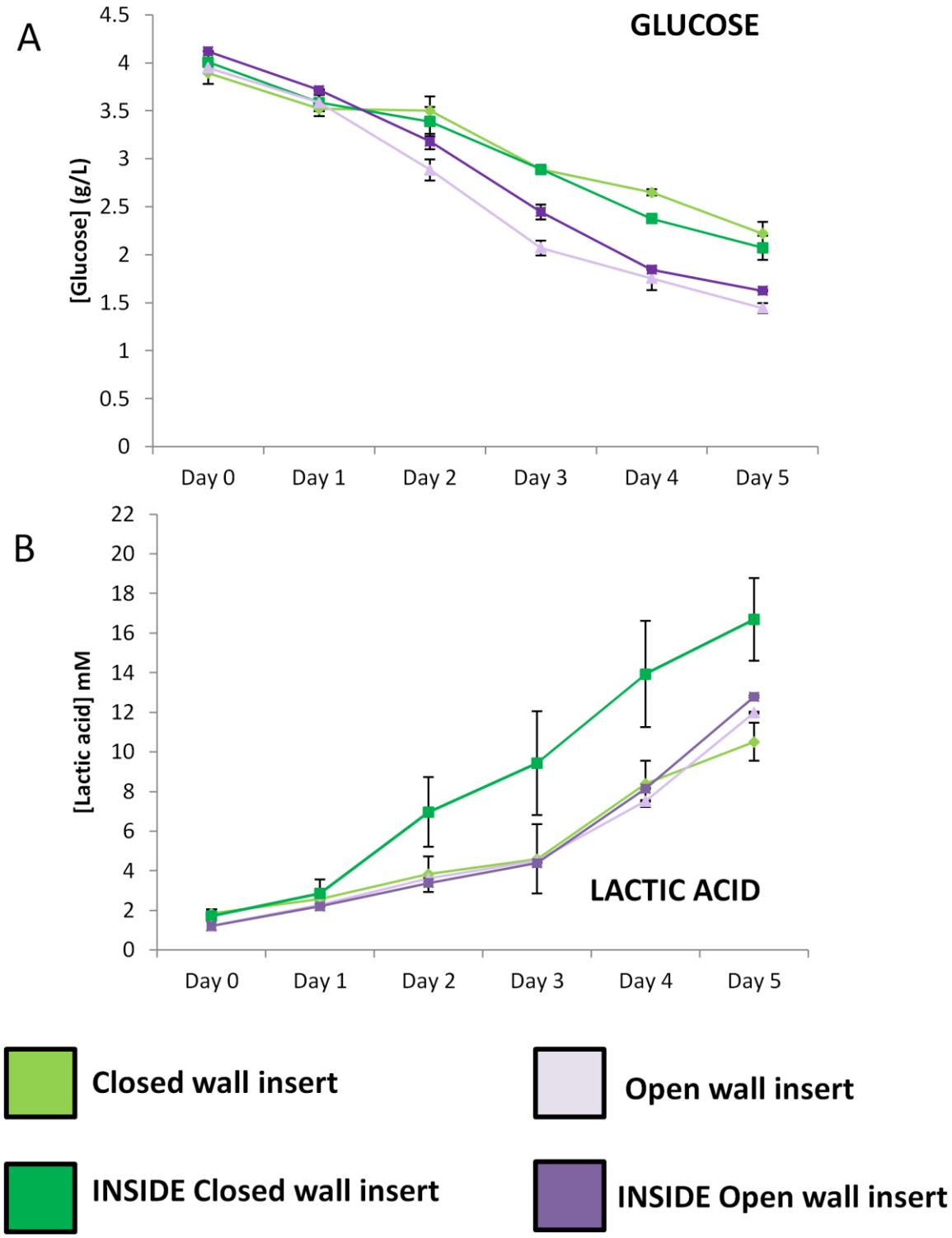

Figure 3.13 Cell culture media quality in the two types of insert. A similar test was performed as in **Figure 3.9** comparing the newly designed open-walled insert and the previously tested closed insert both in the large reservoir system containing three scaffolds. Scaffolds were initially seeded with 0.5 million cells and media samples were tested for glucose **(A)** and lactic acid **(B)** levels each day for five days. Note the difference in lactic acid concentration between the inside and outside of the closed wall inserts. Data represents mean **±SEM, n=3**

3.5.8 Differences in well insert design affect cell distribution within 3D scaffolds

Using the optimised conditions previously described 0.5 x 10^6 TERA2.cl.SP12 cells were seeded onto scaffolds presented in both types of inserts and cultured in the large reservoir Petri dish. Cells were culture for 7 days before being fixed. H&E staining of the scaffolds revealed a difference in cell distribution, cell density and proliferation between cultures grown in the two types of inserts. Cells cultured in the closed-wall inserts infiltrated the scaffold at a low cell density. This led to an even distribution of cells throughout the scaffold. When these cultures are immunostained for the proliferation marker – Ki-67, it is apparent that proliferating cells were present throughout the entire scaffold section (Figure 3.14A). This was in contrast with cells cultured on scaffolds which have been presented in the open-wall inserts. Cells in open-wall cultures had produced a dense cell layer at the surface of the scaffold and cells had begun to produce complex structures at the cell media interface. These cells appeared to penetrate the scaffold at a higher cell density than in the closed-wall cultures. There was also a difference in the localisation of Ki-67 positive cells when compared to the closed-wall inserts. Open-wall cultures only displayed Ki-67-positive cells in the dense areas of cells at the peripheries of the scaffold (Figure 3.14B).

3.5.9 Differentiation of stem cells and the effect of lactic acid concentration

To initially assess the effect of an increase lactic acid concentration on the differentiation of TERA2.cl.SP12 cells, cultures were grown in 2D in T25 flasks. Cultures were treated with 1µM EC23, after 24 hours in culture. In addition to this a range of concentrations of sodium-L-lactate (2.5mM, 5mM, 10mM, & 20mM) were added to separate cultures to simulate a build-up in lactate ions. Cells were cultured in the conditioned media for a further four days before being processed for flow cytometry. The addition of lactate ions affects the differentiation of pluripotent stem cell. The levels of the embryonic stem cell marker – SSEA-3 were decreased by the addition of just 2.5mM lactate. SSEA-3 expression continued to decrease with increasing concentration of lactate ions, at 5mM concentrations of lactic acid there was already a significant difference ($p=0.01$) in expression of the stem cell marker. This difference becomes more significant as lactic acid concentration increases ($p=0.001$ for cultures treated with 20mM lactic acid) (Figure 3.15A).

Expression of the stem cell marker TRA-1-60 was not as sensitive to the lactate concentration as SSEA-3. There was no significant difference in TRA-1-60 expression until the two highest lactic acid concentrations (Figure 3.15B, $p=0.01$). The decrease in TRA-1-60 expression in conjunction with the decrease in SSEA-3 expression suggest that addition of lactate ions teamed with retinoid treatment led to the differentiation of TERA2.cl.SP12 cells. This was confirmed by the increase in the early neuronal cell marker A2B5 (Figure 3.15C). It is expected that levels of A2B5 would increase with the addition of EC23, however significant differences in levels of A2B5 often require

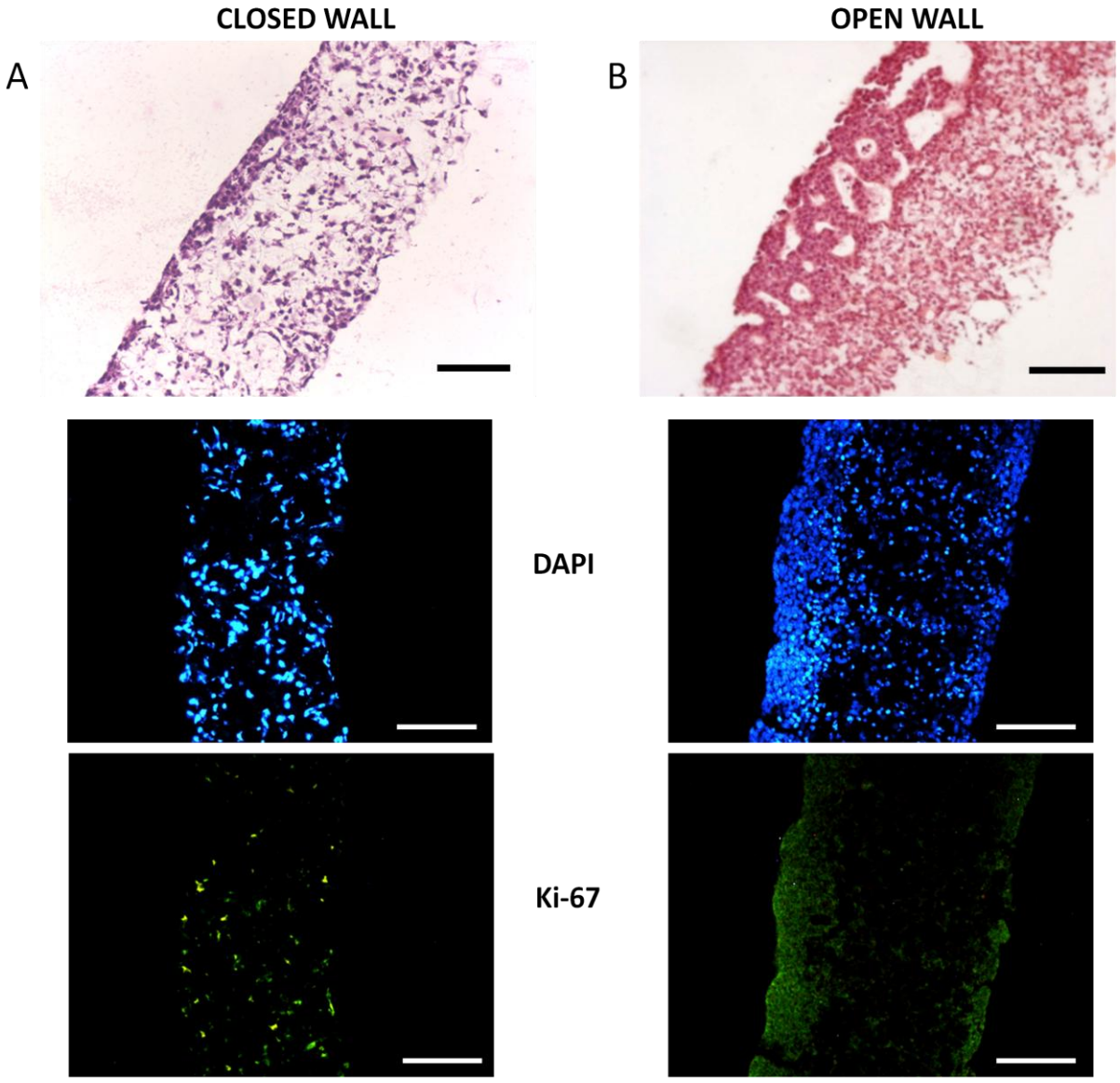

Figure 3.14 Histological and immunofluorescence analysis show a difference between open and closed insert cultures. TERA2.cl.SP12 cells were seeded on to scaffolds in the two types of inserts using identical set up conditions and cultured for 7 days. Cells grown in the scaffold in closed wall inserts **(A)** migrate throughout the scaffold at a low cell density whereas in the open wall inserts **(B)** there is a dense cell layer at the surface of the scaffold which penetrate the scaffold at a high cell density. There is also a difference in the localisation of proliferating cells. Scale bar=100µm

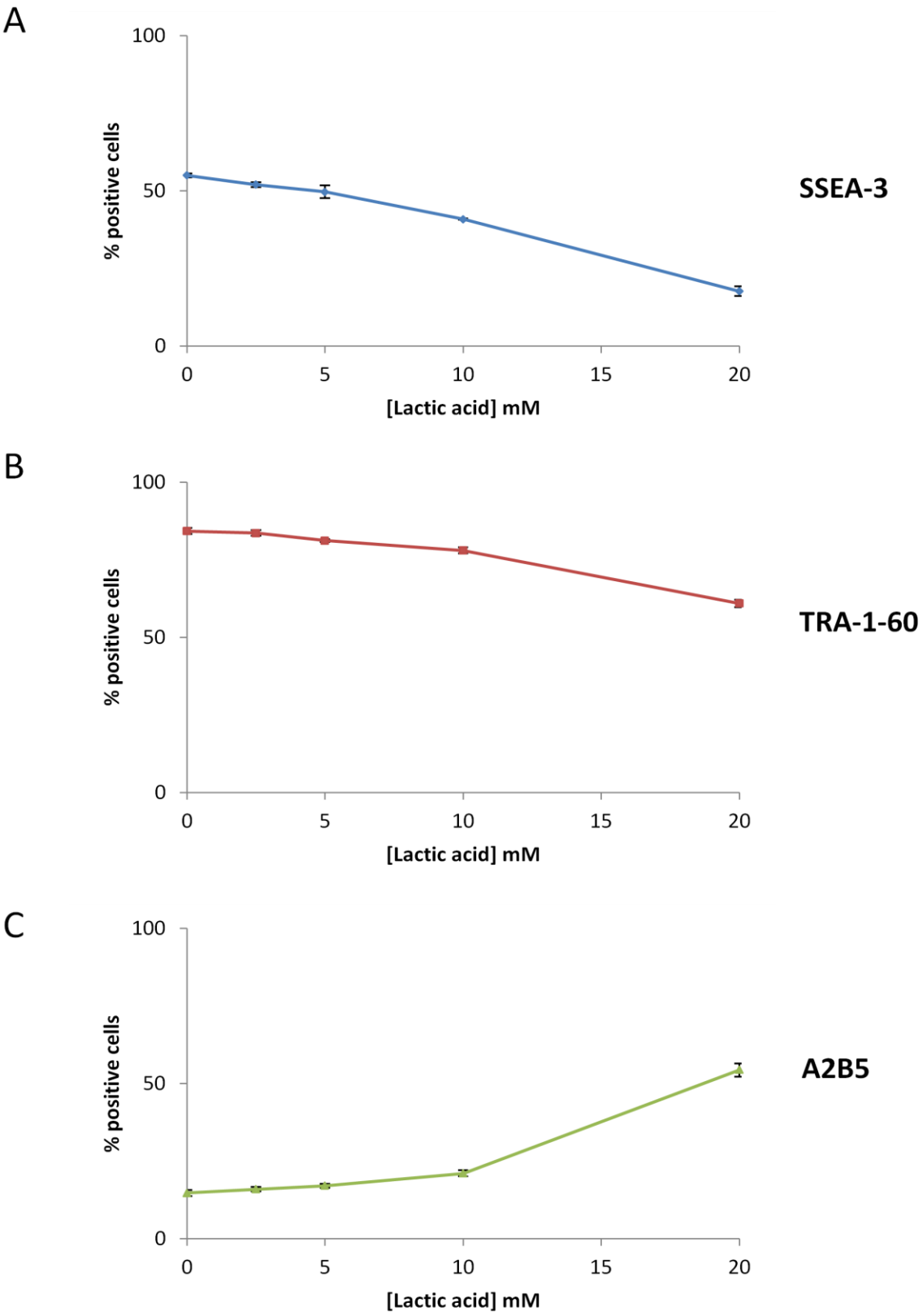

Figure 3.15 Flow cytometric analysis of TERA2.cl.SP12 cells treated with lactic acid. Cells were grown in 2D while be treated with different concentrations of sodium lactate + the synthetic retinoid EC23. After 5 days cells were screened for pluripotency and differentiation markers. Levels of lactic acid similar to those seen in 3D cultures caused upregulation of neural differentiation marker A2B5. **n=3 ±SEM**

at least 7 days of retinoid treatment and the addition of 20mM sodium lactate after 4 days, led to 56% of cells being A2B5 positive.

3.5.10 Stem cell differentiation in 3D.

Due to the data presented in Figure 3.15 on the effect of lactate concentration and the differences in cell distribution highlighted in Figure 3.14, both inserts were used for assessing the differentiation of stem cells in three dimensions. Cultures were processed for flow cytometry 14 days after the addition of either 1μM EC23 or DMSO for the control cultures and fixed for immunostaining at day 7 and 14. The levels of SSEA-3 were approximately 50% for both scaffold presentations with the addition of 1μM EC23 confirming differentiation. The differences caused by insert design were more apparent in the control cultures. At day 14, open insert control cultures displayed high levels of SSEA-3 expression (77%) whereas closed insert control cultures were at similar levels of SSEA-3 expression to the retinoid treated cultures (Figure 3.16A). This suggests that the closed insert control cultures were differentiating. Similar differences were also observed when cultures were analysed for the expression of A2B5. All retinoid treated cultures showed high levels of A2B5 expression (between 86-96%). There was a significant difference in the differentiation marker – A2B5 between the two control cultures. Open insert cultures had 21% of A2B5-positive cells whereas closed insert control cultures were 63.3% A2B5 positive (Figure 3.16B).

Immunostaining for Oct 4 at day 7 also demonstrated that cultures presented in closed wall inserts tend to spontaneously differentiate. Both control and retinoid treated cultures in closed wall inserts displayed no expression of Oct 4 as early as day 7. In contrast to this, control cultures in the open wall inserts showed a dense layer of cells which were almost all positive for Oct 4 and the retinoid treated cultures displayed localised areas of Oct 4 expression at day 7 (Figure 3.17). Both types of cultures were also stained for neuronal class III β-Tubulin (TUJ-1). The neural differentiation marker was not expressed in open insert control cultures but was present in the control cultures in closed wall inserts although there were only small areas of positive cells. The small areas of positive cells in the closed wall control cultures was similar staining to the retinoid-treated cultures presented in the open wall inserts. In contrast to this the closed insert cultures treated with 1μM EC23 showed extensive areas of TUJ-1 positive cells across the entire scaffold section, however at 7 days there was only limited neurite outgrowth (Figure 3.18).

Cultures were maintained for a further 7 days to reach 14 days of retinoid treatment. At this stage the cultures were immunostained for TRA-1-60 (a pluripotency marker which is less sensitive than Oct 4). All cultures displayed areas of TRA-1-60 positive cells at day 14, both the open insert cultures showed a dense area of cells which were all positive for TRA-160, however the EC23-treated cultures had fewer areas of positive cells than the control cultures. Both conditions in the

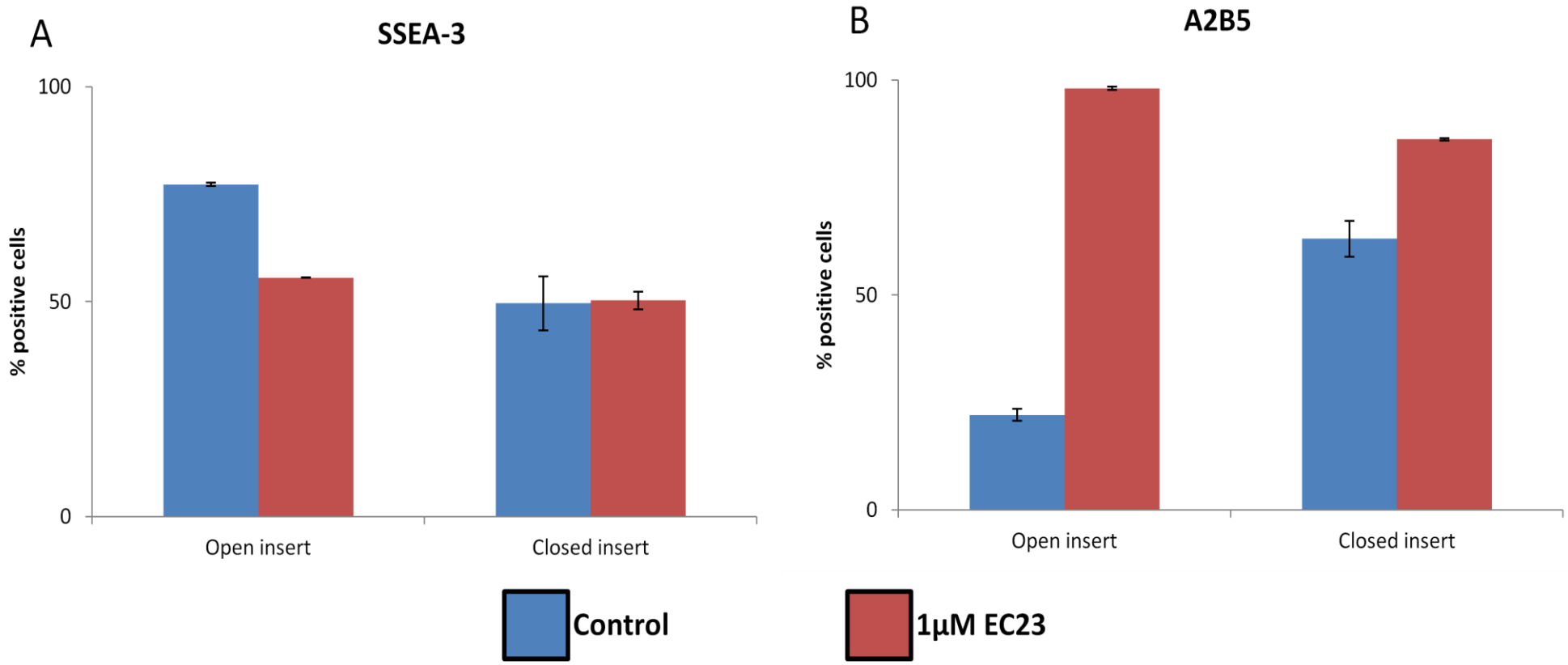

Figure 3.16 Comparison of SSEA-3 and A2B5 expression between open and closed insert cultures. Cultures were grown for 14 days in the two types of inserts. Cells were removed from the scaffold and processed for flow cytometry. Open inserts maintain SSEA-3 expression in the control sample and it is downregulated when treated with retinoid. However in the closed insert cultures there is little difference in SSEA-3 expression between the two types of cultures. Open insert cultures behave as expected: low levels of A2B5 expression in the control and high levels after retinoid treatment. Whereas in the closed insert cultures, the control cultures show high levels of A2B5 expression indicating differentiation. Data represents mean **±SEM, n=3**

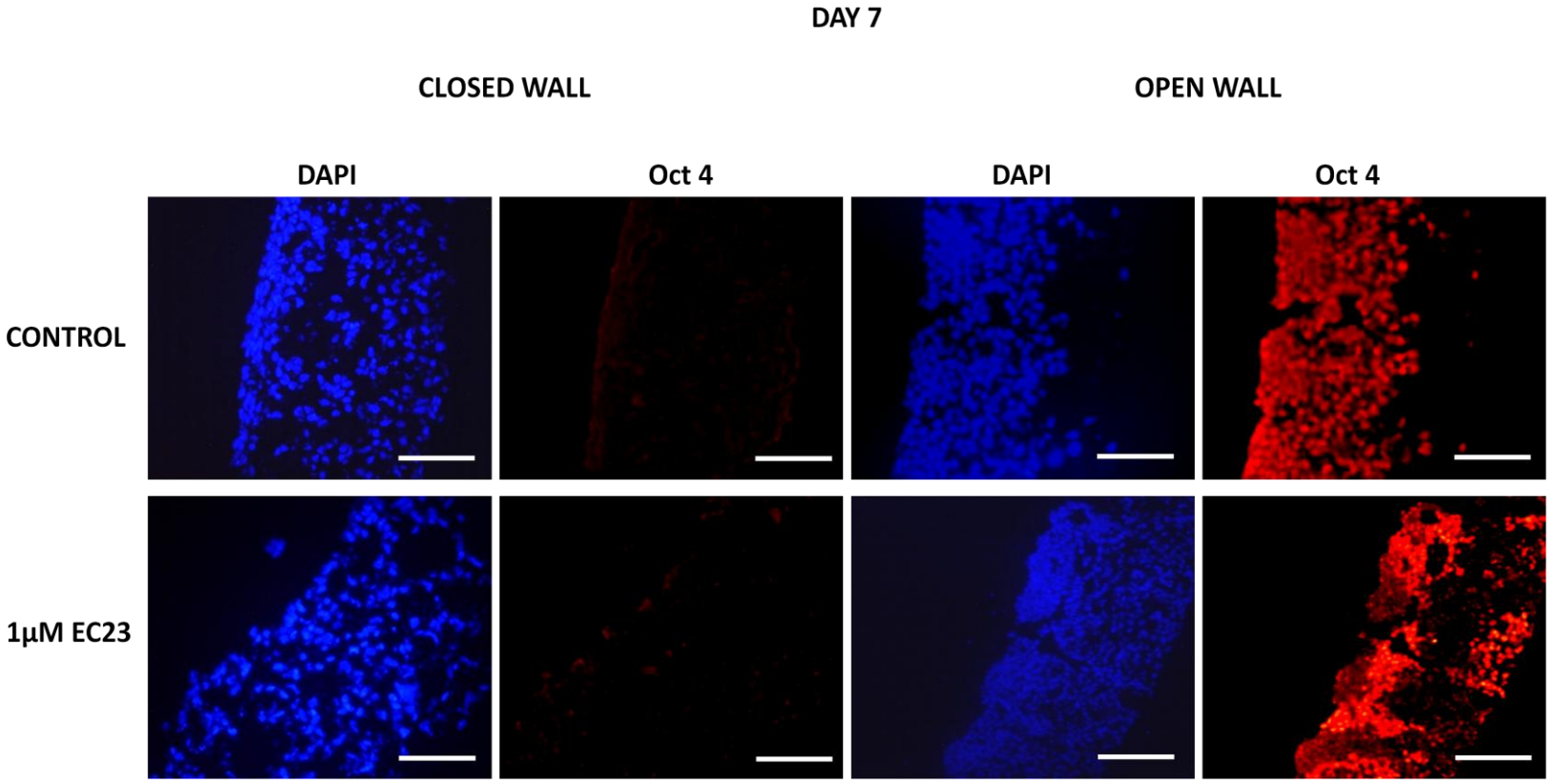

Figure 3.17 Immunostaining shows that open insert cultures maintain Oct 4 at day 7. Closed insert cultures display no Oct 4 positive cells at day 7 in both the control and retinoid treated cultures. Whereas in the open insert cultures there are large areas of Oct 4 positive cells in the control and localised areas in the retinoid-treated scaffolds after 7 days of treatment. **Scale bar: 100µm**

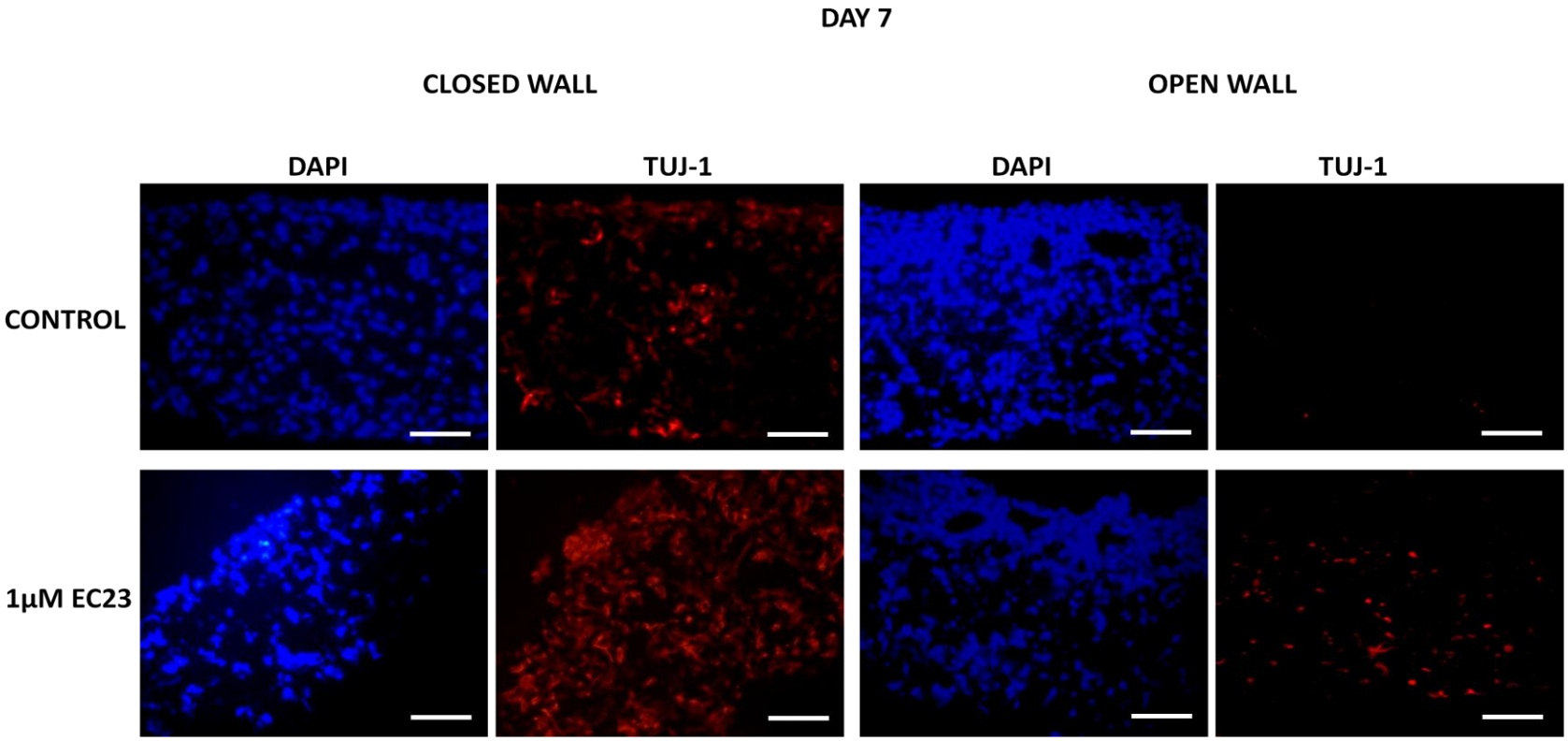

Figure 3.18 Immunofluorescence staining show that closed insert cultures display differentiation marker TUJ-1 at day 7. Closed insert cultures display TUJ-1 positive cells at day 7 in both the control and EC23-treated cultures whereas in the open insert cultures very limited cells expressing TUJ-1 after retinoid treatment and no positive cells in the control. Large areas of TUJ-1 expression demonstrate that the cells in the closed wall inserts differentiate in the control cultures. **Scale bar: 50µm**

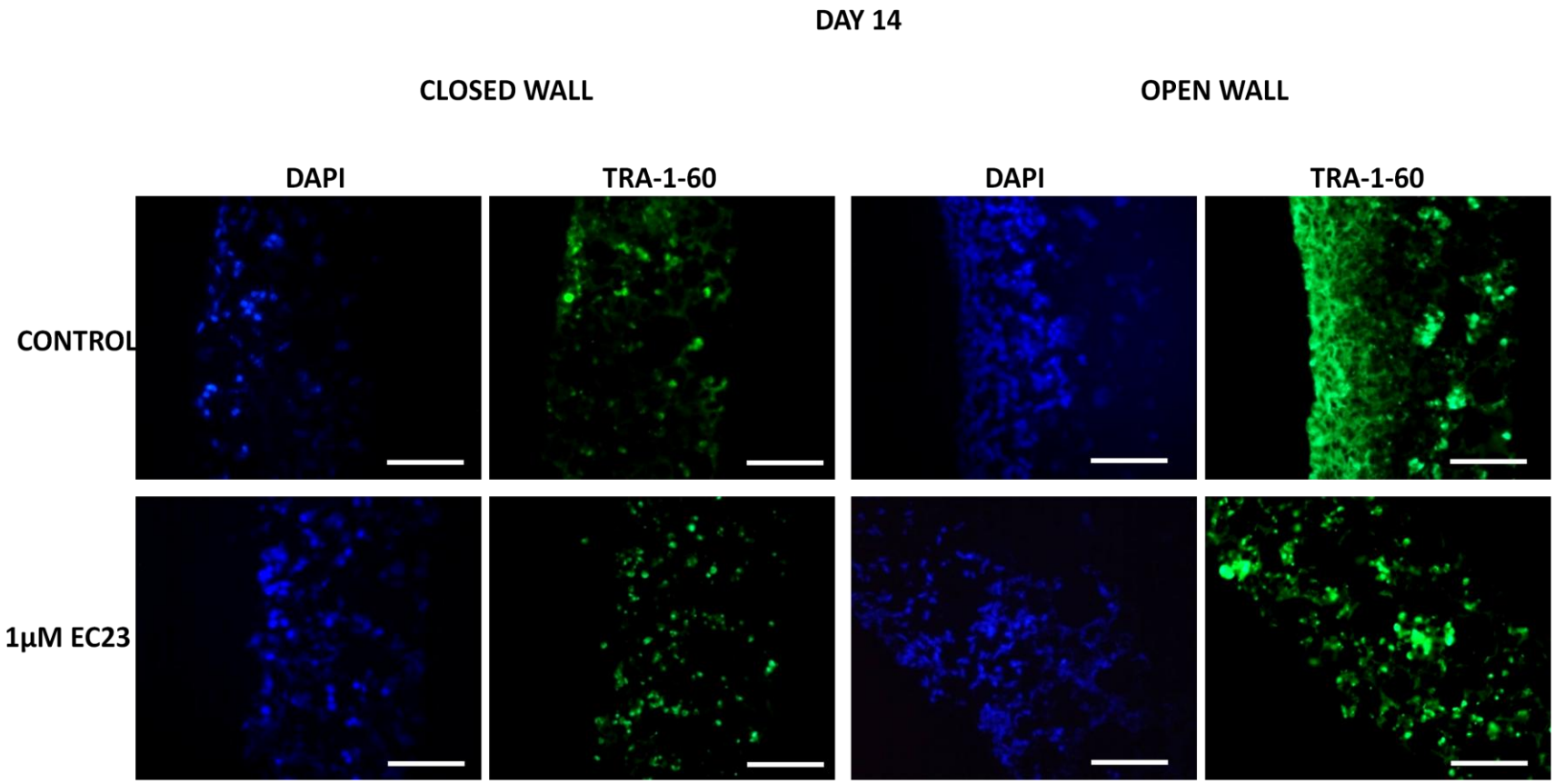

Figure 3.19 Immunofluorescence staining for pluripotent stem cell marker TRA-1-60 in open and closed insert cultures. Closed insert cultures show dispersed TRA-1-60 positive cells at day 14 in both the control and EC23-treated cultures. In contrast, the control open insert cultures show a dense area of high expression TRA-1-60 expression especially in the dense layer of cells at the scaffold surface and more staining for TRA-1-60 in the retinoid treated cultures than in the closed wall insert counterpart. **Scale bar: 100µm**

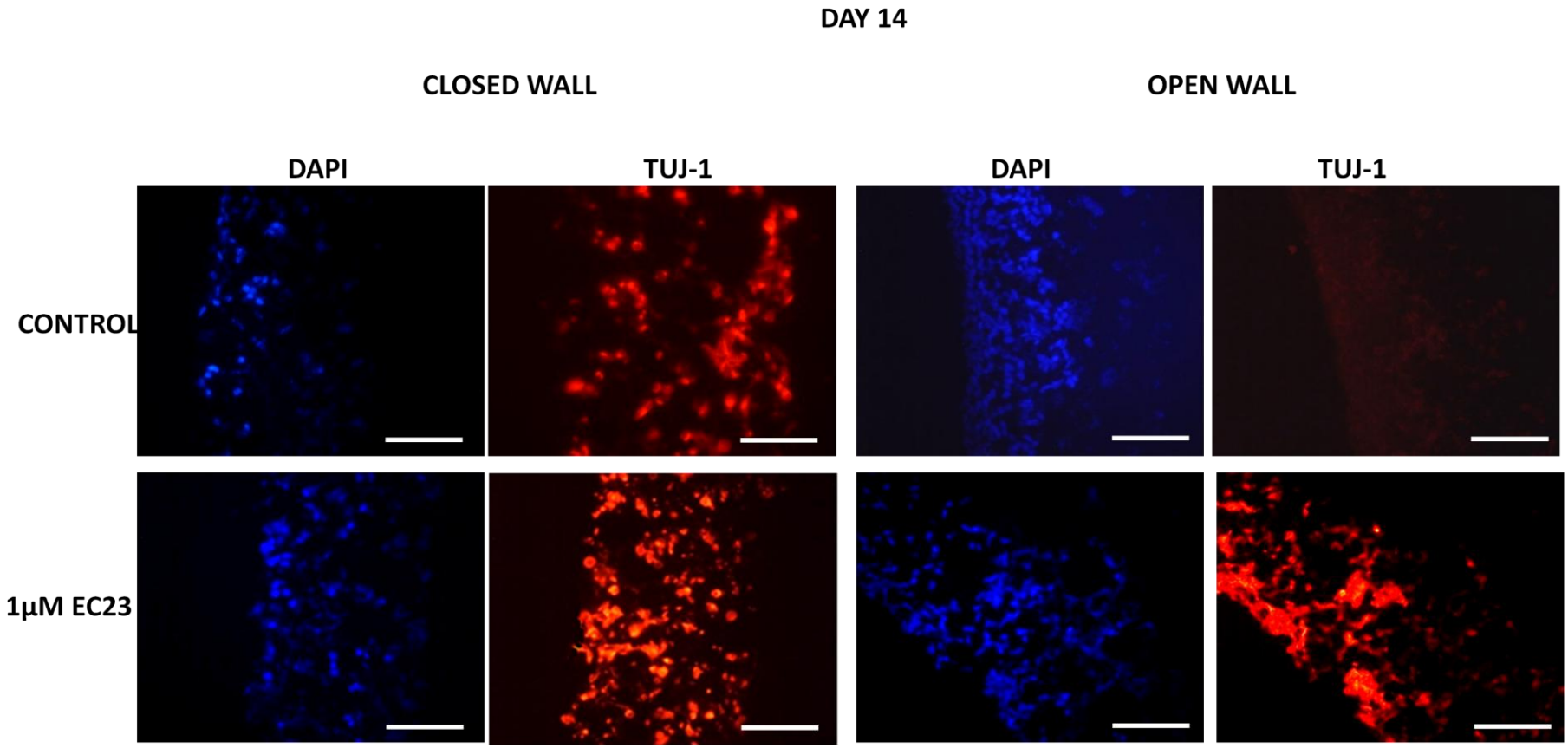

Figure 3.20 Immunofluorescence staining for TUJ-1 in open and closed insert cultures at day 14. Closed insert cultures show positive cells in both the control and EC23-treated cultures. Whereas in the control open insert cultures there no expression of TUJ-1 but comparable TUJ-1 expression in the EC23-treated cultures. Large areas of TUJ-1 expression demonstrate that the cells in the closed wall inserts differentiate in the control cultures. **Scale bar: 100µm**

closed wall inserts showed individual TRA-1-60 positive cells dispersed through the entire scaffold sections (Figure 3.19).

At day 14, all cultures were again immunostained for TUJ-1. Control cultures in the open inserts remained negative for TUJ-1 whereas there were now large areas of TUJ-1 positive cells in the open insert EC23-treated cultures, there was also significantly more positive cells than at day 7 (Figure 3.18). The levels of TUJ-1 staining were similar between the closed insert control culture and two retinoid treated cultures (Figure 3.20). There were more TUJ-1 positive cells compared to day 7 (Figure 3.19).

3.5.11 Neurite outgrowth in 3D cultures

Scaffold cultures in closed wall inserts were cultured for 4 days before the addition of either 1µM all-trans retinoic acid (ATRA) or 1µM of the photostable synthetic retinoid EC23. Retinoid treated cells were cultured for a further 16 days using the large reservoir Petri dish system. TUJ-1 staining of these cultures revealed neurite outgrowth which weaved through voids and interconnects of the scaffold (Figure 3.21). Scaffold cultures treated with EC23 produced higher amounts of neurite outgrowth than ATRA treated cultures. Figure 3.22 shows montages of the entire length of the retinoid treated scaffolds. These montages clearly showed that there is extensive neurite outgrowth which extended across the entire width of the scaffold rather than being confined to the area where the cells were initially seeded. There appeared to be move positive cells in EC23 cultures than ATRA cultures even though the DAPI staining suggested the cells in the two scaffolds are at a similar cell density.

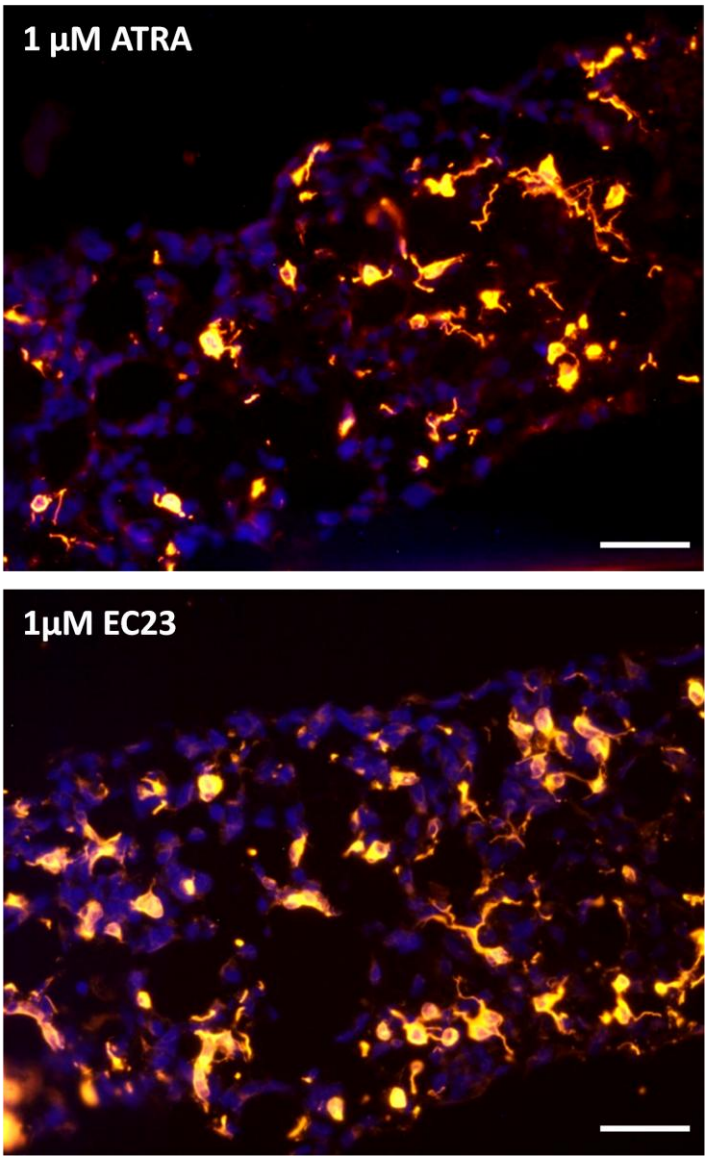

Figure 3.21 Neurite outgrowth in scaffold cultures. High magnification images of closed insert cultures at day 16 show TUJ-1 positive neurons and their neurites weaving through void of the scaffolds in both ATRA- and EC23-treated scaffolds. EC23-treated cultures display more evidence of neurite outgrowth than ATRA-treated cultures. **Scale bars: 50µm**

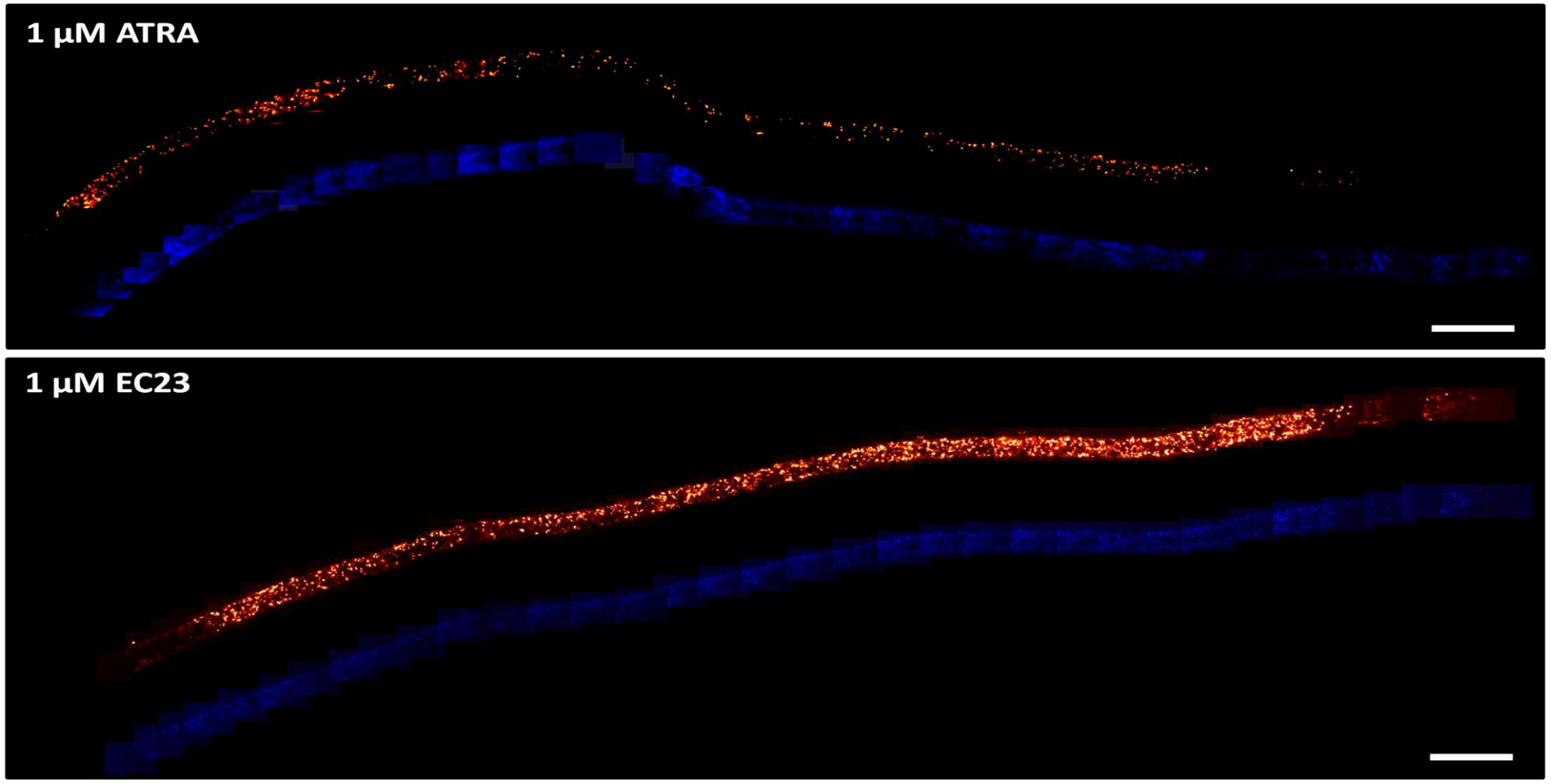

Figure 3.22 Montage of TUJ-1 positive cells along the entire length of the scaffold. Closed insert cultured for 16 days show positive cells distributed reasonably evenly along the whole length of the scaffold in both retinoid cultures. **Scale bar: 500µm.**

3.6 Discussion

During optimisation of 3D cell culture and the growth of pluripotent stem cells in the previous Chapter it became apparent that there were many more parameters that need to be considered when comparing 3D culture to standard monolayer cultures. 3D culture conditions need to be optimised to ensure cell survival, functionality and to allow homogeneous cell distribution across the 3D construct. These parameters are of particular importance when the 3D cultures are used to assess the development potential of stem cells *in vitro.* Sengers et al. reviewed various computational models to assess cell spreading and tissue regeneration in porous scaffolds and from their findings they suggest that controlling cell distribution and density throughout a construct is important for the development of tissues and the maturation of cells *in vitro* [223]. In this study I demonstrate how a viable 3D culture with a uniform cell distribution can be achieved across a porous scaffold within five days of cell seeding. Considerations include how a scaffold is presented/supported and how the cells receive nutrients and maintain high quality of media surrounding the construct.

3.6.1 Assessing the viability of cells in different scaffold presentations.

In order to assess the distribution and viability of cells during this study it is necessary to establish a method to accurately assess these parameters. Biochemical assays are the ideal method due to being a simple and quick method for assessing viability that can often be related to cell number. The MTS assay has been used in the previous Chapter to assess viability but there is increasing evidence of the inaccuracies of this assay especially in the presence of varying amounts of glucose. Huang et al. demonstrated that only in the presence of substantial quantities of glucose (4.5g/l) was the reading truly representative of cell number [224]. Considering that most of the data presented in this Chapter is between cultures varying in glucose concentration this was not considered a suitable assay, this was also confirmed in the cell growth profile in Figure 3.6A. Alternative methods for the assessment of cell viability have been assessed and they include the MTT assay for cell viability and the PicoGreen assay for measuring double-stranded DNA. Both assays proved to be more accurate than the MTS assay (Figure 3.6) and either would be suitable for further experiments. Taking into account the data presented in Figure 3.6 and comparisons of these methods by Ng et al. [222] it was decided that due to only comparing between 3D cultures, the MTT assay was suitable for assessing viability. This is because results from the assay can be obtained within a short time frame (~1 hour 15 minutes) and due to cell lysis there are no problems with the diffusion of the coloured substrate through a dense cell layer. Finally this method is more closely related to the British and European standard for testing *in vitro* cytotoxicity BS EN ISO 10993-5 [225]. When measurements of cell number are required the PicoGreen assay is more suitable but results take longer to obtain. This means that the MTT assay and the PicoGreen assay are both suitable for use with 3D cultures of Alvetex® scaffold. Choosing

between the two assays would depend on the requirements of each individual experiment, the MTT assay provides almost instant results but the PicoGreen assay provides an accurate cell number which is independent of the metabolic differences of each cell line and the metabolic differences that have previously been observed between 2D and 3D culture [222].

3.6.2 Differences between theoretical and experimental media quality profiles.

Figure 3.1 showed predicted media profiles for 2D and 3D culture. These profiles highlight the need for cell cultureware that has been specifically optimised for 3D culture to maintain high cell number due to the increased surface area for cell growth. Experimental profiles presented in Figure 3.8 substantially differ from the theoretical schematics. Figure 3.8 also presents a substantial argument for optimised 3D culture systems and provides data for better recommendation of feeding regimes for 3D cultures. The theoretical profiles do not take into account the increase in cell number that occurs from proliferating cells during culture. The increase in cell number is apparent in both the glucose and lactic acid metabolism of both 2D and 3D culture. Analysis of Figure 3.8B confirms that the standard 2D regimes of media changes every 3 days is not suitable for 3D culture as after three days in 3D cultures the lactic acid concentration is over double the concentration found in 2D cultures. Unfortunately the feeding regime tested in Figure 3.8C is also unsuitable for 3D cultures not only because cells are regularly disturbed leading to cell detachment but also due to the severe drop in media quality in the 24 hours between media changes. The ideal feeding regime for long term culture of cells in 3D would be to initially keep to the 2D culture regime changing the media every 3 days and this time period should be progressively shortened during long term 3D cultures.

3.6.3 Presentation of scaffolds for 3D cell culture.

I have developed simple systems to enhance the growth of stem cells in 3D using standard tissue cultureware. The most basic system is the 12-well system, this is a standard 12-well plate where the scaffold is held in place with polystyrene clips on the bottom of the well. The clips ensure that the cultures are always submerged rather than being cultured at the air-liquid interface but due to the simplicity of this format, cultures are only fed from the top surface of the scaffold as demonstrated by the schematic in Figure 3.3. To allow cells to feed from both surfaces of the scaffold and therefore limit the distance required for the diffusion of nutrients to only 100µm, scaffold were incorporated into a well insert that readily fits into a 6-well plate (Figure 3.3B). This system is similar to other transwell inserts which use porous membranes to either separate cells for co-culture experiments [226] or for the maintenance of organotypic cultures [227]. However such membranes only have pore sizes of approximately 0.45µm and a porosity of 80% meaning the inner and outer reservoirs must be filled separately and there is little diffusion between the two areas. This differs from the scaffold where movement of media occurs freely through the

scaffold. The inserts containing Alvetex® Scaffolds also fit into a 25mm deep Petri Dish using a well insert holder. This allows three inserts to be surrounded by an excess of medium (Figure 3.3C) – a method which was suggested by Heywood et al. to increase cell viability and function of cells in 3D [203]. Heywood et al. used exceptionally high volumes of media (6.4ml per 1 x 10^6 cells) to maintain cellularity and glycosaminoglycan synthesis of chondrocytes in 3D hydrogel constructs.

3.6.4 Scaffold formats affect media quality and cell viability.

As described in the introduction to this chapter there is evidence that three dimensional cultures display differing metabolic activity when compared to two-dimensional cultures, more specifically there is an increase in glycolysis and the build-up of lactic acid [197]. I have observed a rapid decrease in glucose concentration during 3D cell culture especially in the 12-well system (Figure 3.9A) this is due to the large surface area that is available for cell attachment and growth in a scaffold compared to a monolayer culture. Interestingly in the 12-well system at day 5, the cell number has reached 4 million cells (Figure 3.11A), this is equivalent to 1 million cells per ml of media. This is the cell density that Ozturk et al. [199] suggest is the limit for commercial standard cell culture media and may account for why the viability of cells does not increase past day 3 in the 12-well system (Figure 3.9D). Figure 3.10 also shows large areas of cell death in the 12-well plate system between day 3 and day 5 which confirms that the media is no longer able to support further cell growth. The rapid consumption of glucose is teamed with rapid production of lactic acid as would be expected; by day 3 lactic acid concentration has reached more than 20mM (Figure 3.9B) this is also teamed with a drop in pH of the cell culture media (Figure 3.9C). Under these conditions both Fernandes et al. [201] and Patel et al. [202] suggest that further cell growth is inhibited, however Zhu et al. [5] suggest that during 3D culture on collagen-chitosan scaffolds, the inhibitory effect of high lactic acid concentration can be overcome. Analysis of cell viability (Figure 3.9D), cell number (Figure 3.11A) and histological staining of cultures (Figure 3.10) confirms the inhibitory effect of 20mM lactic acid even when cells are cultured in 3D. This is in contrast with the findings of Zhu et al.

3.6.4.1 The effect of pH on cell viability in 3D

The pH of all samples of cell culture media at the beginning of the experiment (0 hours) was higher than the expected pH 7.4 and increased to pH 8.5 after 24 hours in culture in both the 12-well plate and 6-well insert systems but only to pH 8.2 in the large reservoir system (Figure 3.9C). This is due to media being buffered using bicarbonate ions which require the CO_2 atmosphere provided by the incubator in order to maintain pH. This also accounts for the difference between the different scaffold presentations; the large reservoir system has a large surface of media which is in contact with the CO_2 atmosphere in the incubator meaning this system is buffered more

readily than the other two systems. Bicarbonate ions are also thought to regulate the glucose uptake of cells in culture [228]. Lelong and Rebel [229] found that if standard DMEM buffered to a physiological pH 7.4, is placed into a CO_2 incubator, the pH drifts toward pH 8.52. I have also demonstrated the phenomenon in the 12-well and 6-well insert systems (Figure 3.9C). Lelong and Rebel also demonstrated that this change in pH could be overcome by the addition of 20mM HEPES to increase the buffering capacity of DMEM. It is possible that this method could also be used to increase the viability of cells in the 12-well system to allow for longer term cultures in the simple system. An increase in lactic acid concentration is accompanied by a controlled pH there is a lesser effect on cell proliferation [202].

3.6.5 Nutrient diffusion effects cell viability, cell number and infiltration.

To achieve a homogenous cell layer, cells need to maintain metabolic activity even in areas that are deep within the construct. This will ensure that the cells are still capable of synthesising and maintaining extracellular matrix. Unfortunately the uppermost layers of cells in porous scaffolds tend to consume most of the available oxygen and nutrients. This is clearly visible in Figure 3.10 where in the 6-well system there is a dense layer of cells at the surface of the scaffold after 3 days in culture and by day 5 there are areas of cell death which are highlighted by asterisks. This is due to the nutrients in the cell culture media not being able to diffuse through the dense cell layer. This is an alternative factor that affects cell viability and cell penetration other than the build-up of lactic acid in the 12-well plate system. In the 6-well insert system both of these factors have an effect on cell viability as glucose and lactic acid reach similar levels in this system as they do in the 12-well system (Figure 3.9A&B). Interestingly the inhibitory levels of lactic acid teamed with a lack of diffusion through the cell layer lead to a significant decrease in cell viability between days 4 and 5 (Figure 3.9D). The large reservoir system does not reach the inhibitory concentration of lactic acid and still has half the available glucose concentration (2.22g/L) after 5 days, but the MTT data does show a plateau in cell viability between days 4 and 5. This is most likely due to reaching the limits of the cell culture media. Analysis of cell number reveals that a scaffold placed in the large reservoir system contains 1.1 x 10^7 cells (Figure 3.11A) however there are three inserts placed in this system which means the 50ml of media is currently supporting approximately 3.3 x 10^7 cells in total plus any cells that may be growing in 2D on the bottom of the Petri dish. This is equal to at least 6.6 x 10^5 cells per millilitre of media which is beginning to stretch the media capacity.

As predicted by Heywood et al. [203] increasing the volume of media surrounding the 3D constructs does assisting in the production of a homogenous viable cell layer. Figure 3.11B shows the affect that increasing the volume of media and allowing the cells access to media from both sides has on the penetration of cells into the scaffold. In the 12-well plate format the TERA2.cl.SP12 cells are able to penetrate less than halfway through the 200µm thick scaffold.

Whereas once scaffolds are placed into an insert system it is possible for cells to move through the whole 200µm section and on average most cells penetrate over 100µm. By further increasing the media volume more cells are able to infiltrate the whole scaffold and more than three quarters of the scaffold width is filled with cells. Heywood et al. suggested that 6.4ml of media was required per 1 million cells for homogenous distribution of viable cells across their alginate constructs of diameter - 6mm and a height of 4mm (volume = ~113mm^3). Using the cell numbers from day 5 (Figure 3.11A), the 12-well system only has 1 ml of media per 1 million cells and not all these cells are viable as observed in Figure 3.10 and they also are unable to produce a dense cell layer. There is little difference in the number of cells per ml in the two insert systems once the three inserts in the large reservoir Petri dish have been accounted for. The 6-well insert system has 1.51ml per 1 x 10^6 cells and the large reservoir has 1.56ml per 1 x 10^6 cells but the Alvetex® scaffold only has a volume of 76.02mm^3 and the diffusion distance for nutrients is significantly less than the alginate constructs used by Heywood et al., it is therefore possible to produce a homogenous dense viable cell layer with less media per 1 million cells using Alvetex® scaffolds.

The three different formats of Alvetex® Scaffolds each have their own advantages: the 12-well plate system allows for short term culture of many samples in a small volume of media, for purposes such as toxicity screening. The 6-well insert allows cultures to be fed from both above and below. This produces healthier looking cultures than in the 12-well system where a barrier of cells tends to form at the surface as suggested by Sachlos and Czernuska [207]. The large reservoir Petri dish produces large colonies of TERA2.cl.SP12 cells infiltrating the scaffold along its entire length. These cells are healthy throughout due to the high nutrient availability provided by the excess media which allows for fewer media changes. This is ideal for long term (>1 month) culture experiments. The large reservoir system allows three contemporary scaffold samples to be acquired at one time for different applications (e.g. histology, RNA extraction and protein extraction).

3.6.6 Preventing localised build-up of lactic acid

It was recognised that the reservoir above the scaffold in both of the insert systems contains only a small amount of media (~2ml). From this reservoir of media the transfer of nutrients and the removal of waste products can only occur via the cell-filled scaffold. As cells replicate, this become more challenging and may lead to cell death at the top surface of the scaffold. Both the insert systems display a difference in lactic acid concentration between the two areas of the inserts. There is a difference of 1.2mM in the 6-well system and a larger difference of 6.2mM in the large reservoir Petri dish (Figure 3.9B). Localised areas of high lactic acid concentration can act as a signalling molecule rather than just a cell metabolite. The possibility that lactic acid has further importance than just a waste product is reviewed by Philp et al.[230]. There has also been

previous research demonstrating the effect of lactate during cell culture, Green and Goldberg found that incubating fibroblasts in lactate led to a ~2 fold increase in collagen synthesis [231] whereas Constant et al. demonstrated that increased lactate concentrations were able to upregulate vascular endothelial growth factor [232] and finally Zieker et al. demonstrated that lactate modulates gene expression in human mesenchymal stem cells [233] and recently this affect has been shown to be dose dependent [234].

To overcome the problems associated with a build-up of lactic acid, the standard well insert was redesigned to incorporate areas where it was possible for media to exchange between the inside of the insert and the main reservoir of media. Images and schematic of both types of insert are shown in Figure 3.12. The standard well insert is referred to as a closed wall insert whereas the redesigned insert containing windows is the open wall inserts, this system is similar to the windows used in Corning® Costar® snapwell inserts. There are three openings in the walls of the inserts – one between each of the legs used to suspend the insert within the well. To ensure the two reservoirs of the open insert are connected it is necessary to fill the large reservoir Petri dish containing open inserts with 75ml of cell culture media. Analysis of the quality of cell culture media was assessed in this new system in comparison to the standard closed wall inserts containing 75ml DMEM. The addition of windows to the insert has little differences in glucose concentration with the concentration difference between the inside and outside of the insert not greatly differing; however there is a lower glucose concentration in the open insert cultures as early as day 2 when compared to the closed insert cultures (Figure 3.13A). In contrast to this the lactic acid concentration profiles differ greatly between the open and closed insert cultures. There is no longer a significant difference in lactic acid concentration between the two reservoirs when the new open wall insert is used (Figure 3.13B). However the overall lactic acid concentration is higher (12mM) in the open wall insert cultures compared to the media surrounding the closed wall insert (10mM) but a more homogenous cell culture environment is possible when using the open wall inserts.

The localised build-up of lactic acid causes a difference in cell distribution in the scaffold cultures and affects the distribution of proliferating cells. In the closed insert cultures there are cells throughout the scaffold and only a small build-up of cells at the scaffold surface. This is due to cells migrating away from the build-up of waste products. There are proliferating cells throughout the scaffold presented in the closed wall insert (Figure 3.14A). Open insert cultures show a different cell distribution and the cells are able to grow at a high cell density with a large slab of cells at the top surface of the scaffold. Interestingly it is only the cells at the surface of the scaffold which are Ki-67 positive (Figure 3.14B). This distribution of proliferating cells also occurs in other 3D culture models such as tumour spheroids. Monazzam et al. show that spheroids formed from

the MCF-7 breast cancer cell line only have Ki-67 positive cells at the periphery (cell/media interface) of the spheroid [235]. In addition to this Laurent et al. found that the distribution of Ki-67 positive cells was dependent of the size of their Capan-2 pancreatic cancer spheroids. Large spheroids (500µm in diameter) had a similar distribution to the breast cancer spheroids with Ki-67 positive cells mainly at the periphery. This is a similar distribution to open insert cultures. Whereas small pancreatic cancer spheroids (300µm in diameter) had proliferating cells throughout the spheroid this is closer to the distribution of positive cells in the closed wall insert cultures [236]. Further staining of the two sizes of spheroids revealed that the central areas of the large spheroid stained positive for hypoxia marker pimonidazole whereas the small spheroids did not. This could also be the case for the two types of inserts cultures as the dense layer at the surface of the open wall cultures may be causing areas of hypoxic, non-proliferative cells within the scaffold interior.

3.6.7 Impact of metabolites on stem cell differentiation

Sub-optimal culture conditions can influence cell behaviour – specifically stem cell differentiation. From flow cytometrical analysis of TERA2.cl.SP12 monolayer cultures with the addition of lactic acid it is clear that high concentrations of lactic acid (20mM) cause the cells to significantly downregulate stem cell markers (Figure 3.15A&B) and also upregulation of early neuronal markers in monolayers (Figure 3.15C). SSEA-3 is a sensitive marker of the most primitive state for hESCs so would be expected to rapidly downregulate in adverse conditions [237] but the less sensitive pluripotency maker TRA-1-60 is also downregulated with the addition of lactate ions. This is of particular interest due to similar levels of lactic acid being produced in the closed wall insert cultures but not in cultures using the open wall inserts (Figure 3.13). Yanes et al. have previously demonstrated that metabolites affect the differentiation of embryonic stem cells and substrates of pro-oxidative reactions promote neuronal and cardiac differentiation [216].

The effect of lactate ions on nerve cells in culture and *in vivo* has been of particular interest since the proposal of the Astrocyte-Neuron Lactate Shuttle Hypothesis (ANLSH) by Pellerin and Magistretti in 1994 [238] and Tsacopoulos and Magistretti in 1996 [239]. This work has led to the suggestion that lactate is the preferential oxidative substrate for neurons in culture over the use of glucose [240], but there is no indication that lactate can replace glucose and become the unique energy substrate for neurons. However a review of the ANLSH by Chih and Roberts suggest that there is little experimental support for the hypothesis [241].

3.6.8 Lactates effect on differentiation of stem cells

From analysis of SSEA-3 and A2B5 expression in Figure 3.16 and immunostaining for Oct 4 (Figure 3.17), TRA-1-60 (Figure 3.19) and TUJ-1 (Figure 3.18 and Figure 3.20) it is clear that the build-up of lactic acid in the closed wall insert cultures leads to the differentiation of TERA2.cl.SP12 cells

when compared with open insert cultures. This may be due to the reduced metabolic demand of differentiated cells. There have been many studies which suggest that stem cells have a higher metabolic demand than their differentiated counterparts. Birket et al. found that human embryonic stem cells (hESCs) had a higher rate of energy turnover compared to hESC-derived neural stem cells (NSCs) [242]. They also demonstrated that there was a significant difference in the mitochondrial respiration rates used for protein synthesis and nucleic acid synthesis between hESCs and NSCs. In agreement with these finding Folmes et al. established that differentiating stem cells no longer needed to sustain high rates of replication and have lower anabolic demands but may require large amounts of energy for cell functionality [243]. This lower anabolic demand allows differentiated cells to catabolise substrates in a more energy efficient process. Undifferentiated cells require more energy, but Fornazari et al. demonstrated that neuronal differentiated stem cells produce ~200 times more lactate than the undifferentiated cells and underwent a shift from glucose oxidation to fermentation as the cells differentiated [244]. This study used a model embryonal carcinoma cell line in a similar way to this study but used the mouse EC line - P19.

I have established that differentiated cells require less energy but so far have not explained why lactate ions appear to promote neuronal differentiation. Previous studies in monolayer cultures have demonstrated that oxidative phosphorylation is not required for the survival of neuronal cells in culture. This was achieved by culturing neuronal cells in the presence of mitochondrial respiratory inhibitors [245-247]. There is also evidence that neural progenitor cells (NPCs) are able to survive with lactate as their exclusive metabolic substrate. The NPCs remain viable when cultured in 20mM lactate and 0mM glucose, this pure lactate metabolism does not affect caspase activity and appears to increase the viability of NPCs 1.5 fold [217]. This is contrast to the work by Bouzier-Sore et al. that has been previously mentioned [240]. Lampe et al. exposed NPCs isolated from developing brains of rats to lactic acid. This resulted in enhanced neural cell proliferation. They predict that this is due to the ability of lactic acid to scavenge free radicals such as hydroxyl radicals, hydroperoxyl radicals and superoxide radicals (reactive oxygen species – ROS) from the cell culture media [248].

The findings by Lampe et al. help to explain the effect lactic acid is having in the closed insert cultures as research has already demonstrated that hydroxyl radicals induces the differentiation of both the PC12 cell line [249] and SK-N-MC neuroblastoma cell line [250]. Lactic acid is able to scavenge these reactive oxygen species (ROS) [251]. These findings help to explain why control cultures with high lactic acid concentrations begin to differentiate, such as the closed insert control cultures where there is over a 40% difference in cells positive for the early neuronal marker – A2B5 when compared to the open insert control cultures (Figure 3.16B). Oravecz et al.

also demonstrated that treatment of SK-N-MC cells with hydroxyl free radicals for 72 hours caused a 32-fold increase in acetylcholinesterase activity – a marker of terminal neuronal differentiation [250], and may help to explain why closed insert cultures appear to have more developed neurite outgrowth (Figure 3.21) than their counterparts cultured in open inserts (Figure 3.18 & Figure 3.20). Interestingly the well-known inducer of neuronal differentiation – ATRA also increases intracellular reactive oxygen species production in P19 embryonal carcinoma cells [252].

3.6.9 Distribution of differentiated cells in 3D.

The immunostaining in Figure 3.21 suggests that there is increased neuronal differentiation in 3D cultures treated with the photostable synthetic retinoid – EC23 than the naturally derived ATRA. These finding are consistent with 2D cultures of TERA2.cl.SP12 cells [253]. Tonge and Andrews have previously suggested that the neuronal yield of NTERA2 cells was dependent on cell density [193]. An artificial cell density gradient of 2D cells was created using a concentrated seeding technique similar to the method that is used for the seeding on 3D cultures. After 3 weeks of RA-mediated differentiation, TUJ-1 positive neurons were only visible at the centre of the well in the high cell density area and not at the peripheries where cells were at a low cell density. These findings were compared with the TUJ-1 positive cells in 3D scaffold seeded using the concentrated method (Figure 3.22). In contrast to the findings of Tonge and Andrews, positive cells were present across the entire 22mm width of scaffold and not concentrated in the area initially seeded with cells. An even distribution of TUJ-1 positive cells occurs across both ATRA- and EC23-treated scaffolds.

3.7 Conclusion

Using the Alvetex® Scaffold:

- I have assessed the effect of media volume and scaffold presentation on cell metabolism, cell viability, and cell number.
- I have established the ideal culture conditions to produce a homogeneous cell distribution throughout the porous scaffold, this involved significantly less media per 1 x 10^6 cells than had been suggested in previous studies.
- Analysis of media quality has allowed for the development of modified cultureware for minimal disturbance of cells in tissue engineered matrices and recommendation of suitable time frames for media changes.

The cell culture environment that has been further optimised in this Chapter and the previous Chapter influences cell growth, maintenance of stem cell phenotype and differentiation of pluripotent stems cells in 3D. The production of a dense layer of homogenous tissue *in vitro* has allowed for studies into the differentiation of stems cells. It has established that the method chosen to present a scaffold affects neuronal differentiation as waste products and metabolites are able to regulate these processes more than previously anticipated.

4 Development and assessment of a substrate for the long term propagation of pluripotent stem cells in 3D culture.

4.1 Introduction

The environment in which a stem cell resides is known as its stem cell niche. The stem cell niche comprises of physicochemical and biological cues that provide a cell with information to determines its fate. External controls provided by structural, biochemical, mechanical and stimulatory cues make up the stem cell niche and stem cells are defined by their anatomical location [254]. The niche can be broken down into three major components: First cell-cell contacts, these are mediated by integral membrane proteins. For example membrane proteins that are involved in the Notch signalling pathway help mediate the specification of cell fate during development [33]. Second cell-extracellular matrix (ECM) interactions, which include interactions between transmembrane proteins known as integrins and extracellular matrix proteins – alteration of integrin expression ensures departure from the stem cell niche either through differentiation or apoptosis [255]. The third component is cell-soluble factor interactions. This is closely related to the extra-cellular matrix as ECM is thought to sequester and modulate the concentration of secreted factors [256]. A schematic detailing these factors can be seen in the introduction to this thesis (Figure 1.1)

4.1.1 Attempts to mimic the stem cell niche *in vitro*.

There have been many attempts to mimic the stem cell niche *in vivo* and the most basic of these involve culturing human embryonic stem cells (hESCs) on a feeder layer of mouse embryonic fibroblasts (MEFs). Mouse embryonic stem cells (mESCs) are able to grow without feeder layers while in the presence of the cytokine – leukaemia inhibitory factor (LIF). Unfortunately, unlike mESCs, human embryonic stem cells still require the presence of MEFs to maintain pluripotency as murine LIF and IL-6 do not act on human receptors [257] and even human LIF is not able to maintain stem cell pluripotency [187]. Due to this most recent attempts at mimicking the stem cell niche in standard cell culture involve surface modification of the cell culture substrate and conditioned media to replace the MEF feeder layer.

Surface coating for use with stem cells can often be used to promote the differentiation of pluripotent stem cells rather than maintain pluripotency. Specific coatings can be used to promote differentiation towards a specific lineage. These include collagen IV which is used to promote mesodermal differentiation and laminin coating which is mainly used for differentiation toward ectodermal cell fates [258] but can also be used for differentiation to endoderm more specifically pancreatic cells [259]. Other methods of surface modification can also affect stem cell

differentiation as well as stem cell self-renewal. Peerani et al. used BD Matrigel micropatterned surfaces to manipulate colony size and therefore differentiation towards extraembryonic endoderm [25]. This work was built on by Lee et al. where control of colony size was able to direct hESC fate towards either mesodermal or endodermal lineages. Large colonies (~1200μm) gave rise to mesoderm whereas small colonies (~200μm) gave rise to definitive endoderm while circular patterns helped to maintain pluripotency [260].

Coating with ECM proteins has more recently been used to maintain stem cell self-renewal. The first successful attempt at feeder-free culture of undifferentiated human embryonic stem cells was by Xu et al. in 2001 [261]. They were able to subculture undifferentiated hESCs for at least 130 population doublings on BD Matrigel coated tissue culture plates in 100% MEF-conditioned media. Matrigel is a reconstituted basement membrane preparation that is extracted from the Engelbreth-Holm-Swarm (EHS) mouse sarcoma. This tumour is rich in extracellular matrix proteins and the isolated ECM, is approximately 60% laminin, 30% collagen IV, and 8% entactin [262]. Transferring hESCs to the Matrigel coating led to no karyotypic changes. Cells on Matrigel maintained a comparable doubling time to cells grown on feeder layers. The feeder-free cells expressed the stem cell markers – Oct 4, SSEA-4, TRA-1-60 and TRA-1-81 and were also able to form teratomas after implantation into SCID mice. As an alternative to this strategy, well-defined media formulations have been developed to replace MEF condition media. An example of such a formulation is the mTeSR1 media produced by Stem Cell technologies. This media is a serum-free formulation for the maintenance of undifferentiated stem cells [263]. This defined media has been combined with synthetic coatings which are less variable than the Matrigel coating. These coatings include glycosaminoglycan-binding substratum which was used to culture stem cells for 2-3 months while still maintaining pluripotency markers [264]. They also include synthetic polymeric substrates such as poly[2-(methacryloyloxy)ethyl dimethyl-(3-sulfopropyl)ammonium hydroxide] (PMEDSAH) and hydrogel coatings such as aminopropylmethacrylamide (APMAAm). PMEDSAH allowed the hESC cell lines – H9 and BG01 to be cultured for 15 passages in either MEF-conditioned or defined media. Cells remained pluripotent without karyotypic changes [265]. APMAAm synthetic coating allowed H1 and a clone of H9 cells to be cultured for 10 passages in mTeSR1 media. The cells maintained the typical cell morphology seen in Matrigel coated cultures and maintained similar levels of Oct 4 and SSEA-4 [266]. Irwin et al. also noted that the bovine serum albumin (BSA) in the defined media was critical for the adhesion of the cells to the APMAAm surface.

Matrigel coated substrates have more recently been used to produce monolayer cultures of hESCs rather than their standard growth in colonies. It has been suggested that monolayers of pluripotent stem cells provide advantages over standard cultures as they are able to produce

larger numbers of viable cells from a similar cell culture area. Kunova et al. found that monolayer cultures no longer contained Oct 4 expression gradients, the cultures were more homogenous when SSEA-3 expression was assessed and finally the monolayer cells were more efficient at producing teratomas [267]. By being able to mimic the stem cell niche *in vitro* it increases the prospect for the production of the large numbers of cells required for stem cell therapies, regenerative medicine and gene therapy [268].

4.1.2 Adaptation of pluripotent stem cells to cell culture conditions

Indefinite self-renewal is a key feature of human embryonic stem cells but not a property of inner cell mass (ICM) cells from which they are derived. ICM cells eventually give rise to the definitive structures of the fetus, whereas hESCs have selected the ability to self-renewal during the adaptation to the cell culture environment [10]. Interestingly pluripotent stem cells are able to reverse to the ICM state when introduced into the blastocoelic cavity of host fertilized blastocysts [269]. The adaptation of stem cells to the 2D culture environment has become well-documented in recent years. ESCs in long term culture proliferate faster, become easier to maintain in culture [128] and long term culture leads to changes in their cell cycle properties. Barta et al. studied the cell cycle of hESC after short term (50 passages) and long term (240 passages) culture. At high passages there were a higher proportion of cells in G1 phase at the expense of the S phase and the S phase was shortened by approximately a third [270]. A high proliferative rate in stem cells cultures would appear to be advantageous as an increase in proliferation should provide the high number of cells required for downstream processes such as use in regenerative medicine and stem cell therapies. However increase in proliferation is often accompanied with less desirable adaptations to the cell culture environment.

Culture adapted hESCs tend to undergo karyotypic changes [10]. The most frequent karyotypic changes observed are gains of chromosome 12 and 17. Such changes can be compared to testicular germ cell tumours (TGCTs) where these non-random changes are also observed. More specifically the gain of isochromosome 12p is so common it is used as a diagnostic marker of TGCTs [8] and the addition of isochromosome 17q is associated with the nonseminoma germ cell tumours [9]. Baker et al. suggest that the repeated gain of these chromosomes in TGCTs and abnormal hESCs may suggest that these chromosomes contain genes which are critical for cell growth and potentially tumorigenesis [10], which begins to highlight the potential hazards of the clinical use of stem cells. Additionally it is thought that culture adapted ESCs may have a reduced capacity for differentiation. Teratomas formed from culture adapted cells contain histologically recognizable stem cells which grow out once the tumour is explanted and exhibit properties of starting embryonic stem cells [128]. It has also been reported that pluripotent stem cells in culture display high levels of expression for the gene encoding the Notch ligand Dlk-1. Dlk-1

increased 7 fold between normal and culture adapted ESCs [237]. Dlk-1 it is thought to be involved in the proliferation and self-renewal of stem cells [41] and Dlk-1 inhibits Notch signalling *in vitro* and therefore inhibits lateral inhibition. It is also thought to be required for the maturation of various tissue types [271]. Most current approaches to ES cell propagation rely on 2D monolayer cultures which as suggested above lead to changes to cell shape and function.

It has been suggested that a 3D model system is required for self-renewal and propagation of pluripotent stem cells as it will mimic the natural 3D tissue organisation, reduce culture adaptation and a system that allowed for the long term culture of stem cells in 3D may help elucidate the mechanisms of self-renewal [272].

4.1.3 Attempts at developing a 3D artificial stem cell niche *in vitro*.

Once a stem cell is removed from its microenvironment or niche and grown using traditional cell culture methods it loses many of the properties it had *in vivo* including the many exogenous signalling molecules that promote differentiation to a specific lineage. By placing cells back into a 3D culture system they can be fully ensheathed within a new artificial microenvironment [162]. The 3D environment also helps to maintain the 3D shape of stem cells. The shape of cells is particularly important during development as there are many examples of cell shape affecting morphogenesis. An example of a cell shape dependent event is the formation of the neural tube [61].

It has previously been demonstrated that differentiation of stem cells in 3D differs from differentiation in 2D. Such phenomena have been demonstrated in a range of systems including osteogenic [273], haematopoetic [32], neural [172] and chondrogenic [274] differentiation. This is attributed to the cells ability to form more complex structures due to complex interactions between cells achieved by increased cell contact in 3D. Culture in 3D better mimics the temporal and spatial regulation of gene expression and cell signalling that occurs during embryogenesis [27]. It would therefore be ideal to establish these interactions between cells by enabling propagation and self-renewal of stem cells in three dimensions.

As previously reported Kraehenbuehl et al. stated that a 3D model system is required for the self-renewal of pluripotent stem cells. They suggest that this system should have easily tailored mechanical properties, permit the migration of cells through or into the system, be able to adapt to support the expansion of cells, and have the ability to degrade as this property is key to the removal of cells from the matrix after expansion. They conclude by stating that the ideal 3D scaffold should have the capacity to replicate chemical, mechanical, 3D architectural or degradative environment of a specific extracellular matrix [272]. The remainder of this review will highlight a range of 3D systems that attempt to fulfil some of the above criteria.

Firstly, Gerecht et al. designed a single culture system to mimic early development and allow cells to switch to a differentiated state in the same culture setting in an attempt to mimic the ICM and regulate self-renewal and differentiation [275]. They used hyaluronic acid (HA) hydrogels to inhibit the differentiation of ESCs as they produced a homogeneity and structural coherence that is not encountered during embryogenesis. The concentration of hyaluronic acid in humans is at its highest in undifferentiated cells and early embryogenesis, differentiation causes a decrease in HA concentration [276]. Cells were encapsulated into the HA hydrogel using photopolymerisation. This process involves subjecting the cells to low levels of UV light. UV is known to cause DNA damage and tests performed by Gerecht et al. suggest that cells are not affected until exposure reaches 5 hours. However, this may limit the use of this method of 3D culture as encapsulating of cells at each subculture would increase the probability of DNA damage which has the potential to affect karyotype of the culture ESCs.

Culture of pluripotent cells in HA hydrogels appears to have no detrimental effect on ESCs. Cell maintained a doubling time that was comparable with 2D culture systems. However there was the potential for cell loss from the system as colonies close to the surface of the gel were released when cells remodelled the hydrogel matrix. Cells released after 20 days of encapsulation displayed high levels of SSEA-4 and alkaline phosphatase expression although this was not compared to 2D cultures. In line with the suggestions by Kraehenbuehl et al. it was possible to degrade the HA hydrogels for cell removal, however this process was not comparable to the subculture of cells from 2D culture as it required incubating the gels in hyaluronidase for 24 hours [275]. Overall this method of 3D culture fills some of the criteria suggested for an ideal 3D culture system but also contains elements which may be detrimental to long-term self-renewal.

Alternative systems to hydrogels involve fibrous polymeric scaffolds. Two such scaffolds have recently been suggested for the maintenance of stem cells under chemically defined conditions, one for human ESCs and the other for mouse ESCs. Liu et al. used electrospun polymethylglutarimide nanofibres for the culture of 3D mESC in feeder free conditions [277]. Liu et al. were able to achieve a comparable growth rate to 2D cultures and comparable levels of Oct 4 expression (95.4%) compared to cultures on MEFs (93.6%). Unfortunately these experiments were only in the short term (up to 4 days in 3D culture) and the density of the fibres was critical in order to avoid spontaneous differentiation. mESCs on high density fibres remained pluripotent but medium and low density fibres led to poor cell retention and low levels of Oct-4 expression.

A more developed system is presented by Lu et al. They describe an alginate and water soluble chitin (AWC) microfibre scaffold for the propagation, expansion, and cryopreservation of hESCs and induced pluripotent stem cells (iPSCs) [278]. hESCs encapsulated in the microfibres exhibited

a higher proliferation rate than their 2D counterparts. After long term culture in 3D the cells still expressed the stem cell markers Sox 2, Oct 4, nanog, and TRA-1-60, and after 10 passages in 3D, >90% of cells were Oct 4 positive. It was also possible to degrade the scaffold as suggested by Krahenbuehl at al. This processed involved treatment with a mixture of chitinase and alginate lyase and cell retrieval could be achieved within 10 minutes. A novel characteristic of the AWC 3D system is that it can be used for the cryopreservation of hESCs. Cells were frozen *in situ* in defined freezing media, and frozen using conventional methods. Constructs were thawed and cultured using the methods used prior to cryopreservation – this led to 75% hESC viability after thawing.

Lu et al. claim that to establish a truly biomimetic environment, it is necessary for stem cells to be embedded within the environment and not cultured as a monolayer attached to a scaffold structure. They suggest that non-encapsulated cells do not acquire the full benefits of interaction with the ECM but are subjected to fluid shear stresses. Fluid shear stresses and agitation of ESC cultures is known to induce differentiation of pluripotent stem cells [211].

All of the above methods cover at least one of the criteria suggested for an ideal 3D culture system for embryonic stem cells, but all methods are limited in their ability to reach these criteria. One of the main issues being the space for expansion within the 3D systems without producing colonies which are too large and begin to undergo necrosis at their centre, an issue previously described by Gerecht et al. [275]. Another issue arises from the method of cell encapsulation, this method leads to problems of mass transfer and the harvesting of cells without compromising viability or phenotype. Kraehenbuehl et al. also discussed the limitations of 3D culture. These limitations included problems with cellular oxygenation, nutrition and removal of waste products [272]. Considering the data in the previous Chapter to address such issues during 3D scaffold culture, it highlights the possibility of using a similar scaffold based technology to form a 3D artificial stem cell niche for the long term self-renewal of stem cells *in vitro*.

4.2 Aims of chapter

The aim is to establish a method for the culture, propagation, and expansion of pluripotent stem cells in 3D while maintaining their capability for self-renewal and differentiation. This will include the optimisation of a 3D culture system which allows for easy cell removal, ensures maintenance of the stem cell phenotype and causes no detrimental effect on their differentiation capabilities. Once 3D adapted cells are established they will be analysed to see if they more closely mimic cells *in vivo*, in terms of stem cell phenotype, cell shape and their ability to differentiate. This will help to highlight the benefits of 3D cell culture. This system will be established using the EC cell line TERA2.cl.SP12 as a model system to develop methods and the knowledge gained will be transferred to the culture and propagation of human ESCs in 3D.

4.3 Objectives

1. Describe materials to be used for the propagation of pluripotent stem cells in 3D
2. Optimise this 3D culture substrate for seeding method, surface treatment and length of culture as in Chapter 2.
3. Establish methods for the routine 3D propagation of pluripotent stem cells from substrate.
4. Assess cell retrieval, maintenance of stem cell phenotype, and changes of cell shape that occur during 3D culture, compare with 2D cultures and established method of 3D culture.
5. Transfer 3D adapted cells onto Alvetex® Scaffold and differentiate according to protocol established in previous Chapter.
6. Assess the differentiation potential of 3D adapted cells by allowing them to form cell aggregates and teratomas.
7. Use the knowledge gained from the above experiments for the successful propagation of hESCs in 3D culture.

4.4 Methods and Methods

4.4.1 Manufacture of Strata membranes

Highly porous Strata membranes were manufactured using the same materials as described in Chapter 2 for Scaffold membrane production. A basic schematic of the process is detailed in Chapter 2 Figure 2.1. The process was performed on a commercial scale and the difference between the production of Alvetex® Scaffolds and the membranes is an increase in stirrer speed to produce smaller void and interconnect sizes. In contrast to the non-commercial method for the production of Alvetex®, the Strata monoliths are extracted from their moulds and sectioned immediately into 200µm membranes using the vibratome (Leica VT1000S) prior to being washed as individual discs in a specially adapted washing bath. The Strata membranes fit into the open-wall inserts described in Chapter 3. The material produced is known as Strata and a comparison between the Alvetex® Scaffolds and Strata membranes is detailed in Figure 4.1. As with the Scaffold each void is connected to the neighbouring voids via interconnects and when the monolith is cut into 200µm slices there is an open surface structure (Figure 4.1E). The void size is significantly smaller so the material acts as a membrane to support 3D culture primarily on the surface of the membrane rather than allowing the cells to infiltrate into the interior (Figure 4.1H).

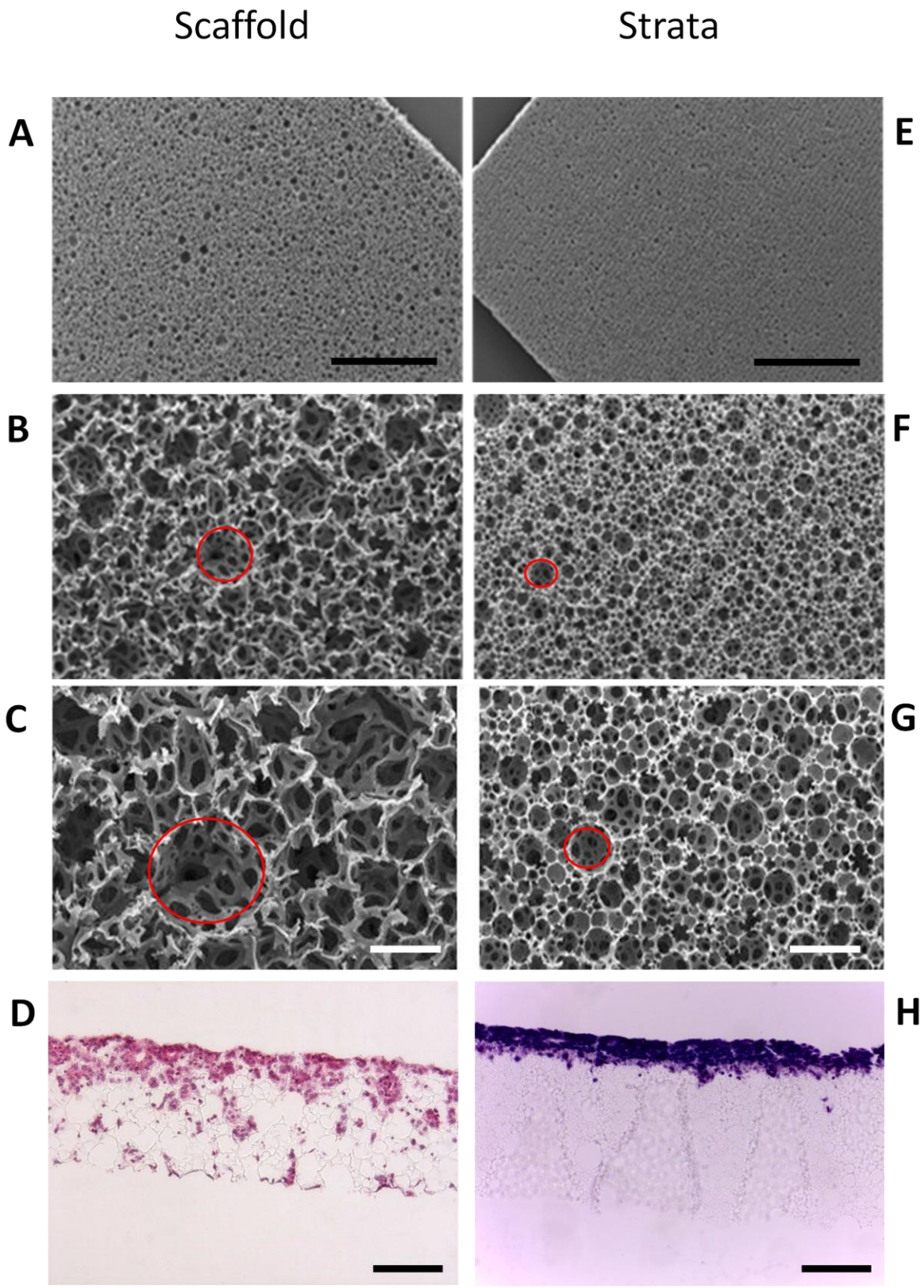

Figure 4.1.Structure of Alvetex® Scaffold compared to Strata membrane. A-C shows scanning electron micrograph of polyHIPE foam. Voids **(red)** are still linked by interconnects. Both can be cut into 200µm thick discs which have an open surface structure. The Strata membrane can also be placed into 6-well inserts ready for cell culture. The key difference between the two materials is the void size. The difference in void leads to a different type of 3D culture as shown in **D** and **H.** TERA2.cl.SP12 cells on Strata produce a dense layer at the membrane surface. TERA2.cl.SP12 cells were fixed after 4 days of culture. Scale bars**: A&E**=100µm, **C&G**=50µm, **D&H**=100µm. SEM images courtesy of Reinnervate Ltd.

4.4.2 Conventional 2D cell culture

4.4.2.1 Culture of TERA2.cl.SP12 EC cells

The pluripotent embryonal carcinoma cell line TERA2.cl.SP12 was cultured as described in the previous Chapter. Cells were maintained in T75 flasks (BD Bioscience) in high glucose Dulbecco's Modified Eagle Medium (DMEM) supplemented with 10% fetal calf serum (DMEM and FCS Invitrogen), 2mM L-glutamine and penicillin/streptomycin (Lonza). Cultures were passaged by rolling acid washed glass beads over the confluent cultures. All cultures were placed in a humidified incubator at 37°C and 5% CO_2. Cells were removed from the T75 flasks using 2ml of 0.2% Trypsin EDTA (Lonza) to form a single cell suspension for further experiments.

4.4.2.2 Culture of RC-10 ES cells

The human embryonic stem cell line RC-10 (Roslin Cellab: http://roslincellab.com/) was cultured as a feeder-free culture using CELLstart coating (Invitrogen) and the StemPro® hESC serum free media kit (Invitrogen). Cells were cultured in 6-well plates coated with CELLstart. The coating was diluted to 1:50 in PBS containing calcium and magnesium prior to the addition of 750µl of the solution to each well of the plate and incubated for 1 hour at 37°C. The StemPro kit is a serum-free and feeder-free media based on DMEM/F12 with Glutamax supplemented with 25% bovine serum albumin (BSA), StemPro hESC growth supplement (50x) and 10µg/ml basic fibroblast growth factor (bFGF). Complete media consists of 454ml DMEM/F12, 10ml of 50x StemPro supplement, 36ml of 25% BSA to a give a final concentration of 8% and finally 400µl of the 10µg/ml stock solution of bFGF to a final concentration of 8ng/ml.

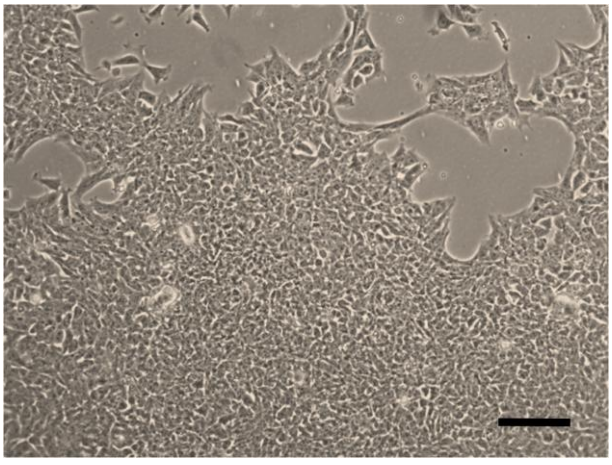

Figure 4.2. Standard 2D monolayer culture of the human embryonic stem cell line – RC-10. A 70 % confluent culture of RC-10 at passage 39. Scale bar: 100µm

RC-10 cells were thawed at 37°C and transferred to a centrifuge tube containing 4.5ml of warmed complete StemPro media. They were centrifuged at 1300 RPM for 3 minutes to pellet the cells. The supernatant was removed and 5ml of complete media was added and the pellet was carefully

broken up by pipetting. CELLStart solution was removed from one well of a 6-well plate and the 5 ml of cell suspension was added. Cells were incubated at 37°C and 5% CO_2 for 24 hours to allow cells to adhere before 100% of the media was changed to remove cell debris.

Cells were passaged using a manual dissociation technique. Media was removed from the cell layer and 3ml of fresh StemPro media was added. RC-10 cells were scraped from the bottom of the well using a 1000µl blue pipette tip, and the resulting cell suspension was split between 8 CELLStart coated wells. Media was changed every 48 hours until cultures reached 70-80% confluent. Cells were split 1:8 once a week. Figure 4.2 shows a 70% confluent culture of RC-10 cells which are ready for splitting 1:8. These cells have previously been documented and used in experiments involving the 3D printing of aggregates [279].

4.4.2.3 Culture of H9 ES cells.

The human embryonic stem cell line – H9 was also grown independent of a feeder layer on growth-factor reduced BD Matrigel (BD Bioscience). Cells were cultured in mTeSR1 serum-free defined media (STEMCELL Technologies) developed by Ludwig et al. [280] but the commercial media contains human FGF rather than the zebrafish FGF originally described. Cells were cultured in only the top three wells of 6-well plates. Each well was coated with growth factor reduced Matrigel, aliquots containing 1mg of Matrigel were defrosted on ice and then added to 12 ml of cold DMEM/F12 media (Sigma Aldrich, UK). A millilitre of this solution was added to each well and incubated at room temperature for 1 hour prior to use. Coated plates can be stored at 4°C for one week but need to be warmed to room temperature prior to use. H9 cells were cultured using the method described by Moody [281].

Cells were thawed in a water bath at 37°C before being transferred to 9ml of warmed DMEM/F12 media. The cell suspension was then centrifuged at 300g for 5 minutes to pellet the cells. The pellets were carefully resuspended in 500µl of complete mTeSR1 media to ensure that cell clumps still remain. Clumps under 60µm in diameter will not adhere to the well plate. Complete mTeSR1 media consists of 400ml mTeSR1 basal media with 100ml of 5x supplement plus 1.1ml penicillin/streptomycin. Each Matrigel-coated well has the remaining solution removed and was topped up with a further 1.5ml of complete media before the 500µl of cell suspension was added. Plates were moved from side to side to evenly distribute cell clumps. Media was changed daily to remove cell debris. Cells were passaged by aspirating the spent media and washing with 1 ml of PBS without calcium and magnesium. A millilitre of room temperature 0.2% EDTA (Versene) (Lonza) was added to each well and incubated at 37°C for two minutes. The EDTA solution was then removed without disturbing the cell layer and 4 ml of mTeSR1 media was added. Cells were scraped from the surface of the plate using a flexible cell scraper (SARSTEDT Ltd) to ensure that

the cells remain as aggregates. 500µl of cell suspension was added to room temperature Matrigel-coated plates and topped up to 2ml with mTeSR1 media. Cells were passaged every 4 days and were routinely split 1:8, ensuring that clumps of cells were maintained and well-distributed across the surface of the well.

4.4.3 Cell seeding onto Strata membranes

Cell seeding onto Strata membranes was optimised for use with pluripotent stem cells in a similar way to how the scaffold was optimised in Chapter 2. Seeding method, seeding density and surface treatment were assessed. The optimal conditions are to seed 0.5 x 10^6 cells onto ethanol-treated membranes using a dispersed seeding method (Figure 4.8).

4.4.3.1 Seeding and passaging of TERA2.cl.SP12 EC cells from Strata membranes

Strata membranes in open wall inserts were ethanol-wetted in 70% ethanol and washed twice in PBS containing calcium and magnesium. The final PBS wash was removed and 9 ml of media was added to the each well containing an insert. Cells were trypsinised from T75 flasks and counted using a haemocytometer and Trypan Blue assay. The cells were centrifuged and resuspended in media to allow for 0.5 x 10^6 cells in 500µl for each Strata disc. The 500µl of cell suspension was added to the well containing Strata inserts and 9 ml of media using a dispersed seeding technique (Figure 4.3 step 1). The plates were then incubated for 30 minutes at 37°C and 5% CO_2 to allow for cells to settle onto the membranes. After incubation, 500µl of fresh media was added down the side of the insert to allow for the two reservoirs of media to become connected (Figure 4.3 step 2). The cell containing membranes were then incubated at 37°C and 5% CO_2 for 24 hours. The media was then removed and replaced with 10ml of fresh media. They were incubated for a further 3 days with no media changes to avoid disturbing the dense cell layer.

After 4 days of growth of TERA2.cl.SP12 cells on 3D Strata membranes were removed from the inserts using a blunt pair of tweezers. The membranes were washed in PBS without calcium and magnesium and placed in the bottom of a 6-well plate. To each well containing a membrane, 2 ml of 0.25% trypsin EDTA was added and the plate was incubated at 37°C on an orbital shaker at 100 RPM for 7 minutes. After incubation the cells were scraped from the membranes using a flexible cell scraper (SARSTEDT Ltd 18.1832 – 16cm length & 1.3cm blade)(Figure 4.3, step 3). The trypsin EDTA was then neutralised using 3ml of cell culture media. Cell suspensions from individual discs were combined in a Falcon tube, centrifuged at 1000RPM for 3 minutes and the cell pellet was resuspended in 5ml of cell culture media. Cells were counted using a Trypan Blue assay and a haemocytometer then resuspended to a dilution of 0.5 x10^6 cells per 500µl and added to the

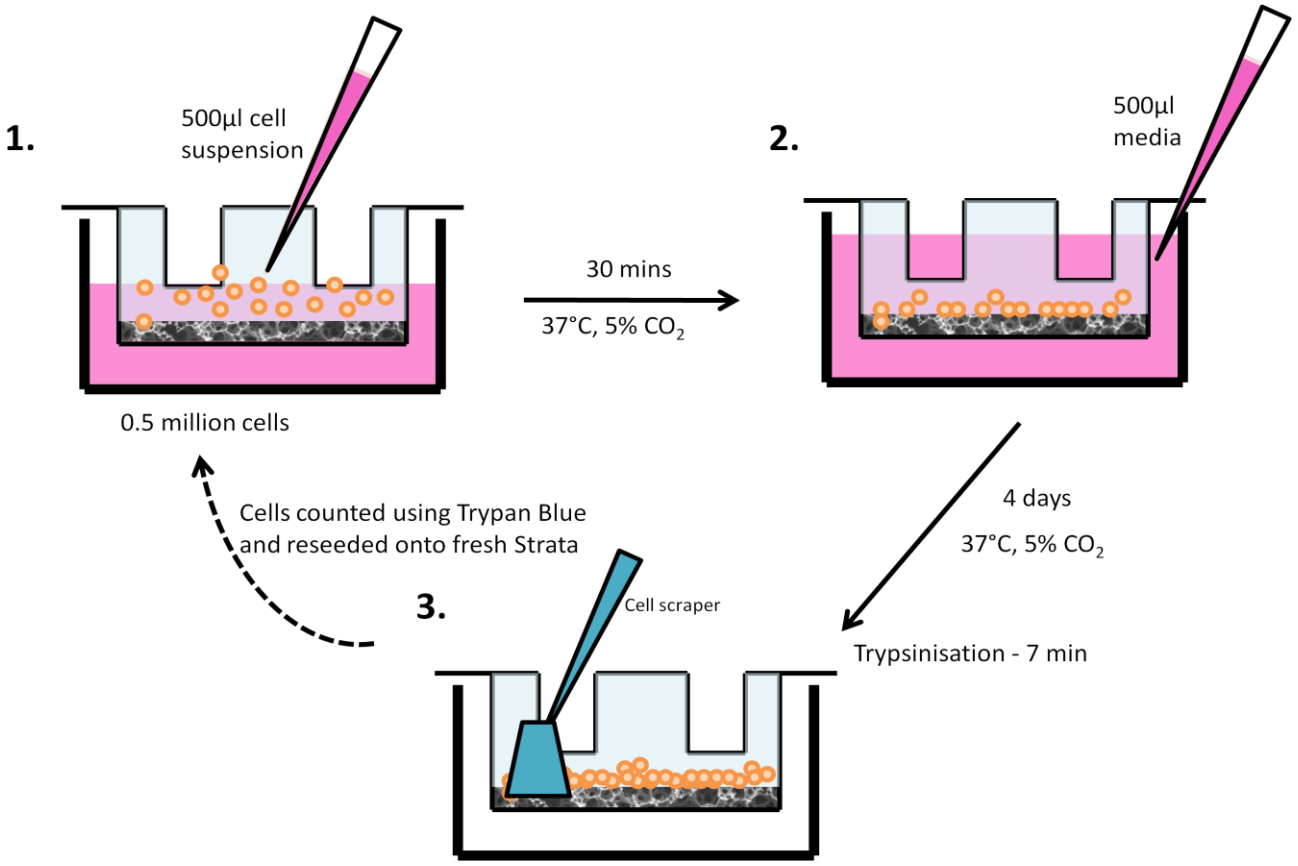

Figure 4.3. Passaging of TERA2.cl.SP12 cells in 3D from Strata. Strata membranes are ethanol treated and suspended in open wall inserts. Prior to cell seeding 9ml of media is added to the insert in a 6-well plate, so the two reservoirs of media are initially separate. In **step 1,** 0.5 million cells are seeded into the media on top of the membrane using the dispersed seeding method. This is then incubated for 15 minutes to allow cells to settle onto the membrane. In **step 2,** 500µl of fresh media is added down the wall of the insert to ensure the two reservoirs of media are now connected. The membrane cultures are incubated at 37°C and 5% CO_2 for 4 days without media changes. After 4 days the media is removed, membranes are washed in PBS and trypsin EDTA is added to the membrane. This is incubated at 37°C on a rotator plate for 7 minutes then the cells are scraped from the membranes using a cell scraper as shown in **step 3.** Trypsin EDTA is neutralised using cell culture media and cells are counted using a haemocytometer and a Trypan Blue exclusion assay . 0.5 million cells are seeded onto fresh membranes as in the first step. Excess cells are seeded onto additional membranes.

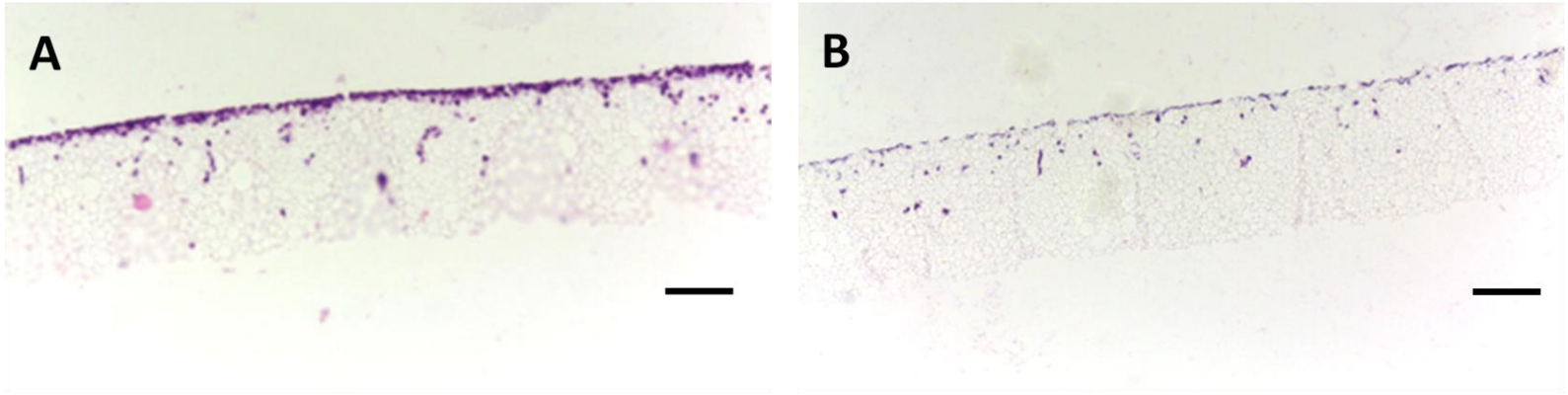

Figure 4.4. Histological analysis of TERA2.cl.SP12 cells grown and removed from Strata. After 4 days of growth on the Strata membrane there is a dense layer of TERA.cl.SP12 cells on the surface of the membrane **(A).** After trypsinisation and scraping only a few cells remain within the interior of the membrane **(B).** Scale bars: 100µm

membranes as previously described. Note that, it is necessary to count cells after every passage as cell proliferation slows after prolonged culture in 3D. This entire process is described schematically in Figure 4.3 and the effect of cell removal protocol is visible in Figure 4.4. The passage number of TERA2.cl.SP12 at the start of all 3D passaging experiments and their 2D counterparts was passage 31. All passage number presented in this Chapter are p31 plus the number of passages in 3D. After each passage, cells were sampled for flow cytometry, and placed into 2D culture to assess cell shape.

4.4.3.2 Passaging RC-10 ES cells from Strata membranes

Strata inserts were treated with 70% ethanol and washed twice in 5ml of sterile deionised water, before being coated with CELLStart. As previously described for 2D cultures, the CELLStart coating was diluted to 1:50 in PBS containing calcium and magnesium prior to the addition of 750µl of the solution to each insert containing Strata which had been placed on the bottom of a Petri dish. Strata membranes were incubated for 1 hour at 37°C. After incubation, excess CELLStart was removed via aspiration, 5ml of StemPro culture medium was added and the plates were placed in a CO_2 incubator to equilibrate. RC-10 cells were removed from the 6-well plate which they had been cultured in, using Accutase solution (Sigma Aldrich, UK). The cells were dissociated to form a single cell suspension and cell number was determined using a Nucleo-counter NC-3000 (ChemoMetec A/S). The inoculation volume was calculated based on the viable cell count only and membranes were seeded with 1 x 10^6 cells each. Membranes containing cells were cultured for either 3.5 days or 7 days between each passage. Media was changed every 48 hours. When cells were ready for passaging, inserts containing membranes were washed twice in PBS with calcium and magnesium and then placed into a Petri dish containing 20ml of warmed Accutase. Inserts were allowed to sit undisturbed at room temperature for 15 minutes. During this time, 5ml of fresh media was placed into each well of a 6-well plate. After incubation the Strata inserts were removed from the Accutase solution and placed into the wells containing media. Using a 1000µl pipette and tilting each individual inserts the cells were removed from the membrane by repeatedly pipetting the media onto the membrane. Cells from multiple membranes were collected into centrifuge tubes and centrifuged at 1300RPM for 3 minutes. Cells were again counted using NC-3000 and reseeded onto fresh membranes as previously described.

4.4.3.3 Passaging H9 ES cells from Strata membranes

Strata membranes were coated with growth factor reduced BD Matrigel in a similar way to 6-well plates. Six inserts containing membranes were placed in the bottom of a deep well Petri dish before the addition of 1ml of the Matrigel diluted in DMEM/F12 was added to the centre of each insert. Inserts were incubated at room temperature for 1 hour prior to use. Cells were removed from the bottom of 6-well plates using 0.2% EDTA and a cell scraper as previously described. This

was to ensure that cells remain in clumps and did not form a single cell suspension. Matrigel-coated inserts were placed in 6-well plates and 7ml of complete mTeSR1 media was added to each well. Clumps of cells were counted using the clump counting method described by Moody [281]. H9 cells were centrifuged at 300g for 5 minutes and were carefully resuspended so as not to break up clumps, at a density of 350 clumps per 500µl. The 500µl suspension was added to the centre of each of the inserts using the dispersed seeding method; membranes containing cells were incubated overnight at 37°C and 5% CO_2. After 24 hours in culture the entire cell culture media was removed and 10ml of room-temperature mTeSR1 media was added to each well. A partial media change was performed every 24 hours by removing 5ml of media from the well so the membrane was at the air liquid interface and then 5ml of fresh mTeSR1 was added to the cultures.

Cells were initially passaged every 4 day using a similar method to the passaging of TERA2.cl.SP12 cells from Strata membranes. Membranes were removed from inserts and placed in the bottom of a 6-well plate. 2ml of 0.2% EDTA was added to each well containing a membrane culture and incubated at 37°C on a orbital shaker at 100RPM for 2 minutes. The EDTA solution was removed and 2 ml of DMEM/F12 was added to each membrane. Cells were gently scraped from the membrane using the flexible cell scraper. Cell clumps were counted and a suitable amount was centrifuged at 300g for 5 minutes to allow for approximately 650 clumps per membrane. Clumps were then resuspended in 500µl mTeSR1 media per membrane and seeded as previously described onto Matrigel®-coated membranes. After 4 passages in 3D, the time between passages was increased to allow for the decrease in cell proliferation. Passage 5 cells were split after 5 days in culture, passage 6 after 6 days and there after cells were passaged every 7 days. During the 7 days between passaging part media changes were performed everyday as previously described apart from on day 4 when a complete media change was performed. All passage numbers of H9 cells presented in this Chapter are p52(8) plus the number of passages in 3D or their 2D counterparts from the beginning of experiments. This passage number refers to 52 passages on fibroblast feeder layer + passages in feeder-free cultures (bracketed number) and then a 3D passage number, For example p52(8) +3D p6.

4.4.4 Suspended cell aggregate formation

Aggregates were formed from TERA2.cl.SP12 cells. Cells were trypsinised from their cultured substrates and counted using the Trypan Blue assay. Cell suspensions were centrifuged at 1000 rpm for 3 minutes and the cell pellet was resuspended to allow for 1 x 10^6 cells per 100µl. This 100µl of cell suspension was added to 10ml of complete DMEM in a non-coated bacteriological Petri dish. After 24 hours, synthetic retinoid EC23 was added to the Petri dishes to a final concentration of 1µM. Cells were allowed to form aggregates and media was changed every 2-3

days by transferring aggregates to a 50ml centrifuge tube and allowing them to settle to the bottom of the tube. After 10 minutes the spent media was removed and aggregates were carefully resuspended in 10ml of fresh media containing 1µM EC23. Aggregates were cultured for 21 days and phase images were captured every few days using the Nikon Diaphoto 300 with connected digital camera and ACT1 image capture software. Images were analysed using the ImageJ software (http://rsb.info.nih.gov/ij/) and setting the scale within the program. The average diameter of aggregates was measured using a range of images.

Cell aggregates that were passaged in conjunction with the 3D passaged cells did not undergo induction of differentiation using EC23 but were dissociated every four days and allowed to reaggregate.

4.4.5 Processing of cell aggregates for immunohistochemistry

Cell aggregates were fixed at suitable time points by placing the media containing aggregates into Falcon tubes and centrifuging at 200 rpm for 5 minutes. Media was removed and aggregates were washed twice in PBS, centrifuging between each wash step. Aggregates were resuspended in 4% PFA and fixed at room temperature for 30 minutes. After fixation, aggregates were wash twice in PBS and then dehydrated through 30% and 50% ethanol for 10 minutes each – it is necessary to centrifuge the aggregates between each step as above. The 70% ethanol dehydration step was replaced with a staining step. Crystal violet was dissolved in 70% ethanol at a concentration of 0.05% (w/v) (Sigma Aldrich, UK). Aggregates were resuspended in 1ml of the Crystal violet solution for 10 minutes. The aggregates were then dehydrated fully with 10 minute incubations in 80%, 90%, 95% and 100% ethanol, aggregates were allowed to settle to the bottom of the tube during each incubation step so the supernatant could easily be removed. Crystal violet-stained aggregates were resuspended in Histoclear for 10 minute then 50:50 Histoclear to paraffin wax solution for 30 minutes and then two 30 minute incubations in paraffin wax. Aggregates were embedded in wax using dispomoulds (CellPath Ltd) and blocks were sectioned at 6µm using a Leica Microtome RM2125RT prior to floating on a 40°C histology water bath and mounting onto electrostatically charged SuperFrost+ slides (Fisher Scientific).

4.4.6 Immunocytochemistry on 2D monolayer cultures.

Monolayer cultures were immunostained in a similar way to previously described for 3D cultures. Cultures were fixed by removing the cell culture media, washing twice in PBS and fixing in 4% PFA for 30 minutes at room temperature. Cultures were washed a further two times with PBS prior to permeabilisation with 0.1% (v/v) Triton X-100 in PBS for 15 minutes. Cells were blocked using blocking buffer (0.1% Tween-20, and 1% normal goat serum in PBS) for 30 minutes prior to the addition of primary antibodies diluted in blocking buffer (See Table 4.1). Primary antibodies were

incubated with the monolayer on ice for 1 hour before washing for 3 x 10 minutes in blocking buffer on a rotator plate at 40rpm. Fluorescent-conjugated secondary antibodies were diluted in blocking buffer with Hoescht 33342 to stain nuclei or phalloidin if required (Table 4.1) and incubated with the monolayer for 1 hour in the dark on ice. Immuno-stained cells were washed as before for 3 x 10 minutes prior to imaging using either a Leica fluorescence microscope DMI 3000B with connected camera – DFC310 FX or Leica SP5 Confocal Laser Scanning Microscope. Negative controls for immunocytochemical staining are shown in Figure 4.5.

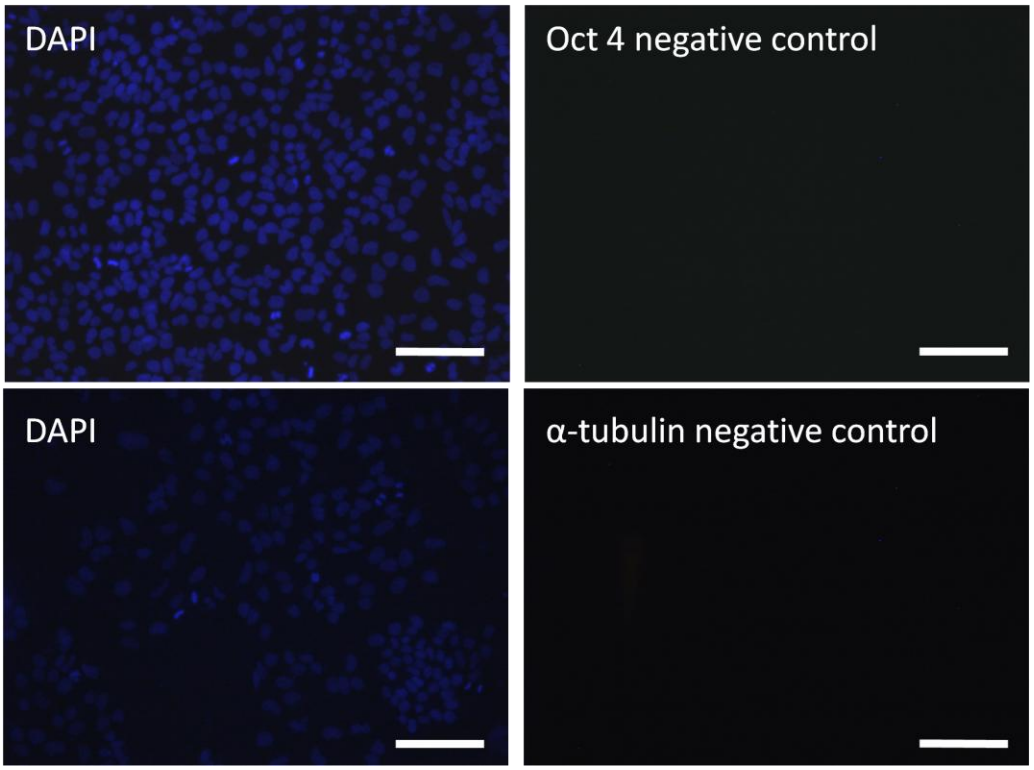

Figure 4.5 Negative control for Oct 4 and α-tubulin immunocytochemistry on standard 2D cultures. The standard immunocytochemistry protocol was performed without the addition of the primary antibody, to demonstrate the degree of background staining. Scale bar=100µm

Primary Antibody	Supplier	Dilution in blocking buffer	Secondary Antibody	Supplier	Dilution in blocking buffer
Oct 4 Rabbit polyclonal	Abcam (ab19857)	1:250	Goat anti-rabbit IgG (H+L) Alexafluor 488	Invitrogen (A11008)	1:600
α-tubulin Rabbit polyclonal	Abcam (ab18251)	1:2500	Cy3-AffiniPure Donkey Anti-Rabbit IgG (H+L)	Jackson ImmunoResearch	1:600
			Acti-stain™ 488 phalloidin (F-actin stain)	Universal Biologicals (Cambridge) Ltd (PHDG1)	1:500
Nuclear stain			Hoescht 33342	Molecular Probes (H3570)	1:1000

Table 4.1 Antibody dilutions for immunocytochemistry on monolayer cultures**.**

4.4.7 Assessing the effect of 3D culture on proliferation and cell shape.

To assess the difference in cell shape, cell density/proliferation between TERA2.cl.SP12 cells cultured in 2D and 3D, cells were transferred to monolayer cultures in 12-well plates. After each passage cells from 2D and 3D were trypsinised from their culture surface as described above, counted using a haemocytometer and 2 x 10^5 viable cells were seeded onto 16mm glass coverslips in 12-well plates. Wells were topped up with 3ml of complete DMEM and cultured for a further four days. Phase contrast images were taken every 24 hours and used to assess cell density of the cultures, from which proliferation can be assessed and also to measure changes in cell shape. Due to being seeded on glass coverslips these cultures can be processed for imaging using the confocal microscope. Cultures were processed for immunocytochemistry as described above. After immunostaining, the coverslips were removed from the well and attached to glass slides using Vectashield immunofluorescence mountant (Vector Labs) and a large rectangular coverslip was placed on the top and sealed using nail varnish.

4.4.7.1 Measuring cell circularity

The change in cell shape that occurs during 3D cultures was assessed using the phase micrographs from the above mentioned cultures on glass coverslips. Individual cells from both 2D and 3D cultures were assessed by measuring their circularity. Cell circularity was measured using the equation previously described by Ballester-Beltrán et al.[282]. The area and perimeter of 10 individual cells in 3 separate phase images was calculated using the ImageJ software (http://rsb.info.nih.gov/ij/) and silhouettes of individual cells were also recorded by cutting individual cells that had been assessed for circularity from the phase images (Figure 4.18). To measure circularity the follow equation was used which is based on the surface area of a sphere:

$$Circularity = 4\pi \times \left(\frac{cell\ area}{cell\ perimeter}\right)^2$$

Circularity of cells was measured at a range of passages on 2D and 3D cells for the four day period after they were reseeded into 12-well plates.

4.4.8 Calculating cell density of 2D cultures

Monolayer cultures were fixed in 4% PFA after 4 days in culture. Cultures were then stained with Hoescht 33342 to highlight nuclei. The number of nuclei was counted in five randomly selected 100µm squares in 5 separate images for every passage number and culture condition. Cell density was calculated as the number of cells per 100µm^2.

4.4.9 Differentiation of cells on Alvetex® Scaffolds

After 10 passages in either 2D or 3D culture, TERA2.cl.SP12 cells were transferred to Alvetex® Scaffolds to assess their ability to differentiate in 3D. Cells were seeded onto the scaffolds using

the optimised protocols previously described using the large reservoir Petri dish and the addition of 1µM EC23 after 4 days to establish the cultures. Cultures were grown for either a further 7 or 14 days before being processed for flow cytometry or being fixed in 4% PFA for immunohistochemistry.

4.4.10 Subcutaneous transplantation of pluripotent stem cells to form teratomas

All procedures involving mice were conducted in accordance with guidelines and permission granted by the Institution and the Home Office, UK. Cells were trypsinised from either 2D or 3D culture using the methods previously described. Viable cells were counted using the Trypan Blue assay and 0.5 x 10^6 cells were resuspended in 100µl of cell culture media. Each cell suspension was combined with 100µl of BD Matrigel (BD Bioscience) to increase the success rate of tumour formation. The resulting 200µl of cell suspension was loaded into 1ml syringes with 21G needles and stored on ice until required. Cells were injected subcutaneously into adult male nude (nu/nu) mice. Each animal received grafts bilaterally on the flanks. To validate the findings 3 mice were injected with each cell type, giving the possibility of 6 tumours per cell type. Mice were examined regularly and when teratoma formation was visible the tumour was measured at least once a week until they reached 1cm^2. At this point mice were sacrificed and teratoma tissue was surgically removed. This was usually between 6-8 weeks after injection.

4.4.11 Processing of teratoma tissue.

Teratoma tissue was immersed in 4% PFA immediately after removal and fixed overnight. Tissue was washed 3 times in PBS and transferred to Falcon tubes before dehydration. Tissue was progressively dehydrated through a range of ethanols (70%, 80%, 90%, 95%, and 2 x 100%) for 2 hours each. When the last 100% ethanol was removed, teratomas were incubated in Histoclear (National Diagnostics) to clear the tissue for 2 hours. Tubes containing tissue were then topped up with paraffin wax to produce a 50:50 solution of Histoclear:Wax. Tubes were incubated at 60°C overnight before the solution was removed and paraffin wax was added and again incubated overnight, this step was repeated a further three times before the teratomas were embedded. Teratomas were sectioned to 6µm using a Leica Microtome RM2125RT prior to floating on a 40°C histology water bath and mounting onto electrostatically charged SuperFrost+ slides. Consecutive sections of each teratoma were cut and the central section was stained with Haemotoxylin and Eosin and neighbouring sections were immunostained for germ layer markers.

4.4.12 Imaging of whole teratoma sections

Teratoma sections were stained using Haemotoxylin and Eosin as described in Chapter 2. To produce montages to highlight the size and complexity of the teratoma, images were taken using the Nikon Diaphoto 300 with connected digital camera and ACT1 image capture software.

Overlapping images were captured across the entire tissue section. Images were digitally 'stitched' together using Microsoft PowerPoint software to produce a montage.

4.4.13 Immunohistochemical staining of teratoma sections

Teratoma sections were de-waxed in Histoclear and rehydrated through 100% ethanol (2 minutes), 95% ethanol (1 minute), 70% ethanol (1 minute) and deionised water (1 minute) before being placed in 10mM citrate buffer at pH6 (10x stock: 19.2g anhydrous citric acid in 1000ml dH_2O). Antigen retrieval was performed by microwaving the slides for 3 x 2 min at 800W. Slides were left to stand in the warm citrate buffer for 20 minutes and subsequently incubated in permeabilisation solution (0.1% (v/v) Triton X-100 in PBS) for 15 minutes. Teratoma sections were blocked in 0.1% Tween-20, and 1% normal goat serum in PBS for 30 minutes. Primary antibodies were diluted in 200µl of blocking buffer per slide as detailed in Table 4.2. Sections were incubated at 4°C in a humidified chamber overnight before washing for 3 x 10 minutes in blocking buffer on a rotator plate at 100rpm. Fluorescent-conjugated secondary antibodies were diluted in blocking buffer with Hoescht 33342 to stain nuclei and incubated on the sections for 1 hour at room temperature. Immuno-stained scaffolds were washed as before for 3 x 10 minutes and mounted in Vectashield mounting media (Vector Labs). Coverslips were attached and sealed using nail varnish. To produce negative controls the tissue was incubated overnight in blocking buffer rather than primary antibody but the remainder of the protocols was consistent (Figure 4.6)

Each teratoma was stained for the ectodermal markers – TUJ-1, nestin, NF-200 and cytokeratin-8, mesoderm marker – smooth muscle actin (SMA), endoderm marker – α-fetoprotein (AFP), and embryonic stem cell marker – Oct 4. The slides were examined using Leica DMI 3000B fluorescence microscopy with connected camera – DFC 31- FX and the Leica AF software.

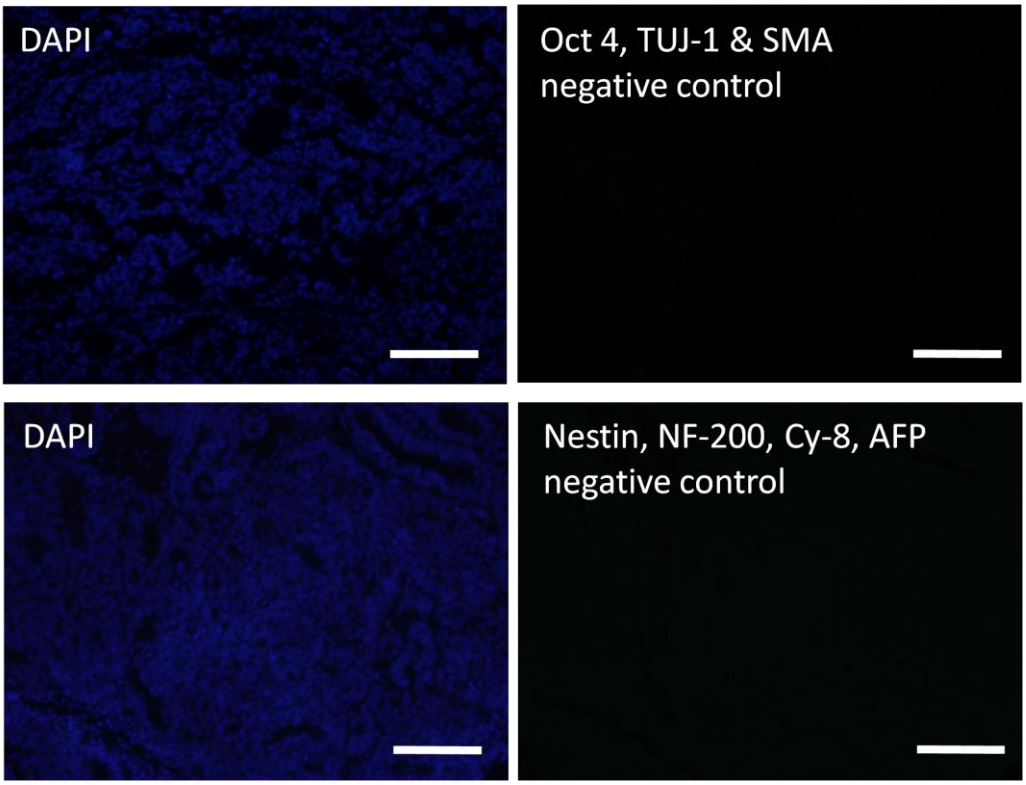

Figure 4.6 Negative control for Oct 4, TUJ-1, SMA, nestin, NF-200, cytokeratin-8, AFP immunohistochemistry on teratoma sections. The standard immunohistochemistry protocol was performed without the addition of the primary antibody, to demonstrate the degree of background staining with Alexfluor 488 anti- Rabbit secondary (top) and Alexafluor 488 anti-mouse (bottom). Scale bar=100µm

Primary Antibody	Supplier	Dilution in blocking buffer	Secondary Antibody	Supplier	Dilution in blocking buffer
Oct 4 Rabbit polyclonal	Abcam (ab19857)	1:250	Goat anti-rabbit IgG (H+L) Alexafluor 488	Invitrogen (A11008)	1:600
Rabbit Polyclonal neuronal Class III β tubulin (TUJ-1)	Cambridge Bioscience (PRB-435P-100)	1:600	Goat anti-rabbit IgG (H+L) Alexafluor 488	Invitrogen (A11008)	1:600
Nestin Mouse monoclonal	Abcam (ab22035)	1:500	Goat anti-mouse IgG (H+L) Alexafluor 488	Invitrogen (A1101)	1:600
Anti-200 kD Neurofilament Heavy antibody, mouse monoclonal	Abcam (ab77745)	1:200	Goat anti-mouse IgG (H+L) Alexafluor 488	Invitrogen (A1101)	1:600
Monoclonal Anti-Cytokeratin Peptide 8 antibody produced in mouse	Sigma Aldrich UK (C5301)	1:200	Goat anti-mouse IgG (H+L) Alexafluor 488	Invitrogen (A1101)	1:600

Rabbit polyclonal to alpha smooth muscle Actin	Abcam (ab5694)	1:100	Goat anti-rabbit IgG (H+L) Alexafluor 488	Invitrogen (A11008)	1:600
Monoclonal Anti-α-Fetoprotein (AFP) antibody produced in mouse	Sigma Aldrich, UK (A8452)	1:500	Goat anti-mouse IgG (H+L) Alexafluor 488	Invitrogen (A1101)	1:600
Nuclear stain			Hoescht 33342	Molecular Probes (H3570)	1:1000

Table 4.2 Antibody dilutions for immunohistochemistry of teratoma sections.

4.5 Results

4.5.1 Characterisation and comparison of 3D scaffolds and Strata membranes

Strata is an inert non-degradable membrane constructed from porous polystyrene polyHIPE. Each void of the scaffold is connected to the neighbouring voids via interconnects, this can be clearly visualised on the SEM micrograph in Figure 4.1E-G, where voids are highlighted in red. Voids are linked to multiple neighbouring voids through a network of smaller interconnects. As with Alvetex® Scaffolds, Strata monoliths were sliced into membranes of 200µm thick and 22mm in diameter, the membranes were then fitted into 6-well sized open-wall inserts. The membranes have an open surface structure which is shown in the SEM micrograph in Figure 4.1E; this ensured the movement of media through the construct to feed the cells from both surfaces. Figure 4.1A presents a comparison of the Strata membrane with the previously used Alvetex® Scaffold. The basic structure of the two materials were identical (Figure 4.1A-C compared to Figure 4.1E-G) apart from a difference in void and interconnect size. These differences in void and interconnect size mean that when cells are added to Strata they produce a different type of culture to the Scaffold cultures (Figure 4.1D compared to Figure 4.1H). In the Alvetex® Scaffold, cells were able to form a layer of supported tissue which can be cultured for long term experiments (Figure 4.1D) whereas the Strata membrane is able to produce a dense layer of tissue where cells were able to interact with each other without interference from a scaffold but it was only possible to culture cells like this in the short term (Figure 4.1H).

Strata membranes undergo quality control procedures using the same methods as the Alvetex® Scaffold testing described in Chapter 2. The void size was determined from analysis of SEM micrographs and statistical correction of the measured diameters. Average void diameter was plotted against frequency to establish the modal void size of the polyHIPE membrane. Figure 4.7A shows an example of void size analysis for the Alvetex® Scaffolds which have a modal void size of 40µm, although the voids ranged from 30µm - 90µm. In contrast to this, Strata membranes had a modal void size of 15µm and only ranged between 13µm-20µm (Figure 4.7B). Interconnect size was also monitored using mercury porosimetry. The diameter of interconnects in Alvetex® Scaffold was between 11µm and 14µm to allow the movement of cells through the construct (Figure 4.7C). To reduce the movement of cells into the interior of the Strata membrane as the membrane was for use as a support matrix the interconnect size is limited to 6.45µm (Figure 4.7C).

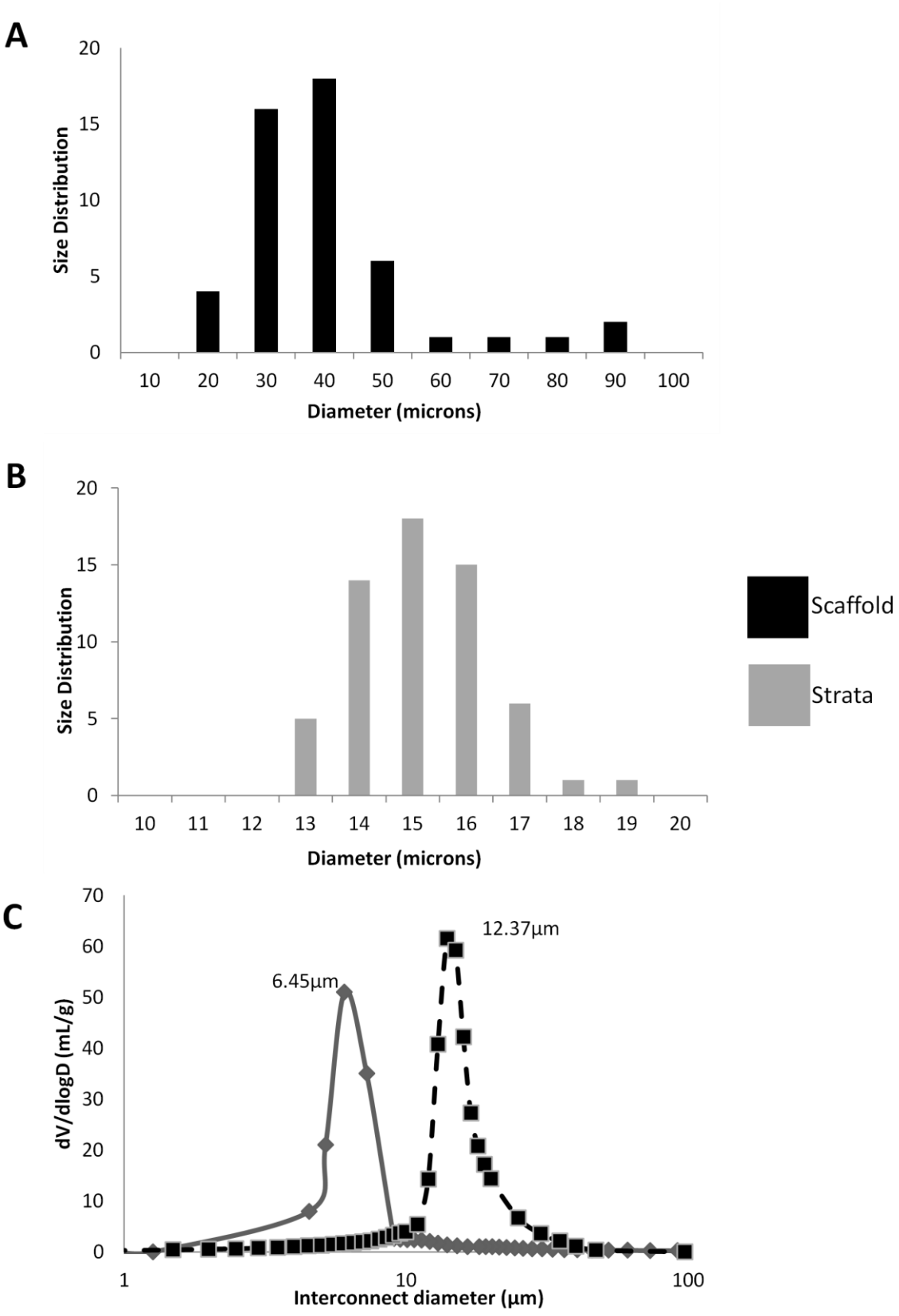

Figure 4.7. Analysis of the structure of Alvetex® Scaffolds compared to Alvetex® Strata membranes. The Scaffolds have a consistent structure with an average void size of 40µm **(A, black)** (determined by measurement of voids from SEM images) and 12.37µm interconnects (**C, black)** which is determined using mercury porosimetry. Whereas Strata membranes have an average void size of only 15µm **(B, grey)** and an interconnect size of 6.45µm **(C, grey).** Data courtesy of Reinnervate Ltd

4.5.2 Optimisation of Strata membranes for the growth of pluripotent stem cells.

As described by the literature review for Chapter 2, the successful culture of 3D constructs requires additional optimisation compared to monolayer cultures to ensure viable cells are observed throughout the construct and a homogenous distribution of cells is achieved. To mimic the optimisation procedures for Alvetex® Scaffolds for the growth of pluripotent stem cells, Strata membranes were assessed to establish the cell numbers which could be achieved using the membranes, the optimal cell seeding method, and surface treatment for the membranes. Finally to produce a growth profile for cells grown in 3D using membrane cultures.

First, surface treatment of membranes was assessed as per previous experiments. The optimised plasma treatment parameters used for the treatment of Alvetex® Scaffold (40W for 5 min) were used with the Strata membranes. Untreated Strata membranes appeared very similar to the Alvetex® Scaffold (Figure 4.8D) but if Strata undergoes plasma treatment the membranes begun to thin and can split (Figure 4.8E). The longer treatment of 10W for 30 minutes was suitable and caused no detrimental effect on the membranes. This method was then compared with ethanol treatment of the membranes. There was very little difference between the two treatments and due to this it was decided that plasma treatment at 10W for 30 minutes was unnecessarily time consuming and promoted more cell growth into the interior of the membrane which was not required.

Second, cell seeding method was assessed again using both an MTT assay (quantification not shown) and a PicoGreen assay. There was no significant difference in cell number after four days of culture between the cell seeding methods, with both membranes holding approximately 4 x 10^6 TERA2.cl.SP12 cells (Figure 4.8A). However the staining of full membrane discs with the MTT substrate showed that there was a difference in viable cell distribution across the membranes seeded using the two different methods. When the concentrated seeding method was used, after 4 days there were very few viable cells at the centre of the membrane in the area where cells were initially seeded. Viable cells had started to congregate at the periphery of the membrane (Figure 4.8B). In contrast to this the dispersed seeding method led to a more even distribution of cells with a dense layer across most of the surface of the disc (Figure 4.8C).

Third, the cell growth profile for TERA2.cl.SP12 cells on membrane was significantly different to that seen on Alvetex® Scaffolds (Figure 2.11) Cells on the membrane were only viable up to approximately day 5 as seen in the graph in Figure 4.9. There was a rapid drop in cell viability from day 5 onwards. Histological analysis of membrane cultures revealed that between days 1 and 5, a dense layer of cells forms at the surface of the membrane. These cells were still present at day 7, but at later timepoints they were no longer present. There were no obvious signs of cell

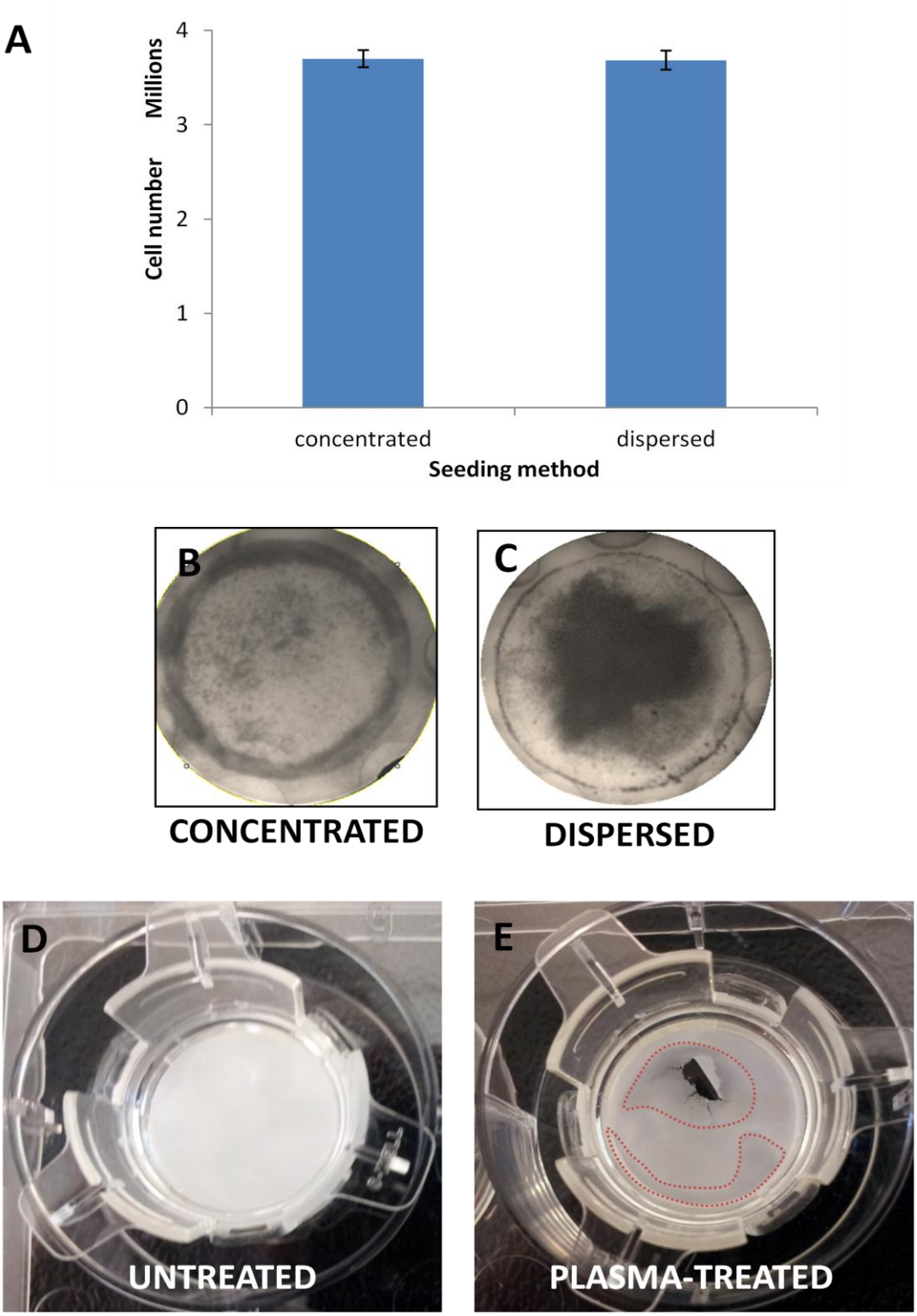

Figure 4.8. Optimisation of TERA2.cl.SP12 cell growth on Strata membranes. The seeding methods originally described in Chapter **2** were assessed for use with Strata. Both seeding methods were assessed at day 4 using the PicoGreen assay. There is little difference in cell number between the two seeding methods **(A**). However staining the entire scaffolds using an MTT solution shows that when seeding using the concentrated methods cells tend to congregate at the periphery of the scaffold **(B)** whereas using the dispersed leads to a more homogeneous cell distribution **(C).** Surface treatment of Strata membranes was also assessed, uncoated strata membranes appear very similar to Alvetex® Scaffolds **(D**) but if Strata membranes are plasma treated at 40W for 5 minutes this causes thinning of the materials and can cause splitting of the membrane **(E)** Red dotted lines highlight areas of degradation on the membrane. Data represents mean ±SEM, n=3

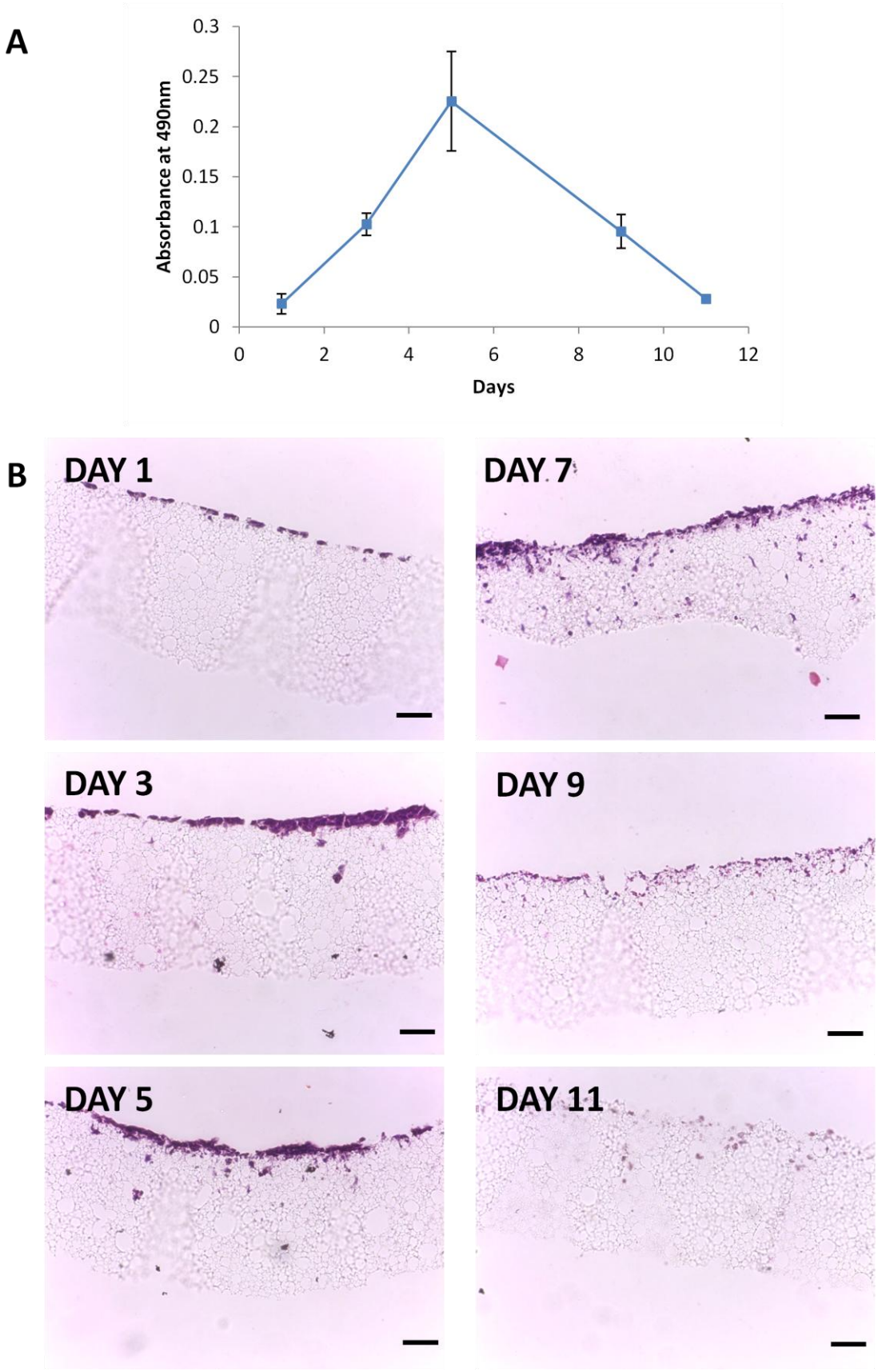

Figure 4.9. Cell growth profile for TERA2.cl.SP12 on Strata membranes. The growth profile using an MTS assay to assess viability for TERA2.cl.SP12 cells on Strata shows an increase in viability up to day 5 but after this there is a rapid decrease in viability **(A).** This is also evident in the H&E stain sections where the cell layer is reduced at day 9 and 11 **(B).** Data represents mean ±SEM n=3 **Scale bars: 50µm**

death on the images suggesting that when the cell layer reached a critical size it no longer attached to the membrane but rather attach to each other and became dislodge from the membrane.

4.5.3 Cell retrieval from Strata membranes.

Passaging of cells from Strata membranes is detailed schematically in Figure 4.3. The process involved enzymatic treatment to loosen the cell layer and manual removal with a cell scraper. This is required due the cells not being attached to a smooth surface. The process was fully optimised and a range of incubation times in trypsin EDTA were tested to ensure complete cell retrieval with limited cell death due to over exposure, both removal methods were included to reduce this time in trypsin EDTA. Figure 4.4 shows the effect of successful cell retrieval from the membranes. After 4 days of cell growth, discs containing TERA2.cl.SP12 cells were cut in half and one of the halves was fixed in 4% PFA. The other contemporary half of the scaffold underwent the retrieval protocol to demonstrate the effectiveness of the cell retrieval process. From the H&E stained images it was clear that the majority of the cell layer had been successfully removed (Figure 4.4A). The remaining cells were in the interior of the membrane and had been grown at a low cell density.

4.5.4 Maintenance of cell viability and proliferation during passaging of cells in 3D.

The cell retrieval protocol did not have any detrimental effect on cell viability. This was evident from the cell counts in Figure 4.10. After each passaging procedure, TERA2.cl.SP12 cells from individual membranes were resuspended in 2ml of media before being counted using a haemocytometer and Trypan Blue assay to assess the number of live and dead cells for reseeding onto fresh membranes. Cell counts were taken from at least 6 individual membranes and averaged to produce the graph. After an initial adaptation period at passages 0 and 1, cell number routinely at least double at each passage. Every 3-4 passages (notably p4 and p10) there was a large increase in cell number to approximately 1.75 x 10^6 cells, but this cell proliferation rate cannot be maintained. At passage 6, cells were removed from the membranes and were frozen down in FBS containing 10% DMSO. After storage at -80°C for two weeks, the 3D cells were thawed counted and reseeded onto membranes for a further four passages. As expected there was a slight increase in the number of dead cells after cell revival, but cells were successfully revived into 3D cultures and continue to at least double every four days. Histological analysis showed the dense layer of cells which is present on the membrane at a range of passage numbers. As passage number increased fewer cells were visible in the interior of the Strata membrane.

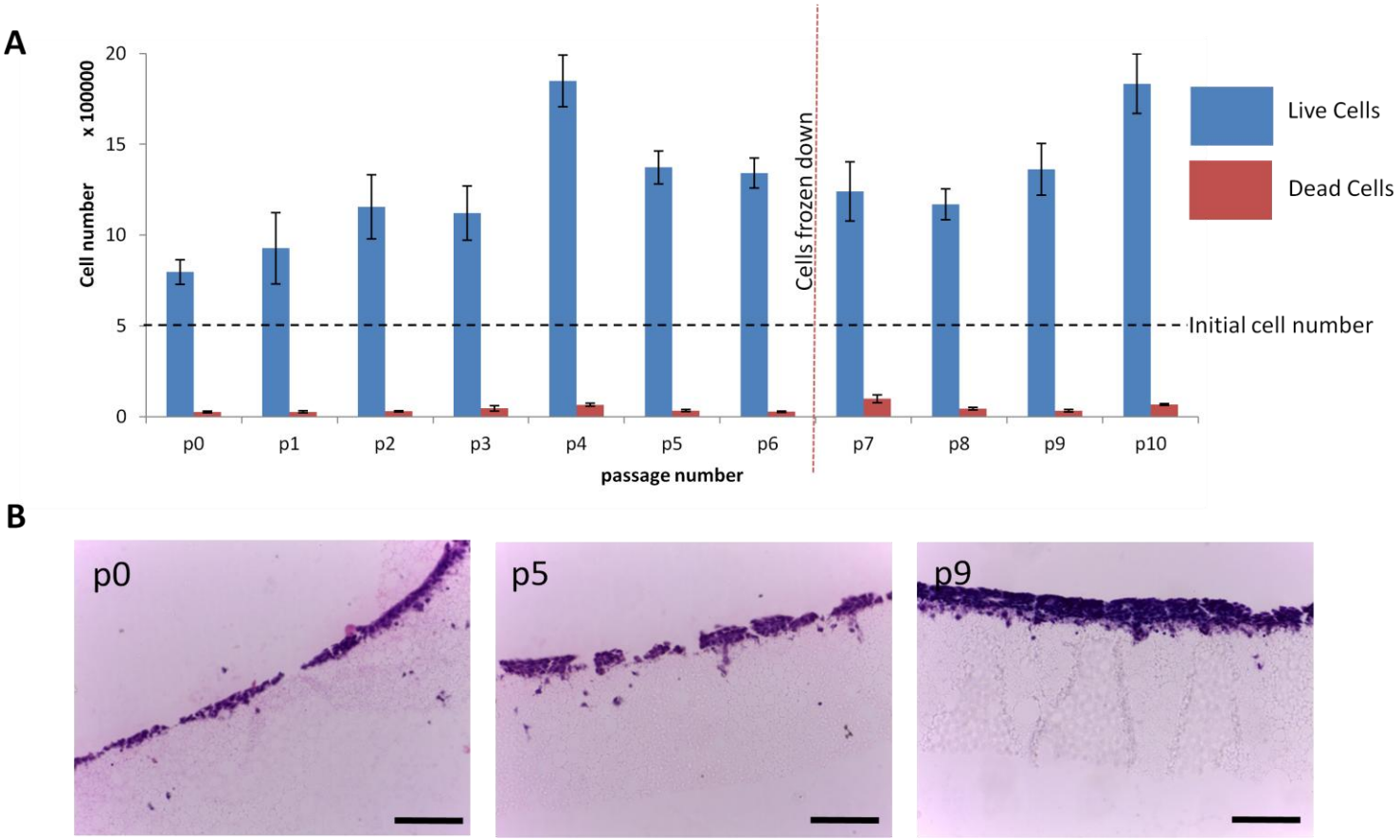

Figure 4.10. Cell proliferation after passaging in 3D on Strata membranes. TERA2.cl.SP12 cells were passaged every 4 days. Cells from individual membranes were counted using a Trypan Blue assay and the number of live and dead cells were recorded **(A**). The graph demonstrates that cell number increases every 4 days although at low passage the increase in cell number is less than doubled this could be due to cells adapting to the 3D environment. At passage 6 cells were removed from the membrane and frozen down, after storage at -80°C for two weeks the cells were revived directly onto Strata membranes. There appears to be no detrimental effect on the number of live cells but a slight increase in the number of dead cells on the cells recovery from cryopreservation. **B** shows Haemotoxylin and Eosin staining of 3D cultures at a range of passage numbers. A thick layer of cells is clearly visible on the membrane surface. This data demonstrates that prolonged cultivation of TERA2.cl.SP12 cells in 3D has no detrimental affect on cell number. Data represents mean, ±SEM, n=10**. Scale bars = 100µm**

4.5.5 Maintaining stem cell phenotype during 3D passaging.

TERA2.cl.SP12 cells of the same original passage number as the 3D cells were passaged in 2D in T25 flasks in conjunction with the 3D passages. The same cells were also grown in suspension culture as aggregates and acted as a positive control of 3D cells that spontaneously differentiate. After each passage in 2D and both types of 3D culture, membranes, flasks or Petri dishes containing aggregates were sampled for flow cytometry. Cells in all formats were trypsinised to form a single cell suspension before staining for flow cytometry with either the stem cell marker – SSEA-3 or the early neuronal differentiation marker – A2B5. Over the range of passage numbers, the 2D cells remained consistent - approximately 60% of 2D cells were SSEA-3 positive (Figure 4.11A) and 15% of cells were A2B5 positive (Figure 4.11B). This represents an undifferentiated monolayer of cells. In contrasts to these results, aggregate cultures spontaneously differentiated. At passage 0, the cells had only spent 4 days in a suspension culture and displayed similar levels of SSEA-3 expression as the 2D cultures (~70%) (Figure 4.11A). As passage number increased the levels of SSEA-3 positive cells rapidly dropped to less than 20% and remained at this level for all other passages (Figure 4.11A). The drop in SSEA-3 positive cells was teamed with an increase in A2B5 expression to 20% at passage 3 and 60% at passage 8. Cells cultured in 3D on Strata membranes did not differentiate like the 3D aggregate cultures but also differred from the 2D cultures. At passage 0 the 2D and 3D cultures displayed similar levels of SSEA-3 positive cells but as the cultures progressed there is a significance difference in SSEA-3 expression with 80% of cells positive at passage 3 which represented a 20% difference in the amount of positive cells ($p=0.01$) and there is a similar difference in expression at passage 8 ($p=0.001$). By passage 8 there was also a significant difference in the percentage of A2B5 positive cells between 2D and 3D cultures with 3D cultured cells displaying a significantly lower level of A2B5-positive cells ($p=0.01$) (Figure 4.11B).

Phase micrographs in Figure 4.12 confirmed that there were no large areas of cell differentiation in the 2D cultures, and cell morphology remained consistent throughout the 8 passages. This was a typical TERA2.cl.SP12 culture with cells closely packed together. Cells are routinely allowed to reach 100% confluent as close cell contact is required to maintain their stem cell phenotype and prevent spontaneous differentiation. To confirm that the 2D cells were able to maintain their stem cell phenotype for multiple passages representative monolayer cultures were immunostained for the embryonic stem cell marker – Oct 4. At both passages the majority of cells were Oct 4 positive (Figure 4.13). 3D cultured cells were also tested in a similar manner. Alvetex® Strata membrane cultures were fixed and processed for histology as previously described for Alvetex® Scaffold cultures. Haematoxylin and Eosin sections showed the dense layer of cells that it was possible to produce on the surface of the membranes. The cell layer was multiple cells thick

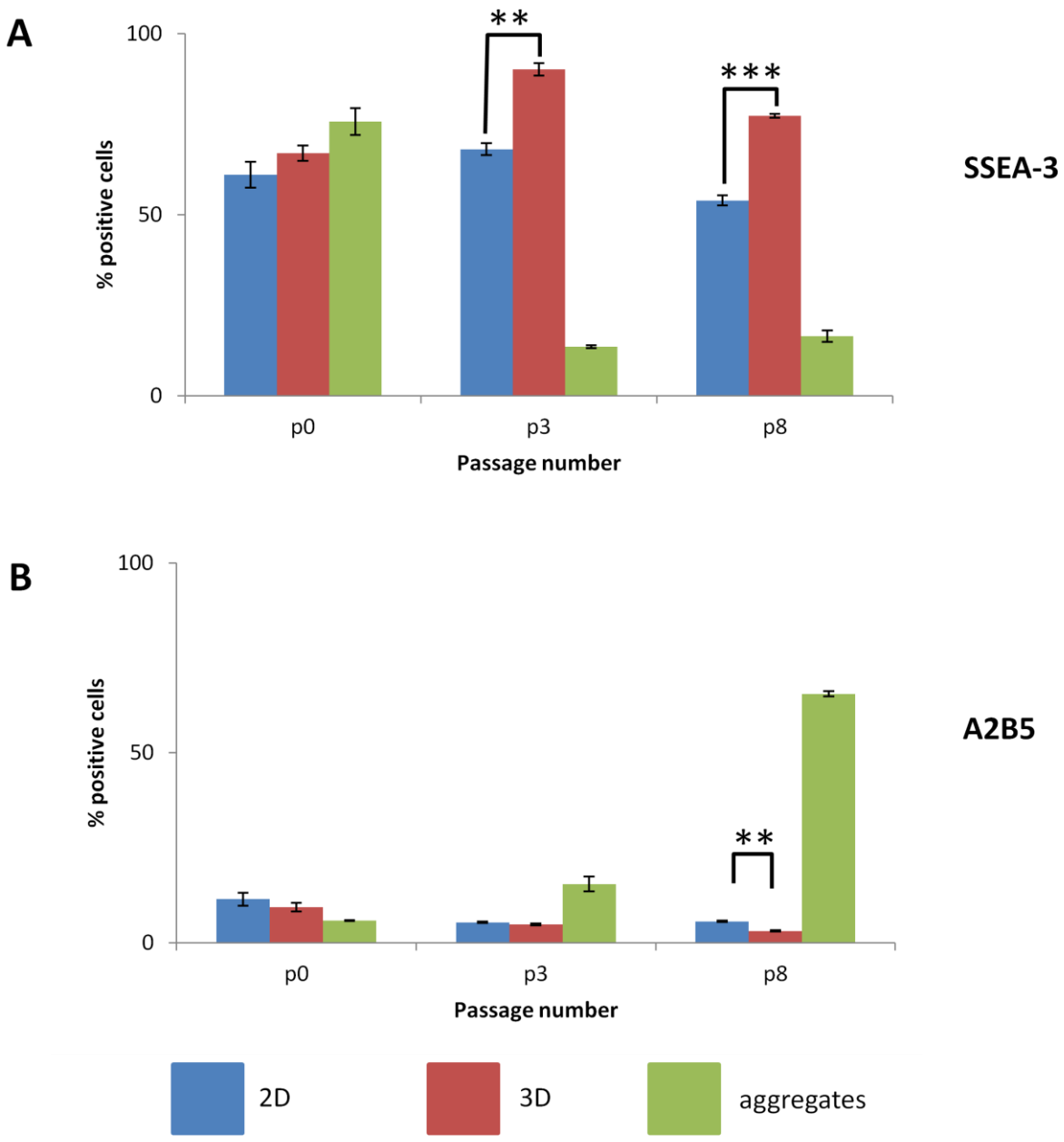

Figure 4.11. Flow cytometrical analysis of TERA2.cl.SP12 cells passaged in 3D compared to 2D monolayer and 3D aggregate cultures. After each passage, cells were sampled using flow cytometry for the stem cell marker SSEA-3 **(A)** and the early neuronal marker A2B5 **(B).** Cells maintained in 3D on membranes maintain high levels of SSEA-3 compared to the aggregate cultures which readily differentiate. By passage 3 there is a significant difference in SSEA-3 expression between 2D and 3D cultures. Data represents mean ±SEM n=3 ****p=0.01, ***p=0.001.**

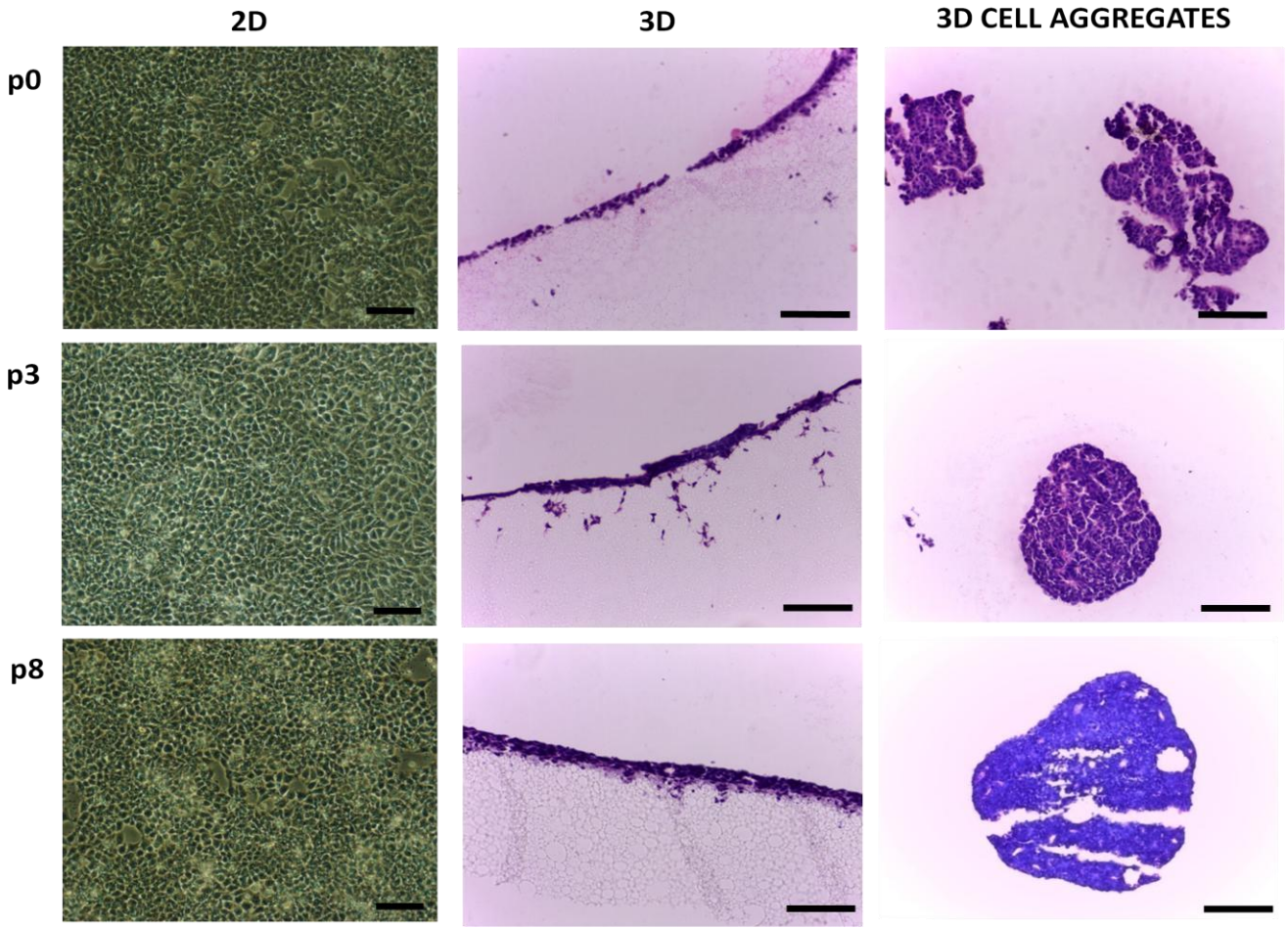

Figure 4.12. Analysis of TERA2.cl.SP12 cells passaged in 2D and 3D. Phase micrographs of cells maintained in continual 2D culture show no difference in cell morphology as passage number increases. Cells grown on the 3D membrane also show little difference as passage number increases apart from fewer cells infiltrate the interior of the membrane. At higher passage numbers the cell aggregates appear to be more densely packed**. Scale bars = 100µm**

and consisted of many more cells than 2D monolayer cultures. As passage number increased the cell layer appeared to thicken and fewer cells enterred the pores in the interior of the membrane (Figure 4.12). For 3D membrane cultures all passages were stained for Oct 4 to ensure that cells that were being passaged were not differentiating between passages and pluripotent cells were being reseeded. Representative sections of the membrane cultures are shown in Figure 4.14, they revealed that the majority of cells were Oct 4 positive in all 10 passages. These results were in contrasts to other methods of 3D cell culture such as the formation of aggregates. At passage 0, aggregates had not been able to form dense sphere of cells and they consisted of loosely bound clumps of cells. As passage number increased they were able to form dense spheres of cells similar to simple embryoid bodies. By passage 8 the aggregates appeared to contain primitive structures indicative of stem cell differentiation (Figure 4.12) and at a similar stage to the formation of cystic embryoid bodies during the differentiation of embryonic stem cells. Aggregates were fixed, section and immunostained for the embryonic stem cell marker - Oct 4 up to passage 3. Initially the majority of cells throughout the loosely formed aggregate were Oct 4 positive at passage 0. As passage number increased fewer cells were positive and at passage 1 and 2, the Oct 4 positive cells remained at the periphery of the cell aggregates. Finally, by passage 3 only individual isolated cells within the aggregates remained Oct 4 positive and at subsequent passages there were no Oct 4 positive cells (Figure 4.15).

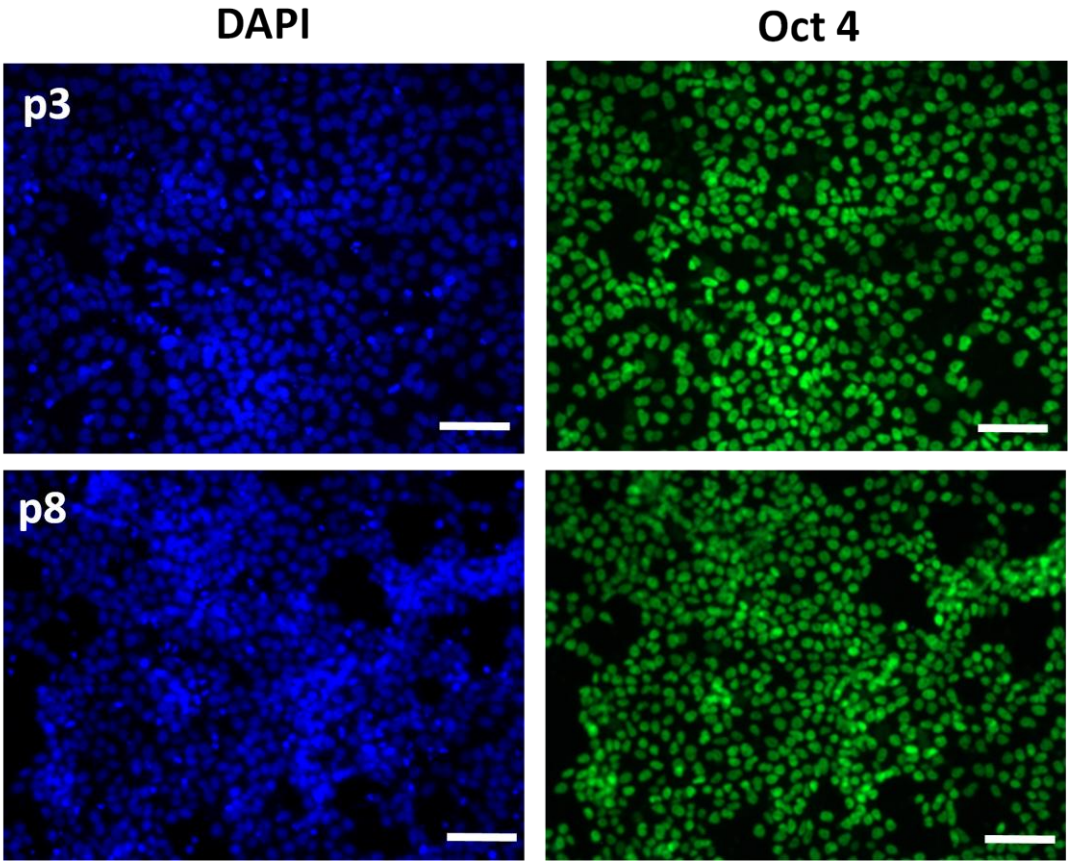

Figure 4.13. Immunostaining of 2D monolayer passaged cultures of TERA2.cl.SP12 cells for the embryonic stem cell marker – Oct 4. At all passage numbers, the majority of 2D cells are Oct 4 positive. **Scale bars=100µm.**

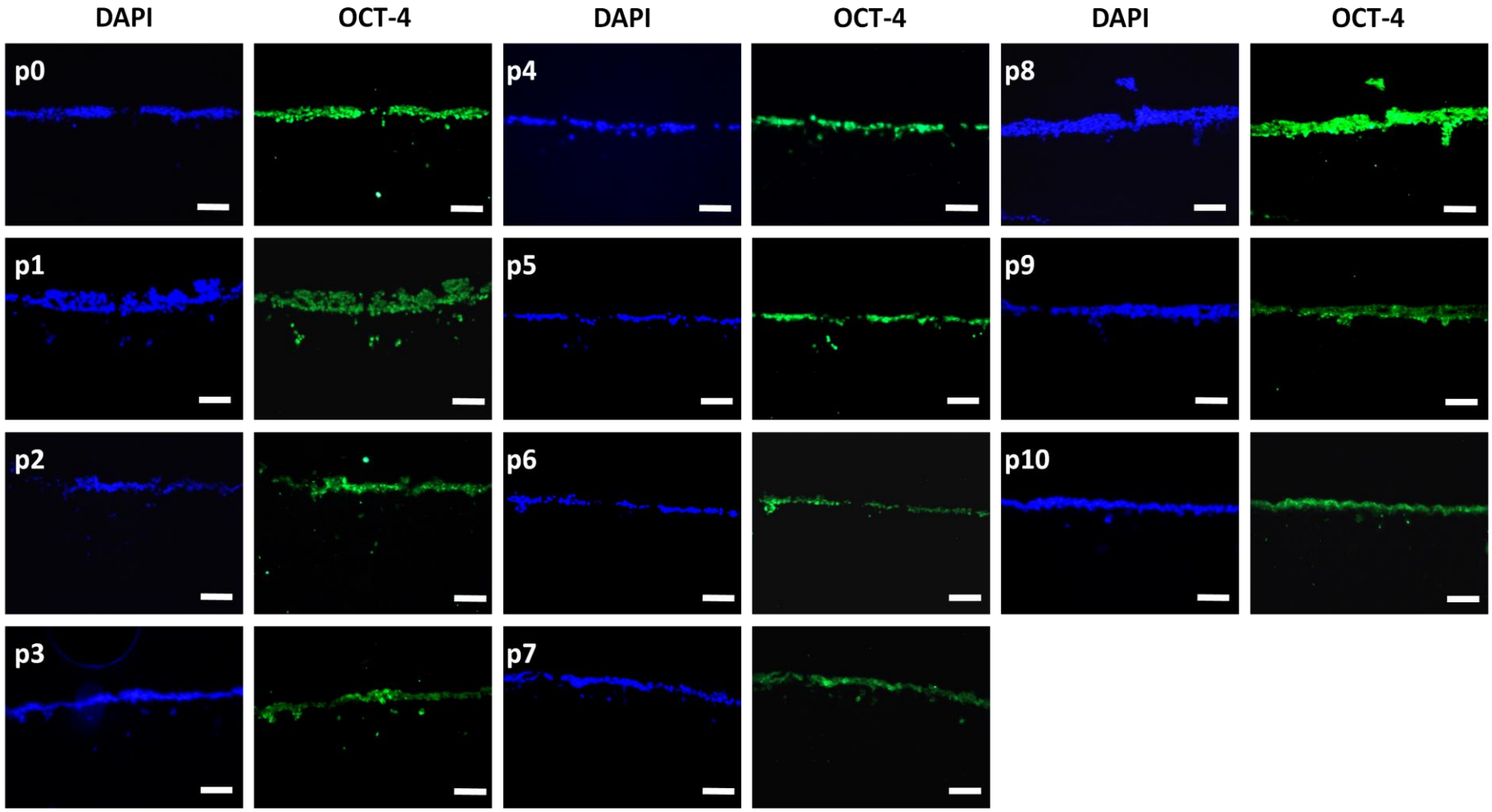

Figure 4.14. Immunostaining of 3D passaged cultures of TERA2.cl.SP12 cells for the embryonic stem cell marker – Oct 4. All passage numbers between 0 and 10 show a dense slab of cells which displays Oct 4 positive cells throughout. **Scale bars = 100µm**

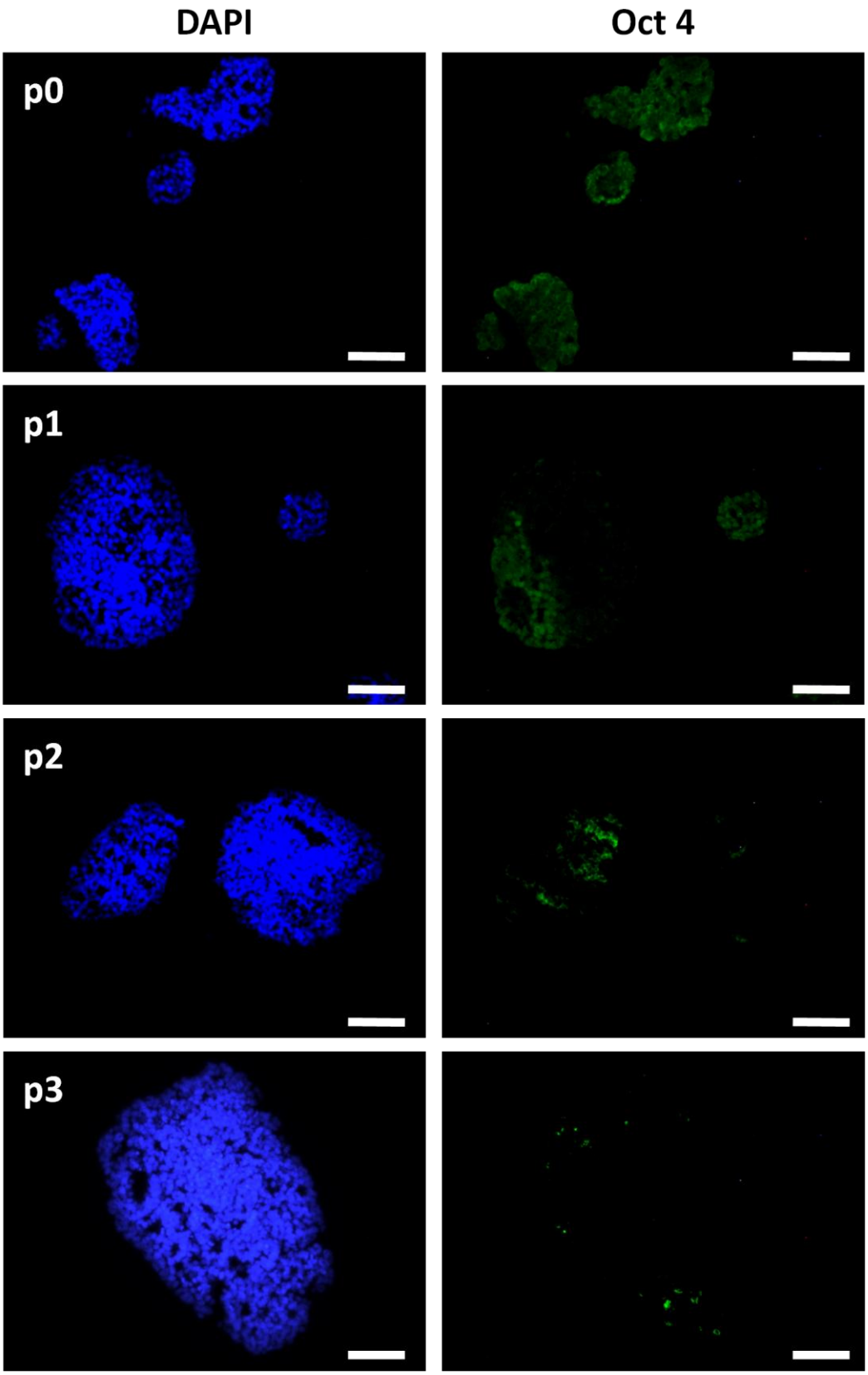

Figure 4.15. Immunostaining of aggregate cultures of TERA2.cl.SP12 cells for stem cell marker – Oct 4. Unlike the 3D cultures on membranes, 3D aggregate cultures display very few cells that are positive for Oct 4 even at the lowest passage numbers indicating spontaneous cell differentiation. **Scale bar=100µm.**

4.5.6 Prolonged passaging in 3D affects cell proliferation rate.

After each passage, samples of cells were removed from T25 flasks, Strata membranes, or aggregates. A single cell suspension was formed from the cells from each method and 2 x 10^5 cells were seeded into 12-well plates. These cells were cultured for 4 days before the cell density of the cultures was assessed using the method described in Chapter 2. At passage 0, cell density was identical in all of the culture methods and the density remained low after 4 days (Figure 4.16). As the number of passages increased the cell density increased (~25 cells per 100µm) in the 2D cultures suggesting that proliferation rate was high as the same initial cell number was seeded. Cell density of 2D cultures remained high up to passage 10 suggesting that proliferation rate remains constant. In contrast to this the 3D passaged cells showed a slight increase in cell density between passage 0 and passage 3 but the cell density did not increase to the levels seen in the 2D passaged cells but remained constant at 13 cells per 100µm up to passage 10. This would indicate that prolonged passaging of cells in a 3D environment caused a decrease in cell proliferation. When aggregates were dissociated to a single cell suspension and seeded back into 2D culture they also did not reach the cell density achieved by the 2D passaged cells but in contrast with the other two culture methods there was a decrease in cell density between passage 0 and passage 3 of approximately 5 cells per 100µm. The low cell density was maintained up to passage 10, presumably due to the cells differentiating and no longer actively proliferating (Figure 4.16).

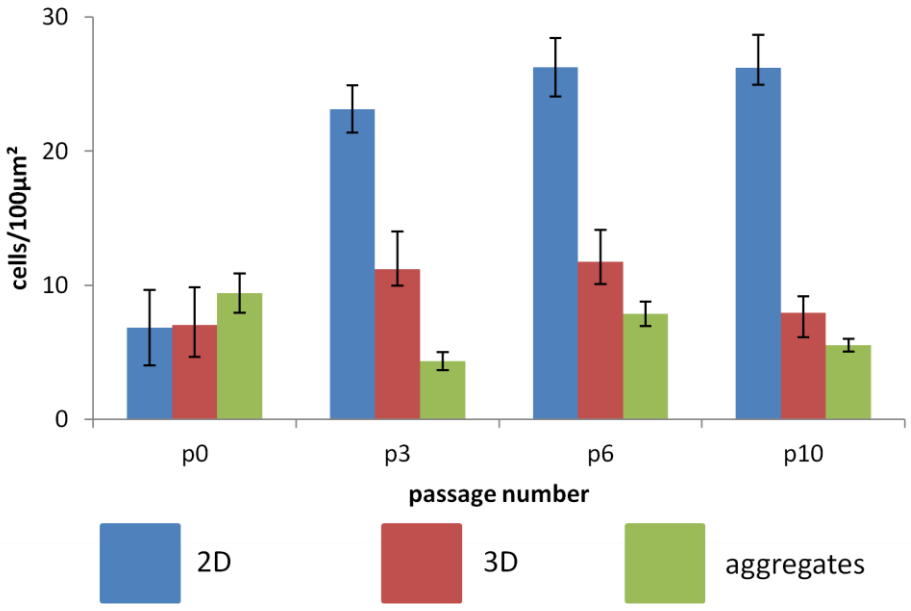

Figure 4.16. Passaging cells in 3D affects cell proliferation rate. After each passage, 200000 cells from each of the three growth methods were seeded back onto standard tissue culture plastic. These cells were cultured for 4 days before the cell density was assessed as in Chapter **2**. As passage number increases the density of the cells grown in 3D decreases suggesting there is a decrease in proliferation rate as identical numbers of cells were initially seeded. Data represent mean, ±SEM, n=10

4.5.7 Long term propagation of cells in 3D cultures results in a change in cell shape.

The 12-well cultures described in the previous section, were photographed every 24 hours over 4 days culture to assess any differences in TERA2.cl.SP12 cell shape/circularity that may occur after culture in 3D. Figure 4.17A shows a typical 2D culture over the 4 day culture period. At day 1, the 2D cells were sparse and stretched out across the cell culture plastic and by day 2 individual colonies of cells had begun to connect to each other. Between days 3 and 4, the TERA2.cl.SP12 cells squashed together to form a 100% confluent layer. TERA2.cl.SP12 cells that had been passaged in 3D showed a difference in cell shape as early as passage 0. After just 4 days in 3D culture the cells were transferred to the 12-well plates and after 24 hours in 2D there was evidence that the cells differ from their 2D counterparts. At 3D passage 0, fewer cells were stretched across the surface of the cell culture plastic and there were single cells that retain a more spherical shape. This change was not retained in 2D culture and by 48 hours the cultures resemble the standard 2D culture (Figure 4.17B). If the TERA2.cl.SP12 cells were passaged in 3D for further passages the difference in cell shape was retained for longer at passage 4 there was visible difference in cell shape up to day 3 before the cells started to resemble their 2D counterparts although cell proliferation was slower so the cells were unable to produce confluent cell layers after 4 days in 2D culture (Figure 4.17C). By 3D passage 8 the stretched cell morphology that was observed in 2D cells was not present after 24 hours and cells remained more rounded up until day 4 where the cells had started to form colonies that resembled the cultures seen in day 2 of the 2D cultures (Figure 4.17D). After prolonged passaging of cells in three-dimensions up to passage 10 all cells had a spherical appearance and even when they began to form colonies between 48 hours and 72 hours they were still rounded and did not resemble the 2D TERA2.cl.SP12 cells (Figure 4.17E). After being returned to 2D culture for 4 days they began to more closely resemble the colonies formed in 2D cultures of human embryonic stem cells such as the H9 cell line shown in Figure 4.46.

To further highlight the difference in cell shape that occurred during prolonged 3D culture, high magnification phase contrast images were captured of passage 10 cultures for both 2D and 3D TERA2.cl.SP12 cells (Figure 4.18A). The 3D cells had fewer processes stretching out and adhering to the cell culture plastic than their 2D counterparts. The 3D passaged cells also appearred more likely to form tightly packed colonies than the 2D passaged cells which formed a monolayer of irregular shaped cells. To quantitatively assess this change in cell shape, cells from phase micrographs were randomly selected and using the ImageJ software it was possible to measure individual cell area and the cell perimeter. An example image showing the selection of cells used for measurements is shown in Figure 4.18B. Using this method it was also possible to cut out individual cells from the phase micrographs to produce silhouette cells which help to highlight

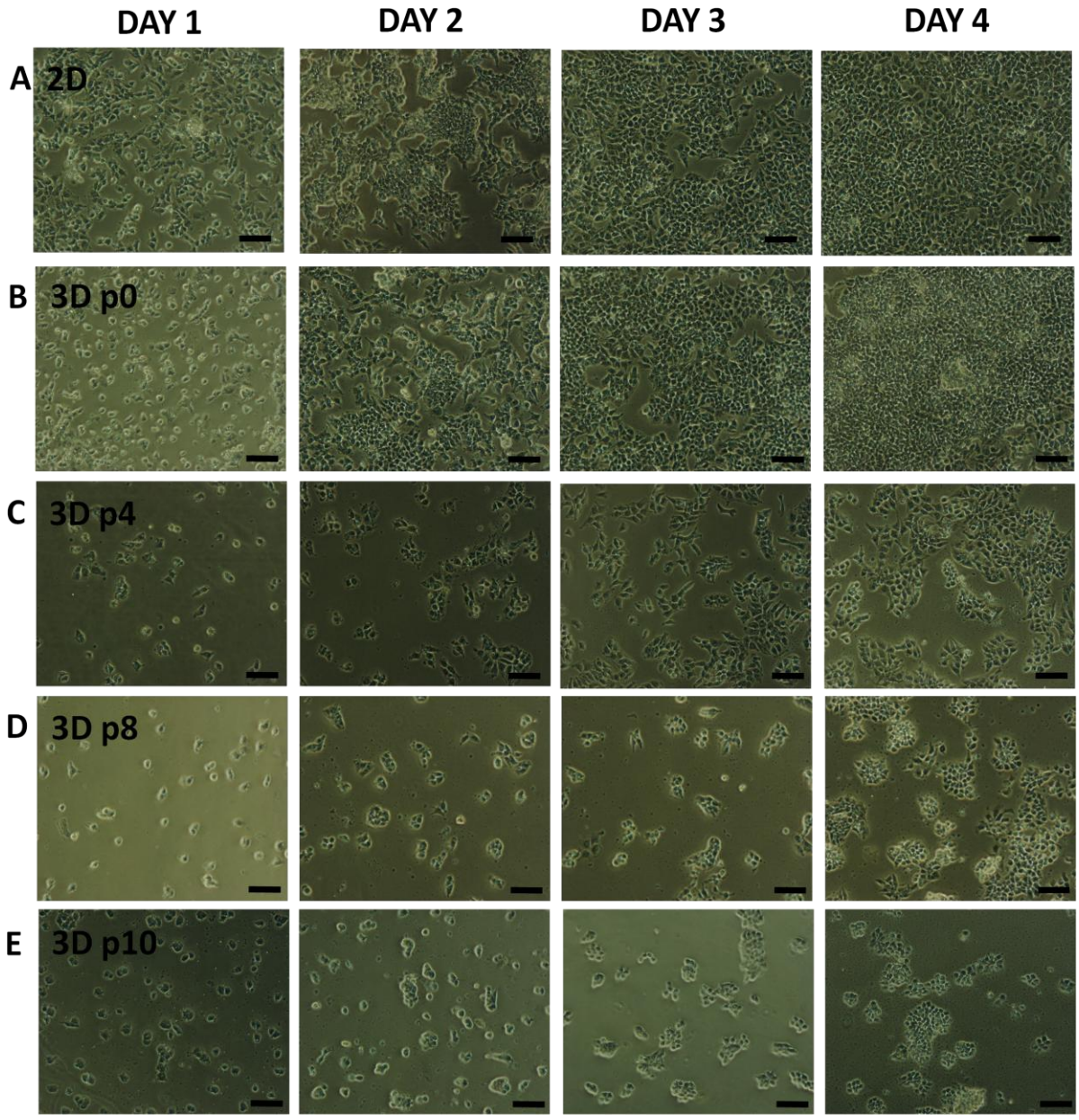

Figure 4.17. Passaging TERA2.cl.SP12 cells in 3D affects cell morphology and the difference in cell morphology is maintained when placed into 2D. After each passage, 200000 cells from both 2D and 3D cultures were seeded onto standard tissue culture plastic. The 3D passaged cells were maintained in 2D for 4 days At every 24 hours these cells were imaged. There is a clear difference in cell shape between the 2D and 3D cells even at p0 but this shape is lost by 1-2 days as the cell proliferate and adapt to the 2D substrate. Whereas cells that have been passaged 10 times in 3D are able to maintain the difference in cell morphology for up to 4 days**.** Passaging cells in 3D affects phenotype with 3D passaged cells appearing more round and having fewer processes that 2D passaged cells. **Scale bars = 100µm.**

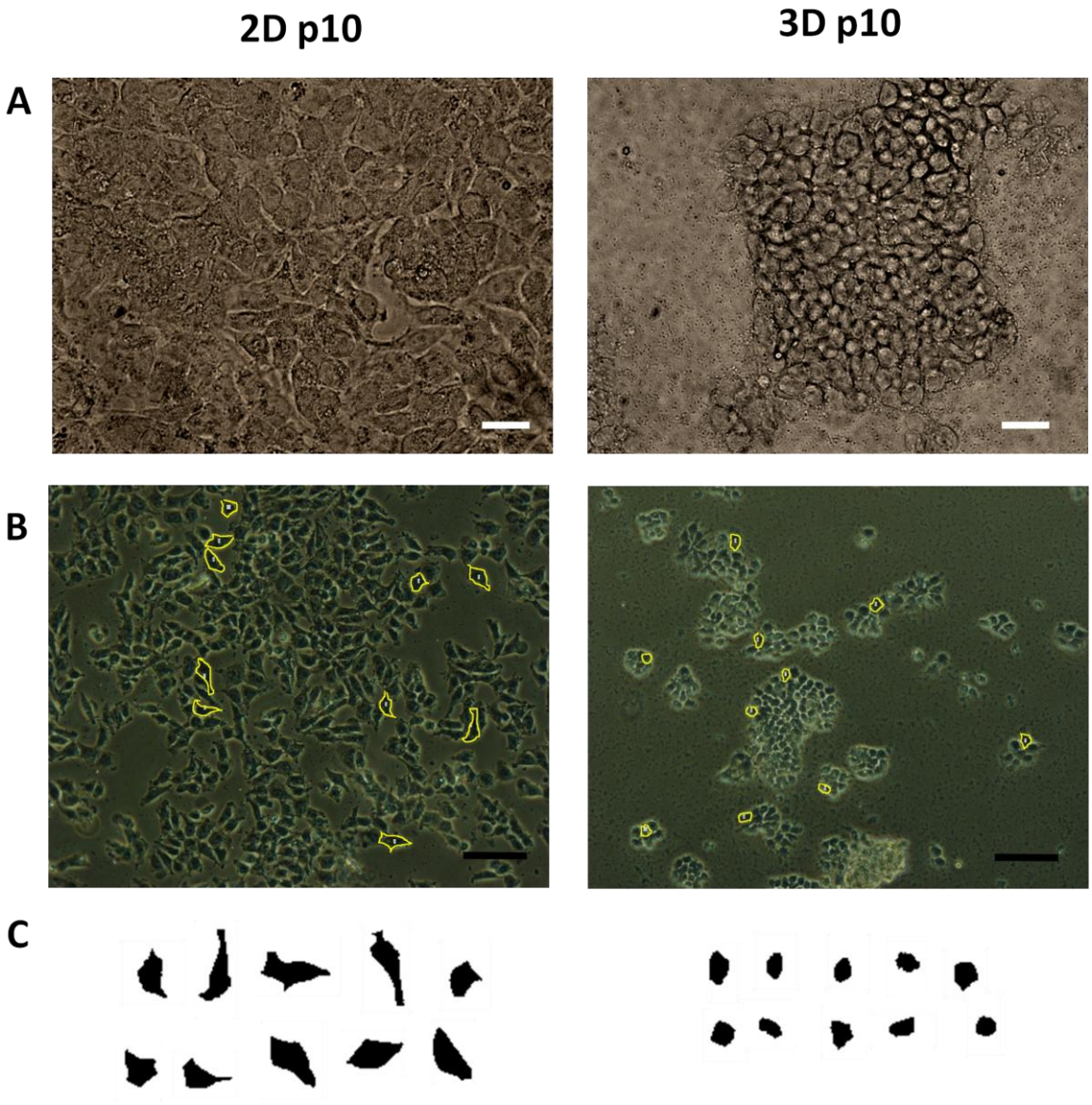

Figure 4.18. High magnification images highlight the differences between 2D and 3D passaged cells after 10 passages. There is a clear difference in cell shape between the 2D and 3D cells after 10 passages. The high magnification phase micrographs reveal that 3D passaged cells appear rounder and are more likely to grow in colonies than the 2D cells which form a monolayer of irregular shaped cells **(A). B** show the sampling method used to assess the circularity off individual cells and C shows silhouettes of each randomly selected individual cells this highlights the difference in cell shape between the 2D and 3D. **Scale bars A=25µm, B=100µm.**

the differences in shape observed between separate cultures. Figure 4.18C shows 10 examples of silhouettes for 2D p10 and 3D p10 12-well plate cultures. As previously mentioned the 3D passaged cells appeared smaller and had fewer processes than 2D cells which were long and thin.

Using the cell area and perimeter measurements from phase micrographs it was possible to assess the cell circularity using a similar method to that used by Ballester-Beltrán et al. [282] This method is based on the surface area of a sphere. If a cell was perfectly spherical it would have a circularity ratio of 1. Cells with multiple processes have a circularity of closer to 0. The circularity measurements in Figure 4.19 quantified the observations from Figure 4.17. At passage 0 the measurements of circularity confirmed observations from the phase micrographs, there was an initial difference in cell shape with the 3D cells having a ratio of 0.76 and 2D cells only 0.51, but after day 2, 2D and 3D cells had similar measurements of approximately 0.62. There was a greater difference in circularity at passage 4 with 3D cells having a circularity of 0.84 and 2D cells of 0.42, this difference in circularity was actually maintained until day 4 rather than the predicted day 3 from Figure 4.17C. It was also interesting that as the 2D cells became confluent and formed close interactions with each other they became more rounded, this occurred at all passages. At passage 8 there was a further increase in cell circularity to 0.87 the more circular shape was maintained for the entire 4 days with the 3D cells still having a circularity of 0.79 after 4 days in culture this was 0.2 higher than at passage 4 at day 4. After 10 passages in 3D plus 4 days of 2D culture, 3D passaged TERA2.cl.SP12 cells still retained a circularity of 0.84 (Figure 4.19).

It is evident from the cell silhouettes that 3D passaged cells appearred smaller than 2D passaged cells; this is especially noticeable at passage 10. The cells were not smaller but more spherical than their 2D counterparts as revealed by the confocal images and Z-stacks in Figure 4.20. Glass coverslips were placed into the bottom of well plates and at passage 10 both 2D and 3D TERA2.cl.SP12 cells were seeded onto the coverslips housed in 12-well plates. After 24 hours of 2D culture the cells were fixed in 4% PFA and stained with phalloidin to investigate the distribution of F-actin and the nuclear stain – DAPI. To highlight the remainder of the individual cells, they were also immunostained for α-tubulin. 2D cells at passage 10 were more stretched out across the glass surface compared to the 3D passaged cells. There was also a difference in F-actin distribution between 2D and 3D cells, with 2D cells showing F-actin only in the cell projections (Figure 4.20A) whereas F-actin was more evenly distributed in the 3D passaged cells (Figure 4.20B). There was also a difference in nuclear shape between the two types of TERA2.cl.SP12 cells. In the 2D passaged cells the nuclei were flattened and sat within the actin fibres whereas in 3D the nuclei appeared more spherical and lay on top of a bed of actin fibres. The 3D passaged cells were taller (~15.36µm) than the 2D passaged cell (~9.90µm), as expected they were more three-dimensional and were a similar size in all directions.

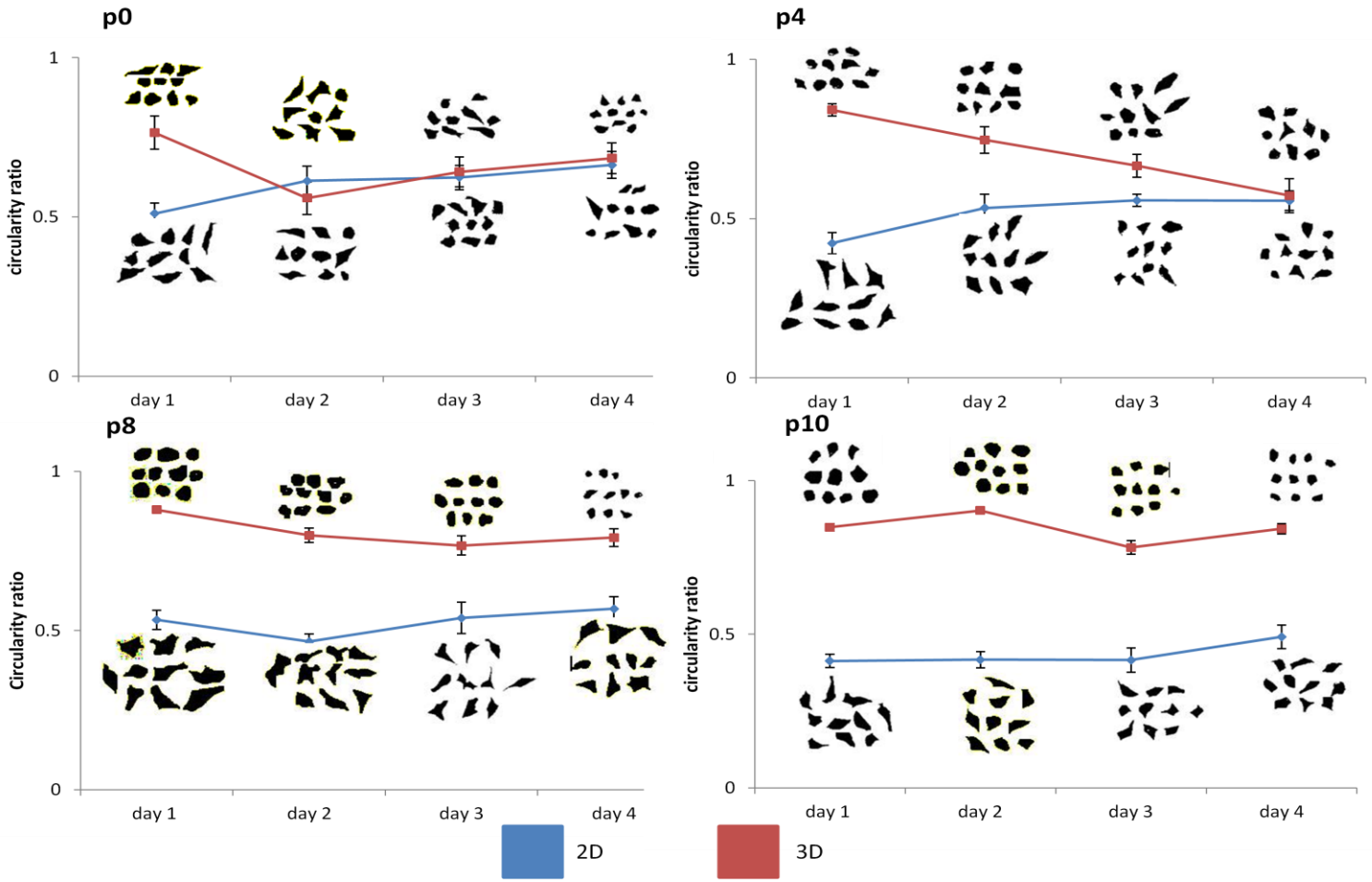

Figure 4.19. Measurements of TERA2.cl.SP12 cell circularity show that there is a change in cell morphology between cells passaged in 2D and 3D. The circularity of cells grown in 2D was assessed by calculating the ratio between the cell perimeter and cell area. The change in cell shape/circularity due to 3D culture is maintained for longer as the passage number increases. Cells stay rounder for longer. This is also evident when examining the silhouettes of cells. n=10, ±SEM.

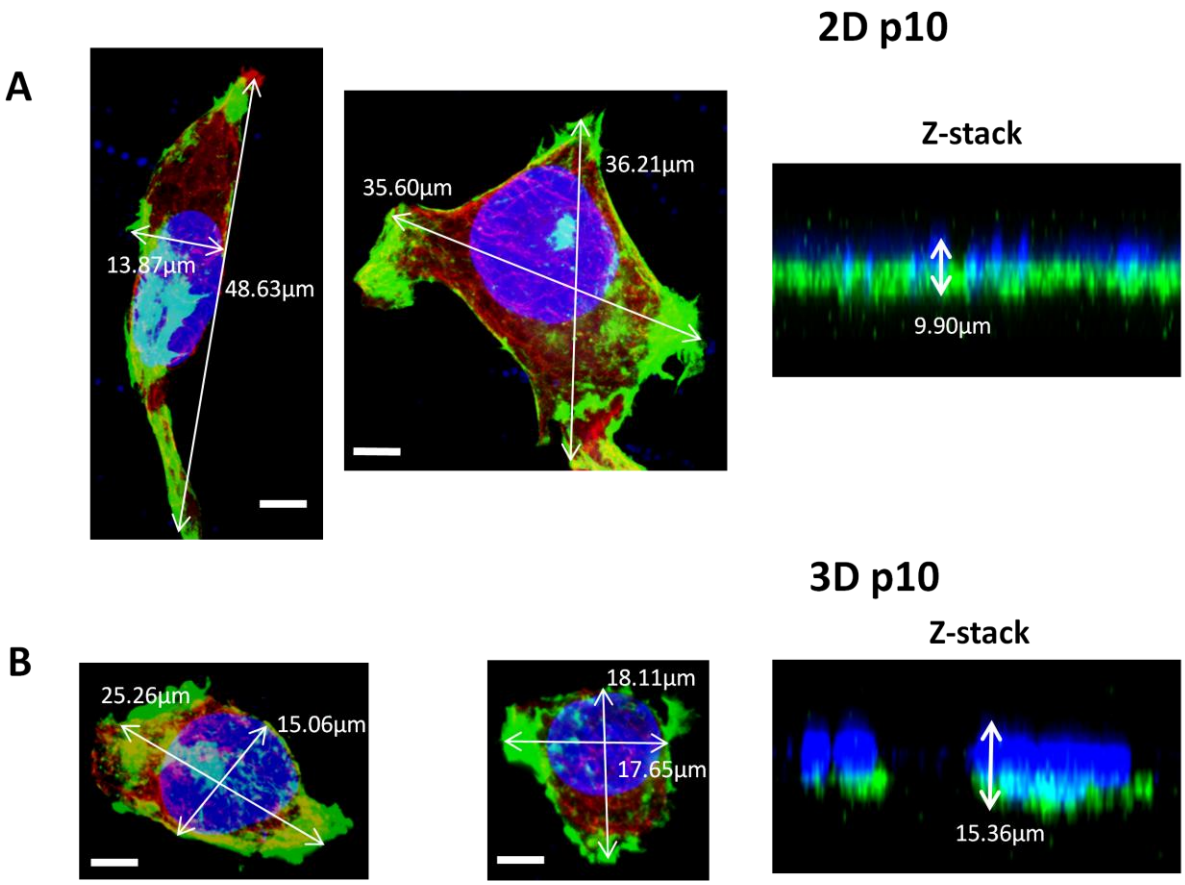

Figure 4.20. Confocal images confirm there is a difference in TERA.cl.SP12 cell size and distribution of cytoskeletal protein between 2D and 3D passaged cells. Passage 10 cells were examined in 2D culture and stained with nuclear DAPI **(blue**), phalloidin to highlight actin cytoskeleton **(green)** and α-tubulin **(red).** There was a difference in cell size and cell spread between 2D **(A**) and 3D passaged **(B)** cells. Z-stacks of the monolayer show that there is a difference in height between the 2D and 3D cells. Note that there is also a difference in nuclear shape the 2D cells are flattened in appearance with the nuclei sitting within the cytoskeleton whereas the 3D passaged cells are more spherical in appearance and appear to be sitting above a bed of actin fibres. **Scale bars = 5µm.**

4.5.8 Prolonged culture in 3D affects the differentiation and distribution of stem cells in 3D scaffolds

After 10 passages in either 2D or 3D culture, TERA2.cl.SP12 cells were seeded onto Alvetex® Scaffold using the optimal seeding conditions described in Chapter 2. The cells were differentiated using 1μM EC23 and the differentiation protocol described in Chapter 3. Flow cytometrical analysis of cultures after 7 days of differentiation revealed a significant difference between 2D and 3D passaged cells. Cells that had undergone 10 passages in 3D were able to differentiate quicker and led to significantly lower levels of SSEA-3 expression (7.46%) at day 7 than 2D passaged cells (18.23%). There was also a difference in the percentage of TRA-1-60 positive cells with 2D passaged cultures containing 32.86% positive cells and 3D passaged cultures containing only 18.86% TRA-1-60 positive cells (Figure 4.21A).

A difference in cell density and distribution was also observed between the scaffold differentiated cultures of 2D and 3D passaged cells. 2D cells had infiltrated the scaffold at a low cell density (Figure 4.21B) and were unable to fill the entire Alvetex® Scaffold even after 14 days in culture (Figure 4.21C). In contrast to these observations the 3D passaged cells infiltrated the entire scaffold as early as day 7 (Figure 4.21D). By 14 days of differentiation in 3D, the 3D passaged cells had reached a very high cell density within the scaffold and there were potential neural rosettes formed within the cultures – highlighted with black arrows (Figure 4.21E). Immunostaining for the neuronal marker – TUJ-1 after 14 days of retinoid-induced differentiation in 3D also revealed the differences between the 2D and 3D passaged cells. The two immunostained images have been selected as the cells are at a similar cell density in the two culture conditions, this was evident from the nuclear staining (Figure 4.22). Even though the cells were at a similar cell density there was significantly higher number of cells that were TUJ-1 positive in the 3D passaged cultures. The 2D passaged cultures did contain TUJ-1 positive cells put they were sparsely arranged individual cells throughout the cell layer whereas the 3D passaged cultures displayed dense areas of TUJ-1 positive cells (Figure 4.22). High magnification montages of the TUJ-1 positive 3D passaged cells shows evidence of extensive neurite outgrowth weaving through the entire width of the scaffold (Figure 4.23) and also confirmed the presence of neural rosettes previously highlighted in Figure 4.21E.

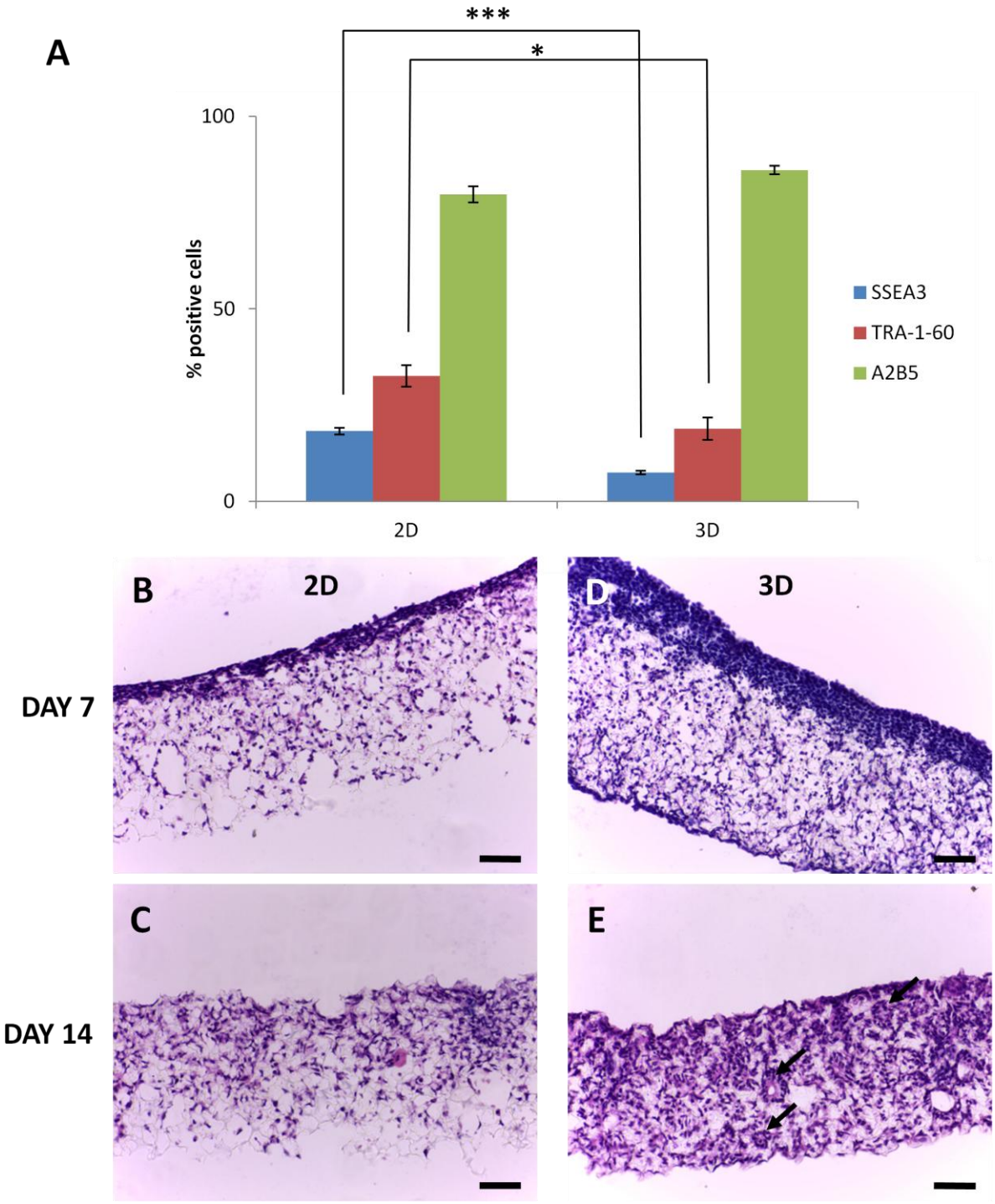

Figure 4.21. Maintaining TERA2.cl.SP12 cells in 3D affects their ability to differentiate. After 10 passages both 2D and 3D cells were placed on to Alvetex® Scaffolds and differentiated in 3D using 1µM EC23. Flow cytometric analysis **(A)** reveals a difference in the levels of stem cell markers between the 2D and 3D cells. There is also a difference in cell distribution and density within the scaffold, with 3D passaged cells appearing to adapt to 3D cultures in Alvetex® Scaffold **(D,E)** more readily than their 2D passaged counterparts **(B,C). B-E** are H&E stained sections of the Scaffold cultures. Black arrows highlight potential neural rosettes in 3D passaged cells **(E) *p=0.05, ***p=0.001,** Data represents mean ±SEM n=3**, Scale bars = 50µm**

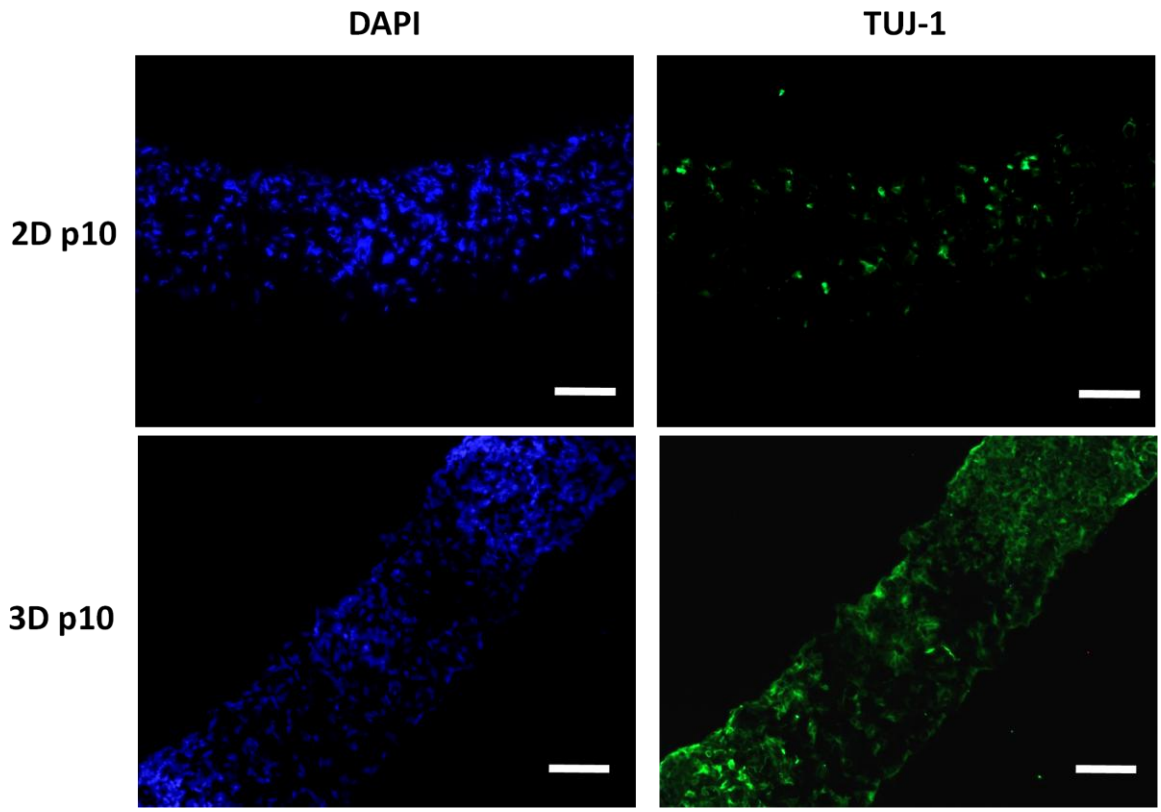

Figure 4.22. Maintaining TERA2.cl.SP12 cells in 3D affects their differentiation in 3D. After 10 passages both 2D and 3D cells were placed on to Alvetex® Scaffolds and differentiated in 3D using 1µM EC23. Immunostaining for β(III)tubulin after 14 days of retinoid treatment showed significantly higher levels of expression when cells have been maintained in 3D**. Scale bars = 100µm**

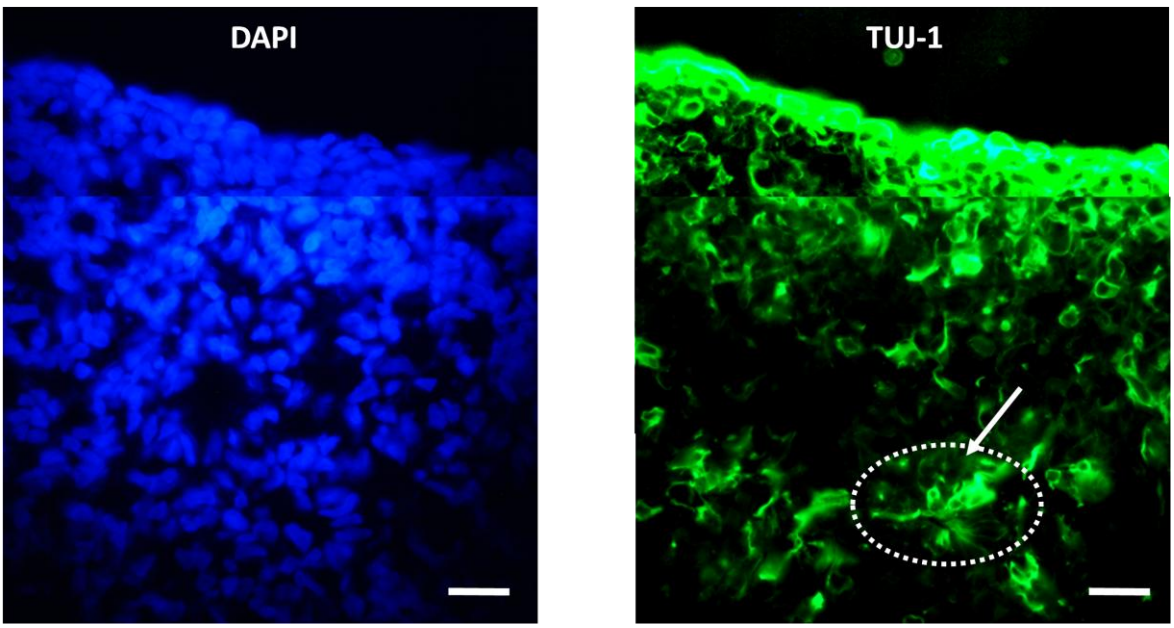

Figure 4.23. High magnification images of 3D passaged TERA2.cl.SP12 cells differentiated and stained with neural marker β(III)tubulin. The high magnification image of immunostaining for β(III)tubulin after 14 days of retinoid treatment showed significant evidence of neuronal differentiation, neurite outgrowth and neural rosettes **(white arrow).** Images represent a composite image of two field of view captures from same specimen. **Scale bars = 25µm**

4.5.9 Passaging TERA2.cl.SP12 EC cells in 3D affects their ability to form cell aggregates

After passages 4, 6, and 10, both 2D and 3D passaged cells were dissociated and placed in non-tissue culture coated Petri dishes to form cell aggregates. Aggregates were treated with 1µM EC23 to assess the cells differentiation potential. The size of aggregates was also measured from phase micrographs over a 21 day period. At passage 4, the 2D and 3D cells showed little difference in their ability to form aggregates. Although aggregates formed from 3D passaged cells appeared larger after 14 days when compared to the 2D passaged cells (Figure 4.24A). After longer culture in 3D up to passage 6, the difference in aggregate size appeared as early as day 1 and after 21 days in suspension culture there was a significant difference between the size of aggregates formed from 2D and 3D passaged cells ($p=0.01$). Aggregates formed from 2D passaged cells were on average 110µm (28%) smaller in diameter than aggregates formed from 3D passaged cells after 21 days in culture (Figure 4.24B). TERA2.cl.SP12 cells which had been passaged in 3D for 10 passages showed a significant difference in their ability to form aggregates as early as day 1, when compared to 2D passaged cells of the same age. After only 24 hours in culture the difference in aggregate diameter between 2D and 3D cells was already 93.05µm ($p=0.01$). This difference in size significantly increased the longer the aggregates were in suspension culture. At day 7 the difference in aggregate size between 2D and 3D passaged cells was 168.55µm, and at day 14 it had increased to 203.71µm ($p=0.001$). This difference in aggregate size continued to the full 21 days in suspension culture with 3D passage 10 cells producing the overall largest aggregate size at 761.30µm in diameter (Figure 4.24C).

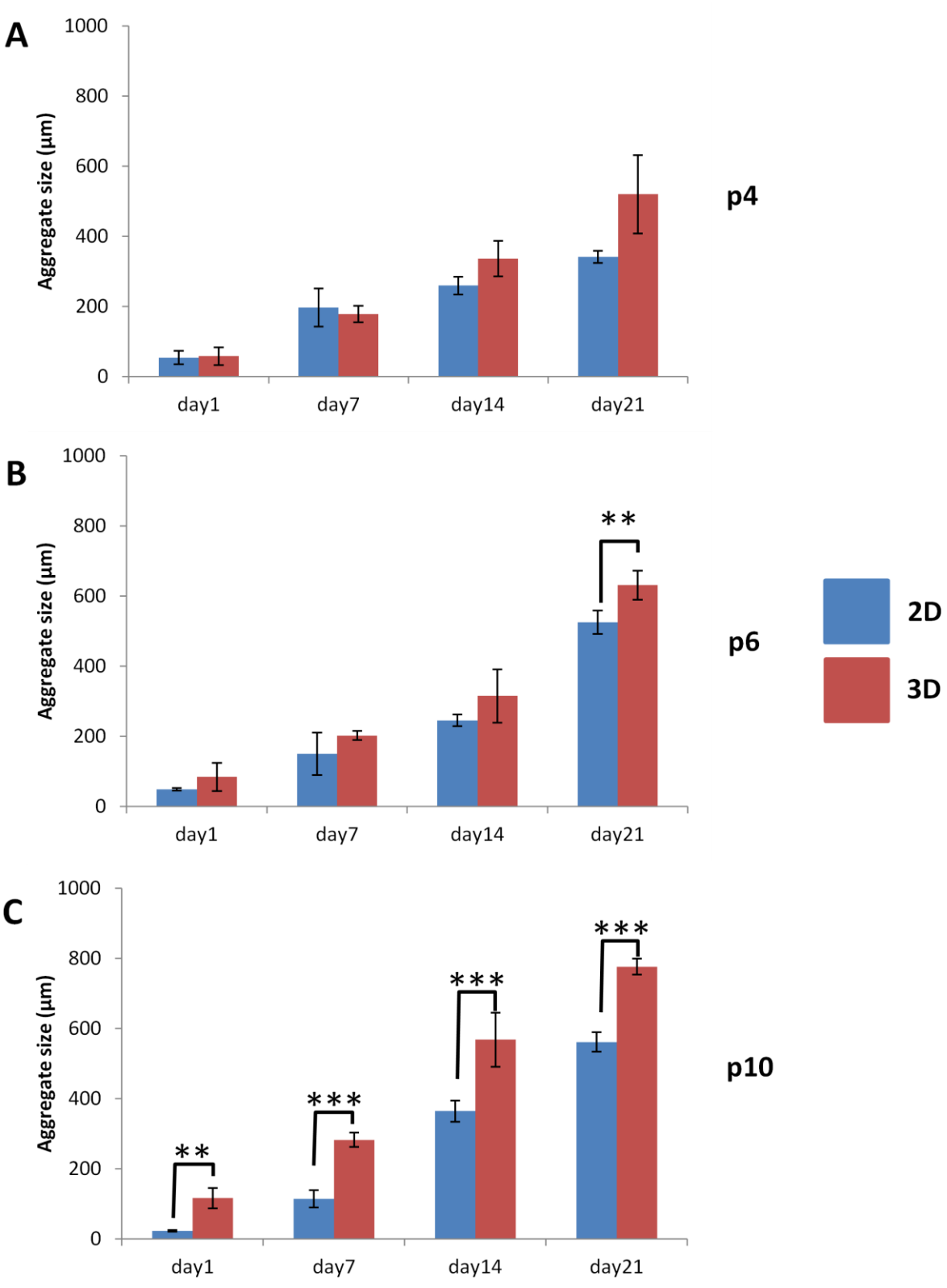

Figure 4.24. Passaging TERA2.cl.SP12 cells in 3D affects their ability to form cell aggregates. At passages 4,6, and 10 **(A-C respectively),** 2D and 3D cells were placed in non-tissue culture treated Petri Dishes to form cell aggregates. Cells were maintained in suspension cultures for 21 days and the size of the aggregate was measured by analysing images using ImageJ. Cells that had been grown in 3D for 4 passages were similar to their 2D counterparts whereas cells maintained in 3D for 10 passages showed a significant difference in aggregate size. Data represents mean ±SEM n=10, ****p=0.01, ***p=0.001.**

4.5.10 Passaging TERA2.cl.SP12 EC cells in 3D affects the differentiation of the cells within aggregates.

The formation of aggregates took 21 days in suspension culture, after this aggregates formed from all types of cells were fixed in 4% PFA, dehydrated and paraffin embedded. Aggregates were then cut into 6µm sections and consecutive sections were immunostained for the neuronal marker – TUJ-1 and epithelial marker – cytokeratin-8. At passage 4 there was no difference in staining between the 2D and 3D passaged cells with the majority of the aggregates staining TUJ-1 positive and no staining for cytokeratin 8 (Figure 4.25A&B). The sections did show a slight difference in aggregate size between the 2D and 3D passaged cells. As the number of passages in 3D increased there was a change in composition of the aggregates formed. After 6 passages in 2D culture the aggregates remained similar to the passage 4 aggregates with the majority of cells being TUJ-1 positive and no staining for cytokeratin-8 (Figure 4.26A). In contrast to this, after 6 passages in 3D culture, cells formed aggregates that displayed greater evidence of neural differentiation and cellular diversity. There were also areas within the aggregates that were negative for TUJ-1; these areas were at a lower cell density to the remainder of the aggregate and also stained for the epithelial marker – cytokeratin-8 (Figure 4.26B). Finally, after 10 passages the sections of aggregates highlighted the significant difference in aggregate size between 2D and 3D passaged cells. The 2D passage 10 aggregates were again mainly composed of TUJ-1 positive cells although there were individual cells within the aggregate which showed weak staining for cytokeratin-8 (Figure 4.27A). In comparison to the 3D p10 aggregates this cytokeratin-8 staining was minimal. At the centre of the aggregates formed from 10th 3D passage TERA2.cl.SP12 cells there was a large area of low density cells which only stained positive for the epithelial marker – cytokeratin-8 whereas the remainder high density cells were TUJ-1 positive (Figure 4.27B).

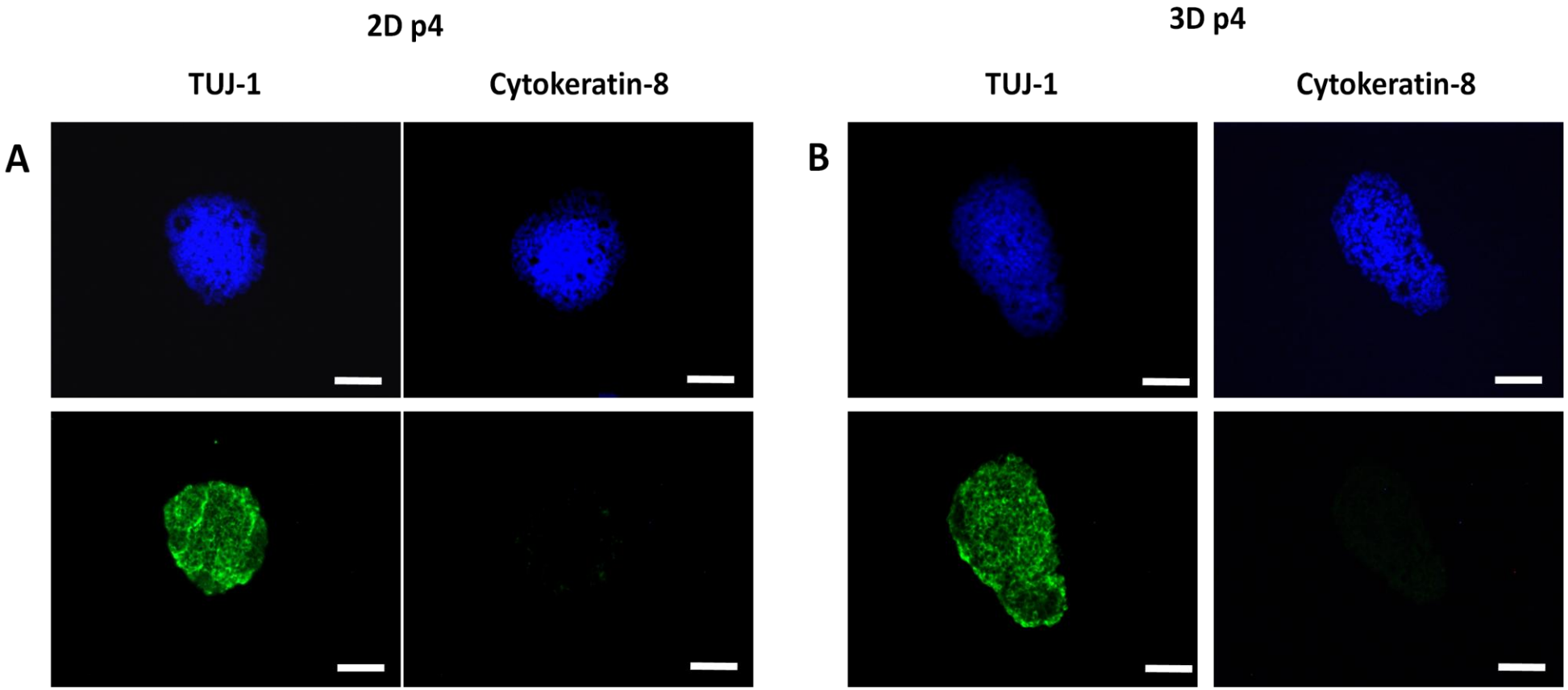

Figure 4.25. Immunohistochemical analysis of TERA2.cl.SP12 cell aggregates formed from 2D and 3D cells at passage 4. Cell aggregates were fixed in PFA at day 21 and processed for histology. They were then stained for the neuronal marker β(III) tubulin and epithelial marker cytokeratin-8. At passage 4 there is very little difference between and **2D (A)** and 3D **(B)** passaged cells. **Scale bars =100μm.**

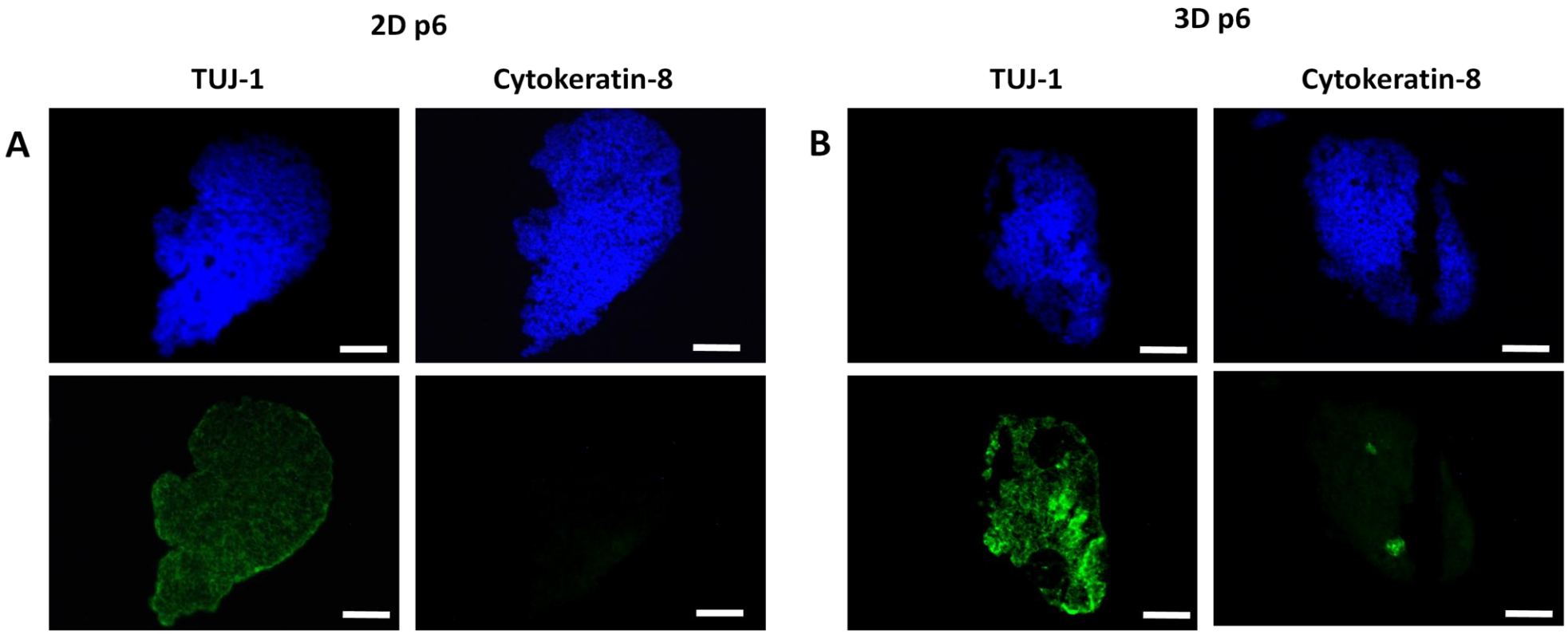

Figure 4.26. Immunohistochemical analysis of TERA2.cl.SP12 cell aggregates formed from 2D and 3D cells at passage 6. Cell aggregates were fixed in PFA at day 21 and processed for histology. They were then stained for the neuronal marker β(III) tubulin and epithelial marker cytokeratin-8. At passage 6 the 3D cells show areas of TUJ-1 and cytokeratin-8 staining **(B)** whereas the 2D cells are only TUJ-1 **positive (A).** Furthermore, 3D passaged cells produce aggregates with greater evidence of neural differentiation and cellular diversity. **Scale bar = 100µm.**

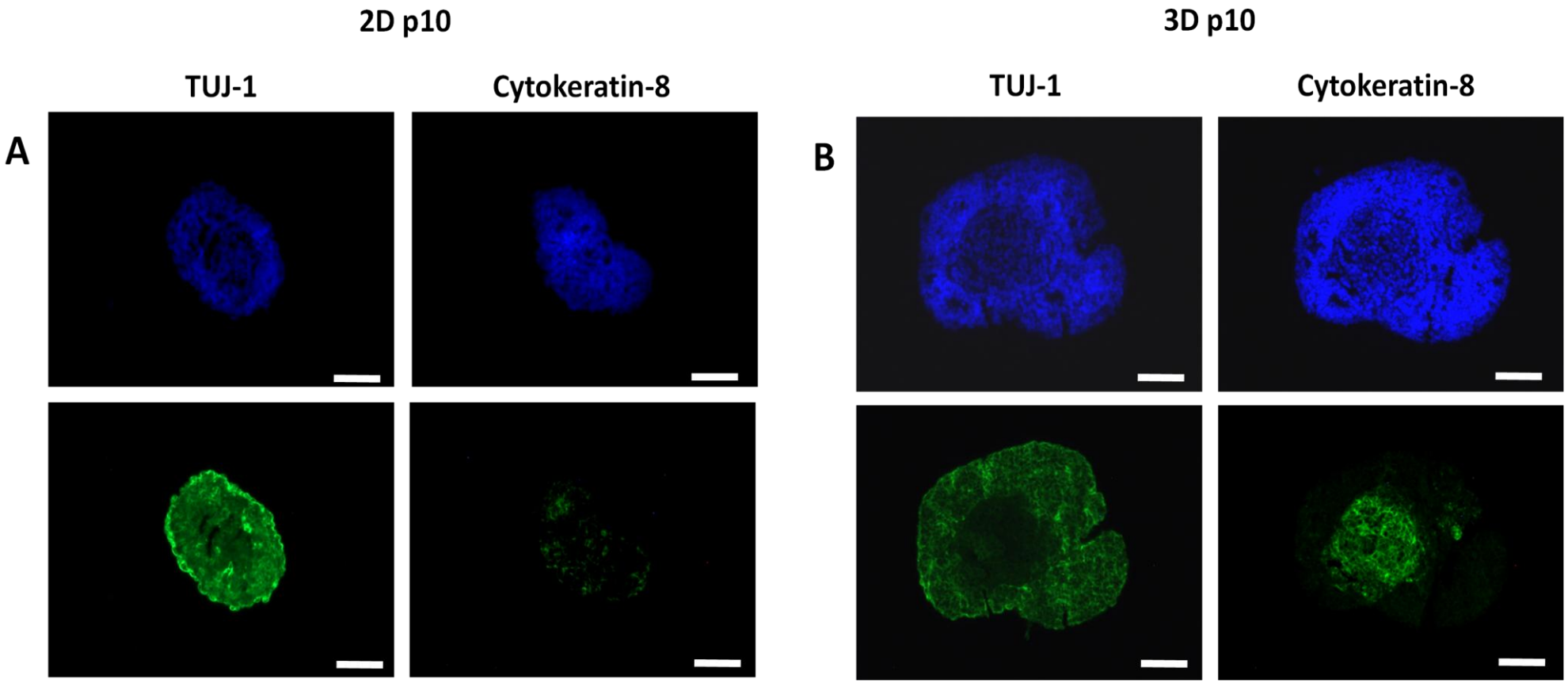

Figure 4.27. Immunohistochemical analysis of TERA2.cl.SP12 cell aggregates formed from 2D and 3D cells at passage 10. Cell aggregates were fixed in PFA at day 21 and processed for histology. They were then stained for the neuronal marker β(III) tubulin and epithelial marker cytokeratin-8. At passage 10 the 3D passaged cells produce significantly larger aggregates than their 2D counterparts **(A).** The aggregates formed from 3D passaged cells have large areas of cells at a lower cell density ,it is these areas which are cytokeratin-8 positive **(B). Scale bar =100µm**

4.5.11 Passaging TERA2.cl.SP12 EC cells in 3D affects the formation of teratomas.

To further test the developmental potential of 3D passaged cells, a teratoma assay was performed. At passages 4, 6, and 10, both 2D and 3D passaged cells were removed from their growth substrate, mixed with BD Matrigel and 0.5 x 10^6 cells were injected subcutaneously into immune-deficient mice to form teratomas. In a similar way to the aggregate size data presented in Figure 4.24, there was a difference in the weight of teratomas formed from 2D and 3D passaged cells. The weight of teratomas was assessed post-fixation and prior to dehydration of the teratomas for paraffin embedding. As with aggregate formation (Figure 4.24A) the difference between 2D and 3D was not visible at passage 4. After 6 passages, the 3D-primed cells formed teratomas that were slightly larger than teratomas formed from cells cultured in standard 2D monolayers. After 10 passages in a 3D environment the cells had been primed for a 3D environment and were able to form teratomas that were significantly heavier than teratomas formed from their 2D counterparts ($p=0.01$) (Figure 4.28).

Histological analysis of teratomas formed from either 2D or 3D passaged cells highlighted their differences in size. On average teratomas formed from passage 4 cells grown on either substrate were approximately 5mm in diameter. Whereas there was a difference of 6mm between teratomas formed from 2D and 3D passage 6 cells and a difference between passage 10 cells of 3mm in diameter. Again, in agreement with the aggregate size data presented in Figure 4.24C, 3D-primed cells at passage 10 formed the largest teratomas of approximately 12.57mm in diameter. The differences in diameter of 2D and 3D teratomas was linked with a difference in their overall weight (Figure 4.28). From the Haematoxylin and Eosin-stained montages of teratoma sections it was also evident that teratomas formed from 3D passaged cells forme a more diverse range of tissues (Figure 4.29).

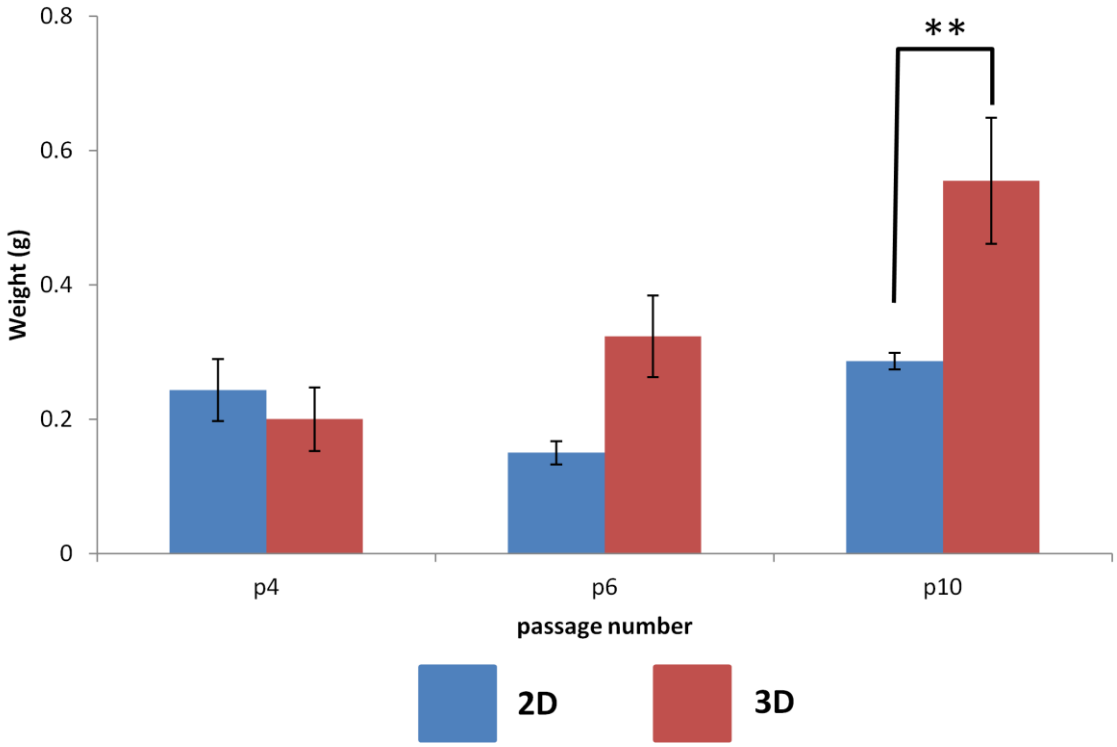

Figure 4.28. Passaging TERA2.cl.SP12 cells in 3D affects the formation of teratomas. At passage 4,6, and 10, 0.5 x 10^6 2D or 3D cells were injected subcutaneously into immune-deficient mice and allowed to form teratomas. Teratomas were removed and weighed prior to dehydration. In a similar way to the aggregate size, teratomas formed from 3D-primed cells were larger than ones formed from 2D cells. Data represents mean ±SEM n=3, ****p=0.01.**

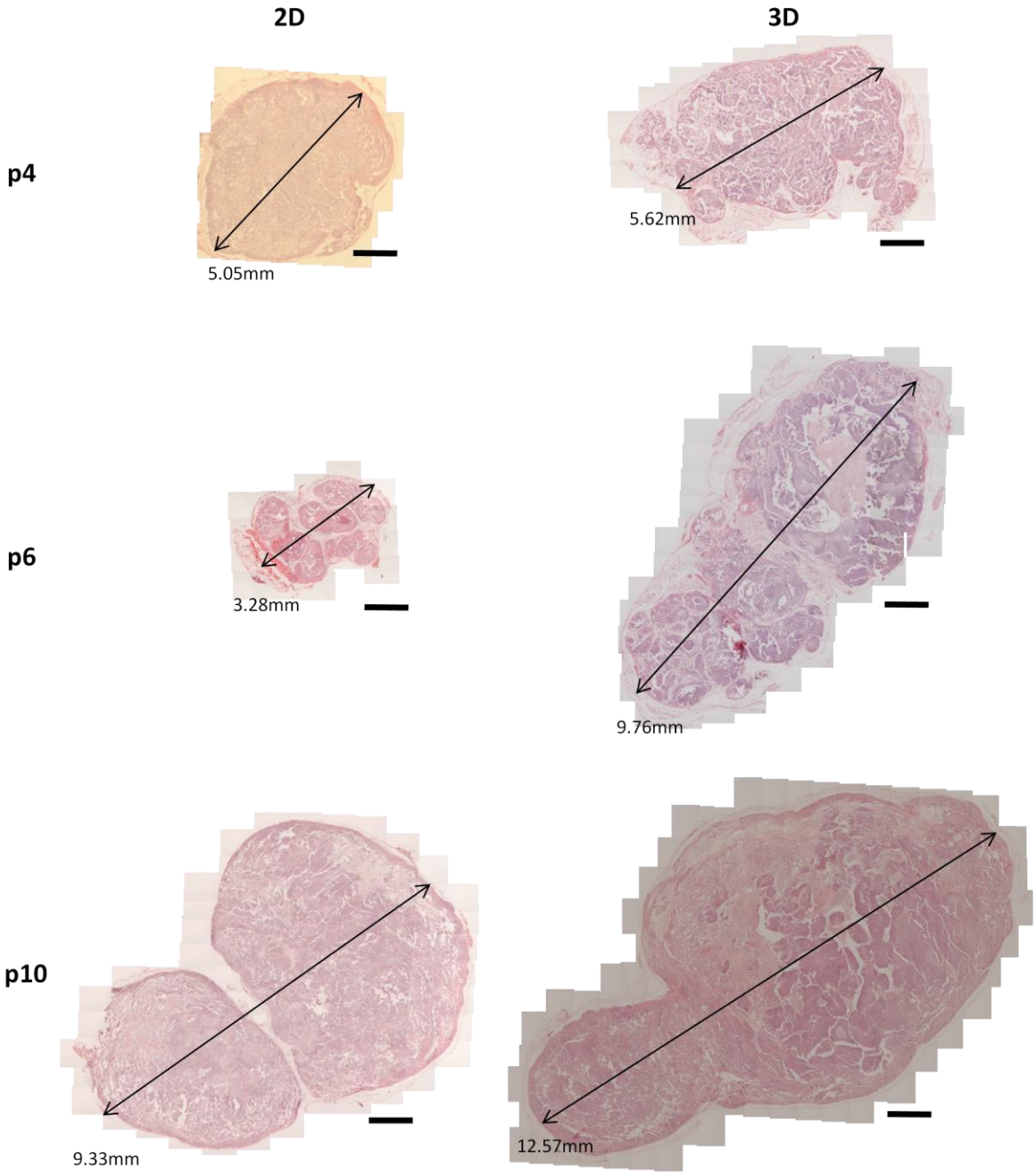

Figure 4.29. Passaging TERA2.cl.SP12 cells in 3D affects the teratoma size and complexity. At passage 4,6, and 10, 2D and 3D cells were injected subcutaneously into immune-deficient mice and allowed to form teratomas. Teratoma were removed and processed for histology. H&E staining demonstrates that teratomas from 3D-primed cells are on average larger than those formed from 2D cells and comprise of a more diverse range of tissue that their 2D counterparts. Example sections/profiles of teratomas shown. Scale bar = 1mm.

4.5.12 Analysis of teratoma sections using immunohistochemistry.

Teratomas were paraffin embedded and sectioned to produce 8 consecutive 6µm sections. Each of these sections were attached to separate microscope slides. Samples of teratomas formed from the 3 different passages and 2 culture conditions were stained with Haematoxylin and Eosin and for all three germ layers. More specifically sections were immunostained for the ectodermal markers: nestin – a neural progenitor cell marker, TUJ-1 – a marker of immature neurons, NF-200 – a mature neuronal marker and cytokeratin-8 – an epithelial marker. They were also stained for the mesodermal marker – smooth muscle actin (SMA), the endoderm marker – alpha-fetoprotein (AFP) and the embryonic stem cell marker – Oct 4.

Staining for ectodermal markers revealed a difference between teratomas formed from 2D and 3D passaged cells as early as passage 4. Teratomas formed from 2D passage 4 cells were primarily TUJ-1 (Figure 4.30A) and nestin positive (Figure 4.30B). They had very limited positive staining for NF-200 and it was limited to isolated cells within the teratomas (Figure 4.30C). There were also individual cells which stained for the epithelial marker cytokeratin-8 (Figure 4.30D). Teratomas formed from 3D passage 4 cells displayed more localised staining for TUJ-1 than their 2D counterparts (Figure 4.32A) and also the majority of cells no longer stained for nestin. In Figure 4.32B there are large areas which do not stain for nestin. There were more cells which stain for NF-200 in the 3D passage 4 teratoma than the tumour formed from 2D cells, with evidence of NF-200 positive neurites within the tumour tissue (Figure 4.32C). There were also noticeably dense areas of cytokeratin-8 positive tissue in the 3D passage 4 teratoma (Figure 4.32D).

Staining for markers of the other two germ layers also displayed a difference between the teratomas formed from TERA2.cl.SP12 cells passaged in 2D and 3D culture. Both the tumours formed from 2D and 3D cells displayed areas of undifferentiated Oct 4 positive cells (Figure 4.31A & Figure 4.33A) and they were also similar in their staining for the endoderm marker – AFP with neither teratoma producing strong staining for AFP (Figure 4.31B and Figure 4.33B). The teratomas differed greatly when stained with the mesodermal marker – smooth muscle actin. Teratomas produced from 2D passage 4 cells had minimal weak staining for SMA (Figure 4.31C) whereas 3D passage 4 cells produced SMA-positive structures within the tumour tissue (Figure 4.33C).

As the passage number of both 2D and 3D cells increased to passage 6 the teratomas contained tissue that was more organised into structures compared to lower passage cells. In the teratomas formed from 2D passage 6 cells there was still large areas of TUJ-1 staining (Figure 4.34A) and fewer nestin positive cells than the lower passage cells (Figure 4.34B). Consistent with the 2D passage 4 cells there was still only isolated cells which were NF-200 positive in the 2D passage 6

teratomas (Figure 4.34C). These higher passages of 2D cells were able to form teratomas which displayed significantly larger amounts of cytokeratin-8 staining than the passage 4 cells (Figure 4.34D). Interestingly after 6 passages in 3D culture, TERA2.cl.SP12 cells were able to form more diverse teratomas and immunostaining for ectodermal markers revealed TUJ-1 positive structures (Figure 4.36A) rather than the majority of cells staining positive for TUJ-1. Nestin-positive cells were also limited to specific structures rather than throughout the tissue (Figure 4.36B) as had been seen in all previous lower passage tissues. There was still only limited staining for NF-200, although there was more evidence of neurites from the 3D passage 6 cells (Figure 4.36C). In contrast to the 2D passage 6 tumours the 3D tissue had formed distinct structures which were cytokeratin-8 positive as highlighted in Figure 4.36D.

By passage 6, there was also a difference in staining for the embryonic stem cell marker – Oct 4. In the 2D passaged tissue there was still staining for Oct 4 in large areas of the tumour although staining was relatively weak (Figure 4.35A) whereas in the 3D passaged tissue, the staining was of a similar intensity but was limited to small structures within the teratoma (Figure 4.37A). Consistent with the findings from the lower passage tissue – 2D cells showed very limited staining for mesoderm (Figure 4.35B) whereas 3D passage 6 cells were able to form structures that stained positive for smooth muscle actin (Figure 4.37B). Again neither the 2D or 3D passage 6 cells stained strongly for the endoderm marker – AFP, although both produced isolated positive cells (Figure 4.35C & Figure 4.37C).

As described for the passage 6 tissue, the passage number of both 2D and 3D passaged cells affected the formation of tissue with passage 10 cells being able to form more complex structures than the lower passages. The vast majority of 2D passage 10 tissue remained either TUJ-1 (Figure 4.38A) or nestin positive (Figure 4.38B) but in contrast to the lower passages there was staining of discrete complex structures for NF-200 (Figure 4.38C) and for cytokeratin-8 although the structures were not as large as in 3D passaged tissue (Figure 4.38D). Staining for all the ectodermal markers in 3D passage 10 tissues highlights complex structures. In both the TUJ-1 (Figure 4.40A) and nestin (Figure 4.40B) positive tissue there were areas containing evidence of neural rosettes. There was more extensive staining for NF-200 than had been seen in the previously mentioned tissue (Figure 4.40C) and there were obvious cytokeratin-8 positive structures (Figure 4.40D). Both the passage 10 teratomas again had weak Oct 4 (Figure 4.39A & Figure 4.41A) staining but there was a more noticeable difference in both mesoderm and endoderm markers between 2D and 3D passaged cells. The tissue formed from 2D passage 10 cells did contain cells that were SMA (Figure 4.40B) and AFP (Figure 4.40C) positive but this staining is likely to be peripheral blood vessels rather than differentiated tissue. Whereas the 3D passage 10 tissue showed complex structures staining for smooth muscle actin (Figure 4.41B) and

areas of significant alpha-fetoprotein staining which had not been evident in any of the other tumours (Figure 4.41C).

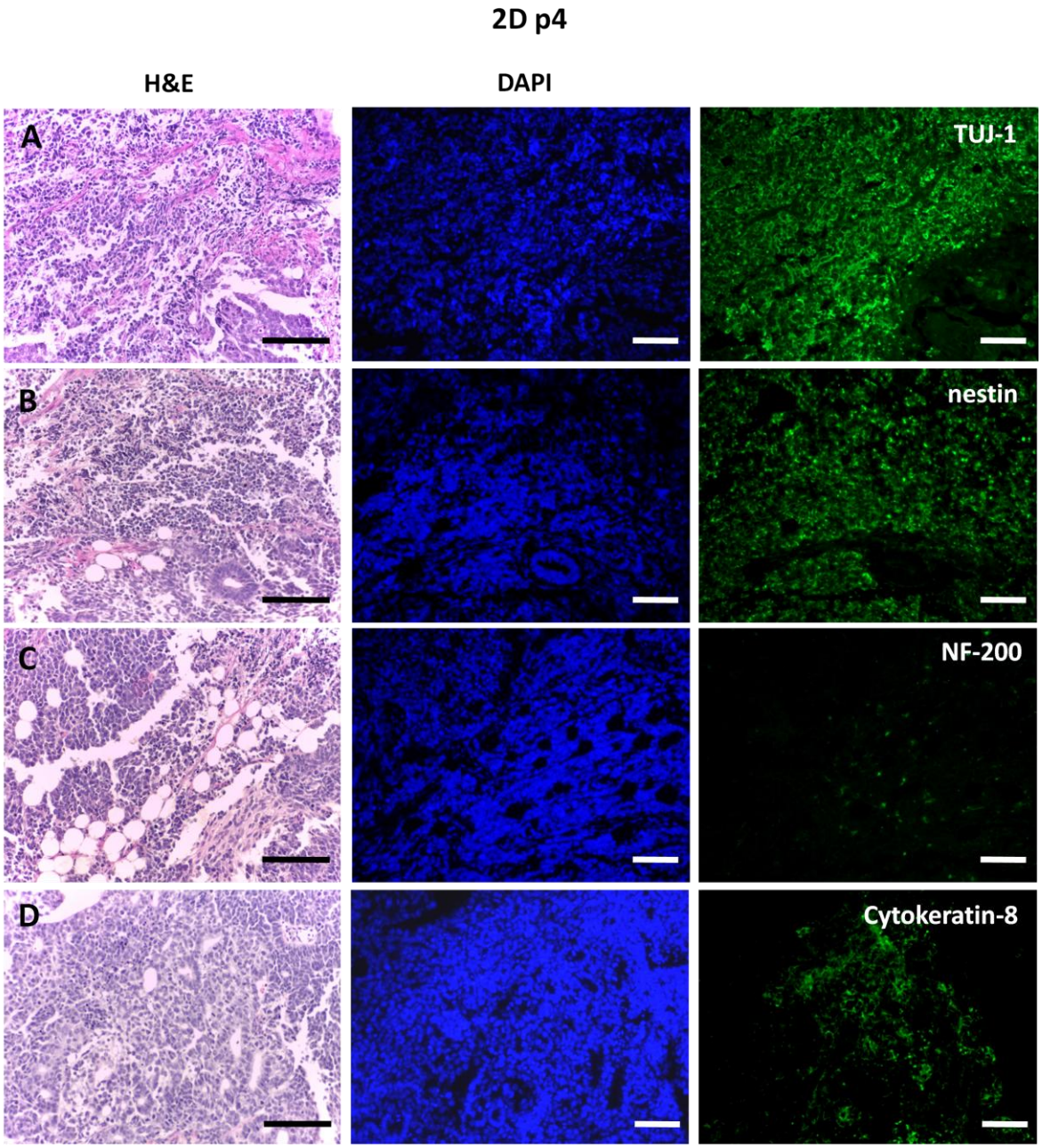

Figure 4.30. Immunostaining for ectodermal markers in teratomas formed from TERA2.cl.SP12 cells cultured in 2D for 4 passages. 2D p4 teratomas show large areas of TUJ-1 positive and nestin- positive cells. There was very limited NF-200 staining and limited production of cytokeratin-8**. Scale bars = 100µm.**

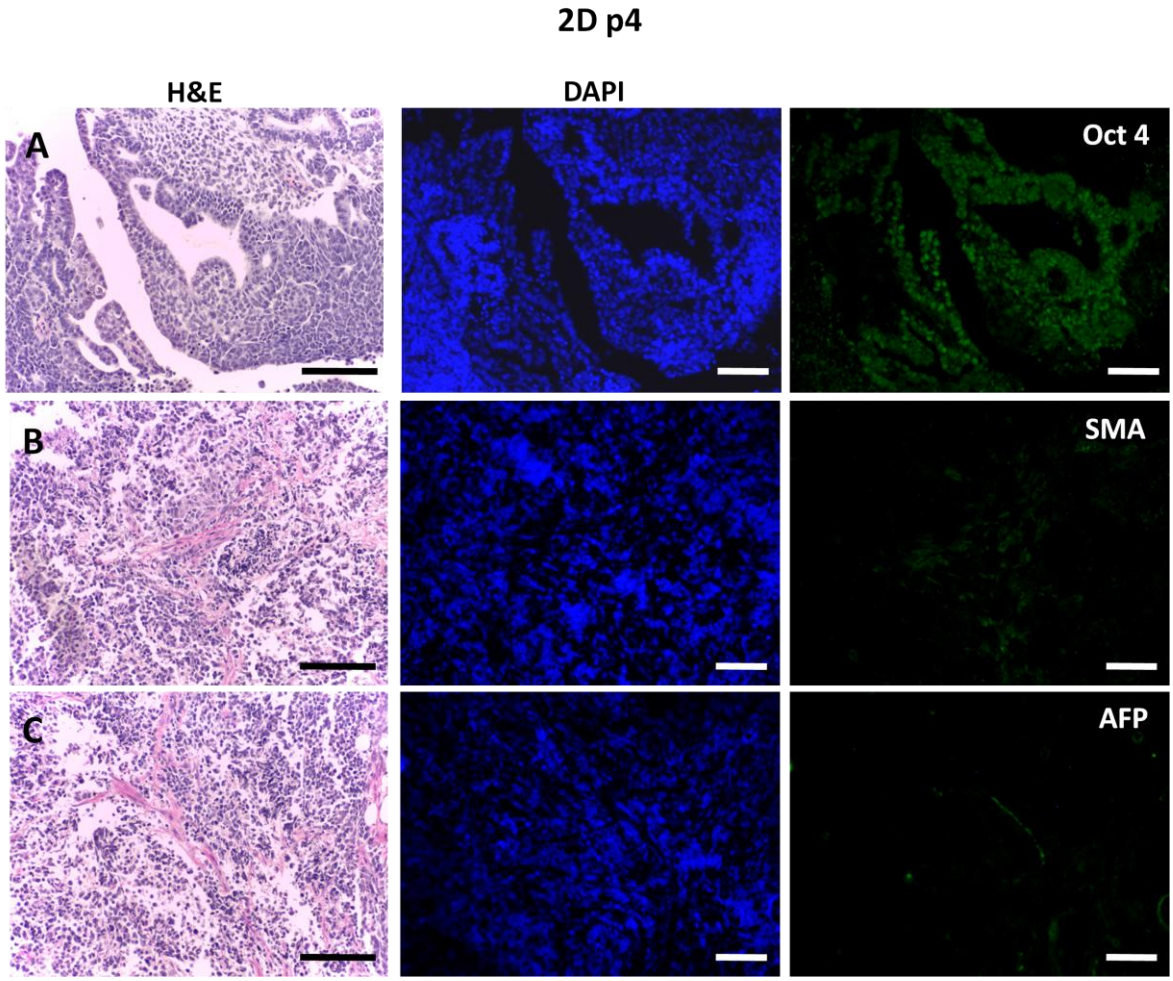

Figure 4.31. Immunostaining for embryonic stem cell marker – Oct-4 and the two other germ layer markers in teratomas formed from TERA2.cl.SP12 cells cultured in 2D for 4 passages. 2D p4 teratomas have large areas of Oct 4 positive cells and minimal staining for mesoderm (SMA) and endoderm (AFP) markers**. Scale bars = 100μm**

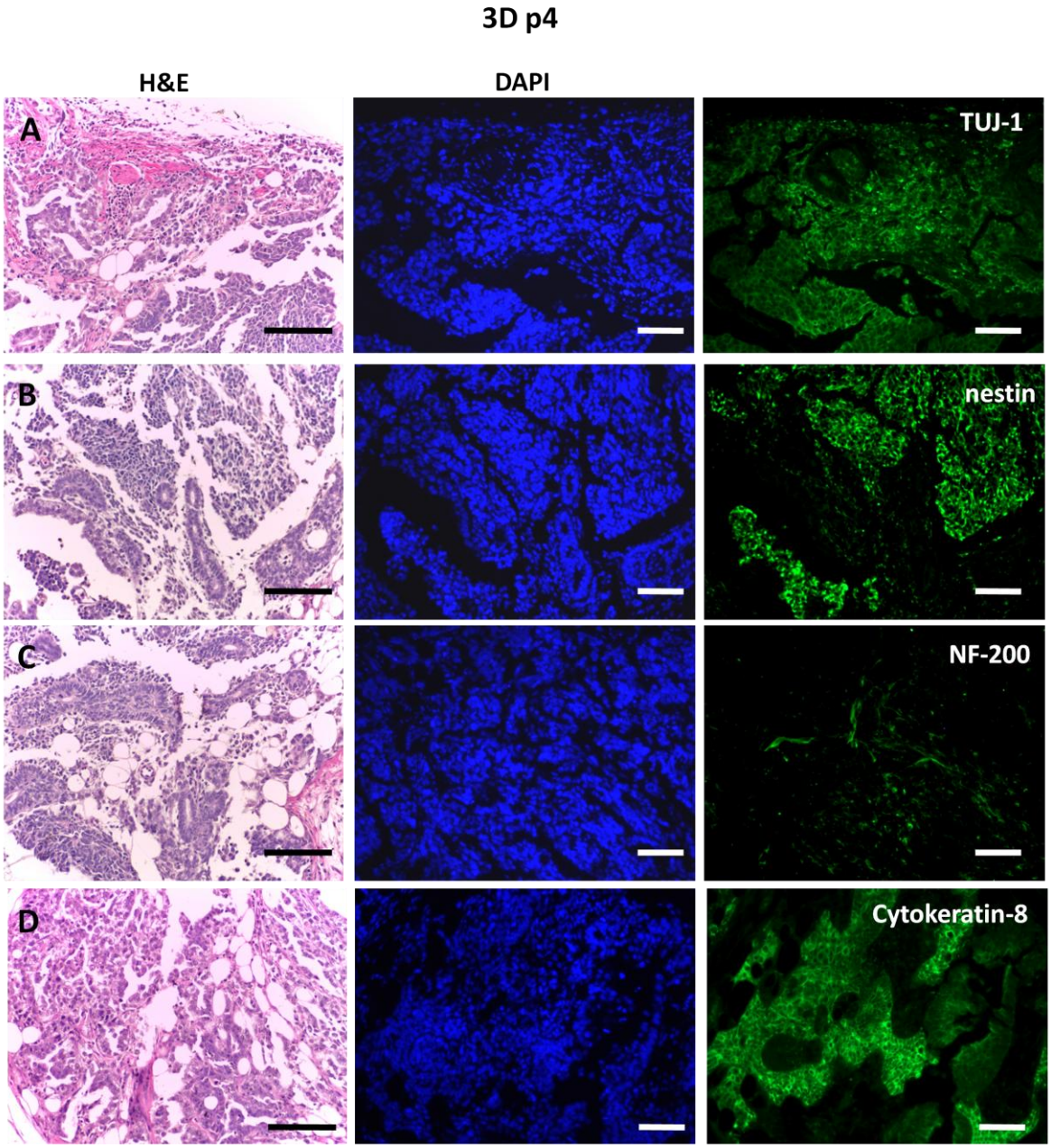

Figure 4.32. Immunostaining for ectodermal markers in teratomas formed from TERA2.cl.SP12 cells cultured in 3D for 4 passages. 3D p4 teratomas show large areas of TUJ-1 positive and nestin- positive cells in a similar way to the 2D p4 teratomas. There is also some NF-200 staining and noticeably dense areas of cytokeratin-8 positive tissue which differs from the 2D p4 teratomas. **Scale bars = 100µm.**

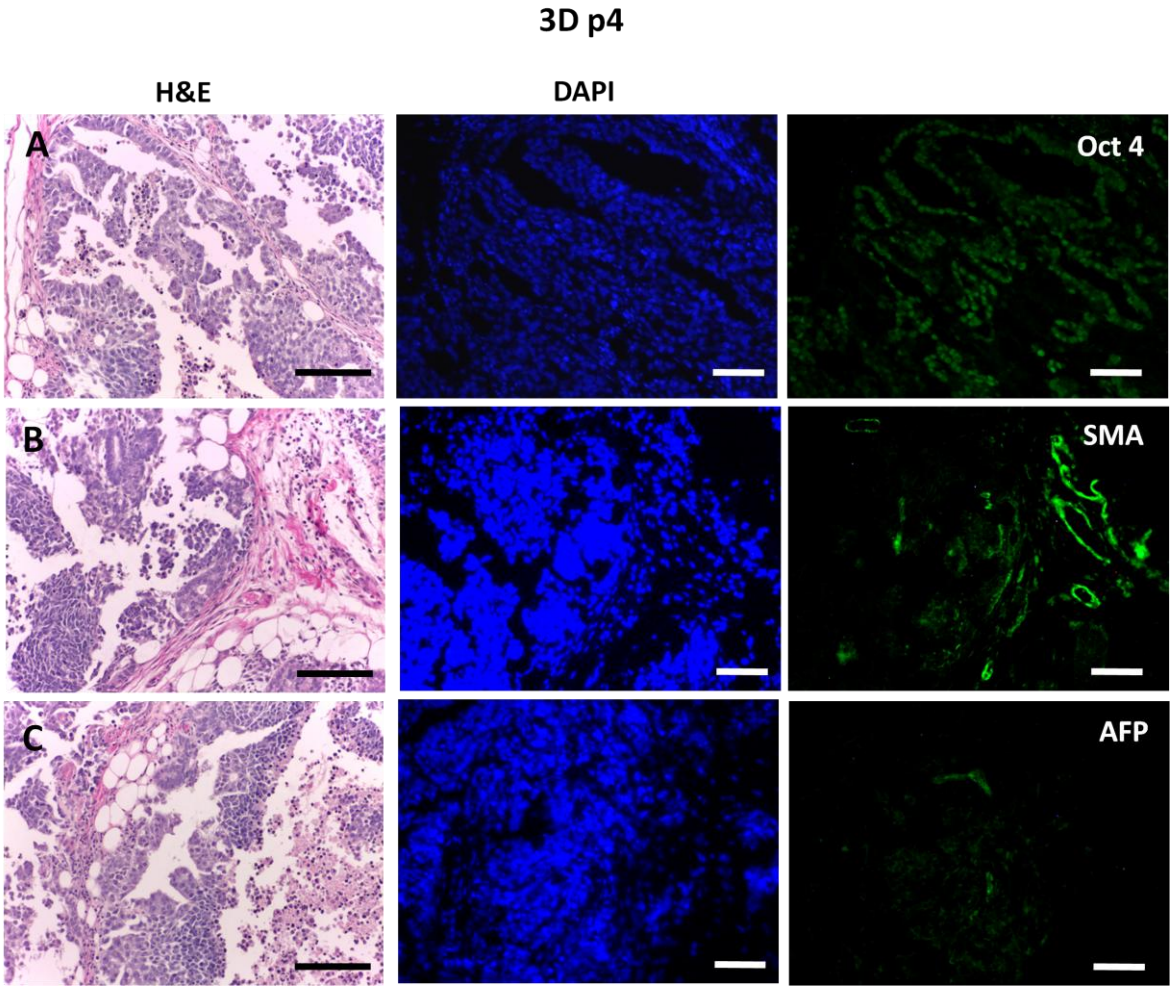

Figure 4.33. Immunostaining for embryonic stem cell marker – Oct 4 and the two other germ layer markers in teratomas formed from TERA2.cl.SP12 cells cultured in 3D for 4 passages. 3D p4 teratomas still have areas of Oct 4 positive cells and structures that stain for the mesoderm marker – smooth muscle actin. This similar to the 2D p4 teratomas but there is also some limited staining for endoderm (AFP) marker**. Scale bar = 100µm.**

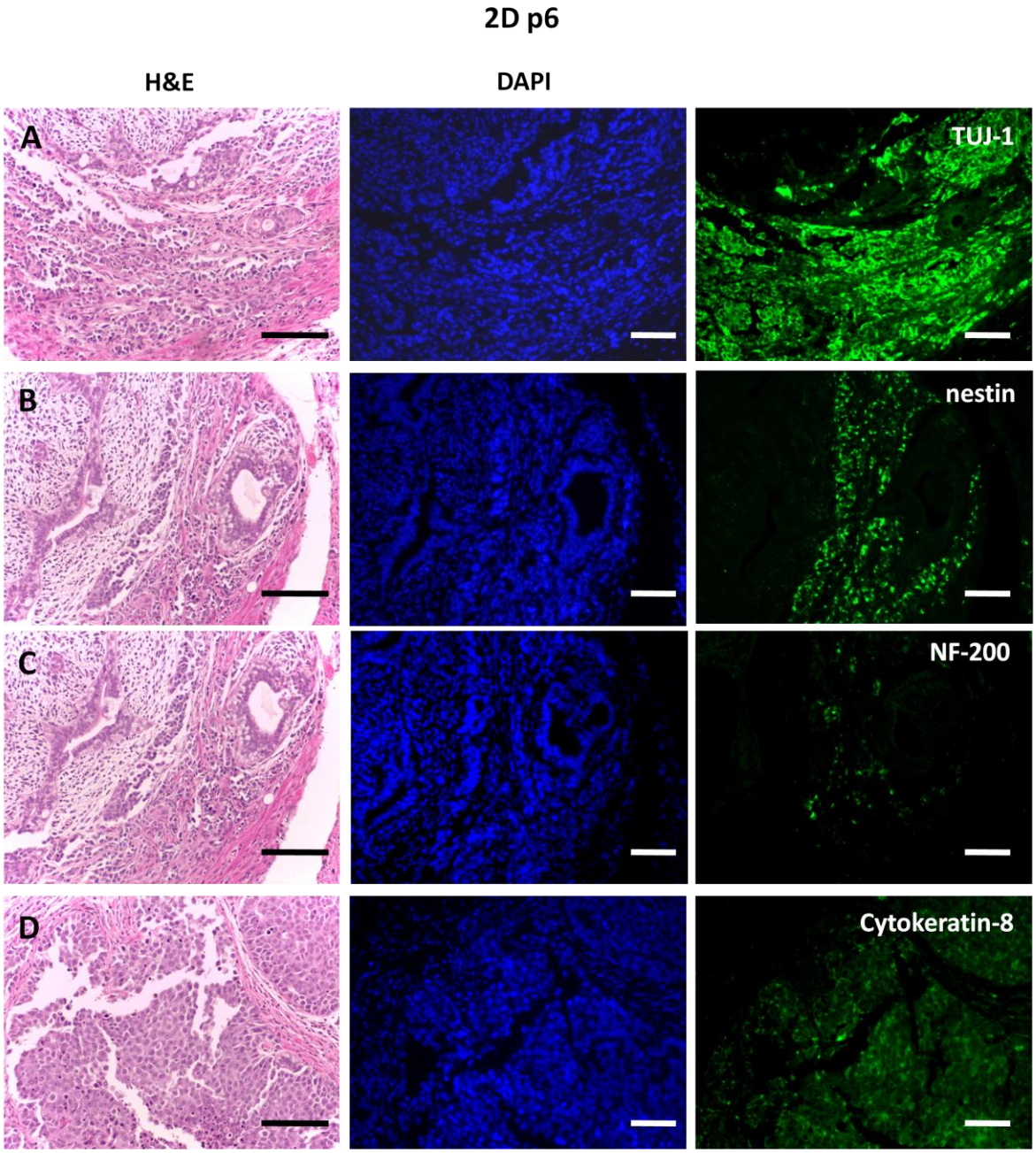

Figure 4.34. Immunostaining for ectodermal markers in teratomas formed from TERA2.cl.SP12 cells cultured in 2D for 6 passages. 2D p6 teratomas show large areas of TUJ-1 positive in a similar way to the lower passage cells but there is now reduced areas of and nestin-positive cells. There are individual cells which stain positive for NF-200 large areas of cytokeratin-8 positive tissue, in contrast to the lower passage counterparts. **Scale bars = 100µm.**

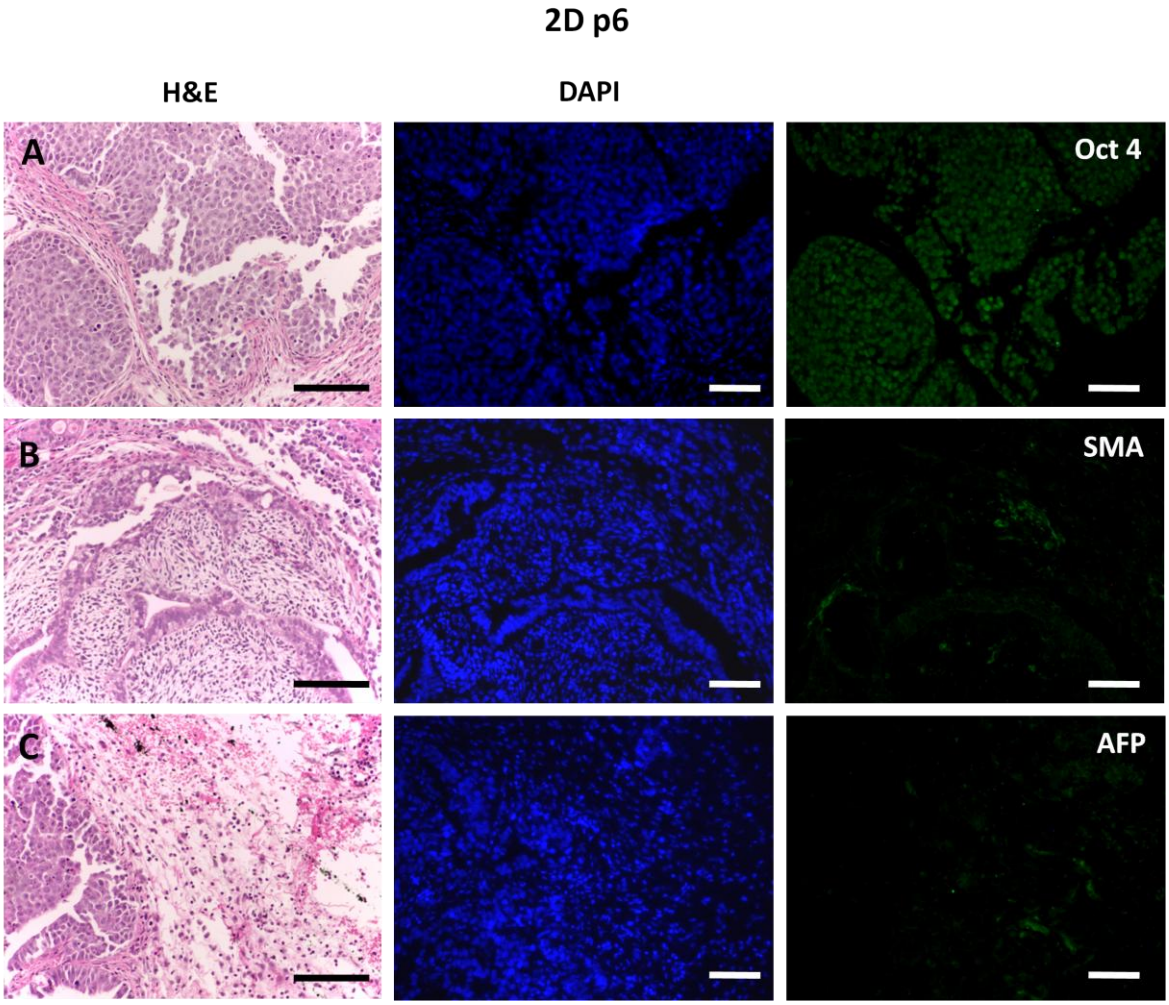

Figure 4.35. Immunostaining for embryonic stem cell marker – Oct 4 and the two other germ layer markers in teratomas formed from TERA2.cl.SP12 cells cultured in 2D for 6 passages. 2D p6 teratomas have large areas of Oct 4 positive cells and limited staining for mesoderm (SMA) and endoderm (AFP) markers similar to the 2D lower passage cells. **Scale bars = 100µm.**

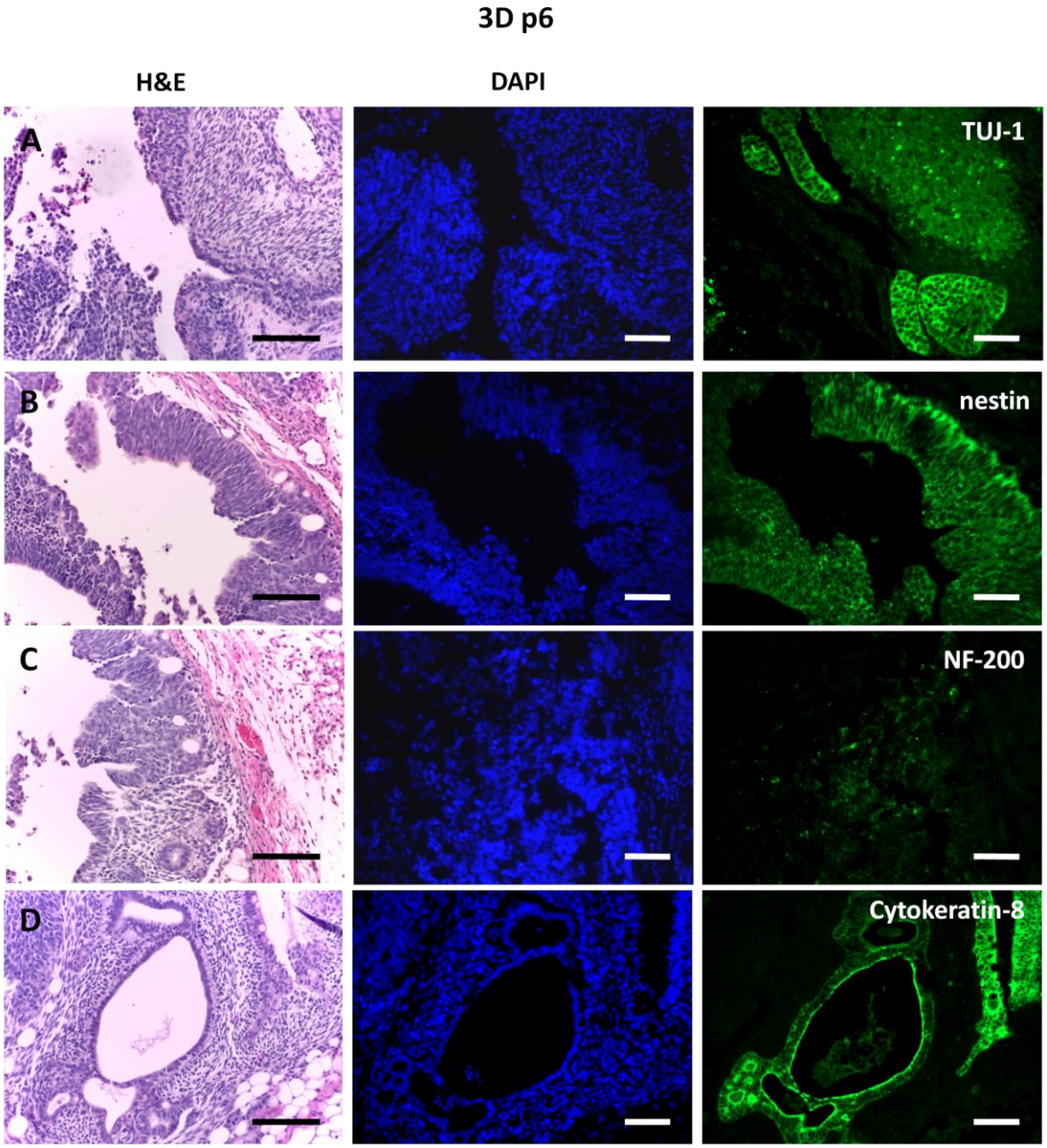

Figure 4.36. Immunostaining for ectodermal markers in teratomas formed from TERA2.cl.SP12 cells cultured in 3D for 6 passages. 3D p6 teratomas show complex structures which are positive for TUJ-1, nestin, and cytokeratin-8. These structures show a degree of organisation not seen in the passage 4 tissues or the 2D p6 tissues. There is still some limited NF-200 staining**. Scale bars = 100µm.**

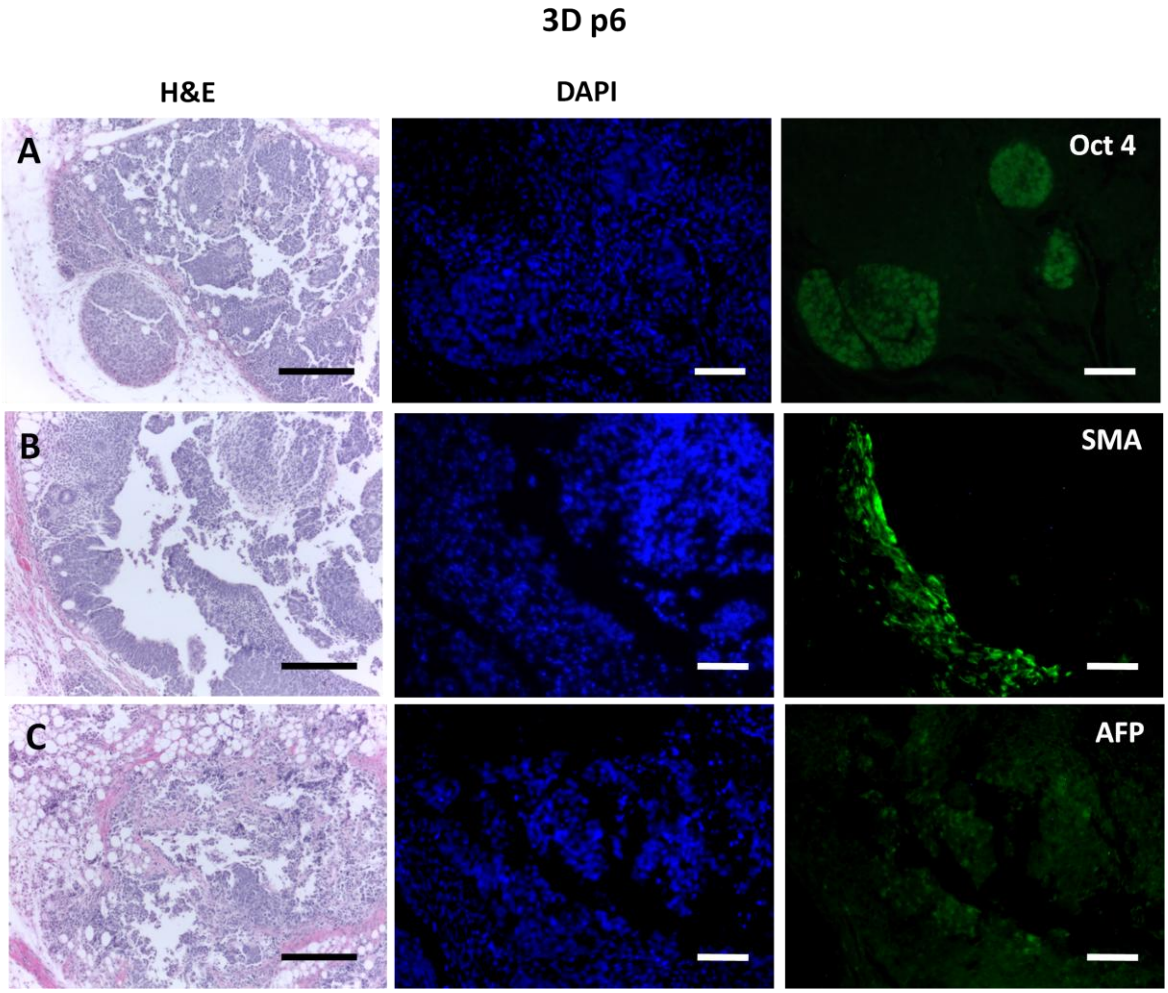

Figure 4.37. Immunostaining for embryonic stem cell marker – Oct 4 and the two other germ layer markers in teratomas formed from TERA2.cl.SP12 cells cultured in 3D for 6 passages. 3D p6 teratomas have fewer structures that are Oct 4 positive cells than their 2D counterparts. There are also complex structures that stain for the mesoderm marker – smooth muscle actin. There is also some positive staining for endoderm marker – alpha fetoprotein, not previously observed. **Scale bars = 100µm.**

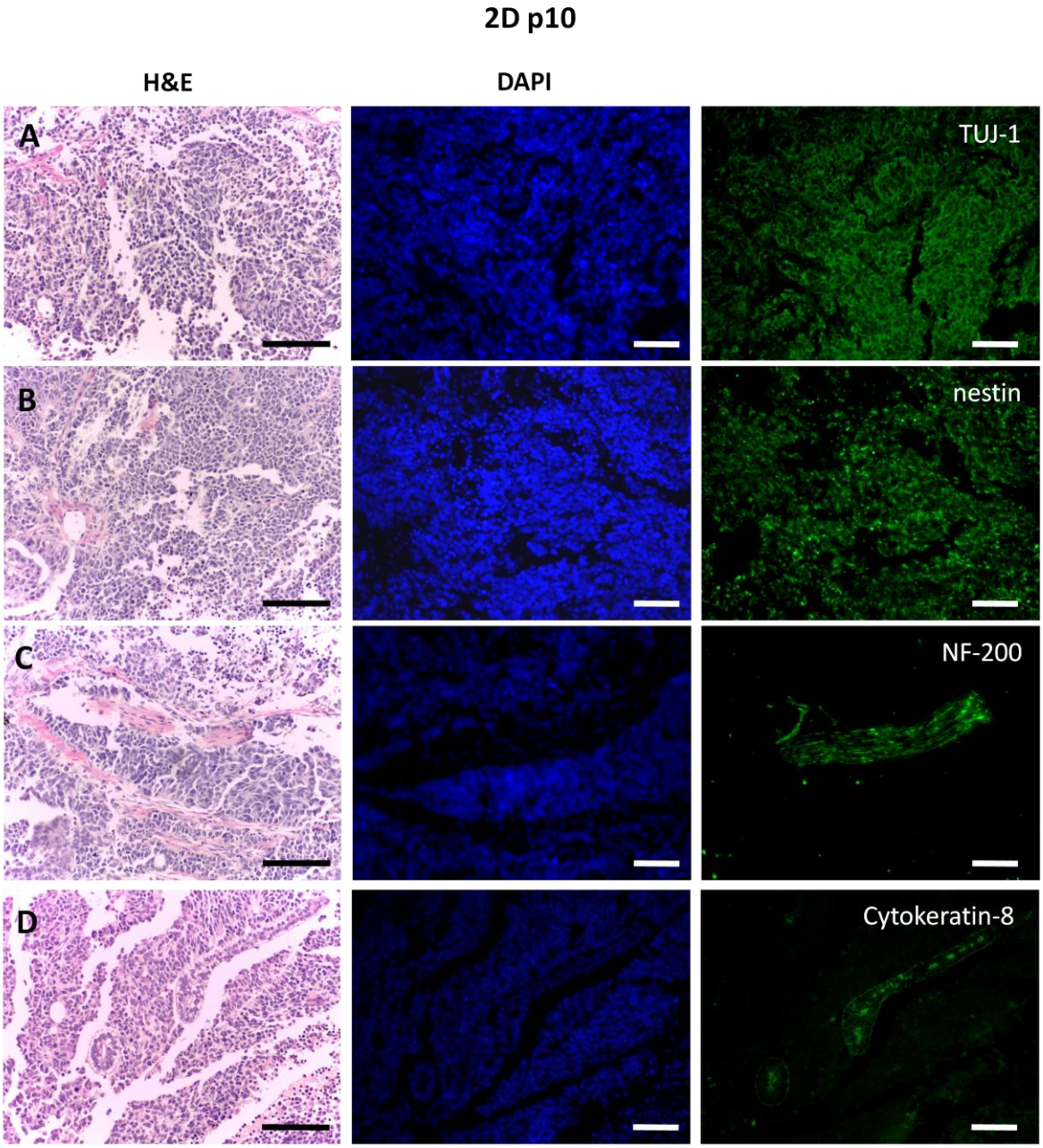

Figure 4.38. Immunostaining for ectodermal markers in teratomas formed from TERA2.cl.SP12 cells cultured in 2D for 10 passages. 2D p10 teratomas still show large areas of TUJ-1 positive and nestin positive cells. There are now structures which stain positive for NF-200 and cytokeratin-8 which had not previously been noted in teratomas from 2D passaged cells. **Scale bars = 100µm.**

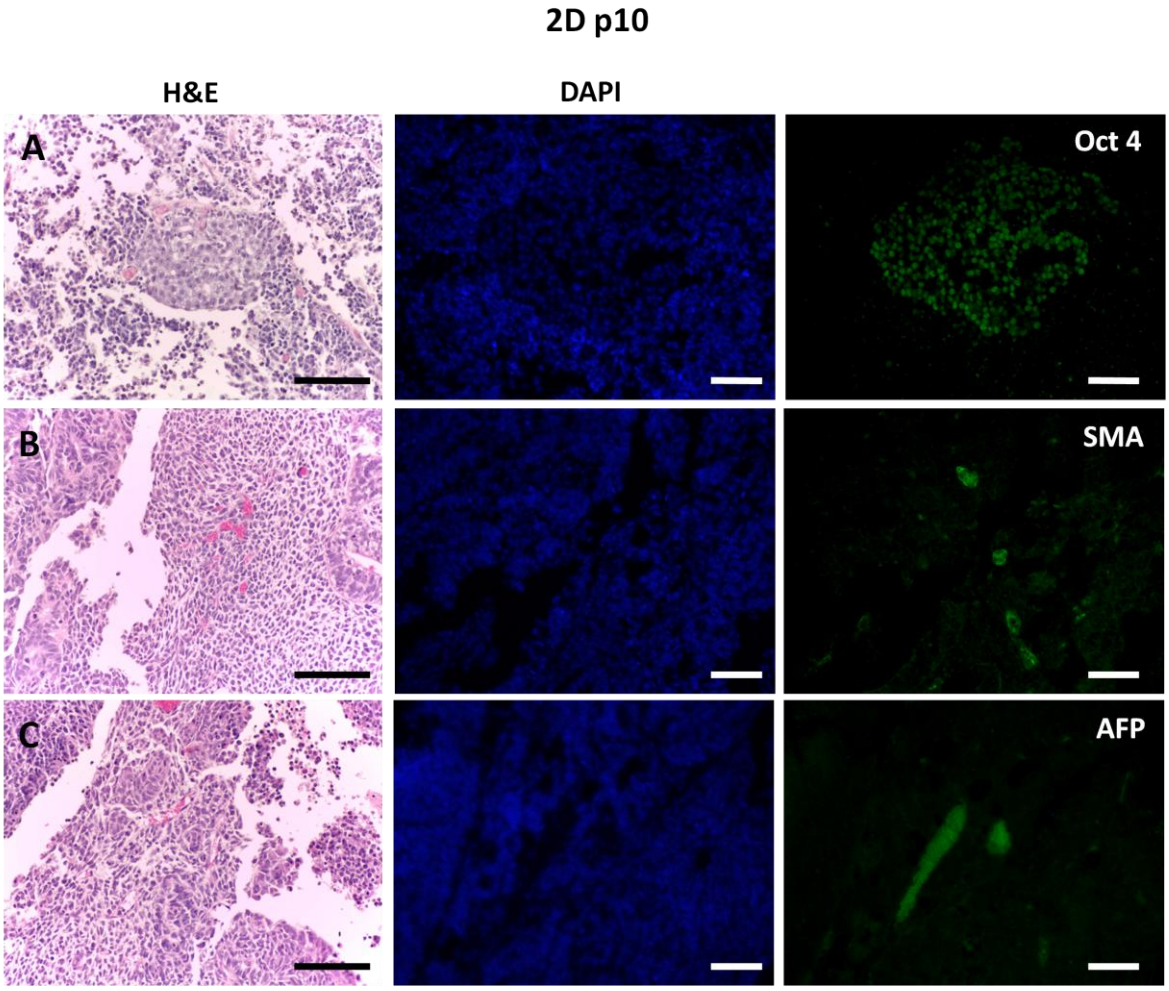

Figure 4.39. Immunostaining for embryonic stem cell marker – Oct 4 and the two other germ layer markers in teratomas formed from TERA2.cl.SP12 cells cultured in 2D for 10 passages. 2D p10 teratomas have areas containing Oct 4 positive cells and still only very limited staining for mesoderm (SMA) and endoderm (AFP) markers. **Scale bars = 100µm.**

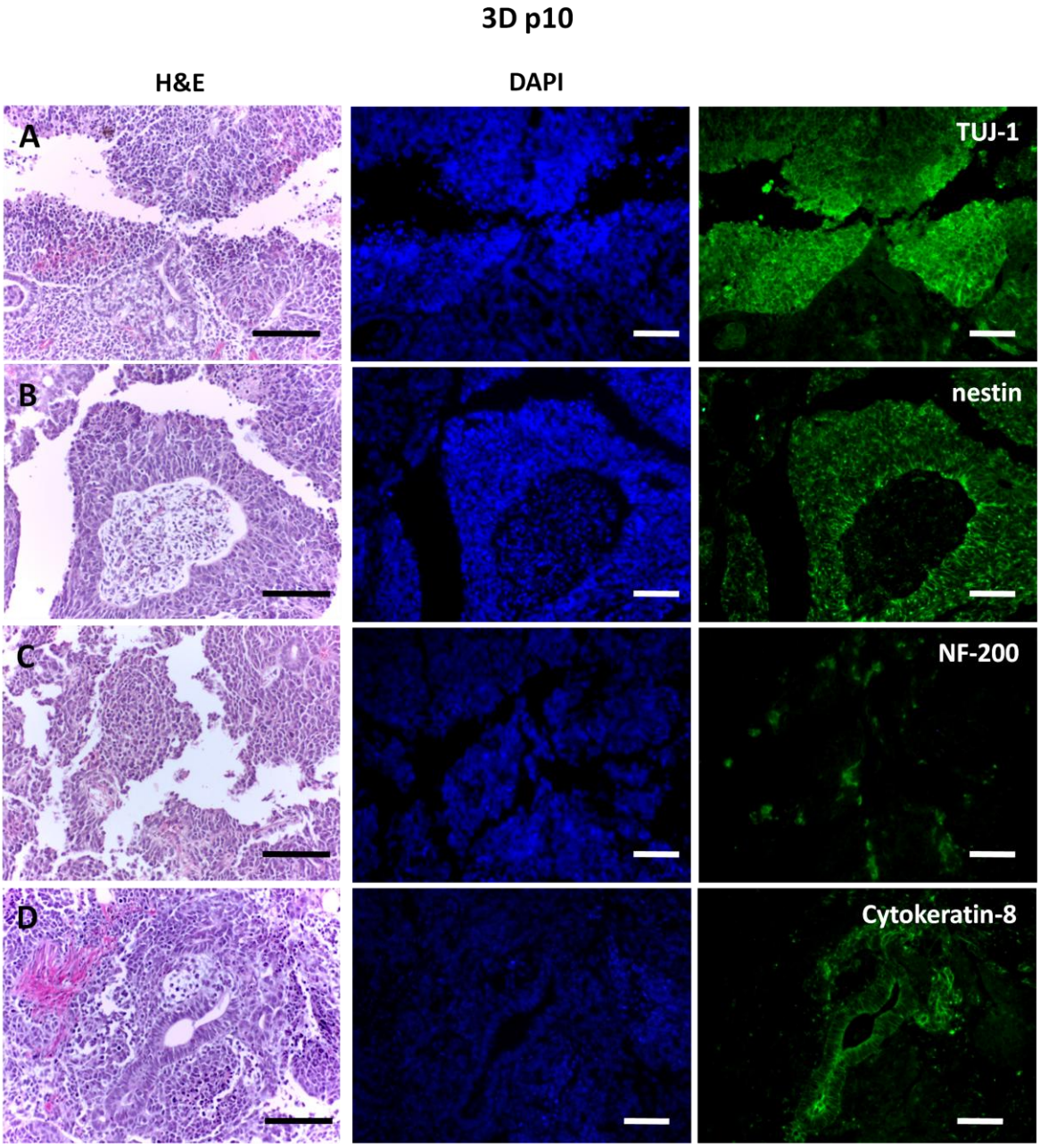

Figure 4.40. Immunostaining for ectodermal markers in teratomas formed from TERA2.cl.SP12 cells cultured in 3D for 10 passages. 3D p10 teratomas show complex structures which are positive for TUJ-1, nestin, and cytokeratin-8, this is in contrast to teratomas formed from 2D p10 cells which do not contain positive structures. There are now NF-200 positive cells across large areas of the teratoma. **Scale bars = 100µm.**

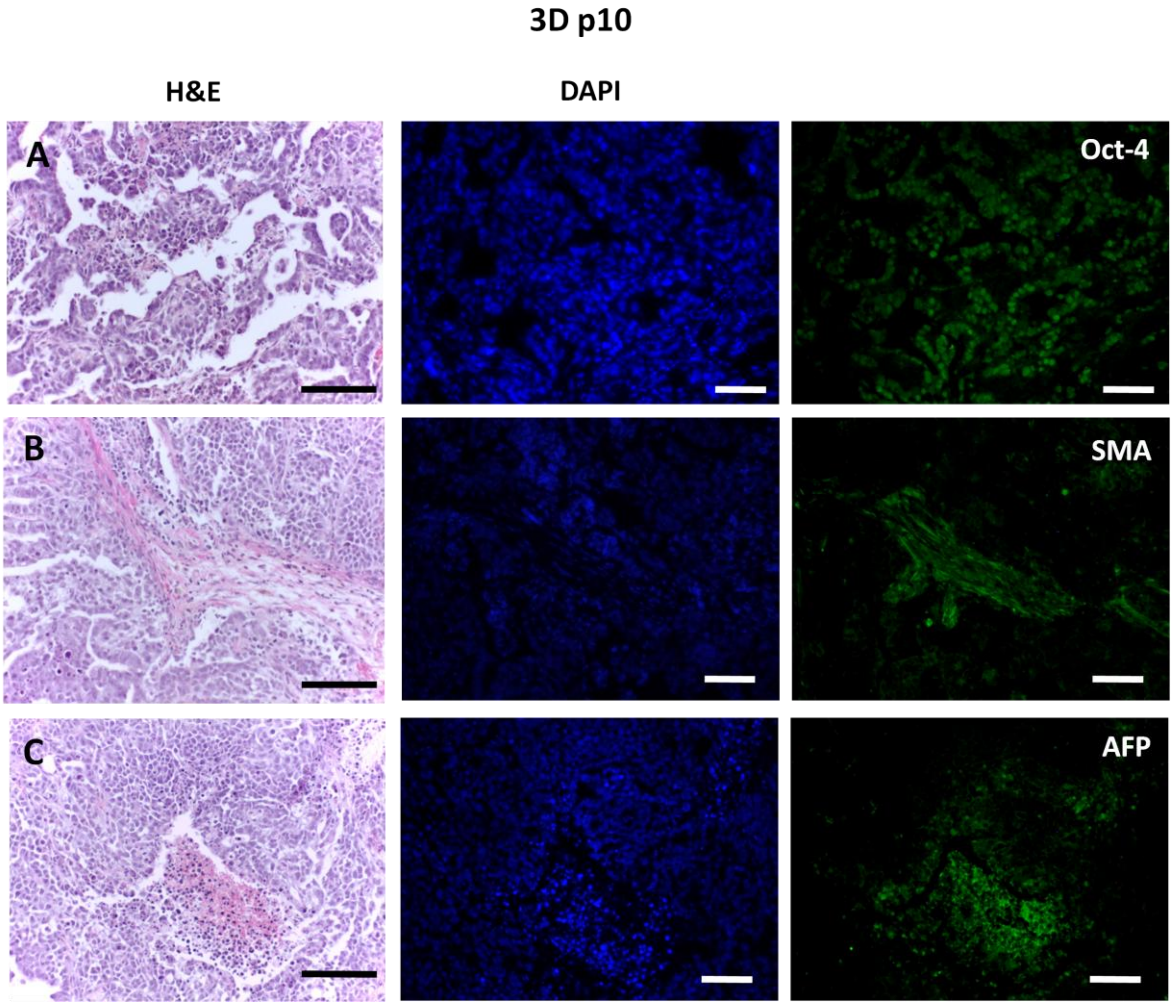

Figure 4.41. Immunostaining for embryonic stem cell marker – Oct 4 and the two other germ layer markers in teratomas formed from cells cultured in 3D for 10 passages. 3D p10 teratomas still have some areas that show some weak Oct 4 staining and now contain many complex structures that stain for smooth muscle actin and some that stain for alpha fetoprotein. **Scale bars = 100μm.**

4.5.13 Passaging embryonic stem cell line in 3D

The findings detailed above provide evidence that growing human pluripotent stem cells in 3D may affect their ability to differentiate. Whilst an excellent, well proven and established model system, this proof of concept work has used the embryonal carcinoma cell line – TERA2.cl.SP12. This is a good model system for pluripotent stem cells, as the cells are less expensive to culture and it is easy to maintain their pluripotency in culture. They are also a useful model of early development and cell fate determination in the embryonic ectoderm [127]. To validate the findings previously described in this Chapter it was necessary to test the system using embryonic stem cells. To do this two cell lines were chosen – one developed by Roslin Cellab (http://roslincellab.com/) called RC-10 and the H9 cell line originally described by Thomson et al. [51] but now cultured using a feeder layer-free method.

4.5.14 Passaging the RC-10 ES cells in 3D on Strata membranes

Due to difference in proliferation rate between the TERA2.cl.SP12 cells and the RC-10 cell line, it was advised that the length of time between passages should be modified for the specific cell line, as would be done during 2D culture. In order to do this, two time periods were tested: passaging at 3.5 day which is close to the TERA2.cl.SP12 cell protocol and passaging at 7 days.

Harvest point (D3.5)	Passage 1	Passage 2	Passage 3
Cells In (Seeding per insert)	1×10^6	1×10^6	1×10^6
Cells Out (Harvest per insert)	4.8×10^6	6.35×10^6	3.7×10^6
Fold Increase	4.8	6.35	3.7

Harvest point (D7)	Passage 1	Passage 2	Passage 3
Cells In (Seeding per insert)	1×10^6	1×10^6	2.35×10^5
Cells Out (Harvest per insert)	5.9×10^6	3.525×10^5	2.165×10^5
Fold Increase	6.0	< inoculum	< inoculum

Table 4.3. Cell retrieval of human embryonic stem cells (RC-10) from 3D passaging. The two alternative passaging protocols (3.5 and 7 day) for RC-10 were assessed for cell number and fold increase of the cell population as a whole, using the NC-3000 cell counter. These data highlight the need for an optimal passaging protocol and the need to adapt the protocol as the cells adapt to the 3D environment.

Haematoxylin and Eosin staining of the first 4 passages using the 3.5 day protocol revealed a dense layer of cells formed on the surface of the Strata membrane at all passages but as the passage number increased the thickness of the cell layer decreased (Figure 4.42N). This was consistent with the number of cells retrieved from the Strata membranes: at passage one there was a 4.8 fold increase in cell number after passage 1 and this increased to a 6.35-fold after passage 2. However at passage 3 the fold increase had started to decrease to less than that at passage 1 (Table 4.3). Consistent with the data for TERA2.cl.SP12 cells, the majority of RC-10 cells passaged every 3.5 days in 3D, stained positive for the embryonic stem cell marker – Oct 4 at all passages. (Figure 4.43).

Increasing the time period between passages in 3D to 7 days had a detrimental effect on the number of cells retrieved from the Strata membranes. At the first passage there was a very dense cell layer on the membrane which was up to 11 cells thick. The majority of these cells are Oct 4 positive although there appears to be a gradient of positive cells with fewer cells staining for Oct 4 as they get further away from the membranes (Figure 4.44). When this cell layer was removed using Accutase after 7 days in culture, cells were counted and there were 5.9×10^6 cells retrieved (Table 4.3). When these cells were reseeded onto fresh Strata membranes they either did not adhere or were unable to proliferate and fewer cells were removed from the membrane than were initially seeded after 7 days in culture (Table 4.3). This was also evident when sections of the membranes were prepared and stained with H&E; there were very few cells on the membranes but the cells that do remain were Oct 4 positive suggesting that this drop in cell number does not appear to be due to differentiation of the stem cells (Figure 4.44).

Further investigation into this decrease in cell number required a growth curve for RC-10 cells cultured on Strata membranes and an assessment of whether embryonic stem cells spontaneously differentiate when placed in the 3D environment. The growth curve was produced using the MTT assay and conducted as previously described to produce the curve for TERA2.cl.SP12 cells in Figure 4.9. The growth profiles on Strata membranes were similar for the two cell lines. They both peaked at day 5 but the profile for RC-10 cells displayed a more rapid decrease in cell viability after 5 days with almost no viable cells on the membranes after 9 days in culture (Figure 4.45).

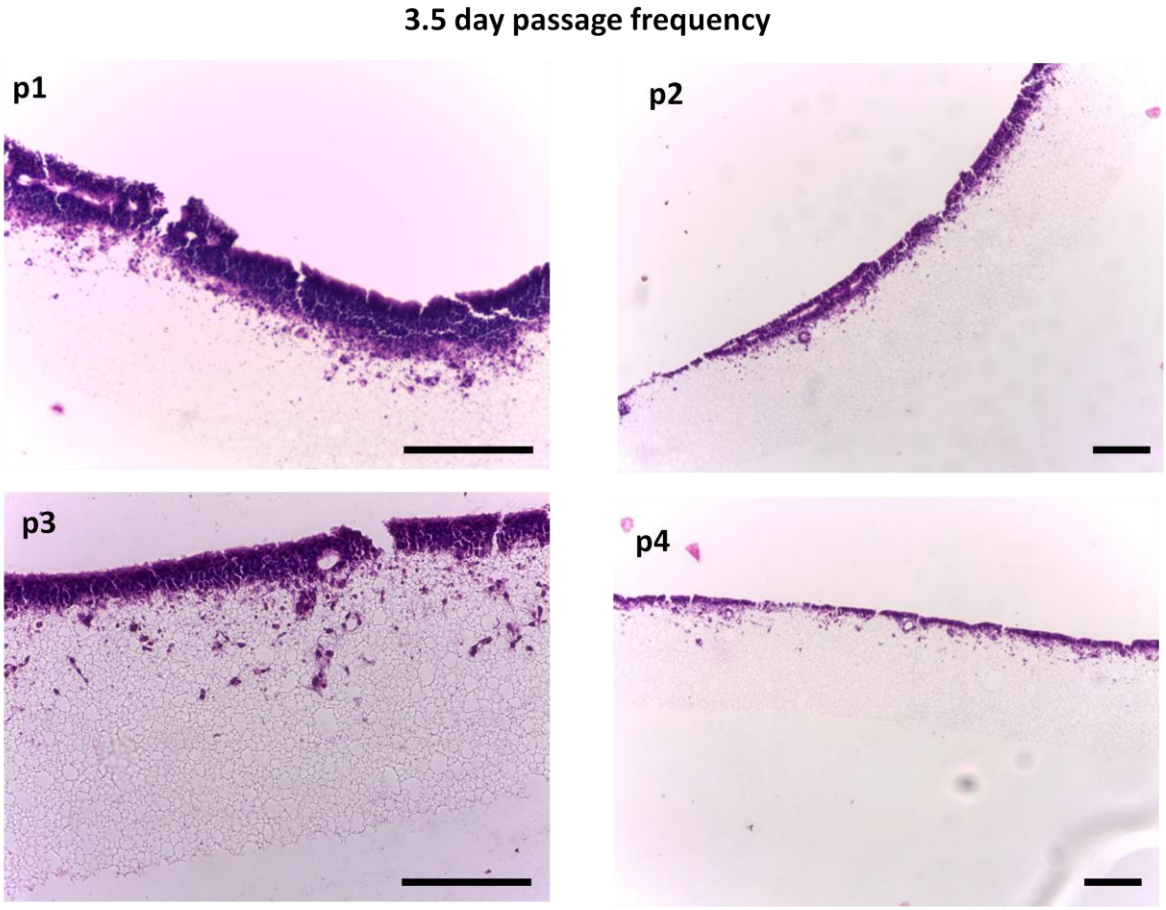

Figure 4.42. Passaging of human embryonic stem cells (RC-10) in 3D. It is possible to passage embryonic stem cells in a similar way to TERA2.cl.SP12 cells. ES cells were passaged every 3.5 days using Accutase. Histological analysis shows a dense layer of cells forming at the surface of the strata membrane. **Scale bars = 100µm**

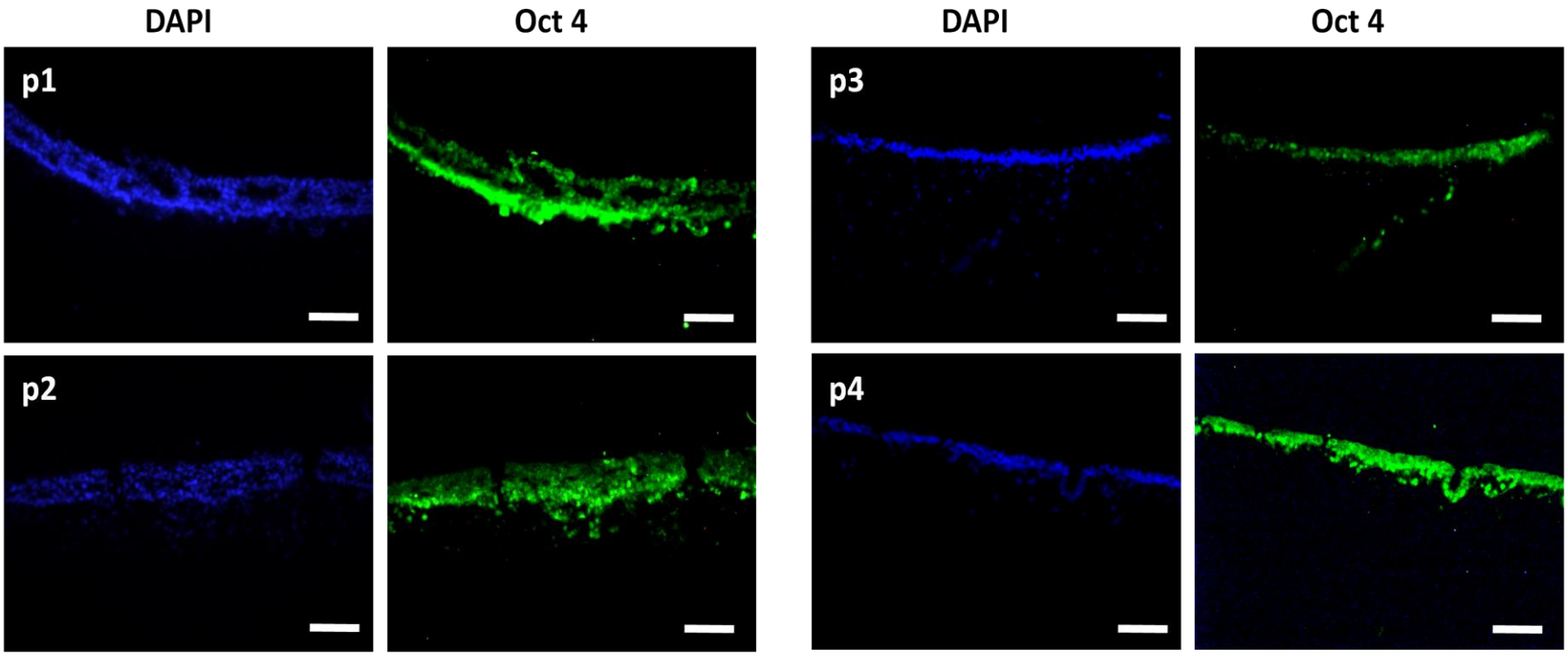

Figure 4.43. Human embryonic stem cells (RC-10) grown in 3D on Strata membranes maintain expression of pluripotent stem cell marker Oct 4. Embryonic stem cells were stained with the stem cell marker Oct 4 at all passage numbers. Even after 4 passages there is still a layer of Oct 4 positive cells on top of the strata membrane**. Scale bars =100µm.**

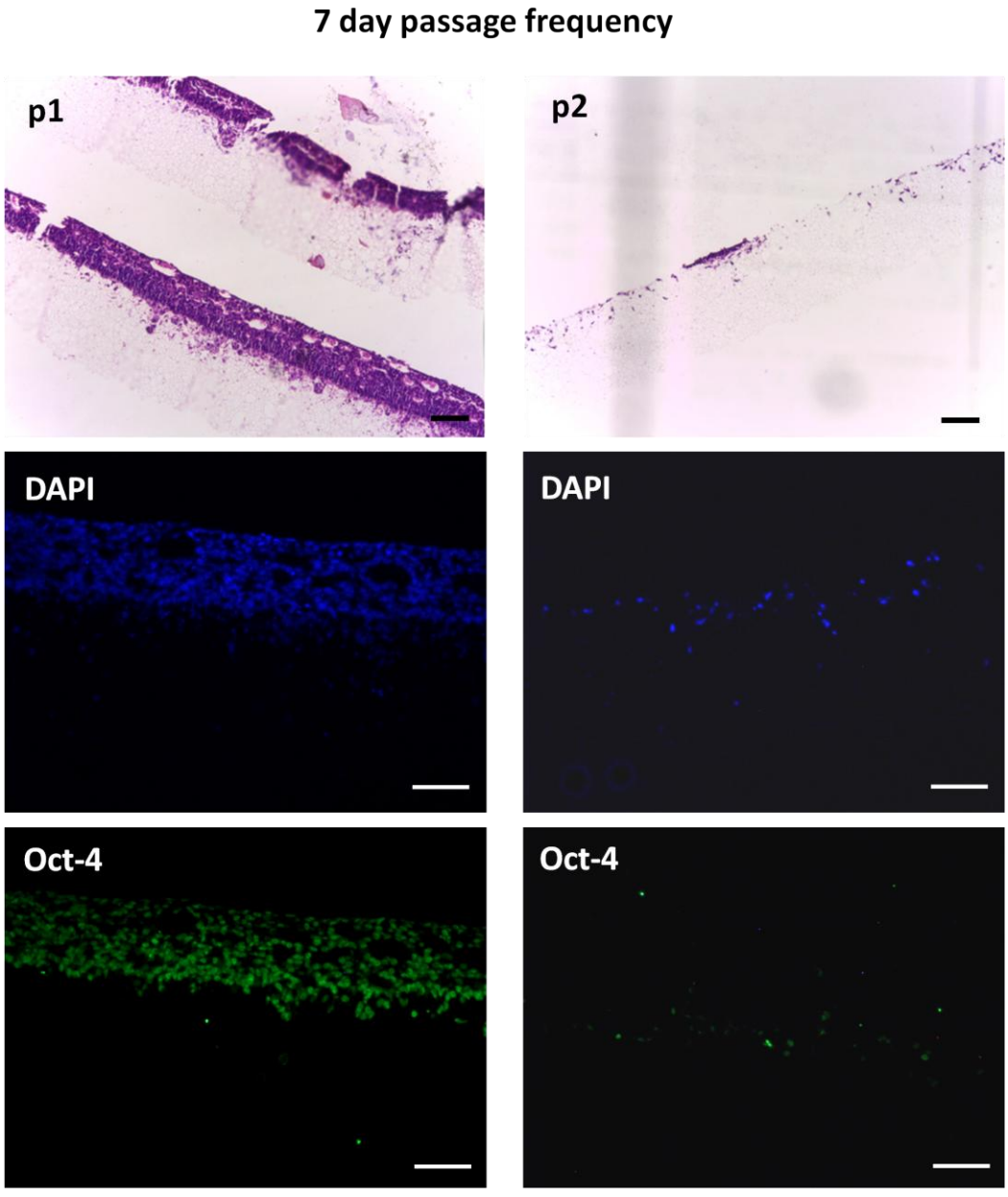

Figure 4.44. Passaging of human embryonic stem cells (RC-10) in 3D. As an alternative passaging protocol, RC-10 cells were passaged every 7 days using Accutase. A dense layer of Oct 4 positive cells is visible during the first passage. However this could not be maintained during subsequent passages using this method. This is due to loss of cells rather than fewer Oct 4 positive cells. **Scale bars = 100µm.**

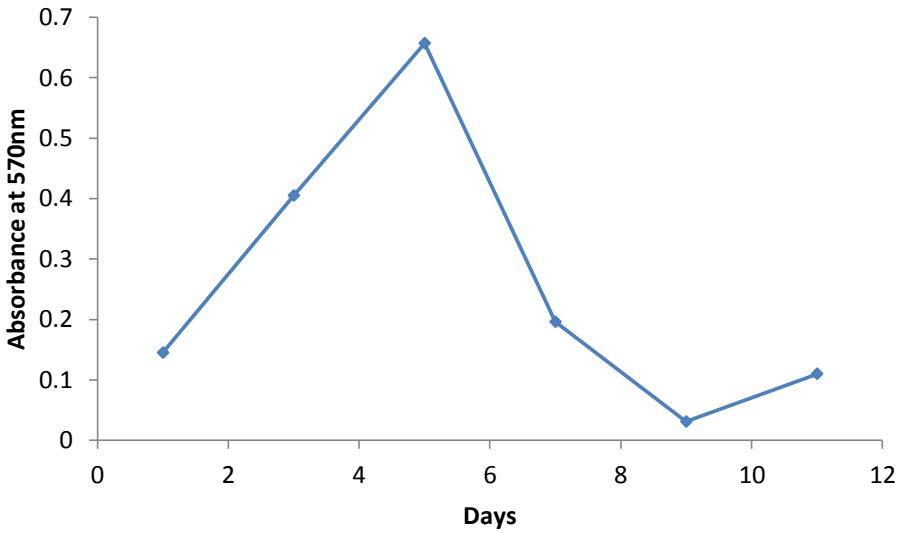

Figure 4.45. Cell growth profile for RC-10 human embryonic stem cells on Strata membranes. The growth profile using an MTT assay to assess viability of RC-10 cells on strata shows an increase in viability up to day 5 but after this there is a rapid decrease. This is a similar profile to that seen for TERA2.cl.SP12 cells in **Figure 4.9**. Data represents mean ±SEM n=3

4.5.15 Passaging the H9 ES cells in 3D on Strata membranes

The embryonic stem cell line – H9 was cultured in 3D on BD Matrigel coated Strata membranes using a protocol which was similar to the culture of TERA2.cl.SP12 cells in 3D (Figure 4.3). The main differences in the procedure were that cells were removed from the membranes non-enzymatically using 0.2% EDTA rather than 0.2% Trypsin EDTA and the cultures were only incubated for 3 minutes. This change in protocol ensured that a single cell suspension was not produced and instead clumps of cells were counted to reseed onto fresh membranes. Cultures were initially passaged every 4 days but the period between passages was increased at later passages.

Unlike the TERA2.cl.SP12 cells which grow as a sheet of cells, the H9 cells grow as colonies during standard 2D culture, such colonies were clearly visible in the phase micrograph in Figure 4.46. When the embryonic stem cells were cultured in 3D at low passages, they remained as colonies as can be seen by the histological analysis of H9 cells at passage 1 (Figure 4.46). As the passage number increased the cells began to form a dense cell layer across the entire surface of the membrane (Figure 4.46). After passage 1 the majority of cells in the 3D colonies were Oct 4 positive and this was also the case for the dense cell layer at passage 8. This was comparable to the Oct 4 positive cell in colonies during 2D culture (Figure 4.47). Low passage cultures of both 2D and 3D cultures displayed a gradient of Oct 4 expression through the colony from low in the centre to high at the periphery. Interestingly this was no longer apparent in the 3D passage 8 cultures.

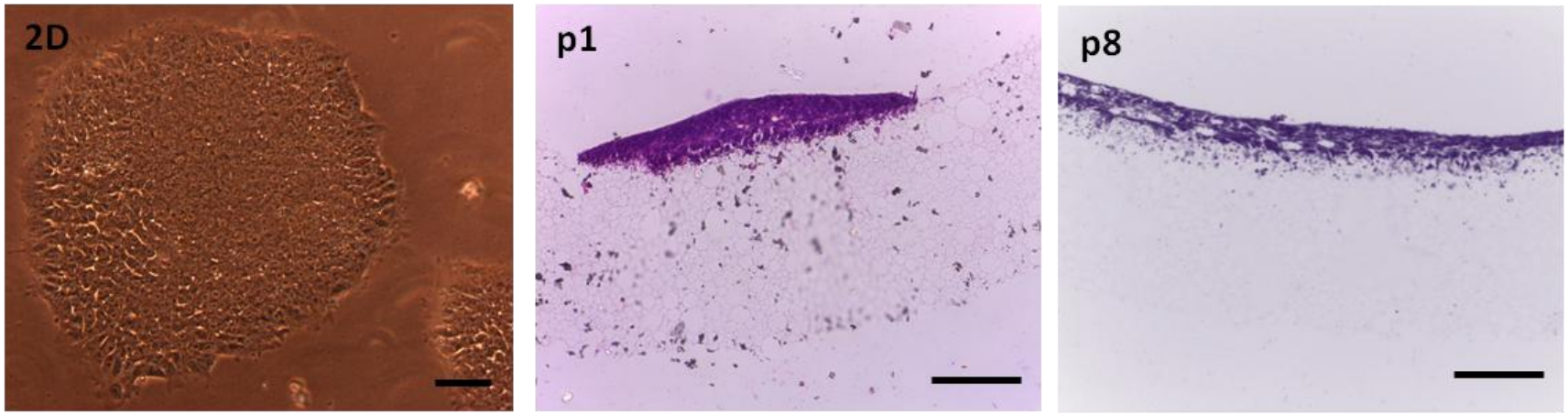

Figure 4.46. Human embryonic stem cell line-H9 grown in 2D without a feeder layer and on Strata membranes. H9 cells were cultured for 52 passages on a standard MEF feeder layer before being adapted to feeder free culture conditions on growth factor reduced BD Matrigel. Cells were then transferred to Strata membrane and passaged up to passage 8 in 3D. At early passages cells grow as small colonies on the membranes as they do in 2D culture but as the number of passages in 3D increase the H9 cells begin to form a dense cell layer. **Scale bars =100µm.**

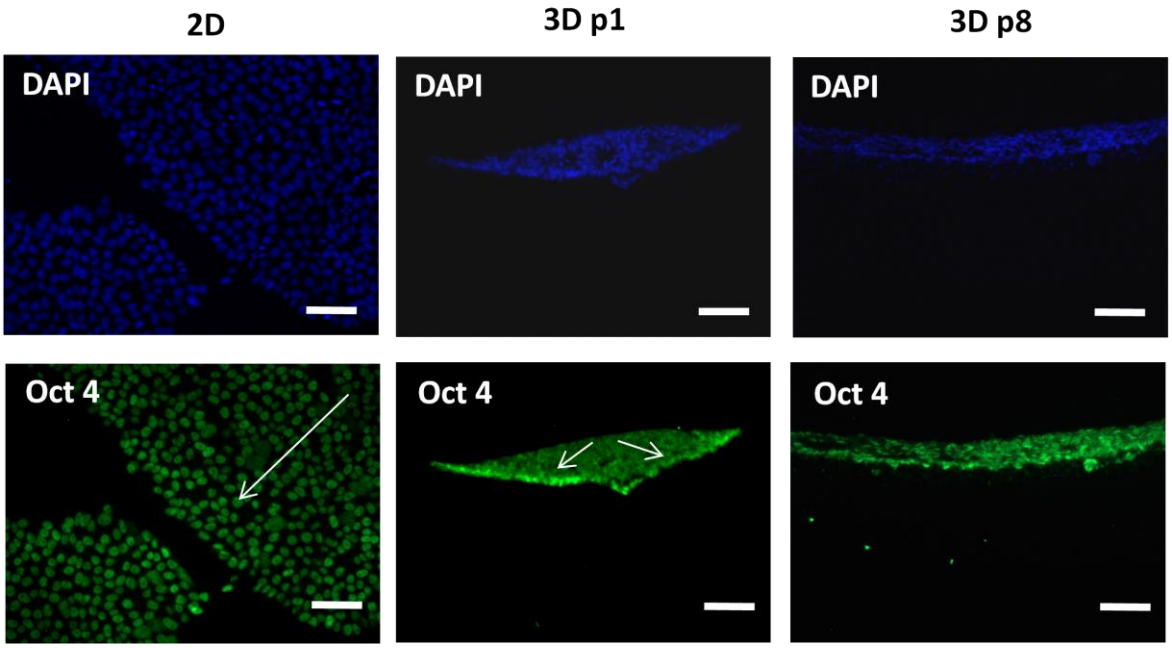

Figure 4.47. H9 human ES cells remain Oct 4 positive when cultured in 3D on strata membranes. H9 cells were stained with the stem cell marker Oct 4 at all passage numbers. 2D cells show colonies of Oct 4 positive cells this is also visible in 3D after 1 and 8 passages. Arrows highlight the gradient in Oct 4 expression from low at the centre of the cultures to high at the periphery. **Scale bars =100µm.**

4.5.16 Flow cytometrical analysis of H9 ES cells cultured in 3D

After every passage for 6 passages, H9 cells were trypsinised from either 2D or 3D culture to form a single cell suspension. Cells were then processed for flow cytometry and were sampled for the presence of the stem cell marker – SSEA-3 and the pluripotency marker – TRA-1-60. There were significant differences in SSEA-3 expression between the 2D and 3D cultured cells as early as passage 0 with 2D samples only containing 10.32% SSEA-3 positive cells (SSEA-3 level in 2D consistent with the original paper on derivation of H9 cells [51]) and 3D cultures containing 27.29% SSEA-3 positive cells at passage 0 ($p=0.01$) (Figure 4.48A). This difference continued through all passages of 2D and 3D cells and by passage 6 there was a difference of 61.85% in SSEA-3 expression ($p=0.001$). There was less of a difference in TRA-1-60 expression. There was a significant difference in expression for the first two passages ($p=0.05$) but as passage number increases this was not the case. Levels of TRA-1-60 remained high in both 2D and 3D culture and did not dip below 73%. In general, expression in 3D cultures was slightly lower than the corresponding 2D culture (Figure 4.48B).

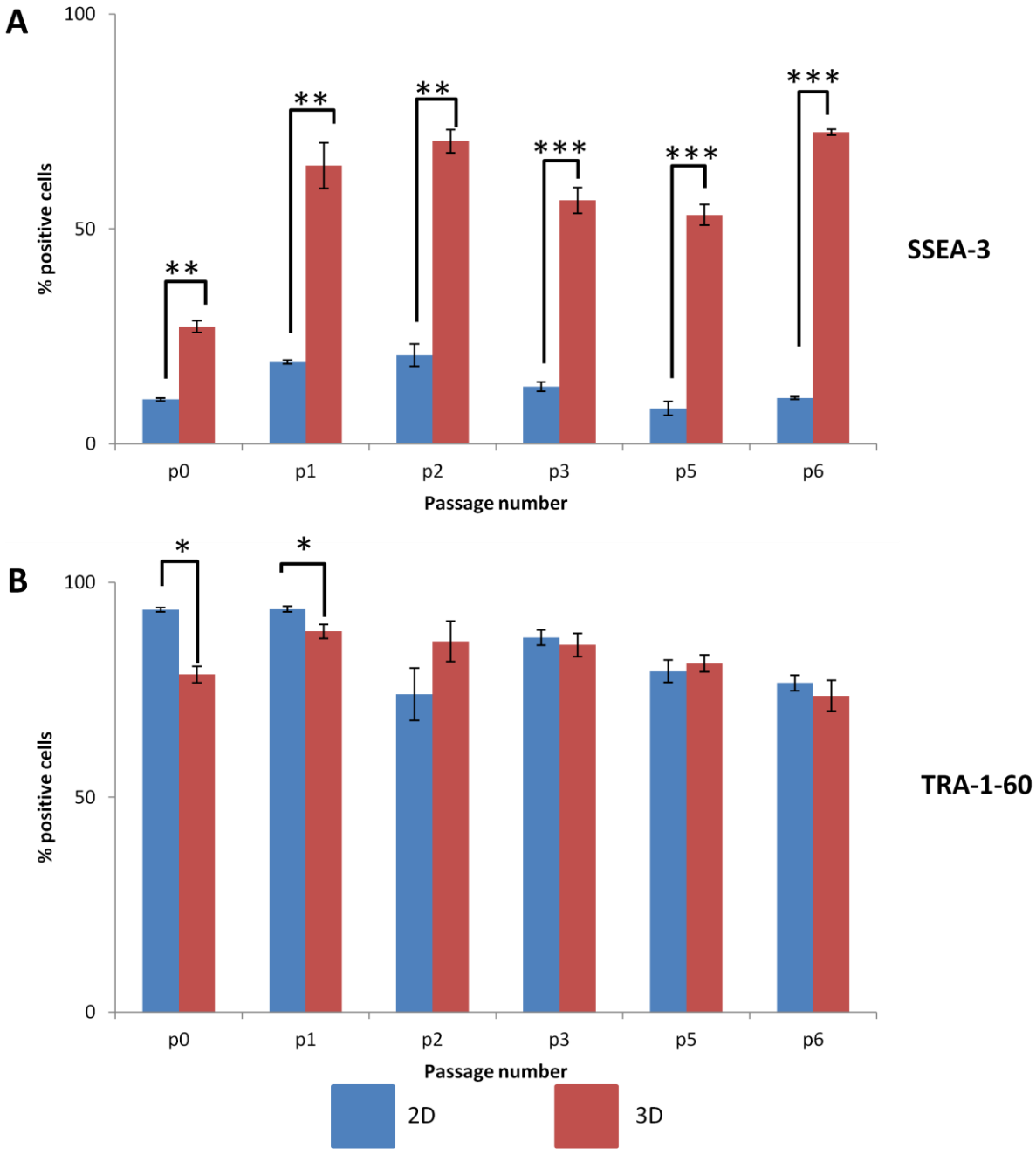

Figure 4.48. Flow cytometrical analysis of H9 human ES cells passaged in 3D compared to 2D. After each passage numbers cell were sampled using flow cytometry for the stem cell marker SSEA-3 **(A)** and TRA-1-60 **(B).** Cells maintained in 3D on Strata membranes have significantly different SSEA-3 expression than their 2D counterparts after only 4 days in 3D. This is a similar finding to the data presented using TERA2.cl.SP12 cells (Figure 4.11). Data represents mean ±SEM, n=3 ***p=0.05, **p=0.01, ***p=0.001**

4.6 Discussion

In the introduction to this Chapter I discussed properties for a 3D model system for the self-renewal of pluripotent stem cell *in vitro* as described by Krahenbuehl et al. [272]. These suggestions included the ability to tailor the mechanical properties of the substrate, migration of cells through or into the system, adaptation of the substrate to support the expansion of cells, and degradability in order to retrieve cells. They concluded by stating that the ideal 3D scaffold should have the capacity to replicate chemical, mechanical, 3D architectural or degradative environment of a specific extracellular matrix. During this discussion I will assess how close I have come to establishing an appropriate 3D culture environment and if these properties are actually necessary for the propagation and self-renewal of pluripotent cells in 3D. In this process I will also establish if cells have adapted to a 3D environment and whether this provides any advantage for the self-renewal and differentiation of pluripotent stem cells.

4.6.1 Production of a substrate suitable for the propagation of stem cells in 3D.

As described in Chapter 2, void size is vitally important during 3D cell culture. Differences in void size affect differentiation of cells [155] and small voids have been proven to promote mineralisation [156]. Reilly and Engler schematically highlight the importance of void size and especially its effects on stem cells – if the pore size is too large, cells can only spread on a strut of the scaffold in a manner that is similar to planar materials, this can cause large forces through the cells. When pore size is small and the cell can attach in three-dimensions, the force developed is smaller [283]. Such observations confirms the suggestion of Zeltinger et al. that pore size could be used to promote or exclude ingrowth of specific cell types [157]. It is this property that I have exploited when producing a 3D substrate for passaging of cells. By decreasing the void size from 40µm to 15µm (Figure 4.7A&B) and interconnect size from 12.37µm to 6.45µm (Figure 4.7C) I have been able to exclude the TERA2.cl.SP12 cells from the interior of the membrane (Figure 4.1D compared to Figure 4.1H). This exclusion of cells from the interior becomes progressively more pronounced as passage number increases and cell shape becomes more rounded (Figure 4.10 & Figure 4.12). By not allowing cells to infiltrate into the interior of the Strata membrane will allow for simple cell removal which in turn will allow for the membrane to be used for 3D cell expansion as an alternative to a 2D T75 flask.

4.6.2 Optimal parameters for the seeding of cells onto Strata membranes

Strata membranes were optimised using similar parameters to the optimisation of Alvetex® Scaffold in Chapter 2. Optimisation parameters tested were seeding method, cell number, surface treatment and culture length. Strata membranes were seeded using a standard dispersed seeding method and the concentrated method described by van den Dolder [159]. The two seeding methods lead to no difference in cell number and after 4 days both Strata membranes seeded

using the two different methods contained almost 4 million cells (a 4-fold increase in cell number) (Figure 4.8A). Staining of the Strata membranes revealed the preferable seeding method as the disperse method. This is in contrast to the optimal seeding method for Alvetex® Scaffold. The concentrated seeding method allowed cells to pool at the periphery of Strata (Figure 4.8B) which was not conducive to producing a homogenous cell layer whereas the dispersed seeding method led to a more even cell distribution across the membrane (Figure 4.8C).

Plasma treatment of the Strata membranes led to a phenomenon not observed when treating Alvetex® Scaffold. After treating Strata at 40W for 5 minutes areas of the polystyrene membranes started to degrade and appear thinner, in some of the membranes the thinning became so severe that the membranes split (Figure 4.8E). The process that is occurring during the surface treatment is described by Chu et al. [147]. During treatment of Strata there is interaction between the plasma and polymer which leads to two competitive reactions, the modification and the degradation of the surface. If degradation becomes the prominent reaction due to the absorbance of heat into the substrate (this is likely to occur due to the dense porous structure) then etching of the substrate occurs. The etching reaction is a degradation reaction at the surface of the polymer, and when polymers are exposed to plasma for a long enough time, the exposed layers of the polymers are etched off. The rate of this weight loss is strongly dependent on the nature of the polymer as well as the energy of the plasma [147]. If the alternative plasma treatment is used (10W for 30 min) this effect is less visible and it is still possible to seed cells onto the surface of the Strata membrane. However this process may still be having a detrimental effect on the structure of the membrane and the treatment only causes more cell ingrowth into the Strata interior. This is not desirable for the passaging of the 3D cultures. Also the additional time which would be required to plasma treat each disc is not conducive to producing a quick method for passaging cells in 3D.

As with the Alvetex® Scaffold cultures, a growth profile for TERA2.cl.SP12 cells was also produced using the MTS assay. This profile was profoundly different to the profile for TERA2.cl.SP12 seeded in Alvetex® Scaffold (Chapter 2 Figure 2.11). The profile of cell growth on Strata shows an initial increase in cell viability but this reaches a peak at day 5 and after this there is a rapid drop in viability – at day 11 there is the same cell viability as day 1 (Figure 4.9). This is presumably because the cells become over-confluent and would rather attach to each other than the growth substrate – this is also observed in over-confluent 2D cultures.

From analysis of Figure 4.8 and Figure 4.9 it was possible to determine optimal conditions for the culture of TERA2.cl.SP12 on Strata. All further experiments were conducted on ethanol treated

membranes and seeded using the dispersed seeding method. Strata cultures were not cultured for longer than 5 days.

The optimal parameters for the culture of TERA2.cl.SP12 were used as a starting point for the culture of the two embryonic stem cell lines – RC-10 and H9 on Strata membranes. However the protocols were further developed for the specific cell needs.

4.6.3 Developing a method for the simple passaging of cells in 3D

In the recent paper from Lu et al. they describe an alginate and water soluble chitin (AWC) microfibre scaffold for the propagation, expansion, and cryopreservation of hESCs [278] - they state that, "to date, the use of 3D scaffolds for cell expansion is limited and is always linked to a tedious process with a low cell recovery efficiency". In contrast to this view, I have developed a 3D scaffold to support the expansion of stem cells. The 3D environment provided by the Strata membrane which allows for the routine propagation, expansion in 3D and the removal of cells for cryopreservation. The process described in Figure 4.3 for the propagation of TERA2.cl.SP12 cells from the Strata membrane demonstrates that cell removal process is not tedious. It takes less than 10 minutes from removal of TERA2.cl.SP12 from spent membranes onto fresh membranes and a shorter length of time for the removal of ES cells. In contrast to the environments provided by Lu et al. [278] and the HA hydrogel used by Gerecht et al. [275] the process of cell removal from Strata does not require the degradation of the support matrix (Figure 4.4). Also cells do not require encapsulation into the 3D environment with seeding on top the 3D substrate being very similar to seeding standard 2D culture. By not requiring the encapsulation of cells, the Strata membrane does not introduce the cells to an extra parameter that may cause DNA damage – For example during the encapsulation of cells in hydrogels by Gerecht et al.[275], stem cells are subjected to low levels of UV light. In addition to this the Strata membrane is stable and inert during cell culture experiments, therefore not introducing an extra variable into the culture system.

In answer to Lu et al.'s final statement the cell recovery process from Strata does not lead to a low cell recovery efficiency. From the H&E images in Figure 4.4 it is evident that the majority of cells have been removed from the membrane suggesting that the recovery efficiency is high. Cells that are remaining in the interior of the membrane are at low cell density and therefore likely to be differentiated cells [133]. The Strata membrane therefore select for cells which have been grown at a high cell density and are more like to remain pluripotent. The graph of the cell numbers removed for the membranes at every passage also suggests that there is no problem with cell recovery. After the first passage cell number routinely at least doubles between each passage

(Figure 4.10). In summary, I have created a novel easy to use system for the 3D culture of stem cells.

The protocol for the passaging of TERA2.cl.SP12 cells in 3D was adapted for use with the embryonic stem cells lines. On suggestion from Roslin Cellab, an extra time period between passages was tested. The passaging protocol in Figure 4.3 was adapted for the RC-10 cells, the following parameters were modified for the specific cell type. Firstly instead of trypsin EDTA to remove cells, Accutase was used. Accutase is a non-enzymatic cell dissociation solution which is often used to produce a single cell suspension as it is less detrimental to cell viability and proliferation rate of hESCs [284]. Secondly cell removal step was increased to 15 minutes and thirdly two passaging protocols were tested at 3.5 and 7 days.

The passaging protocol was also modified for use with the H9 ES cells. In agreement with standard 2D cultures the cells were passaged using 0.2% EDTA as suggested by Moody et al. [281]. This allowed the cells to remain in clumps rather than form a single cell suspension. Treatment with EDTA only required a 3 minute incubation to avoid the dissociation of cell clumps. Initially H9 cells were passaged every 4 days but after passage 4 this time period was increased by 1 day for every passage to take into account a drop in cell proliferation.

4.6.4 Cell removal and cryoperservation from Strata membranes

At every passage, TERA2.cl.SP12 cells were removed from membranes and cells from individual membranes were assessed for cell number and cell viability using the Trypan blue assay. The viability count was necessary to assess the effect of the extended trypsinisation step on stem cells in 3D. The use of 0.2% trypsin EDTA for dissociation of cells from the growth substrates has previously been shown to affect a cells proteome, more specifically it may upregulate proteins associated with apoptosis [285]. The analysis of the number of dead cells reveals no detrimental effect on cell viability. The number of dead cells on average over the 10 passages is less than 7.9% of the original number of cells seeded and approximately 3.2% of the average number of cells retrieved for the scaffold. This is also consistent throughout the ten passages (Figure 4.10). This could be due two possible reasons, firstly trypsin takes a long time to diffuse through the dense cell layer or 3D cells are less susceptible to the damage caused by trypsin. Previous research has suggested that growing cells in 3D rather than 2D improves their ability to survive exposure to cytotoxic agents [64].

The highest increase in dead cells is at passage 7 (~93750 dead cells, 7.8% of total cells), this is most likely due to these cells being bought up directly into 3D culture after cryopreservation (Figure 4.10). This increase in non-viable cells is therefore expected. Previous studies have suggested cryopreserving cells *in situ* [278]. In this situation the cells are slowly released from the

hydrogel as aggregates a few days after thawing. Previous studies have also suggested that it is beneficial to cryopreserve cells *in situ*, especially after the production of 3D organotypic cultures [286]. Costa et al. assessed the effect of cryopreservation on cell laden porous scaffolds formed from a blend of starch and polycaprolactone [287]. The study suggests that a greater porosity and interconnectivity of the scaffold favours the retention of cells and cell viability after cryopreservation in 3D, when compared with nonporous disc cultures. This suggests that it would be possible to cryopreserve the TERA2.cl.SP12 cells on Strata membranes. However due to the intended use of the membrane as a disposable substrate for the expansion of 3D cells, it seems preferable to remove the cells from the substrate for cryopreservation. This will allow 3D adapted cells to be thawed into other 3D systems such as the Alvetex® Scaffold or back onto Strata for further expansion. After cryopreservation at passage 6 the 3D cells do not appear to need a period of adaptation to the 3D environment as the number of viable cells after 4 days in culture is comparable to other passages. During the first passage in 3D (p0) there is the least number of cells after 4 days in culture this is presumably due to the cells adapting to 3D culture (Figure 4.10).

The numbers of RC-10 ES cells removed from Strata membranes was also assessed. The 3.5 day passaging protocol appears to be optimal with an average fold increase between passages of 4.9 for the first 3 passages (Table 4.3), this is interesting as this is a shorter length of time than between subcultures of the cells in 2D. The protocol which is more in line with the 2D sub-culturing method (See Materials and Methods) is the 7 day protocol. However this protocol produces a large number of cells after the first passage. All subsequent passages led to a drop in cell number (Table 4.3). This was further investigated by producing a growth profile for the RC-10 cells in similar way to the profile for TERA2.cl.SP12 cells in Figure 4.9. The growth profile for RC-10 cells on Strata is similar to TERA2.cl.SP12 cells, there is a rapid increase up to the peak at day 5 but after this there is a rapid drop in cell viability (Figure ZQ). From this data it suggest that passaging at day 4 and 5 may produce more cells for subculturing in 3D.

4.6.5 Maintenance of stem cells markers during 2D and 3D cell culture

For 10 passages the stem cell marker SSEA-3 and early neuronal differentiation marker were assessed using flow cytometry in standard 2D cultures, 3D membrane cultures and as a positive control for spontaneous differentiation – 3D aggregate cultures. The two 3D culture systems differ greatly from each other as early as passage 3. It is evident that the 3D Strata cultures do not spontaneously differentiate like the aggregate cultures (Figure 4.11A). Previous systems for the culture of stem cells have reported that they are able to maintain stem cells markers in 3D culture. Gerecht et al. reported high levels of SSEA-3 and alkaline phosphatase in their HA hydrogels but this was not compared to 2D cultures [275]. Lu et al. reported the production of Sox-2, Oct 4, nanog, and TRA-1-60 using immunostaining after 10 passages in their microfiber

culture system and flow cytometric analysis revealed that >90% of 3D cells were Oct-4 positive [278]. Liu et al. directly compared standard 2D cultures with 3D ES cells on electrospun nanofibres and found that the levels of Oct-4 were comparable in both culture systems (2D = 93.6%, 3D = 95.4% Oct 4 positive) [277]. However none of these systems report a significant difference in the expression of stem cell markers between the 2D and 3D cultures. This may be due to the method they use for assessing pluripotency. Sections of Strata membrane cultured for both ES and EC cells were stained for the stem cell marker Oct 4 and compared with their 2D counterparts. From this form of analysis there is very little difference in the number of positive cells. For TERA2.cl.SP12 cells in 2D culture the majority of cells are Oct 4 positive (Figure 4.13) and this is also visible in 3D with all cells staining positive for Oct 4 (Figure 4.14). These results can also be compared with immunostaining of aggregate cultures which display very few Oct 4 positive cells; this demonstrates the cells ability to downregulate Oct 4 (Figure 4.15). Interestingly as passage number increases, aggregates of TERA2.cl.SP12 cells seem to be undergoing a transition which is similar to the transition of embryoid bodies (EBs) described by Itskovitz-Eldor et al.[188]. As the cells differentiate the transition from simple EBs which are masses of densely packed cells to cystic EBs where cells in the centre of the mass begin to undergo apoptosis in order to provide space to form complex structures (Figure 4.12& Figure 4.15)

The majority of 3D cells are also positive for Oct 4 for both of the ES cell lines. RC-10 cells passaged using both 3.5 day and 7 day subculture show dense layers of Oct 4 positive cells. However there appears to be a gradient of positive staining within the 3D cultures (Figure 4.43& Figure 4.44). Such gradients of stem cell marker expression are well documented in 2D ES cell colonies. Kunova et al. highlight the gradient in marker expression from the centre to the outside of ES cell colonies for markers such as Oct 4, nanog and Sox-2 [267]. The gradient in Oct 4 expression is also visible in Strata membranes cultures of H9 ES cells at passage 1 and in the 2D colonies of H9 cells (Figure 4.47). Interestingly there does not appear to be a gradient of Oct 4 expression in 3D culture at passage 8 (Figure 4.47), this may be due to the cells adapting to the 3D environment. After multiple passages in 3D, the H9 cells no longer appear to form colonies on the membrane as seen in 2D and early 3D passages but instead produce a dense layer of tissue (Figure 4.46). This loss in expression gradient is consistent with the findings of Kunova et al. by allowing ES cells to form monolayers on Matrigel coated plastic rather than forming colonies. Monolayer cultures displayed improved cell viability and no longer had a edge to centre gradient of Oct 4 expression, they also produced a more homogenous cell population as they no longer contained SSEA-3 high and SSEA-3 low subpopulations [267].

4.6.6 Differences in SSEA-3 production between 2D and 3D cultures.

SSEA-3 is a cell surface stem cell marker which displays rapid loss on differentiation [288]. Envers et al. suggest that downregulation of SSEA-3 does not necessarily indicate the differentiation of hESCs [289]. Instead they suggest that there are two interchangeable types of embryonic stem cells – SSEA-3^+ and SSEA-3^-. These two subtypes can both self-renew and SSEA-3^+ cells can transition to SSEA-3^- cells. SSEA-3^- cells undergo self-renewal but are biased towards differentiation. Kunova et al. have suggested that by culturing hESCs as monolayer they are able to select for the SSEA-3^+ population and therefore produced less heterogeneity in the cell population [267]. From flow cytometrical analysis of both EC and ES cells on Strata it is likely that the 3D environment provided by Strata also selects for the SSEA-3^+ population and is therefore less likely to spontaneously differentiate. As passage number of TERA2.cl.SP12 cells increases there becomes a significant difference in SSEA-3 expression between the 2D and 3D cultures (Figure 4.11A). At passage 3 there is already a significant difference in levels of SSEA-3 ($p=0.01$) and this becomes more significant at passage 8 ($p=0.001$). This difference is SSEA-3 expression also seems to have an effect on spontaneous differentiation of TERA2.cl.SP12 cells. As previously stated the SSEA-3^- population is biased towards differentiation, due to the 2D cells having a lower percentage of SSEA-3^+ cells it is likely that there are more SSEA-3^- cells within the 2D population of cells which are more likely to spontaneously differentiate. At passage 8, the 2D cells have a significantly higher level of A2B5 positive cells when compared with the cultures on Strata membranes (Figure 4.11B $p=0.01$).

A difference in SSEA-3 levels is also evident in 2D and 3D membrane cultures of the human embryonic stem cell line – H9 over the 6 passages (Figure 4.48A). On average 2D cultures only contain 13.7% SSEA-3 positive cells in contrast to 63.5% positive cells on 3D membrane cultures. The 2D cultures are not differentiated as two culture conditions contain similar TRA-1-60 levels (Figure 4.48B). This is consistent with the finding from Brimble et al. who suggest that SSEA-3 negative cells are not necessarily differentiating cells [289]. The high levels of SSEA-3 in 3D H9 cells is particularly interesting as the original paper describing H9 hESCs states that some small H9 colonies stain uniformly for SSEA-3 but most colonies contained a mixture of weakly stained cells and a majority of non SSEA-3 stained cells [51]. This accounts for the low SSEA-3 expression in 2D cultures.

4.6.7 Proliferation rate of 2D and 3D TERA2.cl.SP12 cells

Culture adapted hESCs tend to show enhanced population growth rates as passage number increases [290]. Park et al. demonstrated that as the cells adapt to the culture environment the population doubling time is reduced for example the hESC line - SNUhES3 at passages up to 40 has a population doubling time of 37.6.hours but by 90 passages this time has decreased to 30 hours.

The change in growth rate is teamed with a difference in actively proliferative cells. At early passages 62.1% of cells are BrdU positive (proliferation marker – bromodeoxyuridine) but by late passages, 94.6% of cells are BrdU positive [291]. In this particular study there is no change in karyotype as passage number increases but other studies such as Harrison et al. have found that the enhanced population growth rate is linked with a change in karyotype [290]. Although an increase in proliferation rate of stem cells may be advantageous in order to produce a large number of cells in a short time frame, any increase in proliferation rate increases the possibility of irreversible damage to the cells.

When TERA2.cl.SP12 are cultured for extended periods of time in 3D culture this leads to a decrease in cell proliferation as demonstrated by the differences in cell density observed in Figure 4.16. From the cell numbers obtained from the 3D cultures at every passage, this change in proliferation does not appear to have a large effect on cell yield in 3D (Figure 4.10). Due to the nature of the EC cells assessing cell karyotype would be less helpful but this feature of Strata 3D cultures may be more relevant during the culture of hESCs. Interestingly, during the passaging of H9 cells a decrease in proliferation was also observed and the number of days between passages was extended to compensate. This is in contrast to previous experiments which expand cells in 3D. Liu et al. [277], Lu et al. [278], and Gerecht et al. [275] all report a comparable growth rate between 2D and 3D culture.

4.6.8 Prolonged 3D culture leads to a difference in cell shape.

It has been proven that cell shape is a regulator of DNA synthesis and cell growth *in vitro* [78]. It is evident that culture in 3D using Strata membranes leads to a gradual change in cell shape, which after prolonged culture in 3D can be maintained when the cells are returned to 2D culture (Figure 4.17 & Figure 4.18). This is presumably due to the increased attachment of cells in all planes which allows cells to tessellate with each other without the influence from a hard tissue culture plastic. 3D cell culture promotes cell interactions and causes the cells to become more spherical especially at higher passage numbers (Figure 4.19). Cell rounding has previously been shown to affect differentiation with rounding of ES cells promoting adipogenesis [148]. However, this cell rounding was caused by disruption of the cytoskeleton using cytochalasin D (inhibits actin polymerisation) or nocodazole (interferes with the polymerisation of microtubules) treatment. Whereas the difference in cell circularity observed due to prolonged 3D culture still allows for the maintenance of actin cytoskeleton and microtubules (Figure 4.20). The 3D culture environment appears to allow cells to maintain a spherical cellular morphology that is more representative of cell shape *in vivo*. Furthermore cells cultured in 3D for 10 passages appear to have spherical nuclei sitting on a dense bed of F-actin. The 3D cells have produced more interactions with surrounding cells than their 2D counterparts and when returned to 2D all the adhesion molecules are forced to

drop to the bottom of the cells to attach to a planar 2D substrate hence the cells become polarised. In conclusion, Feng et al. stated that environment sensing focal adhesion may play an indirect role in stem cell commitment by modulating cell shape [148]. The increased interaction between cells in 3D culture may help in enabling stem cell self-renewal.

4.6.9 Culturing cells in 3D affects developmental potential

As mentioned in the Introduction to this Chapter, 3D environments have previously been shown to enhanced differentiation towards a range of lineages [32, 172, 273, 274]. Hwang et al. suggested that 3D culture may promote cell-cell interactions and therefore differentiation by entrapping secreted ECM matrix, maintaining spherical cellular morphology and providing a structural support for higher order tissue organisation and remodelling [29]. The studies that have previously passaged cells in 3D, report that the extended period of 3D culture has no detrimental effect on stem cell differentiation but also do not highlight specific differences between the 2D and 3D cells [277, 278].

Instead of comparing differentiation directly between 2D and 3D cells in their own environments both the 2D and 3D-primed TERA2.cl.SP12 cells at passage 10 were transferred to Alvetex® Scaffolds for differentiation studies. This allowed any differences in differentiation to be attributed to the method in which the cells had previously been cultured. Any possible enhancements in differentiation attributed to the 3D cells may have been due to the enhanced support provided by the scaffold which gave more opportunities for complex structure formation. Figure 4.21 reveals the difference in the differentiation of 2D and 3D-primed TERA2.cl.SP12 cells. Flow cytometrical analysis reveals that 3D-primed cells downregulate the stem cell markers SSEA-3 and TRA-1-60 earlier than 2D cultured cells (Figure 4.21A). This is a phenomenon that has previously been documented with differences in the differentiation towards hepatocytes of 2D cultured hESCs and those cultured in 3D on collagen scaffolds. Baharvand et al. observed earlier gene expression patterns of albumin and glucose-6-phosphotase as wells as high detection levels of urea and AFP in 3D cultures compared to 2D cultures [292]. They suggest that their 3D tissue culture system provides a microenvironment that is conducive to normal progenitor cell kinetics and enhanced cell differentiation. However unlike the Alvetex® Scaffold differentiation protocol, the procedure used by Baharvand et al. does not compare like-for-like situations.

Interestingly there is also a difference in cell distribution between 2D and 3D primed TERA2.cl.SP12 cells in the Scaffold. The 3D primed/adapted cells grow at a significantly higher density compared to the 2D cells this is presumably because the 3D cells have already adapted to the 3D environment (Figure 4.21B-E). To ensure the difference in neuronal differentiation that occurred between the 2D and 3D primed cells was not cell density dependent, two areas of

approximately the same cell density were immunostained for the neuronal marker TUJ-1. Figure 4.22 reveals a large difference between differentiated 2D and 3D cells, with the majority of 3D-primed cells displaying positive staining for TUJ-1 compared to individual cell staining in the 2D cultures after 14 days of differentiation. There is also evidence of complex structures in Scaffold cultures of 3D cells which are not apparent in the scaffold cultures of 2D cells (Figure 4.23).

To further assess the differentiation potential of 3D-primed cells compared to their 2D counterparts, both types of cells were allowed to formed aggregates in suspension. This method has been previously used to form 3D neurospheres of TERA2.cl.SP12 cells [293]. This method of differentiation promotes neuronal differentiation due to disruption of BMP signalling which is a strong endogenous repressor of neural fate [294]. Treatment with recombinant BMP-2 blocks RA-induced differentiation and up-regulates the expression of epithelial associated proteins.

Aggregates formed from 2D and 3D-primed cells differed in size with the cells which had been cultured for longer in 3D, being able to form significantly larger aggregates than their 2D counterparts (Figure 4.24)($p=0.001$). As suggested by Horrocks and Przyborski [294], the majority of cells in the aggregates are neuronal. This is clearly evident in the staining of passage 4, 2D and 3D aggregates with TUJ-1 and cytokeratin-8 (Figure 4.25). Interestingly as the number of passages in 3D increases, fewer cells within the aggregates are TUJ-1 positive and there are areas of the aggregate that are positive for the epithelial marker – cytokeratin-8 (Figure 4.26 and Figure 4.27) beginning to appear more frequently. This suggests that the increased cell interactions provided during 3D cell culture help the cells to overcome the problems of short range signalling of BMP that occurs during aggregate formation. Interestingly the areas of the aggregates which are cytokeratin-8 positive are at a considerably lower cell density that the TUJ-1 positive areas (Figure 4.27). This difference in cell density could account for the differences in aggregate size observed in Figure 4.24. Previous research on the formation of embryoid bodies from 2D and 3D-primed hESCs has observed a difference in differentiation and downregulation of stem cell markers. Storm et al. found that 2D cells took longer to down regulate stem cell markers such as nanog and also observed lower levels of AFP staining from EBs formed from 3D-primed cells [295].

4.6.10 Formation of teratomas from 2D and 3D-passaged cells

Consistent with the sizes of aggregates formed from 2D and 3D-primed cells, there was also a difference in the mass and dimensions of teratomas formed. Teratomas formed from 3D passage 10 cells were significantly larger than their 2D counterparts (Figure 4.28) ($p=0.01$). To our knowledge this is a phenomenon that is previously undocumented. Previous studies such as that by Lu et al. have used the teratoma assay to confirm the pluripotency of 3D-primed cells *in vivo* but have not observed differences between 2D and 3D cells [278]. Analysis of teratomas formed

from 2D cells and 3D-primed cells using Strata membranes show a difference in tissue complexity between the two types of cells. This is initially evident in the montages of teratoma sections, 3D primed cells at all passages form complex structures compared to their 2D counterparts that have formed smaller dense tumours with fewer distinct tissue types (Figure 4.29).

Using the model EC system for assessing the changes during 3D culture has been advantageous as their more limited differentiation capabilities has made it easier to observe the changes between the 2D and 3D cultured cells. TERA2.cl.SP12 cells preferentially differentiate towards ectodermal derivatives [127, 294] and this is evident in the formation of teratomas. However, remarkably *in vivo* differentiation of 3D TERA2.cl.SP12 has shown evidence of differentiation towards all three germ layers. Teratomas formed from 2D cells are primarily nestin or TUJ-1 positive (Figure 4.30, Figure 4.34 & Figure 4.38) with limited NF-200 and cytokeratin-8 staining. There is minimal evidence of SMA and AFP staining in teratomas formed from 2D cells and positive staining is at the periphery of the tumours and can be attributed to vascularisation from mouse cells rather than differentiation of the injected cells. In contrast to the immunostaining of 2D teratomas, teratomas formed from 3D-primed cells show enhanced differentiation as early as passage 4 (Figure 4.32& Figure 4.33). Teratomas formed from 3D p4 cells show more localised areas of TUJ-1 positive cells (Figure 4.32A) than their 2D counterparts and significantly less nestin staining suggesting that the 3D cells are further on their way to terminal differentiation (Figure 4.32B). This is confirmed by the presence of NF-200 positive neurites (Figure 4.32C) and there are also areas of noticeable cytokeratin-8 staining (Figure 4.32D). Teratomas formed from 3D-primed cells also display areas of SMA positive cells which are not observed in the 2D cell teratomas (Figure 4.33B).

As the number of passages in 3D increases the teratomas appear to display more complex differentiation. At 3D passage 6 there are obvious TUJ-1 positive (Figure 4.36A) and cytokeratin-8 positive structures (Figure 4.36D). Nestin expression is now limited to specific structures rather than in the majority of the teratoma (Figure 4.36B). There is also less widespread staining for the embryonic stem cell marker – Oct 4 (Figure 4.37A) and discrete structures that stain for smooth muscle actin (Figure 4.37B). There are isolated cells which stain weakly for the endoderm maker – AFP, this was not observed in the lower passage 3D cells or 2D cells (Figure 4.37C). The teratomas formed from cells that have undergone 10 passages in 3D are similar to the 3D passage 6 teratomas apart from there is more extensive staining for NF-200 (Figure 4.40C), complex structures which are SMA positive (Figure 4.41B) and distinct areas of AFP staining (Figure 4.41C)

4.7 Conclusion

The aim of this Chapter was to establish a method for the culture and expansion of pluripotent stem cells while maintaining their self-renewal capabilities. I have achieved this aim in the model EC cell line – TERA2.cl.SP12 and have been able to potentially translate the knowledge gained from these experiments for use with two human embryonic stem cell lines – RC-10 and H9. In the Introduction to this Chapter we highlighted the conditions required for a 3D model system for self-renewal as described by Krahenbuehl et al. [272], I have met many of these conditions or proven that some of the requirements are not necessary for our method of 3D passaging of pluripotent stem cells. They suggest that the 3D system should permit the migration of cells either through or into the system – as is clearly visible in Figure 4.1, Figure 4.10, and Figure 4.12, this is not a feature of Strata membranes. Strata is used as a support matrix that permits the 3D culture of cells at the surface of the membrane and therefore does not need to permit migration into the interior. The 3D layer of cells is able to form its own ECM and without the structural support of a scaffold between cells they are able to form close cell-cell contact. Another requirement of the model 3D system was to be able to adapt to support the expansion of cells. Strata membranes are inert synthetic membranes that do not adapt in the presence of cells. This may appear as a disadvantage but due to the cells growing in their own 3D layer at the interface between the polymer and the media rather than being encapsulated in the matrix there is a considerable space for cell expansion as long as enough media is provided, therefore the matrix does not need to adapt. Kraehenbuehl et al. also suggested that the 3D support matrix would need to be biodegradable to allow for cell removal. As demonstrated in Figure 4.3 it is not necessary to degrade the Strata membrane for cell removal and this is advantageous as it means that cells are not subjected to the degradation of the scaffold or spend prolonged periods of time in enzyme solution as is the case in the degradation of other support matrices [275, 278].

In conclusion, I have demonstrated the use of a 3D culture system for the successful self-renewal of stem cells during long term passaging in 3D. Using the optimised system I have established that prolonged culture in 3D affects levels of SSEA-3 expression in both EC and ES cells, proliferation rate, and cell shape. Three dimensional culture affects differentiation potential of pluripotent stem cell as early as passage 6, demonstrated by a difference in differentiation between 2D and 3D cultures on Alvetex® Scaffold and differences in aggregate formation and teratoma formation.

5 The use of 3D culture systems to assess the differentiation potential of hESCs

5.1 Introduction

In stem cell research, the teratoma assay is used to demonstrate the pluripotency of the stem cells *in vivo.* The 'gold standard' pluripotency test as stated by the International Stem Cell Bank initiative is that human embryonic stem cells must at least form teratomas in SCID mice [121]. The National Institutes of Heatlh (NIH) human pluripotent stem cell registry also calls on researchers submitting new cell lines to provide evidence of teratoma formation "because it is currently the gold standard for determining whether a human line is pluripotent" [296]. In addition to this a multi-national study to evaluate human embryonic stem (hES) cells worldwide by the International Stem Cell Initiative included data on teratoma formation [297]. Even though this is considered a requirement for the testing of pluripotency, a comprehensive review of the literature on human pluripotent cell lines between 1998 and 2009 by Muller et al. [298] revealed that 56% of published hESC lines and 64% of induced pluripotent stem cell (iPSC) lines included no data on teratoma formation. There were also hESC lines being reported that failed to form teratomas and others that were mainly fluid filled cysts. Muller et al. go on to call for standards to be established to make the teratoma assay worthy of its ''golden'' status. There have been many recent attempts at such standardisation

5.1.1 Attempts at standardisation of the teratoma assay.

The formation of teratomas is required to confirm the pluripotency of new hES and iPS cells but there is currently no standardised method for their production. Gropp et al. state that a teratoma assay needs to be sensitive, quantitative, easy to perform and monitor. To meet these requirements it is necessary to have standardised the number of implanted cells, characterisation of the phenotype and genotype of the transplanted cells, the mode of transplantation and finally the site of transplantation. In addition to these parameters it is also necessary to consider the choice of recipient animal, the duration of monitoring teratoma formation and to define histological criteria for teratoma analysis [299]. Previously Gertow et al. presented protocols to assess the developmental potency of human embryonic stem cells (hESCs) by performing xenografting into immunodeficient mice to induce teratoma formation. They provided various alternative protocols for different graft sites such as in the testis capsule, kidney capsule or subcutaneous injection [300]. However the graft site has been shown to effect the differentiation of teratomas with subcutaneous injection leading to enhanced differentiation [134]. The standard procedure suggested by Gropp et al. [299] suggests karyotyping and FACS analysis of cells prior to transplantation of a single cell suspension of between 1 x 10^5 and 5 x10^5 hES cells with the

addition of feeder cells leading to a final concentration of 1 x 10^6 cells into NOD/SCID mice. Cells should be transplanted subcutaneously using Matrigel into 3-5 mice per condition. Tumours should be observed weekly until they reach <1cm or up to 30 weeks after transplantation.

Even with these recently defined criteria there are still criticisms of the procedures used. For example the addition of feeder cells. This was suggested by Hentze et al. as it was found to give enhanced reproducibility of teratoma formation however with the increasing number of feeder-free systems for the growth of hES cells [280, 281], this part of the standard procedure may no longer be suitable. Alternatively, the use of extracellular matrix proteins such as Matrigel helps to enhance teratoma formation [301, 302].

Due to the lack of standardisation, plus the fact that the teratoma assay is considered technically challenging, both resource and time intensive, costly and primarily qualitative an alternative to the teratoma assay would be beneficial. Finding such an alternative to provide an initial screen for pluripotent cells would also be in line with the 3Rs principle suggested by Russell and Burch in 1959 to replace, reduce and refine scientific experiments using animals [120].

5.1.2 Alternative methods for the assessment of pluripotency.

Recently Buta et al. questioned the need for the teratoma assay and suggested a range of alternatives [303]. These alternative methods include characterisation of the expression of pluripotency markers within the cell cultures. Such markers include Oct 4 [304], Nanog [305], and Sox 2 [306]. However these markers are also present in embryonal carcinoma cell lines as shown in previous chapters and are therefore not a definitive marker of hES cells. Buta et al. also suggest computer based predictive models of pluripotency. Potential *in silico* assays could be a cost effective alternative to teratoma assays and may also enable exploratory bioinformatic downstream applications. One such bioinformatic assay of pluripotency has been described by Muller et al. and is known as PluriTest (http://www.pluritest.org/). This is an online open-access database that compares novel data sets with existing known pluripotent cells to determine pluripotency based on their gene expression profile [307]. Although such an approach is promising, this method also requires standardisation as only microarray data using specific chips can be assessed and microarrays can be costly experiments.

In a recent editorial by Dolgin in Nature Medicine he quotes that “Only the teratoma test can investigate differentiation in a living animal, thereby taking advantage of all the incompletely understood factors that help create three-dimensional tissue architectures”[296]. The two methods mentioned above do not allow for the formation of complex 3D structures; however an alternative *in vitro* method that does allow for the formation of complex structure is the formation of embryoid bodies (EBs). EBs provide 3D structures which are most similar to the *in*

vivo environment as they involve gradients of secreted factor such as hedgehog signalling proteins and other morphogens. The EB environment also allows 3D structure formation that better represents structures observed *in vivo*. The formation of EBs also helps to recapitulate the early stages of human embryonic development *in vitro*. Recently Sheridan et al. suggested the use of EBs to assess the pluripotency of iPSCs [308]. Buta et al.[303] stated that EBs provide an ideal *in vitro* test for pluripotency as they can provide multiple endpoints which may be more informative that the final endpoint provided by teratoma. Due to being able to produce large quantities of EBs they are more statistically significant and more reproducible than teratomas as well as having a significantly lower cost.

Unfortunately the formation of EBs to test for pluripotency does have drawbacks. These include the limited supply of nutrients in culture which has led to suggestion that it is only possible to form aggregates that are limited to 7 layers thick [303]. Also expression of the pluripotency marker – Oct 4 persists for an unexpectedly long time in differentiating EBs and studies have shown that there is noticeably low expression of mesodermal marker – Brachyury in many hESC lines and this is limited to single cells [309]. This is explained by Fuchs et al. [310] and is shown schematically in Figure 5.1. In suspension, aggregated ESCs form an outer layer of endoderm which resembles the hypoblast [311]. Inner cells adopt and ectodermal fate which resembles the epiblast and mesoderm is limited in a localised and asymmetric manner in EBs kept in suspension [312]. When EBs are transferred to gelatin coated tissue culture plastic, the gelatin assists with the attachment of the primitive endoderm. Unfortunately if the EBs are kept in suspension for too long before plating, the majority of the EB becomes encapsulated and blocked by the overgrowing endoderm. This limits mesodermal differentiation which can also be influenced by the proximity of neighbouring EBs [310] . The formation of EBs has great potential for use as a pluripotency test as they are able to form complex structures and show evidence of all three germ layers, it is limited by the terminal differentiation stage being in 2D culture and being extremely dependent on the length of time cells have been grown in suspension which leads to areas of necrosis.

Due to the limitations of the embryoid body culture system mentioned above it would be ideal to establish an *in vitro* pluripotency test which would allow terminal differentiation in 3D. Buta et al. [303] suggest organotypic models such as skin models which would be cultured *in vitro* and stem cells could be injected into skin pads and allowed to develop and differentiate. Although this is a potential suggestion, it requires a fully functioning skin model to be produced prior to the addition of the stem cells for testing. This potentially could be a very time consuming method for testing *in vitro* pluripotency as many skin models can take up to 12 weeks to differentiate [313]. Other suggestions have included confining EBs to 3D microenvironments produce from

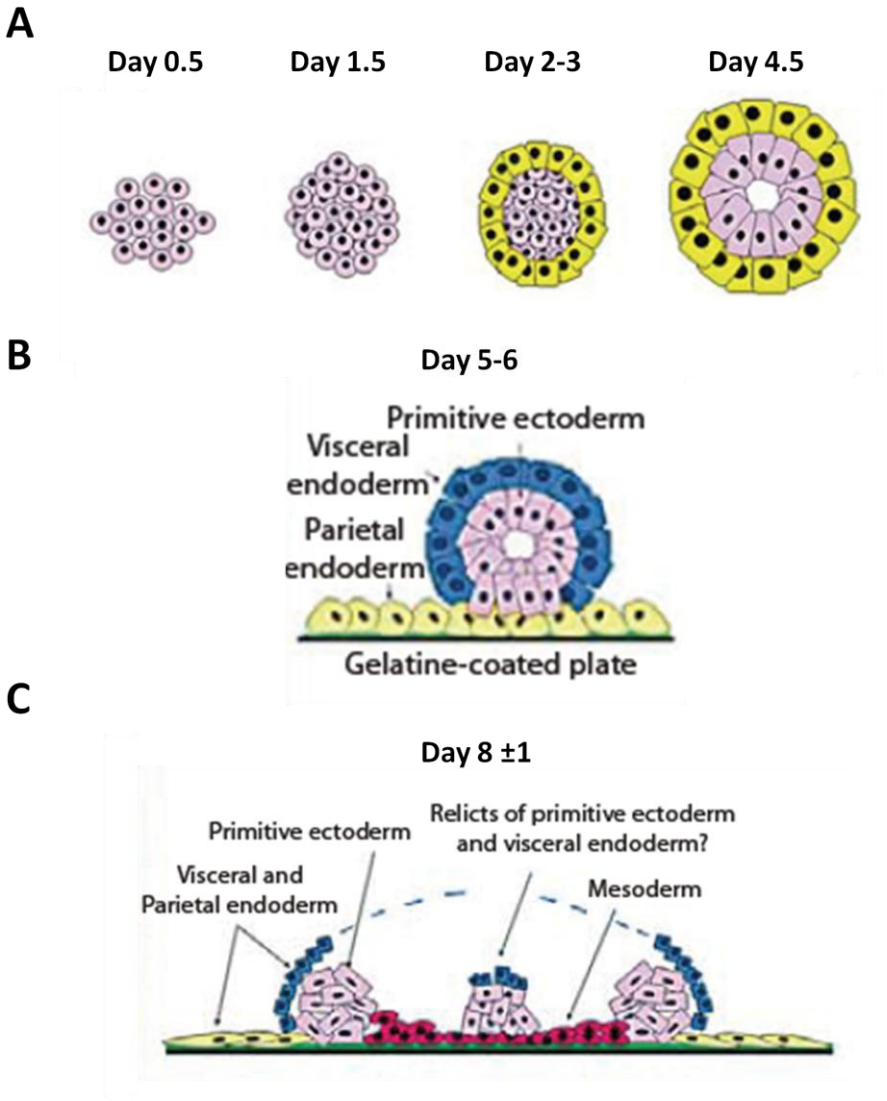

Figure 5.1 Schematics demonstrating the development of embryoid bodies *in vitro*. A - the early development of cell types in EBs. Pink: ESCs and primitive ectodermal cells; yellow: primitive endoderm. **B** - cross section of a typical EB at days 5 and 6 after transfer to gelatin coated tissue culture plastic. Inner cells of primitive ectoderm (pink) are surrounded by primitive endoderm (blue) which differentiates upon contact with the gelatin-coated tissue culture plate (green) into parietal endoderm (yellow) and visceral endoderm on top of the primitive ectoderm, respectively. **C** - transverse section through the centre of the EB at day 8 of differentiations. Images adapted from Fuchs et al. 2011 [310].

polyacrylamide hydrogels however these were also demonstrated to prevent mesodermal differentiation of both hESCs and iPSCs as shown by immunostaining and from microarray analysis. It was demonstrated that the confinement of EBs leads to specification of genes involved in ectoderm and endoderm formation [314]. Giobbe et al. suggest that this is due to the size of mesoderm inducing factors which are able to diffuse away from the EBs. Alternatively, both Gerlach et al. [315] and Stachelscheid et al. [316] describe the use of a perfusion bioreactor for the differentiation of mESCs and hESCs respectively. Gerlach et al. show spontaneous differentiation of mESCs which form aggregates of heterogeneous size in the bioreactor, however necrosis is evident in the larger aggregates even though there is media perfusion. However, they are able to suggest that bioreactor cultures more closely resemble mouse fetal tissue development than the control mESCs cultured in Petri dishes. Stachelscheid et al. use the same bioreactor for teratoma formation *in vitro*. They compare the differentiation of hESCs and hiPSCs cultured *in vitro* as embryoid bodies, in the bioreactor, and during teratoma formation. Results from immunohistological analysis reveal that hESCs cultured in bioreactors formed tissue-like structures containing derivatives of all three germ layers. When these structures are compared with embryoid bodies and the teratomas, there was a high degree of similarity of tissues formed in the bioreactor to those observed in teratomas. These results show potential for the development of an *in vitro* teratoma assay, however the bioreactor methods are expensive and on a large scale. Stachelscheid et al. do suggest a method for the scale down of their bioreactor [317] but such systems may need significant standardisation before it could be used for widespread assessment of pluripotency.

The aim of this study will be to attempt to produce a simple 3D culture alternative to the teratoma assay. Any model produced must be based on cell-cell and cell-matrix interactions so as to provide knowledge of complex *in vitro* differentiation. The purpose of such a model would be as a quick screening method in order to limit the number of cell lines requiring analysis using the teratoma assay. The teratoma assay will still be required as it is needed to demonstrate the lack of tumorigenic potential in stem cells to be used in stem cell therapies.

5.2 Aims

The aim is to produce a simple 3D model of stem cell differentiation using both Alvetex® Scaffold and Strata. This model needs to have the potential for use as a pluripotency assay and therefore assessing differentiation into all three germ layers is required. Any model produced for the differentiation of hESC will be compared to both standard *in vitro* differentiation of EBs and teratoma formation.

5.3 Objectives

1. Assess the suitability of both Alvetex® Scaffold and Strata for supporting the differentiation of EBs.

2. Test the need for coating of the 3D culture membranes for such purpose.

3. Compare 3D culture methods with existing standard methods for EB formation and teratoma formation.

4. Confirm the production of a 3D *in vitro* teratoma assay by assessing multiple hESC lines

5.4 Materials and Methods

5.4.1 Monolayer cultures of RC-10 and RC-6 embryonic stem cells

The embryonic stem cell lines, RC-6 (Figure 5.2A) and RC-10 (Figure 5.2B) were provided by Roslin Cellab (http://roslincellab.com/) and were both cultured using the same method. This method has previously described in Chapter 4. They were cultured as a feeder-free culture using CELLstart coating (Invitrogen) and the StemPro® hESC serum free media kit (Invitrogen). Both cell lines were cultured in 6-well plates coated with CELLstart as described in the previous Chapter. The StemPro kit is based on DMEM/F12 with Glutamax supplemented with 25% bovine serum albumin (BSA), StemPro hESC growth supplement (50x) and 10µg/ml basic fibroblast growth factor (bFGF). Complete media consists of 454ml DMEM/F12, 10ml of 50x StemPro supplement, 36ml of 25% BSA to a give a final concentration of 8% and finally 400µl of the 10µg/ml stock solution of bFGF to give a final concentration of 8ng/ml.

Both the cell lines – RC-6 & RC-10 were thawed at 37°C, transferred to individual centrifuge tubes containing warmed complete StemPro media and centrifuged at 1300 RPM for 3 minutes to pellet the cells. The pellets were carefully broken up by pipetting in fresh StemPro. CELLStart solution was removed from one well of a 6-well plate and 5 ml of cell suspension was added. Cells were incubated at 37°C and 5% CO_2 for 24 hours to allow cells to adhere before 100% of the media was changed to remove cell debris.

Cells were passaged using a manual dissociation technique and the resulting cell suspension was split between 8 CELLStart coated wells. Media was changed every 48 hours until cultures reached 70-80% confluency. Cells were split 1:8 once a week.

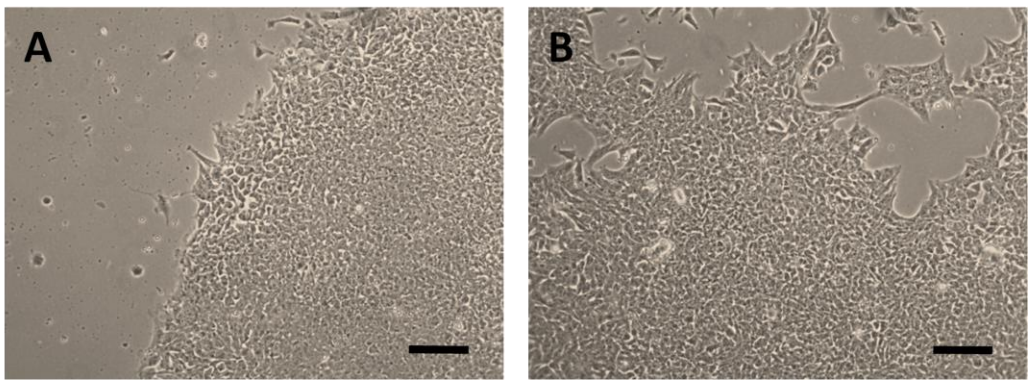

Figure 5.2 Standard 2D monolayer cultures of the human embryonic stem cells: RC-6 (A) and RC-10 (B) grown in feeder-free conditions in StemPro media. Scale bars = 100µm

5.4.2 Formation of embryoid bodies from RC-10 and RC-6 hES cells

Embryoid bodies were formed using both the AggreWell™ 400 and AggreWell™ 800 system (Stem Cell technologies) as previously by Antonchuk [318]. The media used for the formation and

maintenance of embryoid bodies (EBs) was Knock-Out DMEM (Invitrogen) supplemented with 50ml hESC qualified FBS, 5ml of 200mM L-glutamine (Invitrogen); 5ml Non-Essential Amino Acids (Invitrogen); and 1ml 2-mercaptoethanol (Invitrogen). This media was aliquoted and either frozen or stored at 4°C for up to 2 weeks.

Both sizes of AggreWell™ plates were prepared to remove any trapped air bubbles. The 8 centre wells of the AggreWell™ plates contain inverse pyramidal microwells of 400µm or 800µm. The size of the microwells determines the size of the embryoid bodies which are formed. The AggreWell™ plate was removed from the packaging in a sterile environment and each well was washed with 1ml of PBS containing calcium and magnesium. This was replaced with 0.5 ml of the EB media and the plate was centrifuged at 2000g for 5 minutes to force air bubbles out of the wells. Plates were then observed on a phase microscope to ensure all bubbles had been removed. Figure 5.3A shows the 800µm microwells in the AggreWell™ plate after this preparation process, the plate is then placed in an incubator at 37°C and 5% CO_2 to equilibrate while cells are harvested.

A 70-80% confluent, RC-6 and RC-10 cells were selected for the formation of EBs. Prior to cell harvesting the ROCK inhibitor - Y-27632 (Tocris Bioscience) was added to the cultures to a final concentration of 10µm for 1 hour. This helps to prevent cell death when the cells are dissociated into a single cell suspension. The single cell suspension of both cell lines was achieved by treating the hESCs with TrypLE™ Select CTS™ solution (Invitrogen). This is a non-animal alternative to Trypsin EDTA. 1.5ml of EB media was added to neutralise the enzyme and cells were centrifuged at 1300rpm for 3 minutes before being resuspended in 1ml of EB media. Cells were counted using a haemocytometer.

Cells were added directly to the pre-warmed media in the AggreWell™ plates. For the formation of 400µm embryoid bodies, 2.4 x 10^6 cells were added to each well of the AggreWell™ 400 plate which contains approximately 1200 microwells. Assuming an even distribution, this should produce EBs containing approximately 2000 cells each. For the formation of 800µm EBs, 9.0 x 10^5 cells were added per well of the AggreWell™ 800 plate containing 300 microwells. This formed embryoid bodies containing approximately 3000 cells each. The EB media was topped up to a final volume of 2ml per well and supplemented with 10µM Y-27632. The cells were pipetted up and down to evenly distribute the cells and the plate was immediately centrifuged at 300g for 2

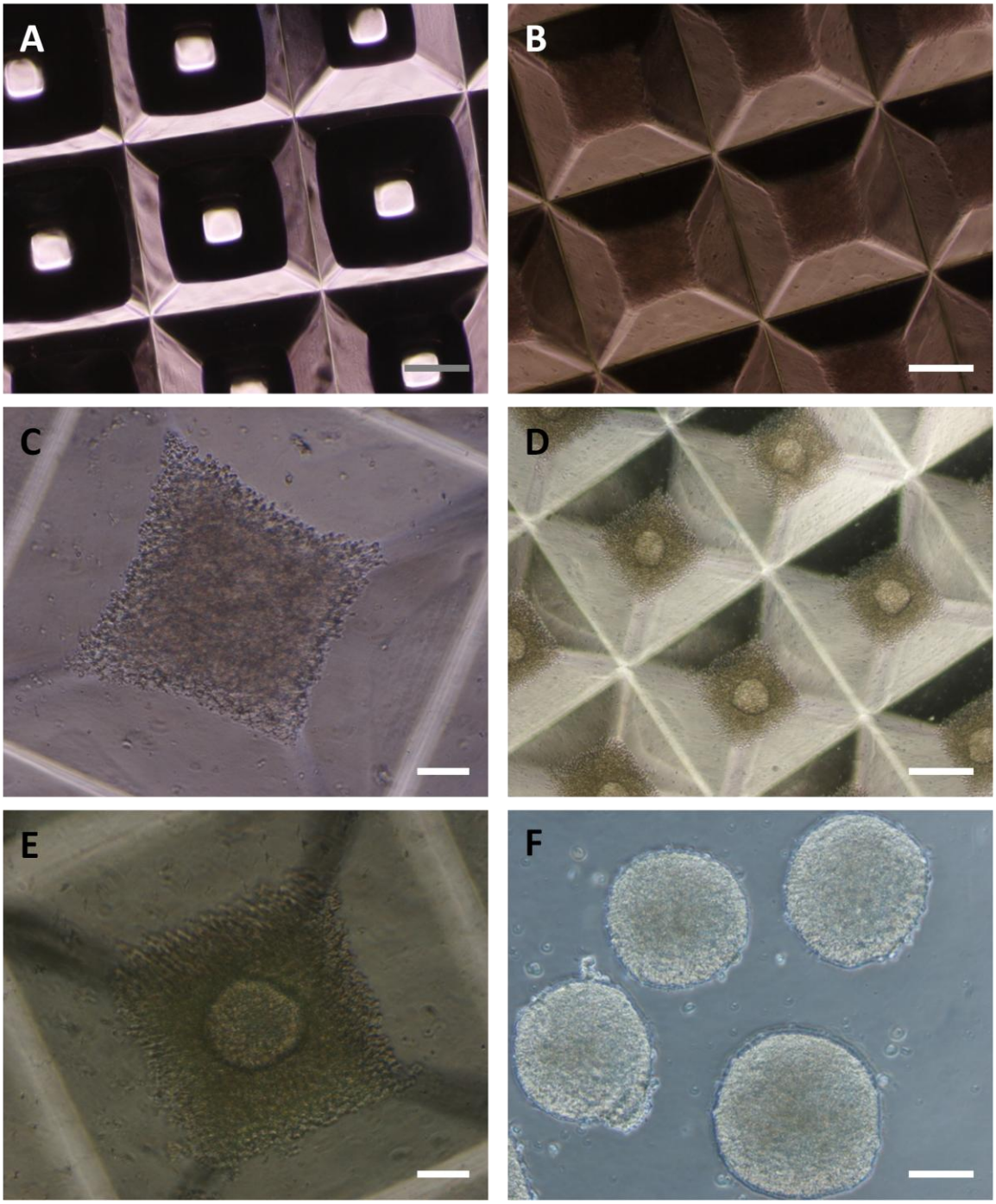

Figure 5.3 Formation of embryoid bodies from human embryonic stem cells using Aggrewell 800™plates. Aggrewell plates contain large amounts of microwells on the surface of the plate that help to promote the formation of EBs **(A).** Cells are initially centrifuged in the plate to force them to sit in the microwells **(B).** The microwells are full of cells after initial seeding the stem cells, this is visible at both low **(B)** and high magnification **(C).** Cells are maintained in the wells for 48 hours to allow EBs to form **(D,E).** The low magnification image clearly shows one EB formed inside each microwell. After 48 hours, the EBs are removed from the wells put through a cell strainer to remove single cells and then placed into low adherency plates for a further 7 days in suspension culture. **F** shows the EBs formed from this method which are relatively uniform in size. Scale bars: **A,B,D** = 100µm, **C,E,F**=50µm**.**

minutes to force the cells into the microwells. Microwells containing cells are visible throughout the plate and can be seen in Figure 5.3B &C.

The cells were cultured for 48 hours at 37°C and 5% CO_2. After 48 hours incubation, EBs are clearly visible within each microwell (Figure 5.3D&E). Embryoid bodies were harvested by firmly pipetting the medium up and down three times using a blue pipette tip to dislodge the EBs from the microwells. The resulting suspension was passed through a 40µm cell strainer to remove any remaining single cells. The strainer was then inverted and fresh media was used to wash the aggregates into a 50 ml falcon tube. Embryoid bodies were counted and 1000 EBs per well were added to non-tissue culture treated 6 well plates. Plates were placed at 37°C and gently moved in a side to side motion to evenly distribute the EBs. The resulting uniformly sized EBs can be seen in Figure 5.3F. EBs were cultured as a suspension culture for 7 days before being moved to a subsequent differentiation protocol.

5.4.3 Seeding embryoid bodies onto tissue culture plastic

After 7 days in suspension culture, embryoid bodies were plated onto either coated or non-coated tissue culture plastic to differentiate. Half of the wells of a 12-well plate were coated with 1ml of 0.1% gelatin solution (Sigma Aldrich, UK) for 1 hour prior to use. Gelatin solution was removed and 2 ml of EB media was added to all the wells of the 12-well plate. Embryoid bodies were evenly distributed between coated and non-coated wells. The embryoid bodies were cultured for a further 7 days with a media change after 3.5 days. After 7 days of culture the resulting monolayers were washed and fixed in 4% PFA. They were then washed twice with PBS and processed for immunocytochemistry to confirm the presence of all three germ layers.

5.4.4 Seeding embryoid bodies onto Alvetex® Scaffold and Strata

Alvetex® Scaffold and Strata were ethanol-treated and washed twice in PBS prior to use. Both types of Alvetex® were placed on the bottom of a Petri dish and coated with 0.1% gelatin solution for 1 hour prior to the seeding of embryoid bodies. Inserts were removed for the gelatin solution and placed in a 6-well plate, excess gelatine was removed via aspiration. Inserts were topped up with 7 ml of EB differentiation media and placed in the incubator to equilibrate until required. Embryoid bodies were collected from their suspension culture and allowed to settle in 15ml centrifuge tubes, spent media was then removed. EBs were topped up with 1ml of fresh media and EBs were distributed evenly between gelatin-coated and non-coated Scaffold and Strata using a blue pipette tip. EBs were cultured on Scaffold and Strata for a further 7 days before being fixed in 4% PFA overnight.

5.4.5 Subcutaneous cell transplantation to form teratomas

Teratomas were formed from ES cells using the method described for EC cells in the previous Chapter. All procedures involving mice were conducted in accordance with guidelines and permission granted by the Institution and the Home Office, UK. Cells were trypsinised from monolayer cultures and viable cells were counted using the Trypan Blue assay and 0.5 x 10^6 cells were resuspended in 100µl of cell culture media. Each hES cell suspension was combined with 100µl of BD growth factor reduced Matrigel (BD Bioscience) to increase the success rate of tumour formation. The resulting 200µl of cell suspension was loaded into 1ml syringes with 21G needles and stored on ice until required. Cells were injected subcutaneously into adult male nude (nu/nu) mice. Each animal received grafts bilaterally on the flanks. Mice were examined regularly and when teratoma formation was visible the tumour was measured at least once a week until they reached 1cm^2. At this point mice were sacrificed and teratoma tissue was surgically removed.

5.4.6 Processing of teratomas

Teratomas formed from embryonic stem cells were processed as described for EC cells in the previous chapter. Teratomas were immersed in 4% PFA immediately after removal and fixed overnight. Tissue was washed 3 times in PBS and transferred to Falcon tubes before dehydration. Tissue was progressively dehydrated through a range of ethanols (70%, 80%, 90%, 95%, and 2 x 100%) for 2 hours each. When the last 100% ethanol was removed, teratomas were incubated in Histoclear (National Diagnostics) for 2 hours. Tubes containing tissue were then topped up with paraffin wax to produce a 50:50 solution of Histoclear : paraffin wax. Tubes were incubated at 60°C overnight before the solution was removed and wax was added and again incubated overnight, this step was repeated a further three times before the teratomas were embedded. Teratomas were sectioned to 6µm using a Leica Microtome RM2125RT prior to floating on a 40°C histology water bath. Sections were mounted onto electrostatically charged SuperFrost+ slides. Consecutive sections of each teratoma were cut and the central section was stained with Haemotoxylin and Eosin and neighbouring sections were immunostained for germ layer markers.

5.4.7 Immunocytochemistry on embryoid bodies grown on tissue culture plastic

EBs grown in 2D were washed twice in PBS and fixed in 4% PFA for 30 minutes. Separate wells were stained for three germ layer markers – β (III) Tubulin, smooth muscle actin and α-fetoprotein and stem cell marker – Oct 4 using the method described in the previous chapter. Antibody dilutions are shown in Table 5.1. For negative controls see previous Chapters.

5.4.8 Processing of embryoid bodies cultured on 3D substrates and teratomas.

After fixation, Scaffold and Strata were washed twice in PBS and dehydrated through 30% and 50% ethanol for 15 minutes each. The 70% ethanol dehydration step was replaced with a Crystal

Violet staining step. 0.05% Crystal Violet was dissolved in 70% ethanol and 3D cultures were stained for 15 minutes prior to the following 80% dehydration step. Further dehydration and embedding steps were identical to those describe for 3D cultures in previous Chapters. After embedding Scaffold and Strata containing EBs was sections into 6µm sections and stained for all three germ layers and Oct 4 as well as Haemotoxylin and Eosin. Teratomas were also sectioned to 6µm and immunostained using the same method. Antibody dilutions are detailed in Table 5.1.

Primary Antibody	Supplier	Dilution in blocking buffer	Secondary Antibody	Supplier	Dilution in blocking buffer
Oct 4 Rabbit polyclonal	Abcam (ab19857)	1:250	Goat anti-rabbit IgG (H+L) Alexafluor 488	Invitrogen (A11008)	1:600
Rabbit Polyclonal neuronal Class III β tubulin (TUJ-1)	Cambridge Bioscience (PRB-435P-100)	1:600	Goat anti-rabbit IgG (H+L) Alexafluor 488	Invitrogen (A11008)	1:600
Rabbit polyclonal to alpha smooth muscle Actin	Abcam (ab5694)	1:100	Goat anti-rabbit IgG (H+L) Alexafluor 488	Invitrogen (A11008)	1:600
Monoclonal Anti-α-Fetoprotein (AFP) antibody produced in mouse	Sigma Aldrich, UK (A8452)	1:500	Goat anti-mouse IgG (H+L) Alexafluor 488	Invitrogen (A1101)	1:600
Nuclear stain			Hoescht 33342	Molecular Probes (H3570)	1:1000

Table 5.1 Antibody dilutions for the staining of 2D cultures, 3D cultures and teratomas

5.5 Results

5.5.1 Analysis of embryoid bodies terminally differentiated in 2D

Embryoid bodies were formed in Aggrewell™ plates, grown in suspension culture for 7 days and finally terminally differentiated in 2D on non-coated or gelatin-coated tissue culture plastic. The cultures were fixed in 4% PFA and stained for ectoderm using TUJ-1, mesoderm using SMA, and endoderm using AFP and the embryonic stem cell marker – Oct 4. There were noticeable differences between the two sizes of embryoid bodies. EBs derived from RC-10 cells formed using the Aggrewell 400™ plates produced dense networks of neurite outgrowth (Figure 5.4A & Figure 5.6A) whereas the 800µm sized EBs displayed large β(III)-tubulin positive cells (Figure 5.5A & Figure 5.7A). There was very little difference in alpha fetoprotein between large (800µm) and small (400µm) embryoid bodies (Figure 5.4B & Figure 5.6B compared with Figure 5.5B & Figure 5.7 B). However there was a difference in the smooth muscle actin even though positive staining was very limited. Staining of the 800µm EBs (Figure 5.5C & Figure 5.7C) is significantly less than the 400µm EBs (Figure 5.4C & Figure 5.6C). None of the EBs which had been terminally differentiated in 2D showed any evidence of Oct 4 staining (Figure 5.4D – Figure 5.7D)

Coating tissue culture plastic with gelatin also affected the differentiation of RC-10 cells in 2D. Although EBs were normally plated onto gelatin, it appeared the non-coated cultures of RC-10 cells displayed more complex structures. This was most apparent in the 400µm EBs where non-coated cultures had formed complex structures that were positive for the endoderm marker – α-fetoprotein (Figure 5.6B) and SMA-positive cells were more dense (Figure 5.6C) than their gelatin-coated counterparts (Figure 5.4C). There was also more staining for SMA in the 800µm sized EBs (Figure 5.7C).

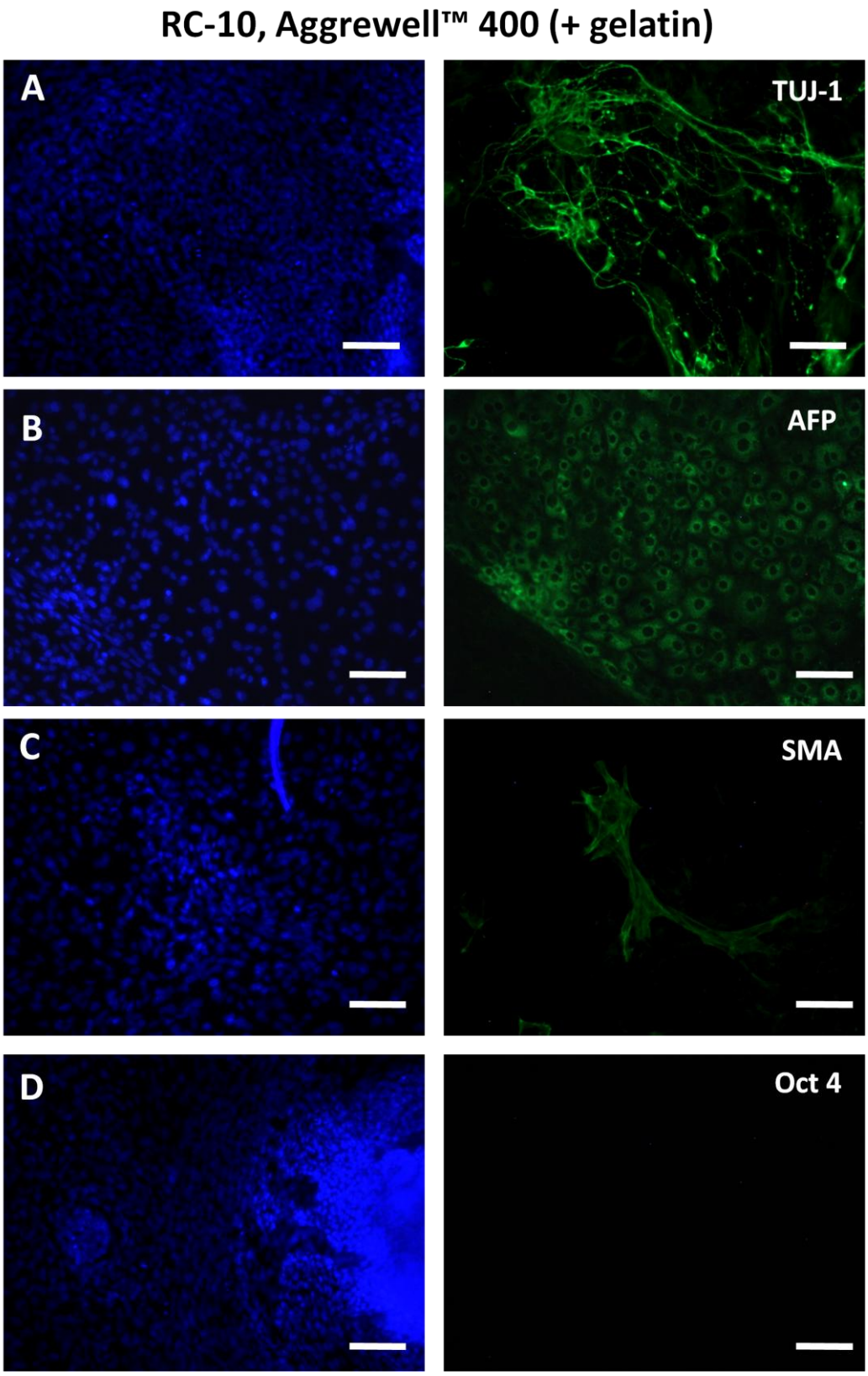

Figure 5.4 Analysis of Aggrewell™ 400 RC-10 derived embryoid bodies cultured on 2D gelatin-coated tissue culture plastic. After 7 days in suspension culture the embryoid bodies were seeded into 12-well plates and were allowed to adhere to the surface and differentiate for a further 7 days in culture before being fixed in PFA and stained for all three germ layers. The 400µm EBs grown on gelatin coating show large areas of TUJ-1 positive neurites **(A)** and also dense areas of AFP positive cells **(B).** However there were only individual cells that stained for SMA **(C)** and no evidence of Oct 4 positive cells **(D).** Scale bars = 100µm

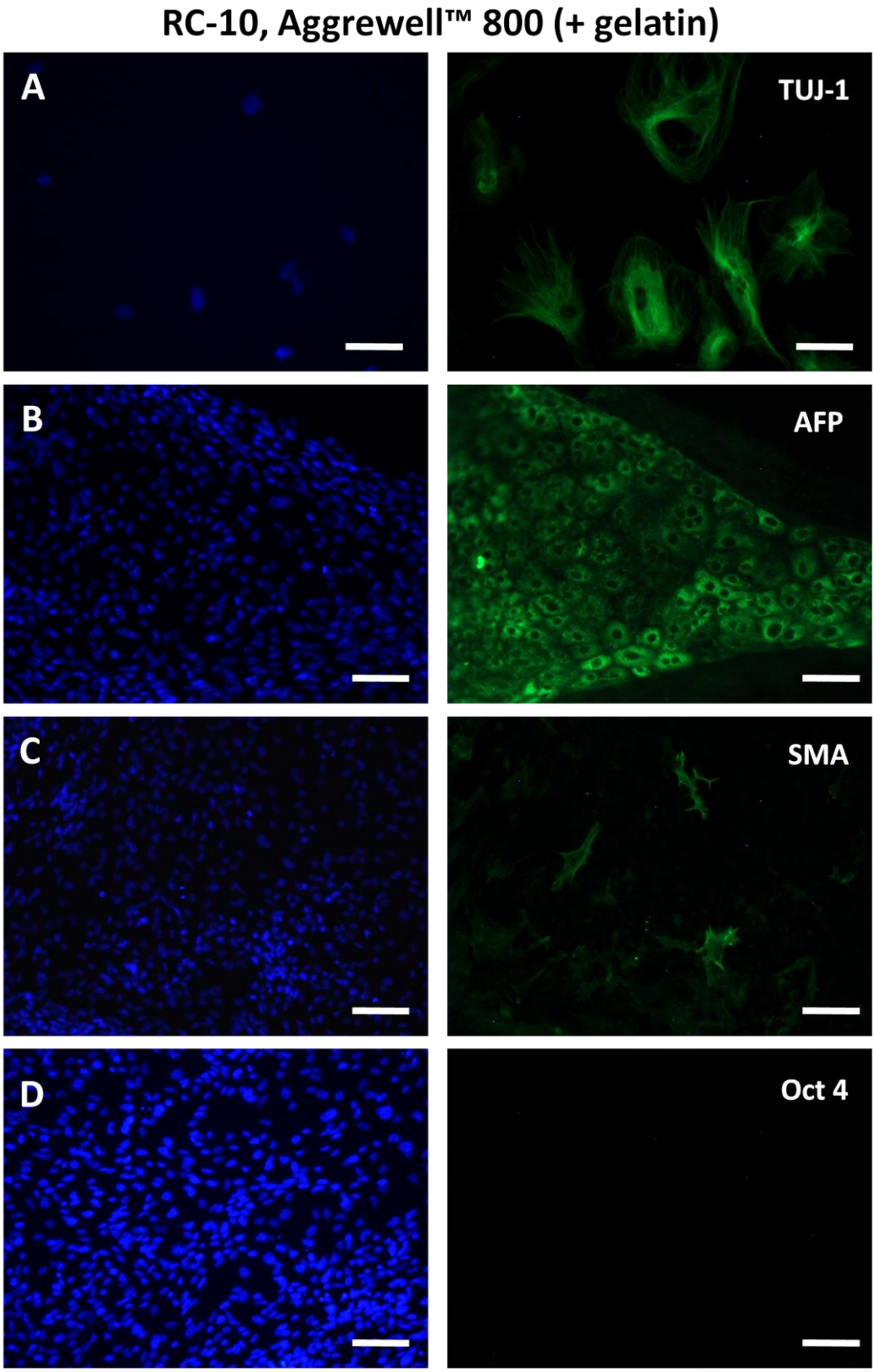

Figure 5.5 Analysis of Aggrewell™ 800 RC-10 derived embryoid bodies cultured on 2D gelatin-coated tissue culture plastic. After 7 days in suspension culture the embryoid bodies were seeded into 12-well plates coated with gelatin and were allowed to adhere to the surface and differentiate for a further 7 days in culture before being fixed in PFA and stained for all three germ layers. The 800µm EBs grown on gelatin coating show individual cells that stain for TUJ-1 **(A)** instead of neurites of neurites which were visible in the 400-sized EBs. In a similar way to the 400 µm EBs they display large areas of AFP positive cells **(B)** and very limited staining for the mesoderm marker –SMA **(C).** Again there is no staining for the embryonic stem cell marker - Oct 4 **(D).** Scale bars = 100µm

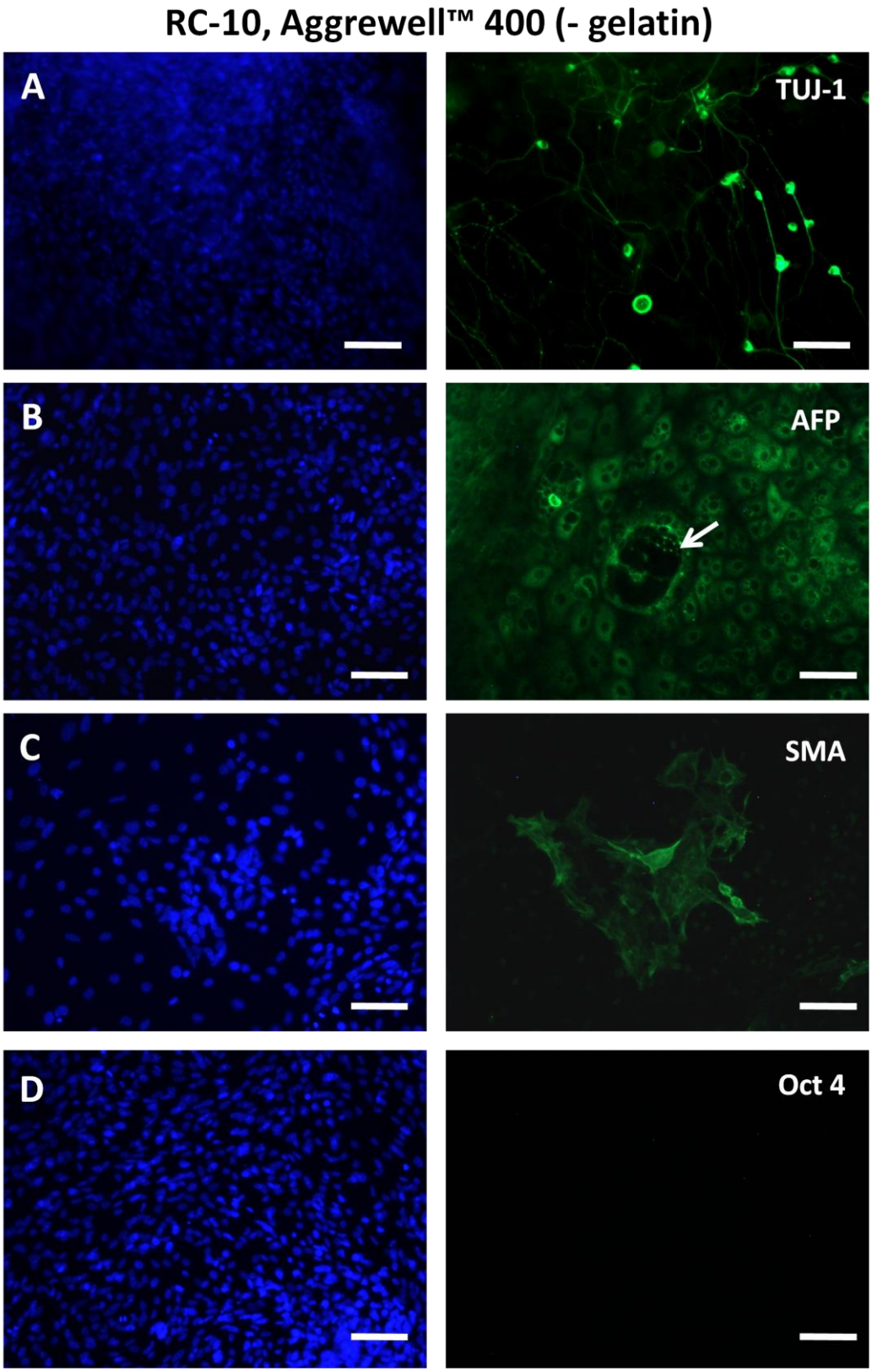

Figure 5.6 Analysis of Aggrewell™ 400 RC-10 derived embryoid bodies cultured on 2D standard tissue culture plastic. After 7 days in suspension culture the EBs were seeded in 12-well tissue culture plates and allowed to adhere and differentiate for a further 7 days. Then fixed in PFA and stained for all three germ layers. The 400µm EBs grown without additional surface coating show TUJ-1 positive neurites **(A)** similar to the large networks observed using the gelatin coating. There are also areas that stain for the endodermal marker – AFP and highlight complex structures. **(B, white arrow)** Without the gelatin coating there are more SMA positive cells (C) but still no staining for the embryonic stem cell marker - Oct 4 **(D).** Scale bars = 100µm

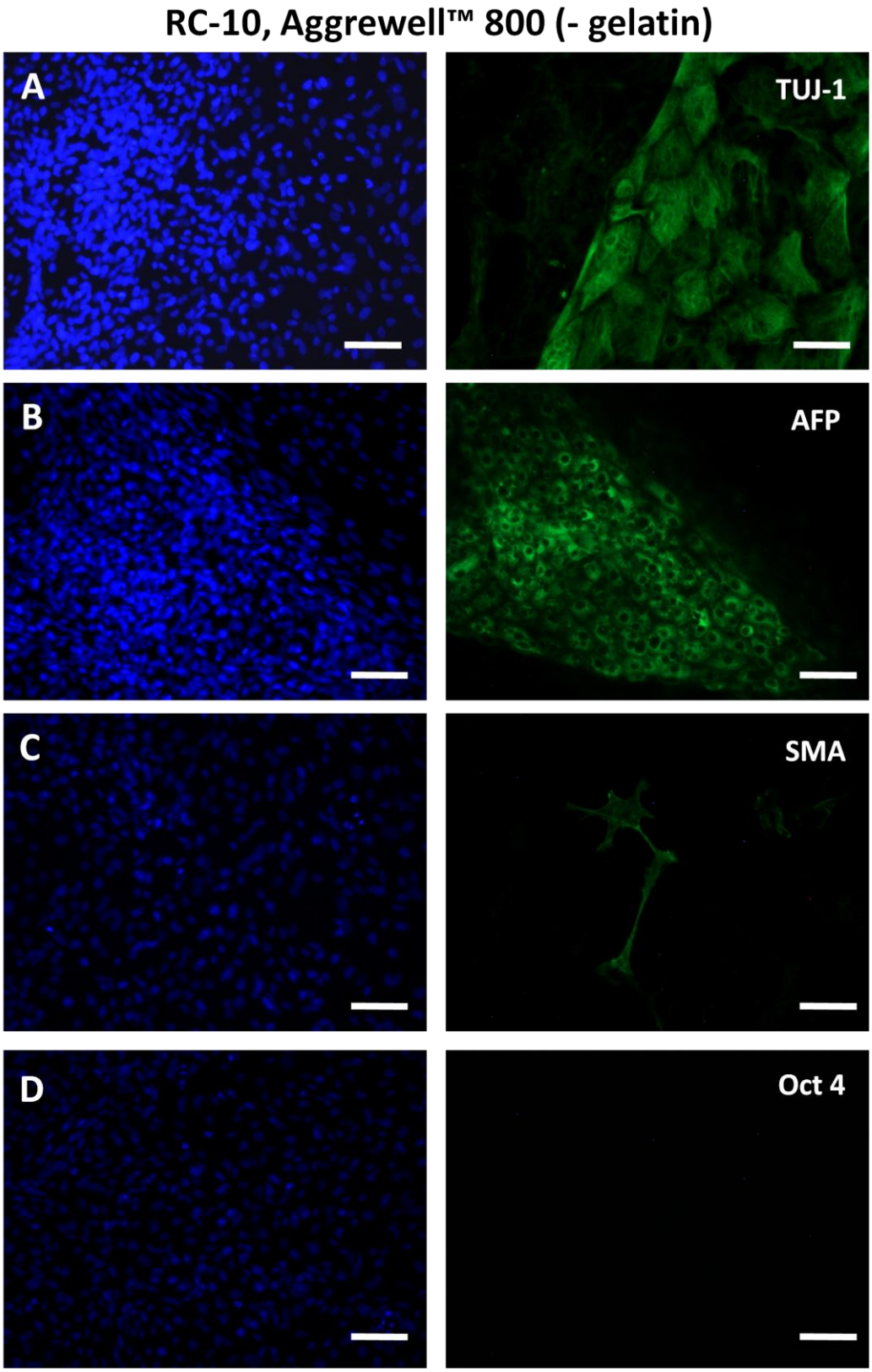

Figure 5.7 Analysis of Aggrewell™ 800 RC-10 derived embryoid bodies cultured on 2D standard tissue culture plastic. After 7 days in suspension culture the EBs were seeded in 12-well tissue culture plates and allowed to differentiate for a further 7 days. Then fixed in PFA and stained for all three germ layers. The 800µm EBs grown without additional surface coating show dense areas of cells positive for the ectodermal marker – TUJ-1 **(A)** similar to cells observed in the 800µm EBs with gelatin coating. There are also large areas that stain for AFP **(B)** and only individual cells which are SMA positive **(C)** and no staining for the embryonic stem cell marker - Oct 4 **(D).** Scale bars = 100µm

5.5.2 Immunostaining of teratomas derived from embryonic stem cells in 2D

For comparison with the embryoid bodies that were differentiated in both 2D and 3D, teratomas formed from ES cells were also stained for all three germ layers and Oct 4. Human embryonic stem cell lines were injected into immune-deficient mice as previously described for the EC cells and allowed to form teratomas. Unlike the teratomas formed from EC cells in the previous chapters. ES teratomas displayed a wider variety of tissue types and large area of tissue stained for TUJ-1 (Figure 5.8A), alpha fetoprotein (Figure 5.8B) and smooth muscle actin (Figure 5.8C). In contrast to the EBs described in Figure 5.4– Figure 5.7 the teratomas also displayed extensive staining for the embryonic stem cell marker – Oct 4 (Figure 5.8D).

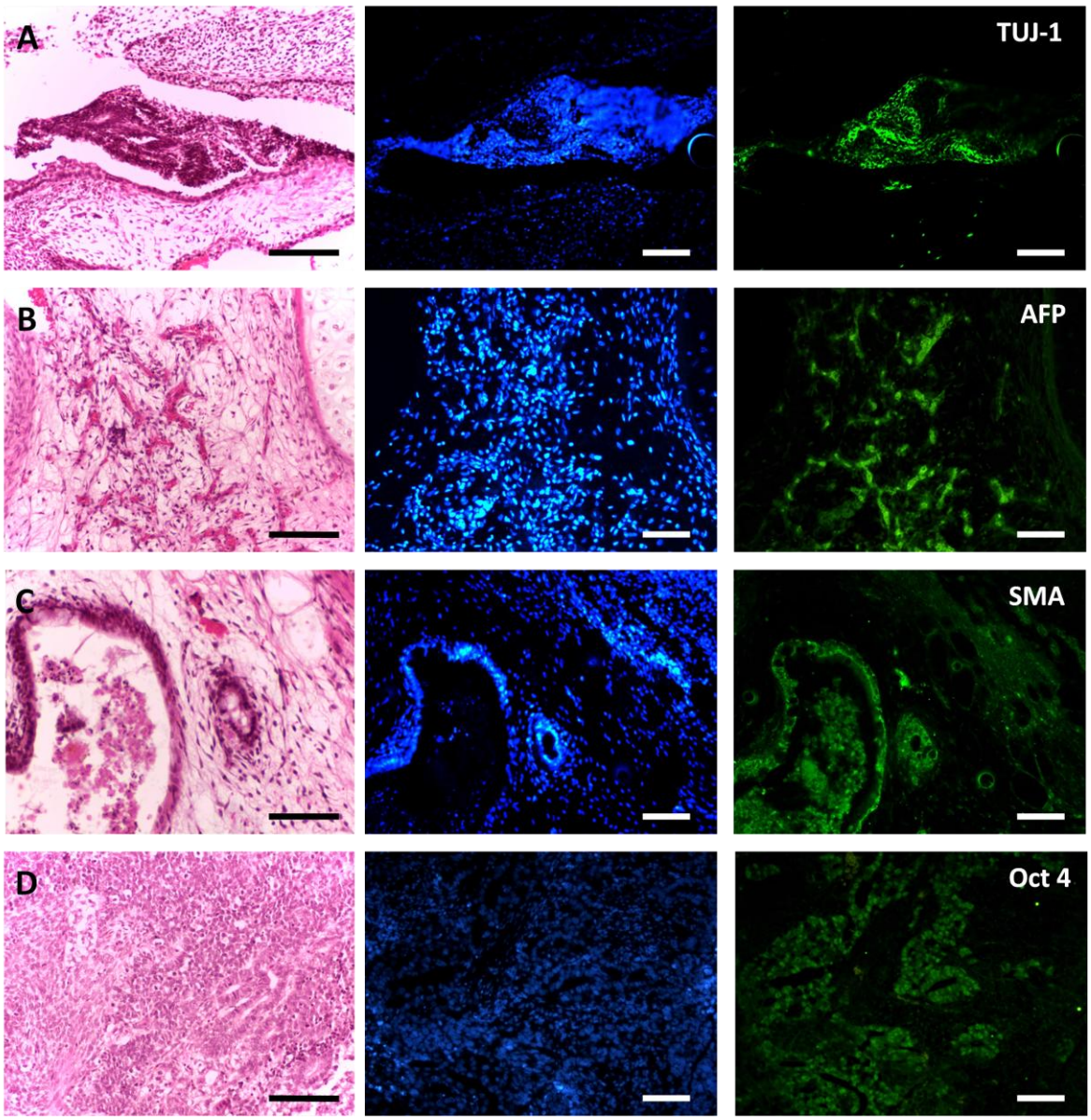

Figure 5.8 Immunostaining of a subcutaneous teratoma formed from engrafted 2D embryonic stem cells cultured on feeder layers: formation of three germ layers. Teratomas formed in SCID mice were stained for the ectoderm marker – β(III) tubulin (TUJ-1) **(A),** endoderm marker – α-fetoprotein **(B),** mesoderm marker – smooth muscle actin **(C)** and embryonic stem cell marker – Oct 4 **(D)** as well as with H&E for comparison with embryoid bodies cultured in 2D and 3D. Scale bars = 100µm

5.5.3 Analysis of RC-10 derived embryoid bodies terminally differentiated in 3D on Alvetex® Strata and Scaffold.

After the 7 days in suspension culture, RC-10 derived embryoid bodies were seeded onto ethanol-treated Strata and Scaffold which was either non-coated or gelatin-coated. The EBs were terminally differentiated in 3D for a further 7 days before being fixed in 4% PFA. They were processed for histology with an additional Crystal Violet staining step to ensure the EBs were easily located. Haematoxylin and Eosin staining revealed that the EBs were sitting on the surface of both the gelatin-coated (Figure 5.9B) and non-coated (Figure 5.9A) Strata membranes. The cells were able to migrate from the initial seeding areas and into the interior of the Strata membrane. Coating the Strata with gelatin allowed the embryoid body to become flattened so fewer complex structures were visible when compared with the non-coated membrane. Gelatin-coating also appeared to prevent cells from growing in the interior of the membrane (Figure 5.9B). The non-coated Strata membranes displayed an embryoid body at the surface containing many complex structures and cells were also present within the membrane (Figure 5.9A). When RC-10 cells were seeded onto the Alvetex® Scaffold, after 7 days on the Scaffold the original embryoid bodies were not visible (Figure 5.9C and Figure 5.9D). There was very little difference between the non-coated and coated scaffold with them both allowing cells throughout the Scaffold interior with areas of differing cell density.

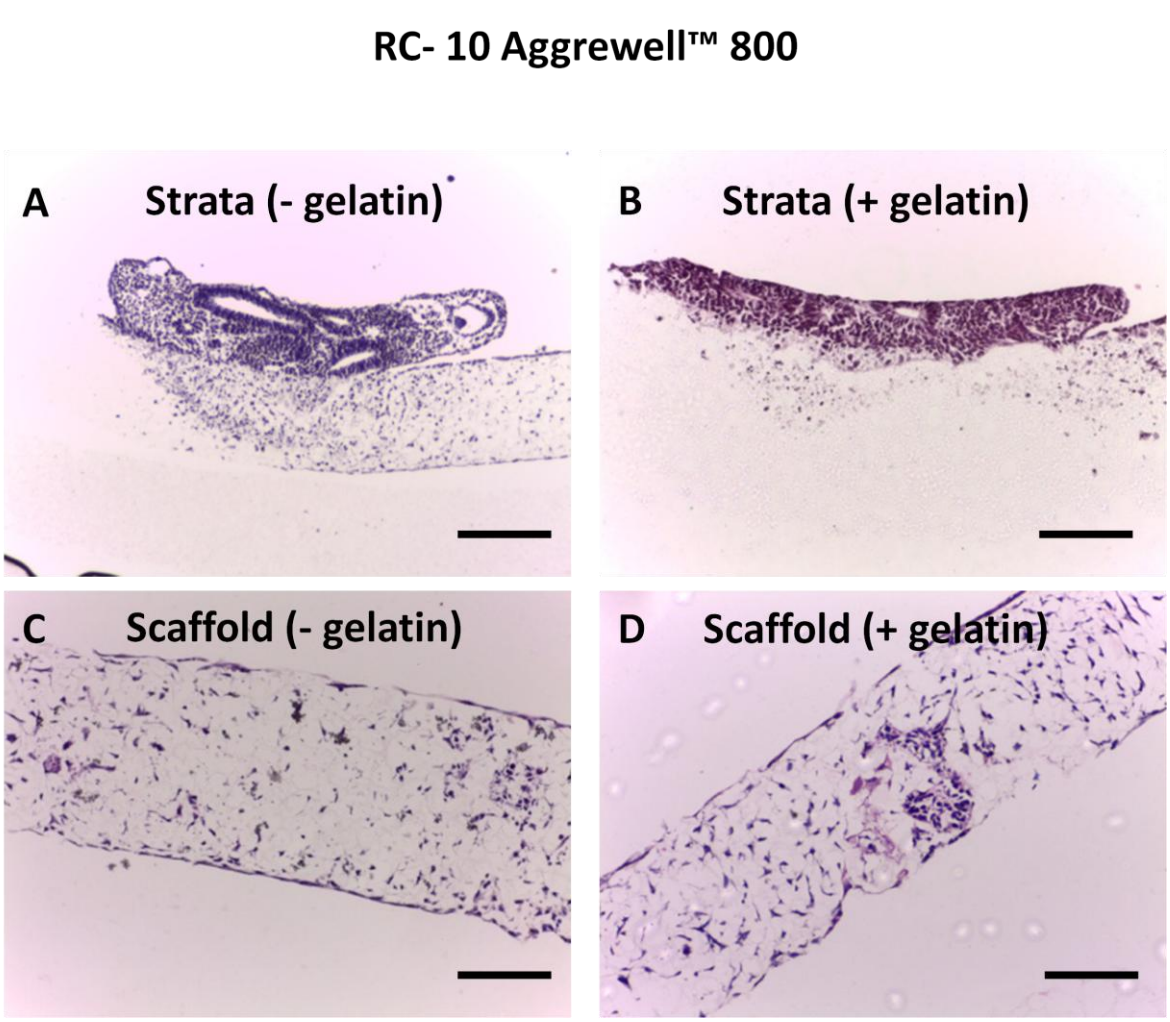

Figure 5.9 Histological analysis of Aggrewell™800 RC-10 derived embryoid bodies cultured in 3D on Alvetex® Scaffold and Strata. After 7 days in suspension culture, embryoid bodies were transferred to Strata **(A,B)** and Scaffold **(C,D)** with **(B,D)** and without **(A,C)** gelatin coating and cultured for a further 7 days. When the EBs are cultured on Strata they are able to retain their shape and complex structures are visible **(A)** when the Strata is gelatin coated the EBs begin to flatten **(B).** If EBs are grown in 3D on Scaffold, after the 7 days there is no evidence of the EB as cells have infiltrated the membrane with **(D)** and without **(C)** gelatin coating. Scale bars = 100µm

Immunostaining of the RC-10 embryoid bodies showed some evidence of all three germ layers and staining for the stem cell marker – Oct 4. Staining for the ectodermal marker TUJ-1 revealed neural rosettes and neurite outgrowth from EBs seeded on non-coated Strata (Figure 5.10A). There was also evidence of neural rosettes on the gelatin-coated Strata but no neurite outgrowth (Figure 5.11A). There was evidence of TUJ-1 positive cells in both of the Scaffold cultures. On the non-coated Scaffolds, TUJ-1 positive cells were visible at the media interfaces of the Scaffold and in areas of high cell density within the Scaffold (Figure 5.12A). Whereas on gelatin-coated Scaffolds, TUJ-1 positive cells were limited to the surface of the scaffold, where cells were at a high cell density (Figure 5.13A).

There was a greater difference in staining for endodermal marker – alpha fetoprotein between Strata and Scaffold than was visible in the TUJ-1 staining. RC-10 EBs seeded onto non-coated Strata displayed areas of AFP staining in both the initial EB and within the interior of the membrane (Figure 5.10B). These structures were similar to those visible in 2D non-coated plates (Figure 5.6B). In contrast to this there were no definite structures that were AFP positive on the gelatin-coated Strata and few positive cells within the interior (Figure 5.11B). Interestingly allowing EBs to migrate into the Alvetex® Scaffold led to no AFP positive cells on the non-coated membranes (Figure 5.12B) and weak staining when the Scaffold is gelatin-coated (Figure 5.13B).

The distribution of the mesoderm marker – smooth muscle actin was limited to the interior of the membranes in all cases. On Strata there was no evidence of SMA positive cells in the original EB in either the gelatin-coated (Figure 5.11C) or non-coated membranes (Figure 5.10C). The SMA positive cells infiltrated the entire width of the Strata membrane and were also visible throughout the Scaffold cultures (Figure 5.12C & Figure 5.13C). There was also evidence of staining for the embryonic stem cell marker – Oct 4 in the EBs with positive cells being limited to a structure on the top surface of the non-coated Strata membrane (Figure 5.10D) and at the periphery of a complex structure in the EB on the gelatin-coated membrane (Figure 5.11D). The Scaffold cultures of RC-10 cells showed very limited evidence of Oct 4 staining with two cells showing positive staining in the non-coated culture (Figure 5.12D) and no positive cells in the gelatin-coated cultures (Figure 5.13D).

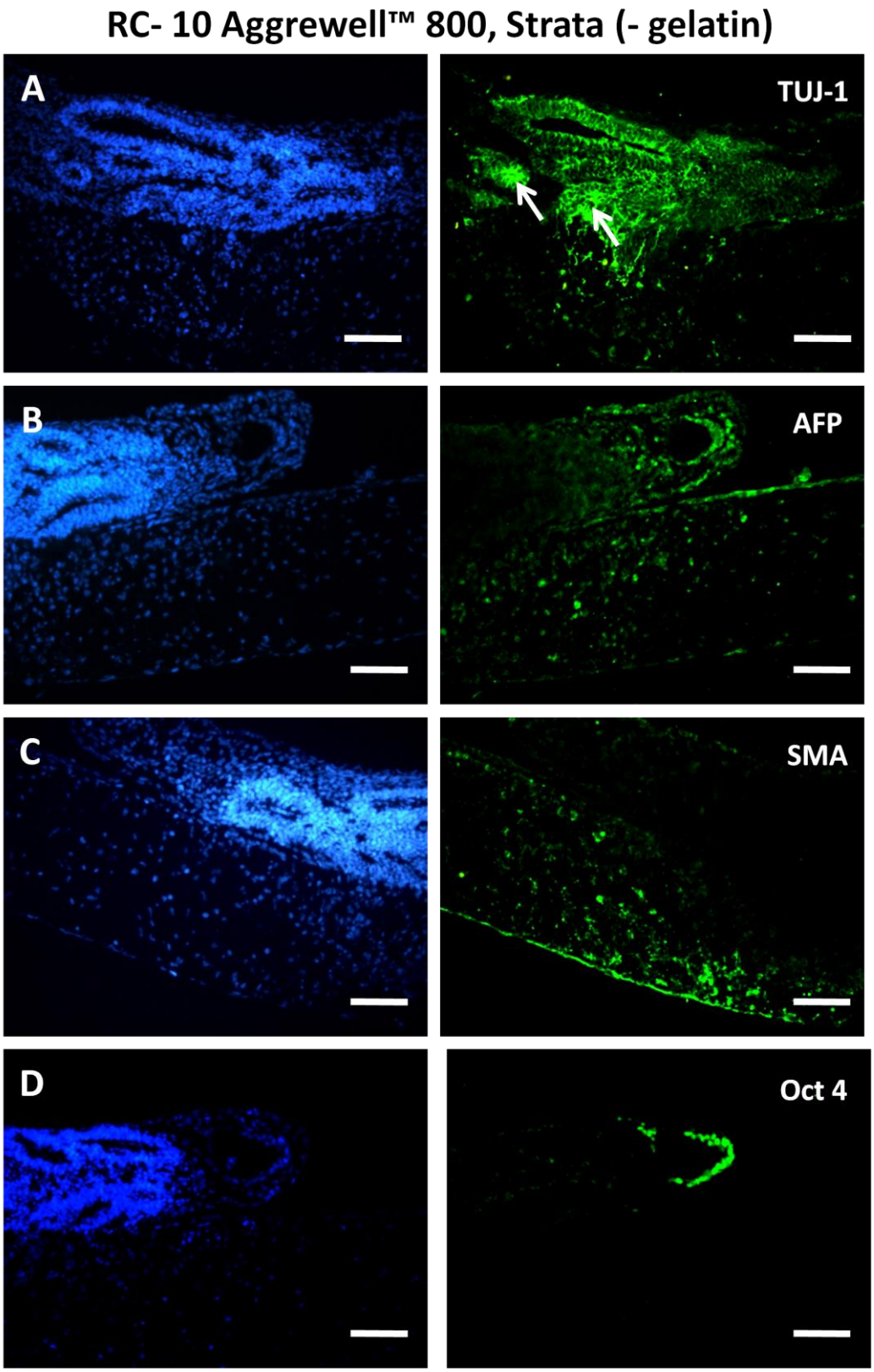

Figure 5.10 Immunostaining of Aggrewell™ 800 RC-10 derived embryoid bodies cultured in 3D on <u>non-coated</u> Strata. After 7 days in suspension culture EBs were transferred to Strata membranes and cultured for 7 days before being fixed and immunostained for the 3 germ layers and stem cell marker – Oct 4. Complex structures are clearly visible with the EB and there is also evidence of neural rosettes **(A, white arrows**) and AFP-positive cells **(B).** Interestingly staining for SMA only occurs within the interior of the membrane **(C)** and unlike the 2D counterparts (**Figure 5.7**) there are Oct 4 positive cells **(D).** Scale bars = 100µm

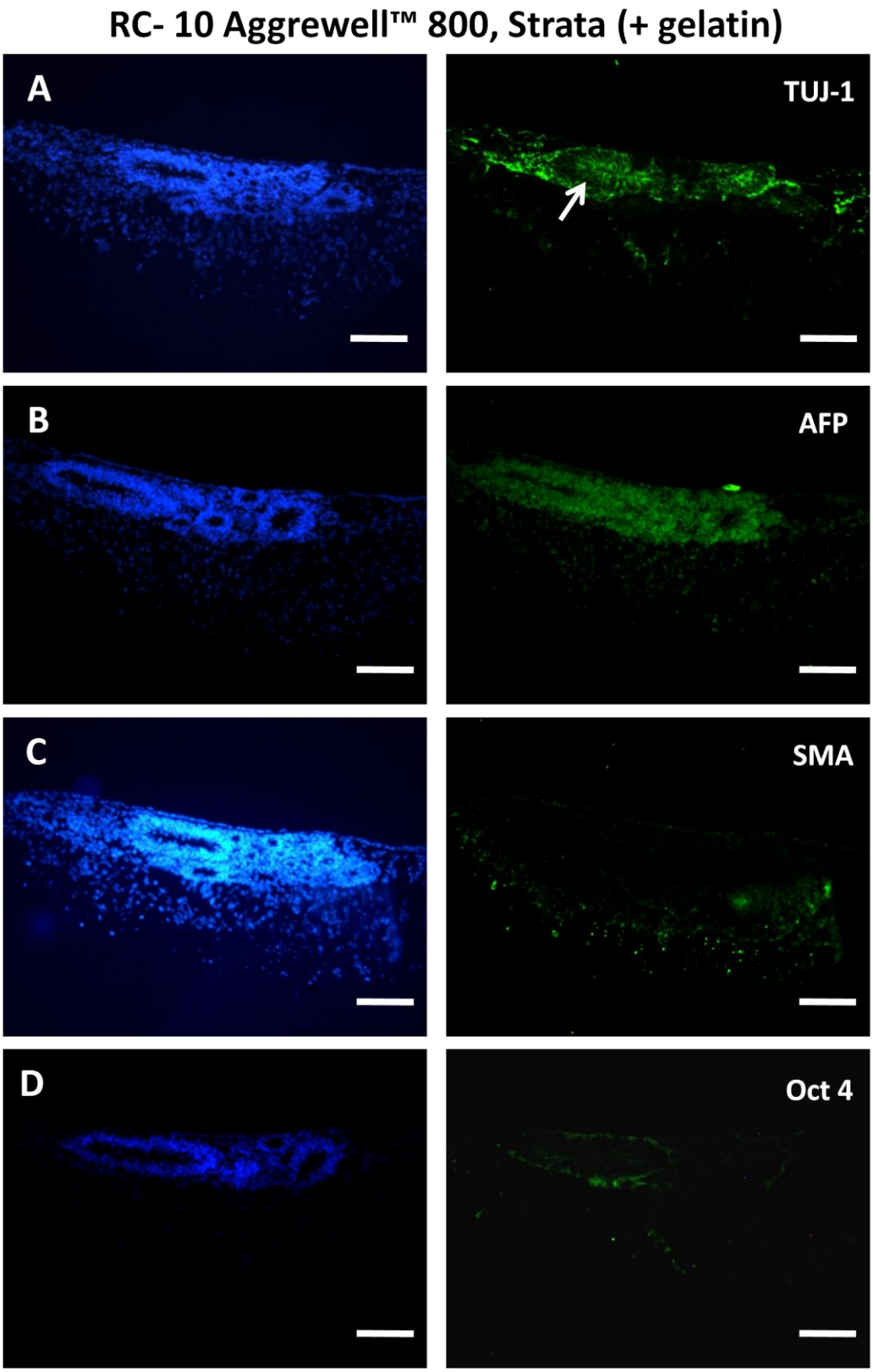

Figure 5.11 Immunostaining of Aggrewell™ 800 RC-10 derived embryoid bodies cultured in 3D on gelatin coated Strata. After 7 days in suspension culture EBs were transferred to Strata membranes coated with gelatin and cultured for 7 days before being fixed and immunostained for the 3 germ layers and stem cell marker – Oct 4. Complex structures are less visible when compared to the non-gelatin coated EB (Figure I) although there still evidence of neural rosettes **(A, white arrows)** and more AFP-positive cells **(B).** Similar to the non-coated Strata, staining for SMA also only occurs within the interior of the membrane **(C)** and there is weak staining for Oct 4**(D).** Compared with its non-coated counterpart these EBs on gelatin coating appear more flattened. Scale bars = 100µm

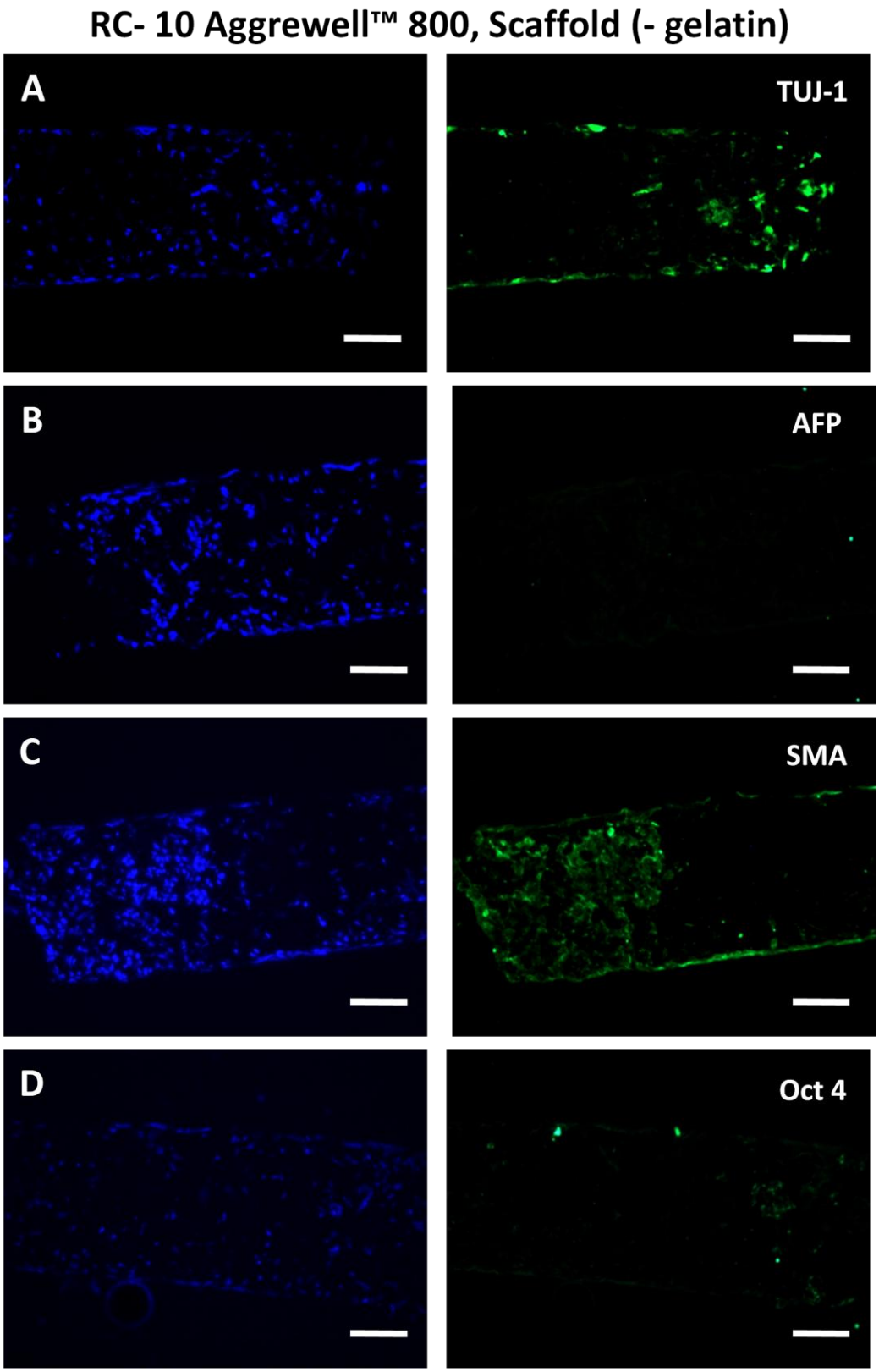

Figure 5.12 Immunostaining of Aggrewell™ 800 RC-10 derived embryoid bodies cultured in 3D on <u>non-coated</u> Scaffold. After 7 days in suspension culture EBs were transferred to Alvetex® Scaffolds and cultured for 7 days before being fixed and immunostained for the 3 germ layers and a stem cell marker. There is no evidence of the original EB that had been seeded onto the scaffold but there are TUJ-1 positive cells **(A)** and interestingly no staining for AFP **(B).** Unlike the Strata cultures and the 2D cultures there is dense areas of SMA positive cells **(C)** and limited Oct 4 staining **(D).** Scale bars = 100µm

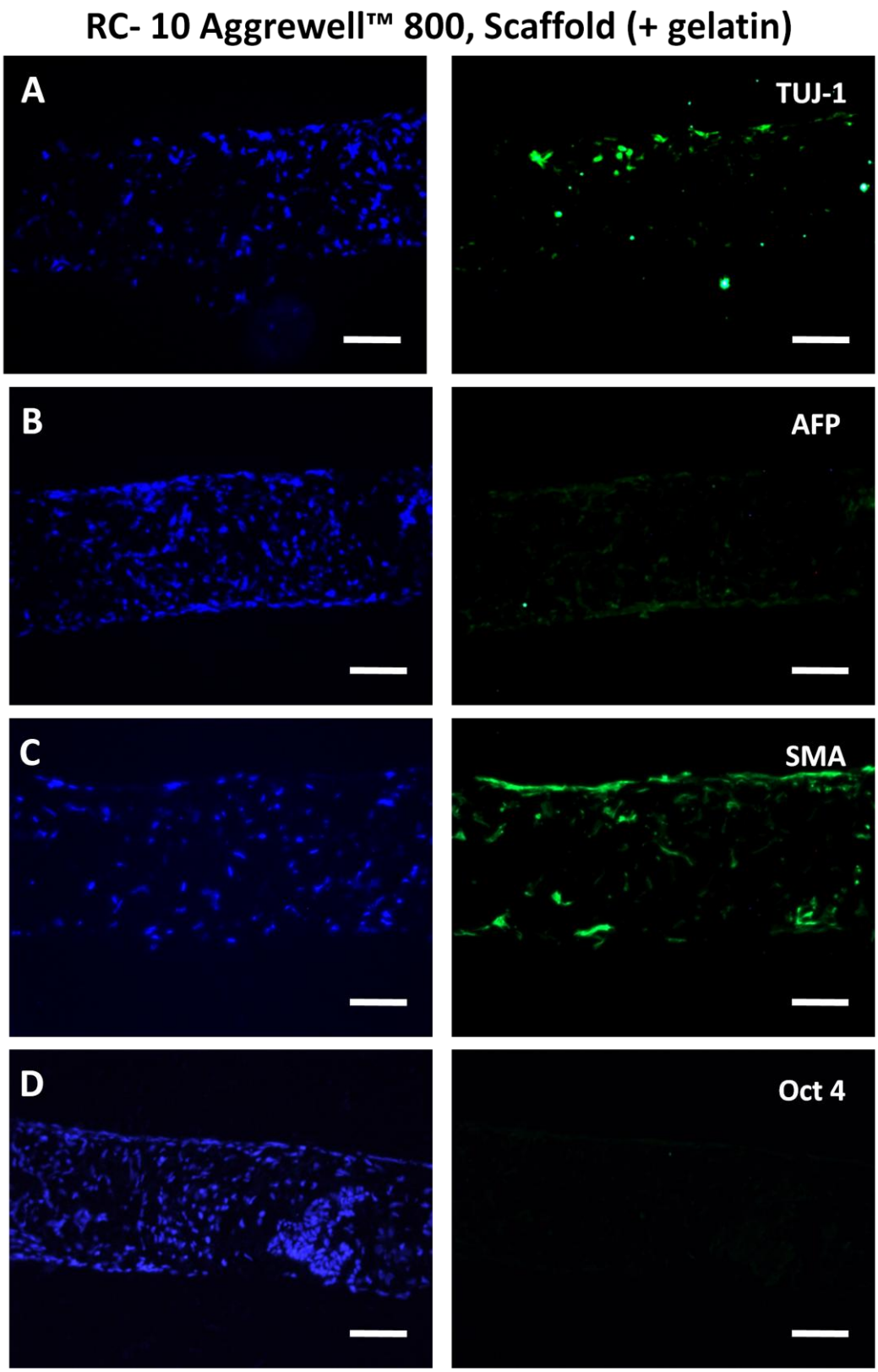

Figure 5.13 Immunostaining of Aggrewell™ 800 RC-10 derived embryoid bodies cultured in 3D on gelatin-coated Scaffolds. After 7 days in suspension culture EBs were transferred to gelatin-coated Alvetex® Scaffolds and cultured for 7 days before being fixed and immunostained for the 3 germ layers. As with the non-coated Scaffold there is no evidence of the original EB. There are areas TUJ-1 positive cells **(A)** within the scaffold and interestingly there is still no staining for AFP **(B).** Again there are large numbers of cells that stain for the mesoderm marker - SMA **(C)** and no Oct 4 staining **(D).** Scale bars = 100µm

5.5.4 Analysis of RC-6 derived embryoid bodies terminally differentiated in 3D on Alvetex® Strata and Scaffold.

After the 7 days in suspension culture, RC-6 derived embryoid bodies were also seeded onto ethanol-treated Strata and Scaffold which was either non-coated or gelatin-coated. The RC-6 EBs were terminally differentiated in 3D for a further 7 days before being fixed in 4% PFA, and processed for histology with an additional Crystal Violet staining step to ensure the EBs were easily located. In a similar way to the RC-10 EBs on Strata, the RC-6 cells were also able to form complex structures at the surface of the membrane and both the non-coated (Figure 5.14A) and gelatin-coated (Figure 5.14B) membranes allowed for the infiltration of cells into the interior of the membranes. The non-coated membranes appeared to allow the EBs to retain the structures within the mass of cells (Figure 5.14A) whereas the gelatin coating allowed the EB to flatten. RC-6 cells were able to migrate into the interior even with the additional gelatin coating (Figure 5.14B). In contrast to the previously described RC-10 EBs on Scaffold, RC-6 derived EBs still showed evidence of the original cell mass at the surface of the Scaffold membrane (Figure 5.14C&D) as well as a dense cell layer within the Scaffold interior this was in contrast with the RC-10 derived EBs (Figure 5.9C&D). However the RC-6 EBs on Scaffold also shows little difference between gelatin-coating (Figure 5.14C) and no coating (Figure 5.14D).

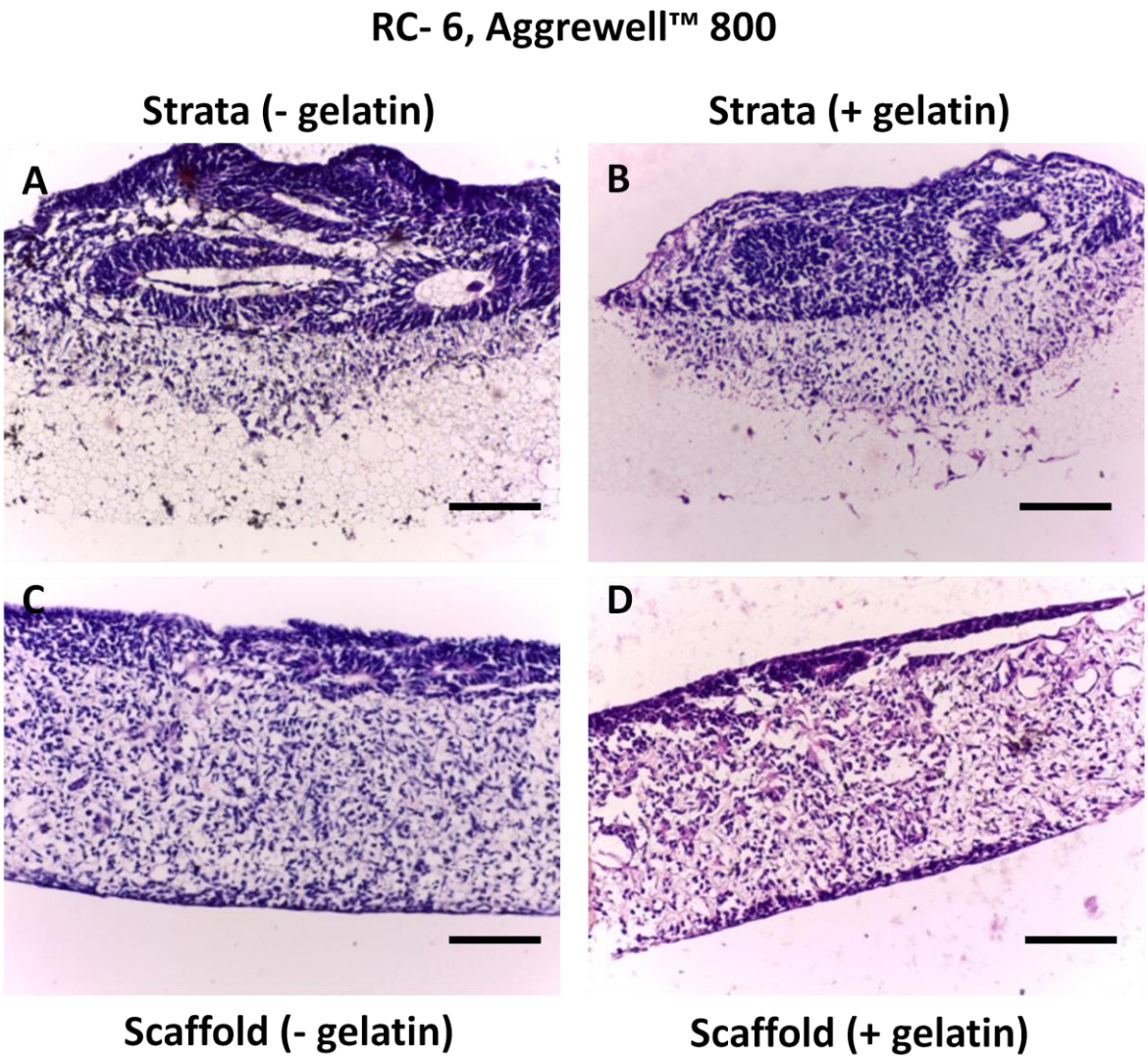

Figure 5.14 Histological analysis of Aggrewell™800 RC-6 derived embryoid bodies cultured in 3D on Alvetex® Scaffold and Strata. After 7 days in suspension culture, RC-6 embryoid bodies were transferred to Strata **(A,B)** and Scaffold **(C,D)** with **(B,D)** and without **(A,C)** gelatin coating and cultured for a further 7 days. In a similar way to the previous EBs in Figure H, when the RC-6 EBs are cultured on Strata they are able to retain their shape and complex structures are visible **(A)** and are also still evident on gelatin-coated Strata **(B).** If EBs are grown in 3D on Scaffold, after the 7 days there is still evidence of the EB unlike the RC-10 cultures. Cells are also able to infiltrated the membrane with **(D)** and without **(C)** gelatin coating. Scale bars = 100µm

Immunostaining for ectoderm in the RC-6 derived EBs that were grown on non-coated Strata showed large complex structures which were TUJ-1 positive (Figure 5.15A). Most of TUJ-1 positives cells were in the mass of cells on the top of membrane, there was no evidence of neurite outgrowth from these cells. The gelatin coating led to fewer TUJ-1 positive cells on Strata (Figure 5.16A) and this was consistent with the findings from the RC-10 derived EBs (Figure 5.11A). In the non-coated Scaffold cultures, there were TUJ-1 positive cells in both the dense areas of cells at the surface of the Scaffold and also long thin TUJ-1 positive cells within the Scaffold interior (Figure 5.17A), these types of cells were also evident in the interior of the gelatin coated scaffold but there were none visible at the surface (Figure 5.18A).

Immunostaining for the endoderm marker – AFP was restricted in all conditions for RC-6 derived EBs. On non-coated Strata there was weak AFP staining in the original EB (Figure 5.15B) but when the Strata membranes were coated with gelatin there was a band of stronger staining for AFP at the interface between the membrane and the EB (Figure 5.16). This band of positive staining was also visible on non-coated Scaffold and extended into the high density cells within the Scaffold interior but only in areas directly underneath the EB (Figure 5.17B). This distribution of AFP positive cells was also apparent in the gelatin-coated Scaffold (Figure 5.18B).

Immunostaining for SMA to highlight mesodermal differentiation of RC-6 cells showed an extremely restricted pattern of positive cells. This pattern was similar to that observed in the RC-10 cells (Figure 5.10C & Figure 5.11C). In the Strata cultures both the non-coated (Figure 5.15C) and gelatin-coated (Figure 5.15C) showed SMA positive cells only in low density areas in the interior of the membrane directly below the original EB. This differed from the Scaffold cultures where SMA positive cells were not directly under the EB due to these cells still being at a high cell density but positive areas were to the sides of the originally seeded EB (Figure 5.17C) and were also visible at the interface between the media and the Scaffold (Figure 5.18C). This very restricted pattern of SMA positive staining was highlighted in the montage in Figure 5.19. This displays the area of the Scaffold containing the original EB and the surrounding area. As cell density increased the levels of SMA staining decreased.

There was very limited staining for the embryonic stem cell marker – Oct 4 in all cultures of the RC-6 cells. Non-coated Strata membranes showed a few positive cells at the surface of the membranes (Figure 5.15D) whereas the gelatin coated Strata cultures showed isolated positive cells within high cell density areas in the membrane interior (Figure 5.16D). Oct 4 staining was limited to individual isolated cells in both of the Scaffold cultures and again it tended to be within the high cell density areas (Figure 5.17D & Figure 5.18D).

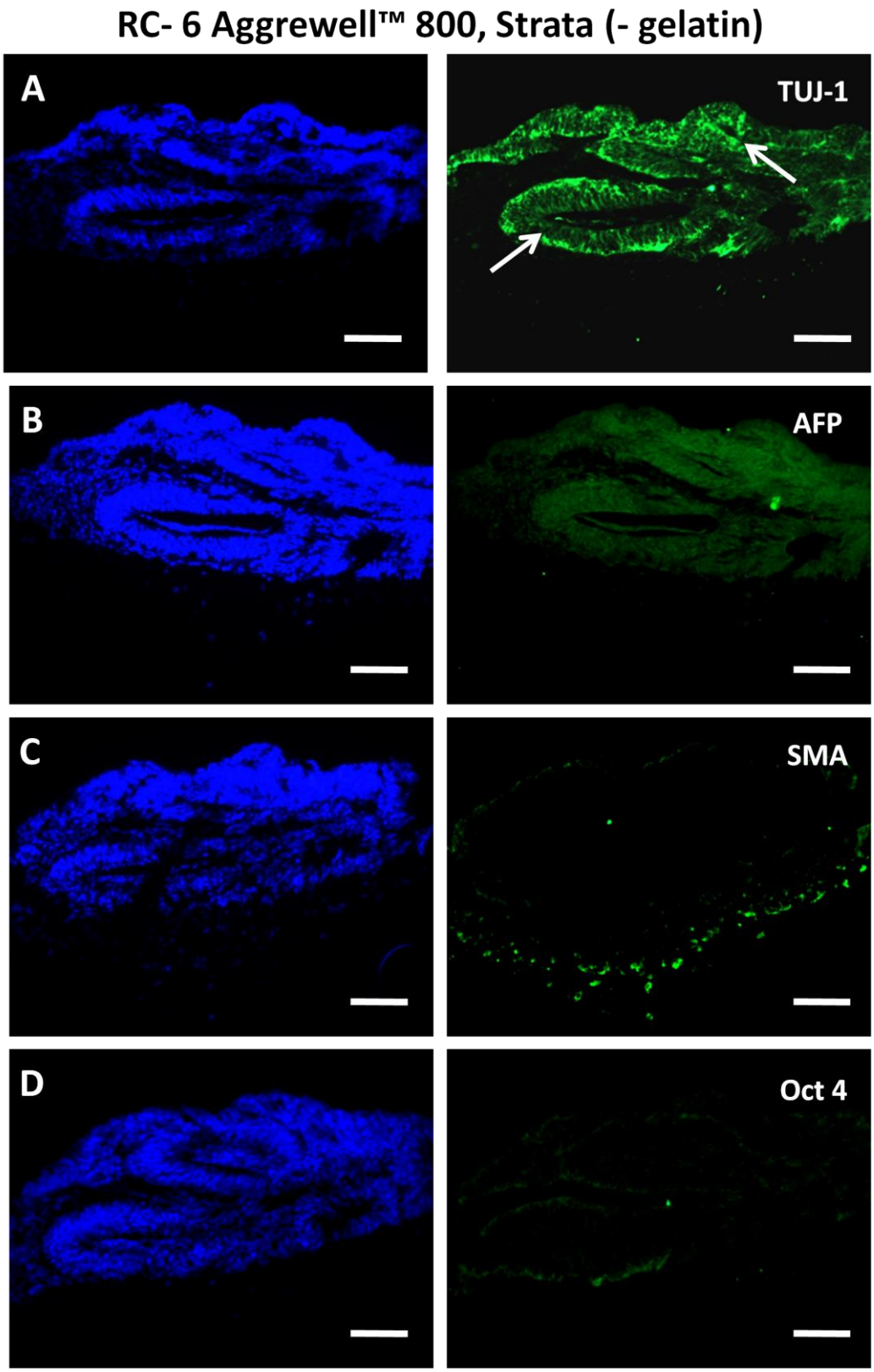

Figure 5.15 Immunostaining of Aggrewell™ 800 RC-6 derived embryoid bodies cultured in 3D on <u>non-coated</u> Strata. After 7 days in suspension culture EBs were transferred to Alvetex® Strata and cultured for 7 days before being fixed and immunostained . As seen with RC-10 cells the non-coated Strata cultures have complex structures and neural rosettes which are TUJ-1 positive **(A, white arrows),** these cells remain on top of the membrane. The rest of the cells on top of the membrane stain positive for the endoderm marker – AFP **(B).** Again SMA- positive cells are only seen within the Strata membranes **(C)** and there are few Oct 4 –positive cells **(D).** Scale bars = 100µm

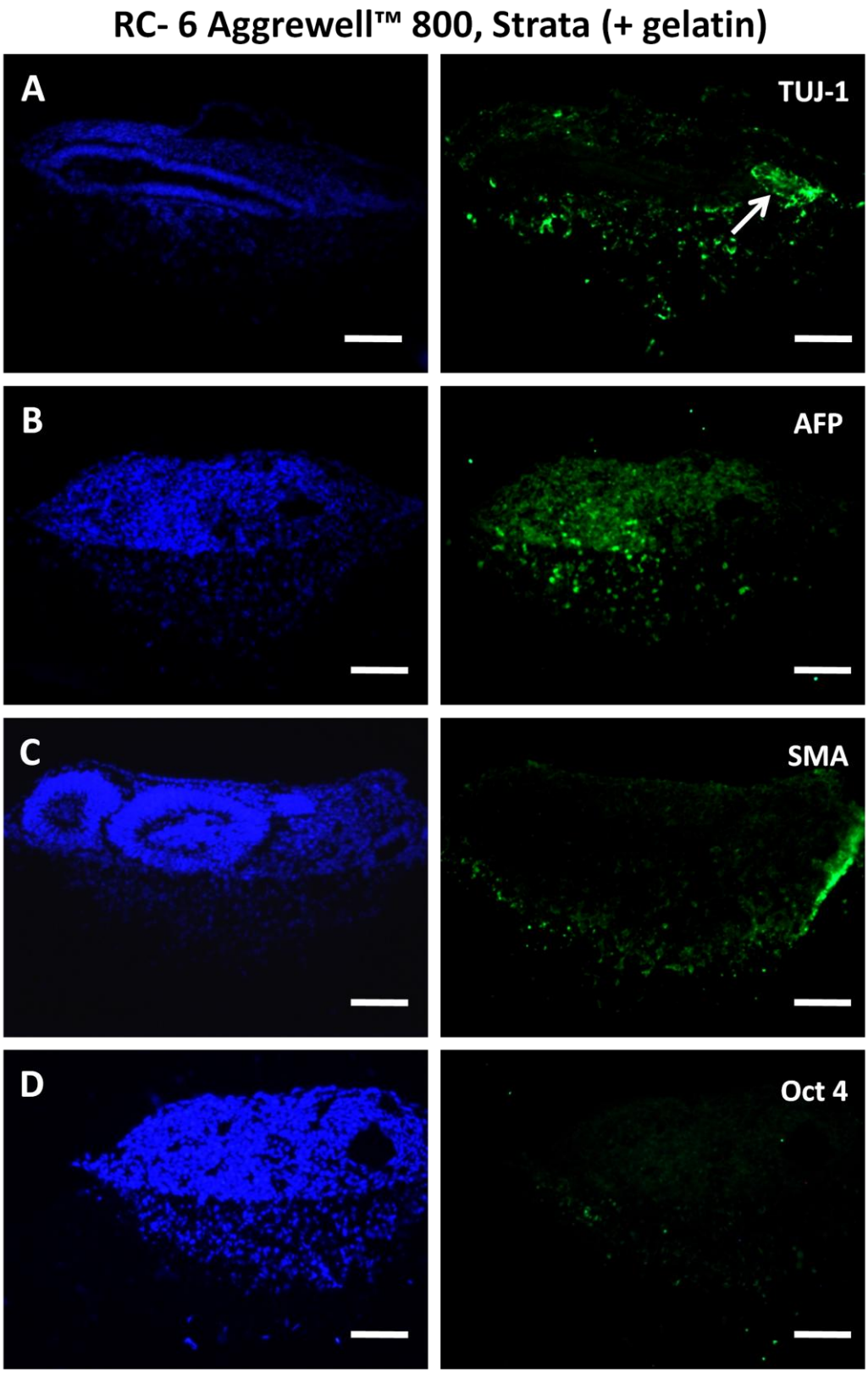

Figure 5.16 Immunostaining of Aggrewell™ 800 RC-6 derived embryoid bodies cultured in 3D on gelatin-coated Strata. After 7 days in suspension culture EBs were transferred to Alvetex® Strata coated with gelatin and cultured for 7 days before being fixed and immunostained. RC-6 cells do not flatten on gelatin-coated Strata as much as the RC-10 cells and complex structures are still visible. There is less TUJ-1 positive cells with only a small neural rosette being visible **(A, white arrow)** and the majority of cells are AFP positive **(B).** SMA staining is only seen in the cells grown at a low cell density in the interior of the membrane **(C)** and this EB shows no evidence of Oct 4 staining, this is similar to EBs culture in 2D **(D).** Scale bars = 100µm

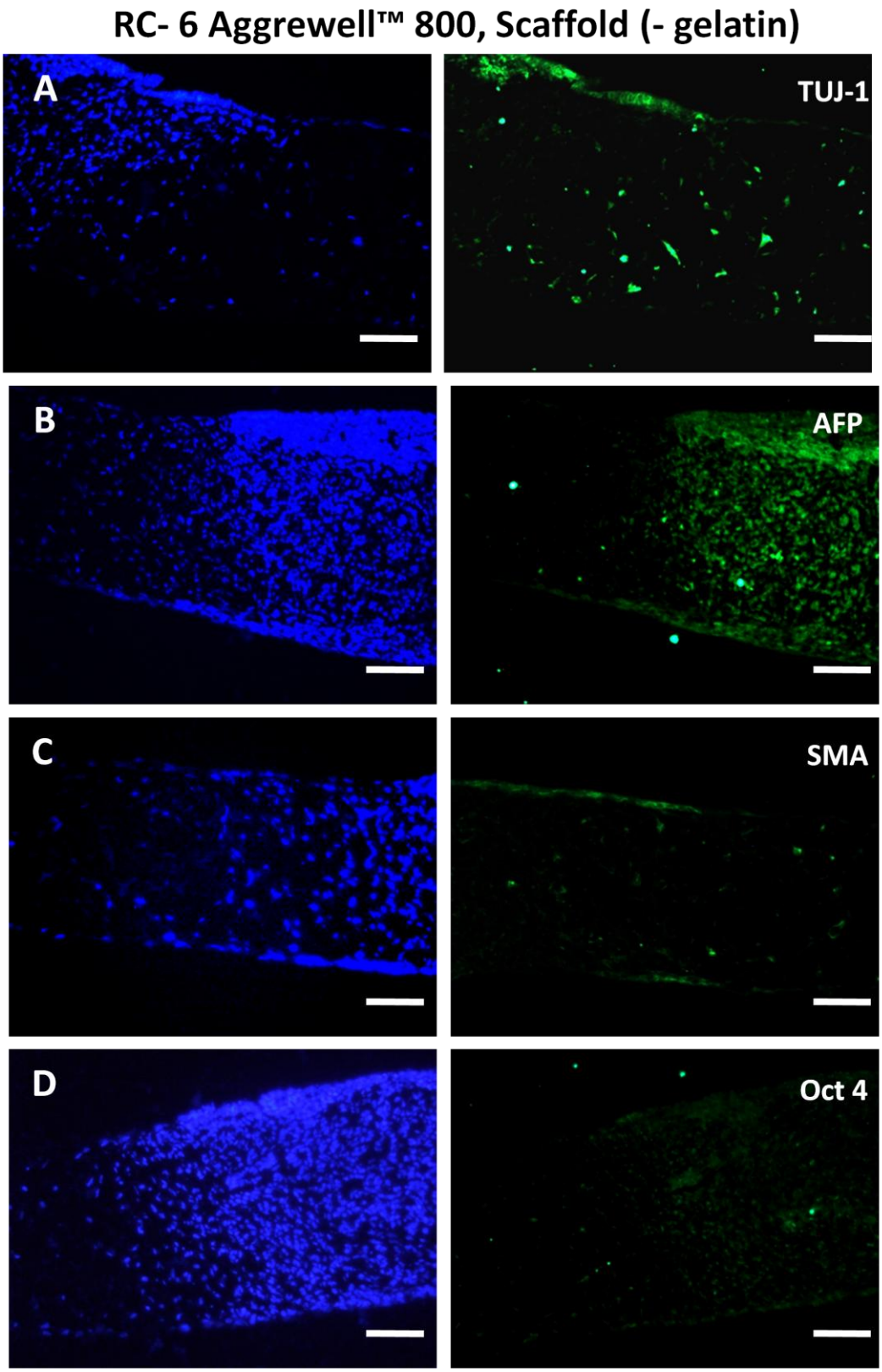

Figure 5.17 Immunostaining of Aggrewell™ 800 RC-6 derived embryoid bodies cultured in 3D on <u>non-coated</u> Scaffold. After 7 days in suspension culture EBs were transferred to Alvetex® Scaffold and cultured for 7 days before being fixed and immunostained . Unlike RC-10 cultures there is still evidence of the original EB. There are areas TUJ-1 positive cells **(A)** in contrast to the RC-10 cells there are large amounts of AFP staining especially when cells are at a high cell density **(B).** There is limited staining for both SMA **(C)** and Oct 4 **(D).** Scale bars = 100µm

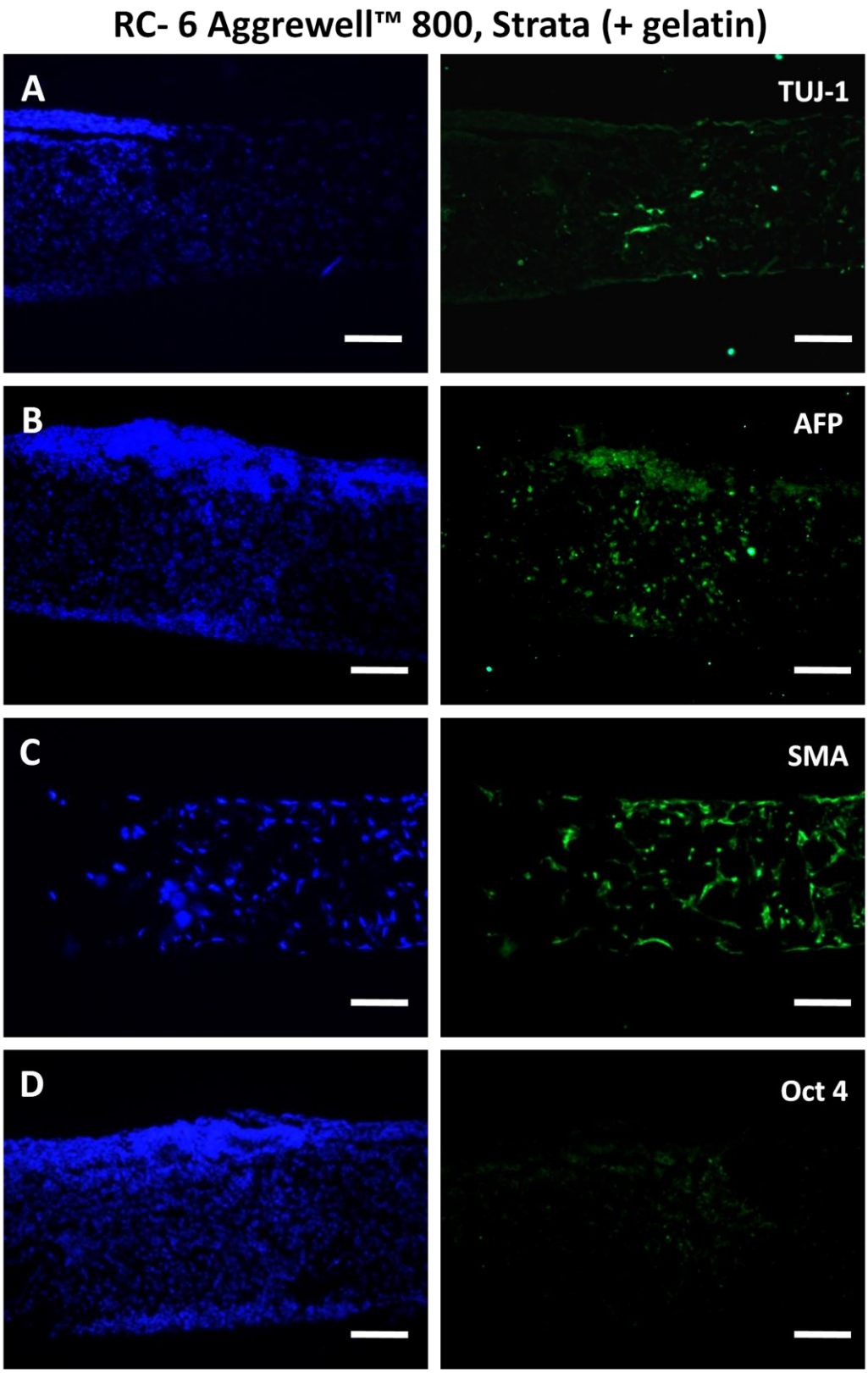

Figure 5.18 Immunostaining of Aggrewell™ 800 RC-6 derived embryoid bodies cultured in 3D on gelatin-coated Scaffold. After 7 days in suspension culture EBs were transferred to Alvetex® Scaffold coated with gelatin and cultured for 7 days before being fixed and immunostained. There is evidence of ectodermal differentiation **(A),** mesodermal differentiation **(C)** and the embryonic stem cell marker – Oct 4 **(D),** AFP staining is limited to the EB –Scaffold interface and the high cell density area directly underneath the EB **(B).** Scale bars = 100µm

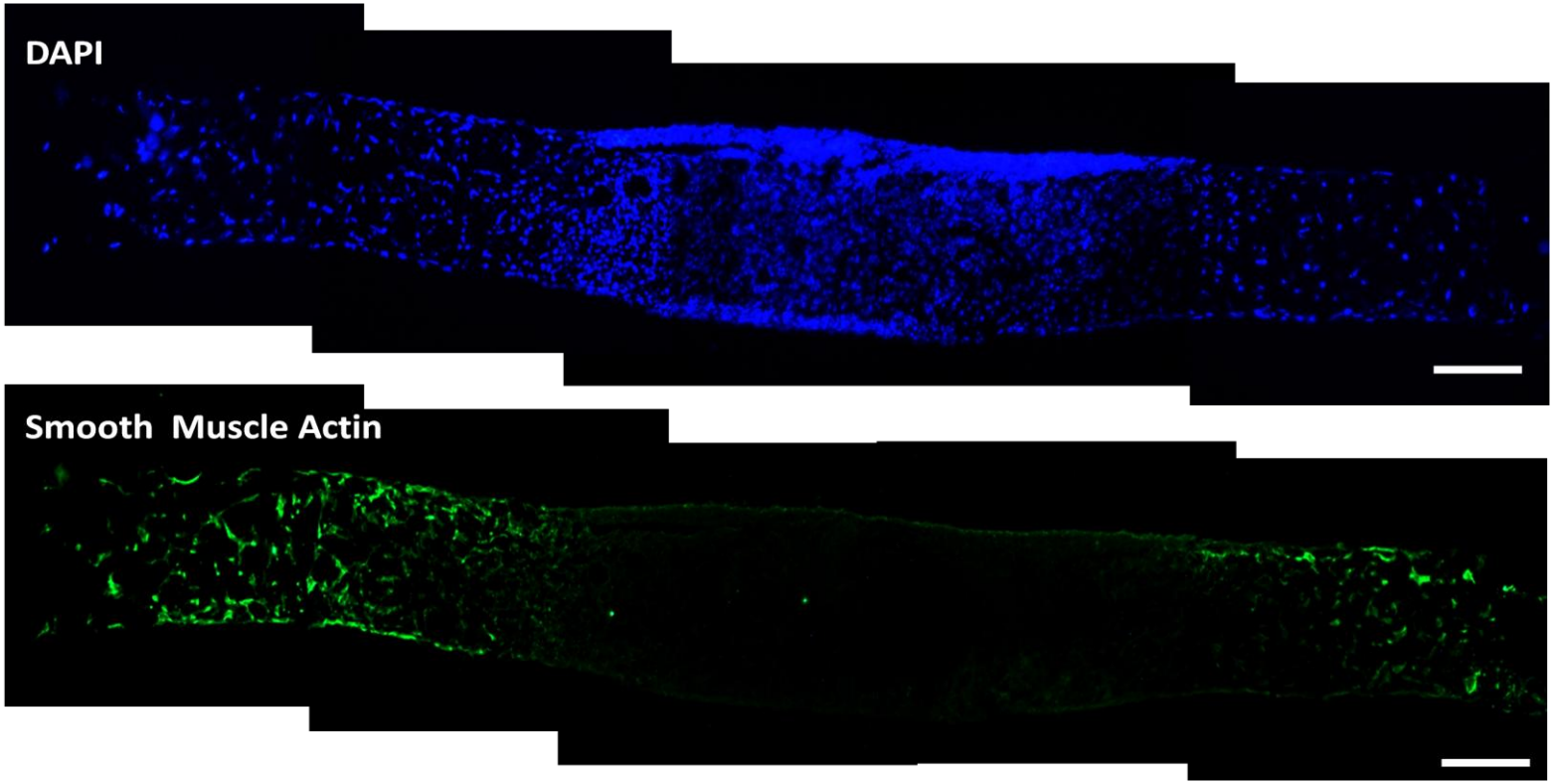

Figure 5.19 Cells positive for the mesodermal marker – smooth muscle actin are only present when the cells are at a low cell density within the membranes. A montage example image of RC-6 cells grown on gelatin coated scaffolds highlighting the distribution of SMA-positive cells. In all conditions involving both RC-10 and RC-6 cells on both Scaffold and Strata , SMA-positive cells are only in low cell density areas and only within the membranes and not with the embryoid body. Scale bars = 100µm

5.6 Discussion

During the introduction to this Chapter it became apparent that there are limited methods for the assessment of pluripotency *in vitro*. This is partly due to the limitations of 2D culture but many of the 3D methods are unnecessarily complex for a standardised procedure. During this discussion I demonstrate a simple procedure that overcomes some of the limitations of 2D culture such as limited mesodermal differentiation and endoderm encapsulation [310].

5.6.1 Comparison of the differentiation of embryoid bodies in 2D and 3D and teratoma formation.

Firstly, two different sizes of EBs were assessed for their differentiation potential in 2D. The size of EBs has previously been documented to affect the differentiation of stem cells [319, 320]. This was also observed in the RC-10 cell line. The smaller EBs produced using the Aggrewell™400 produced extensive neurite networks on both gelatin-coated (Figure 5.4) and non-coated (Figure 5.6) tissue culture plastic. Whereas the EBs produced using the Aggrewell™800 led to large TUJ-1 positive cells (Figure 5.5A &Figure 5.7A). As suggested by Fuchs et al. [310] the majority of cells in all 2D conditions, are endoderm-derived and therefore stain positive for AFP (Figure 5.4B, Figure 5.5B, Figure 5.6B & Figure 5.7B). Normally EBs are seeded onto gelatin-coated surfaces after differentiation in suspension. The gelatin coating assists in the attachment of the outer layer of primitive endoderm [321]. Interestingly the RC-10 cells do not appear to require the gelatin coating to attach to the surface and they are also able to form AFP-positive complex structures without the gelatin coating (Figure 5.6B). Finally, there is minimal mesodermal differentiation which is limited to localised areas in the Aggrewell™400 EB (Figure 5.4C & Figure 5.6C) and to individual cells in the Aggrewell™800 RC-10 derived EBs (Figure 5.5C & Figure 5.7C). This is consistent with previous literature which suggests that mesodermal differentiation is localised and asymmetric in the EBs [312, 322]. These issues highlight the limitations of standard embryoid body production as a pluripotency assay as there is limited differentiation into all three germ layers. However, plating RC-10 derived EBs into 2D leads to terminal differentiation with no evidence of Oct 4 staining in any of the conditions tested (Figure 5.4D – Figure 5.7D) this suggests that if the similar phenomena occurred in the formation of teratomas then the cells would have potential for use in stem cell therapies. However analysis of the EBs differentiated in 3D environments reveals that there are structures which are clearly positive for the pluripotency marker – Oct 4 (Figure 5.10D & Figure 5.11D). This is consistent with the findings of Pekkanen-Mattila et al. who found that EBs cultured in suspensions maintain Oct 4 expressions for unexpectedly long time [309].

By allowing RC-10 derived EBs to undergo the final stages of differentiation in 3D using the Strata membrane, they are able to form and maintain many more complex structures than their 2D

counterparts (Figure 5.9A&B). These structures include neural rosettes (Figure 5.10A and Figure 5.11A) which had not been observed in the 2D differentiation and areas of neurite outgrowth from the original EB (Figure 5.10A). Evidence of neurite outgrowth only occurs in non-coated membranes presumably due to the gelatin coating blocking the pores of the material. This is in contrast to previous reports of neurite outgrowth in 3D on electrospun gelatin coated scaffolds. Gelatin has previously been shown to enhance cell adhesion and neurite outgrowth [323]. These TUJ-1 positive structures are not seen in 2D and they more closely resemble structures derived from hES cells *in vivo* (Figure 5.8A).

It is standard protocol to differentiate EBs on gelatin-coated surfaces [324]. However on the 3D membranes, the lack of gelatin coating appears to enhance differentiation potential. From the H&E stained images there is more evidence of complex structures due to the EB not flattening on the top of the Strata assisted by the attachment of primitive endoderm to the gelatin coating [321]. On the non-coated membrane the primitive endodermal layer which encapsulated the EB is seen stretching across the surface of the membrane (Figure 5.10B). Due to this the original EB is not encapsulated and SMA positive cells are able to infiltrate into the Strata interior at a low cell density. Fuchs et al. previously demonstrated that the lack of mesodermal differentiation can be due to the endoderm encapsulation and the proximity of neighbouring EB [310]. This lack of mesodermal differentiation was evident in the 2D RC-10 derived EBs. However there are large areas of SMA–positive cells in 3D non-coated Strata cultures (Figure 5.10C). There is less evidence of mesodermal differentiation on Strata membranes coated with gelatin (Figure 5.11C) and high levels of AFP-positive cells (Figure 5.11B) suggesting that the attachment of endodermal cells to the membranes is preventing mesodermal differentiation. Giobbe et al. suggested that the lack of mesodermal differentiation in their 3D differentiation system was due to diffusion of mesoderm inducing agents. In general, the mesodermal inducing factors were of lower molecular weight than endodermal and ectodermal inducing factors and were therefore able to diffuse away from the EB [314]. This is unlikely to be the mechanism in EBs cultured on Strata membrane as they would also allow for the diffusion of inducing factors such as EGF and bFGF.

Differentiation of EBs on Alvetex® Scaffold does not allow for the formation of complex structures. Cells from the EB are able to rapidly migrate into the Scaffold interior. Considering this was the intended use of the Scaffold as optimised in Chapters 2 and 3 of this work, this is not a surprising. Embryoid bodies cultures on Scaffold (Figure 5.12 & Figure 5.13) therefore closely imitate the cultures of dissociated EBs on PLGA/PLA porogen leached scaffolds produced by Levenberg et al. [3]. If the culture of EBs on Scaffold was extended for a further 14 days, it may be possible for similar complex structures to be allowed to form.

From analysis of RC-10 derived EBs presented above, there is a set of conditions that stands out as the obvious candidate for the testing of pluripotency. These are to seed EBs onto non-coated Strata membranes for further differentiation to occur in 3D. Although these results are convincing as they allow for formation of all three germ layers *in vitro*, it was necessary to test these conditions using other human embryonic stem cells. For this purpose the same conditions were tested using another cell line – RC-6. Although undifferentiated monolayer cultures of the RC-10 and RC-6 cell lines appear similar (Figure 5.1), they produce significantly different 3D EB cultures especially on Alvetex® Scaffold.

The Strata membrane cultures containing RC-6 derived EBs are still able to form complex structures (Figure 5.14) at the surface of the membrane which include neural rosettes (Figure 5.15A & Figure 5.16A) and derivatives of all three germ layers (Figure 5.15& Figure 5.16). As with the RC-10 derived EBs, the addition of a gelatin coating leads to flattening of the EB and therefore less evidence of complex structures (Figure 5.14B & Figure 5.16). In contrast to the RC-10 derived EBs, the RC-6 derived EBs grown on Alvetex® Scaffold are able to form complex structures at the surface of the Scaffold as well as infiltrate at a high density into the scaffold interior (Figure 5.14C&D). This resulted in cultures that closely mimic those observed by Levenberg et al. [3] but in a much shorter timeframe. These cultures also produce structures which are similar to those observed in ES cell derived teratomas (Figure 5.8). Embryoid Bodies derived from the RC-6 cell line also help to highlight the lack of mesodermal differentiation close to the original EB seeding site (Figure 5.19). This suggests that mesodermal differentiation is only possible at low cell density

5.7 Conclusion

Allowing embryoid bodies to differentiate while being supported by a 3D culture matrix allows for differentiation into all three germ layers. The non-coated Strata system appears to be the most promising method of support. The structures produced on the Strata membranes resemble structures that were previously observed by Stachelscheid et al. using their bioreactor system [316]. However the Strata supported EBs are a less complex and therefore more reproducible system than the use of bioreactors. Buta et al. highlighted some drawbacks of a EB-based pluripotency assay which included problems with the nutrient supply leading to necrotic areas and that aggregates are limited to 7 cell layers thick [303]. Due to the fully optimised insert system used for the support of Alvetex®, I have not observed areas of necrosis at the centre of the EBs. The embryoid bodies are also not limited to 7 cell layers thick (Figure 5.9& Figure 5.14).

Allowing the terminal differentiation of EBs in 3D on Strata membranes provides a simple, reproducible method for assessing the differentiation potential of human ES cells. This approach could easily be teamed with genetic profiling of contemporary samples to produce a robust pluripotency assay.

6 General discussion and Future Work

Key Findings

- The 3D environment provided by the scaffold has been fully optimised for a range of cell lines
- Optimisation of scaffold presentation and media requirements leads to the production of homogenous slabs of tissue *in vitro*.
- The method by which a porous scaffold is presented affects neuronal differentiation in 3D.
- Prolonged propagation of both ES and EC cells in 3D leads to high levels of pluripotency markers in comparison to their 2D counterparts and a change in cell shape.
- Prolonged propagation of pluripotent stem cells in 3D enhances their developmental potential compared to their 2D counterparts.
- The 3D environment provided by the scaffold combined with embryoid bodies has a potential application in the production of an *in vitro* alternative to the teratoma assay.

The 3D environment provided by the Alvetex® polystyrene Scaffold has been fully optimised for a range of cell lines and recommended culture conditions produced for mouse embryonic fibroblasts – NIH 3T3, squamous cell carcinoma cells – MET 4 and pluripotent stem cells – TERA2.cl.SP12. The optimised conditions allow the culture of cells in three dimensions without the need for the daily monitoring using phase microscopy. The range of cells optimised provides a solid basis for the development of protocols for the 3D culture of other cell types.

These 3D models of each cell line produce a dense cell layer which is more representative of native tissue. However properties of the cells that are observed during standard 2D culture are also apparent in their 3D counterparts. For example, the NIH 3T3 cells still display contact inhibition when placed in the 3D microenvironment, and may be more inhibited in 3D due to the increased capability of intercellular signalling. In addition low seeding density also has a detrimental effect on cell growth.

These developed models of 3D cell growth can now be readily incorporated into more complex models to mimic tissue *in vitro*. For example the 3D growth of fibroblasts could be teamed with keratinocytes to develop a 3D epidermal model. Such a model could be utilised for testing the

penetration of chemicals into the skin and for *in vitro* irritation tests. The advantage of the polystyrene scaffold for such tests is that it provides a chemically inert support which does not degrade into other products. I have demonstrated that 3D cultures can be processed for a range of techniques including biochemical assays which have been specifically optimised for 3D cultures, standard histology, and immunohistochemistry. Commandeur et al. also suggested that development of a representative *in vitro* squamous cell carcinoma model system would allow for a better understanding of the carcinogenesis mechanism and could be used as a validated pre-screening platform for drugs [182]. By combining the fibroblast model with the optimal conditions for MET 4 culture in 3D it may be possible to develop an *in vitro* cancer model, not only for the pre-screening of drugs, but also as a cell invasion model. A simple technique for measuring cell penetration using the Alvetex® Scaffold is described in Chapter 2 but further development may be necessary for these specific requirements. Once these models are developed including the pluripotent stem cell model they could lead to the development of models for wound healing, tumour progression, and also the remodelling of bioengineered tissues.

The above mentioned models would require further detailed investigation to fully establish the model and testing methods. However the pluripotent stem cell model was further optimised to investigate how the 3D environment affects stem cell differentiation.

Although much has been learned on the growth and differentiation of pluripotent stem cells using standard monolayer cultures, it is widely recognised that the formation of complex structures is not possible in 2D culture. In an attempt to produce such structures, embryonic stem cells are often removed from their feeder layer or ECM coated substrate and cultured in suspension. This allows for the formation of embryoid bodies (EBs). As a result the cells are able to differentiate into all three germ layers [188] and provide a 3D environment for the formation of complex structures. However EBs have many disadvantages when studying stem cell differentiation including: limited control of both cell aggregation and density, and the techniques unsuitability for the large scale production of differentiated cells. [189]. Consequently the technique offers a low efficiency of EB formation and EBs have a tendency to differentiate towards ectodermal lineages and forms a layer of visceral endoderm at the periphery [190]. Finally there are also issues of a limited supply of nutrients during the culture of dense EBs. This leads to suggestion that it is only possible to form aggregates no more than 7 layers thick [303] before areas of necrosis occur at the centre of the mass of cells. Using a scaffold for the differentiation of stem cells gives more support to any structures formed and, through modification of how the scaffold is presented, preventing both spontaneous differentiation and allowing cell layers more than 7 cells thick without spontaneous cell death at the centre of the construct.

Using the Alvetex® Scaffold, I have assessed the effect of media volume and scaffold presentation on cell viability, cell number and stem cell differentiation. I have established the ideal culture conditions to produce a homogeneous cell distribution throughout the porous scaffold. This involved significantly less media per 1 x 10^6 cells than had been suggested in previous studies [88]. It was also not necessary to differentiate the cells prior to seeding onto the scaffold to achieve a homogenous cell layer, even though this had been the case with other porous polymeric scaffolds [3]. I tested standard methods for ensuring an even distribution of nutrients around a scaffold including the standard well insert [19] and developed modified cultureware to ensure a uniform cell distribution. Such modifications allowed for the production of scaffold presentations that minimise the disturbance of cells in tissue engineered matrices. This is ideal for stem cell culture as it reduces the loss of cells and limits the effect of the frequent media changes which are associated with stem differentiation due to removal of secreted factors.

This has allowed an analysis of the 3D culture of pluripotent stem cells to a degree not previously achieved. This has led to a well-defined 3D culture method that includes recommendation of a suitable time frame for media changes. This analysis of cell culture media quality during 3D culture will be of particular importance when the system is adapted for the use of human embryonic stem cells. In addition the data gathered allows for the calculation of media requirements in future experiment, which will be especially useful when using expensive defined media such as mTeSR1 (Stem Cell Technologies) [281] or StemPro (Invitrogen) [325] both of which have been examined in this thesis.

The production of a dense layer of homogenous tissue *in vitro* allowed for studies into the neuronal differentiation of stems cells supported on 3D matrices. Further characterisation of the 3D cultures in comparison to 2D differentiated TERA2.cl.SP12 cells is necessary to identify the further benefits of the 3D culture system. Protocols for the extraction of RNA from Alvetex® Scaffolds have previously been optimised. The extracted RNA was shown to be of high quality and suitable for use for qPCR analysis [326]. As a result further experiments could include the extraction of RNA from both 2D and 3D cultures for microarray analysis. Previous microarray analysis of 2D and 3D spheroid cultured hepatocellular carcinoma cell line – HepG2 demonstrated differences in genes for extracellular matrix production, cytoskeleton and cell adhesion [327]. Analysis of 2D and 3D cultures of differentiated TERA2.cl.SP12 cells could potentially highlight differences in the levels of genes involved in the Notch signalling pathway. As described in the background (Section 1.2) to this thesis, the 3D environment provided by the scaffold leads to more complex cell-cell interactions and to more sites for the interaction of notch ligands. Such interactions between cells could lead to enhanced neuronal differentiation via the notch signalling pathway [43]. Further characterisation of neuronal differentiation in 3D should also include

assessing the functionality of neuronal populations in comparison to 2D cultures. In particular microelectrode array recordings, as previously described by Illes et al., would detect functionality in embryonic stem cell derived neural populations [328]. However such techniques would require significant development for use with 3D cultures.

The culture of pluripotent stem cells on Alvetex® Scaffolds has also been optimised to ensure that spontaneous differentiation of cultures does not occur in 3D. This is possibly due to optimisation of parameters such as seeding method, initial seeding density, and the modification of well inserts to produce an open wall insert. Optimisation of these parameters may allow the differentiation of pluripotent stem cells toward alternative lineages. Being able to maintain the stem cell phenotype in Alvetex® Scaffold cultures may help to identify factors which are necessary to maintain stem cell phenotype *in vitro*. This could again be achieved by microarray analysis of 2D and 3D undifferentiated cultures and may provide insights in to the importance of cell-cell contact for signalling pathways such as Notch.

The optimisation of a 3D culture environment using model pluripotent stem cells such as the EC cell line TERA2.cl.SP12 will lead to an easy transition to a hESC 3D model. Initial experiments on the 3D culture of hESCs using Alvetex® Scaffold would require a cell line that has previously been adapted to feeder-free conditions. The H9 cells grown on mTeSR1 media which are described in Chapter 4 would be ideal for such experiments. Differentiation of hESCs on Alvetex® Scaffold would further demonstrate the potential of 3D culture.

As demonstrated in Figure 2.11, pluripotent stem cells require a period of adaptation when transferred to 3D culture systems. Taking this into account, it would be beneficial to establish a 3D alternative to the T75 flask which allows for prolonged cultivation in 3D. The aim would be to reduce the time required for cell adaptation from 4 days during which the cells are susceptible to toxic agents. This was particularly apparent during attempts to differentiate TERA2.cl.SP12 cells in scaffolds and led to the addition of both ATRA and EC23 to the 3D cultures after a 4 day settling period. The production of 3D-adapted cells may also display advantages when cultured cells are introduced to the *in vivo* environment. Finally adapted cells may also display increased proliferation rates as Notch signalling regulates proliferation of both hESC and EC cells [41] and may be enhanced by the 3D culture environment. This would be of particular advantage for the production of large numbers of cells for personalised stem cell therapies.

To produce a 3D-primed cell line it is necessary to maintain the cells self-renewal capabilities in 3D culture. This has been achieved using Alvetex® Strata membranes and the model EC cell line – TERA2.cl.SP12. The knowledge gained from these experiments was used to establish two 3D-primed hESC lines using RC-10 and H9 cells. A 3D model system for self-renewal had previously

been suggested by Krahenbuehl et al. in which they describe the properties such a system should have which includes: easily tailored mechanical properties, permit the migration of cells through or into the system, able to adapt to support the expansion of cells, and degradability to allow for cell removal.[272]. The Alvetex® Strata system for the maintenance of pluripotent stem cells has met many of these conditions or proven that some of the requirements are unnecessary. Such unnecessary parameters include the migration of cells either through or into the system. Strata is used as a support matrix that permits the 3D culture of cells at the surface of the membrane and therefore does not permit migration into the interior, rather the 3D layer of cells is formed using its own ECM for support and without the structural support of a scaffold. Kraehenbuehl et al. also suggested that the 3D support matrix needs to be biodegradable to allow for easy cell removal [272]. Such a biodegradable scaffold would lead to an undefined environment which potentially leads to areas cells that undergo differentiation due to a build-up of waste products. Localised areas of high levels of lactic acid can be produced through the degradation of commonly used biodegradable scaffold manufactured from PLA. This can lead to spontaneous differentiation of stem cells as demonstrated in Figure 3.15. It is not necessary to degrade the Strata membrane for cell removal therefore cells are not subjected to scaffold degradation products or to prolonged periods in enzyme solution as is the case in other support matrices [275, 278].

I have demonstrated the advantages of 3D-primed cells over 2D cultured cells using a range of methods including aggregate formation, differentiation on Alvetex® Scaffolds and the formation of teratomas. All of these methods have demonstrated clear advantages of 3D-adapted cells, with 3D TERA2.cl.SP12 cells being capable of differentiation into a wider range of cell types after prolonged propagation in 3D. It is now necessary to characterise the 3D hESC cells in the same manner. This will require the formation of teratomas from 3D-adapted hESCs. A study is currently in progress to compare teratoma formation of 2D H9 cells at passages 52(8) and 52(15) (bracketed numbers refers to number of passages in feeder-free culture) with 3D cells of passage p52(8) + 7 passages in 3D. Results of this study will confirm that prolonged culture in 3D affects the differentiation potential of cultured stem cells.

Although, clear differences between 2D and 3D cells have been demonstrated. Including in stem cell marker expression, proliferation rate, cell shape and differentiation potential. It would be ideal to perform more in-depth analysis of the two culture systems such as genome-wide analysis using microarray technology. Such information would detail the levels of difference of stem cell marker expression and will also highlight any differences in signalling pathways between the two culture systems. Such analysis may help to determine the mechanisms of self-renewal *in vitro.* Further work is also needed to demonstrate that the 3D-primed cells do not require an adaptation period when transferred to other 3D culture systems and also test the differentiation potential of

the cells during 3D culture. It may be that the functionality of neurons derived from 3D adapted cells is enhanced compared to both 2D and 3D cells which still require adaptation. If the production of 3D-primed cells is considered advantageous it may also be necessary to adapt the Strata membrane from the insert system to a system that more closely resembles a T75 flask. This will provide many challenges as the membrane will still need feeding from both above and below and also be accessible to allow for the scraping of the cells from the membranes.

Finally the synthetic 3D microenvironment provided by Alvetex® was assessed as potential method for screening the pluripotency of stem cells without the use of an expensive teratoma assay. While it is recognised that an *in vitro* screening system will not negate the use of SCID mice for the teratoma assay, it has the potential to reduce the number of animals required. This will be achieved by using a Strata or Scaffold based system to highlight potential failures at an early stage.

Previously I have highlighted some of the disadvantages of embryoid body formation for the differentiation of stem cells. However, by allowing EBs to differentiate and be supported by a 3D culture matrix such as Alvetex®, it is possible for cells to differentiate into all three germ layers. The non-coated Strata system appears to be the most promising method of support. Non-coated Strata membranes allow for both the formation of complex structures at the surface which do not flatten and the migration of cells into the membrane interior. The structures produced on Strata membranes resemble structures that have previously been observed in bioreactor systems [316], with the advantage of the system being considerably less complex. The simplicity of the system improves reproducibility and is therefore ideal as a standard pluripotency assay.

Buta et al. highlighted the drawbacks of an EB-based pluripotency assay which included insufficient nutrient supply leading to the dense cell aggregates [303]. The optimised insert system used to support Alvetex® as described in Chapter 3 involves the use of a modified open wall insert. It ensures a nutrient rich environment for stem cell differentiation. As a result, there have been no observable issues with nutrient transfer and no evidence of necrosis in all of the systems tested in Chapter 5. Allowing the terminal differentiation of EBs in the 3D environment provided by Strata membranes gives a simple, reproducible and easy-to-process method for assessing the differentiation potential of human ES cells *in vitro*. This approach could readily be teamed with genetic profiling of contemporary samples to produce a robust pluripotency assay. Such genetic profiling is most likely to involve qPCR analysis to detect evidence of all three germ layers and downregulation of stem cell markers.

In order to implement a standardised *in vitro* test for pluripotency, it will be necessary to fully validate the system. Therefore further work should concentrate on testing a range of known

pluripotent ES cell lines including the H9 cells using the non-coated Strata membrane system teamed with qPCR analysis. Screening should then be widened to include known pluripotent iPSC lines, and finally unknown newly-derived hESCs and iPSCs and results compared with the 'gold standard' teratoma assay. If the Strata system withstands these tests then it should be suggested as an alternative to the teratoma assay. This in turn will reduce the number of animals used in stem cell research, although it must be recognised that stem cells intended for human therapies would still require the teratoma assay to ensure malignant cells do not remain *in vivo*. This is due to differentiating EBs displaying the pluripotency marker – Oct 4 for unexpectedly long time *in vitro* [309].

In conclusion, I have demonstrated novel methods for the culture of stem cells which show an apparent enhancement in cell signalling, improved performance for the propagation of stem cells, and potential as a pluripotency assay. As a result there is the opportunity to test the hypothesis of differences in the Notch pathway activity between 2D and 3D. The further experiments suggested above will also provide insights into other signalling mechanisms which may be involved in both stem cell differentiation and self-renewal. They will also allow for the production of new technologies for the propagation of stem cells in 3D. Finally, the use of Alvetex® Strata has the potential to be used as a standardised pluripotency assay. This will assist in the implementation of the 3Rs framework in stem cell biology.

7 Bibliography

1. Smalley, K.S.M., M. Lioni, and M. Herlyn, *Life isn't flat: Taking cancer biology to the next dimension.* In Vitro Cellular & Developmental Biology-Animal, 2006. **42**(8-9): p. 242-247.
2. Pierret, C., et al., *Developmental cues and persistent neurogenic potential within an in vitro neural niche.* Bmc Developmental Biology, 2010. **10**.
3. Levenberg, S., et al., *Differentiation of human embryonic stem cells on three-dimensional polymer scaffolds.* Proceedings of the National Academy of Sciences of the United States of America, 2003. **100**(22): p. 12741-12746.
4. Cao, Y., et al., *Scaffolds, stem cells, and tissue engineering: A potent combination!* Australian Journal of Chemistry, 2005. **58**(10): p. 691-703.
5. Zhu, Y., et al., *Collagen-chitosan polymer as a scaffold for the proliferation of human adipose tissue-derived stem cells.* J Mater Sci Mater Med, 2009. **20**(3): p. 799-808.
6. Comley, J., *3D cell culture: easier said than done.* DDW Drug Discovery World, 2010: p. 25-41.
7. Knight, E., et al., *Alvetex (R): Polystyrene Scaffold Technology for Routine Three Dimensional Cell Culture*, in *3d Cell Culture: Methods and Protocols*, J.W. Haycock, Editor. 2011, Humana Press Inc: Totowa. p. 323-340.
8. Reuter, V.E., *Origins and molecular biology of testicular germ cell tumors.* Modern Pathology, 2005. **18**: p. S51-S60.
9. Kraggerud, S.M., et al., *Genome profiles of familial/bilateral and sporadic testicular germ cell tumors.* Genes Chromosomes and Cancer, 2002. **34**(2): p. 168-174.
10. Baker, D.E.C., et al., *Adaptation to culture of human embryonic stem cells and oncogenesis in vivo.* Nature Biotechnology, 2007. **25**(2): p. 207-215.
11. Baker, B.M. and C.S. Chen, *Deconstructing the third dimension - how 3D culture microenvironments alter cellular cues.* Journal of Cell Science, 2012. **125**(13): p. 3015-3024.
12. Ortinau, S., et al., *Effect of 3D-scaffold formation on differentiation and survival in human neural progenitor cells.* Biomedical Engineering Online, 2010. **9**.
13. Perrimon, N., C. Pitsouli, and B.Z. Shilo, *Signaling Mechanisms Controlling Cell Fate and Embryonic Patterning.* Cold Spring Harbor Perspectives in Biology, 2012. **4**(8).
14. Debnath, J. and J.S. Brugge, *Modelling glandular epithelial cancers in three-dimensional cultures.* Nature Reviews Cancer, 2005. **5**(9): p. 675-688.
15. Bissell, M.J., A. Rizki, and I.S. Mian, *Tissue architecture: the ultimate regulator of breast epithelial function - Commentary.* Current Opinion in Cell Biology, 2003. **15**(6): p. 753-762.
16. Zegers, M.M.P., et al., *Epithelial polarity and tubulogenesis in vitro.* Trends in Cell Biology, 2003. **13**(4): p. 169-176.
17. Roskelley, C.D., P.Y. Desprez, and M.J. Bissell, *Extracellular matrix-dependent tissue-specific gene-expression in mammary epithelial-cells requires both physical and biochemical signal-transduction.* Proceedings of the National Academy of Sciences of the United States of America, 1994. **91**(26): p. 12378-12382.
18. Haque, M.A., et al., *Artificial extracellular matrix for embryonic stem cell cultures: a new frontier of nanobiomaterials.* Science and Technology of Advanced Materials, 2010. **11**(1).
19. Griffith, L.G. and M.A. Swartz, *Capturing complex 3D tissue physiology in vitro.* Nature Reviews Molecular Cell Biology, 2006. **7**(3): p. 211-224.
20. Scadden, D.T., *The stem-cell niche as an entity of action.* Nature, 2006. **441**(7097): p. 1075-1079.
21. Marthiens, V., et al., *Adhesion molecules in the stem cell niche - more than just staying in shape?* Journal of Cell Science, 2010. **123**(10): p. 1613-1622.
22. Wong, V.W., et al., *Stem cell niches for skin regeneration.* International journal of biomaterials, 2012. **2012**.

23. Urciuolo, A., et al., *Collagen VI regulates satellite cell self-renewal and muscle regeneration.* Nature communications, 2013. **4**.
24. Bentzinger, C.F., et al., *Fibronectin Regulates Wnt7a Signaling and Satellite Cell Expansion.* Cell Stem Cell, 2013. **12**(1): p. 75-87.
25. Peerani, R., et al., *Niche-mediated control of human embryonic stem cell self-renewal and differentiation.* Embo Journal, 2007. **26**(22): p. 4744-4755.
26. Xu, Y., et al., *Revealing a core signaling regulatory mechanism for pluripotent stem cell survival and self-renewal by small molecules.* Proceedings of the National Academy of Sciences of the United States of America, 2010. **107**(18): p. 8129-8134.
27. Tam, P.P.L. and D.A.F. Loebel, *Gene function in mouse embryogenesis: get set for gastrulation.* Nature Reviews Genetics, 2007. **8**(5): p. 368-381.
28. Shvartsman, S.Y., et al., *Autocrine loops with positive feedback enable context-dependent cell signaling.* American Journal of Physiology-Cell Physiology, 2002. **282**(3): p. C545-C559.
29. Hwang, N.S., S. Varghese, and J. Elisseeff, *Controlled differentiation of stem cells.* Advanced Drug Delivery Reviews, 2008. **60**(2): p. 199-214.
30. Tanaka, H., et al., *Chondrogenic differentiation of murine embryonic stem cells: Effects of culture conditions and dexamethasone.* Journal of Cellular Biochemistry, 2004. **93**(3): p. 454-462.
31. Hwang, N.S., et al., *Effects of three-dimensional culture and growth factors on the chondrogenic differentiation of murine embryonic stem cells.* Stem Cells, 2006. **24**(2): p. 284-291.
32. Liu, H. and K. Roy, *Biomimetic three-dimensional cultures significantly increase hematopoietic differentiation efficacy of embryonic stem cells.* Tissue Engineering, 2005. **11**(1-2): p. 319-330.
33. Artavanis-Tsakonas, S., K. Matsuno, and M.E. Fortini, *Notch Signaling.* Science, 1995. **268**(5208): p. 225-232.
34. Perdigoto, C.N. and A.J. Bardin, *Sending the right signal: Notch and stem cells.* Biochimica Et Biophysica Acta-General Subjects, 2013. **1830**(2): p. 2307-2322.
35. Wakamatsu, Y., T.M. Maynard, and J.A. Weston, *Fate determination of neural crest cells by NOTCH-mediated lateral inhibition and asymmetrical cell division during gangliogenesis.* Development, 2000. **127**(13): p. 2811-2821.
36. Logeat, F., et al., *The Notch1 receptor is cleaved constitutively by a furin-like convertase.* Proceedings of the National Academy of Sciences of the United States of America, 1998. **95**(14): p. 8108-8112.
37. Taniguchi, Y., et al., *Notch receptor cleavage depends on but is not directly executed by presenilins.* Proceedings of the National Academy of Sciences of the United States of America, 2002. **99**(6): p. 4014-4019.
38. Hatakeyama, J., et al., *Hes genes regulate size, shape and histogenesis of the nervous system by control of the timing of neural stem cell differentiation.* Development, 2004. **131**(22): p. 5539-5550.
39. Poulson, D.F., *Chromosomal control of embryogenesis in drosophila.* American Naturalist, 1945. **79**(783): p. 340-363.
40. Noggle, S.A., D. Weiler, and B.G. Condie, *Notch signaling is inactive but inducible in human embryonic stem cells.* Stem Cells, 2006. **24**(7): p. 1646-1653.
41. Fox, V., et al., *Cell-cell signaling through NOTCH regulates human embryonic stem cell proliferation.* Stem Cells, 2008. **26**(3): p. 715-723.
42. Androutsellis-Theotokis, A., et al., *Notch signalling regulates stem cell numbers in vitro and in vivo.* Nature, 2006. **442**(7104): p. 823-826.
43. Lowell, S., et al., *Notch promotes neural lineage entry by pluripotent embryonic stem cells.* PLoS Biology, 2006. **4**(5): p. 805-818.
44. Oda, T., et al., *Mutations in the human Jagged1 gene are responsible for Alagille syndrome.* Nature Genetics, 1997. **16**(3): p. 235-242.

45. Ellisen, L.W., et al., *TAN-1, The human homolog of the drosophila Notch gene, is broken by chromosomal translocations in t-lymphoblastic neoplasms.* Cell, 1991. **66**(4): p. 649-661.
46. Maier, E., et al., *A Balance of BMP and Notch Activity Regulates Neurogenesis and Olfactory Nerve Formation.* Plos One, 2011. **6**(2).
47. Hynes, R.O., *Cell adhesion: old and new questions.* Trends in Biochemical Sciences, 1999. **24**(12): p. M33-M37.
48. Rozario, T. and D.W. DeSimone, *The extracellular matrix in development and morphogenesis: A dynamic view.* Developmental Biology, 2010. **341**(1): p. 126-140.
49. Watt, F.M., *Epidermal stem cells: markers, patterning and the control of stem cell fate.* Philos Trans R Soc Lond B Biol Sci, 1998. **353**(1370): p. 831-7.
50. Quesenberry, P.J. and P.S. Becker, *Stem cell homing: Rolling, crawling, and nesting.* Proceedings of the National Academy of Sciences of the United States of America, 1998. **95**(26): p. 15155-15157.
51. Thomson, J.A., et al., *Embryonic stem cell lines derived from human blastocysts.* Science, 1998. **282**(5391): p. 1145-1147.
52. Keller, G., *Embryonic stem cell differentiation: emergence of a new era in biology and medicine.* Genes & Development, 2005. **19**(10): p. 1129-1155.
53. Korin, N. and S. Levenberg, *Engineering human embryonic stem cell differentiation.* Biotechnology & genetic engineering reviews, 2007. **24**.
54. Spagnoli, F.M. and A. Hemmati-Brivanlou, *Guiding embryonic stem cells towards differentiation: lessons from molecular embryology.* Current Opinion in Genetics & Development, 2006. **16**(5): p. 469-475.
55. Sasai, Y., *Next-generation regenerative medicine: organogenesis from stem cells in 3D culture.* Cell stem cell, 2013. **12**(5): p. 520-30.
56. Briscoe, J. and J. Ericson, *The specification of neuronal identity by graded sonic hedgehog signalling.* Seminars in Cell & Developmental Biology, 1999. **10**(3): p. 353-362.
57. Towers, M. and C. Tickle, *Growing models of vertebrate limb development.* Development, 2009. **136**(2): p. 179-190.
58. Ingham, P.W. and A.P. McMahon, *Hedgehog signaling in animal development: paradigms and principles.* Genes & Development, 2001. **15**(23): p. 3059-3087.
59. Moore, D.C.P., M. Stanisstreet, and G.E. Evans, *Morphometric analyses of changes in cell-shape in the neuroepithelium of mammalian embryos.* Journal of Anatomy, 1987. **155**: p. 87-99.
60. Sadler, T.W., *Embryology of neural tube development.* American Journal of Medical Genetics Part C-Seminars in Medical Genetics, 2005. **135C**(1): p. 2-8.
61. Sawyer, J.M., et al., *Apical constriction: A cell shape change that can drive morphogenesis.* Developmental Biology, 2010. **341**(1): p. 5-19.
62. Jessell, T.M., *Neuronal specification in the spinal cord: Inductive signals and transcriptional codes.* Nature Reviews Genetics, 2000. **1**(1): p. 20-29.
63. Bhadriraju, K. and C.S. Chen, *Engineering cellular microenvironments to cell-based drug testing improve.* Drug Discovery Today, 2002. **7**(11): p. 612-620.
64. Sun, T., et al., *Culture of skin cells in 3D rather than 2D improves their ability to survive exposure to cytotoxic agents.* Journal of Biotechnology, 2006. **122**(3): p. 372-381.
65. Cukierman, E., R. Pankov, and K.M. Yamada, *Cell interactions with three-dimensional matrices.* Current Opinion in Cell Biology, 2002. **14**(5): p. 633-639.
66. Brizzi, M.F., G. Tarone, and P. Defilippi, *Extracellular matrix, integrins, and growth factors as tailors of the stem cell niche.* Current Opinion in Cell Biology, 2012. **24**(5): p. 645-651.
67. Kulangara, K. and K.W. Leong, *Substrate topography shapes cell function.* Soft Matter, 2009. **5**(21): p. 4072-4076.
68. Bettinger, C.J., R. Langer, and J.T. Borenstein, *Engineering Substrate Topography at the Micro- and Nanoscale to Control Cell Function.* Angewandte Chemie-International Edition, 2009. **48**(30): p. 5406-5415.

69. Hu, W., et al., *Effects of nanoimprinted patterns in tissue-culture polystyrene on cell behavior.* Journal of Vacuum Science & Technology B, 2005. **23**(6): p. 2984-2989.
70. Yim, E.K.F., S.W. Pang, and K.W. Leong, *Synthetic nanostructures inducing differentiation of human mesenchymal stem cells into neuronal lineage.* Experimental Cell Research, 2007. **313**(9): p. 1820-1829.
71. Nagaoka, M., et al., *E-Cadherin-Coated Plates Maintain Pluripotent ES Cells without Colony Formation.* PLoS One, 2006. **1**(1).
72. Pierret, C., et al., *Elements of a neural stem cell niche derived from embryonic stem cells.* Stem Cells and Development, 2007. **16**(6): p. 1017-1026.
73. Ingber, D.E., *Tensegrity: The architectural basis of cellular mechanotransduction.* Annual Review of Physiology, 1997. **59**: p. 575-599.
74. Chen, C.S., et al., *Micropatterned surfaces for control of cell shape, position, and function.* Biotechnology Progress, 1998. **14**(3): p. 356-363.
75. McBeath, R., et al., *Cell shape, cytoskeletal tension, and RhoA regulate stem cell lineage commitment.* Developmental Cell, 2004. **6**(4): p. 483-495.
76. Mei, Y., et al., *Combinatorial development of biomaterials for clonal growth of human pluripotent stem cells.* Nature Materials, 2010. **9**(9): p. 768-778.
77. Schoenwolf, G.C. and J.L. Smith, *Epithelial cell wedging: a fundamental cell behavior contributing to hinge point formation during epithelial morphogenesis.* Seminars in Developmental Biology, 1990. **1**(5): p. 325-334.
78. Folkman, J. and A. Moscona, *Role of cell-shape in growth-control.* Nature, 1978. **273**(5661): p. 345-349.
79. Bokhari, M., et al., *Culture of HepG2 liver cells on three dimensional polystyrene scaffolds enhances cell structure and function during toxicological challenge.* Journal of Anatomy, 2007. **211**: p. 567-576.
80. van Vliet, E., *Current Standing and Future Prospects for the Technologies Proposed to Transform Toxicity Testing in the 21(st) Century.* Altex-Alternatives to Animal Experimentation, 2011. **28**(1): p. 17-44.
81. Keller, G.M., *In-vitro differentiation of embryonic stem-cells.* Current Opinion in Cell Biology, 1995. **7**(6): p. 862-869.
82. Yoshii, Y., et al., *The use of nanoimprinted scaffolds as 3D culture models to facilitate spontaneous tumor cell migration and well-regulated spheroid formation.* Biomaterials, 2011. **32**(26): p. 6052-6058.
83. Banerjee, M. and R.R. Bhonde, *Application of hanging drop technique for stem cell differentiation and cytotoxicity studies.* Cytotechnology, 2006. **51**(1): p. 1-5.
84. De Smedt, A., et al., *Optimisation of the cell cultivation methods in the embryonic stem cell test results in an increased differentiation potential of the cells into strong beating myocard cells.* Toxicology in Vitro, 2008. **22**(7): p. 1789-1796.
85. Szczepny, A., et al., *Identification of Hedgehog Signaling Outcomes in Mouse Testis Development Using a Hanging Drop-Culture System.* Biology of Reproduction, 2009. **80**(2): p. 258-263.
86. Tibbitt, M.W. and K.S. Anseth, *Hydrogels as Extracellular Matrix Mimics for 3D Cell Culture.* Biotechnology and Bioengineering, 2009. **103**(4): p. 655-663.
87. Jongpaiboonkit, L., et al., *An adaptable hydrogel array format for 3-dimensional cell culture and analysis.* Biomaterials, 2008. **29**(23): p. 3346-3356.
88. Heywood, H.K., et al., *Cellular utilization determines viability and matrix distribution profiles in chondrocyte-seeded alginate constructs.* Tissue Engineering, 2004. **10**(9-10): p. 1467-1479.
89. Topman, G., et al., *A new technique for studying directional cell migration in a hydrogel-based three-dimensional matrix for tissue engineering model systems.* Micron (Oxford, England : 1993), 2013. **51**.

90. Semino, C.E., et al., *Functional differentiation of hepatocyte-like spheroid structures from putative liver progenitor cells in three-dimensional peptide scaffolds.* Differentiation, 2003. **71**(4-5): p. 262-270.
91. Sun, T., et al., *Development of a 3D cell culture system for investigating cell interactions with electrospun fibers.* Biotechnology and Bioengineering, 2007. **97**(5): p. 1318-1328.
92. Zhang, X.H., M.R. Reagan, and D.L. Kaplan, *Electrospun silk biomaterial scaffolds for regenerative medicine.* Advanced Drug Delivery Reviews, 2009. **61**(12): p. 988-1006.
93. Yu, C.C., et al., *Electrospun scaffolds composing of alginate, chitosan, collagen and hydroxyapatite for applying in bone tissue engineering.* Materials Letters, 2013. **93**: p. 133-136.
94. Zhang, Y.Z., et al., *Electrospinning of gelatin fibers and gelatin/PCL composite fibrous scaffolds.* Journal of Biomedical Materials Research Part B-Applied Biomaterials, 2005. **72B**(1): p. 156-165.
95. Saraf, A., et al., *Regulated non-viral gene delivery from coaxial electrospun fiber mesh scaffolds.* Journal of Controlled Release, 2010. **143**(1): p. 95-103.
96. Kim, K., et al., *Incorporation and controlled release of a hydrophilic antibiotic using poly(lactide-co-glycolide)-based electrospun nanofibrous scaffolds.* Journal of Controlled Release, 2004. **98**(1): p. 47-56.
97. Xie, J.W. and C.H. Wang, *Electrospun micro- and nanofibers for sustained delivery of paclitaxel to treat C6 glioma in vitro.* Pharmaceutical Research, 2006. **23**(8): p. 1817-1826.
98. Sun, T., et al., *Investigation of fibroblast and keratinocyte cell-scaffold interactions using a novel 3D cell culture system.* Journal of Materials Science-Materials in Medicine, 2007. **18**(2): p. 321-328.
99. Ma, P.X. and J.W. Choi, *Biodegradable polymer scaffolds with well-defined interconnected spherical pore network.* Tissue Engineering, 2001. **7**(1): p. 23-33.
100. Wei, G. and P.X. Ma, *Macroporous and nanofibrous polymer scaffolds and polymer/bone-like apatite composite scaffolds generated by sugar spheres.* Journal of Biomedical Materials Research Part A, 2006. **78A**(2): p. 306-315.
101. Zimmermann, H., S.G. Shirley, and U. Zimmermann, *Alginate-based encapsulation of cells: past, present, and future.* Curr Diab Rep, 2007. **7**(4): p. 314-20.
102. Lutolf, M.P. and J.A. Hubbell, *Synthetic biomaterials as instructive extracellular microenvironments for morphogenesis in tissue engineering.* Nature Biotechnology, 2005. **23**(1): p. 47-55.
103. Nicodemus, G.D. and S.J. Bryant, *Cell encapsulation in biodegradable hydrogels for tissue engineering applications.* Tissue Engineering Part B-Reviews, 2008. **14**(2): p. 149-165.
104. Lau, T.T. and D.A. Wang, *Bioresponsive hydrogel scaffolding systems for 3D constructions in tissue engineering and regenerative medicine.* Nanomedicine, 2013. **8**(4): p. 655-668.
105. Gerecht, S., et al., *Hyaluronic acid hydrogen for controlled self-renewal and differentiation of human embryonic stem cells.* Proceedings of the National Academy of Sciences of the United States of America, 2007. **104**(27): p. 11298-11303.
106. Marklein, R.A. and J.A. Burdick, *Controlling Stem Cell Fate with Material Design.* Advanced Materials, 2010. **22**(2): p. 175-189.
107. Toole, B.P., *Hyaluronan: from extracellular glue to cell signaling cue.* International Journal of Experimental Pathology, 2009. **90**(2): p. A96-A96.
108. Nisbet, D.R., et al., *Review Paper: A Review of the Cellular Response on Electrospun Nanofibers for Tissue Engineering.* Journal of Biomaterials Applications, 2009. **24**(1): p. 7-29.
109. Guex, A.G., et al., *Fine-tuning of substrate architecture and surface chemistry promotes muscle tissue development.* Acta Biomaterialia, 2012. **8**(4): p. 1481-1489.
110. Bokhari, M., et al., *Emulsion-templated porous polymers as scaffolds for three dimensional cell culture: effect of synthesis parameters on scaffold formation and homogeneity.* Journal of Materials Chemistry, 2007. **17**: p. 4088-4094.

111. Carnachan, R.J., et al., *Tailoring the morphology of emulsion-templated porous polymers.* Soft Matter, 2006. **2**(7): p. 608-616.
112. Bokhari, M., et al., *Novel cell culture device enabling three-dimensional cell growth and improved cell function.* Biochemical and Biophysical Research Communications, 2007. **354**(4): p. 1095-1100.
113. Hayman, M.W., et al., *Enhanced neurite outgrowth by human neurons grown on solid three-dimensional scaffolds.* Biochemical and Biophysical Research Communications, 2004. **314**(2): p. 483-488.
114. Hayman, M.W., et al., *Growth of human stem cell-derived neurons on solid three-dimensional polymers.* Journal of Biochemical and Biophysical Methods, 2005. **62**(3): p. 231-240.
115. Busby, W., N.R. Cameron, and C.A.B. Jahoda, *Emulsion-derived foams (PolyHIPEs) containing poly(epsilon-caprolactone) as matrixes for tissue engineering.* Biomacromolecules, 2001. **2**(1): p. 154-164.
116. Maltman, D.J. and S.A. Przyborski, *Developments in three-dimensional cell culture technology aimed at improving the accuracy of in vitro analyses.* Biochem Soc Trans, 2010. **38**(4): p. 1072-5.
117. Tremblay, P.L., et al., *Inosculation of tissue-engineered capillaries with the host's vasculature in a reconstructed skin transplanted on mice.* American Journal of Transplantation, 2005. **5**(5): p. 1002-1010.
118. Levenberg, S., et al., *Engineering vascularized skeletal muscle tissue.* Nature Biotechnology, 2005. **23**(7): p. 879-884.
119. *Biological evaluation of medical devices Part 10:Tests for irritation and skin sensitization (ISO 10993-10:2010)*, in *ISO 10993-10:2010*, B. Standard, Editor. 2010, BSI group.
120. Russell, W.M.S. and R.L. Burch, *The principles of humane experimental technique*, ed. R.L. Burch. 1959, London: Methuen.
121. Andrews, P.W., et al., *Consensus Guidance for Banking and Supply of Human Embryonic Stem Cell Lines for Research Purposes.* Stem Cell Reviews and Reports, 2009. **5**(4): p. 301-314.
122. Andrews, P.W., *From teratocarcinomas to embryonic stem cells.* Philosophical Transactions of the Royal Society of London Series B-Biological Sciences, 2002. **357**(1420): p. 405-417.
123. Kleinsmith, L.J. and G.B. Pierce, *Multipotentiality of single embryonal carcinoma cells.* Cancer Research, 1964. **24**(9): p. 1544-&.
124. Evans, M.J. and M.H. Kaufman, *Establishment in culture of pluripotential cells from mouse embryos.* Nature, 1981. **292**(5819): p. 154-156.
125. Martin, G.R., *Isolation of a pluripotent cell-line from early mouse embryos cultured in medium conditioned by teratocarcinoma stem-cells.* Proceedings of the National Academy of Sciences of the United States of America-Biological Sciences, 1981. **78**(12): p. 7634-7638.
126. Lensch, M.W. and T.A. Ince, *The terminology of teratocarcinomas and teratomas.* Nature Biotechnology, 2007. **25**(11): p. 1211-1211.
127. Przyborski, S.A., et al., *Human embryonal carcinoma stem cells: Models of embryonic development in humans.* Stem Cells and Development, 2004. **13**(4): p. 400-408.
128. Andrews, P.W., et al., *Embryonic stem (ES) cells and embryonal carcinoma (EC) cells: Opposite sides of the same coin.* Biochemical Society Transactions, 2005. **33**: p. 1526-1530.
129. Pera, M.F., et al., *Isolation and characterization of a multipotent clone of human embryonal carcinoma-cells.* Differentiation, 1989. **42**(1): p. 10-23.
130. Pleasure, S.J. and V.M.Y. Lee, *NTERA-2 cells - a human cell-line which displays characteristics expected of a human committed neuronal progenitor-cell.* Journal of Neuroscience Research, 1993. **35**(6): p. 585-602.

131. Stewart, R., V.B. Christie, and S.A. Przyborski, *Manipulation of human pluripotent embryonal carcinoma stem cells and the development of neural subtypes.* Stem Cells, 2003. **21**(3): p. 248-256.
132. Schopperle, W.M. and W.C. DeWolf, *The TRA-1-60 and TRA-1-81 human pluripotent stem cell markers are expressed on podocalyxin in embryonal carcinoma.* Stem Cells, 2007. **25**(3): p. 723-730.
133. Przyborski, S.A., *Isolation of human embryonal carcinoma stem cells by immunomagnetic sorting.* Stem Cells, 2001. **19**(6): p. 500-504.
134. Cooke, M.J., M. Stojkovic, and S.A. Przyborski, *Growth of teratomas derived from human pluripotent stem cells is influenced by the graft site.* Stem Cells and Development, 2006. **15**(2): p. 254-259.
135. Andrews, P.W., et al., *Pluripotent embryonal carcinoma clones derived from the human teratocarcinoma cell-line TERA-2 - differentiation in vivo and in vitro.* Laboratory Investigation, 1984. **50**(2): p. 147-162.
136. Andrews, P.W., et al., *Cell-surface antigens of a clonal human embryonal carcinoma cell line: Morphological and antigenic differentiation in culture.* International Journal of Cancer, 1982. **29**(5): p. 523-531.
137. Lewis, J., *Neurogenic genes and vertebrate neurogenesis.* Current Opinion in Neurobiology, 1996. **6**(1): p. 3-10.
138. Przyborski, S.A., et al., *Developmental regulation of neurogenesis in the pluripotent human embryonal carcinoma cell line NTERA-2.* European Journal of Neuroscience, 2000. **12**(10): p. 3521-3528.
139. Smalley, K.M., M. Lioni, and M. Herlyn, *Life ins't flat: Taking cancer biology to the next dimension.* In Vitro Cellular & Developmental Biology - Animal, 2006. **42**(8-9): p. 242-247.
140. Kleinman, H.K., et al., *Use of extracellular matrix components for cell culture.* Analytical Biochemistry, 1987. **166**(1): p. 1-13.
141. Tamada, Y. and Y. Ikada, *Cell-adhesion to plasma-treated polymer surfaces.* Polymer, 1993. **34**(10): p. 2208-2212.
142. Cooke, M.J., et al., *Enhanced cell attachment using a novel cell culture surface presenting functional domains from extracellular matrix proteins.* Cytotechnology, 2008. **56**(2): p. 71-79.
143. Curtis, A.S.G., et al., *Adhesion of cells to polystyrene surfaces.* Journal of Cell Biology, 1983. **97**(5): p. 1500-1506.
144. Barker, S.L. and P.J. Larocca, *Method of production and control of a commercial tissue culture surface.* Journal of Tissue Culture Methods, 1994. **16**(3-4): p. 151-153.
145. Maroudas, N.G., *Sulfonated polystyrene as an optimal substratum for adhesion and spreading of mesenchymal cells in monovalent and divalent saline solutions.* Journal of Cellular Physiology, 1977. **90**(3): p. 511-519.
146. Klemperer, H.G. and P. Knox, *Attachment and growth of BHK and liver cells on polystyrene: effect of surface groups introduced by treatment with chromic acid.* Laboratory Practice, 1977. **26**: p. 179-180.
147. Chu, P.K., et al., *Plasma-surface modification of biomaterials.* Materials Science & Engineering R-Reports, 2002. **36**(5-6): p. 143-206.
148. Feng, T.S., et al., *Cytoskeletal Disassembly and Cell Rounding Promotes Adipogenesis from ES Cells.* Stem Cell Reviews and Reports, 2010. **6**(1): p. 74-85.
149. Xu, L.C. and C.A. Siedlecki, *Effects of surface wettability and contact time on protein adhesion to biomaterial surfaces.* Biomaterials, 2007. **28**(22): p. 3273-3283.
150. Goddard, J.M. and J.H. Hotchkiss, *Polymer surface modification for the attachment of bioactive compounds.* Progress in Polymer Science, 2007. **32**(7): p. 698-725.
151. Thevenot, P., W.J. Hu, and L.P. Tang, *Surface chemistry influences implant biocompatibility.* Current Topics in Medicinal Chemistry, 2008. **8**(4): p. 270-280.
152. Cretel, E., et al., *How Cells Feel Their Environment: A Focus on Early Dynamic Events.* Cellular and Molecular Bioengineering, 2008. **1**(1): p. 5-14.

153. van Kooten, T.G., H.T. Spijker, and H.J. Busscher, *Plasma-treated polystyrene surfaces: model surfaces for studying cell-biomaterial interactions.* Biomaterials, 2004. **25**(10): p. 1735-1747.
154. Hoshino, T., et al., *Improvement of neuronal cell adhesiveness on parylene with oxygen plasma treatment.* Journal of Bioscience and Bioengineering, 2012. **113**(3): p. 395-398.
155. Kuboki, Y., Q.M. Jin, and H. Takita, *Geometry of carriers controlling phenotypic expression in BMP-induced osteogenesis and chondrogenesis.* Journal of Bone and Joint Surgery-American Volume, 2001. **83A**: p. S105-S115.
156. Aronin, C.E.P., et al., *Comparative effects of scaffold pore size, pore volume, and total void volume on cranial bone healing patterns using microsphere-based scaffolds.* Journal of Biomedical Materials Research Part A, 2009. **89A**(3): p. 632-641.
157. Zeltinger, J., et al., *Effect of pore size and void fraction on cellular adhesion, proliferation, and matrix deposition.* Tissue Engineering, 2001. **7**(5): p. 557-572.
158. Yang, J., et al., *Fabrication and surface modification of macroporous poly(L-lactic acid) and poly(L-lactic-co-glycolic acid) (70/30) cell scaffolds for human skin fibroblast cell culture.* Journal of Biomedical Materials Research, 2002. **62**(3): p. 438-446.
159. van den Dolder, J., P.H.M. Spauwen, and J.A. Jansen, *Evaluation of various seeding techniques for culturing osteogenic cells on titanium fiber mesh.* Tissue Engineering, 2003. **9**(2): p. 315-325.
160. Bokhari, M.A., et al., *Enhancement of osteoblast growth and differentiation in vitro on a peptide hydrogel - polyHIPE polymer hybrid material.* Biomaterials, 2005. **26**(25): p. 5198-5208.
161. Kimlin, L.C., G. Casagrande, and V.M. Virador, *In vitro three-dimensional (3D) models in cancer research: An update.* Molecular Carcinogenesis, 2013. **52**(3): p. 167-182.
162. Lutolf, M.P. and H.M. Blau, *Artificial Stem Cell Niches.* Advanced Materials, 2009. **21**(32-33): p. 3255-3268.
163. Lutolf, M.P., P.M. Gilbert, and H.M. Blau, *Designing materials to direct stem-cell fate.* Nature, 2009. **462**(7272): p. 433-441.
164. Cory, A.H., et al., *Use of an aqueous soluble tetrazolium formazan assay for cell-growth assays in culture.* Cancer Communications, 1991. **3**(7): p. 207-212.
165. Proby, C.M., et al., *Spontaneous keratinocyte cell lines representing early and advanced stages of malignant transformation of the epidermis.* Experimental Dermatology, 2000. **9**(2): p. 104-117.
166. Mitchell, S.A., M.R. Davidson, and R.H. Bradley, *Glow discharge modified tissue culture polystyrene: role of surface chemistry in cellular attachment and proliferation.* Surface Engineering, 2006. **22**(5): p. 337-344.
167. Herbert, C.B., G.D. Bittner, and J.A. Hubbell, *Effects of fibrinolysis on neurite growth from dorsal root ganglia cultured in two- and three-dimensional fibrin gels.* Journal of Comparative Neurology, 1996. **365**(3): p. 380-391.
168. Schense, J.C. and J.A. Hubbell, *Three-dimensional migration of neurites is mediated by adhesion site density and affinity.* Journal of Biological Chemistry, 2000. **275**(10): p. 6813-6818.
169. Cox, S., M. Cole, and B. Tawil, *Behavior of human dermal fibroblasts in three-dimensional fibrin clots: Dependence on fibrinogen and thrombin concentration.* Tissue Engineering, 2004. **10**(5-6): p. 942-954.
170. Tuan, T.L., et al., *In vitro fibroplasia: Matrix contraction, cell growth, and collagen production of fibroblasts cultured in fibrin gels.* Experimental Cell Research, 1996. **223**(1): p. 127-134.
171. Bensaid, W., et al., *A biodegradable fibrin scaffold for mesenchymal stem cell transplantation.* Biomaterials, 2003. **24**(14): p. 2497-2502.
172. Willerth, S.M., et al., *Optimization of fibrin scaffolds for differentiation of murine embryonic stem cells into neural lineage cells.* Biomaterials, 2006. **27**(36): p. 5990-6003.

173. Wake, M.C., C.W. Patrick, and A.G. Mikos, *Pore Morphology Effects on the Fibrovascular Tissue-Growth in Porous Polymer Substrates.* Cell Transplantation, 1994. **3**(4): p. 339-343.
174. Jainchil.Jl, S.A. Aaronson, and G.J. Todaro, *Murine Sarcoma and Leukemia Viruses - Assay Using Clonal Lines of Contact-Inhibited Mouse Cells.* Journal of Virology, 1969. **4**(5): p. 549-&.
175. Yannas, I.V., et al., *Synthesis and Characterization of a Model Extracellular-Matrix That Induces Partial Regeneration of Adult Mammalian Skin.* Proceedings of the National Academy of Sciences of the United States of America, 1989. **86**(3): p. 933-937.
176. Maroudas, N.G., *Chemical and mechanical requirements for fibroblast adhesion.* Nature, 1973. **244**(5415): p. 353-354.
177. Thevenot, P., et al., *Method to Analyze Three-Dimensional Cell Distribution and Infiltration in Degradable Scaffolds.* Tissue Engineering Part C-Methods, 2008. **14**(4): p. 319-331.
178. Bhattarai, S.R., et al., *Novel biodegradable electrospun membrane: scaffold for tissue engineering.* Biomaterials, 2004. **25**(13): p. 2595-2602.
179. Detomaso, L., et al., *Stable plasma-deposited acrylic acid surfaces for cell culture applications.* Biomaterials, 2005. **26**(18): p. 3831-3841.
180. Mackintosh, L.J., C.C. Geddes, and R.M. Herd, *Skin tumours in the West of Scotland renal transplant population.* The British journal of dermatology, 2013. **168**(5).
181. Krynitz, B., et al., *Risk of skin cancer and other malignancies in kidney, liver, heart and lung transplant recipients 1970 to 2008-A Swedish population-based study.* International Journal of Cancer, 2013. **132**(6): p. 1429-1438.
182. Commandeur, S., et al., *An in vitro three-dimensional model of primary human cutaneous squamous cell carcinoma.* Experimental Dermatology, 2009. **18**(10): p. 849-856.
183. Nystrom, M.L., et al., *An in vitro 3D-model of invasive squamous cell carcinoma (SCC) recapitulates in vivo pathology.* Clinical Science (London), 2003. **104**(Supplement 49): p. 28P-29P.
184. Borchers, A.H., et al., *Fibroblast-directed expression and localization of 92-kDa type IV collagenase along the tumor-stroma interface in an in vitro three-dimensional model of human squamous cell carcinoma.* Molecular Carcinogenesis, 1997. **19**(4): p. 258-266.
185. Pera, M.F., B. Reubinoff, and A. Trounson, *Human embryonic stem cells.* Journal of Cell Science, 2000. **113**(1): p. 5-10.
186. Kaufman, D.S., et al., *Hematopoietic colony-forming cells derived from human embryonic stem cells.* Proceedings of the National Academy of Sciences of the United States of America, 2001. **98**(19): p. 10716-10721.
187. Reubinoff, B.E., et al., *Embryonic stem cell lines from human blastocysts: somatic differentiation in vitro.* Nature Biotechnology, 2000. **18**(4): p. 399-404.
188. Itskovitz-Eldor, J., et al., *Differentiation of human embryonic stem cells into embryoid bodies comprising the three embryonic germ layers.* Molecular Medicine, 2000. **6**(2): p. 88-95.
189. Cameron, C.M., W.S. Hu, and D.S. Kaufman, *Improved development of human embryonic stem cell-derived embryoid bodies by stirred vessel cultivation.* Biotechnology and Bioengineering, 2006. **94**(5): p. 938-948.
190. Doetschman, T.C., et al., *The in vitro development of blastocyst-derived embryonic stem-cell lines - formation of visceral yolk-sac, blood islands and myocardium.* Journal of Embryology and Experimental Morphology, 1985. **87**(JUN): p. 27-&.
191. Thomas, P. and R. Beddington, *Anterior primitive endoderm may be responsible for patterning the anterior neural plate in the mouse embryo.* Current Biology, 1996. **6**(11): p. 1487-1496.
192. Vacanti, J.P. and R. Langer, *Tissue engineering: the design and fabrication of living replacement devices for surgical reconstruction and transplantation.* Lancet, 1999. **354**: p. SI32-SI34.

193. Tonge, P.D. and P.W. Andrews, *Retinoic acid directs neuronal differentiation of human pluripotent stem cell lines in a non-cell-autonomous manner.* Differentiation, 2010. **80**(1): p. 20-30.
194. Zeyfert, C.M., S.A. Przyborski, and N.R. Cameron, *Surface functionalized emulsion-templated porous materials for in vitro cell culture in 3D.* Abstracts of Papers of the American Chemical Society, 2009. **238**.
195. Yildirim, E.D., et al., *Enhanced Cellular Functions on Polycaprolactone Tissue Scaffolds by O-2 Plasma Surface Modification.* Plasma Processes and Polymers, 2011. **8**(3): p. 256-267.
196. Hu, W.S., et al., *Effect of glucose on the cultivation of mammalian cells.* Dev Biol Stand, 1987. **66**: p. 279-90.
197. Santini, M.T., et al., *MG-63 human osteosarcoma cells grown in monolayer and as three-dimensional tumor spheroids present a different metabolic profile: a 1H NMR study.* FEBS Letters, 2004. **557**(1-3): p. 148-154.
198. Hassell, T., S. Gleave, and M. Butler, *Growth inhibition in animal cell culture. The effect of lactate and ammonia.* Appl Biochem Biotechnol, 1991. **30**(1): p. 29-41.
199. Ozturk, S.S., *Engineering challenges in high density cell culture systems.* Cytotechnology, 1996. **22**(1-3): p. 3-16.
200. Ozturk, S.S., et al., *Real-time monitoring and control of glucose and lactate concentrations in a mammalian cell perfusion reactor.* Biotechnol Bioeng, 1997. **53**(4): p. 372-8.
201. Fernandes, A.M., et al., *Mouse embryonic stem cell expansion in a microcarrier-based stirred culture system.* J Biotechnol, 2007. **132**(2): p. 227-36.
202. Patel, S.D., et al., *The lactate issue revisited: novel feeding protocols to examine inhibition of cell proliferation and glucose metabolism in hematopoietic cell cultures.* Biotechnol Prog, 2000. **16**(5): p. 885-92.
203. Heywood, H.K., D.L. Bader, and D.A. Lee, *Glucose concentration and medium volume influence cell viability and glycosaminoglycan synthesis in chondrocyte-seeded alginate constructs.* Tissue Engineering, 2006. **12**(12): p. 3487-3496.
204. Razaq, S., R.J. Wilkins, and J.P.G. Urban, *The effect of extracellular pH on matrix turnover by cells of the bovine nucleus pulposus.* European Spine Journal, 2003. **12**(4): p. 341-349.
205. Badylak, S.F., *The extracellular matrix as a scaffold for tissue reconstruction.* Seminars in Cell & Developmental Biology, 2002. **13**(5): p. 377-383.
206. Tilkorn, D.J., et al., *Implanted Myoblast Survival Is Dependent on the Degree of Vascularization in a Novel Delayed Implantation/Prevascularization Tissue Engineering Model.* Tissue Engineering Part A, 2010. **16**(1): p. 165-178.
207. Sachlos, E. and J.T. Czernuszka, *Making tissue engineering scaffolds work: Review on the application of solid freeform fabrication technology to the production of tissue engineering scaffolds.* European Cells & Materials, 2003. **5**(January-June Cited July 25, 2003): p. 29-40.
208. Gstraunthaler, G., T. Seppi, and W. Pfaller, *Impact of culture conditions, culture media volumes, and glucose content on metabolic properties of renal epithelial cell cultures - Are renal cells in tissue culture hypoxic?* Cellular Physiology and Biochemistry, 1999. **9**(3): p. 150-172.
209. Heywood, H.K., et al., *Cellular utilization determines viability and matrix distribution profiles in chondrocyte-seeded alginate constructs.* Tissue Engineering, 2004. **10**(9-10): p. 1467-1479.
210. Cartmell, S.H., et al., *Effects of medium perfusion rate on cell-seeded three-dimensional bone constructs in vitro.* Tissue Engineering, 2003. **9**(6): p. 1197-1203.
211. Toh, Y.C. and J. Voldman, *Fluid shear stress primes mouse embryonic stem cells for differentiation in a self-renewing environment via heparan sulfate proteoglycans transduction.* Faseb Journal, 2011. **25**(4): p. 1208-1217.
212. Yamamoto, K., et al., *Fluid shear stress induces differentiation of Flk-1-positive embryonic stem cells into vascular endothelial cells in vitro.* American Journal of Physiology-Heart and Circulatory Physiology, 2005. **288**(4): p. H1915-H1924.

213. Ahsan, T. and R.M. Nerem, *Fluid Shear Stress Promotes an Endothelial-Like Phenotype During the Early Differentiation of Embryonic Stem Cells.* Tissue Engineering Part A, 2010. **16**(11): p. 3547-3553.
214. Wolfe, R.P. and T. Ahsan, *Shear stress during early embryonic stem cell differentiation promotes hematopoietic and endothelial phenotypes.* Biotechnology and Bioengineering, 2013. **110**(4): p. 1231-1242.
215. Raghavan, S., et al., *Decoupling diffusional from dimensional control of signaling in 3D culture reveals a role for myosin in tubulogenesis.* J Cell Sci, 2010: p. jcs.055079.
216. Yanes, O., et al., *Metabolic oxidation regulates embryonic stem cell differentiation.* Nature Chemical Biology, 2010. **6**(6): p. 411-417.
217. Wohnsland, S., et al., *Neurons and Neuronal Stem Cells Survive in Glucose-Free Lactate and in High Glucose Cell Culture Medium During Normoxia and Anoxia.* Neurochemical Research, 2010. **35**(10): p. 1635-1642.
218. Wang, I.K., K.M. Chang, and L. Ho, *Glucose measurement for cell culture - GlucCell, a modified blood glucose meter.* Genetic Engineering News, 2006. **26**(10): p. 40.
219. Klawitter, J., et al., *Metabolic characteristics of imatinib resistance in chronic myeloid leukaemia cells.* British Journal of Pharmacology, 2009. **158**(2): p. 588-600.
220. Mosmann, T., *Rapid colorimetric assay for cellular growth and survival - application to proliferation and cyto-toxicity assays.* Journal of Immunological Methods, 1983. **65**(1-2): p. 55-63.
221. Rye, H.S., et al., *Fluorometric assay using dimeric dyes for double-stranded and single-stranded-dna and rna with picogram sensitivity.* Analytical Biochemistry, 1993. **208**(1): p. 144-150.
222. Ng, K.W., D.T.W. Leong, and D.W. Hutmacher, *The challenge to measure cell proliferation in two and three dimensions.* Tissue Engineering, 2005. **11**(1-2): p. 182-191.
223. Sengers, B.G., et al., *Computational modelling of cell spreading and tissue regeneration in porous scaffolds.* Biomaterials, 2007. **28**(10): p. 1926-1940.
224. Huang, K.T., Y.H. Chen, and A.M. Walker, *Inaccuracies in MTS assays: major distorting effects of medium, serum albumin, and fatty acids.* Biotechniques, 2004. **37**(3): p. 406, 408, 410-2.
225. *BS EN ISO 10993-5:2009 Biological evaluation of medical devices, Part 5: Tests for in vitro cytotoxicity*. BSI group.
226. Khodarev, N.N., et al., *Tumour-endothelium interactions in co-culture: coordinated changes of gene expression profiles and phenotypic properties of endothelial cells.* Journal of Cell Science, 2003. **116**(6): p. 1013-1022.
227. Gahwiler, B.H., et al., *Organotypic slice cultures: a technique has come of age.* Trends in Neurosciences, 1997. **20**(10): p. 471-477.
228. Miller, M.H., H. Amos, and D.A. Sens, *Regulation of glucose-utilization in chick-embryo fibroblasts by bicarbonate ion.* Journal of Cellular Physiology, 1981. **107**(2): p. 295-302.
229. Lelong, I.H. and G. Rebel, *pH drift of "physiological buffers" and culture media used for cell incubation during in vitro studies.* Journal of Pharmacological and Toxicological Methods, 1998. **39**(4): p. 203-210.
230. Philp, A., A.L. Macdonald, and P.W. Watt, *Lactate - a signal coordinating cell and systemic function.* Journal of Experimental Biology, 2005. **208**(24): p. 4561-4575.
231. Green, H. and B. Goldberg, *Collagen + cell protein synthesis by established mammalian fibroblast line.* Nature, 1964. **204**(495): p. 347-&.
232. Constant, J.S., et al., *Lactate elicits vascular endothelial growth factor from macrophages: a possible alternative to hypoxia.* Wound Repair and Regeneration, 2000. **8**(5): p. 353-360.
233. Zieker, D., et al., *Lactate modulates gene expression in human mesenchymal stem cells.* Langenbecks Archives of Surgery, 2008. **393**(3): p. 297-301.
234. Schneider, C.C., et al., *Lactate Influences the Gene Expression Profile of Human Mesenchymal Stem Cells (hMSC) in a Dose Dependant Manner.* Cellular Physiology and Biochemistry, 2012. **30**(6): p. 1547-1556.

235. Monazzam, A., et al., *Application of the multicellular tumour spheroid model to screen PET tracers for analysis of early response of chemotherapy in breast cancer.* Breast Cancer Research, 2007. **9**(4).
236. Laurent, J., et al., *Multicellular tumor spheroid models to explore cell cycle checkpoints in 3D.* Bmc Cancer, 2013. **13**.
237. Enver, T., et al., *Cellular differentiation hierarchies in normal and culture-adapted human embryonic stem cells.* Human Molecular Genetics, 2005. **14**(21): p. 3129-3140.
238. Pellerin, L. and P.J. Magistretti, *Glutamate uptake into astrocytes stimulates aerobic glycolysis - a mechanism coupling neuronal-activity to glucose-utilization.* Proceedings of the National Academy of Sciences of the United States of America, 1994. **91**(22): p. 10625-10629.
239. Tsacopoulos, M. and P.J. Magistretti, *Metabolic coupling between glia and neurons.* Journal of Neuroscience, 1996. **16**(3): p. 877-885.
240. Bouzier-Sore, A.K., et al., *Lactate is a preferential oxidative energy substrate over glucose for neurons in culture.* Journal of Cerebral Blood Flow and Metabolism, 2003. **23**(11): p. 1298-1306.
241. Chih, C.P. and E.L. Roberts, *Energy substrates for neurons during neural activity: a critical review of the astrocyte-neuron lactate shuttle hypothesis.* Journal of Cerebral Blood Flow and Metabolism, 2003. **23**(11): p. 1263-1281.
242. Birket, M.J., et al., *A reduction in ATP demand and mitochondrial activity with neural differentiation of human embryonic stem cells.* Journal of Cell Science, 2011. **124**(3): p. 348-358.
243. Folmes, C.D.L., et al., *Energy metabolism plasticity enables stemness programs*, in *Evolving Challenges in Promoting Cardiovascular Health*. 2012, Blackwell Science Publ: Oxford. p. 82-89.
244. Fornazari, M., et al., *Neuronal differentiation involves a shift from glucose oxidation to fermentation.* Journal of Bioenergetics and Biomembranes, 2011. **43**(5): p. 531-539.
245. Budd, S.L. and D.G. Nicholls, *Mitochondria, calcium regulation, and acute glutamate excitotoxicity in cultured cerebellar granule cells.* Journal of Neurochemistry, 1996. **67**(6): p. 2282-2291.
246. Castilho, R.F., et al., *Mitochondrial control of acute glutamate excitotoxicity in cultured cerebellar granule cells.* Journal of Neuroscience, 1998. **18**(24): p. 10277-10286.
247. Nicholls, D.G. and S.L. Budd, *Mitochondria and neuronal glutamate excitotoxicity.* Biochimica Et Biophysica Acta-Bioenergetics, 1998. **1366**(1-2): p. 97-112.
248. Lampe, K.J., et al., *Impact of Lactic Acid on Cell Proliferation and Free Radical-Induced Cell Death in Monolayer Cultures of Neural Precursor Cells.* Biotechnology and Bioengineering, 2009. **103**(6): p. 1214-1223.
249. Oravecz, K., et al., *The involvement of hydroxyl free radicals in differentiation of the PC-12 rat pheochromocytoma cell line.* Archives of Gerontology and Geriatrics, 2001. **33**(1): p. 61-69.
250. Oravecz, K., et al., *Hydroxyl free radicals induce cell differentiation in SK-N-MC neuroblastoma cells.* Tissue & Cell, 2002. **34**(1): p. 33-38.
251. Groussard, C., et al., *Free radical scavenging and antioxidant effects of lactate ion: an in vitro study.* Journal of Applied Physiology, 2000. **89**(1): p. 169-175.
252. Konopka, R., et al., *Alternation of retinoic acid induced neural differentiation of P19 embryonal carcinoma cells by reduction of reactive oxygen species intracellular production.* Neuroendocrinology Letters, 2008. **29**(5): p. 770-774.
253. Christie, V.B., et al., *Synthesis and evaluation of synthetic retinoid derivatives as inducers of stem cell differentiation.* Organic & Biomolecular Chemistry, 2008. **6**(19): p. 3497-3507.
254. Watt, F.M. and B.L.M. Hogan, *Out of Eden: Stem cells and their niches.* Science, 2000. **287**(5457): p. 1427-1430.
255. Zhu, A.J., I. Haase, and F.M. Watt, *Signaling via beta 1 integrins and mitogen-activated protein kinase determines human epidermal stem cell fate in vitro.* Proceedings of the

National Academy of Sciences of the United States of America, 1999. **96**(12): p. 6728-6733.
256. Czyz, J. and A.M. Wobus, *Embryonic stem cell differentiation: The role of extracellular factors.* Differentiation, 2001. **68**(4-5): p. 167-174.
257. Owczarek, C.M., et al., *Inter-species chimeras of leukaemia inhibitory factor define a major human receptor-binding determinant.* EMBO J, 1993. **12**(9): p. 3487-95.
258. Ma, W., et al., *Cell-extracellular matrix interactions regulate neural differentiation of human embryonic stem cells.* Bmc Developmental Biology, 2008. **8**.
259. Dickinson, L.E., S. Kusuma, and S. Gerecht, *Reconstructing the Differentiation Niche of Embryonic Stem Cells Using Biomaterials.* Macromolecular Bioscience, 2011. **11**(1): p. 36-49.
260. Lee, L.H., et al., *Micropatterning of human embryonic stem cells dissects the mesoderm and endoderm lineages.* Stem Cell Research, 2009. **2**(2): p. 155-162.
261. Xu, C.H., et al., *Feeder-free growth of undifferentiated human embryonic stem cells.* Nature Biotechnology, 2001. **19**(10): p. 971-974.
262. Hughes, C.S., L.M. Postovit, and G.A. Lajoie, *Matrigel: A complex protein mixture required for optimal growth of cell culture.* Proteomics, 2010. **10**(9): p. 1886-1890.
263. Ludwig, T.E., et al., *Derivation of human embryonic stem cells in defined conditions.* Nature Biotechnology, 2006. **24**(2): p. 185-187.
264. Klim, J.R., et al., *A defined glycosaminoglycan-binding substratum for human pluripotent stem cells.* Nature Methods, 2010. **7**(12): p. 989-U72.
265. Villa-Diaz, L.G., et al., *Synthetic polymer coatings for long-term growth of human embryonic stem cells.* Nature Biotechnology, 2010. **28**(6): p. 581-583.
266. Irwin, E.E., et al., *Engineered polymer-media interfaces for the long-term self-renewal of human embryonic stem cells.* Biomaterials, 2011. **32**(29): p. 6912-6919.
267. Kunova, M., et al., *Adaptation to Robust Monolayer Expansion Produces Human Pluripotent Stem Cells With Improved Viability.* Stem Cells Translational Medicine, 2013. **2**(4): p. 246-254.
268. Dellatore, S.M., A.S. Garcia, and W.M. Miller, *Mimicking stem cell niches to increase stem cell expansion.* Current Opinion in Biotechnology, 2008. **19**(5): p. 534-540.
269. Bradley, A., et al., *Formation of germ-line chimeras from embryo-derived teratocarcinoma cell-lines.* Nature, 1984. **309**(5965): p. 255-256.
270. Barta, T., et al., *Cell cycle regulation in human embryonic stem cells: links to adaptation to cell culture.* Experimental Biology and Medicine, 2013. **238**(3): p. 271-275.
271. Falix, F.A., et al., *Possible roles of DLK1 in the Notch pathway during development and disease.* Biochimica Et Biophysica Acta-Molecular Basis of Disease, 2012. **1822**(6): p. 988-995.
272. Kraehenbuehl, T.P., R. Langer, and L.S. Ferreira, *Three-dimensional biomaterials for the study of human pluripotent stem cells.* Nature Methods, 2011. **8**(9): p. 731-736.
273. Garreta, E., et al., *Osteogenic differentiation of mouse embryonic stem cells and mouse embryonic fibroblasts in a three-dimensional self-assembling peptide scaffold.* Tissue Engineering, 2006. **12**(8): p. 2215-2227.
274. Hwang, N.S., et al., *Enhanced chondrogenic differentiation of murine embryonic stem cells in hydrogels with glucosamine.* Biomaterials, 2006. **27**(36): p. 6015-6023.
275. Gerecht, S., et al., *Hyaluronic acid hydrogel for controlled self-renewal and differentiation of human embryonic stem cells.* Proceedings of the National Academy of Sciences of the United States of America, 2007. **104**(27): p. 11298-11303.
276. Toole, B.P., *Hyaluronan in morphogenesis.* Seminars in Cell & Developmental Biology, 2001. **12**(2): p. 79-87.
277. Liu, L., et al., *Chemically-defined scaffolds created with electrospun synthetic nanofibers to maintain mouse embryonic stem cell culture under feeder-free conditions.* Biotechnology Letters, 2012. **34**(10): p. 1951-1957.

278. Lu, H.F., et al., *A 3D microfibrous scaffold for long-term human pluripotent stem cell self-renewal under chemically defined conditions.* Biomaterials, 2012. **33**(8): p. 2419-2430.
279. Faulkner-Jones, A., et al., *Development of a valve-based cell printer for the formation of human embryonic stem cell spheroid aggregates.* Biofabrication, 2013. **5**(1).
280. Ludwig, T.E., et al., *Feeder-independent culture of human embryonic stem cells.* Nature Methods, 2006. **3**(8): p. 637-646.
281. Moody, J., *Feeder-independent culture systems for human pluripotent stem cells.* Methods in molecular biology (Clifton, N.J.), 2013. **946**.
282. Ballester-Beltran, J., et al., *Dorsal and Ventral Stimuli in Cell-Material Interactions: Effect on Cell Morphology.* Biointerphases, 2012. **7**(1-4).
283. Reilly, G.C. and A.J. Engler, *Intrinsic extracellular matrix properties regulate stem cell differentiation.* Journal of Biomechanics, 2010. **43**(1): p. 55-62.
284. Bajpai, R., et al., *Efficient propagation of single cells accutase-dissociated human embryonic stem cells.* Molecular Reproduction and Development, 2008. **75**(5): p. 818-827.
285. Huang, H.L., et al., *Trypsin-induced proteome alteration during cell subculture in mammalian cells.* Journal of Biomedical Science, 2010. **17**.
286. Rupf, T., et al., *Cryopreservation of organotypical cultures based on 3d scaffolds.* Cryoletters, 2010. **31**(2): p. 157-168.
287. Costa, P.F., et al., *Cryopreservation of Cell/Scaffold Tissue-Engineered Constructs.* Tissue Engineering Part C-Methods, 2012. **18**(11): p. 852-858.
288. Henderson, J.K., et al., *Preimplantation human embryos and embryonic stem cells show comparable expression of stage-specific embryonic antigens.* Stem Cells, 2002. **20**(4): p. 329-337.
289. Brimble, S.N., et al., *The cell surface glycosphingolipids SSEA-3 and SSEA-4 are not essential for human ESC pluripotency.* Stem Cells, 2007. **25**(1): p. 54-62.
290. Harrison, N.J., D. Baker, and P.W. Andrews, *Culture adaptation of embryonic stem cells echoes germ cell malignancy.* International Journal of Andrology, 2007. **30**(4): p. 275-281.
291. Park, Y.B., et al., *Alterations of proliferative and differentiation potentials of human embryonic stem cells during long-term culture.* Experimental & molecular medicine, 2008. **40**(1).
292. Baharvand, H., et al., *Differentiation of human embryonic stem cells into hepatocytes in 2D and 3D culture systems in vitro.* International Journal of Developmental Biology, 2006. **50**(7): p. 645-652.
293. Horrocks, G.M., et al., *Formation of neurospheres from human embryonal carcinoma stem cells.* Biochemical and Biophysical Research Communications, 2003. **304**(2): p. 411-416.
294. Horrocks, G.M. and S.A. Przyborski, *Determination of neural and epithelial cell fate in the human embryonic ectoderm: the role of bone morphogenetic proteins.* Journal of Anatomy, 2004. **205**(6): p. 525.
295. Storm, M.P., et al., *Three-dimensional culture systems for the expansion of pluripotent embryonic stem cells.* Biotechnology and Bioengineering, 2010. **107**(4): p. 683-695.
296. Dolgin, E., *Putting Stem Cells to the Test.* Nature Medicine, 2010. **16**(12): p. 1354-1357.
297. Adewumi, O., et al., *Characterization of human embryonic stem cell lines by the International Stem Cell Initiative.* Nature Biotechnology, 2007. **25**(7): p. 803-816.
298. Muller, F.J., et al., *A Call to Standardize Teratoma Assays Used to Define Human Pluripotent Cell Lines.* Cell Stem Cell, 2010. **6**(5): p. 412-414.
299. Gropp, M., et al., *Standardization of the Teratoma Assay for Analysis of Pluripotency of Human ES Cells and Biosafety of Their Differentiated Progeny.* Plos One, 2012. **7**(9).
300. Gertow, K., et al., *Isolation of human embryonic stem cell-derived teratomas for the assessment of pluripotency.* Current protocols in stem cell biology, 2007. **Chapter 1**.
301. Prokhorova, T.A., et al., *Teratoma Formation by Human Embryonic Stem Cells Is Site Dependent and Enhanced by the Presence of Matrigel.* Stem Cells and Development, 2009. **18**(1): p. 47-54.

302. Cooke, M.J., *The influence of the extracellular matrix on cell behaviour*. 2009, Durham University.
303. Buta, C., et al., *Reconsidering pluripotency tests: Do we still need teratoma assays?* Stem Cell Research, 2013. **11**(1): p. 552-562.
304. Pesce, M. and H.R. Scholer, *Oct-4: Gatekeeper in the beginnings of mammalian development.* Stem Cells, 2001. **19**(4): p. 271-278.
305. Mitsui, K., et al., *The homeoprotein Nanog is required for maintenance of pluripotency in mouse epiblast and ES cells.* Cell, 2003. **113**(5): p. 631-642.
306. Fong, H.L., K.A. Hohenstein, and P.J. Donovan, *Regulation of self-renewal and pluripotency by Sox2 in human embryonic stem cells.* Stem Cells, 2008. **26**(8): p. 1931-1938.
307. Muller, F.J., et al., *A bioinformatic assay for pluripotency in human cells.* Nature Methods, 2011. **8**(4): p. 315-U54.
308. Sheridan, S.D., V. Surampudi, and R.R. Rao, *Analysis of embryoid bodies derived from human induced pluripotent stem cells as a means to assess pluripotency.* Stem cells international, 2012. **2012**.
309. Pekkanen-Mattila, M., et al., *Spatial and temporal expression pattern of germ layer markers during human embryonic stem cell differentiation in embryoid bodies.* Histochemistry and Cell Biology, 2010. **133**(5): p. 595-606.
310. Fuchs, C., et al., *Self-Organization Phenomena in Embryonic Stem Cell-Derived Embryoid Bodies: Axis Formation and Breaking of Symmetry during Cardiomyogenesis.* Cells Tissues Organs, 2012. **195**(5): p. 377-391.
311. Rula, M.E., et al., *Cell autonomous sorting and surface positioning in the formation of primitive endoderm in embryoid bodies.* Genesis, 2007. **45**(6): p. 327-338.
312. ten Berge, D., et al., *Wnt Signaling Mediates Self-Organization and Axis Formation in Embryoid Bodies.* Cell Stem Cell, 2008. **3**(5): p. 508-518.
313. Brohem, C.A., et al., *Artificial skin in perspective: concepts and applications.* Pigment Cell & Melanoma Research, 2011. **24**(1): p. 35-50.
314. Giobbe, G.G., et al., *Confined 3D microenvironment regulates early differentiation in human pluripotent stem cells.* Biotechnology and Bioengineering, 2012. **109**(12): p. 3119-3132.
315. Gerlach, J.C., et al., *Dynamic 3D Culture Promotes Spontaneous Embryonic Stem Cell Differentiation In Vitro.* Tissue Engineering Part C-Methods, 2010. **16**(1): p. 115-121.
316. Stachelscheid, H., et al., *Teratoma formation of human embryonic stem cells in three-dimensional perfusion culture bioreactors.* Journal of tissue engineering and regenerative medicine, 2013. **7**(9).
317. Zeilinger, K., et al., *Scaling Down of a Clinical Three-Dimensional Perfusion Multicompartment Hollow Fiber Liver Bioreactor Developed for Extracorporeal Liver Support to an Analytical Scale Device Useful for Hepatic Pharmacological In Vitro Studies.* Tissue Engineering Part C-Methods, 2011. **17**(5): p. 549-556.
318. Antonchuk, J., *Formation of embryoid bodies from human pluripotent stem cells using AggreWell plates.* Methods in molecular biology (Clifton, N.J.), 2013. **946**.
319. Messana, J.M., et al., *Size of the embryoid body influences chondrogenesis of mouse embryonic stem cells.* Journal of Tissue Engineering and Regenerative Medicine, 2008. **2**(8): p. 499-506.
320. Bratt-Leal, A.M., R.L. Carpenedo, and T.C. McDevitt, *Engineering the Embryoid Body Microenvironment to Direct Embryonic Stem Cell Differentiation.* Biotechnology Progress, 2009. **25**(1): p. 43-51.
321. Bader, A., et al., *Paracrine promotion of cardiomyogenesis in embryoid bodies by LIF modulated endoderm.* Differentiation, 2001. **68**(1): p. 31-43.
322. Kopper, O., et al., *Characterization of Gastrulation-Stage Progenitor Cells and Their Inhibitory Crosstalk in Human Embryoid Bodies.* Stem Cells, 2010. **28**(1): p. 75-83.
323. Alvarez-Perez, M.A., et al., *Influence of Gelatin Cues in PCL Electrospun Membranes on Nerve Outgrowth.* Biomacromolecules, 2010. **11**(9): p. 2238-2246.

324. Kurosawa, H., *Methods for inducing embryoid body formation: In vitro differentiation system of embryonic stem cells.* Journal of Bioscience and Bioengineering, 2007. **103**(5): p. 389-398.
325. Wang, L., et al., *Self-renewal of human embryonic stem cells requires insuhn-like growth factor-1 receptor and ERBB2 receptor signaling.* Blood, 2007. **110**(12): p. 4111-4119.
326. Schutte, M., et al., *Rat Primary Hepatocytes Show Enhanced Performance and Sensitivity to Acetaminophen During Three-Dimensional Culture on a Polystyrene Scaffold Designed for Routine Use.* Assay and Drug Development Technologies, 2011. **9**(5): p. 475-486.
327. Chang, T.T. and M. Hughes-Fulford, *Monolayer and Spheroid Culture of Human Liver Hepatocellular Carcinoma Cell Line Cells Demonstrate Distinct Global Gene Expression Patterns and Functional Phenotypes.* Tissue Engineering Part A, 2009. **15**(3): p. 559-567.
328. Illes, S., et al., *Niche-dependent development of functional neuronal networks from embryonic stem cell-derived neural populations.* Bmc Neuroscience, 2009. **10**.